Ba 58

Synthesis of the bedrock geology in the Bergslagen region, Fennoscandian Shield, south-central Sweden

Michael B. Stephens, Magnus Ripa, Ingmar Lundström, Lena Persson, Torbjörn Bergman, Martin Ahl, Carl-Henric Wahlgren, Per-Olof Persson & Linda Wickström

SGU
Sveriges geologiska undersökning
Geological Survey of Sweden

Ba 58

Synthesis of the bedrock geology in the Bergslagen region, Fennoscandian Shield, south-central Sweden

Michael B. Stephens, Magnus Ripa, Ingmar Lundström, Lena Persson, Torbjörn Bergman, Martin Ahl, Carl-Henric Wahlgren, Per-Olof Persson & Linda Wickström

Sveriges geologiska undersökning
2009

ISSN 0373-2657
ISBN 978-91-7158-883-8

Cover: View of the main frame at the Garpenberg Zn-Pb-Ag-(Cu-Au) sulphide deposit in the central part of the Bergslagen region, owned and operated by Boliden AB.

Layout: Jeanette Bergman Weihed
Tryck: AB Danagårds Grafiska, Ödeshög, 2009

Preface

The Bergslagen region in south-central Sweden is one of Sweden's important metallic mineral provinces with three currently operating mines (see cover photograph). Digital databases for bedrock geological information for the Bergslagen region were released by the Geological Survey of Sweden (SGU) during 2001 for public usage, following completion of the so-called Bergslagen project. Geophysical maps over the region were published 2002 and bedrock geological maps that addressed different themes were published during 2007. This report presents an evaluation of the various data sets used in the map compilation work and a modern, integrated synthesis of the bedrock geology in the region. It has been written for a professional audience, in particular geoscientists employed in exploration and mining companies, consultant agencies and universities.

Following a short introduction, the aims, scope and products of the work within the Bergslagen project are described. Some nomenclatural considerations and the regional tectonic framework of the Bergslagen region are subsequently presented. The data available for use in the project as well as new data acquired in connection with its execution are summarized in later sections. Methodological aspects that concern the acquisition and interpretation of new data are also addressed.

The key results of the work within the project are presented in three separate sections, each of which opens with an overview of the content in the respective section. The character, spatial distribution, geochronology, geochemical signature, petrophysical characteristics and regional geophysical signature of the different bedrock units in the region are addressed in the first section. This section also includes a detailed description of Svecofennian metavolcanic rocks and their relationship to metasedimentary rocks in twelve selected sub-areas in the Bergslagen region. The mineral and bedrock deposits that have been a focus for exploration and mining activities in historical time are described in the second section. Finally, the deformation and metamorphism in the bedrock as well as the mechanism of emplacement of one of the suites of intrusive rocks are addressed in the third section. On the basis of the results in the previous sections, a tectonic model for Svecokarelian orogenic activity in the Bergslagen region between 1.9 and 1.8 Ga is subsequently presented and key geological issues that require more attention in future work are identified.

The report is completed with a description of excursion stops in the Bergslagen region, four errata and a clarification to the published geological maps, a reference list and an appendix. The appendix presents eleven new age determinations using U-Pb analyses of zircon, monazite and titanite at ten different sites in this region.

Different sections or parts of sections have been written by different people at SGU. Michael Stephens has been responsible for the homogenization of both the text and figures in these different contributions and the necessary editorial amendments of the text. The contribution of the authors of the report is as follows:

- Summary: *Michael Stephens.*
- Introduction: *Michael Stephens*.
- Aims, scope and products: *Michael Stephens*.
- Nomenclature: *Michael Stephens*.
- Regional tectonic framework: *Michael Stephens*.
- Data input: *Michael Stephens with complementary text from Martin Ahl (geochemistry) and Lena Persson (geophysics).*
- Acquisition of new data and data interpretation – methodological aspects: *Michael Stephens with complementary text from Martin Ahl (geochemistry), Ingmar Lundström (hydrothermal alteration) and Lena Persson (geophysics).*
- Character, spatial distribution, geochronology, geochemical signature, petrophysical characteristics and regional geophysical signature of rock units: *Martin Ahl, Ingmar Lundström, Lena Persson, Magnus Ripa, Michael Stephens, Carl-Henric Wahlgren and Linda Wickström*.
- Mineral and bedrock deposits: *Torbjörn Bergman and Magnus Ripa*.
- Deformation, metamorphism and mechanism of emplacement of the 1.87–1.84 Ga GSDG suite of intrusive rocks: *Michael Stephens with complementary text from Lena Persson (gravity modelling).*
- Tectonic model for Svecokarelian orogenic activity in the Bergslagen region: *Michael Stephens*.
- Key issues for future work: *Michael Stephens*.
- Description of excursion stops: *Ingmar Lundström, Michael Stephens and Carl-Henric Wahlgren with complementary text from Torbjörn Bergman and Lena Persson*.
- Errata and some clarification to the geological maps: *Michael Stephens*.
- Appendix. Age determinations using U-Pb analyses of zircon, monazite and titanite: *Michael Stephens, Per-Olof Persson and Ingmar Lundström*.

Vladislav Stejskal (formerly SGU) and Torbjörn Wikström (formerly SGU) carried out digitization of the bedrock geological maps in the Bergslagen region under the leadership of Michael Stephens. Besides the

authors of the report, the following people have kindly provided photographs and figures: Rodney Allen (Boliden AB), Jan-Olof Arnbom (SGU), Stefan Bergman (SGU), Tobias Hermansson (Boliden AB), Erik Jonsson (SGU), Benno Kathol (SGU), Sven Lundqvist (SGU), Lars Malmström (Zinkgruvan Mining AB) and Malin Sträng (Golder Associates AB, formerly SGU). Svensk Kärnbränslehantering AB (SKB) and, in particular, Anders Lindblom (SKB) are also thanked for providing some figures published earlier in SKB reports. Many of the figures in the text that show geological maps were produced by Jeanette Bergman Weihed (SGU).

Lars Malmström (Zinkgruvan Mining AB) is thanked for his comments on the text that describes Zinkgruvan. Rodney Allen and Erik Lundstam (Boliden AB) are thanked for discussion on the geology at Garpenberg, and John Berge (JB MinQuest) and Jan-Erik Björklund (Lovisagruvan AB) for discussion on the geology at Lovisagruvan. Stefan Bergman (SGU) and Benno Kathol (SGU) are thanked for a review that radically improved the manuscript. Jenny Andersson (SGU) is also thanked for a constructive review of the appendix.

Michael Stephens

Contents

Summary

The Bergslagen region in central Sweden forms one of Sweden's important provinces for the exploitation of metallic mineral deposits, with three currently operating mines at the base metal sulphide deposits Garpenberg, Zinkgruvan and Lovisagruvan. The current synthesis of the bedrock geology in this region complements the regional geological and geophysical maps that were published by the Geological Survey of Sweden (SGU) during 2002 and 2007.

The synthesis and map compilation work have made use of primary data available in various databases at SGU as well as published descriptions. The results of the detailed investigations in the north-eastern part of the region around Forsmark, concerned with the characterization of a possible site for the disposal of highly radioactive nuclear waste, have also been utilized. The work has also involved the acquirement of new data that have radically updated several databases or even generated, for the first time, digital cartographic information at a scale of resolution of 1:250 000. Furthermore, new data have been acquired concerning the physical volcanology and age of the metamorphosed, volcanic and subvolcanic intrusive rocks (1.91–1.89 Ga), the stratigraphic relationships between this important ore-bearing unit and surrounding metasedimentary rocks, and the structural geology in different domains inside the Bergslagen region.

CHARACTER AND TECTONIC SETTING OF ROCK UNITS IN TIME SEQUENCE

The Bergslagen region is situated predominantly in the south-western part of the Svecokarelian orogen in the Fennoscandian Shield. The region is dominated by Palaeoproterozoic rocks formed between 1.9 and 1.8 Ga. These rocks were variably affected by Svecokarelian deformation and metamorphism over the whole region during the same time period and, to variable extent in western areas, by a Sveconorwegian tectonic overprint between 1.0 and 0.9 Ga. Subordinate rocks consist of an alkaline intrusive rock of uncertain age and rocks that formed around or after 1.7 Ga. The latter include Proterozoic rocks that formed after the Svecokarelian orogenic activity but are variably affected, in western areas, by Sveconorwegian deformation and metamorphism. Fault-bounded outliers of Neoproterozoic and Lower Palaeozoic sedimentary rocks are also present and form a cover to the crystalline bedrock in this part of the shield.

Rocks formed between 1.9 and 1.8 Ga

Turbiditic metagreywacke dominates the oldest part of the supracrustal sequence in the region. These clastic metasedimentary rocks shallow upwards into quartzite and subsequently into metavolcanic rocks that are predominantly rhyolitic or dacitic and medium-K in composition. Metamorphosed, well-sorted sandy rocks or even conglomerate are also intercalated with the volcanic rocks in several parts of the region. Calcite- or dolomite-rich, crystalline carbonate rock and calc-silicate rock (skarn) are spatially associated with the upper part of the volcanic succession, where also most of the metallic mineral deposits are located. A younger sequence of clastic metasedimentary rocks, including meta-argillite, metamorphosed, sandy to muddy turbidite and, in places, quartzite and metaconglomerate lie stratigraphically above the volcanic rocks. Felsic subvolcanic intrusions and cryptodomes are a conspicuous feature in the supracrustal succession, while mafic dykes or sills intruded during deposition of the younger clastic metasedimentary rocks.

Both Archaean (3.0–2.5 Ga) and Palaeoproterozoic (2.1–1.9 Ga) detrital zircons have been identified in the clastic metasedimentary rocks that lie stratigraphically beneath or are intercalated with the volcanic rocks. Negative ε_{Nd} values in the metasedimentary rocks are consistent with the age data for the detrital zircons. The U-Pb (zircon) ages for the metamorphosed, felsic volcanic and subvolcanic rocks span from 1906±3 Ma to 1887±5 Ma.

In accordance with the conceptual understanding of the region as presented in earlier publications, the supracrustal succession described above records ambient, deep water sedimentation that was interrupted at 1.9 Ga by a volcanic episode accompanied by thermal doming. Shallow water or, locally, even subaerial eruptive and depositional environments prevailed during an intense volcanism and extension stage. Volcanism during this stage was explosive and produced thick successions of massive, poorly bedded volcanic sandstone and breccia. The waning volcanic stage, represented in the upper part of the volcanic succession, was characterized by regional subsidence and the deposition of bedded successions of volcanic siltstone to sandstone and carbonate rocks. Transgression and resumed deep water sedimentation generally prevailed during the concluding sedimentary, thermal subsidence stage.

Prior to the ductile deformation under greenschist- or predominantly amphibolite-facies metamorphic

conditions, the volcanic rocks were affected, to variable extent, by different types of regional hydrothermal alteration. Sodium or potassium alteration mainly caused readjustments of feldspar compositions in the volcanic rocks. Magnesium ± iron ± potassium ± silicon alteration ("magnesium alteration") resulted in the destruction of feldspar in the volcanic rocks and replacement by phyllosilicates. Calcium ± magnesium ± iron alteration ("skarn alteration") gave rise to calc-silicate blastesis and is, in many places, linked to the intrusion of mafic dykes. The effects of hydrothermal alteration are also prominent in the geochemical composition and gamma radiation characteristics of the volcanic rocks.

The 1.91–1.89 Ga and older supracrustal rocks were intruded by several different suites of igneous rocks that can be distinguished using a combination of compositional trend, intrusion–deformation relationships and absolute age. Three different compositional suites have been identified, referred to as the Granitoid-dioritoid-gabbroid (GDG), Granite-syenitoid-dioritoid-gabbroid (GSDG) and Granite-pegmatite (GP) intrusive rock suites.

Mingling relationships between rocks with felsic composition and rocks with more primitive compositions are a conspicuous feature of the intrusive rocks in the GDG and GSDG suites. The GDG rocks show a calc-alkaline to calcic trend, while the GSDG rocks show an alkali-calcic trend and an alkali composition similar to shoshonitic rocks. A compositionally more homogeneous character and high concentrations of uranium and thorium form the distinctive features of the intrusive rocks in the GP suite. Furthermore, the latter are distinguished from the rocks in the other suites on the basis of their conspicuous geophysical signatures, not least in the gravity and airborne radiometric data. The GP rocks also show an alkali composition similar to shoshonitic rocks. Gravity modelling of some GSDG and GP intrusive bodies indicates their sheet-like character with a vertical extension considerably less than the horizontal extension at the ground surface.

Metamorphosed, pre-tectonic GDG rocks, with U-Pb (zircon) ages that span from 1901±6 Ma to 1867±4 Ma, comprise the oldest intrusive rock suite in the Bergslagen region (1.90–1.87 Ga GDG intrusive rock suite). This suite also strongly dominates the bedrock in the region. Metamorphosed quartz monzodiorite to quartz monzonite and granite that belong to the GSDG rocks, with a U-Pb (zircon) age of 1875±4 Ma, comprise a subordinate, pre-tectonic component.

Younger intrusive rocks, which crystallized between different phases of or completely after Svecokarelian ductile deformation and metamorphism (late Svecokarelian intrusive rocks), are dominated by GSDG and GP rocks. On the basis of U-Pb (zircon) age determinations, two separate suites of late Svecokarelian, GSDG intrusive rocks with age spans of 1869±9 Ma to 1842^{+23}_{-13} Ma and 1812±14 Ma to 1783±10 Ma, respectively, have been identified (1.87–1.84 Ga and 1.81–1.78 Ga GSDG intrusive rock suites, respectively). Volcanic, subvolcanic and sedimentary rocks are also spatially and temporally associated with the 1.81–1.78 Ga GSDG suite. The intrusive rocks in the GP suite range in age from 1855±6 Ma to 1750±10 Ma and predominantly overlap temporally with the late Svecokarelian, GSDG rocks. GDG rocks with ages of 1864±4 and 1850±1 Ga, which also intruded after some Svecokarelian ductile deformation and metamorphism, comprise a younger and subordinate GDG suite (1.87–1.85 Ga GDG intrusive rock suite). This suite is spatially associated with the 1.87–1.84 Ga GSDG rocks.

A tectonic setting that involved extensional back-arc rifting along an active continental margin has previously been proposed for the 1.91–1.89 Ga volcanic and subvolcanic rocks. Furthermore, a continental arc setting rather than an inherited signature from previous subduction events has also been proposed for the generation of at least the GSDG rocks. An evaluation of the geochemical data for the different 1.9 to 1.8 Ga igneous suites in the Svecokarelian orogen indicates the influence of one or more source regions that were affected by subduction-related processes. Deposition and intrusion of the rocks in a continental back-arc setting along a convergent, active continental margin is inferred.

The ε_{Nd} values for the 1.91–1.89 Ga volcanic and subvolcanic rocks are mildly depleted and follow the same evolutionary trend on a ε_{Nd} versus age diagram as the intrusive rocks in the GDG, GSDG and GP suites. These values indicate a homogenous source and the incorporation of relatively juvenile mantle material. There are no indications of an influence from Archaean crust in any of these rocks. These features are consistent with models for a juvenile volcanic-arc crust that probably comprised a 2.1–1.9 Ga continental basement to the Bergslagen region.

Alkaline intrusive rock of uncertain age

An alkaline intrusive rock of uncertain age, which is associated spatially with fenitization of the country rock, forms an isolated intrusive body in the eastern part of the Bergslagen region. Although previous work tentatively indicated a post-Svecokarelian age for this rock, recent field and radiometric age data suggest that it is similar in age to the country rocks, which have been included in the 1.90–1.87 Ga GDG intrusive rock suite.

Rocks formed around and after 1.7 Ga

The post-Svecokarelian, geological evolution in the Bergslagen region initiated with the intrusion of a fourth suite of GSDG rocks with an age span of 1699±7 Ma to 1676±7 Ma (1.70–1.67 Ga GSDG intrusive rock suite). Volcanic and sedimentary rocks are also spatially and temporally associated with these rocks. Similarities of some of the volcanic rocks to shoshonitic lavas that were formed along the Andean continental margin at a considerable distance from a subduction trench have been proposed in the literature.

Mesoproterozoic sandstone, four different suites of dolerites that formed at 1.60–1.56 Ga, 1.48–1.46 Ga, 1.27–1.26 Ga and 0.98–0.95 Ga, and isolated bodies of granite and quartz syenite dated at 1.50 Ga and 1.47 Ga, respectively, form minor components in the region. In virtually all cases, it is possible to relate the post-Svecokarelian igneous events temporally to more widespread tectonic activity outside the Bergslagen region as a so-called far-field tectonic response. The crystalline rocks in the region are locally covered by fault-bounded outliers of Neoproterozoic sandstone as well as Lower Palaeozoic sandstone, black shale and limestone.

MINERAL AND BEDROCK DEPOSITS

Most of the metallic mineral deposits, including the Garpenberg, Zinkgruvan and Lovisagruvan base metal sulphide deposits, which are of economic importance at the current time, are hosted by the metamorphosed and hydrothermally altered, 1.91–1.89 Ga felsic volcanic rocks and the spatially associated skarn or crystalline carbonate rock. The most important groups of mineral deposit include iron oxide deposits in manganese-poor (<1% MnO) or manganese-rich (>1% MnO) skarn or crystalline carbonate rock (e.g. Persberg ore field and Dannemora, respectively), quartz-rich iron oxide deposits including banded iron formation (e.g. Striberg), apatite-bearing iron oxide deposits (e.g. Grängesberg), stratiform manganese oxide deposits spatially associated with iron oxide deposits in manganese-poor skarn or crystalline carbonate rock (e.g. Långban), contact metasomatic tungsten oxide skarn deposits (e.g. Yxsjöberg) and base-metal sulphide deposits rich in zinc, lead and silver. Well-constrained age data show that at least some of the tungsten oxide skarn deposits are related to the intrusion of granites in the GP suite around 1.8 Ga. Minor, molybdenum sulphide deposits, which can be classified as climax-type, are also hosted by such granites, while minor, polymetallic greisen mineralizations rich in tin have been documented in the 1.70–1.67 Ga GSDG intrusive rock suite.

Two types of base metal sulphide deposits can be distinguished in the Bergslagen region on the basis of their character of occurrence, metal content and host rock. Stratiform, sheet-like, Zn-Pb-Ag-rich and Fe-Cu-poor deposits (e.g. Zinkgruvan) are hosted by rhyolitic, ash-siltstone metavolcanic rock in the 1.91–1.89 Ga volcanic sequence. Crystalline carbonate rock, skarn and beds of siliceous chemical sediment are also present. The footwall lithologies generally show conspicuous potassium and silicon alteration, and subordinate magnesium alteration. The second type of deposit consists of irregular, multi-lens and podiform, stratabound, massive and disseminated Zn-Pb-Ag-(Cu-Au) deposits (e.g. Garpenberg and Falun) that are hosted by felsic metavolcanic rock interbedded with crystalline carbonate rock in the 1.91–1.89 Ga volcanic sequence. The deposits in this group are closely associated with magnesium-rich skarn and intense footwall magnesium ± iron alteration. Several iron oxide deposits in the Bergslagen region contain, to variable extent, iron and base metal sulphides and some of these deposits have had a mining history for both iron oxides and base metals (e.g. Dannemora and Stollberg).

The Bergslagen region also contains non-metallic mineral and bedrock deposits which have had or, in some cases, even continue to have economic importance. Examples include the exploitation of minerals in pegmatite (e.g. feldspar at the Forshammar deposit) and the quarrying of Palaeoproterozoic crystalline carbonate rock (e.g. Kolmården), Ordovician limestone (e.g. Kvarntorp) and Cambrium to Lower Ordovician alum shale. Alum shale has been exploited as a source of fuel in the production of cement as well as a source of oil and alum. Locally, this shale also contains high contents of uranium and vanadium.

STRUCTURAL DOMAINS AND MULTIPHASE DUCTILE STRAIN

The Bergslagen region is divided into four structural domains that were established in a ductile tectonic régime. They are referred to as the northern, central, southern and western structural domains. These domains have been defined primarily on the basis of differences in the style and orientation of the multiphase ductile strain within them. To some extent, these differences correspond to differences in the grade of metamorphism as well as to differences in the timing of the deformation and metamorphism. As far as the northern domain is concerned, only data from the eastern part of this domain, around Forsmark and Östhammar, have been used in the current synthesis. Structural data that have been used in the other three domains are more evenly distributed over each of these domains.

Northern and southern structural domains

The northern and southern structural domains contain steeply dipping high-strain belts that formed under amphibolite-facies metamorphic conditions and more discrete steeply dipping zones that formed under lower-grade metamorphic conditions. All these structural features strike west-north-west–east-south-east. Kinematic data indicate a combination of dextral strike-slip and south-side-up shear. These structures can be followed for several tens of kilometres and anastomose around sub-domains where the planar grain-shape fabric strikes east-north-east–west-south-west to north-east–south-west or is affected by major folding that verges north to north-west. Both fold axes and a mineral stretching lineation plunge gently to moderately, predominantly to the east and south-east. Sheath folding that accounts for an eye-shaped geometry on the ground surface at different scales has been inferred in a part of the northern domain. Younger, more open and upright folds, with axial surface traces that strike approximately north–south, occur in the southern structural domain.

The penetrative, ductile grain-shape fabric and the high-strain belts in the eastern part of the northern structural domain formed between 1.87 and 1.86 Ga and all these structures are deformed by the later folding. Ductile deformation after 1.85 Ga, probably around 1.8 Ga, occurred along the discrete high-strain zones. Amphibolite-facies deformation and metamorphism affected the bedrock in the southern structural domain prior to 1.85 Ga and is inferred to be most conspicuous in the sub-domains between the ductile high-strain zones (or belt). However, there is a strong influence of penetrative ductile deformation under amphibolite-facies metamorphic conditions after 1.85 Ga along a ductile high-strain belt. This younger ductile strain affected the 1.87–1.84 Ga GSDG suite of intrusive rocks. Thus, the tectonic evolution of the southern structural domain is different from that in the eastern part of the northern structural domain.

An evaluation of data from the 1.87–1.84 Ga GSDG suite of intrusive rocks and their country rock in the southern structural domain raises question-marks around earlier interpretations that these rocks were forcefully emplaced by diapirism. An alternative mechanism is proposed whereby emplacement was controlled solely by the space created in connection with significant dextral strike-slip movement along west-north-west–east-south-east structures in the Bergslagen region at this time.

Central structural domain

Early-stage folding and stratigraphic inversion of the bedrock has been recognized in parts of the central structural domain. However, a second generation folding of an early, planar grain-shape fabric in the bedrock and constrictional ductile strain are the most prominent structural geological features in this domain. The folding is apparent on different scales, not least on a larger-scale, as inferred from an inspection of the form line and magnetic anomaly maps as well as the spatial distribution of the boundary between different metamorphic domains. In the major part of the central structural domain, the folds show axial surface traces that strike east–west to north-east–south-west, verge to the north to north-west and deform the planar grain-shape fabric in the rocks. Fold axes and a mineral stretching lineation vary in orientation but generally show a moderate to steep plunge in an easterly direction. In western areas, the axial surface traces to the second generation structures are refolded by more open, upright folds. These third generation structures show axial surface traces that strike north-west–south-east to north-north-west–south-south-east.

Ductile high-strain belts that formed under amphibolite-facies metamorphic conditions were established prior to the second generation of folding. A combination of sinistral and north-west-side-up shear dominates in a folded high-strain belt that strikes north-east–south-west in the eastern part of the central structural domain. It has been suggested that this shear strain is conjugate to that along a high-strain belt in the northern structural domain. Ductile high-strain belts and more discrete high-strain zones are also present along the flanks of the second generation folds. It has been inferred that the folded ductile grain-shape fabric in the central structural domain formed between 1.88 and 1.86 Ga.

Western structural domain

The western structural domain shows a complex interference of older, pre-Sveconorwegian structures that strike west-north-west–east-south-east and structures that strike approximately north–south that are steered by Sveconorwegian tectonics. The domain is inferred to belong to the frontal, easternmost part of the Sveconorwegian orogen.

An earlier phase of Sveconorwegian ductile strain consists of a grain-shape fabric that varies in intensity from spaced to semi-penetrative to penetrative from east to west across the domain. This gradient in strain intensity corresponds to a change in syn-deformational metamorphic conditions from greenschist facies in the

east to amphibolite facies further west. Kinematic indicators along this ductile shear fabric indicate a consistent west-side-up sense of shear. In combination with the strongly asymmetric fan-like geometry shown by the grain-shape fabric, the kinematic data indicate apparent extensional ductile strain in western areas, where the fabric elements dip or plunge to the east, and apparent compressional strain in eastern areas, where the fabric elements dip or plunge to the west.

There remains an uncertainy concerning whether this earlier phase of Sveconorwegian deformation was related to the build-up of an imbricate thrust stack in a compressional tectonic setting or to regional east–west extension. Bulk extensional strain in an east–west direction is indicated around 0.98–0.95 Ga, with the intrusion of a suite of dolerites in a north–south direction along the frontal part of and to the east of the Sveconorwegian orogen. Furthermore, such strain has been proposed to explain the decompression and exhumation of high-pressure rocks in the southern part of the orogen.

A later phase of Sveconorwegian ductile strain is prominent in the easternmost part of the domain. This phase of ductile deformation accounts for the distinctive variation in strike direction of the early Sveconorwegian grain-shape fabric. It also affected dolerites in the 0.98–0.95 Ga dyke swarm. The later phase of deformation consists of a high frequency of steeply dipping, ductile high-strain zones that formed under greenschist-facies metamorphic conditions and strike predominantly north-east–south-west or north–south. The sense of shear along these zones has been inferred to be caused by bulk shortening in an approximately east–west direction.

SVECOKARELIAN METAMORPHIC DOMAINS AND PEAK METAMORPHISM RELATED TO MAFIC UNDERPLATING

The Bergslagen region is divided into four metamorphic domains that were established during the Svecokarelian orogeny (1.9–1.8 Ga). They are referred to as the northern migmatitic, central low-grade, central medium-grade and southern migmatitic metamorphic domains. All domains except the northern migmatitic domain are overprinted in their western parts by Sveconorwegian, syn-deformational metamorphism. Furthermore, contact metamorphism related to a 1.7 Ga intrusive body has also been identified. The peak of Svecokarelian metamorphism followed establishment of penetrative fabric development in the different structural domains. For this reason, the metamorphic evolution needs to evaluated separately. In this context, it is worthwhile noting that the spatial distributions of the structural domains described above and the Svecokarelian metamorphic domains are similar but are not fully compatible with each other. Furthermore, the boundary between at least the central medium-grade and southern migmatitic domains is deformed by the second generation folding in the central structural domain.

Quantitative determinations of pressure–temperature conditions of metamorphism in the central medium-grade and southern migmatitic domains indicate low-pressure conditions in both domains, with metamorphism generally at depths close to or shallower than c. 20 km. Temperatures of metamorphism correspond to upper greenschist or amphibolite facies conditions in the central medium-grade domain, and to amphibolite or granulite facies conditions in the southern migmatitic domain, confirming inferences based on mineral assemblages.

An older, metamorphic event in the southern migmatitic domain at or prior to 1.85 Ga is inferred to be equivalent to a 1.88 (1.87)–1.86 Ga event in the central medium-grade domain. This metamorphic event is referred to as the M_1 event. A younger, 1.8 Ga metamorphic event (or events) has been identified in the southern part of the Bergslagen region and is referred to as M_2. However, the northern boundary of the M_2 metamorphism is not constrained. An evaluation of spatial variations in grade of metamorphism, crustal thickness and gravity data suggest that peak high-grade metamorphism at relatively shallow pressures in the southern part of the Bergslagen region, with formation of migmatites, is steered by the thermal input from the injection of hot, mafic igneous material at or prior to 1.85 Ga and around 1.8 Ga, i.e. by two separate phases of mafic underplating. Geochronological data confirm that these events are temporally related to the emplacement of the two suites of late Svecokarelian GSDG rocks.

TECTONIC MODEL FOR SVECOKARELIAN OROGENIC ACTIVITY

The Bergslagen region is characterized by a significant strike-slip component of shear deformation, with dextral displacement along west-north-west–east-south-east structures, combined with a variable inclination of a mineral stretching lineation. The first generation (D_1) of Svecokarelian fabric in the region, with both planar and linear components, and the early, folded high-strain belts are inferred to have developed initially in a transpressive tectonic régime around 1.86 Ga. The kinematic data along the high-strain belts are consistent with bulk horizontal shortening in an approximately north–south direction in combination with east–west

extension, as suggested earlier, partly or wholly, by several workers. It is suggested that mafic underplating and the establishment of the metamorphic peak shortly after D_1, and not least migmatization, corresponded to a changeover to a transtensional tectonic régime.

The tectonic evolution that occurred around 1.86 Ga repeated itself approximately 50 million years later around 1.8 Ga and the effects of this reworking are most conspicuous in the southern structural domain. However, the driving mechanism appears to have been similar during both events. A conceptual driving mechanism that involved a cyclic tectonic evolution in the region is inferred.

There are major uncertainties concerning the mechanism, tectonic setting and timing of the regional second generation folds (D_2). Several workers have suggested that both the D_1 deformation and the D_2 folding formed as a result of progressive, bulk horizontal shortening in a north–south direction. However, if the D_2 folding formed as a result of strike-slip shear deformation rather than by bulk horizontal shortening of the crust, then it is also possible that this folding developed in a regional-scale, transtensional tectonic régime. A transtensional D_2 tectonic régime in Bergslagen is attractive since it explains the poor development of an axial surface fabric and the continued development of a pronounced linear grain-shape fabric during the D_2 event. Alternative hypotheses for the development of the D_2 folding that take account of the above considerations and, not least, the poor time constraints for their formation are proposed.

A conceptual driving mechanism that takes account of separate tectonic cycles between 1.91 and c. 1.86 Ga and between c. 1.86 Ga and 1.8 Ga, with long time periods of transtensional tectonics and two short time periods of transpression, is described. This mechanism involved migration of what has been described in the literature as tectonic switching in the younger accretionary orogenic systems of eastern Australia (Lachlan orogen) and New Zealand. Approximately northward-directed oblique subduction beneath an active continental margin to the north-east is inferred.

BRITTLE DEFORMATION AND INFERRED METEORITE IMPACT STRUCTURES

^{40}Ar-^{39}Ar (hornblende, biotite) cooling ages indicate that the bedrock in the Bergslagen region cooled into the subgreenschist-facies metamorphic realm and was able to respond to deformation in the brittle régime some time between 1.8 and 1.7 Ga. The influence of the ancient Svecokarelian and Sveconorwegian structural anisotropies in the bedrock (ductile high-strain zones, boundaries between rock units) on the orientation of lineaments and faults is apparent in several parts of the region. Phanerozoic faulting is evident from the stratigraphic control provided by the Lower Palaeozoic sedimentary cover rocks or the disturbance of the exhumed, sub-Cambrian unconformity (peneplain). Two circular structures in the southern part of the Bergslagen region have been inferred to represent meteorite impact structures that formed during the Ordovician.

Data bearing on the character, timing and kinematics of brittle deformation at Forsmark in the north-eastern part of the region, where the detailed investigations in connection with site characterization for the possible disposal of highly radioactive nuclear waste have recently been completed, are summarized in the current synthesis. However, in general, relatively little is known about the structural development in the Bergslagen region in the brittle régime from approximately 1.7 Ga to the Quaternary period, i.e. throughout nearly 1 700 million years of Earth history.

Introduction

The area of investigation addressed in this report, which is referred to here as the Bergslagen region, is situated in the central part of Sweden, between Linköping in the south and Falun and Hofors in the north, and from Kristinehamn in the west to the Baltic Sea in the east (Fig. 1). The area of investigation corresponds to map-sheets 8.5 to 13 (south–north direction) and E to J (west–east direction) in the Swedish national grid (RT 90 system), an area of 82 500 km^2. A gentle relief and a landscape situated below the highest shoreline, which developed after the latest Weichselian glaciation, characterize the eastern part of the Bergslagen region, whereas a more varied relief and a landscape situated above the highest shoreline characterize the north-western part of the region (Fig. 1 and Lidmar-Bergström 1994, Lundqvist 1994). Furthermore, the current bedrock surface beneath the unconsolidated Quaternary cover in much of this area corresponds to the morphological structure referred to as the sub-Cambrian peneplain (Lidmar-Bergström 1994). Geologically this surface forms a substantial gap in the geological record and corresponds to a sub-Cambrian unconformity.

The Bergslagen region forms one of Sweden's important provinces for the exploitation of mineral deposits (Fig. 2). During the 18th and 19th centuries, iron ore from over 3 000 workings in this area provided much of Sweden's wealth, and the region is historically the most prosperous mining district in the country. When the Falun mine in the north-western part of the province closed during 1992, a history of over 700 years of mining activ-

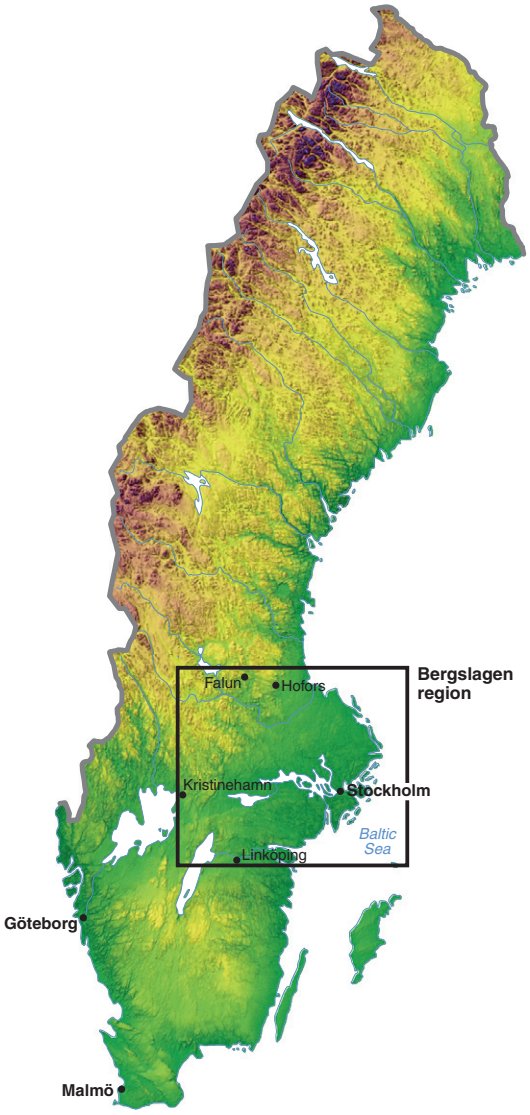

Fig. 1. Outline of the area of investigation marked on a digital relief map of Sweden. The area is referred to in the text as the Bergslagen region.

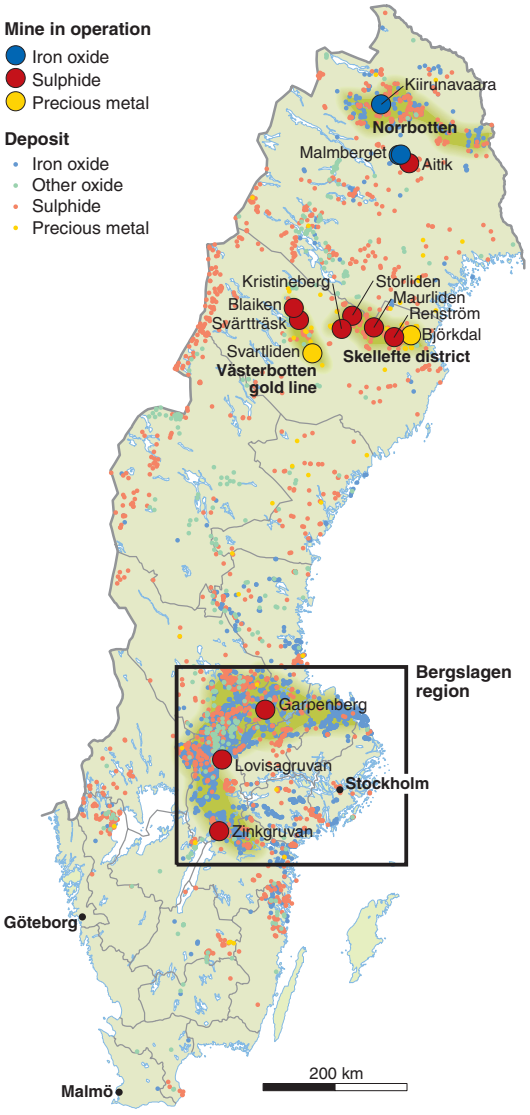

Fig. 2. Major mineral resource provinces in Sweden including the Bergslagen region.

ity ended at this deposit. At the current time, three base-metal sulphide deposits are in operation (Garpenberg, Zinkgruvan and Lovisagruvan) and the area is an active field for mineral exploration (Fig. 3). The iron oxide deposit at Dannemora, north of Uppsala, is currently being prepared for a renewed phase of mining activity.

During the later half of the 1990's, the Geological Survey of Sweden (SGU) initiated regional bedrock geological projects in the mineral provinces of Norrbotten, the Skellefte district in Västerbotten and in Bergslagen (Fig. 2), in order to provide public support to ongoing mineral exploration and mining activities in the private sector. Digital map compilations, published geological and geophysical maps, and written map descriptions for northern Norrbotten and the Skellefte district were all completed by 2005 (see descriptions in Bergman et al. 2001 and Kathol & Weihed 2005). In the Bergslagen project, digital map information was available for use by the public including private companies during 2001, geophysical maps were published during 2002, bedrock geological maps during 2007 and finally this description of the area during 2009. Reports that documented ongoing progress with the project were also published by SGU (Stephens et al. 1998, 1999, 2000, 2001).

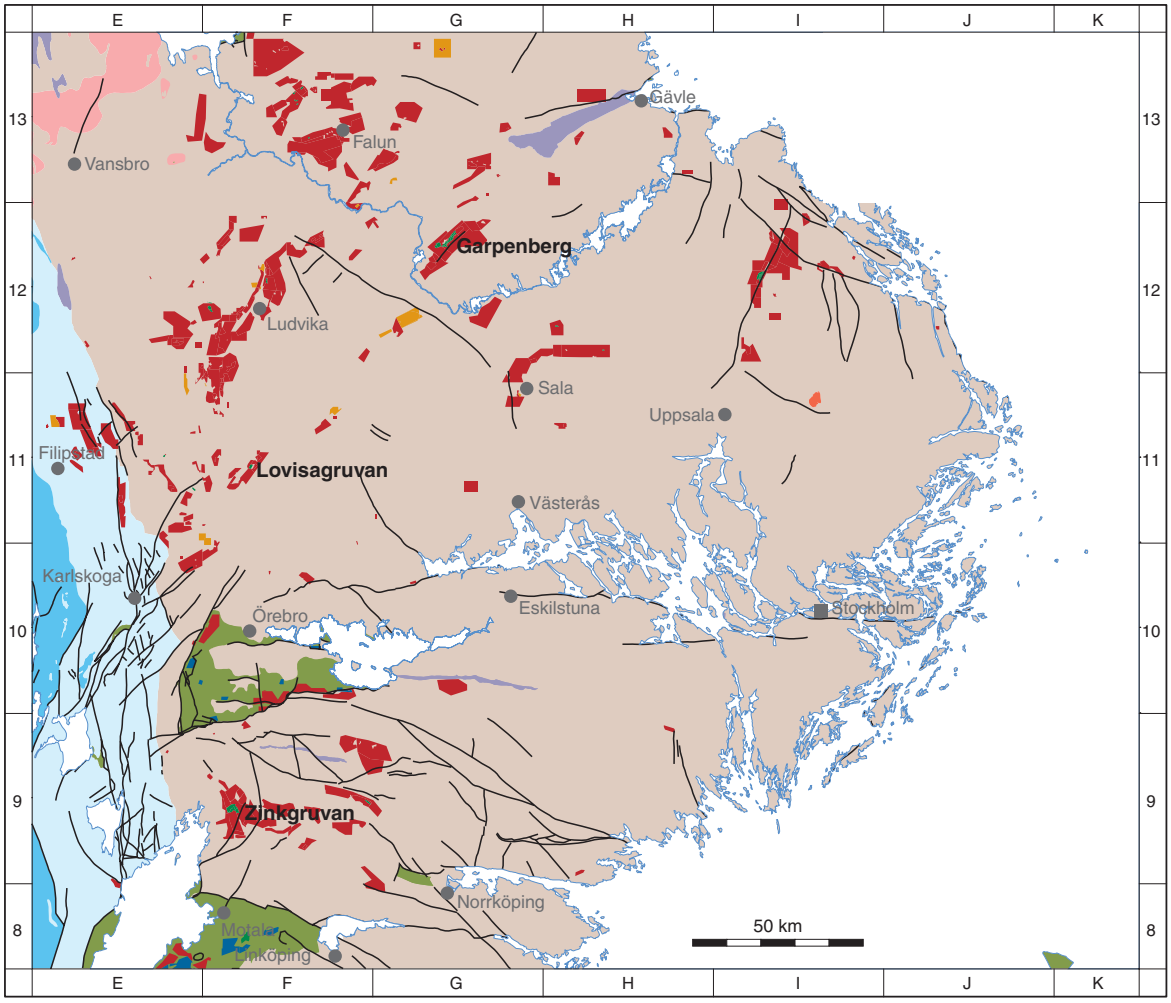

Mining concession granted

Exploration permit for oil, gas or diamonds granted

Exploration permit for metallic or non-metallic mineral deposit granted

Exploration permit for metallic or non-metallic mineral deposit submitted

Fault, ductile shear zone

Sedimentary cover rocks

Neoproterozoic and Lower Palaeozoic sedimentary rocks

Sveconorwegian orogen

Palaeoproterozoic (1.7 Ga) and Mesoproterozoic rocks affected, to variable extent, by Sveconorwegian ductile deformation and metamorphism

Palaeoproterozoic rocks (1.9–1.8 Ga) affected, to variable extent, by Sveconorwegian and older ductile deformation and metamorphism

Post-Svecokarelian rocks

Mesoproterozoic rocks

Palaeoproterozoic rocks (1.7 Ga)

Alkaline intrusive rock (uncertain age)

Alkaline intrusive rock (uncertain age)

Svecokarelian orogen

Palaeoproterozoic rocks (1.9–1.8 Ga) affected, to variable extent, by Svecokarelian ductile deformation and metamorphism

Fig. 3. Mineralizations that are currently (December 2008) being explored or mined in the Bergslagen region. The different rock units shown on the map are distinguished on the basis of their tectonic status.

Aims, scope and products

AIMS AND SCOPE

The aims of the study in the Bergslagen project were primarily two-fold:

- To compile and to update bedrock geological and geophysical information in the area referred to as the Bergslagen region (Fig. 1) and to archive the results of this work in a number of accessible databases at SGU.
- To present a new, integrated synthesis of the bedrock geology in the Bergslagen region.

The following work in the Bergslagen region was planned in order to improve the status of some of the databases at SGU:

- Produce a digital compilation of the areas that 1. are inferred to be exposed (outcrop) or covered by a thin cover of Quaternary deposits (JORDDB_JOGI/JOLC) or 2. fulfil this condition and also include some form of observation in the context of SGU's bedrock mapping programme or are simply outcrops with a bedrock observation point (BERGDB_BELO/BELA).
- Produce a digital compilation of the most up-to-date, published geological maps in the region (BERGDB_BELO/BELA).
- Complete field studies on selected outcrops (BERGDB_HALL) in order to address some specific geological issues that were identified at the initiation of the project (see below). This field work also included sampling for geochemical, geochronological or petrophysical analytical work.
- Integrate and carry out an interpretation of the airborne geophysical and digital elevation data in the Bergslagen region with focus on lineaments and dykes (BERGDB_BELO/BELA).
- Complete an update of the bedrock geochronology database (BERGDB_ALDR) with focus on U-Pb (zircon) age determinations of felsic metavolcanic rocks. Compile Sm-Nd analyses in the region.
- Complete a radical update of the bedrock geochemical database (BERGDB_BLAB_KEM).
- Complete a radical update of the petrophysical database (FYSIK_DB_MAGN and BERGDB_PETR_SPK) with measurements of density, magnetic susceptibility and contents of potassium (^{40}K), uranium (^{238}U) and thorium (^{232}Th).
- Complete a radical update of the mineral and bedrock resources database (BERGDB_MDEP) with focus on some specified attributes (see later text).
- Compile the data that provide some quantitative constraints on pressure-temperature conditions during metamorphism of the bedrock (BERGDB_BLAB).

The results of the synthesis work were ultimately planned to be presented in the form of printed geological and geophysical maps extracted from the digital map database and a detailed printed description of the bedrock geology, with an excursion guide that addresses the geology at some key localities. The maps are essentially 2-D models for the distribution of different geological and geophysical attributes at the ground surface.

It is important to emphasize that the scope of the work was strongly compilationary in character, making use of and complementing the results of already published work. There was no ambition to produce a completely new bedrock geological map of the Bergslagen region. This approach was motivated by the urgent need to compile and digitize the available bedrock geological maps and to radically update the database for mineral and bedrock resources in the region. At the start of the project, such digital information was virtually absent in the region. Bearing in mind this strategy, field work was restricted to a focussed input during short intervals spread over three field seasons (1998–2000). Apart from the sampling for complementary analytical work, the field work aimed to address the following specific geological issues:

- The physical volcanology of the metamorphosed, Svecofennian volcanic and subvolcanic intrusive rocks (1.91–1.89 Ga) and their stratigraphic relationships to surrounding metasedimentary rocks. Selected sites focussed on areas that had not been addressed in earlier studies (e.g. Glanshammar, Falun, Uppsala-Östhammar, Kolsva-Kungsör-Strängnäs, Linköping).
- The regional structural geology in different structural domains inside the Bergslagen region.

Work with the first issue has built heavily on and made use of the results of earlier work financed by Närings- och teknikutvecklingsverket (NUTEK), the mining industry and SGU in the context of the research programme entitled "Ore geology related to prospecting (Prospekteringsinriktad malmgeologi – PIM)" and the internal research and development project at SGU entitled "Physical volcanology in Bergslagen (Fysisk vulkanologi i Bergslagen)" (SGU project code 8657).

Work with the second issue has made use of and directly incorporated the results of earlier work with

the internal research and development project at SGU entitled "Kinematics and timing of major deformation zones, south-central Sweden" (SGU project code 5082). This project addressed structural geological aspects in one of the structural domains in the Bergslagen region (southern structural domain, see section "Deformation, metamorphism and mechanism of emplacement of the 1.87–1.84 Ga GSDG suite of intrusive rocks"). Finally, the project helped to initiate, proceeded contemporaneously with and made use of the results of three projects financed by SGU's external research and development programme. These projects bear the following titles and codes:

- Age and P-T paths of metamorphism in the Bergslagen region, southern Sweden (SGU project code 03-1025/97 implemented by U.B. Andersson).
- Deformation zones in eastern Bergslagen (Uppland-Södermanland), (SGU project code 03-1026/97 implemented by H. Sjöström and K.S. Persson).
- Regional stratigraphy, basin evolution and the setting of stratbound Zn-Pb-Cu-Ag-Au deposits in Bergslagen, Sweden (SGU project code 03-1203/99 implemented by R. Allen, S. Bull, M. Ripa and R. Jonsson).

PRODUCTS

The following products have emerged as a result of the work with the Bergslagen project:

- An update and, in some cases, a radical update of several of SGU's bedrock geological and geophysical databases (see sections entitled "Data input" and "Acquisition of new data and data interpretation – methodological aspects").
- Two published regional geophysical maps. A magnetic anomaly map at the scale 1:400 000 over the whole Bergslagen region, derived from airborne magnetic data, was presented (Stephens et al. 2002a). The second geophysical product was a geophysical and topographic cartographic montage with four separate inset maps at the scale 1:750 000 – a topographic relief map, a Bouguer gravity anomaly map, an electromagnetic map (VLF) and a composite radiometric map for potassium, uranium and thorium (Stephens et al. 2002b). The electromagnetic and radiometric maps were also derived from airborne data. These 2-D models at the ground surface are naturally sensitive to the degree of data resolution.
- Three published regional geological maps, at the scale 1:400 000, including a bedrock geological map (Stephens et al. 2007a), a metamorphic, structural and isotopic age map (Stephens et al. 2007b) and a mineral resources map (Stephens et al. 2007c). Since these maps are 2-D models that compile and extrapolate a particular set of data, they will change with the acquisition of new data or new concepts.
- An exploration package on CD-ROM that contains databases covering gravity and airborne magnetic measurements in the Bergslagen region, the bedrock geological map of the region, and mineralizations and Cu geochemistry in the region. It also contains metadata covering other SGU databases, together with documentation and general information. Much of the material in the exploration package is a direct product of the Bergslagen project.
- A description of the bedrock geology of the Bergslagen region, which integrates geological, geochronological, geochemical and geophysical data sets and presents a tectonic model for the Svecokarelian orogenic development in the region (see sections in the main text entitled "Character, spatial distribution, geochronology, geochemical signature, petrophysical characteristics and regional geophysical signature of rock units", "Mineral and bedrock deposits", "Deformation, metamorphism and mechanism of emplacement of the 1.87–1.84 Ga GSDG suite of intrusive rocks", "Tectonic model for Svecokarelian orogenic activity in the Bergslagen region" and "Key issues for future work" as well as the appendix to this report).
- Descriptions of some excursion localities that are considered to be of importance in the Bergslagen region (see section "Description of excursion stops"). These localities have been selected and are addressed under specific geological themes.

Nomenclature

The prefix "meta" has, in general, not been used in the headings for different groups of rock; simple reference to the general character of the inferred protolith (sedimentary, volcanic or intrusive) being preferred. This procedure follows that used in the legend to the published geological maps. However, it needs to be kept in mind that the major part of the bedrock in the Bergslagen region has been affected by metamorphism and ductile deformation, predominantly under amphibolite-facies conditions. For this reason, the prefix "meta" (e.g. metagreywacke) or specific metamorphic rock names (e.g. amphibolite, paragneiss) have commonly been used in the text when referring to individual lithologies. This is once again consistent with the legend to the published geological maps.

Some definitions are provided below for terms or acronyms that are used in this publication.

Bergslagen region: Term used here to define the area of study. It includes the area in the central part of Sweden where extensive mining activity has taken place since the Middle Ages. The Bergslagen region is defined by the following coordinates in the Swedish national grid (RT 90 system, Northing/Easting): 6475000/1400000, 6475000/1700000, 6750000/1400000, 6750000/1700000.

Ga: Acronym used for giga-annum, i.e. billion of years before present.

Ma: Acronym used for mega-annum, i.e. million of years before present.

Svecokarelian orogen or orogeny: The term "Svecokarelian orogen" refers to the part of the Fennoscandian Shield in Sweden, Finland, northernmost Norway and north-western Russia that was affected by ductile deformation, metamorphism and extensive igneous activity, i.e. tectonic activity, between 1.9 and 1.8 Ga (Koistinen et al. 2001). The term "Svecokarelian orogeny" refers to the processes by which structures within this orogenic belt were formed. Different phases of deformation, metamorphism and igneous activity affected different parts of the Svecokarelian orogen between 1.9 and 1.8 Ga. Recently, an attempt has been made to define different tectonic events and belts inside the Svecokarelian orogen (see, for example, Lahtinen et al. 2008).

Use of the term "Svecokarelian" follows the conceptual understanding in Rankama & Welin (1972). These authors recognized the need to use separate names for groups of rock and for deformational events. This principle was abandoned by Gaál & Gorbatschev (1987). They proposed use of the term "Svecofennian" for an "orogenic sequence" of supracrustal and intrusive rocks with an age between 2.0 and 1.75 Ga, and also introduced the terms "Svecofennian orogeny" and "Svecofennian Domain".

Sveconorwegian orogen or orogeny: The term "Sveconorwegian orogen" refers to the part of the Fennoscandian Shield (Koistinen et al. 2001) in south-western Sweden and southern Norway that was affected by ductile deformation, metamorphism and igneous activity between 1.14 and 0.90 Ga (see review in Bingen et al. 2008). The term "Sveconorwegian orogeny" refers to the processes by which structures within this orogenic belt were formed. Different phases of metamorphism and deformation have been recognized in different parts of the Sveconorwegian orogen during the time period 1.14 to 0.90 Ga (Bingen et al. 2008). Bedrock affected by older (pre-Sveconorwegian) orogenic events is also present inside this orogen.

Svecofennian supracrustal rock suite: The term "Svecofennian" was used by Rankama & Welin (1972) for a sequence of supracrustal rocks of complex composition and origin inside the Fennoscandian Shield without any clear basement. The term was extended in Gaál & Gorbatschev (1987) to include, amongst other features, an "orogenic sequence" of supracrustal and intrusive rocks with an age between 2.0 and 1.75 Ga. In the context of the description of the Bergslagen region presented here, the term is used for the volcanic and subvolcanic intrusive rocks with an age of 1.91–1.89 Ga and the sedimentary rocks that are 1.9 Ga or, in part, possibly older, i.e. use of the term here follows that perceived in Rankama & Welin (1972).

GDG intrusive rock suite: Acronym used here for an intrusive rock suite consisting of granitoid, dioritoid and gabbroid as defined in Le Maitre (2002). The felsic rocks in this rock suite are variable in composition but are consistently rich in quartz (granitoids). Enclaves of mafic or intermediate rocks are common in especially the tonalitic and granodioritic rocks. Different suites have been recognized here on the basis of a combination of intrusion–deformation relationships and absolute age.

GSDG intrusive rock suite: Acronym used here for an intrusive rock suite consisting of granite, syenitoid, dioritoid and gabbroid as defined in Le Maitre (2002). The felsic rocks in this rock suite are variable in composition including quartz content (granites and syenitoids) and commonly contain enclaves of mafic or intermediate rocks. Different suites have been recognized here on the basis of a combination of intrusion–deformation relationships and absolute age.

GP intrusive rock suite: Acronym used for an intrusive rock suite consisting of granite and in places pegmatitic

granite as defined in Le Maitre (2002). The rocks in this suite show a limited range in composition, are consistently rich in quartz (granites) and commonly exhibit a higher gamma radiation related to higher contents of uranium and thorium. Enclaves of mafic or intermediate rocks are absent or uncommon in this rock suite.

Structural domain: Bedrock area at the current level of erosion identified primarily on the basis of the style and orientation of the ductile structures. To some extent, the differences between structural domains also correspond to differences in the grade of metamorphism and the timing of the ductile strain in the bedrock. However, these features have not been used as a prerequisite for their identification. Four such domains have been recognized in the Bergslagen region. These are referred to as the northern, central, southern and western structural domains and are described in the section "Deformation, metamorphism and mechanism of emplacement of the 1.87–1.84 Ga GSDG suite of intrusive rocks".

Metamorphic domain: Bedrock area at the current level of erosion identified on the basis of the grade of Svecokarelian metamorphism that occurred between 1.9 and 1.8 Ga. Four such domains have been recognized in the Bergslagen region. These are referred to as the central low-grade, the central medium-grade, the southern migmatitic and the northern migmatitic metamorphic domains and are described in the section "Deformation, metamorphism and mechanism of emplacement of the 1.87–1.84 Ga GSDG suite of intrusive rocks".

Tectonic domain: Concept used in Hermansson et al. (2007, 2008a) and developed further in Stephens & Wahlgren (2008) for a bedrock area at the current level of erosion in the south-western part of the Svecokarelian orogen identified on the basis of either the timing of tectonic activity, i.e. the timing of ductile deformation, metamorphism and igneous activity, or the character and intensity of ductile strain.

Transscandinavian Igneous Belt (TIB): The term "Transscandinavian Igneous Belt" (Patchett et al. 1987) refers to a belt of predominantly intrusive and volcanic rocks with ages between c. 1.85 and 1.67 Ga (Gorbatschev 2004). These rocks are dominant in the western part of the Fennoscandian Shield and in windows inside the Caledonian orogen. The igneous rocks are alkali-calcic in composition and can be classified as I- or A-type or transitional between these compositions (Gorbatschev 2004). The spatial distribution of this belt as proposed in Figure 1 in Högdahl et al. (2004) excludes the gneissic rocks of similar composition dated at 1.7 Ga in the Sveconorwegian orogen as well as calc-alkaline intrusive rocks formed around or after 1.85 Ga in south-eastern Sweden. However, the spatial distribution presented in Högdahl et al. (2004) includes the suite of intrusive rocks referred to as *Revsund granite* with different rock composition in the central part of Sweden. For reasons evaluated in more detail in the text, the term is generally avoided here.

Local terms for geological features: Several local terms, which have been used earlier on an informal basis for, for example, specific intrusions (e.g. *Hedesunda granite*), individual mineral deposits or ore fields (e.g. *Striberg deposit, Riddarhyttan ore field*) or specific structures (e.g. *Guldsmedshyttan syncline*), are included in the appropriate part of the following text, primarily to provide the reader with some help to link the nomenclature used here (e.g. *GSDG intrusive rock suite*) with that used in the older literature. Several of these geological features are referred to or discussed in the overview of the geology of Sweden in Lindström et al. (2000). These local, generally poorly defined terms are consistently marked in italics in the text. No attempt is made here to provide formal definitions.

Regional tectonic framework

The Palaeoproterozoic Svecokarelian orogen comprises a major part of the Fennoscandian Shield, which is one of the ancient continental nuclei on the planet Earth (Fig. 4). The deformed and metamorphosed rocks in the Lapland-Kola region, which are situated in the northernmost part of the Fennoscandian Shield, are also included here in this orogen. The Svecokarelian orogen is bordered by an Archaean continental nucleus in the north-east, by the Sveconorwegian orogen in the south-west and by Neoproterozoic and Phanerozoic sedimentary cover rocks of the East European Platform to the south-east (Fig. 4). In the west and north-west, it is overthrust by rocks that belong to the Caledonian orogen (Fig. 4). The Bergslagen region is situated predominantly in the south-western part of the Svecokarelian orogen (Fig. 4).

Intrusive and meta-intrusive rocks, felsic metavolcanic rocks and subordinate metasedimentary rocks dominate the Svecokarelian orogen at the current level of erosion inside the Bergslagen region and in its immediate surroundings to the north and south (Koistinen et al. 2001). This part of the orogen has been divided into five tectonic domains (tectonic domains 1 to 5 in Fig. 5). These domains have been separated on the basis of differences in either the timing of tectonic activity, i.e. the timing of ductile deformation, metamorphism and igneous activity, or in the character and intensity of the ductile strain (Hermansson et al. 2007, 2008a, Stephens & Wahlgren 2008).

Tectonic domains 1 and 3 (Fig. 5) are characterized by major folding of rock units and a ductile planar fabric, and, in general, constrictional strain that formed under variable metamorphic conditions. Ductile high-strain zones or broader belts are also present. However, these two domains show a contrasting tectonic evolution. In tectonic domain 1, penetrative ductile deformation and metamorphism under amphibolite- and, locally, granulite-facies conditions affected a volumetrically important suite of intrusive rocks with ages between 1.86 and 1.84 Ga. Migmatization and ductile deformation have been dated at 1.82–1.80 Ga (Högdahl & Sjöström 2001, Högdahl et al. 2001, 2008). By contrast, in tectonic domain 3, in the heart of Bergslagen, an older suite of supracrustal and intrusive rocks that formed between 1.91 Ga (and possibly earlier) and 1.87 Ga was affected by pervasive, yet variable ductile deformation under predominantly amphibolite-facies metamorphic conditions between 1.88 and 1.86 Ga (Hermansson et al. 2008a).

Tectonic domains 2 and 4 (Fig. 5) contain broad belts of highly strained rocks, which were deformed under amphibolite-facies metamorphic conditions and are strongly anisotropic. These ductile high-strain belts, which strike approximately west-north-west to north-

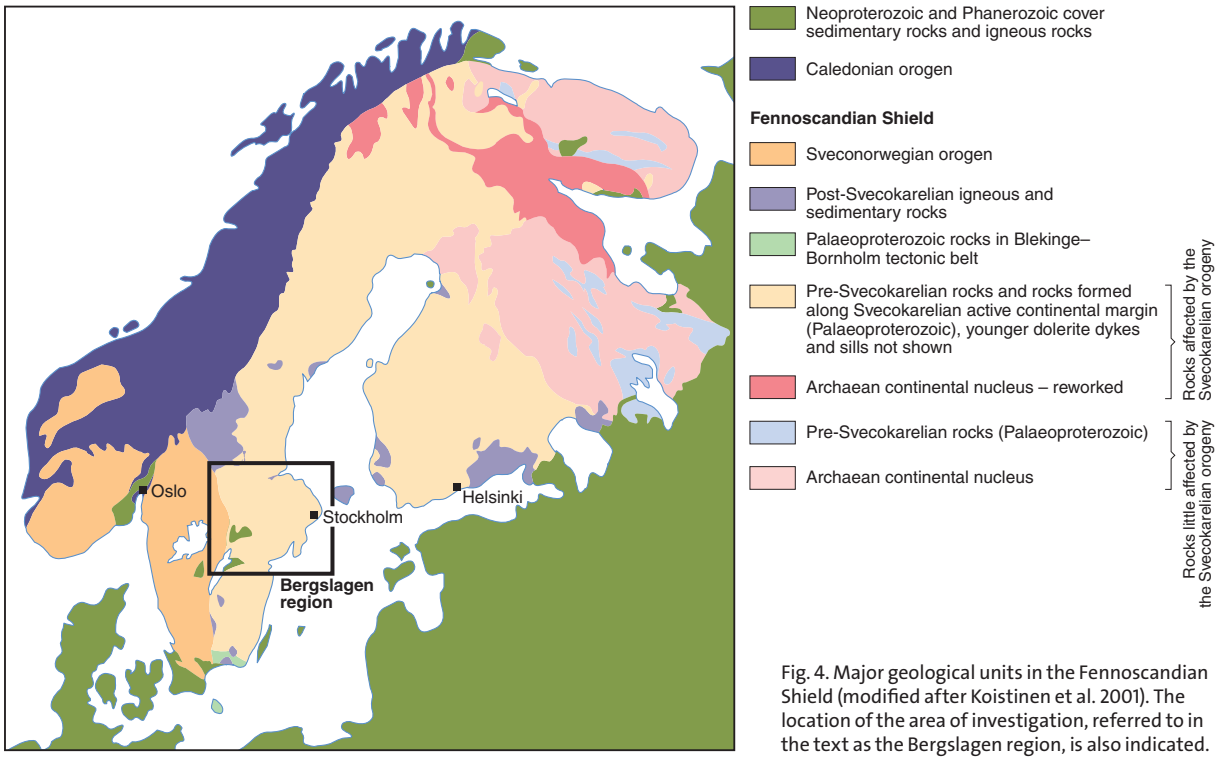

Fig. 4. Major geological units in the Fennoscandian Shield (modified after Koistinen et al. 2001). The location of the area of investigation, referred to in the text as the Bergslagen region, is also indicated.

west and are subvertical, anastomose around tectonic lenses in which the bedrock is commonly folded and, in general, affected by lower ductile strain. The high-strain belts also contain retrograde deformation zones. The post- and pre-1.85 Ga tectonic signatures observed in domains 1 and 3, respectively, appear to be present in the complex, high-strain belts in each of the domains 2 and 4 (Hermansson et al. 2007, 2008a, Stephens & Wahlgren 2008). In particular, ductile deformation and amphibolite- and locally granulite-facies metamorphism after 1.85 Ga are conspicuous in the southern part of the Bergslagen region inside tectonic domain 4.

In its northern part, close to the Bergslagen region, tectonic domain 5 contains intrusive rocks that formed between 1.86 and 1.84 Ga and were affected by ductile deformation under amphibolite-facies metamorphic conditions. However, further to the south, this domain is dominated by an even younger, igneous bedrock that formed around 1.8 Ga and was only affected by ductile strain along low-temperature, high-strain zones after 1.8 Ga.

Bearing in mind the considerations above, it can be inferred that at least tectonic domains 1 and 3 comprise separate tectonostratigraphic terranes (Howell 1989, p. 214). Palaeogeogeographic speculations for the time interval prior to 1.86 Ga, when the bedrock either had started to form or had formed, respectively, in these two domains, need to bear in mind the high ductile strain around and after 1.86 Ga along the intermediate tectonic domain 2.

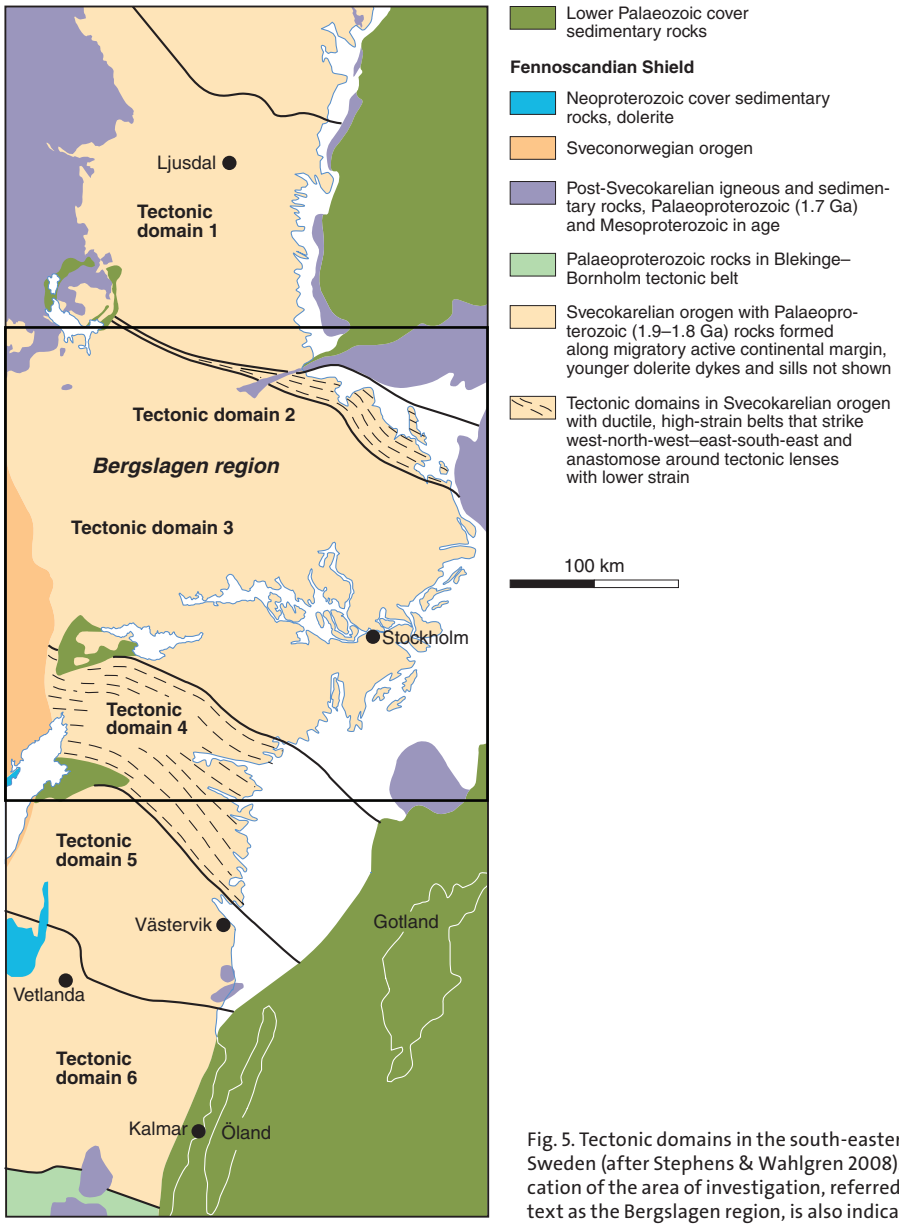

Fig. 5. Tectonic domains in the south-eastern part of Sweden (after Stephens & Wahlgren 2008). The location of the area of investigation, referred to in the text as the Bergslagen region, is also indicated.

Data input

BEDROCK GEOLOGICAL MAPS, DESCRIPTIONS AND OUTCROP DISTRIBUTION

The bedrock geological information that was available at the time of the compilation work, in the form of maps and detailed descriptions, is summarized in Figure 6. In general, there is a profound difference in the quality of data between the material that has been derived from published and preliminary bedrock maps at the scale 1:50 000 with or without descriptions (green colours on Fig. 6) and that derived from regional and county bedrock maps at the reduced scales 1:250 000 or 1:200 000 (beige colour on Fig. 6). The latter are generally based on older (pre-1965) field data and, in some cases, have involved only a limited or no field check in connection with their production. Bedrock maps at the scale 1:50 000 are referred to as local scale or local model scale maps, while bedrock maps at the scale 1:200 000 or 1:250 000 are referred to as regional scale or regional model scale maps.

An understanding of the geology is radically improved when a description of a 1:50 000 local map-sheet is available (all dark green colours on Figure 6). Map-sheet 10I Stockholm at the scale 1:100 000 is included here, since a detailed description of this map-sheet is available and updated geological maps at the scale 1:50 000 have recently been completed. Such descriptions provide a documentation of the composition of the

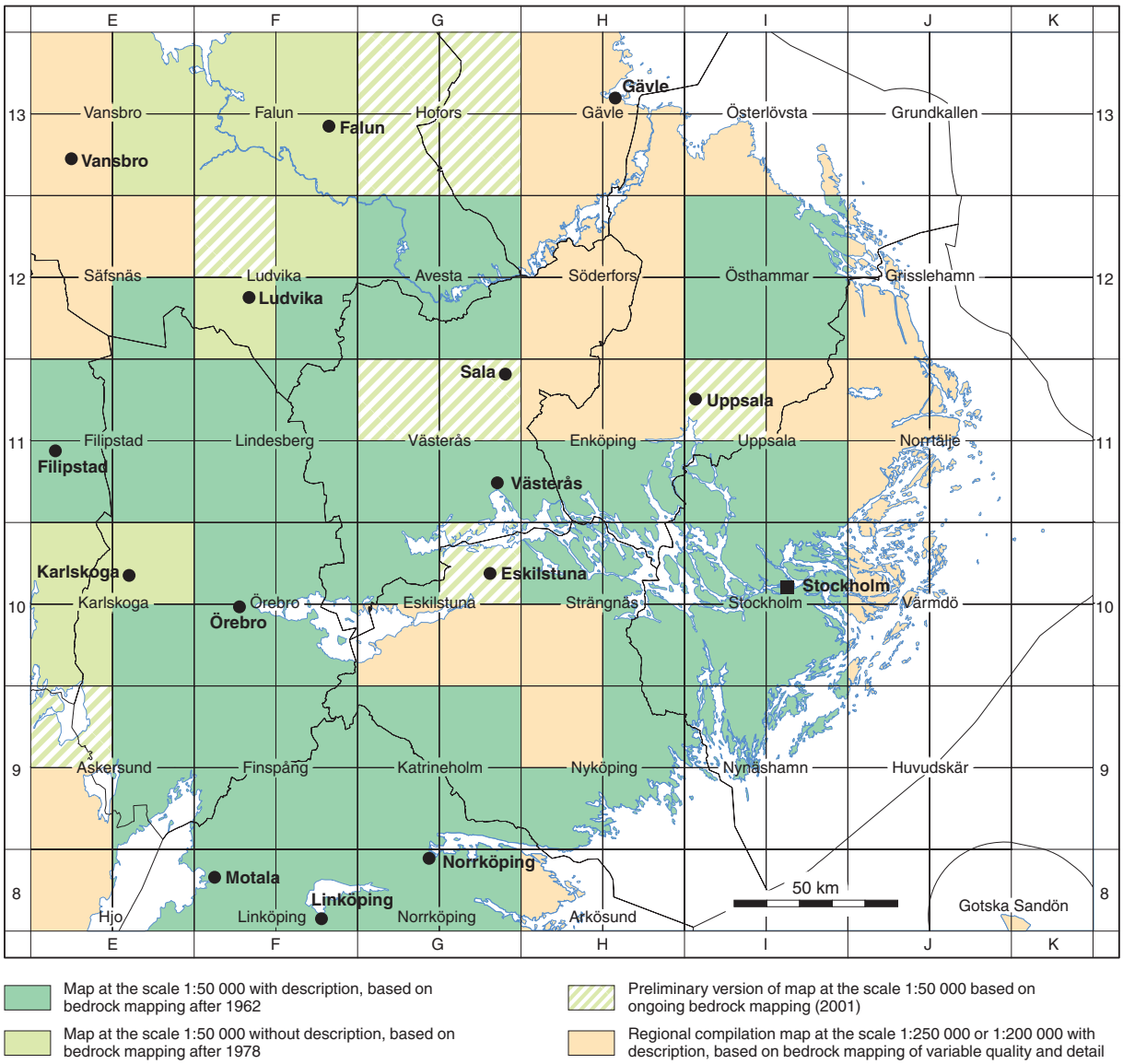

Fig. 6. Base geological maps used in the compilation of the bedrock geology in the Bergslagen region that was completed during 2001. Descriptions of map sheets 11G Västerås NO and 11I Uppsala NV were published after the compilation of the bedrock map.

different rock types, with both modal and geochemical analyses, the field relationships between the different rock types, their structure and metamorphism, and the mineral deposits inside the area represented by the map-sheet. They are also an important source to the earlier geological work carried out in the Bergslagen region prior to the 1960's. A reference list to all these local map descriptions is presented in Table 1.

At the time of the compilation work, descriptions of the bedrock geology were available for the regional maps at 1:250 000 and 1:200 000 in the counties of Dalarna (Kopparberg), Gävleborg, Östergötland, Södermanland and Värmland. The compilation and description work for the counties of Östergötland and Södermanland was carried out in connection with SGU's programme for the documentation of mineral deposits on a county by county basis. For this reason, these two descriptions were also an important source of information for the compilation of mineral and bedrock deposits. A regional description of the geology in the north-eastern part of the Bergslagen region, in the counties of Stockholm and Uppsala, was also available. Descriptions of the mineral deposits in the counties of Stockholm, Uppsala and Västra Götaland were published after 2001, but it was only possible to make use of information on the deposits in Stockholm and Västra Götaland prior to the deadline for the publication of the mineral resources map (Stephens et al. 2007c). A reference list to all these regional map descriptions is provided in Table 1.

A country-wide inventory of the geology by the Swedish Nuclear Fuel and Waste Management Company (SKB), in connection with their search for sites potentially suitable for the disposal of highly radioactive nuclear waste, was completed during 1998 and

Table 1. Local and regional map descriptions used in the synthesis of the bedrock geology in the Bergslagen region.

Local map (SGU)	Reference to description
8E Hjo NO	Wikman et al. 1982
8F Linköping NV	Wikman et al. 1980
8F Linköping NO	Gorbatschev et al. 1976
8G Norrköping NV	Kornfält 1975
8G Norrköping NO	Wikström 1975
9E Askersund NO, SO	Wikström & Karis 1998
9F Finspång NV, NO, SV, SO	Wikström & Karis 1991
9G Katrineholm SV	Wikström 1976
9G Katrineholm SO	Wikström 1979
9G Katrineholm NV, NO	Wikström 1983
9H Nyköping NO	Stålhös 1975
9H Nyköping SV	Lundström 1974
9H Nyköping SO	Lundström 1976
9I Nynäshamn NV, SV	Stålhös 1979
9I Nynäshamn NO, SO	Stålhös 1982a
10E Karlskoga SO	Wikström & Karis 1997
10F Örebro NV	Lundegårdh et al. 1972
10F Örebro NO	Gorbatschev 1972
10F Örebro SV	Lundegårdh & Fromm 1971
10F Örebro SO	Lundegårdh et al. 1973
10G Eskilstuna NV	Lundegårdh 1974
10H Strängnäs NV, NO	Stålhös 1984
10H Strängnäs SO	Stålhös 1982b
10I Stockholm NV, NO, SV, SO	Stålhös 1969
11E Filipstad NV	Björk 1986
11E Filipstad NO, SO	Lundström 1995
11E Filipstad SV	Lundegårdh 1987
11F Lindesberg NV	Lundström l985
11F Lindesberg NO	Ambros l983a
11F Lindesberg SV	Lundström 1983
11F Lindesberg SO	Lundegårdh 1983
11G Västerås NO	Ripa et al. 2002
11G Västerås SV	Lundegårdh & Nisca 1978
11G Västerås SO	Arnbom 1999
11H Enköping SV	Stålhös 1976
11H Enköping SO	Stålhös 1974
11I Uppsala NV	Arnbom & Persson 2002
11I Uppsala SV, SO	Stålhös 1972
12E Säfsnäs SO	Ripa 1998
12F Ludvika SO	Strömberg & Nisca 1983
12G Avesta NV, SV	Ambros l988
12G Avesta SO, NO	Persson 1997
12I Östhammar NV, NO, SV, SO	Stålhös 1991

Regional county map (SGU)	Reference to description
Dalarna (Kopparberg)	Hjelmqvist 1966
Gävleborg	Lundegårdh 1967
Östergötland	Bruun et al. 1995 with focus on mineral deposits in the description
Södermanland	Wik et al. 1999 with focus on mineral deposits in the description
Stockholm	Wik et al. 2004 with focus on mineral deposits in the description. See also Persson & Stålhös 1991
Uppsala	Wik et al. 2006 with focus on mineral deposits in the description. See also Persson & Stålhös 1991
Värmland	Lundegårdh 1995
Västra Götaland	Wik et al. 2002 with focus on mineral deposits in the description

County description (SKB)	Reference to description
Dalarna	Gierup et al. 1999
Gävleborg	Antal et al. 1998a
Södermanland	Antal et al. 1998b
Stockholm	Antal et al. 1998c
Örebro	Bergman et al. 1999a
Östergötland	Antal et al. 1998d
Uppsala	Antal et al. 1998e
Värmland	Fredén et al. 1999
Västmanland	Bergman et al. 1999b
Västra Götaland	Antal et al. 1999

1999. This study provided short, modern descriptions of the geology in the Bergslagen region, on a county by county basis. A reference list to these descriptions of the bedrock geology in the ten counties that lie inside the Bergslagen region is provided in Table 1.

All the bedrock geological maps and descriptions referred to above formed a significant base input to the compilation of the bedrock geology in the Bergslagen region, as presented in the published geological maps (Stephens et al. 2007a, b, c), and in the bedrock synthesis, as presented in this report. The compilation work has also made use of various publications in the scientific literature that are referred to directly in the text that follows.

Following completion and release of the Bergslagen map database in 2001, outcrop mapping and production of 2-D bedrock geological models at the local scale 1:50 000, in the form of geological maps, has been carried out on map-sheets 11H Enköping NV, 11H Enköping NO, 11I Uppsala NO, 12E Säfsnäs NO, 12H Söderfors (all four map-sheets) and 13H Gävle (all four map-sheets). New bedrock information has also been obtained by SGU in the context of bedrock mapping activities south of Eskilstuna, around Värmdö and south of Norrtälje as well as in previously mapped areas around Falun and Borlänge, around Örebro and around Katrineholm and Nyköping. The present (2009) coverage of bedrock geological information that is of sufficient detail to merit usage at the scale 1:50 000 or less is shown in Figure 7. Full descriptions of the bedrock geology with evaluation of data acquired during these mapping exercises have not been published and are not planned to be published by SGU.

The results of the mapping work completed during and after the summer 2001 are not included in the map compilations presented here. This work provides a new model for the distribution of rock units at the ground surface in the newly mapped areas that is more up-to-date and presumably better than the compilations presented here. However, inspection of these maps reveals

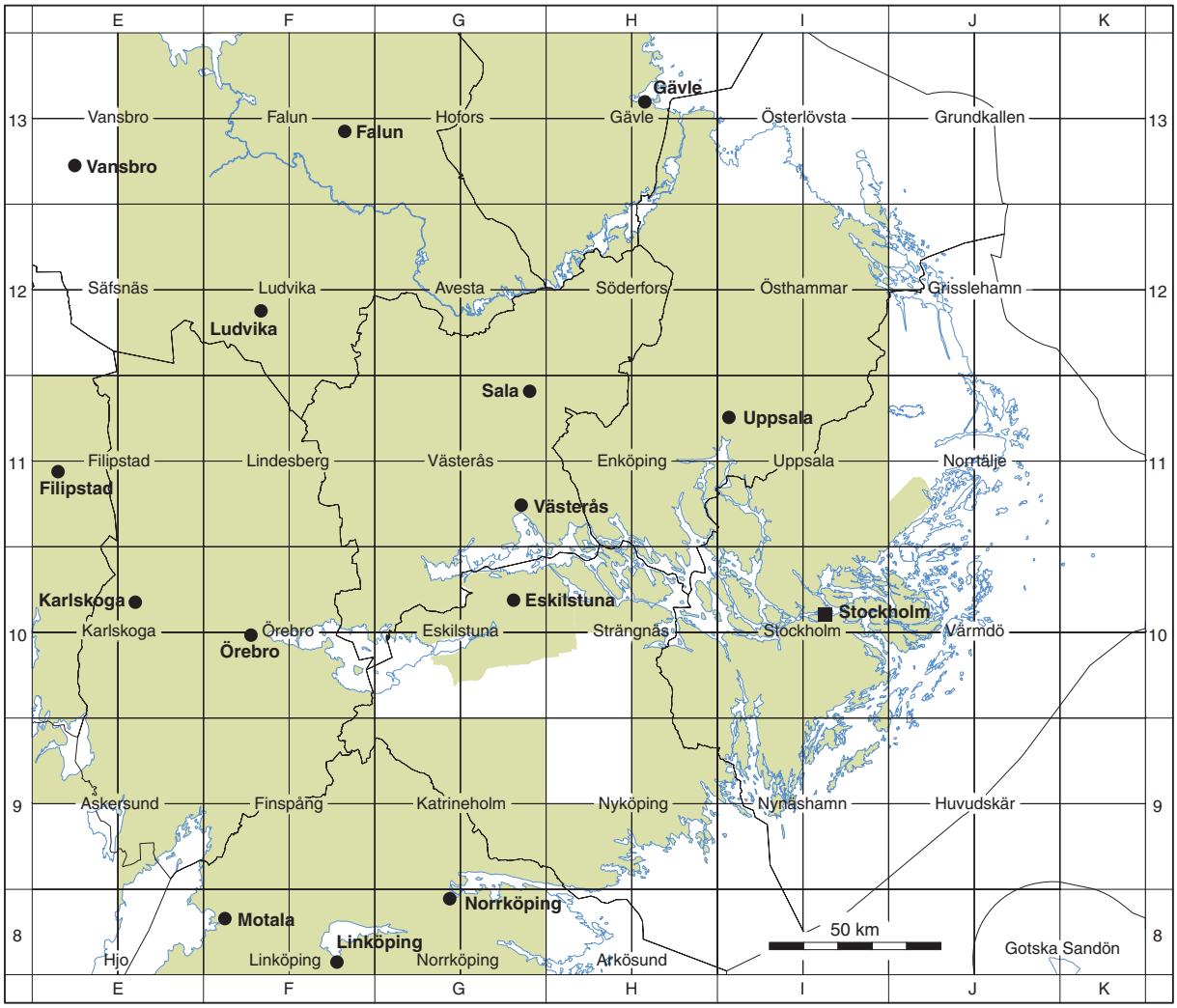

Fig. 7. Coverage of bedrock geological information in the Bergslagen region at the scale 1:50 000 during 2009.

no changes to the regional geological understanding of the Bergslagen region as presented in this description.

The results of the detailed geological mapping work around Forsmark (Stephens et al. 2008a), in the north-eastern part of the Bergslagen region, which was completed by the Swedish Nuclear Fuel and Waste Management Company (SKB) during 2002 and 2003, in connection with the characterization of a potential site for the disposal of highly radioactive nuclear waste, are also not included in the map compilation. However, the wealth of geological information, including data acquisition, data analysis and 3-D modelling work, published in open reports on SKB's web site (www.skb.se), has been of significant value for the description presented here. In particular, a wealth of geochronological data has emerged from this site that has had a profound impact on our understanding of the tectonic development in the Bergslagen region.

The digital compilation of inferred outcrops, inferred outcrops with some sort of bedrock observation at one or more points inside them and outcrops with a bedrock observation are shown in Figure 8. This image provides an overview at the time of completion of data compilation during 2001. Notwithstanding that the scale of presentation yields a somewhat misleading view, some general trends are apparent. Firstly, the area beneath the highest shoreline after the latest Weichselian glaciation and nearer to the Baltic Sea coast is much better

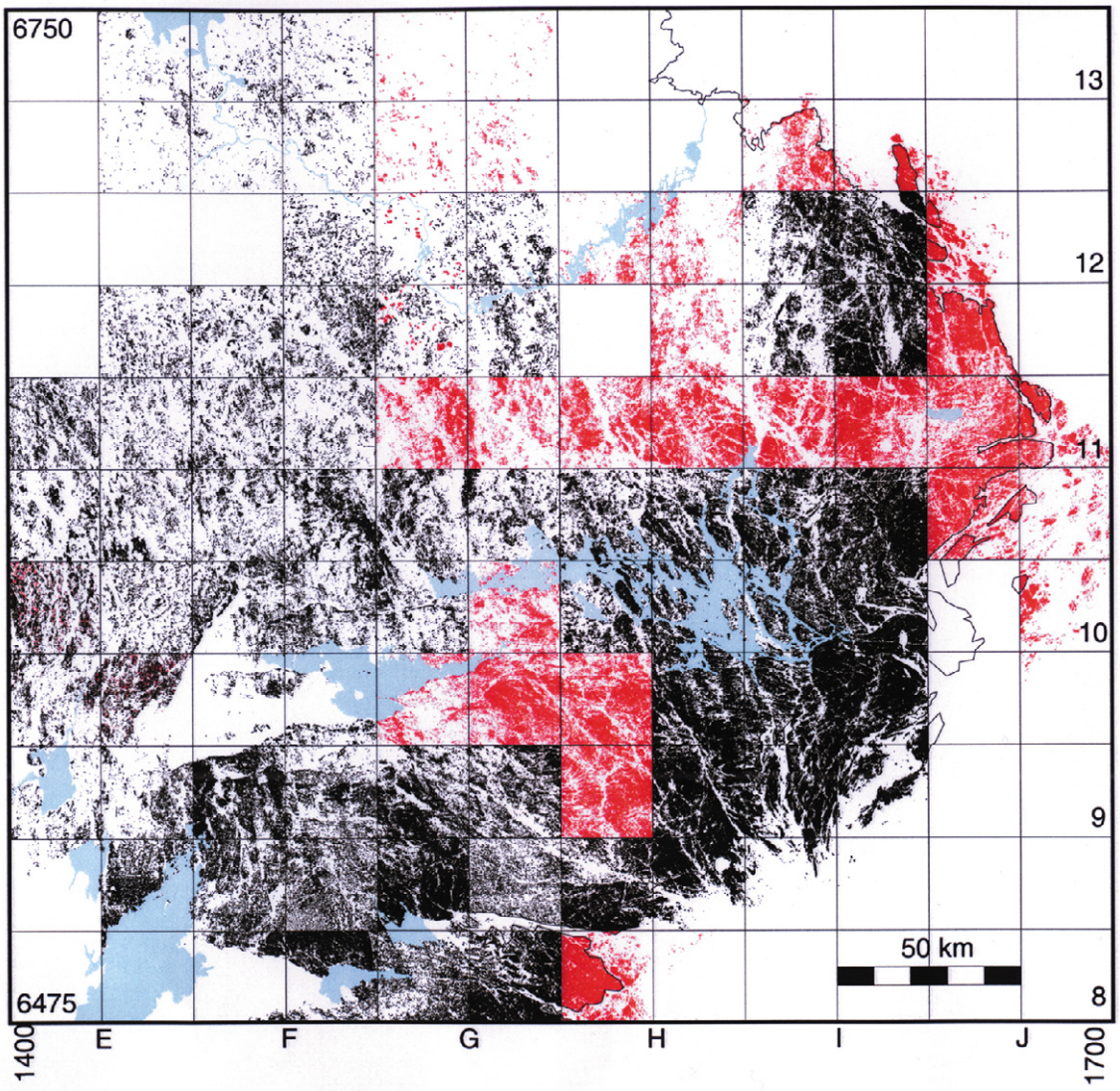

Fig. 8. Outcrops in the Bergslagen region. The black ornament shows inferred outcrops which also include some form of observation in the context of SGU's bedrock mapping programme or are simply outcrops with a bedrock observation point. The red ornament shows inferred outcrops where the bedrock had not been studied by modern bedrock geological mapping at the time of the compilation work (2001). Areas covered by thin Quaternary deposits, i.e. where the bedrock is not exposed, are also included in both the areas marked black or red. Map squares without shading (e.g. 12H Söderfors SV) and most of 9E Askersund SV were covered neither by modern Quaternary geology mapping with inferred outcrops nor by modern bedrock geological mapping at the time of the compilation work (2001). This compilation is in digital format.

exposed than the area further north-west. Secondly, the areas covered by Lower Palaeozoic sedimentary rocks on map-sheets 10E Karlskoga SO and 10F Örebro as well as on map-sheets 8E Hjo NO, 8F Linköping NV and 8F Linköping NO are very poorly exposed.

AIRBORNE GEOPHYSICAL, TOPOGRAPHIC AND GRAVITY DATA

The work within the Bergslagen project has made use of airborne geophysical and topographic data, and, to a more limited extent, gravity data. The 2-D compilations of especially the airborne geophysical and topographic data form a second, significant base input to the geological work in this project. The gravity data have been used by earlier workers for the assessment of specific geological problems in the Bergslagen region, for example, 3-D modelling of the shape of granitic bodies and major fold structures. These aspects are addressed in the sections entitled "Character, spatial distribution, geochronology, geochemical signature, petrophysical characteristics and regional geophysical signature of rock units", and "Deformation, metamorphism and mechanism of emplacement of the 1.87–1.84 Ga GSDG suite of intrusive rocks", respectively.

The airborne geophysical data were collected during 1964 to 1999 by SGU, Nämnden för statens gruvegendom (NSG) and Luossavaara–Kiirunavaara AB (LKAB). Prior to 1995, data were collected with a ground clearance of c. 30 m and a sampling interval of 40 m. From 1995 and onwards, all data were collected with a ground clearance of c. 60 m and a sampling interval of 17 m. Most of the data have been acquired with a line spacing of 200 m. Over the lake Vättern, the line spacing is 400 m and, over the Baltic Sea to the east, the line spacing is 1 000 m.

During work with the Bergslagen project, airborne magnetic data were available over the whole Bergslagen region, apart from a small area along the coast to the Baltic Sea, in the easternmost part of the region (Fig. 9).

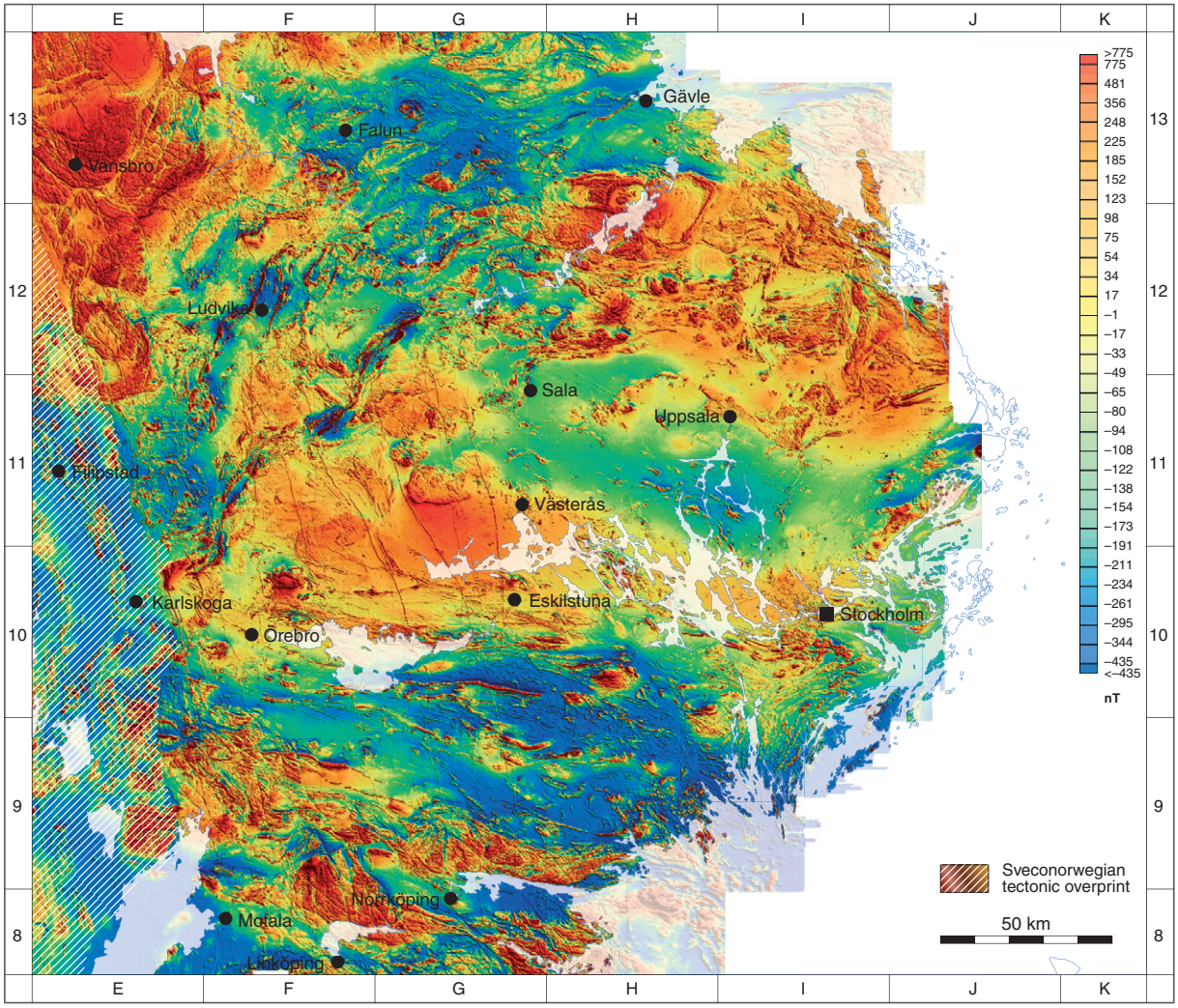

Fig. 9. Magnetic anomaly map over the Bergslagen region inferred from airborne magnetic data.

Airborne electromagnetic (VLF) and gamma radiation data were lacking over some map sheets (Figs. 10 and 11, respectively). Topographic data from the digital 50 m elevation database from the National Land Survey of Sweden have been used in the project.

The Bergslagen region is covered with gravity measurements with a sampling distance that varies from 0.3 to 5 km. At the current time, the distance between measurement points is 1–2 km. About 36 000 points cover the Bergslagen region. The locations of all gravity measurements used in the map compilation work in the Bergslagen region are shown in Figure 12. The Bouguer gravity anomaly map is shown in Figure 13.

DATABASE FOR RADIOMETRIC AGE DETERMINATIONS

Geochronological data have been compiled from the database for radiometric age determinations at SGU and from some publications that have recently been published or are in press (Hermansson 2007, 2008a, 2008b, Page et al. 2007, Söderlund et al. 2008, in press). Only published U-Pb (zircon, monazite, columbite, titanite, baddelyite, uraninite), Re-Os (molybdenite), ^{40}Ar-^{39}Ar (hornblende, biotite, white mica) and (U-Th)/He (apatite) data from predominantly the ground surface, with an uncertainty that does not exceed ±20 Ma, have been included in this compilation work. In addition, new U-Pb (zircon, monazite, titanite) age determinations from eleven samples, acquired in the context of the Bergslagen project at ten separate

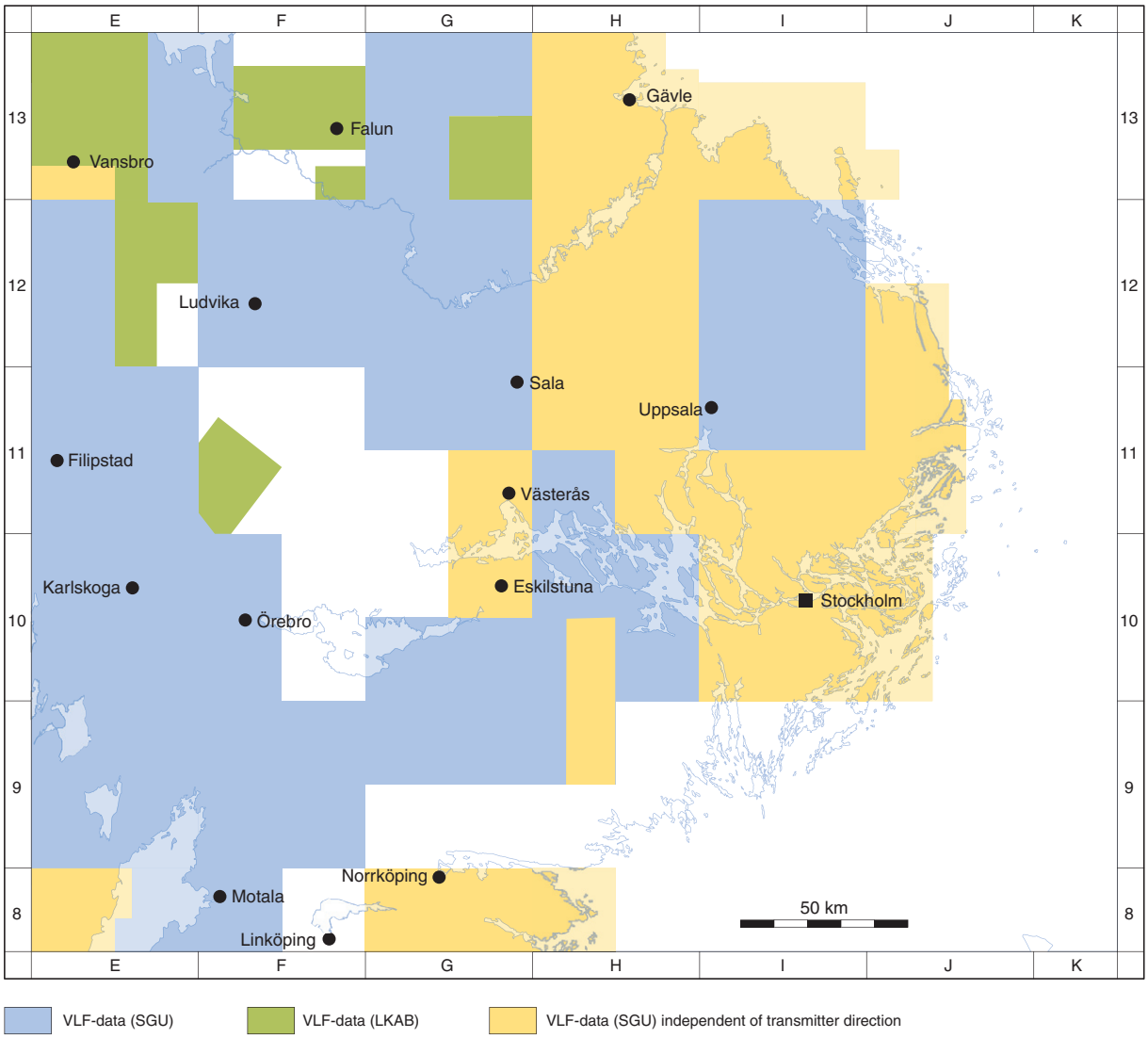

Fig. 10. Coverage of airborne electromagnetic (VLF) data over the Bergslagen region. Current measurements of the VLF field are collected from two different transmitters. With this option, a response can be calculated which is independent of the transmitter direction.

locations, are described for the first time in this report (see also following section). These data have also been used in the compilation work.

Ninety U-Pb (zircon, columbite, monazite, baddeleyite and uraninite) and Re-Os (molybdenite) age determinations, which are inferred to constrain the timing of crystallization of igneous and meta-igneous rocks in the Bergslagen region, are included in the compilation and are shown on the metamorphic, structural and isotope age map (Stephens et al. 2007b). In addition, U-Pb (zircon) data that address the age of detrital zircons in some metasedimentary rocks and U-Pb (monazite, titanite, zircon), ^{40}Ar-^{39}Ar (hornblende, biotite, white mica) and (U-Th)/He (apatite) ages, which have been inferred to date geological events other than the protolith age, are also present. All sample sites where geochronological data are present are shown in Figure 14. The age data are presented in tabular format and their geological significance discussed in the relevant parts of the text below (see sections entitled "Character, spatial distribution, geochronology, geochemical signature, petrophysical characteristics and regional geophysical signature of rock units", and "Deformation, metamorphism and mechanism of emplacement of the 1.87–1.84 Ga GSDG suite of intrusive rocks").

U-Pb ages strongly dominate in the database for radiometric age determinations. Most of these data have been acquired using the Thermal Ionization Mass Spectrometry (TIMS) technique on multiple grains at the Laboratory for Isotope Geology in Stockholm, Sweden. More recently, analyses of single grains using either the Secondary Ion Mass Spectrometry (SIMS) technique at the same laboratory or the TIMS technique at the University of Oslo, Norway, have become available.

Attention was focussed in the database for radiometric age determinations on seven attributes – lithology, rock unit (see also nomenclatural considerations presented earlier), age determination method, age in

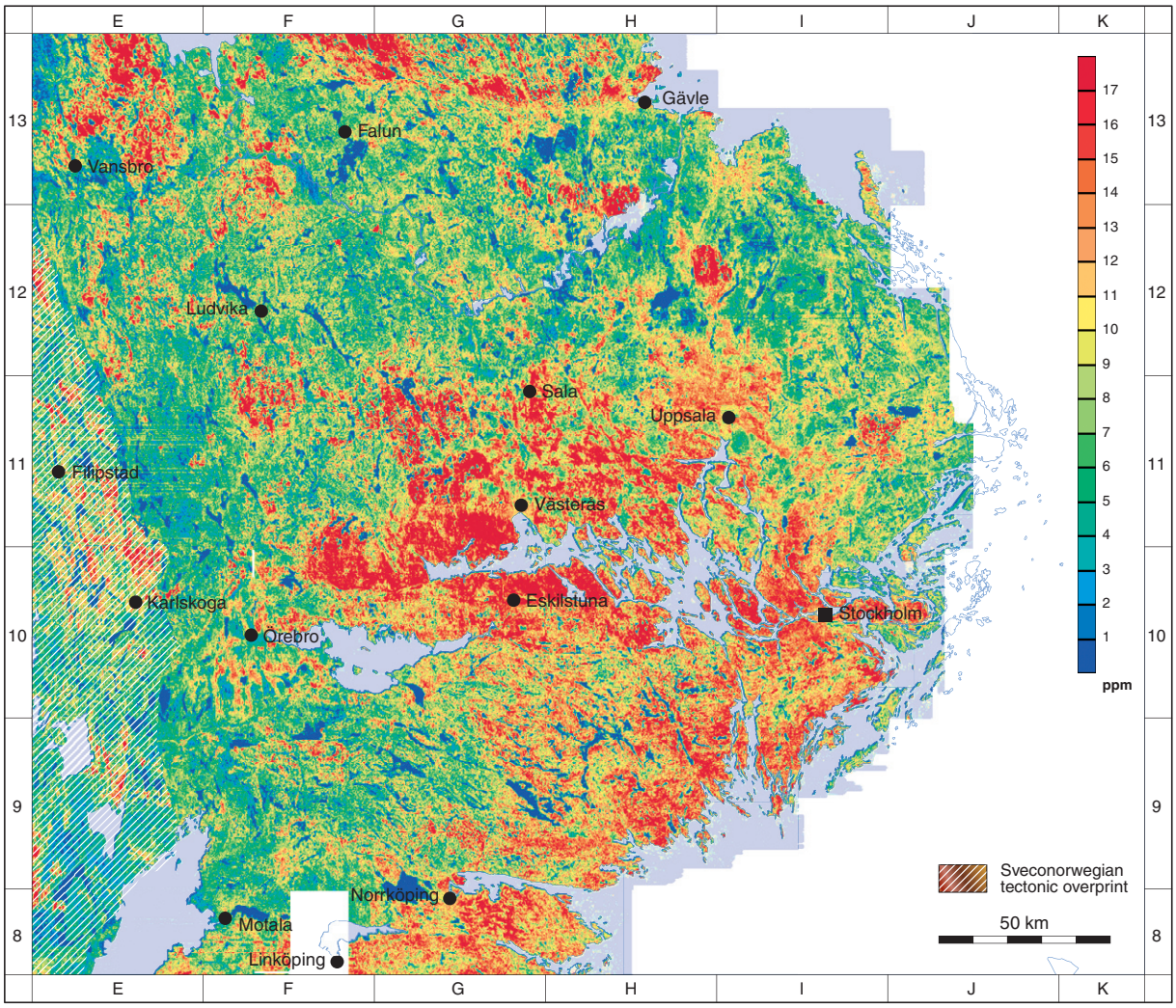

Fig. 11. Radiometric map over the Bergslagen region inferred from airborne data. The map displays the spatial distribution of thorium in the uppermost part of the bedrock and in the Quaternary cover.

million years (Ma) with uncertainty, coordinates at the ground surface in the Swedish national grid (RT 90), publication year and reference. The quality of the data needs to be judged by inspection of the published reference material. No attempt was made during this study to grade the quality of the age determination data. However, a systematic evaluation of the quality of U-Pb radiometric age determinations from metamorphosed, 1.91 to 1.84 Ga volcanic and intrusive rocks in central Sweden, including data from the Bergslagen region, has recently been presented in Hermansson et al. (2008a).

Sm-Nd ANALYSES

Sm-Nd whole-rock analyses in the Bergslagen region have been compiled from five sources (Patchett et al. 1987, Valbracht 1991, Valbracht et al. 1994, Kumpulainen et al. 1996, Andersson 1997a). 116 analyses have been included in the data compilation.

The original rock name used in each publication has been adopted in the data compilation and an inspection of the literature has permitted the assignment of each analysis to the specific igneous rock suite used in this report (see nomenclatural considerations presented earlier). There is naturally some uncertainty with this procedure and some mistakes may have occurred. Data have been acquired from the Svecofennian sedimentary rocks (12 samples), the Svecofennian volcanic and subvolcanic intrusive rocks (40 samples), the GDG intrusive rock suites (23 samples) and the combined GSDG intrusive rocks, with ages of 1.87–1.84 Ga and 1.81–1.78 Ga, and GP intrusive rocks with ages between 1.85 and 1.75 Ga (41 samples). The Sm-Nd analytical data for each group of rocks are presented in tabular format and their geological significance discussed in the section "Sm-Nd analyses of rock suites in the Svecokarelian orogen formed between 1.9 and 1.8 Ga".

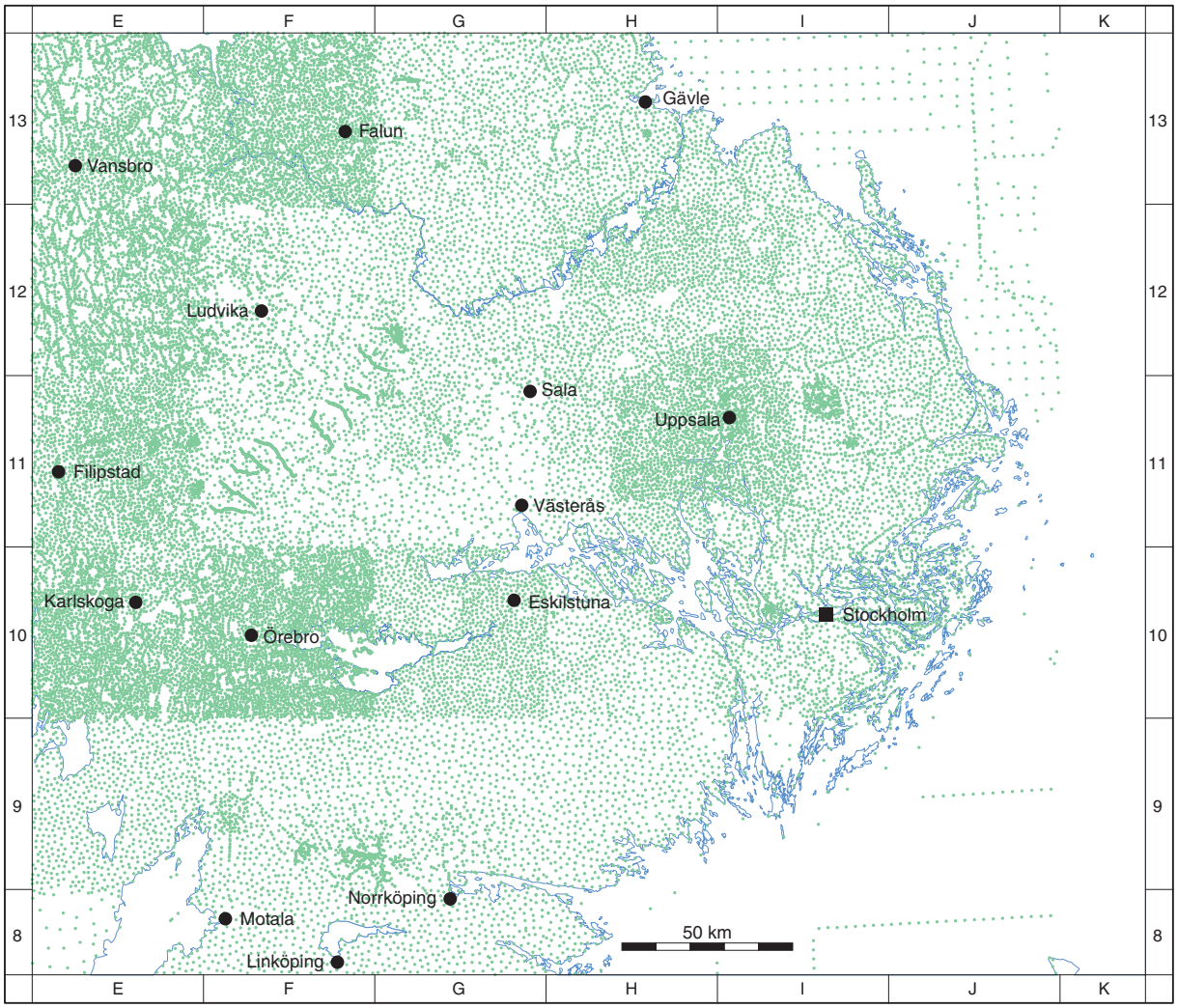

Fig. 12. Location of gravity measurement points in the Bergslagen region.

DATABASE FOR BEDROCK GEOCHEMICAL ANALYSES

At the time of completion of data compilation during 2001, the bedrock geochemical database for the Bergslagen region contained 967 analyses of igneous and meta-igneous rocks. Only high quality analyses of major, minor and trace (including rare earth) elements, determined with the help of the ICP-AES, ICP-MS and XRF techniques, and with coordinates in the Swedish national grid (RT 90), were chosen.

The database includes both older analyses compiled during the Bergslagen project as well as 111 new analyses acquired during the project (see section "Acquisition of new data and data interpretation – methodological aspects"). Older bedrock geochemical data have been extracted from the data assembled during bedrock mapping projects at SGU, from published scientific papers, from internal and external research reports produced by SGU and NFR ("Naturvetenskapliga forskningsrådet") and from unpublished information kindly provided by colleagues at the universities of Luleå, Stockholm and Uppsala. The principal references (in alphabetical order) from which data have been extracted outside SGU's standard bedrock mapping activities are: Ahl et al. (1997, 1999, 2001), M. Ahl (personal communication 2000), Allen et al. (1996), Andersson (1991, 1997a, 1997b), U.B. Andersson (personal communication 2000), Bergman et al. (1995), Billström et al. (1988), Björk (1986), Kumpulainen et al. (1996), Kresten (1986), Lundqvist & Persson (1999), Öhlander & Romer (1996), Öhlander & Zuber (1988), B. Öhlander (personal communication 2000), Persson (1993, 1997), Persson & Persson (1997, 1999), Persson & Ripa (1993), Ripa (1998), Ripa & Persson (1997), Stephens et al. (1993), Sundblad et al. (1993), Sundblad & Bergman (1997) and Wikström & Karis (1991, 1997).

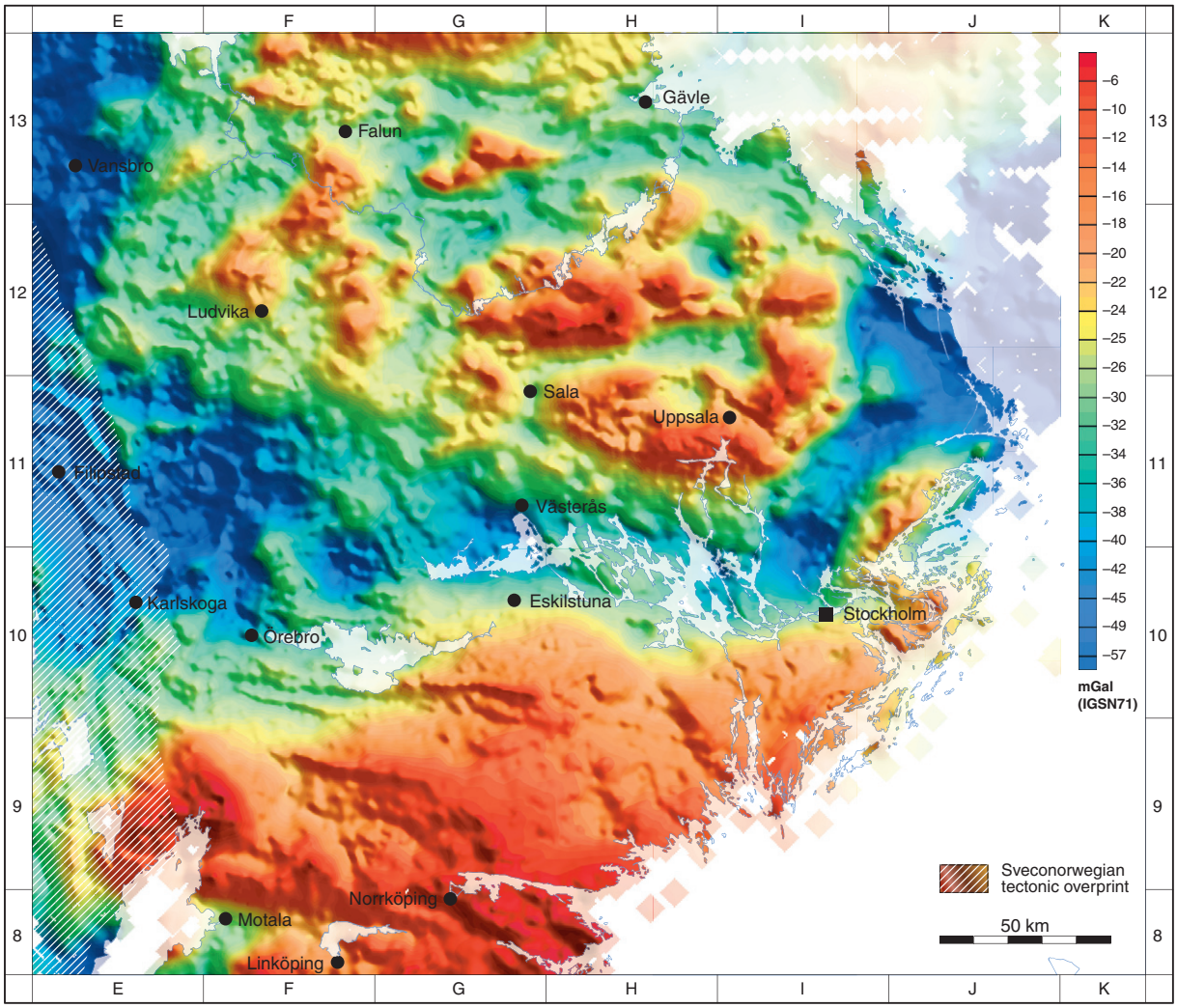

Fig. 13. Bouguer gravity anomaly map over the Bergslagen region. The scale is in mGal (IGSN71).

The original rock name and rock classification used in the primary reports and data assemblies are adopted in the database and each analysis has been assigned to the specific igneous rock suite used in this report (see nomenclatural considerations presented earlier). As for the Sm-Nd whole-rock analyses, there is naturally some uncertainty with this procedure and some mistakes may have occurred. The locations of the bedrock geochemical sample sites are shown in Figure 15 and the data from each rock group are evaluated in the relevant

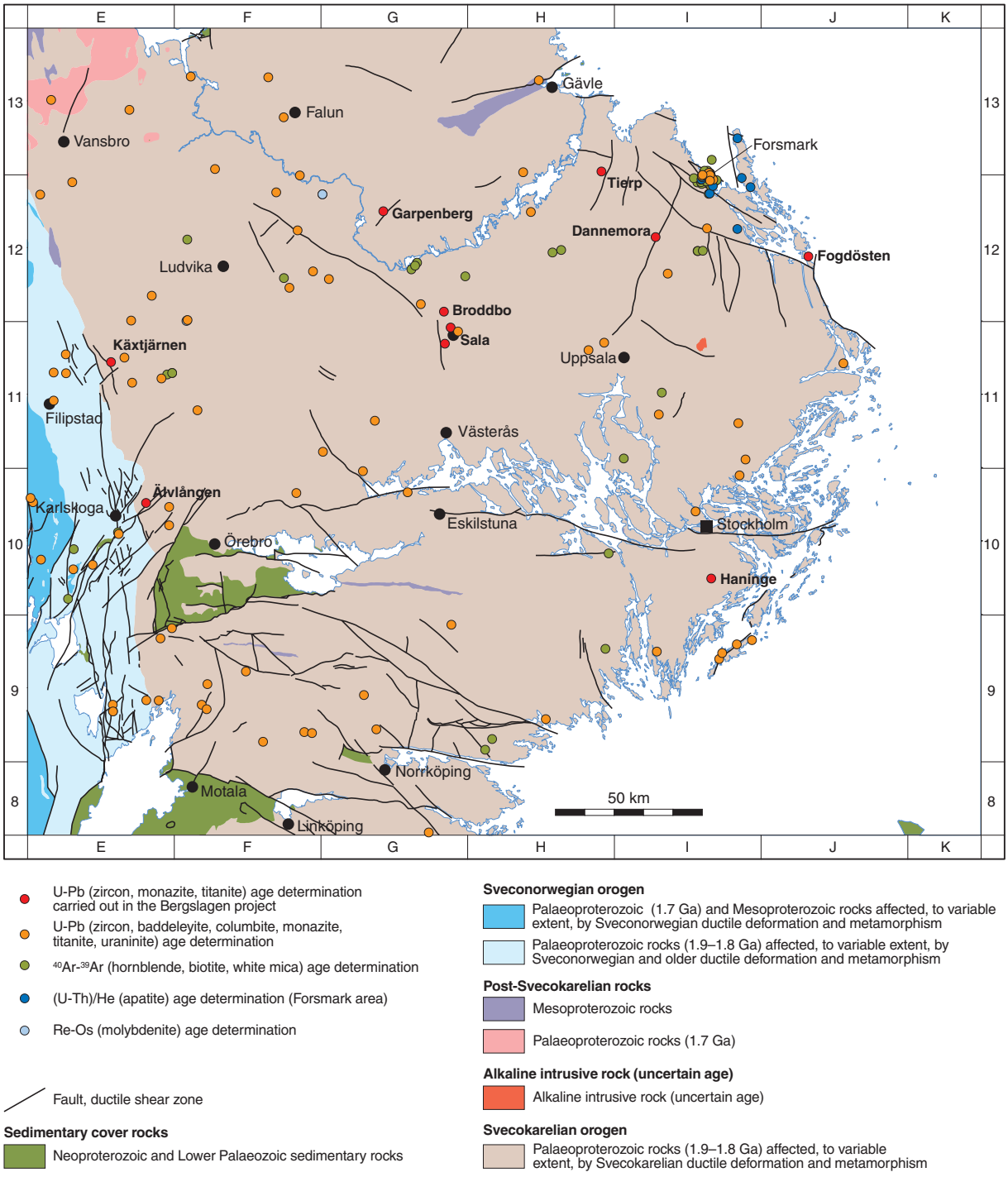

Fig. 14. Location of sample sites for radiometric age determinations. Only published ages or ages acquired in the context of the Bergslagen project, and published in this report, are shown here. Furthermore, ages with an uncertainty that exceeds ±20 Ma have been omitted. At some localities, different minerals have been analysed with the same age determination technique (e.g. U-Pb zircon and monazite) or even with different techniques (e.g. ^{40}Ar-^{39}Ar biotite and (U-Th)/He apatite). These multiple analyses are not distinguished in the figure. The reader is referred to the radiometric age data tables in the text. The sites where U-Pb age determinations have been carried out in the context of the Bergslagen project are named in bold text (see also Appendix). The different rock units shown on the map are distinguished on the basis of their tectonic status.

parts of the section "Character, spatial distribution, geochronology, geochemical signature, petrophysical characteristics and regional geophysical signature of rock units".

DATABASE FOR PETROPHYSICAL ANALYSES

At the time of completion of data compilation during 2001, petrophysical measurements from c. 9 000 localities and gamma radiation measurements from c. 1 400 field sites existed inside the Bergslagen region (Fig. 16). 628 of these measurements were acquired in connection with the Bergslagen project (see section "Acquisition of new data and data interpretation – methodological aspects"). Each analysis has been assigned to the specific rock unit identified in this report (see also nomenclatural considerations presented earlier). As discussed above for other data sets, some mistakes may have occurred during the execution of this procedure, especially where it concerns the majority of the analyses completed prior to the Bergslagen project.

The petrophysical database at SGU includes data from petrophysical measurements of rock samples carried out in the laboratory as well as gamma radiation measurements carried out in situ on outcrop. The point information included in the database consists of sample ID number, coordinates at the ground surface in the Swedish national grid (RT 90), a description of the bedrock geology, density, magnetic susceptibility, natural remanent magnetization (NRM) and, in

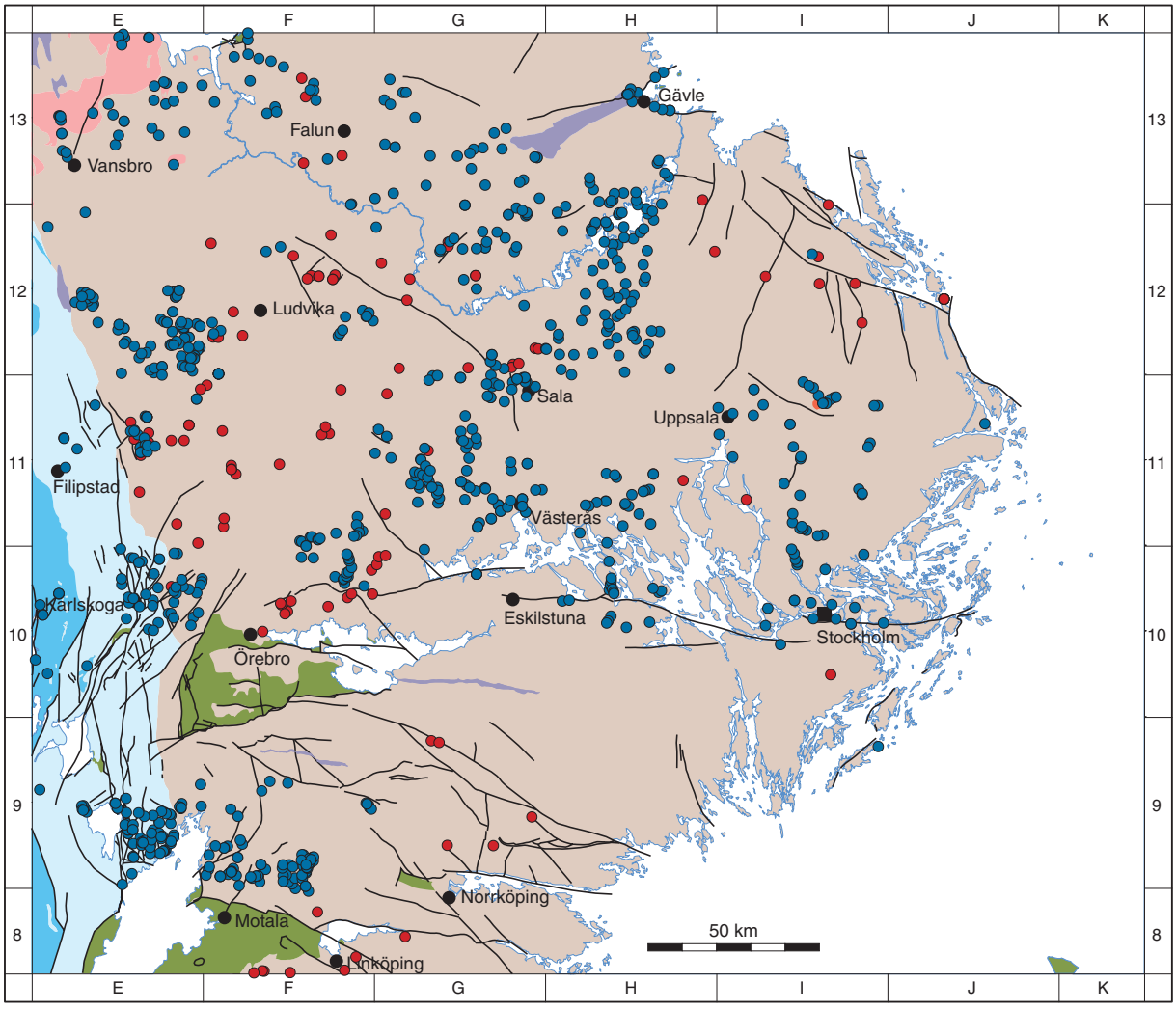

Sample site for bedrock geochemical analysis. Analysis completed during the Bergslagen project

Sample site for bedrock geochemical analysis

Fig. 15. Location of sample sites for bedrock geochemical analyses within the Bergslagen region at the time of completion of data compilation during 2001. The different rock units shown on the map are distinguished on the basis of their tectonic status. The legend is identical to that shown in Figure 14.

some cases, the orientation of NRM. Gamma radiation measurements include total radiation measurements as well as values for potassium (^{40}K), uranium (^{238}U) and thorium (^{232}Th). The petrophysical data are evaluated in the relevant parts of the section "Character, spatial distribution, geochronology, geochemical signature, petrophysical characteristics and regional geophysical signature of rock units".

DATABASE FOR MINERAL AND BEDROCK RESOURCES

The mineral and bedrock resources database at SGU was established prior to the initiation of data compilation work in the Bergslagen region during 1997. However, relatively few deposits from the Bergslagen region were included in this database when the Bergslagen project initiated. Indeed, the database only contained information on mineral deposits in Bergslagen assembled during production of the National Atlas of Sweden (Åkerman 1994). A prime task of the work within the Bergslagen project concerned the build-up of a far more complete mineral and bedrock resources database for this region (see section "Acquisition of new data and data interpretation – methodological aspects"). The mineral and bedrock deposits in the Bersgslagen region are described in the section "Mineral and bedrock deposits".

PRESSURE AND TEMPERATURE ESTIMATES DURING METAMORPHISM

Data bearing on the pressure and temperature conditions (P-T conditions) during metamorphism of the bedrock in the Bergslagen region have been compiled from various publications (Andersson et al. 1992, Wikström & Larsson 1993, Andersson 1997c, Sjöström &

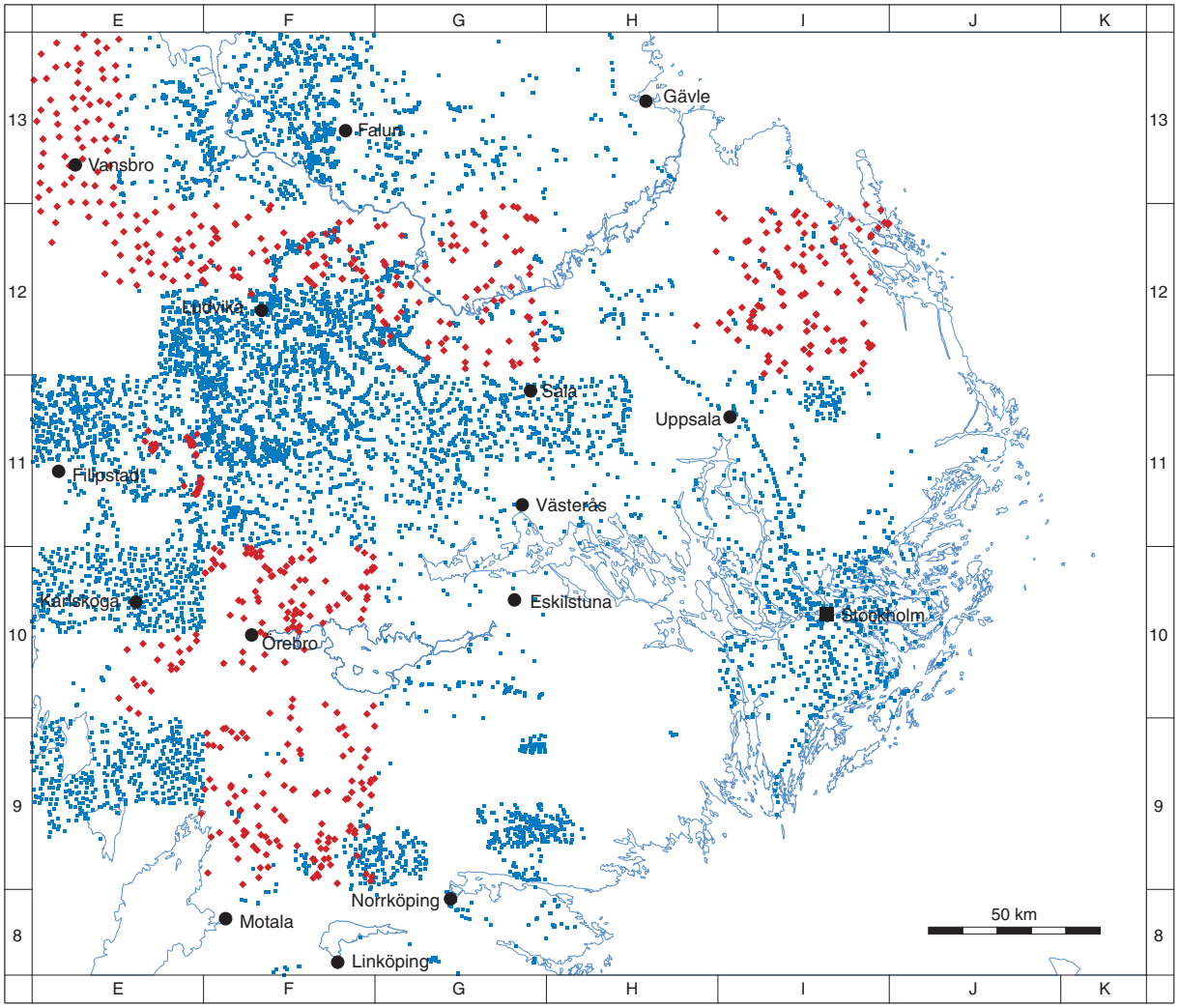

Fig. 16. Location of sample sites for petrophysical or gamma radiation measurements (or both) within the Bergslagen region at the time of completion of data compilation during 2001. Red diamonds indicate measurements completed during the Bergslagen project. Blue squares indicate measurements completed outside this project.

Bergman 1998). 50 analyses have been included in a database that was constructed during the execution of the Bergslagen project. Data were acquired using different techniques that include the garnet-orthopyroxene-plagioclase-quartz (Perkins & Chipera 1985, Reche & Martinez 1996) and garnet-plagioclase-biotite-quartz (Hoisch 1989, 1990, Reche & Martinez 1996) geobarometers, the garnet-orthopyroxene (Perchuk et al. 1985, Reche & Martinez 1996) and garnet-biotite (Hodges & Spear 1982, Reche & Martinez 1996) geothermometers, and the combined garnet-cordierite geothermobarometer (Perchuk et al. 1985, Reche & Martinez 1996). The locations of the sample sites are shown in Figure 17. The P-T data at these 50 locations are also shown on the metamorphic, structural and isotope age map (Stephens et al. 2007b). The data are discussed in the section "Deformation, metamorphism and mechanism of emplacement of the 1.87–1.84 Ga GSDG suite of intrusive rocks".

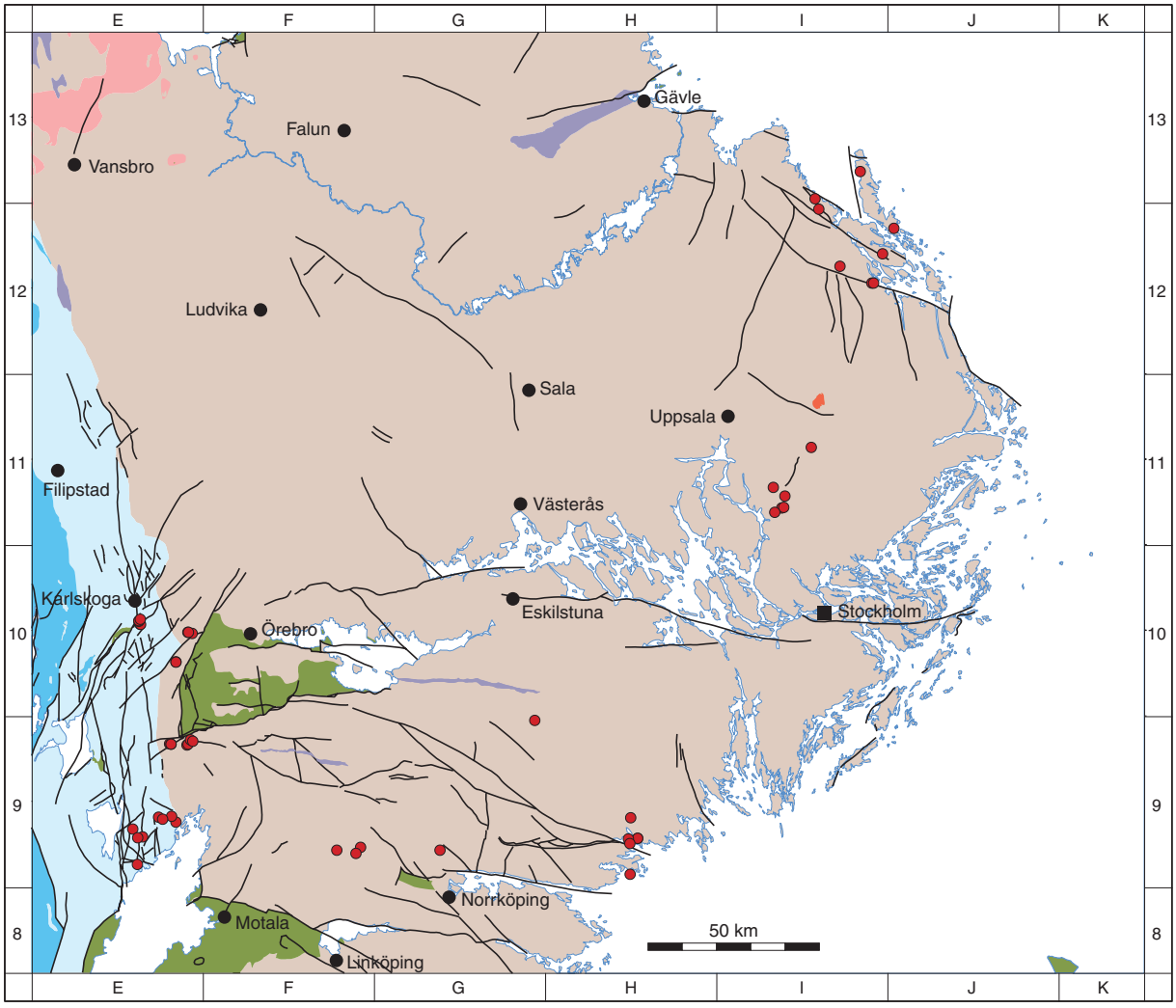

● Sample site for P-T determination

Fig. 17. Location of sample sites where P-T determinations have been completed in the Bergslagen region. The map shows the situation at the time of completion of data compilation during 2001. The different rock units shown on the map are distinguished on the basis of their tectonic status. The legend is identical to that shown in Figure 14.

Acquisition of new data and data interpretation – methodological aspects

INTEGRATED STRUCTURAL FIELD AND GEOPHYSICAL STUDY IN THE SOUTHERN PART OF THE BERGSLAGEN REGION

During an earlier part (1989–1990) of the internal research and development SGU project 5082 entitled "Tectonothermal evolution of the Protogine Zone and the adjacent Bergslagen province, south-central Sweden", attention was focussed on the geometry, kinematic signature and timing of deformation of ductile high-strain zones in the Sveconorwegian orogen in the western part of and to the west of the Bergslagen region (Wahlgren et al. 1994, Page et al. 1996, Stephens et al. 1996). The implications of the results from these publications for our understanding of the regional structural geology in the western part of the Bergslagen region are addressed in the section "Deformation, metamorphism and mechanism of emplacement of the 1.87–1.84 Ga GSDG suite of intrusive rocks".

During a later part (1991–1992) of the SGU project 5082 entitled "Kinematics and timing of major deformation zones, south-central Sweden", an integrated structural geological and geophysical study was completed in the southern part of the Bergslagen region, in order to investigate the occurrence and character of ductile high-strain zones. This area was judged to be suitable for a detailed structural study since the area is relatively well exposed and is covered by modern bedrock geological maps with descriptions (SGU Af series) as well as digital airborne magnetic and topographic data. Field data acquired during this research and development project were incorporated into the work with the Bergslagen project and are evaluated here (see section "Deformation, metamorphism and mechanism of emplacement of the 1.87–1.84 Ga GSDG suite of intrusive rocks").

Initially, a systematic desk-top analysis of structural form-line data, digital airborne magnetic data and topographic data in the southern part of the Bergslagen region was completed. The desk-top analysis indicated the presence of markedly asymmetric structures and discrete, deformation zones in this area. These findings had profoundly new implications for the influence of simple shear deformation in the structural framework of this part of the Svecokarelian orogen. Field checks were subsequently carried out at 92 observation points (Fig. 18) mostly along but also between some of the inferred deformation zones, in order to establish the character of these zones. Particular attention was focussed on kinematic studies (for a review of techniques, see, for example, Hanmer & Passchier 1991). An attempt was also made to qualitatively constrain the grade of metamorphism along these zones at the time when the rocks had deformed in a ductile manner. Microstructural studies were completed on a suite of oriented samples from the deformation zones in order to complement and refine the kinematic and metamorphic studies initiated by the field investigations.

PHYSICAL VOLCANOLOGICAL AND STRUCTURAL FIELD DATA

Field work that provided base information related to the specific geological issues selected for special study (see earlier section) was carried out in connection with the Bergslagen project during c. 40 man-weeks in 1998, 1999 and 2000. Field localities were chosen in areas where published Af or Ai geological maps, with or without descriptions, already existed and the focus of the work was on the parts of the Bergslagen region that are not affected by high-grade metamorphism including migmatization. Furthermore, the field work aimed to complement similar studies that had already been completed in other parts of the region (see Allen et al. 1996 and above). For this reason, field work was mainly centred in the area between Örebro, Eskilstuna, Sala and Falun and field data from 841 observation points were recorded (Fig. 18). The broader geological implications of these data are included in the relevant parts of the sections entitled "Character, spatial distribution, geochronology, geochemical signature, petrophysical characteristics and regional geophysical signature of rock units" and "Deformation, metamorphism and mechanism of emplacement of the 1.87–1.84 Ga GSDG suite of intrusive rocks".

INTERPRETATION OF AIRBORNE GEOPHYSICAL AND TOPOGRAPHIC DATA

The use of airborne geophysical and topographic data has primarily concerned the interpretation of lineaments that are, in general, longer than 10 km and which possibly represent regionally more significant, brittle deformation zones including faults. Three different sets of data have been used for the interpretation of lineaments: Airborne magnetic data, airborne electromagnetic VLF data and topographic data. Each inferred lineament was stored in a database and coded according to which set (sets) of data was (were) used in the interpretation. Relative horizontal dislocations in, for example, the magnetic data were recognized across some lineaments and this information was also included in the database. Such information strengthens the

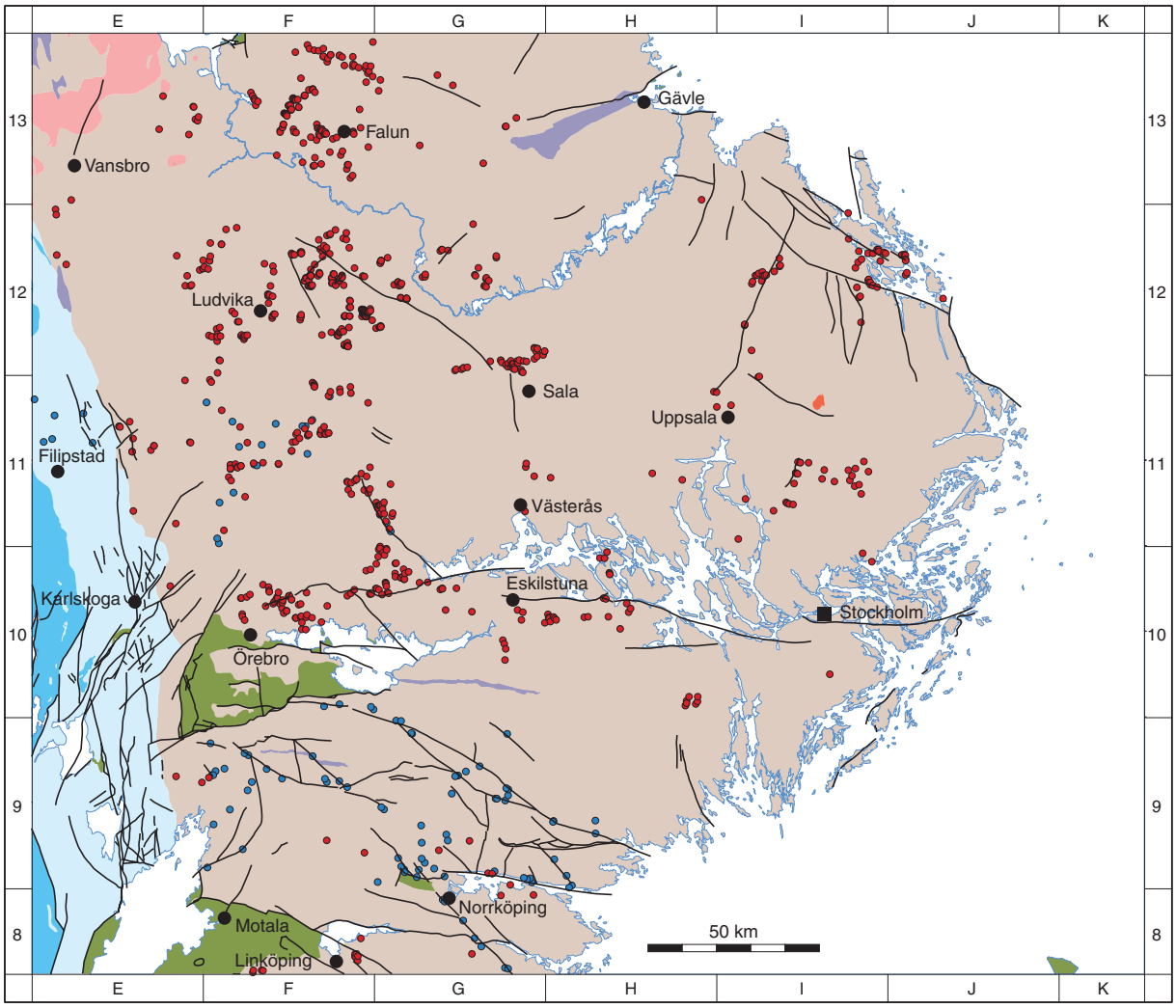

Fig. 18. Field observation points for geological work carried out during the internal research and development project at SGU entitled "Kinematics and timing of major deformation zones, south-central Sweden" (1991–1992) as well as in connection with the Bergslagen project (1998–2000). The different rock units shown on the map are distinguished on the basis of their tectonic status.

interpretation of the lineament as a deformation zone with a shear sense of movement. Dolerite dykes were also recognized with the help of the airborne magnetic data. Furthermore, the airborne radiometric data were used as an aid in the compilation of the bedrock map, for example to delineate the surface extension of granitic intrusions with relatively high gamma radiation.

The interpretations described above have been incorporated in the published geological maps (Stephens et al. 2007a, b, c) and are addressed in the relevant parts of the sections entitled "Character, spatial distribution, geochronology, geochemical signature, petrophysical characteristics and regional geophysical signature of rock units" and "Deformation, metamorphism

and mechanism of emplacement of the 1.87–1.84 Ga GSDG suite of intrusive rocks". The text that follows below addresses technical aspects in the interpretation work for the different sets of data.

Airborne magnetic data

Brittle deformation zones in the bedrock commonly correspond to low-magnetic lineaments due to the hydrothermal alteration of magnetite along such zones. Linear high-magnetic anomalies are commonly related to dolerite dykes that intruded the older crystalline bedrock.

Prior to the interpretation of lineaments, the magnetic data were processed in several steps. Initially, levelling of all airborne magnetic data was carried out. In the levelling process, the programme "kartkorr" developed at SGU was used. All other processing of the data was performed with the Oasis Montaj (Geosoft Inc.) software. The magnetic dataset was gridded using a cell size of 50 m. The different grids were then linked together using the grid knitting function in Oasis Montaj. Several filters were then applied for the interpretation of linear structures. The horizontal derivatives were calculated for different angles in order to enhance different directions in the data. An upward continuation filter was applied in order to emphasize variations in the magnetic field that originate from the shallowest parts of the bedrock. In this process, the data were upward continued to 500 m and the result was then subtracted from the original data. Finally, the "grid peak" function in Oasis Montaj was used as an aid to define linear features in the data, both for low-magnetic lineaments and for high-magnetic anomalies inferred to be related to dolerite dykes.

Airborne electromagnetic VLF data

Crystalline bedrock is often characterized by very high electrical resistivities. However, in fractured bedrock, the resistivity may decrease due to increased water content or clay alteration. For this reason, water-bearing brittle deformation zones can be observed in electromagnetic data due to their relatively low electrical resistivity. Metallic deposits also show low electrical resistivity.

At the time of the investigations, the Bergslagen region was covered by airborne electromagnetic VLF data collected by SGU and LKAB during the years 1972 to 1999. In the SGU system, the real and imaginary parts of the magnetic field were measured simultaneously in three orthogonal directions (i.e. Hx, Hy and Hz). From 1995 and onward, the electromagnetic VLF field was measured from two different transmitters. With this option, a response can be calculated that is independent of the transmitter direction.

The processing of the VLF data was performed using the Oasis Montaj (Geosoft Inc.) software. The VLF data were again gridded using a cell size of 50 m. For older VLF data, which made use of only one transmitter, the square root sum of all three orthogonal components (total field) was employed in the interpretation. For the part of the region covered with modern VLF data, which made use of two transmitters, the Peaker function (Pedersen et al. 1994) was calculated. This function is independent of the geometrical relations between the anomaly source and the two transmitters. The "grid peak" function in Oasis Montaj (Geosoft Inc.) was used as an aid to define linear structures in the VLF data and man-made disturbances from, for example, electrical power lines were removed.

Airborne radiometric data

The airborne radiometric data were used in the compilation of the bedrock map in some areas where modern bedrock geological information was lacking. The data were mainly used to define granitic intrusions with high uranium or thorium concentrations.

At the time of the investigations, radiometric data were present over more or less the entire Bergslagen region. From these measurements, the ground content of the naturally occurring radioactive isotopes of potassium, uranium and thorium were calculated. The data were again gridded using a cell size of 50 m for the different isotopes. The potassium, uranium and thorium maps were then correlated with information from outcrops.

Topographic data

Strongly fractured bedrock may correlate with topographic depressions in the terrain due to the intrinsically weak and more easily eroded character of such rock. In the interpretation of topographic data, the digital 50 m elevation database from the National Land Survey of Sweden was used and the data were once again gridded using a cell size of 50 m. The horizontal derivatives were calculated for different angles in order to enhance different directions in the data. As for the other sets of data, the "grid peak" function in Oasis Montaj (Geosoft Inc.) was used as an aid to define linear features in the data.

DIGITAL COMPILATION OF THE GEOLOGICAL MAPS

At the start of the Bergslagen project, only the 1:50 000 map-sheets 10E Karlskoga NO and 12E Säfsnäs SO

were in digital format. Bedrock geological information in digital format, which was derived from preliminary versions of the 1:50 000 map-sheets produced by ongoing map projects, was incorporated into the Bergslagen compilation work as soon as this information became available (diagonal green lines on the map in Figure 6). Digitization of the bedrock information from all the other published 1:50 000 map-sheets (66 map-sheets, each with an area of 625 km^2) was a key, time-consuming task included in the Bergslagen project. The bedrock geological information in the remaining areas, covered solely by maps at the scale 1:250 000 and 1:200 000, were also digitized.

The major part of the digitization work was carried out at the scale 1:100 000 on scanned copies of the 1:50 000 base geological maps, bearing in mind an established legend and a planned publication at the scale 1:250 000. Since the geological maps were subsequently published at the scale 1:400 000 (Stephens et al. 2007a, b, c), some simplification of the database for the bedrock map (Stephens et al. 2007a) had to be completed prior to publication. Thus, it is important to keep in mind that the underlying database for this product is even more detailed than the printed map. The areas covered solely by maps at the scale 1:250 000 and 1:200 000 were digitized directly at this scale.

All rock units on the bedrock map (Stephens et al. 2007a) are defined on the basis of the dominant rock type (or types) inside each unit. A simplified version of this map is shown in Figure 19. The confidence in the definition of rock units naturally depends on several factors, not least the quality of the background material and the grade of subsequent metamorphism as shown in the metamorphic, structural and isotope age map (Stephens et al. 2007b and Fig. 20). Some necessary modifications to the base geological material were carried out during the compilation work with these maps. These modifications honoured the distribution of outcrops on the printed maps, took account of relevant new field data assembled during the Bergslagen project and the internal research and development project at SGU entitled "Kinematics and timing of major deformation zones, south-central Sweden" (SGU project 5082), and also made use of the information supplied by the interpretations of the airborne geophysical and topographic data described above.

There is a tendency for the occurrence of metasedimentary rocks to be somewhat over-represented on the base geological maps. The extent of this problem is not known but should not be over-exaggerated; examples of metasedimentary rocks with preserved primary structures are common in several parts of the Bergslagen region. Field studies within the project indicated that some mica-rich felsic volcanic rocks, which have been affected by both hydrothermal alteration and later metamorphic processes, and even reworked, felsic metavolcanic rocks have both been interpreted as metasedimentary rocks on some of SGU's published bedrock maps at the scale 1:50 000. This problem is especially conspicuous in the Falun (Stephens et al. 1999) and Kungsör-Köping-Kolsva (Stephens et al. 2000) areas and has motivated significant changes in the geological interpretation in the Bergslagen bedrock geological map described here (Stephens et al 2007a). Furthermore, some mica-rich meta-igneous rocks affected by strong ductile strain have been mapped as metasedimentary rocks.

Field studies in some of the areas affected by migmatization (e.g. around Eskilstuna, north-east of Falun) highlighted the difficulties to define the character of the palaeosome in such high-grade rocks. For example, there are problems in the SGU bedrock mapping work at local model scale concerning the distinction between strongly altered para- and orthogneisses in the area affected by migmatization north-east of Falun (see Stephens et al. 2001). Some changes have been carried out in the Bergslagen bedrock geological map presented here (Stephens et al. 2007a). However, where new information that motivates a reinterpretation is lacking or is restricted in extent, the original classification has been retained in the compilation of the Bergslagen bedrock geological map. Furthermore, the use of metamorphic rock terms where the protolith is not specified was motivated in some areas (see, for example, legend to the bedrock map in Stephens et al. 2007a). Hopefully, more detailed work in future mapping work, for example around Eskilstuna, will improve this situation.

In general, there is a poor documentation of broader belts and narrower zones of high ductile strain on the base geological maps. Some attempt has been made to rectify this deficiency in the present compilation work (see section "Deformation, metamorphism and mechanism of emplacement of the 1.87–1.84 Ga GSDG suite of intrusive rocks"), but much more detailed work needs to be carried out. For this reason, it should be kept in mind that several structures of this type are almost certainly not represented on the bedrock geological maps produced here.

The mineral resources map (Stephens et al. 2007c) contains an inset map that shows a 2-D model for the spatial distribution of different types of hydrothermal alteration in the Bergslagen region, i.e. sodium alteration, potassium alteration, "magnesium alteration" and "skarn alteration" (see section "Character, spatial distribution, geochronology, geochemical signature, petrophysical characteristics and regional geophysical

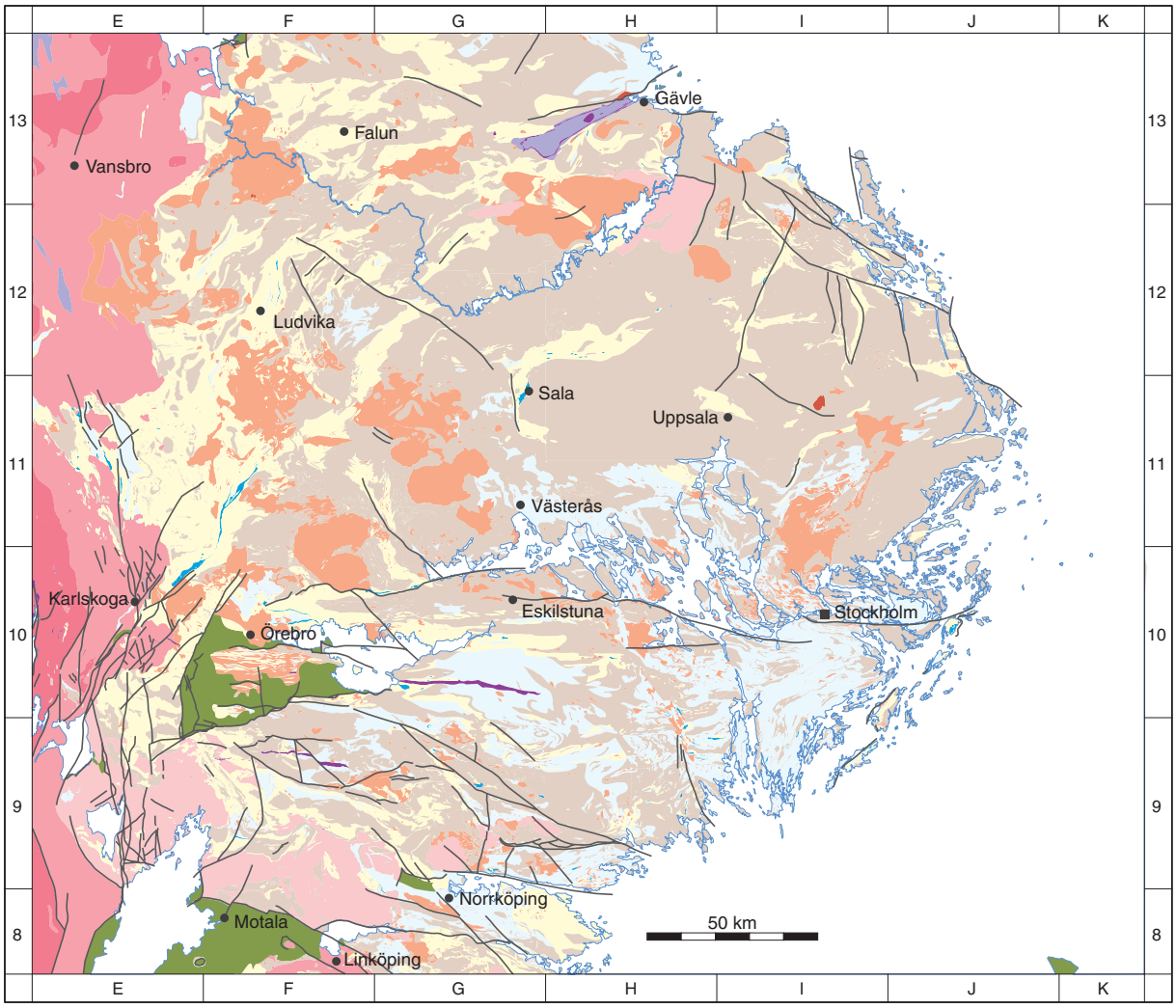

Fault, ductile shear zone

Neoproterozoic and Lower Palaeozoic sedimentary rocks

Granite, quartz syenite (Mesoproterozoic), alkaline intrusive rock of uncertain age

Dolerite (Mesoproterozoic)

Clastic sedimentary rock (Mesoproterozoic)

GSDG intrusive or meta-intrusive rock suite and associated supracrustal rock (1.70–1.67 Ga)

GP intrusive rock suite (1.85–1.75 Ga)

GSDG intrusive or meta-intrusive rock suite and associated supracrustal rock (1.81–1.78 Ga)

GSDG and subordinate GDG intrusive or meta-intrusive rock suites (1.87–1.84 Ga)

GDG and subordinate GSDG meta-intrusive rock suites (1.90–1.87 Ga), undifferentiated gneiss

Svecofennian metavolcanic and subvolcanic meta-intrusive rocks (1.91–1.89 Ga), granofels of uncertain origin

Crystalline carbonate rock

Svecofennian clastic metasedimentary rock

GDG = Granitoid–dioritoid–gabbroid
GSDG = Granite–syenitoid–dioritoid–gabbroid
GP = Granite–pegmatite

Fig. 19. Simplified bedrock geological map of the Bergslagen region. For purposes of clarity, the different types of deformation zone (fault, ductile shear zone) have not been distinguished and lineaments have not been shown on the map. In addition, only the thicker dykes or sills, which are Mesoproterozoic in age, are shown. Neoproterozoic dykes have not been displayed. Compare Figure 18 where the different rock units shown on the map are distinguished on the basis of their tectonic status.

signature of rock units"). Both alteration type and specific alteration minerals are specified in the legend to this map. The compilation of this map was based on the following sources:

- Bedrock geological maps belonging to SGU's Af and Ai series. The more modern maps show different types of alteration according to the principles adopted here and, thereby, could be used directly. However, in other maps, indications of, for example, "magnesium alteration" have been inferred from map symbols that denote the occurrence of, for example, cordierite or anthophyllite, particularly if marked on metavolcanic rocks. In addition, information on so-called "skarn alteration" is predominantly derived directly from the maps.

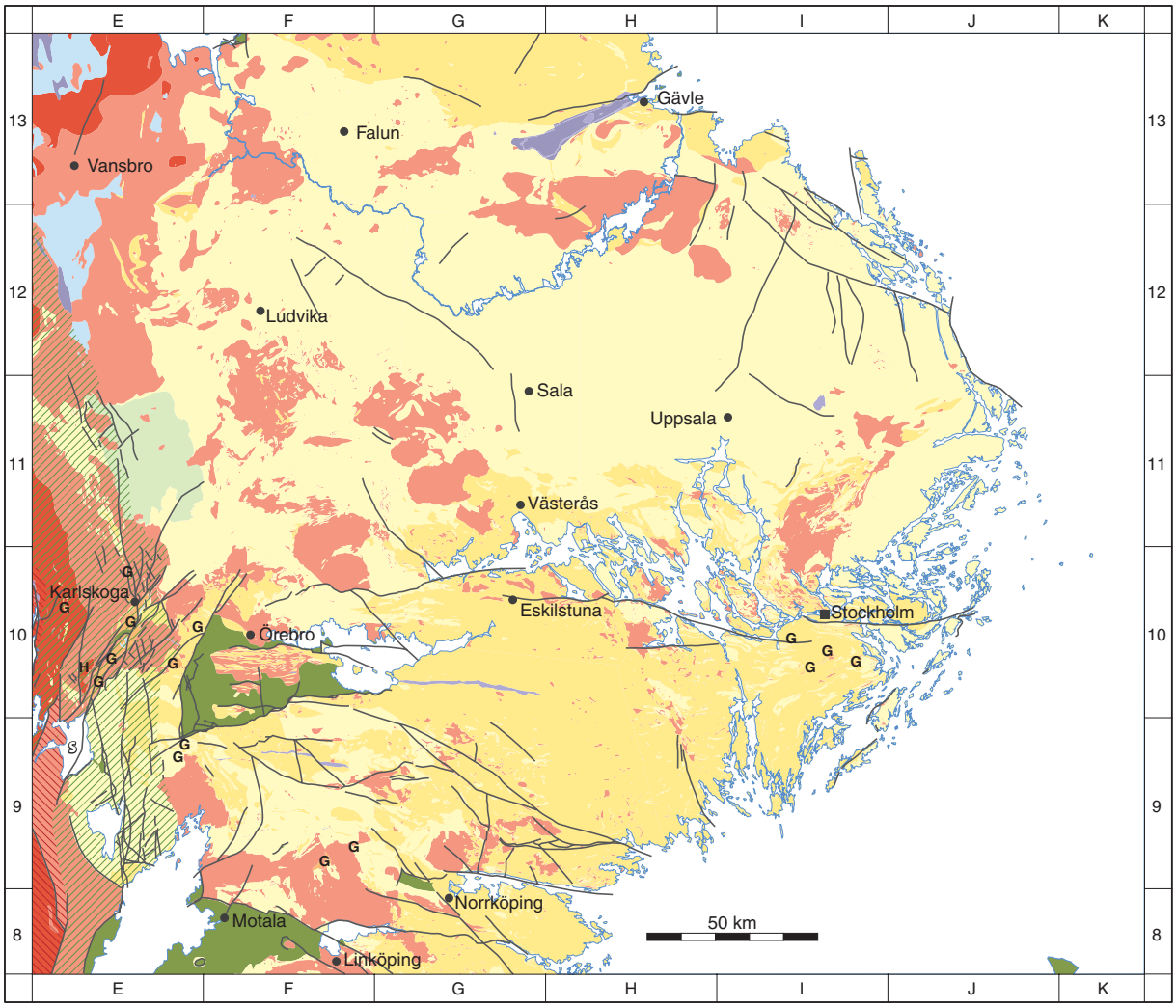

Fault, ductile shear zone

Neoproterozoic and Lower Palaeozoic sedimentary rocks (non-metamorphic)

Sveconorwegian tectonic overprint (1.0–0.9 Ga)

Greenschist facies (non-penetrative deformation)

Amphibolite facies (penetrative deformation), amphibolite-facies metamorphism and deformation directly west and south-west of Skagern either Sveconorwegian or older

Post-Svecokarelian, Mesoproterozoic rocks and alkaline intrusive rock of uncertain age

Non-metamorphic or subgreenschist facies

Post-Svecokarelian, Palaeoproterozoic (1.7 Ga) rocks and associated contact metamorphism (1.7 Ga)

Post-Svecokarelian, 1.70–1.67 Ga GSDG intrusive rock suite and associated supracrustal rocks (non-metamorphic or subgreenschist facies)

H — Contact metamorphism, granulite facies

Svecokarelian metamorphism (1.9–1.8 Ga) which affects, to variable extent, Palaeoproterozoic (1.9–1.8 Ga) rocks

Non-metamorphic, subgreenschist facies or greenschist facies

Greenschist facies

Amphibolite facies

Amphibolite facies, migmatitic

G — Granulite facies, partly migmatitic

Fig. 20. Metamorphic map of the Bergslagen region. For purposes of clarity, the different types of deformation zone (fault, ductile shear zone) have not been distinguished and lineaments have not been shown on the map. In addition, only the thicker dykes or sills, which are Mesoproterozoic in age, are shown. Neoproterozoic dykes have not been displayed. S = Skagern.

- Map descriptions that are only available for SGU's Af series. The written text, geochemical and modal analyses, illustrations and various diagrams were scrutinized for information.
- Literature sources including Magnusson (1936), Lundqvist & Hjelmqvist (1937), Hjelmqvist (1943), Hjelmqvist & Lundqvist (1953) and Lagerblad et al. (1987).
- Field notes from the Bergslagen and earlier projects.
- Bedrock geochemical analyses completed within the Bergslagen project.
- Radiometric maps inferred from airborne data,

which show anomalies in the distribution of potassium in the bedrock, have helped to delineate areas affected by potassium alteration.

The presentation of the different types of alteration in the hydrothermal alteration map was completed, as far as possible, according to the following guidelines. The symbols for sodium or potassium alteration were used for rocks that have or could be suspected to have compositions falling outside the igneous spectrum of Hughes (1973). They were also used for rocks loosely denoted "sodic" or "potassic" in older literature. The symbol for "magnesium alteration" was used primarily for feldspar-poor, magnesium-, iron- or silicon-enriched, alkali-poor but relatively potassium-enriched rocks, and preferably in rocks with transitional relations to recognizable metavolcanic rocks. The symbol for "skarn alteration" was used for areas with calc-silicate blastesis. In addition to larger areas, small isolated occurrences are shown with dots with the same colour.

It is important to keep in mind that hydrothermal alteration was generally not recognized in the Bergslagen region until the beginning of the 1980's. For this reason, it has not been possible to show all areas that are affected by hydrothermal alteration on the map. Furthermore, the distribution of different types of hydrothermal alteration on the alteration map (Stephens et al. 2007c) is uncertain, and should be understood to mean that indications of alteration exist but are not necessarily verified.

AGE DETERMINATIONS USING U-Pb TIMS ANALYSES OF ZIRCON, MONAZITE AND TITANITE

New U-Pb (zircon, monazite and titanite) age determinations were carried out on 11 samples in the Bergslagen region in the context of the present study (Fig. 14). A description of the analysed samples and the results of the analyses are presented in the appendix to this report. The broader geological implications of all the geochronological data are presented in the relevant parts of the sections entitled "Character, spatial distribution, geochronology, geochemical signature, petrophysical characteristics and regional geophysical signature of rock units", and "Deformation, metamorphism and mechanism of emplacement of the 1.87–1.84 Ga GSDG suite of intrusive rocks". Protolith ages are shown on the metamorphic, structural and isotope age map (Stephens et al. 2007b). The text here addresses the procedures used in the analytical work.

Zircons were separated using standard magnetic and heavy liquid techniques. Most fractions were abraded, according to the method described in Krogh (1982), and they were dissolved in HF:HNO_3 in Teflon® capsules in autoclaves, according to the method described in Krogh (1973). After decomposition, a mixed ^{205}Pb-$^{233–236}$U tracer was added. The spiked samples were then dissolved in 3.1 N HCl and loaded onto anion exchange columns with 50 µl resin volume for extraction of Pb and U. Pb was loaded on Re single filaments with silica gel and H_3PO_4. U was loaded on Re double filaments with HNO_3. For the most recently analysed samples, U and Pb were loaded together on single Re filaments with silica gel and H_3PO_4.

The isotopic ratios were measured on a Finnigan MAT 261 mass spectrometer equipped with five faraday cups. Most samples were measured in the static mode on these cups. Small Pb and U amounts, yielding low signals, were measured in peak jumping mode on a secondary electron multiplier. The calculation of the corrected isotope ratios and the uncertainty propagation were made using the PBDAT programme of Ludwig (1991a), and the decay constants recommended by Steiger & Jäger (1977) were used. Calculation of the intercept ages and the drawing of the concordia plot were carried out using the ISOPLOT programme of Ludwig (1991b). The total Pb blank was 2–4 pg and the U blank less than 1 pg. The assigned composition of common Pb is calculated according to the Pb evolution model of Stacey & Kramers (1975). The mass fractionation for Pb is 0.10±0.04% per atomic mass unit. U mass fractionation was monitored and corrected for by means of the $^{233–236}$U ratio of the spike. All analytical uncertainties are given as 2σ.

Monazite was analysed in the same manner as zircon with the exception of being decomposed in 6N HCl. Titanite was analysed in the same manner as zircon, apart from the ion exchange procedure, where a HBr step was added for better purification of lead and a second HCl-HNO_3 cycle was added for purification of uranium.

GEOCHEMICAL ANALYSES

Complementary sampling of different rock types for geochemical analysis has been completed during the Bergslagen project and 111 new analyses have been carried out (Fig. 15). All these analyses contain a SGU identification code that permits a link between the geochemical analysis and a corresponding age determination (e.g. BERGDB_ALDR) or outcrop observation (e.g. BERGDB_HALL) in SGU's database system, where this exists. The new samples were analysed at SGAB Luleå during 1999 and 2000 using the ICP-AES and ICP-MS/QMS analytical techniques.

All samples have been classified with confidence in the different igneous rock suites used in this report (see

nomenclatural considerations presented earlier). The majority of samples have been taken from the Svecofennian, felsic volcanic and subvolcanic intrusive rocks (1.91–1.89 Ga), whereas the mafic and intermediate rocks in this rock suite are less well represented. Standard geochemical classification and discrimination diagrams have been employed to evaluate all the bedrock geochemical data and the results of this evaluation are provided in the relevant parts of the section "Character, spatial distribution, geochronology, geochemical signature, petrophysical characteristics and regional geophysical signature of rock units".

PETROPHYSICAL ANALYSES

The main objective of the geophysical field activities was to collect petrophysical and gamma radiation data from different rock units, in order to radically update the compilation of petrophysical data within the Bergslagen region. The work focussed on areas where petrophysical data were absent or very sparse. In total, 628 sites were measured during the geophysical field activities (Fig. 16). The field work was completed between 1998 and 2000.

The geophysical field activities included gamma radiation measurements and magnetic susceptibility measurements on outcrops. Gamma radiation measurements include total radiation measurements as well as values for potassium (^{40}K), uranium (^{238}U) and thorium (^{232}Th). Furthermore, a bedrock sample was collected from every site for additional measurements in the petrophysical laboratory at SGU.

All samples have been classified with confidence in the different units identified in this report (see also nomenclatural considerations presented earlier). Furthermore, standard petrophysical diagrams have been used to evaluate all the petrophysical data and the results of this evaluation are provided in the relevant parts of the section "Character, spatial distribution, geochronology, geochemical signature, petrophysical characteristics and regional geophysical signature of rock units".

DOCUMENTATION OF MINERAL AND BEDROCK RESOURCES

A radical update of SGU's mineral and bedrock resources database in the Bergslagen region was completed during the Bergslagen project. Data were extracted from SGU's published geological maps and descriptions (see Table 1), published papers and unpublished exploration reports. In particular, the important monographs presented by Tegengren et al. (1924) and Geijer & Magnusson (1944) as well as the reports written in connection with exploration by SGU prior to 1982 and by the state exploration company Swedish Geological AB, between 1982 and 1992, deserve particular attention. The reports produced in connection with exploration work carried out by the Swedish state are archived at SGU's office in Malå, Sweden, and are open for public scrutiny.

After consultation with several exploration companies, the following seven attributes were extracted from the literature and included in the database: Name of deposit, coordinates at the ground surface in the Swedish national grid (RT 90) with an uncertainty of ±50 m, type of deposit (e.g. sulphide deposit), commodity (e.g. Fe, Zn, Pb), economic status, host-rock and reference to source literature. The attributes of approximately 6 550 deposits in the Bergslagen region were compiled in the mineral and bedrock resources database during the Bergslagen project. It is important to emphasize that the contents of this database are continuously under revision as more information is acquired.

The locations of deposits that were present in the resources database during 2004 are shown in the overview map in Figure 21. Each deposit has been classified on the main mineral resources map (Stephens et al. 2007c) according to type of deposit (see section "Mineral and bedrock deposits"). Some attributes of the larger deposits are listed in tabular format on this map and the distribution of these larger deposits in the Bergslagen region is shown on an inset map. The larger deposits are also displayed on the bedrock and metamorphic, structural and isotope age maps (Stephens et al. 2007a, b). Only these deposits have been classified according to size. This attribute refers to either estimated million tonnes of produced ore or estimated million tonnes of potential ore resources. Size estimates have been extracted from Åkerman (1994) or from production statistics provided by the Swedish mining industry up to 2004.

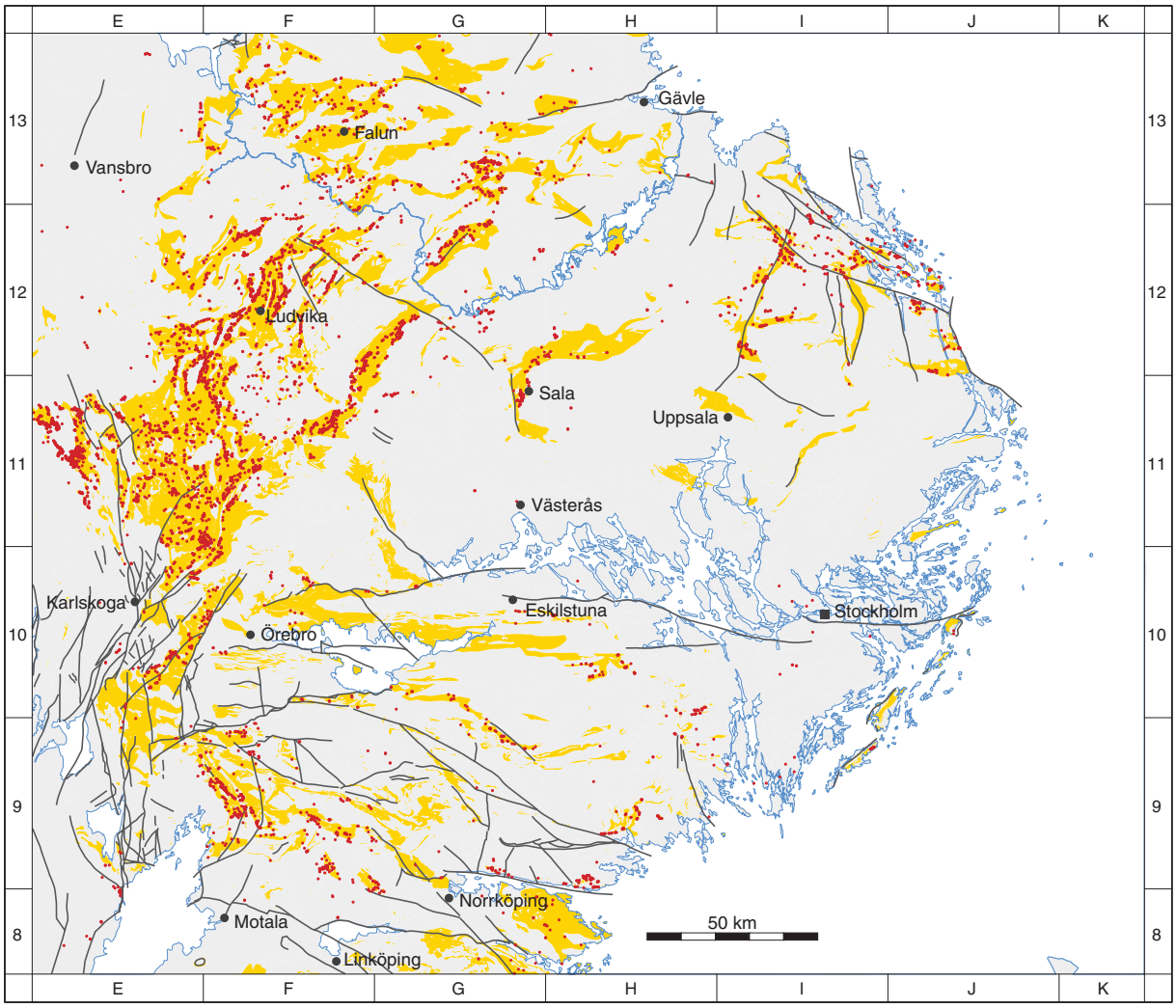

Fault, ductile shear zone

Metallic mineral deposit

Svecofennian metavolcanic and subvolcanic meta-intrusive rocks (1.91–1.89 Ga)

Fig. 21. Distribution of metallic mineral deposits and their close spatial relationship to Svecofennian, metavolcanic and subvolcanic meta-intrusive rocks (1.91–1.89 Ga) in the Bergslagen region. The metallic mineral deposits included in the mineral and bedrock resources database during 2004 are shown on the map.

Character, spatial distribution, geochronology, geochemical signature, petrophysical characteristics and regional geophysical signature of rock units

OVERVIEW OF CONTENT

This section provides a description of the different rock types and their spatial distribution as mappable rock units in the Bergslagen region as shown on the bedrock map (Stephens et al. 2007a). The structure of the legend to this map differs slightly from that adopted in the description here. Furthermore, the age range of two rock units shown in the legend to the bedrock (Stephens et al. 2007a) and mineral resources (Stephens et al. 2007c) maps is different from that used here.

The bedrock in the Bergslagen region is divided and described separately in three major tectonic complexes (see, for example, Fig. 4):

- Palaeoproterozoic rocks that are variably affected by Svecokarelian deformation and metamorphism, i.e. form a part of the Svecokarelian orogen in the Fennoscandian Shield. These rocks are also affected in part by Sveconorwegian deformation and metamorphism in western areas.
- Post-Svecokarelian rocks in the Fennoscandian Shield. These rocks are affected in part by Sveconorwegian deformation and metamorphism in western areas.
- Neoproterozoic and Lower Palaeozoic sedimentary cover rocks.

On the basis of new geochronological data that have emerged following compilation of the geological maps, the highly subordinate unit that is referred to as "alkaline intrusive rock of uncertain age" is also presented separately. Other differences between the legend to the bedrock map and the description here are summarized in the following eight bullets:

- The supracrustal rocks referred to as "granofels of uncertain origin" and shown on the map are not addressed in the following text. However, they are discussed briefly in the section "Metamorphism".
- The rocks referred to as "gneissic rocks, undifferentiated" and shown on the map are only addressed briefly in the following text together with the GDG intrusive rocks.
- The prefix "c." before the range in age of a rock unit has been omitted. The uncertainty in the age of each rock unit is discussed in the appropriate section below.
- On the basis of new geochronological data that have emerged following compilation of the geological maps, the range in age of the younger GDG suite of intrusive rocks is modified from c. 1.85 Ga to 1.87–1.85 Ga.
- The subordinate suite of younger, 1.87–1.85 Ga GDG intrusive rocks is described here together with the dominant suite of older, 1.90–1.87 Ga GDG intrusive rocks.
- Metadolerite, which commonly occurs as amphibolite and does not form a separate rock unit on the bedrock map, is described in a separate section in the following text.
- The range in age of one of the GSDG suites of intrusive rocks is modified from c. 1.81–1.76 Ga to 1.81–1.78 Ga. In accordance with the methodology adopted here (see section "Database for radiometric age determinations"), an unpublished age of 1763±2 Ma has not been included in the range used here.
- Volcanic, subvolcanic and sedimentary rocks that are spatially and temporally associated with the 1.81–1.78 Ga and 1.70–1.67 Ga suites of GSDG intrusive rocks are described in separate sections in the following text.

A detailed description of the age of crystallization, geochemical signature, petrophysical characteristics and regional geophysical signature of the Palaeoproterozoic igneous rocks included in the Svecokarelian orogen is provided. These attributes are addressed in the same manner for each rock unit in this part of the Bergslagen region. Furthermore, special attention is focussed on the physical volcanology, depositional environment and hydrothermal alteration of the Svecofennian volcanic and subvolcanic intrusive rocks (1.91–1.89 Ga), the intrusion–deformation relationships shown in the field by the different suites of intrusive rocks, gravity modelling work to constrain the 3-D shape of intrusive bodies, and a compilation and evaluation of Sm-Nd analyses of different rock suites. The character of the post-Svecokarelian rocks, the Neoproterozoic and Lower Palaeozoic sedimentary cover rocks and the rock unit consisting of alkaline intrusive rocks, all of which are spatially more subordinate in character, is described more briefly.

Place names referred to in the text that describes each rock suite or suites in the Bergslagen region are located in the respective figure that shows the distribution of the rock suite(s) at the ground surface in this region.

PALAEOPROTEROZOIC ROCKS VARIABLY AFFECTED BY SVECOKARELIAN DEFORMATION AND METAMORPHISM AND PARTLY AFFECTED BY SVECONORWEGIAN DEFORMATION AND METAMORPHISM

Svecofennian sedimentary rocks

Rock type and spatial distribution

Palaeoproterozoic metasedimentary rocks, including metagreywacke, meta-argillite, quartzite, feldspathic metasandstone, meta-arkose and crystalline carbonate rock (marble), form an important bedrock component in the Bergslagen region (Fig. 22). They comprise both well-preserved as well as strongly altered, migmatitic varieties. These rocks belong to the Svecofennian supracrustal sequence in the western part of the Fennoscandian Shield.

Metagreywacke

Metagreywacke that commonly displays well-developed bedding with alternating argillitic and sandy layers of varying thickness form the volumetrically most significant metasedimentary rock in the project area. In the main area of occurrence, from Norrköping in

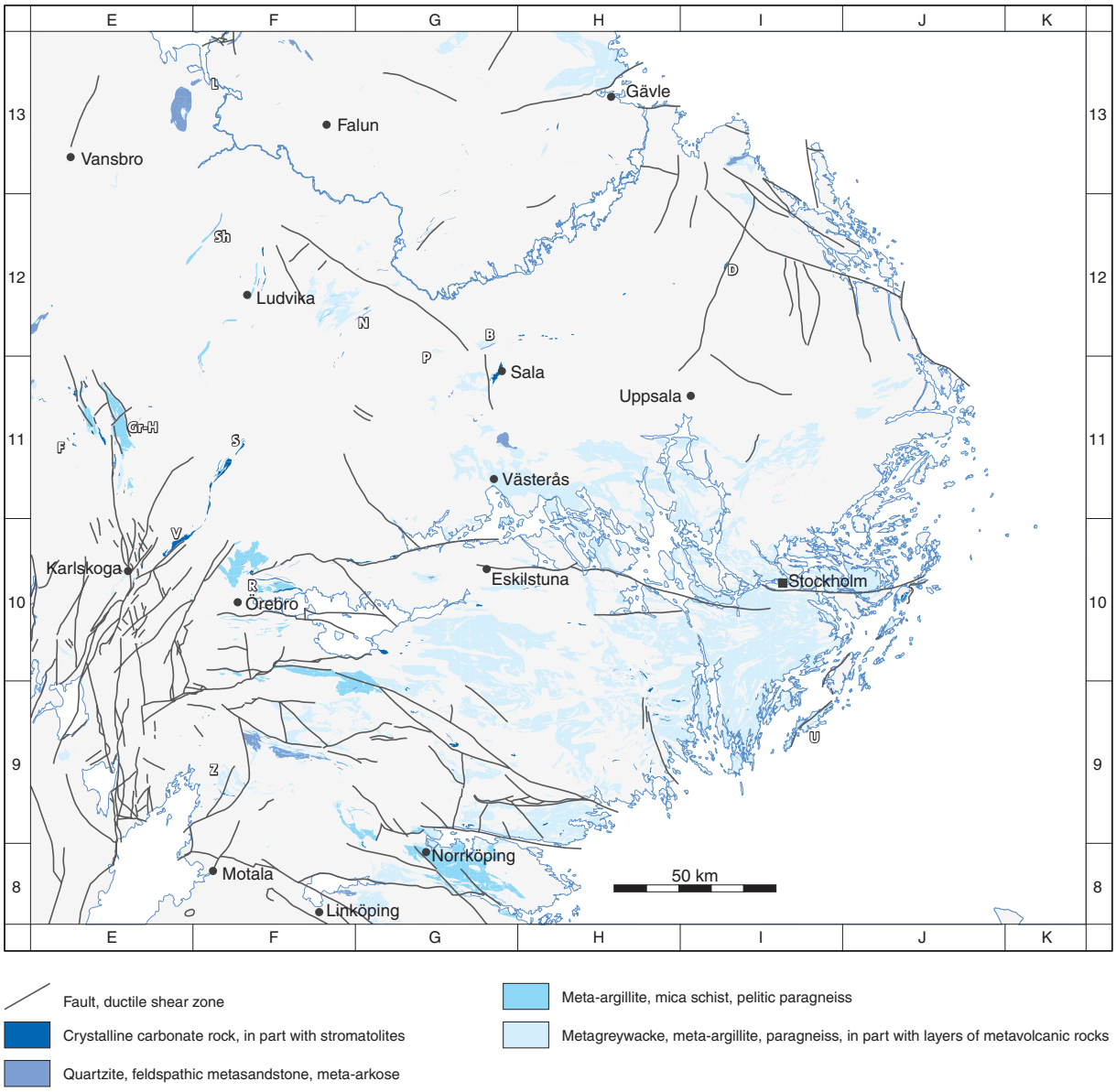

Fig. 22. Distribution of Svecofennian sedimentary rocks at the ground surface in the Bergslagen region. The location of place names referred to in the section "Svecofennian sedimentary rocks" is also shown on the map. B = Broddbo, D = Dannemora, F = Filipstad, Gr–H = Grythyttan–Hällefors, L = Leksand, N = Norberg, P = Prästhyttan, R = Rinkaby–Glanshammar, Sh = Saxhyttan, S = Stråssa, U = Utö, V = Vikern, Z = Zinkgruvan.

the south to the Västerås and Stockholm areas in the north (Fig. 22), the metagreywackes are usually altered to migmatitic paragneisses (Fig. 23a). However, despite the strong metamorphic alteration in this area, the bedding in these rocks is, at least locally, still recognizable, since the sandy layers are not as responsive to veining and migmatization as the argillitic layers. Use of sedimentary rock rather than metamorphic rock terminology is motivated in these instances. In the northernmost part of the project area, north-east of Falun and north of Gävle, migmatitic metagreywacke also constitutes an important bedrock component. The migmatitic paragneisses south of Zinkgruvan, in the *Vintergölen formation*, are inferred to be turbiditic in origin (Kumpulainen et al. 1996).

Metagreywacke comparable to that described above, but affected by metamorphism under lower amphibolite-facies conditions, constitutes a significant bedrock component in the area east of Ludvika, in the central part of the study area (Fig. 22). These rocks are traditionally referred to as the *Larsbo series* (Hjelmqvist 1938) or *Larsbo formation* (Strömberg & Nisca 1983). The occurrence of graded bedding (Fig. 23b) suggests that these rocks were also deposited as turbidites. Minor occurrences of metagreywacke of similar character are also present in, for example, the areas around

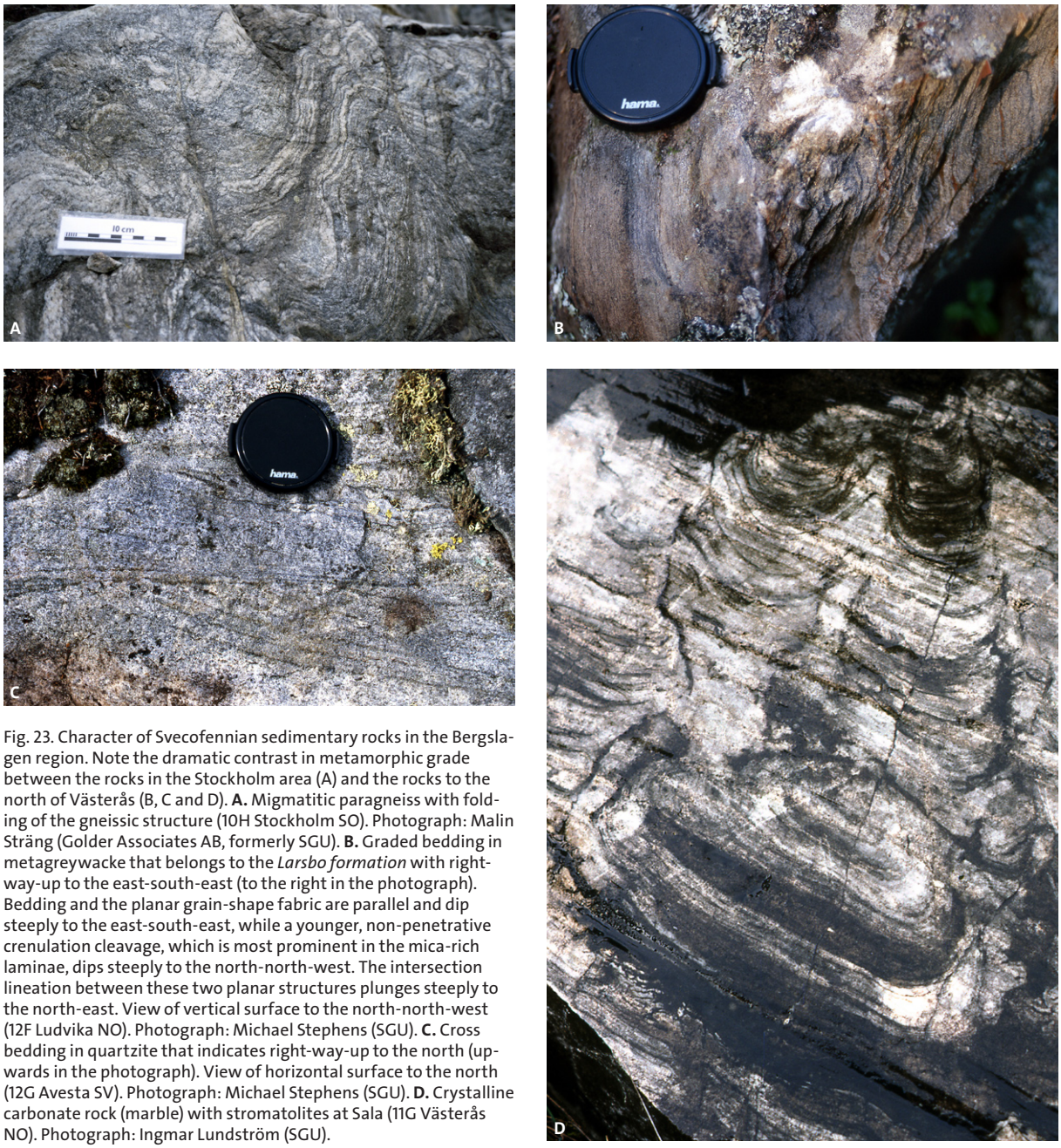

Fig. 23. Character of Svecofennian sedimentary rocks in the Bergslagen region. Note the dramatic contrast in metamorphic grade between the rocks in the Stockholm area (A) and the rocks to the north of Västerås (B, C and D). **A.** Migmatitic paragneiss with folding of the gneissic structure (10H Stockholm SO). Photograph: Malin Sträng (Golder Associates AB, formerly SGU). **B.** Graded bedding in metagreywacke that belongs to the *Larsbo formation* with right-way-up to the east-south-east (to the right in the photograph). Bedding and the planar grain-shape fabric are parallel and dip steeply to the east-south-east, while a younger, non-penetrative crenulation cleavage, which is most prominent in the mica-rich laminae, dips steeply to the north-north-west. The intersection lineation between these two planar structures plunges steeply to the north-east. View of vertical surface to the north-north-west (12F Ludvika NO). Photograph: Michael Stephens (SGU). **C.** Cross bedding in quartzite that indicates right-way-up to the north (upwards in the photograph). View of horizontal surface to the north (12G Avesta SV). Photograph: Michael Stephens (SGU). **D.** Crystalline carbonate rock (marble) with stromatolites at Sala (11G Västerås NO). Photograph: Ingmar Lundström (SGU).

Broddbo-Prästhyttan, in the vicinity of Sala. Locally, metavolcanic rocks are intercalated in the metagreywackes. The turbiditic metagreywackes included in the *Larsbo formation* are of fundamental importance concerning regional stratigraphical correlations (see below), and possibly represent better preserved varieties of the strongly metamorphosed, migmatitic paragneisses described above.

Meta-argillite

In westernmost Bergslagen, between Filipstad and Ludvika (Fig. 22), meta-argillite, including graphite-bearing black slate, occurs in the area close to Grythyttan and Hällefors, where the rocks are affected by greenschist-facies metamorphism, and further west, where the rocks are affected by amphibolite-facies metamorphism. Except for minor intercalations of metaconglomerate, these areas exemplify occurrences of homogeneous meta-argillite. However, a larger coherent occurrence of metaconglomerate, the *Älvestorp conglomerate*, occurs immediately south of the meta-argillite in the Grythyttan–Hällefors area (Lundström 1995). Meta-argillite, metamorphosed under amphibolite-facies conditions, is also present close to the lake Glan, north-west of Norrköping, as well as in several areas between Örebro and Ludvika (Fig. 22). Migmatitic meta-argillite also constitutes an important bedrock component close to Norrköping, (Fig. 22).

Quartzite, feldspathic metasandstone, meta-arkose

In contrast to the metagreywackes, these more well-sorted sedimentary rocks form a subordinate bedrock component in the Bergslagen region (Fig. 22). The occurrence of cross bedding (Fig. 23c) indicates deposition under relatively shallow water conditions above the wave base.

The two most extensive occurrences are in the *Leksand formation* (Kresten & Aaro 1987a), in the north-western part of the Bergslagen region, and in the *Gryt formation* (Wikström & Karis 1991), also named *Närkesberg formation* (Kumpulainen et al. 1996), east of Zinkgruvan, in the south-western part of the region. The *Leksand formation* consists of quartzite and metaconglomerate with minor intercalations of micaceous quartzite and muscovite schist. Possible equivalents have also been recognized in the area north of Saxhyttan. The *Gryt (Närkesberg) formation* is dominated by meta-arkose, but quartzite and meta-argillite as well as minor units of metaconglomerate and sedimentary metabreccia occur at lower stratigraphic levels. Feldspathic metasandstone and quartzite are present in the Norberg and Broddbo–Prästhyttan areas as well as between Västerås and Sala, where a spatial association with metagreywacke, similar to that observed in the *Larsbo formation*, has been documented (Stephens et al. 2001). North-east of Falun, quartzite in the *Ärtknubben formation* (Kresten & Aaro 1987b) is also spatially associated with metagreywacke.

Crystalline carbonate rock

Calcite- or dolomite-rich, crystalline carbonate rock and calc-silicate rock (skarn) are present throughout the Bergslagen region as scattered, usually minor occurrences (Fig. 22). They are spatially associated and intercalated with felsic metavolcanic rocks as well as iron oxide mineral deposits in what is inferred to be the stratigraphic upper part of the volcanic succession (see later text). According to Allen et al. (1996), the crystalline carbonate rocks include both hydrothermal exhalites and marine precipitates. In many of these carbonate rocks, bedding-parallel stylolites are the only occurring primary structure, but locally, for example at Dannemora (north-east of Uppsala), Sala and Hällefors, stromatolites are present indicating an organogenic origin (Fig. 23d, Allen et al. 1996 and references therein, Lager 2001, Allen et al. 2003). The most continuous occurrence of carbonate rock in the Bergslagen region extends for c. 44 km from Vikern north-east of Karlskoga north-eastwards to Stråssa (Fig. 22).

Stratigraphic position and age constraints

The occurrence of primary structures, including graded bedding and cross bedding, permits the establishment of way-up determinations. On the basis of these field data, the stratigraphic position of the metasedimentary rocks is, at least locally, possible to determine. However, regional correlations are highly uncertain, due to the large volume of intrusive rocks that have disrupted the original supracrustal succession. Based on spatial relationships and lithological similarities, only some tentative regional correlations are presented below. Metasedimentary rocks that lie stratigraphically both beneath and above the Svecofennian volcanic and subvolcanic intrusive rocks (1.91–1.89 Ga) are inferred to be present in the Bergslagen region (Fig. 24).

Metasedimentary rocks older than the metavolcanic rocks

On the island of Utö, in the southern part of the Stockholm archipelago, volcanogenic metagreywackes deposited as turbidites lie stratigraphically beneath quartzite that, in turn, is stratigraphically overlain by felsic metavolcanic rocks (Gavelin et al. 1976, Stålhös 1982a, Allen et al. 1996). Felsic metavolcanic rocks

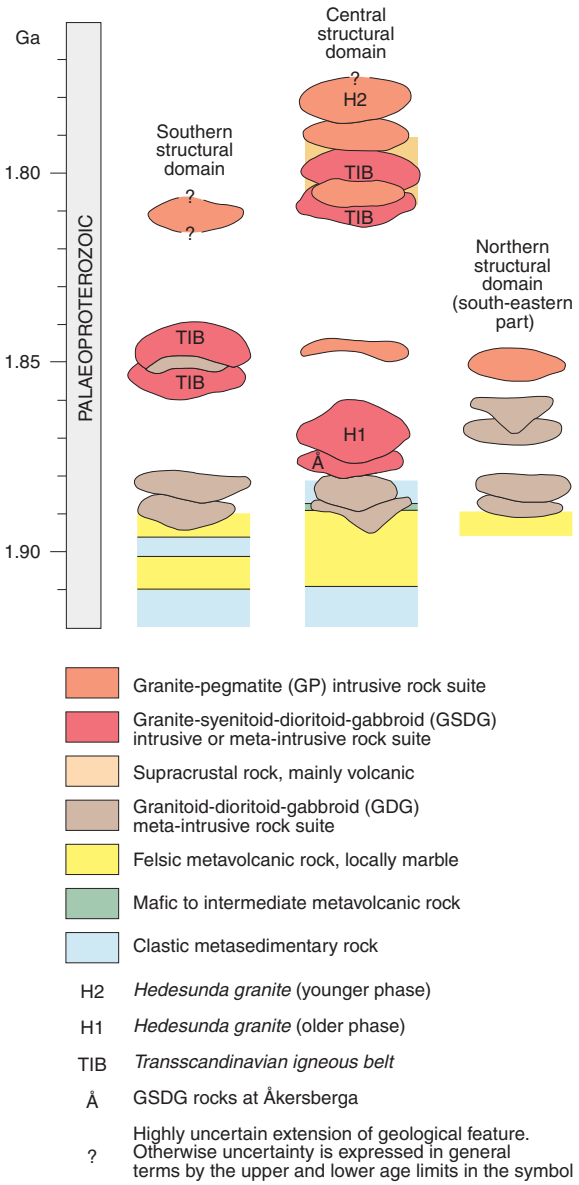

Fig. 24. Simplified sketch that shows a stratigraphic model for the time period 1.91–1.78 Ga in the Bergslagen region. The different structural domains are described later in the text.

also occur as intercalations in the metasedimentary succession. The succession has the overall character of a prograde, sandy sediment system (Allen et al. 1996). A major mylonite zone occurs along the north-western boundary of the metavolcanic succession. For this reason, the stratigraphic position of the metasedimentary rocks in the western part of Utö remains unclear (e.g. Allen et al. 1996). Turbiditic metagreywackes are also inferred to stratigraphically underlie felsic metavolcanic rocks in the northern part of the Stockholm archipelago (Lundqvist 1962).

Similar stratigraphic relationships between metasedimentary rocks with intercalations of meta-andesite and younger, felsic metavolcanic rocks have been recognized in the Norberg area (Ambros 1988). Furthermore, field investigations during the present study in, for example, the Broddbo–Prästhyttan area (Stephens et al. 2000) confirm that turbiditic metagreywackes (*Larsbo formation*) and quartzite lie stratigraphically beneath felsic metavolcanic rocks. The continuous exposure at Prästhyttan indicates a gradual transition from turbiditic metagreywacke (*Larsbo formation*) into stratigraphically younger impure quartzite. Once again a prograde, shallowing-upward character of the sedimentary succession beneath the felsic metavolcanic rocks, similar to that on Utö, is apparent.

Lithological similarities and a spatial relationship between metagreywacke and quartzite tentatively suggest that the migmatitic paragneisses and subordinate quartzites in the south-eastern and northern parts of the Bergslagen region also represent the basal part of the lithostratigraphy. Thus, it is suggested that the large areas of paragneiss in Södermanland and, for example, the *Ärtknubben quartzite*, which is exposed north-east of Falun, can be correlated with the *Larsbo formation* and its overlying quartz-rich rocks, respectively.

U-Pb dating of detrital zircons in a quartzite in the Norberg area, using the Secondary Ion Mass Spectrometry (SIMS) technique, has yielded a population of Palaeoproterozoic zircons in the age range 2.04 to 1.90 Ga as well as Archaean zircons in the age range 2.97 to 2.60 Ga (Claesson et al. 1993). Similar results were obtained by Andersson et al. (2006) using U-Pb SIMS data from detrital zircons in two samples of inferred metasedimentary rocks. Both studies indicate an apparent gap in detrital zircon ages between 2.45 and 2.1 Ga. These data indicate that the metasedimentary rocks were deposited after 1.90 Ga. U-Pb (zircon) ages in the range 1.91 to 1.90 Ga for metavolcanic rocks at Broddbo and Utö (see later text), which lie stratigraphically above metasedimentary rocks, indicate that the pre-volcanic metasedimentary rocks in these two areas were deposited prior to 1.90 Ga. Thus, it is inferred that the pre-volcanic metasedimentary rocks in the Bergslagen region were deposited close in time to the Svecofennian volcanic activity in the region, i.e. around 1.9 Ga (Fig. 24).

Metasedimentary rocks similar in age to or younger than the metavolcanic rocks

In contrast to the stratigraphic relationships described in the previous section, the well-sorted sandy rocks in the *Gryt (Närkesberg) formation* in the south-western part of the study area are both underlain and overlain by felsic metavolcanic rocks. Crystalline carbonate rocks are also intimately associated with felsic metavolcanic

rocks. In areas with more well-preserved bedrock, they can be shown to be interbedded with metamorphosed, volcaniclastic siltstone and sandstone, the so-called ash-siltstone unit of Allen et al. (1996), high up in the volcanic succession (see later text).

Whereas the metasedimentary rocks that underlie the metavolcanic rocks in the Bergslagen region are dominated by turbiditic metagreywackes, the metasedimentary rocks that overlie the metavolcanic rocks, and, thus, constitute the upper part of the Svecofennian stratigraphy (Fig. 24), are dominated by meta-argillite in the Grythyttan–Hällefors area, between Filipstad and Ludvika, and in the Rinkaby–Glanshammar area, north of Örebro. These rocks are located at approximately the same stratigraphic level as the quartzites and metaconglomerates in the *Leksand formation*, in the north-western part of the region, and the turbiditic rocks in the *Vintergölen formation* south of Zinkgruvan. It is apparent that well-sorted metasandstones in the Bergslagen region do not represent one and the same stratigraphic level.

Sundius (1923) suggested that the *Älvestorp conglomerate* in the Grythyttan–Hällefors area lies unconformably above both the metavolcanic and meta-argillitic rocks. However, since there is some interfingering between meta-argillite and conglomerate, Lundström (1995) inferred that these rocks are similar in age and that the locally discordant relationships are tectonic in character.

Petrophysical characteristics and regional geophysical signature

The localities where data bearing on the petrophysical properties of Svecofennian sedimentary rocks have been acquired and used in this report are shown in Figure 25. Samples from 248 localities have been analysed in the laboratory, whereas in situ gamma radiation measure-

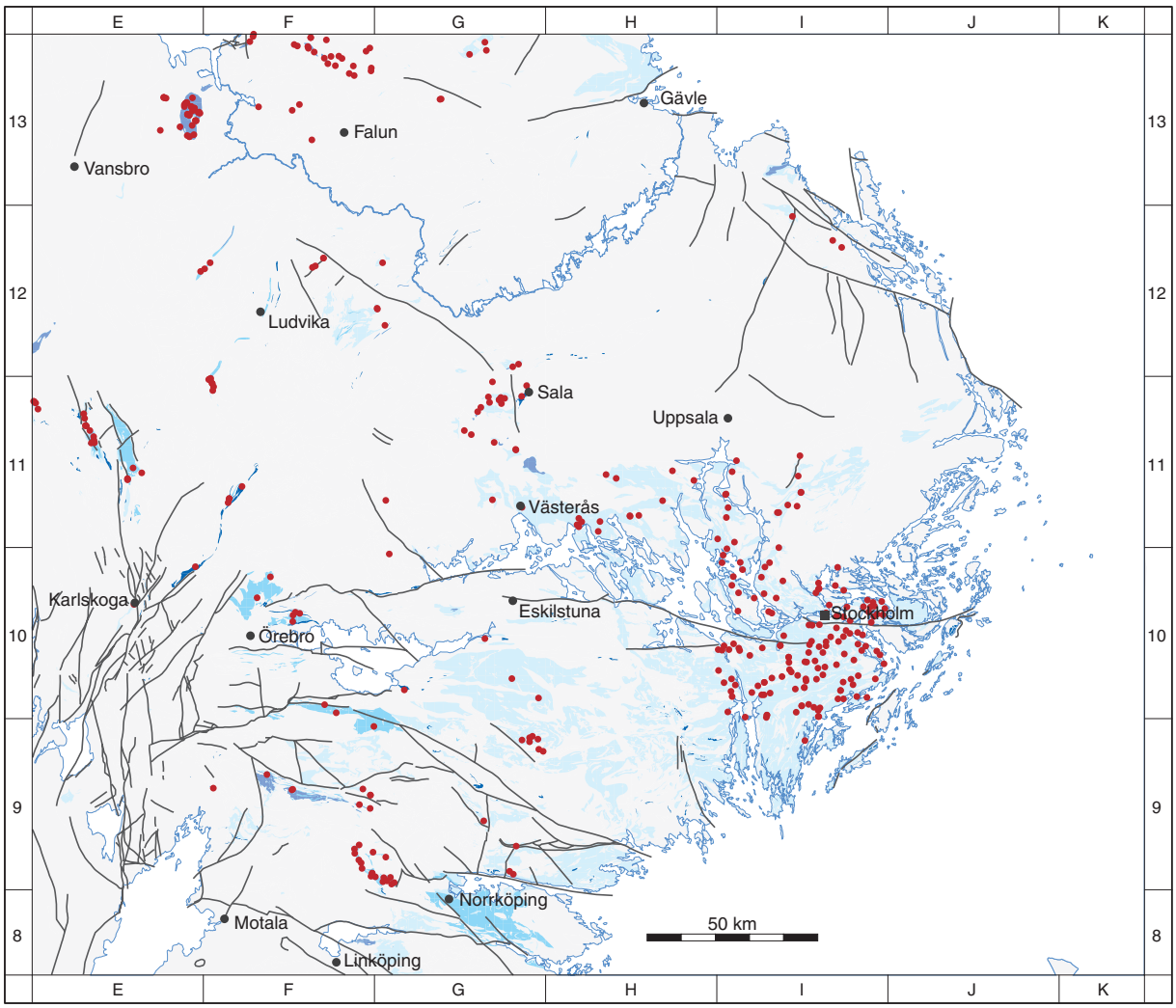

Fig. 25. Location of sample sites of Svecofennian sedimentary rocks in the Bergslagen region for petrophysical and gamma radiation measurements (red dots). See Figure 22 for legend to the base geological map.

ments have been carried out at 186 sites. All these data, both those generated prior to and those generated in connection with the Bergslagen project, have been extracted from SGU's petrophysical database.

Density

The density distribution for the Svecofennian sedimentary rocks compared with all rocks in the study area is shown in Figure 26a. The density values for the metasedimentary rocks show a peak around 2 700–2 750 kg/m^3, and a mean density of 2 733 kg/m^3. A few samples show a density that exceeds 3 000 kg/m^3. The somewhat higher mean density compared with the total population (2 713 kg/m^3), as well as the more extreme values, are related to a number of features. These include:

- A generally high content of mica.
- The presence of crystalline carbonate rock.
- The presence of samples that contain disseminations of pyrite and pyrrhotite.

Magnetic susceptibility

The density–susceptibility diagram is shown in Figure 26b. The metasedimentary rocks show a large variation in magnetic susceptibility. A few rock samples that show a high density (c. 2 850 kg/m^3) and a low magnetic susceptibility (<100 × 10^{-6} SI) can be distinguished (Fig. 26b). These samples correspond to crystalline carbonate rocks that contain the minerals calcite and dolomite with relatively high density and low susceptibility.

Gamma radiation

The gamma radiation characteristics of the Svecofennian sedimentary rocks are shown in Figure 27. The concentration of potassium varies from almost zero to over 6%. However, most of the samples are well concentrated in both the potasium–uranium (Fig. 27a) and potassium–thorium (Fig. 27b) diagrams, with between 1 and 4.5% potassium and generally low concentrations of uranium (<10 ppm) and thorium (<25 ppm).

A small group of samples with concentrations of potassium, uranium and thorium close to zero occur consistently in the crystalline carbonate rocks (Fig. 27). By contrast, several samples measured in the eastern part of the Bergslagen region show anomalously high concentrations of uranium and especially thorium. All samples with a uranium concentration larger than 10 ppm (Fig. 27a) or a thorium concentration larger than 25 ppm (Fig. 27b) have been collected within map sheet 10I Stockholm. The highest concentrations of potassium (>4.5%) are also found in the Stockholm area. The metasedimentary rocks in this region are migmatitic and it is the leucosome in these rocks that accounts for the anomalous values. Furthermore, an increased proportion of mica-rich bands may account for the higher concentration of potassium. It also needs to be kept in mind that gamma radiation data are lacking in the neighbouring areas to map sheet 10I Stockholm.

Regional geophysical signature

Due to their relatively higher density, the Svecofennian sedimentary rocks mainly correlate with local gravity highs on the Bouguer anomaly map (cf. Figs. 22 and 13, respectively). Inspection of the radiometric thorium map inferred from airborne radiometric measurements (Fig. 11) shows a relatively large area around the lake Mälaren, west of Stockholm, that shows a high thorium concentration. Metasedimentary rocks build a prominent component in the bedrock in this region (Fig. 22).

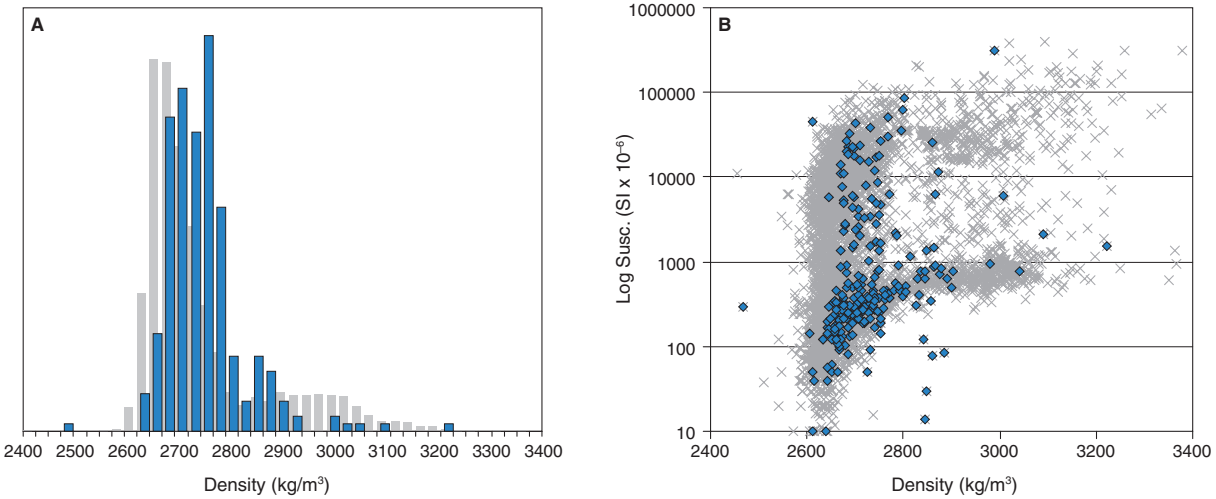

Fig. 26. **A.** Density distribution and **B.** magnetic susceptibility–density diagrams for Svecofennian sedimentary rocks (blue). For purposes of comparison, all samples from the Bergslagen region are shown in grey. The magnetic susceptibility is shown on a logarithmic scale.

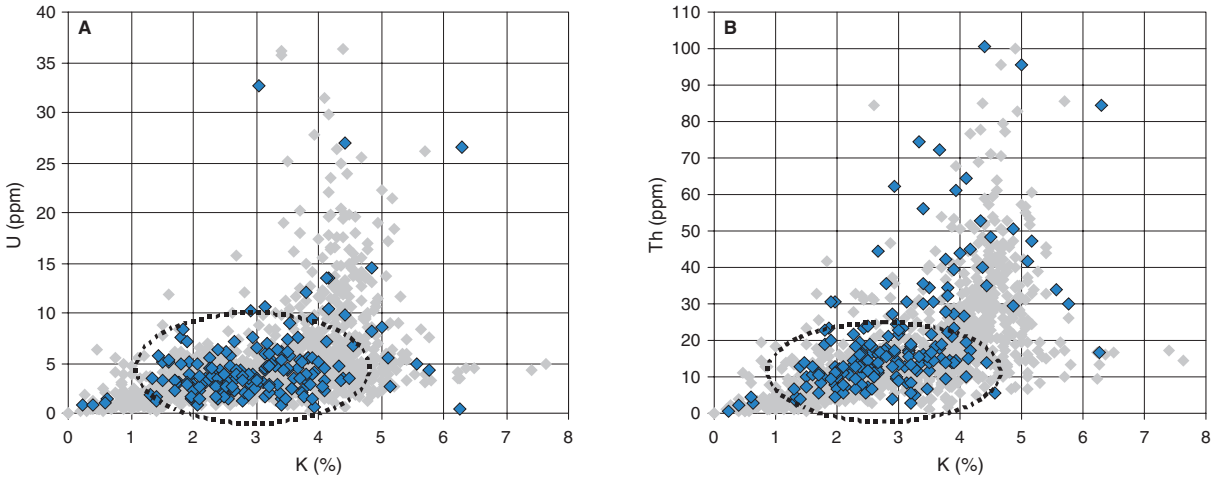

Fig. 27. Concentrations of **A.** uranium versus potassium and **B.** thorium versus potassium for Svecofennian sedimentary rocks (blue). For purposes of comparison, all samples from the Bergslagen region are shown in grey.

However, to a large extent, the thorium anomaly is related to thorium in the Quaternary cover, especially in the post-glacial clays. In some parts, the anomaly is also related to 1.85–1.75 Ga old granites of the GP intrusive suite (see later text).

Svecofennian volcanic and subvolcanic intrusive rocks (1.91–1.89 Ga)

Nomenclature, rock type and spatial distribution

Fine-grained, granoblastic, equigranular felsic rocks are common in the Bergslagen region. These rocks are dominated by quartz and feldspar, are devoid of any instructive primary features and are generally metamorphosed under amphibolite-facies conditions. The interpretation of these rocks is difficult, and, historically, geologists have been hesitant to use a too detailed genetic nomenclature for them. Instead, local, yet neutral names such as "leptite" and "hälleflinta" (see Geijer & Magnusson 1944, Gorbatschev 1969 for a discussion of these concepts) have been employed. However, there is a good reason to regard many of these rocks as volcanic or subvolcanic in origin, since such rocks, interpreted to have been well-sorted and to have had silt to fine sand grain sizes originally, would not have retained a rhyolitic composition if sedimentary processes had been influential. Instead, sedimentary processes would rather have produced more argillitic compositions. In the Bergslagen project, these rocks are regarded as metamorphosed equivalents to precursors rich in volcanic glass. The occurrence of better preserved volcanic rocks, especially in areas that have been affected by a lower grade of metamorphism, confirms this interpretation.

Prior to the regional metamorphism, large volumes of the volcanic rocks in Bergslagen were affected by pervasive, synvolcanic hydrothermal alteration, which resulted in the formation of phyllosilicates, so-called magnesium±iron±potassium±silicon alteration (see below). The phyllosilicate-rich composition approaches that of a meta-argillite, from which it can be difficult to distinguish. Hence, mica-rich rocks in areas that are affected by a higher grade of metamorphism may either be derived isochemically from an argillitic sedimentary rock or from a phyllic-altered volcanic rock. Uncertainties concerning this feature exist in the available geological maps. In rocks affected by a lower grade of metamorphism, relict primary (e.g. porphyritic) textures, gradational contacts or hydrothermal, "jig saw fit" in situ brecciation towards less altered rocks may indicate the precursor. In this study, such criteria have been the basis for the reinterpretation of some rocks, earlier regarded as sedimentary in origin, as altered and metamorphosed volcanic rocks (see also section "Digital compilation of the geological maps").

The volcanic rocks were affected by different grades of metamorphism in different parts of the study area. In westernmost parts, well-preserved, up to 8 km thick successions of metavolcanic rocks, affected only by greenschist-facies metamorphism, occur. Delicate volcanic textures are present in these rocks and permit a detailed volcanic analysis. In the Sala, Dannemora (north-east of Uppsala) and easternmost, coastal areas, metavolcanic rocks characterized by low to medium grade, amphibolite-facies metamorphism provide some opportunities for the recognition of primary textures and structures. However, in most other areas, the volcanic rocks were altered under high grade, amphibolite-facies metamorphic conditions, and, locally, even the classification of

the rocks as volcanic in origin is uncertain (see also section "Digital compilation of the geological maps").

Since much of the field evidence used for volcanic rock analysis in recent successions has been lost in the altered and metamorphosed rocks in the Bergslagen region, recognition must rely also on textural, structural and compositional observations. McPhie et al. (1993) listed some criteria for the recognition of and distinction between the successive steps from juvenile, syn-eruptive deposits (step 1), through resedimented, but syn-eruptive volcaniclastic deposits (step 2) to volcanogenic sedimentary deposits (step 3). Since the formation of step 3 rocks involves weathering, erosion and post-eruptive resedimentation, it causes more profound compositional changes than the preceding steps. These changes can, to variable extent, be recorded in low-, medium- and, locally, even in high-grade metamorphic rocks. Hence the break between steps 2 and 3 is a convenient borderline between metavolcanic and metasedimentary rocks, respectively, even in ancient supracrustal successions and has been utilized in this study.

Metavolcanic rocks are distributed throughout the entire project area with a dominance in the westernmost part (Fig. 28). In most other parts of Bergslagen, they mainly occur as large-scale xenoliths within and between intrusive rocks, predominantly metagranitoids (see later text). The metavolcanic rocks are dominated by rocks with a rhyolitic composition (Fig. 28). Metadacites and meta-andesites occur in some areas, but are notably absent in the westernmost part of Bergslagen (Fig. 28 and Fig. 6 in Allen et al. 1996). It has been suggested that the spatial distribution of dacitic compositions reflects different magma sources in the eastern and western parts of the region (see Gorbatschev 1969, Lagerblad 1988 and Allen et al. 1996 for details). Minor occurrences of metabasite associated with the felsic metavolcanic rocks are common, but only locally is it possible to verify their volcanic character.

Physical volcanology and depositional environment

Allen et al. (1996) interpreted the supracrustal successions in Bergslagen to record ambient, deep water sedimentation that was interrupted at 1.9 Ga by a volcanic episode accompanied by thermal doming. This process was divided into separate stages (Allen et al. 1996). Shallow water or, locally, even subaerial eruptive and depositional environments prevailed during the intense volcanism and extension stage. The ensuing waning volcanic stage, was characterized by regional subsidence, leading to transgression and to resumed deep water sedimentation during the concluding sedimentary, thermal subsidence stage. Superposed, second order variations led to local and regional variations to this pattern. Age dating work undertaken in this and other projects (see below and Lundström et al. 1998 for references) indicates a rapid evolution in which the various stages were approximately synchronous in different parts of the Bergslagen region. Field work in this project has adopted and mainly confirmed the facies model of Allen et al. (1996).

Volcanology and modes of eruption

The felsic volcanism during the intense volcanism stage was explosive and produced thick successions of massive, poorly bedded volcanic sandstones and breccias. Many of these volcanic successions were probably deposited from pyroclastic flows related to huge caldera-related eruptions. Such deposits mostly dominate the lower parts of the volcanostratigraphic sections. Following Allen et al. (1996), these lower, massive, sandstone and breccia sequences are thought to be more or less proximal, juvenile or somewhat resedimented volcanic deposits. In many places, they apparently grade through granite porphyries into coarser, more deep-seated granitoid intrusions. The relationship suggests proximity to a volcanic centre, which, locally, is further corroborated by the occurrence of coherent, lava-like metavolcanic rocks. The explosive character of the volcanism, some indications of subaerial deposition and scattered accretionary lapilli suggest that eruptions took place under limited water depths or subaerially.

The massive sandstone and breccia part of the volcanic pile is overlain by a planar-bedded or laminated succession of volcanic siltstones to sandstones interbedded with crystalline carbonate rocks, calc-silicate rocks (skarn) or clastic metasedimentary rocks, all of which formed during the waning volcanic stage. In rocks of lower metamorphic grade, vitriclastic texture as well as pumice clasts can be observed in the volcanic rocks of the waning volcanic stage. A fairly juvenile volcanic origin is inferred, but the fine bedding or lamination precludes an origin as pyroclastic flow deposits. Allen et al. (1996) suggested that these rocks either originated as distal ash fall or suspension deposits. Thus, they were deposited in distal positions in relation to the particular volcanic centre from which they once erupted. As they record fairly peaceful depositional environments, volcanism cannot have been exceptionally vigorous at this time or locality, but permitted depositional basins of significant extent to develop. Nevertheless, subvolcanic intrusions and lavas were emplaced into this stratigraphic level.

Metabasites locally accompany the felsic metavolcanic rocks. In general, their mode of emplacement is unknown due to lack of diagnostic field evidence.

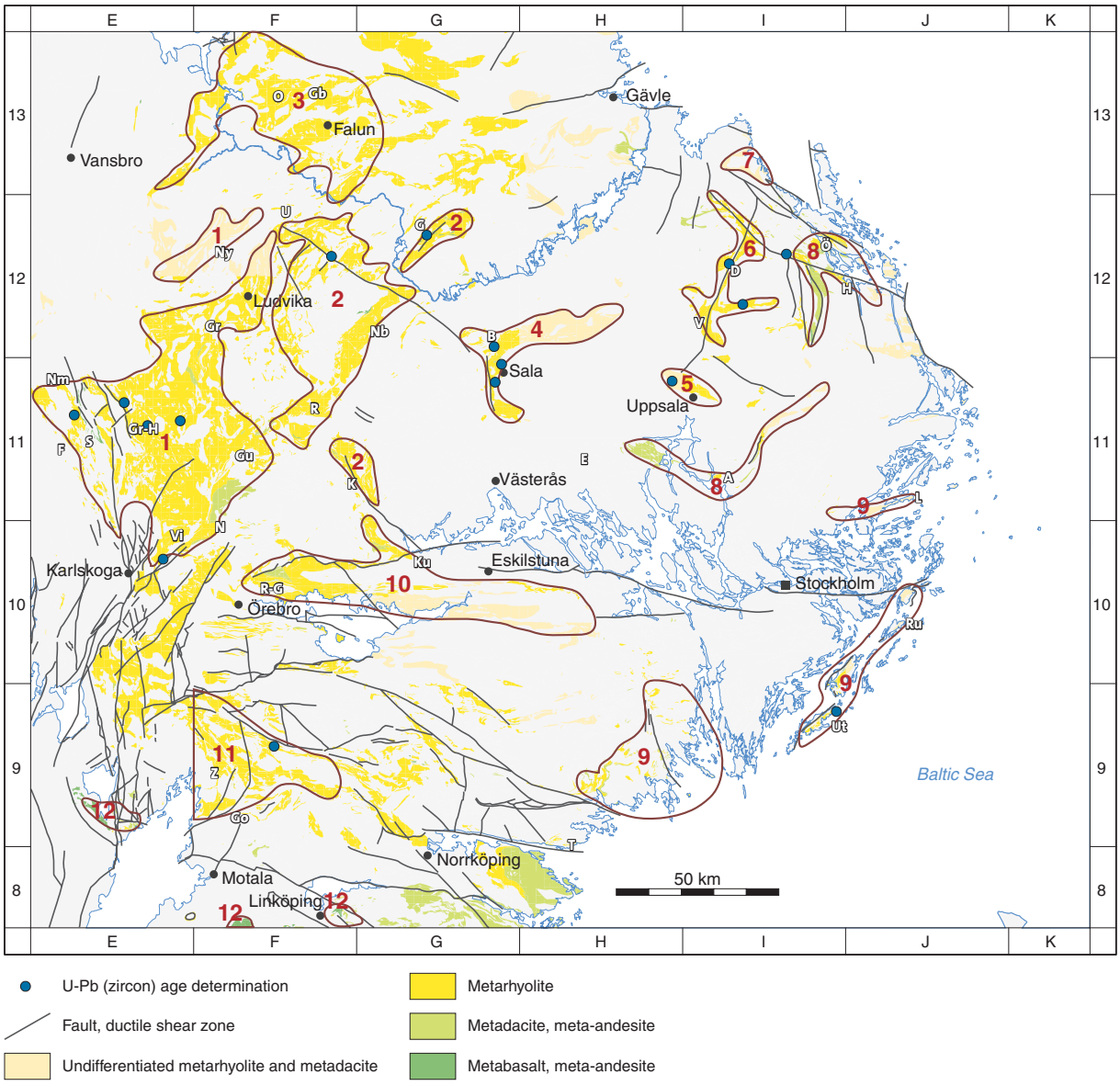

Fig. 28. Distribution of Svecofennian volcanic and subvolcanic intrusive rocks at the ground surface in the Bergslagen region. The map also shows the selected sub-areas (1–12) where such rocks have been described and interpreted in the context of the Bergslagen project, the location of samples that have been dated using the U-Pb (zircon) technique, and the location of place names referred to in the section "Svecofennian volcanic and subvolcanic intrusive rocks (1.91–1.89 Ga)". A = Arlanda, B = Broddbo, D = Dannemora, E = Enköping, F = Filipstad, G = Garpenberg, Gr–H = Grythyttan–Hällefors, Go = Godegård, Gr = Grängesberg, Gb = Grycksbo, Gu = Guldsmedshyttan, H = Harg, K = Kolsva, Ku = Kungsör, L = Ljusterö–Rödlöga, N = Nora, Nb = Norberg, Nm = Nordmark, Ny = Nyhammar, Ö = Östhammar, O = Oxberg, R = Riddarhyttan, R–G = Rinkaby–Glanshammar, Ru = Runmarö–Ornö, S = Saxån, T = Tunaberg, U = Ulvshyttan, Ut = Utö, V = Vattholma, Vi = Vikern, Z = Gryt–Zinkgruvan.

Metabasites also intruded the well-preserved *Grythyttan slate* in the Grythyttan–Hällefors area which belongs to the sedimentary, thermal subsidence stage. Since the metabasites show a spilitic alteration, the slate was probably not yet lithified at the time of intrusion and the metabasites are inferred to have intruded during the deposition of the clastic sedimentary rocks. In the Saxån area, close to Filipstad, a mafic pillow lava extruded close to the start of the sedimentary, thermal subsidence stage. East of the Grythyttan–Hällefors area, most field evidence is inconclusive, but mafic, fragmental, peperitic or hyaloclastic rocks demonstrate that basic magmatism occurred here as well, although at unknown stratigraphic levels.

Depositional environment

The shallow depositional environments recorded by the upper parts of the *Larsbo formation* (see above) persisted in many places into the intense volcanism and extension stage. Thus, eroded tops, scours, stromatolites and cross

bedding are documented in this part of the stratigraphy. Although eruptions most probably occurred under limited water depths, Allen et al. (1996) stressed that the preservation of thick volcanic deposits requires deposition at, or rapid subsidence to, substantial water depths. Subsidence is corroborated by the general scarcity of conglomerates in the Bergslagen region. However, some volcanic units apparently managed to fill in the depositional basin up to wave base and to maintain a limited water depth.

As the depositional basins subsided, water depth increased with time, and the planar-bedded, sediment-interbedded deposits of the waning volcanic stage could be formed. However, second order variations on this evolution caused subaerial depositional conditions to persist locally also during this stage, e.g. at Dannemora (north-east of Uppsala), where gypsum and halite pseudomorphs indicate evaporite formation at this time (Lager 2001).

In the Glanshammar and Guldsmedshyttan areas, north of Örebro, thick crystalline carbonate rocks occur. Their eastward increasing thicknesses have been suggested to indicate an eastward deepening of the depositional basins (Gorbatschev 1969). Furthermore, in the Glanshammar area, Gorbatschev (1969) observed that both the thickness and clast size of some conglomerates decreased towards the south and east, which he interpreted to record either an eastward deepening of the depositional basins or a more distal deposition. As the thickness of the metavolcanic rocks is greater west of the Glanshammar area than to the east, these lateral variations may be due to the transition from a western volcanic area to an eastern sedimentary area.

Hydrothermal alteration

Nomenclature and historical overview

Synvolcanic alteration on both a regional and more local scale is common in the Bergslagen region, particularly in the areas that contain abundant mineral deposits. Four types of alteration affected the volcanic rocks, referred to here as sodium alteration, potassium alteration, magnesium±iron±potassium±silicon alteration (simplified to "magnesium alteration") and calcium±magnesium±iron alteration (simplified to "skarn alteration"). These correspond to the terms sodium metasomatism, potassium metasomatism, magnesium metasomatism and skarn alteration, respectively, in older literature.

In the early 1960's, the extreme alkali-rich compositions of large areas of metavolcanic rocks were thought to reflect stratigraphically controlled, primary magmatic compositions. Furthermore, magnesium metasomatism was thought to be related to alteration associated with fluids derived from granitoid intrusions and the formation of sulphide mineralization. Koark (1962) showed that "magnesium alteration" in rocks at the Falun mine predated the intrusion of granitoids and concluded that the ore was syngenetic. Schermerhorn (1978) discussed similarities between magnesium metasomatic rocks and some rocks in the Iberian pyrite belt, and Wolter & Seifert (1984) suggested that the rocks of the Falun alteration zone had formed from metasomatically altered felsic rocks that, subsequently, were metamorphosed under essentially isochemical conditions. Frietsch (1982a) and Lagerblad & Gorbatschev (1985) showed that the chemical composition of the mineralized metavolcanic rocks was related to hydrothermal metasomatic alteration rather than to primary magmatic variations. A seafloor and sub-seafloor environment model for the alteration and associated mineralization was presented by Oen et al. (1982).

Sodium or potassium alteration

Sodium or potassium alteration mainly caused readjustments of feldspar compositions in the volcanic rocks, and the compositions were subsequently retained during later regional metamorphism.

The development of extremely alkali-rich rocks is more common in mineralized metavolcanic rocks relative to barren areas. Indeed, regional sodium alteration appears to be restricted to the metal-rich areas. Assessment of geochemical data in western Bergslagen (Lundström 1985, 1995) indicates that stratigraphically higher levels in the volcanic sequence tend to be somewhat more potassium-rich in contrast to lower stratigraphic levels, which are more sodium-rich. However, the stratigraphic control is not fully consistent. The pattern is thought to have formed as rising geotherms promoted sodium enrichment to overprint, in some cases, already potassium-rich rocks in a sub-seafloor environment. Potassium-rich rocks retained their composition predominantly because they never experienced sodium alteration. At lower stratigraphic levels, textural factors such as crystallinity, porosity etc. may also have been critical in the alteration process. Volcanic glass is known to be easily enriched in potassium (Lipman 1965), and glass-rich volcanic siltstones deposited during the waning volcanic stage (higher stratigraphic level) were probably more susceptible to potassium alteration relative to the crystal-rich rocks deposited during the intense volcanism and extension stage (lower stratigraphic level).

Both the sodium and potassium alterations apparently occurred by a replacement process without disrupting primary feldspar lattices. Lundström (1995) presented examples of both sodium and potassium re-

placements which left the original textures unaffected. The susceptibility of volcanic glass to potassium alteration may also explain potassium-enrichment in the matrices of some porphyritic rocks. The chemical and thermodynamic prerequisites for alkali alteration were discussed by de Groot (1990).

"Magnesium alteration"

"Magnesium alteration" resulted in the destruction of feldspar in the volcanic rocks, and a depletion of sodium, potassium and calcium is apparent. The feldspars were replaced by various phyllosilicates (Baker & de Groot 1983, Trägårdh 1991, de Groot & Baker 1992). However, the original alteration assemblages are not known, since they were subsequently transformed during regional metamorphism to chlorite, phlogopite, biotite, muscovite, gedrite, anthophyllite and cordierite (Helmers 1984, Trägårdh 1991, Ripa 1994). These minerals indicate a general enrichment in magnesium (cf. Guilbert & Park 1986), but iron, manganese and titanium, for example, were also locally enriched (Ripa 1988). Furthermore, some phyllosilicates that are considered to replace feldspar may host some of the potassium that was removed from the feldspar molecules. Hence an apparent enrichment in potassium may be found in these rocks. The rocks affected by "magnesium alteration" typically plot in the lower, right hand corner of the Hughes (1973) diagram (see below).

The field relations of the "magnesium alteration" are poorly constrained, but this alteration seems to have had a more regional extension in the stratigraphically lower parts of the volcanic sequence. Local, cross-cutting bodies of altered rocks, which are spatially associated with mineralization, are only present at higher stratigraphic levels. Metavolcanic rocks in the Riddarhyttan–Norberg area, between Ludvika and Sala, show a particularly spectacular example of regional-scale, "magnesium alteration" (cf. Trägårdh 1988). At Stollberg, the relationship between more regional and more local zones of alteration was discussed by Ripa (1994).

In places, the "magnesium alteration" can be shown to have started along permeable zones where the water/rock ratios were presumably high. It commonly overprinted an earlier enrichment in sodium, as indicated by the presence of gedrite or chlorite overgrowths in already sodium-altered rocks (Figs. 29a and 29b). More intense alteration initiated with the replacement of feldspar in the matrix (Fig. 29b). At more advanced stages of alteration, all feldspars were consumed and only relict quartz remains in a matrix of magnesium-rich silicates. As expected, fine-grained matrices were more susceptible to alteration than phenocrysts. The "magnesium alteration" selectively attacked particular rock components, including matrix, certain beds (Fig. 29c) etc., thereby revealing primary structures not visible in the unaltered rock.

The replacement of feldspar by phyllosilicates locally makes the hydrothermally altered volcanic rocks deceptively similar to argillitic metasedimentary rocks (see also above). In the marginal parts of some areas that contain rocks affected by "magnesium alteration", hydrothermal brecciation produced monomict, jig-saw fit breccias (Fig. 29d). In the older literature, such breccias were often regarded as volcanic breccias or agglomerates. Many breccias suggested to be volcanic by earlier investigators are consequently regarded as metasomatic in situ breccias in this work (see also Hjelmqvist 1946).

"Skarn alteration"

In the Bergslagen region, calc-silicate blastesis occurred in response to both regional metamorphism of calcareous, volcano-sedimentary rocks and as a consequence of alteration by fluids from intrusions. The alteration is frequently referred to as skarn formation.

In rocks affected by greenschist-facies metamorphism, "skarn alteration" is, in many places, demonstrably cross-cutting and linked to the intrusion of mafic dykes. At some distance from a dyke, scattered sheaves of actinolite overprint the volcanic textures. Closer to the dyke, the actinolites merge together, in many places leaving relict areas, similar to clasts, set in an amphibole matrix (Lundström 1995). In this manner, the alteration created deceptive, pseudoclastic textures (Fig. 29e). Baker et al. (1988) described zones of "skarn alteration" around a mafic dyke and suggested that amphibole growth post-dated earlier "magnesium alteration". In several cases, the alteration was associated with magnetite growth and mineralization (Sundius 1923, Baker et al. 1988).

Field and time relationships between the different alteration types

Although detailed field relations between the various hydrothermal alterations and their relationship to metallic mineralization are not known in many areas, some aspects are revealed in the well-preserved, metavolcanic rocks in the western part of the Bergslagen region (see sub-area 1 below and Fig. 28). Zones of sodium enrichment transect stratigraphic boundaries and encroach upon overlying volcanic units. Furthermore, incipient "magnesium alteration" apparently followed sodium alteration. An alteration sequence is documented in ovoidal structures (Fig. 29f), which demonstrate three successive stages of alteration. In

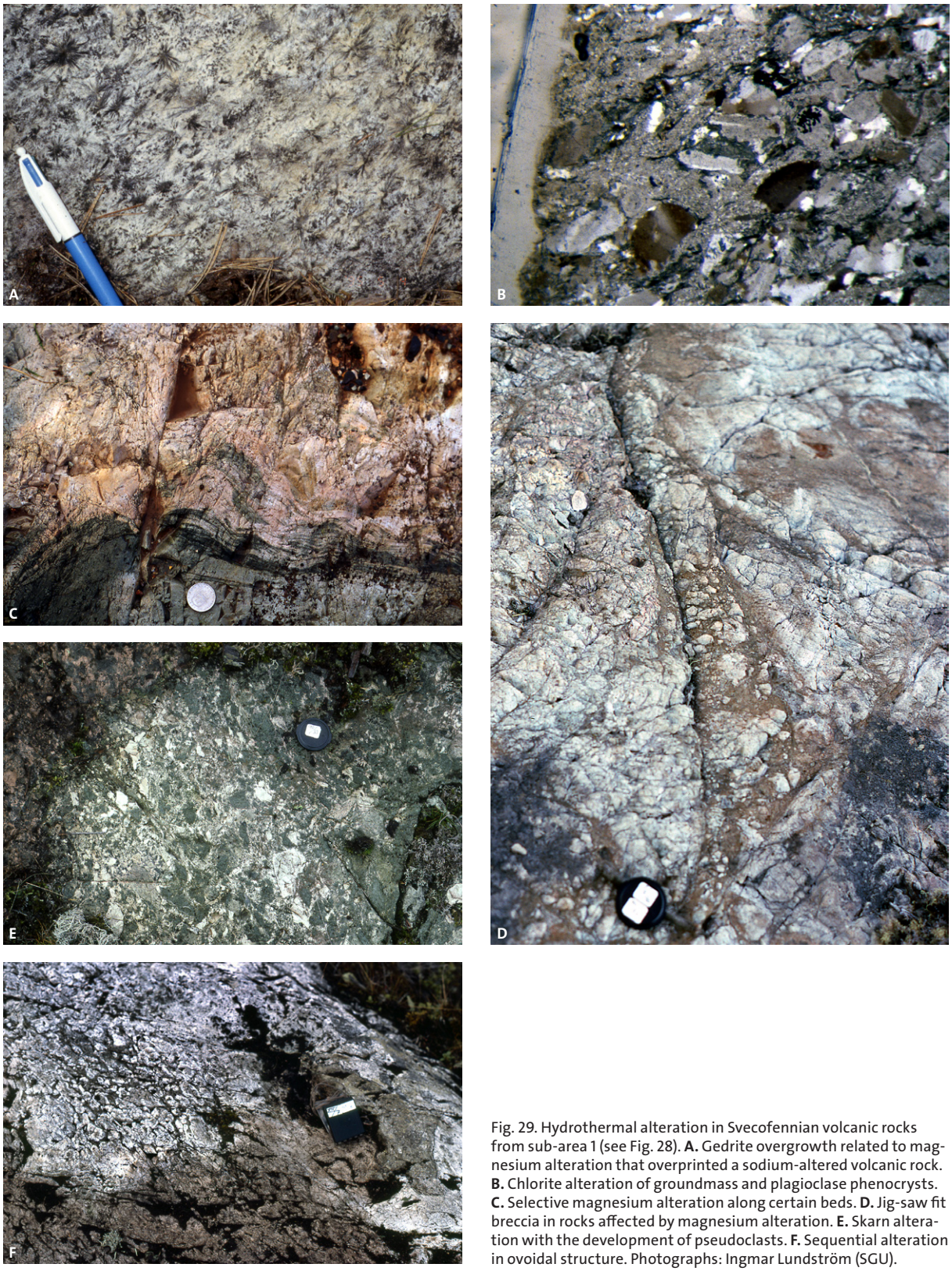

Fig. 29. Hydrothermal alteration in Svecofennian volcanic rocks from sub-area 1 (see Fig. 28). **A.** Gedrite overgrowth related to magnesium alteration that overprinted a sodium-altered volcanic rock. **B.** Chlorite alteration of groundmass and plagioclase phenocrysts. **C.** Selective magnesium alteration along certain beds. **D.** Jig-saw fit breccia in rocks affected by magnesium alteration. **E.** Skarn alteration with the development of pseudoclasts. **F.** Sequential alteration in ovoidal structure. Photographs: Ingmar Lundström (SGU).

these structures, relict, potassium-enriched cores are overprinted and surrounded by an albitized rock, which in turn is corroded in a jig-saw fit fashion by a magnesium-rich micaceous matrix.

Metabasic intrusions occur in the lower part of the stratigraphic sequence, in the central part of the Bergslagen region, and are spatially associated with rocks affected by sodium alteration and by intense "mag-

nesium alteration". By contrast, potassium-enriched rocks occur in adjacent areas that are almost devoid of metabasic intrusions. It is suggested that sodium and "magnesium" alterations occurred in response to the thermal anomaly conveyed by the abundant metabasic intrusions, whereas the earlier potassium alteration persisted in rocks situated distal to these intrusions. The metallogenetic significance of numerous metabasic intrusions was recognized by Sundius (1923) in the western part of the Bergslagen region. Among others, Hellingwerf (1984), Baker et al. (1988) and Lundström (1995) have later studied these features.

Detailed field work during the last twenty years has revealed field evidence for the timing of the various alterations. Rocks affected by sodium, potassium and "magnesium" alterations occur as clasts in conglomerates and breccias in the Grythyttan area (Lundström 1995). Furthermore, "magnesium alteration" is overprinted by regional metamorphism (Helmers 1984, Trägårdh 1990, 1991), which is isochemical in character (Trägårdh 1988, Ripa 1994). Since rocks affected by sodium and potassium alteration in many places show an overprinting by "magnesium alteration", the alkali alterations must also be pre-metamorphic, i.e. most probably synvolcanic. Although most of the alterations can be assumed to be synvolcanic, their syn- or epigenetic nature is generally not obvious. Furthermore, epigenetic field relations are documented from e.g. Garpenberg, where a zone with "magnesium alteration" cross-cuts bedding and encroaches into the stratigraphic hanging wall of the ore (Allen et al. 1996). Even post-deformational and post-metamorphic sodium and "magnesium" alterations have been reported by Lundqvist (1962) from rocks in coastal areas close to the Baltic Sea and by Lundström (1995) from the Nora area, north-east of Karlskoga.

Stratigraphic relationships and physical volcanology in selected sub-areas

Twelve sub-areas within the volcanic rock successions in Bergslagen (Fig. 28) have been selected for more detailed study and description in the context of the Bergslagen project. They have been chosen to illustrate the variable character of the volcanic rock succession at different grades of metamorphism and, to less extent, under different degrees of hydrothermal alteration. Furthermore, where appropriate, attention was focussed on the relationship of the metavolcanic rocks to metasedimentary rocks in a sub-area. Stratigraphic profiles for each sub-area are presented in Figure 30. The rock types and stratigraphic sequences described in more general terms in the earlier part of this section occur, to a variable extent, in each of the sub-areas. Apparently, some volcanic sequences were of major lateral as well as significant stratigraphic extent.

Sub-area 1. Karlskoga–Filipstad–Lindesberg–Ludvika

Sub-area 1 is the largest continuous metavolcanic rock domain in the Bergslagen region (Fig. 28). In part, it contains the best preserved rocks in the region, and it has been described by several authors (Lundström 1995 and references therein). Allen et al. (1996) have also presented detailed stratigraphic columns for the sub-area. Traditionally, the rocks in the Hällefors area, which were metamorphosed under greenschist-facies conditions, have been regarded as type localities for the Svecofennian supracrustal stratigraphy in Bergslagen. The well-preserved rocks in this area grade into more recrystallized, amphibolite-facies rocks toward the east. Rocks belonging to the three different stages in the volcanic development (see above) all occur in sub-area 1 (Fig. 30).

Felsic metavolcanic deposits dominate sub-area 1. The stratigraphically lower parts consist of proximal, massive, volcaniclastic deposits that are several kilometres thick and belong to the intense volcanism and extension stage. Clastic textures, possible pumice clasts and diffuse or thick bedding suggest a pyroclastic flow origin for the majority of these rocks. Furthermore, coherent lavas or subvolcanic rocks have been identified in what are inferred to be proximal areas. In the upper parts of the stratigraphy, planar-bedded, sediment-interbedded volcanic ash-siltsones that belong to the waning volcanic stage are frequent. Observations of accretionary lapilli indicate that subaerial eruptions occurred, and local eroded bed tops provide evidence for subaerial deposition. However, the significant thickness of originally unconsolidated volcaniclastic material indicates that deposition was mostly subaqueous. Rare carbonate and clastic metasedimentary interbeds in the massive volcaniclastic material confirm this conclusion. Porphyritic metadacite with plagioclase phenocrysts (*Storsjön formation* of Lundström 1983) occurs in a few small areas. These rocks show intrusive to peperitic field relations to planar-bedded rocks belonging to the waning volcanic stage (Fig. 31a).

Metabasic rocks in the area are mostly cross-cutting and intrusive, even at high stratigraphic levels. However, in the Saxån area, a pillow lava (Fig. 31b) is interbedded close to the base of the metasedimentary rocks that were deposited during the sedimentary, thermal subsidence stage. The spilitized metabasic rocks in the Grythyttan area provide further support for syndepositional emplacement. Furthermore, peperitic to hyaloclastic con-

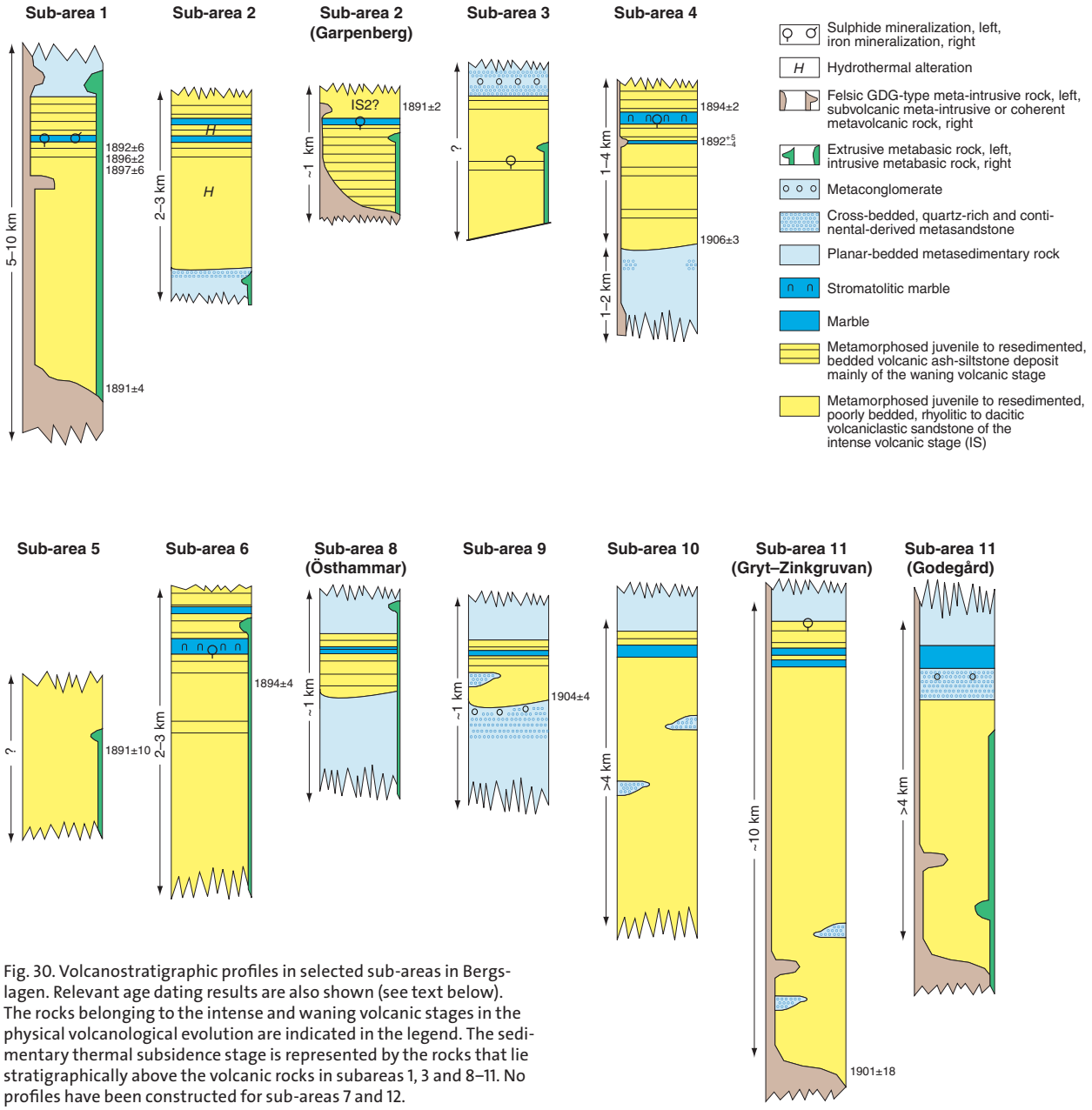

Fig. 30. Volcanostratigraphic profiles in selected sub-areas in Bergslagen. Relevant age dating results are also shown (see text below). The rocks belonging to the intense and waning volcanic stages in the physical volcanological evolution are indicated in the legend. The sedimentary thermal subsidence stage is represented by the rocks that lie stratigraphically above the volcanic rocks in subareas 1, 3 and 8–11. No profiles have been constructed for sub-areas 7 and 12.

Fig. 31. Svecofennian volcanic and subvolcanic intrusive rocks in sub-area 1. **A.** Porphyritic metadacite with peperitic contact against bedded, volcanic metasiltstone. **B.** Metabasalt with inferred pillow lava structure at Saxån. Photographs: Ingmar Lundström (SGU).

tacts of metabasic rocks in the Nyhammar area corroborate the largely syndepositional ages for these rocks.

The occurrence of crystalline carbonate rocks with variable thickness and lateral extension is a significant feature of sub-area 1. One carbonate horizon, which is probably greater than 1 km thick, can be followed c. 40 km from Vikern to Stråssa. In the *Grythyttan slate*, peperitic contacts and vitriclasts suggest that volcanism continued during the sedimentary, thermal subsidence stage and that the material in the slates is volcanogenic in character. East of Nyhammar, cross-bedded quartzite and metaconglomerate with abundant clasts of volcanic rock are present. These rocks resemble the metasedimentary rocks in Leksand and Nordmark. They are surrounded by felsic metavolcaniclastic rocks and were interpreted to be intraformational by Ripa & Kübler (2005). At Nordmark, the metavolcanic rocks are overlain by quartzite and conglomeratic metasedimentary rocks.

Sub-area 2. Lindesberg–Avesta–Säter

The metavolcanic rocks in sub-area 2 (Fig. 28) were metamorphosed under low to middle amphibolite-facies conditions and, consequently, volcanic textures and structures are, in general, poorly preserved. In addition, stratigraphic details are locally obscured by various types of hydrothermal alteration (see below). Nevertheless, volcanic rocks similar to the ones deposited during the intense volcanism and waning volcanic stages can be identified (Fig. 30). Apart from studies of the relatively well-preserved rocks in the Garpenberg area (Allen et al. 1996), little volcanological information exists from sub-area 2.

Synvolcanic, hydrothermal alteration is widespread in the rocks of sub-area 2. Particularly the rocks in large areas between Riddarhyttan and Norberg are pervasively affected by "magnesium alteration" (see above). Peripheral to this area, the rocks may be significantly less altered. Locally (e.g. Kolsva area), rocks that previously were interpreted as sedimentary in character have been reinterpreted in this study as altered metavolcanic rocks.

As originally suggested by Ambros (1983b), a bed of cross-bedded quartzite underlies the metavolcanic rocks in the Norberg area. The quartzite is suggested to be the uppermost unit in the *Larsbo formation* and represents the deepest stratigraphic level. Ambros (1983a, 1988) described both massive and bedded, fine-grained felsic rocks that are predominantly rhyolitic in composition. These are probable equivalents to the more juvenile deposits of the intense volcanism and extension stage and the ash-siltstone deposits of the waning stage, respectively. Clastic, possibly pyroclastic textures and supposed pumice clasts have been observed in poorly bedded, volcanic sandstones, which are inferred to be a pyroclastic flow deposit. At Garpenberg, such rocks overlie the mineralized carbonate horizon and associated waning stage volcanic ash-siltstones (Allen et al. 1996), and this juvenile, pyroclastic mass-flow deposit forms the highest stratigraphic unit in the major synclinal fold structure at Garpenberg (see section "Mineral and bedrock deposits"). It is interpreted to represent a possible, second phase of intense volcanism (IS2? in Fig. 30).

Fig. 32. Metabasic, hyaloclastic lava at Garpenberg in sub-area 2. Photograph: Ingmar Lundström (SGU).

Metadacites are rare in sub-area 2, but locally form a clastic bed, close to the underlying metasedimentary rocks in the *Larsbo formation*. According to Allen et al. (1996), metadacite also intruded the possible second phase of intense volcanism at Garpenberg. South of Ulvshyttan, a metagabbro shows a very fine-grained, peperitic border facies towards the surrounding felsic, metavolcanic ash-siltstones and, at Garpenberg, mafic lava with peperitic to hyaloclastic margins occurs immediately beneath the mineralized carbonate horizon (Figs. 28 and 32).

Sub-area 3. Falun–Leksand–Hofors

Regional metamorphism generally reached lower amphibolite-facies in sub-area 3 (Fig. 28), and primary textures and structures are relatively well-preserved. Kresten (1986) and Bromley-Challenor (1988) reported occurrences of felsic lavas, tuffs and tuffites, but did not present volcanological details. Some information may be found in older literature (see references in Kresten 1986 and Bromley-Challenor 1988). However, this information mainly comes from the area adjacent to the Falun mine. The volcanology in the remaining part of the sub-area is poorly known. Rocks belonging to all three stages in the volcanological evolution occur in sub-area 3 (Fig. 30).

Fig. 33. Svecofennian supracrustal rocks in sub-area 3. **A.** Fiamme-like structure in volcanic mass-flow rock. **B.** Bedded and folded rocks in the *Oxberg formation* possibly of sedimentary origin. **C.** Metabasic dyke showing possible peperite contact against volcanic metasiltstone at Oxberg. Photographs: Ingmar Lundström (SGU).

Weak but regionally extensive "magnesium alteration" affected the rocks south-west of Grycksbo. These rocks are referred to as the *Oxberg formation* by Kresten & Aaro (1987b), who regarded them as sedimentary in origin. Andalusite-bearing mica schists of sedimentary origin do occur in the area, but the majority of the rocks are felsic and fine-grained and have been reinterpreted in this study as altered volcanic rocks.

Massive, poorly bedded felsic metavolcanic rocks locally contain quartz and feldspar phenoclasts together with elongate, fiamme-like segments that are poorer in phenoclasts or phenocrysts (Fig. 33at). They are interpreted to be pyroclastic flow deposits. Rare interbeds of thin, crystalline carbonate rock, hyaloclastic metabasic rock and pillow lava (Koark 1962) indicate at least temporary, subaqeous deposition. Previous work (Geijer 1917, Kresten & Aaro 1987b) reported occurrences of agglomerate. However, some of these occurrences are more or less incipient hydrothermal breccias related to the "magnesium alteration". Bedded, mica-rich, possibly sedimentary strata (the *Oxberg formation* of Kresten & Aaro 1987b; Fig. 33b), with crystalline carbonate interbeds, lie stratigraphically above the massive, inferred pyroclastic flow deposits (Kresten & Aaro 1987b, Bromley-Challenor 1988). The massive and bedded rocks are inferred (Fig. 30) to represent the intense volcanism and waning volcanic stages of Allen et al. (1996), respectively. According to Kresten & Aaro (1987b), metabasic rocks that are volcanic in origin are common in stratigraphically higher parts, and, in the Falun area, hyaloclastic varieties and pillow lavas are present. In the Oxberg area, mafic dykes with bulbous, possibly peperitic contacts against finely bedded metavolcanic rocks (Fig. 33c) occur.

Metavolcanic rocks are overlain by a locally conglomeratic, cross-bedded quartzite referred to as the *Leksand quartzite* by Hjelmqvist (1966). This unit belongs to the sedimentary, thermal subsidence stage in the Svecofennian supracrustal sequence. Cross bedding and clast material in the conglomeratic units show that the main part of the quartzite overlies the metavolcanic rocks, but the upper parts of the volcanic sequence contain some interbeds of quartzite. Hence, there is no unconformity. Interbeds of calc-silicate rock, crystalline carbonate rock and metasedimentary rock also occur in this part of the sequence (Fig. 30). The crystalline carbonate rocks have a smaller volume than those present in sub-areas 1 and 2.

Sub-area 4. Sala

Few publications that address the geology of sub-area 4 at Sala (Fig. 28) exist, but recent mapping and a description of the geology in the area have provided some new

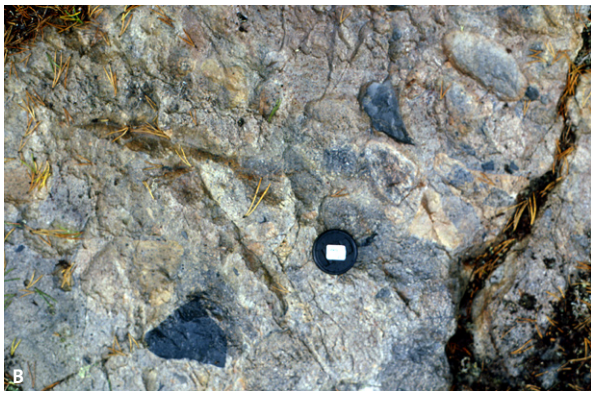

Fig. 34. Svecofennian supracrustal rocks in sub-area 4. **A.** Quartz-feldspar-phyric metarhyolitic mass-flow at Broddbo (top right in photograph). **B.** Arkosic metaconglomerate at Sala. A granite pebble forms a clastic component in this metaconglomerate. **C.** Volcanic metasiltstone with accretionary lapilli at Sala. Photographs: Ingmar Lundström (SGU).

information (Ripa et al. 2002). The stratigraphic section in the Sala mega-xenolith is unusually complete and well-preserved. It contains volcanic deposits that belong to both the intense volcanism and extension stage and the waning volcanic stage (Fig. 30). Sedimentary rocks that lie stratigraphically beneath the volcanic strata are also present (Fig. 30). The bedrock in the north-eastern part of the sub-area was metamorphosed under lower amphibolite-facies conditions. Metamorphic grade increases southwards and, in the southern part of sub-area 4, the rocks are affected by upper amphibolite-facies metamorphic conditions. Hence, textures and structures are only locally well-preserved.

In the area close to Broddbo, in the north-eastern part of the sub-area, metagreywacke similar to that observed in the *Larsbo formation* comprises the lowest stratigraphic unit. These rocks are feldspar-rich and apparently volcanogenic. Locally, they are intruded by plagioclase-phyric, subvolcanic rocks. The metagreywackes are overlain by cross-bedded quartzite, which, in turn, is overlain by a planar-bedded volcanic siltstone. The top bed of the volcanic siltstone was eroded and infilled by a porphyritic rhyolite with coarser crystals of both quartz and feldspar (Fig. 34a), interpreted to be a pyroclastic mass-flow deposit. This rhyolite marks the initial pulse of juvenile volcanism in the area. The metavolcanic rocks at Broddbo are stratigraphically overlain by a volcanic sequence that is several kilometres thick. The top of the stratigraphic sequence is truncated by younger GDG metagranitoids. Southwards, the metavolcanic rocks in sub-area 4 border, via a sheared contact, upon another metasedimentary unit, the *Östrom formation* of Ripa et al. (2002), which probably corresponds stratigraphically to the *Larsbo formation*.

The metavolcanic rocks consist of rhyolitic to dacitic volcanic breccias, sandstones and siltstones, locally intruded by subvolcanic intrusions. Ripa et al. (2002) informally subdivided these rocks into four formations. The lowest part was called the *Sommarhagen formation* and is dominated by volcanic sandstones, which are interbedded with volcanic siltstones and breccias. At least three repeated breccia-sandstone-siltstone successions, which are each some several hundred metres thick, have been recorded and interpreted as depositional units. The dominant, massive rhyolitic sandstones contain clast-like quartz and feldspar phenoclasts that are locally unevenly distributed, suggesting relics of pumice. These rocks are interpreted as rather juvenile, pyroclastic mass-flow deposits and represent the intense volcanism and extension stage. The formation also contains an interbed of polymict, matrix-supported metaconglomerate with a sandy, feldspar-rich and cross-bedded matrix, and locally granitoid clasts (Fig. 34b). The conglomerate indicates that volcanic

activity was temporarily restricted and that intrusive rocks reached erosion level.

Interbeds of crystalline carbonate rock and planar-bedded, volcanic metasiltstone increase in frequency stratigraphically upwards. This part of the stratigraphic pile is referred to as the *Sandtorpet formation* (Ripa et al. 2002). The uppermost part of the supracrustal succession starts with a c. 300 m thick, dolomitic and stromatolitic crystalline carbonate horizon, which is the host rock to the Sala base-metal deposit. This horizon is overlain by alternating planar-bedded volcanic siltstone to sandstone and stromatolitic crystalline carbonate rock, similar to the rocks present in the *Sandtorpet formation* and the whole unit is referred to as the *Finntorpet formation* (Ripa et al. 2002). Subaerial volcanism was active at this time, as indicated by accretionary lapilli in one of the uppermost beds of the *Finntorpet formation* (Fig. 34c). Both the *Sandtorpet* and *Finntorpet formation*s show characteristics typical of the waning stage of volcanic activity. The planar-bedded volcanic siltstones of the *Sandtorpet formation* are locally intruded by subvolcanic intrusions (*Eklövstorp formation* of Ripa et al. 2002), which, in places, show peperitic contacts.

The accretionary lapilli beds, the polymictic metaconglomerate and its cross-bedded matrix, the eroded bottom contacts at Broddbo, and the stromatolites all indicate subaerial to shallow subaqeous environments during the deposition of the volcanic rocks at Sala. Furthermore, water depths were restricted to the range for stromatolite growth. However, the thickness of the volcanic units suggests that the basins of final deposition subsided at a rate that approximately matched the rate of deposition. Hence, the development of the individual depositional basins was highly variable.

Sub-area 5. Uppsala

Wiman (1930), Lundegårdh (1956) and Lundegårdh & Lundqvist (1956) provided some data on the metavolcanic rocks in sub-area 5 in the vicinity of Uppsala (Fig. 28). In addition, SGU's bedrock mapping programme in the Uppsala and Enköping areas (Arnbom & Persson 2002, Ripa & Persson 2007) has provided some new information. Only rocks of the intense volcanism and extension stage as well as subvolcanic intrusions have been identified, but some lithologies have an unclear origin (Fig. 30). The metamorphic grade is middle amphibolite facies.

In the western part of the sub-area, the metavolcanic rocks are dominated by dacitic, sparsely clast-bearing volcanic breccias with a sandy matrix. Lithic clasts are centimetre to decimetre in size and comprise felsic volcanic siltstone, argillite, mafic rock and felsic, rather coarse-grained, possibly subvolcanic intrusive rock. According to Lundegårdh (1956), some "conglomeratic varieties" contain clasts of granitoid and quartzite, which may indicate a pre-volcanic basement similar to that at Broddbo in sub-area 4. In addition, the dacitic rocks contain up to cm-size crystal clasts of quartz and feldspar. The top of one dacitic breccia unit is normal-graded through sandstone to siltstone. Probable interbeds of more rhyolitic volcanic breccia also occur. Furthermore, in places, grey or red, very fine-grained, aphanitic to sparsely feldspar-phyric metarhyolite is also present. It is most likely a coherent rock type, but its relation to the volcanic breccias is unclear. Locally associated with, and probably intrusive into the breccias are hornblende- and feldspar-phyric dacitic to andesitic rocks. In places, the volcanic rocks grade into more deep-seated rocks with a granitoid composition, inferred to represent subvolcanic intrusions. In the eastern part of the sub-area, undifferentiated felsic metavolcanic rocks with quartz and feldspar phenocysts are present (Arnbom & Persson 2002)

Sub-area 6. Dannemora–Vattholma

The metavolcanic rocks in sub-area 6 close to Dannemora and Vattholma (Fig. 28) are well-preserved and regional metamorphism did not exceed lower amphibolite-facies conditions. A summary of relevant older literature as well as a description of the geology in the area north of Uppsala can be found in Stålhös (1991). A description of the iron ore deposit and its host rock at Dannemora is available in Lager (2001). The volcanic succession in the Dannemora mine area has been divided into lower and upper formations that correspond more or less to the volcanic deposits of the intense volcanism and waning stages, respectively (Fig. 30).

Rhyolitic, mostly volcaniclastic rocks dominate the volcanic sequence. They are silty to sandy in grain size and, locally, have quartz and feldspar phenoclasts as well as shards, pumice and lithic clasts. The lower formation of Lager (2001) comprises a few hundred metres of coarsely bedded, pyroclastic flow and fall deposits interbedded with cogenetic planar-bedded, turbiditic, resedimented varieties, which indicate a subaqeous environment. Lager (2001) identified three depositional cycles within the uppermost few hundred metres of the volcanic sequence in the Dannemora mine area. Juvenile, accretionary lapilli-bearing beds occur and demonstrate subaerial volcanic activity.

The mineralized upper formation of Lager (2001) consists of planar-bedded volcanic siltstones, which are interbedded with crystalline carbonate and calc-silicate rocks (Fig. 35). In places, these rocks contain shards as well as pumice clasts and accretionary lapilli. They

Fig. 35. Volcanic metasiltstone with interbeds of crystalline carbonate rock and calc-silicate rock in the upper part of the Svecofennian supracrustal sequence at Dannemora in sub-area 6. Photograph: Ingmar Lundström (SGU).

Fig. 36. Amygdaloidal metadacitic to meta-andesitic mass-flow in sub-area 8. Photograph: Ingmar Lundström (SGU).

are inferred to represent juvenile volcanic deposits. The crystalline carbonate rocks are stromatolite-bearing and Lager (2001) also reported the occurrence of halite and gypsum pseudomorphs. Thus, the depositional environment is inferred to have been rather shallow and temporally even evaporitic. Lager (2001) recognized 14 depositional cycles within the upper formation, which were interpreted to be related to cyclic uplift and subsidence due to subjacent igneous activity. The evidence for shallow to subaerial environments presented by Lager (2001) shows that the waning stage of volcanic activity was not ubiquitously connected with large-scale crustal subsidence. Metavolcanic rocks with a basaltic to andesitic composition are reported by Stålhös (1991). Pillow lavas that grade into hyaloclastic sandstones occur interbedded with rhyolitic siltstones belonging to the waning stage of volcanic activity.

Sub-area 7. Hållnäs

The volcanic rocks in sub-area 7 (Fig. 28), which is equivalent to the Barknåre area in older geological literature, are affected by medium to upper amphibolite-facies metamorphism and are poorly understood. However, the description of Sund (1957) provides some indications of the stratigraphic relationships in the area.

The supracrustal rocks have been interpreted to lie within an open, easterly plunging syncline (Sund 1957). The core of the syncline is occupied by feldspathic quartzite that passes stratigraphically downwards into rhyolitic metavolcanic rocks. Hence, the lithostratigraphy indicates that metasedimentary rocks overlie metavolcanic rocks. However, the nature of the metasedimentary rocks is insufficiently well understood to permit confident conclusions concerning the stratigraphy. Persson & Stålhös (1991) interpreted the quartzites as hydrothermally altered rocks.

Sub-area 8. Southern and eastern parts of the county of Uppsala

The metavolcanic rocks in the southern and eastern parts of the county of Uppsala in sub-area 8 (Fig. 28) contain a high proportion of intermediate to mafic rocks. This is unique for the Bergslagen region and its surroundings. In most places, the metamorphic grade of the rocks is too high for meaningful volcanological studies. However, rocks that belong to the intense volcanism and waning volcanic stages, and probably even the sedimentary, thermal subsidence stage are tentatively inferred to be present.

Dacitic, andesitic and basaltic, massive metavolcanic rocks dominate. The metadacites are quartz- och plagioclase-phyric and resemble the rocks of the *Storsjön formation* in sub-area 1 (Lundström 1983). Locally, it can be demonstrated that these rocks are intrusive in character. However, large areas of massive or poorly bedded metavolcanic rocks with a dacitic to andesitic composition are inferred to be volcaniclastic, most probably pyroclastic mass flow deposits belonging to the intense volcanism and extension stage. Beyer (1954) and Stålhös (1991) described some of these rocks that include partly amygdaloidal tuff-breccias (Fig. 36) as well as coherent metavolcanic rocks with a dacitic to basaltic composition. At Harg, such lava shows peperitic contacts against a bedded volcanic siltstone.

Finely planar-bedded, rhyolitic metavolcanic siltstones with local crystalline carbonate and calc-silicate interbeds, belonging to the waning volcanic stage, as well as more massive and intermediate to basic metavolcanic rocks are present in the Arlanda and Östhammar areas (Fig. 30). Locally, the metavolcanic rocks are overlain by metasedimentary rocks belonging to the later sedimentary, thermal subsidence stage (Fig. 30), including metaconglomerate with volcanic clasts. The

metasedimentary rocks are intruded by a plagioclase-phyric metadacite, similar to the material that comprises the clasts in the metaconglomerate (Stålhös 1972).

Sub-area 9. Stockholm archipelago

The metavolcanic rocks on some of the islands in the Stockholm archipelago (Fig. 28) were metamorphosed under middle amphibolite-facies conditions. However, on the islands of Utö and Ljusterö, a transition to high amphibolite-facies conditions towards the north-west is apparent (see also section "Deformation, metamorphism and mechanism of emplacement of the 1.87–1.84 Ga GSDG suite of intrusive rocks"). Thus, rocks in the mainland area suffered upper amphibolite-facies metamorphism and their volcanic character is difficult to determine. Volcanological aspects of the rocks on the Utö island were discussed in Allen et al. (1996), whereas Lundqvist (1962) provided information on the metavolcanic rocks in the Ljusterö–Rödlöga area. Sundius (1939) described the Runmarö–Ornö area, but few volcanological details were presented.

In contrast to most other sub-areas, the metavolcanic rocks in sub-area 9 are subordinate in relation to metasedimentary rocks. As indicated by numerous way-up observations, the metavolcanic rocks on Utö, and probably also on Ljusterö, lie stratigraphically above metasedimentary rocks with primary depositional contacts. Metasedimentary rocks with primary contacts above metavolcanic rocks have not been verified, but were suggested by Gavelin et al. (1976).

Dacitic rocks on Ljusterö are interpreted as tuffs and both rhyolitic and dacitic, pyroclastic mass flow deposits occur on Utö (Allen et al. 1996). The mass flow deposits on Utö are interbedded with an upward shallowing sequence of metamorphosed mudstone and rippled sandstone as well as cross-bedded quartzite, interpreted to have formed in a prograding delta lobe. The depositional environment is interpreted to have been shallow water to subaerial, which is corroborated by one of the few instances of true welding documented inside the Bergslagen region. These units are interpreted to represent the intense volcanism and extension stage of the volcanic activity (Fig. 30). However, the deposits belonging to this stage in the Stockholm archipelago are much thinner in the Stockholm archipelago compared with the equivalent deposits in the sub-areas in western Bergslagen (e.g. sub-area 1). In the mainland part of sub-area 9, meta-andesite and metabasalt occur, but their volcanic character and stratigraphic position are both uncertain.

Equigranular and planar-bedded, rhyolitic metavolcanic rocks, with interbeds of crystalline carbonate rock, calc-silicate rock and metasedimentary rock are common in sub-area 9. Although the rocks have granoblastic textures or are locally migmatitic in character, it is inferred that they represent metamorphosed volcanic siltstones of the type deposited during the waning volcanic stage (Fig. 30). Lundqvist (1962) reported interbeds of metaconglomerate in the Ljusterö area. On Utö and Ljusterö, the bedded metavolcanic rocks rest upon dacitic and rhyolitic metavolcanic rocks with metasedimentary interbeds.

Sub-area 10. Hjälmaren–Mälaren

The metavolcanic rocks in sub-area 10 north-east of Örebro (Fig. 28) were metamorphosed under amphibolite-facies conditions and primary volcanic features can be observed in the better preserved western areas. The grade of metamorphism increases eastwards into migmatized, upper amphibolite facies and primary volcanic textures and structures are poorly preserved in the eastern areas. Gorbatschev (1969) and Wikman (1972) described the geology in the western areas and attention is focussed here on the supracrustal rocks in these areas.

Svecofennian supracrustal rocks are situated in an antiformal syncline (*Glanshammar antiform*, see section "Deformation, metamorphism and mechanism of emplacement of the 1.87–1.84 Ga GSDG suite of intrusive rocks"). The stratigraphic order within the antiform is demonstrated by several primary structures in the metavolcanic rocks as well as by stromatolites in a laterally extensive, crystalline carbonate bed (S. Sädbom, personal communication 1999). The character of the rocks suggests that they represent the three different stages in the volcanic activity of the Bergslagen region (Fig. 30). Possible high-grade equivalents are found in the eastern part of the sub-area, where rhyolitic metavolcanic rock, crystalline carbonate rock and garnet-bearing metasedimentary rock occur. In the area north-west of Kungsör, rocks similar to the stratigraphically lowest parts in western areas, such as plagioclase-phyric metadacite and quartzite, are present.

Weak "magnesium alteration" of volcanic rock to mica quartzite followed by metamorphism is present in the Rinkaby area to the west (Wikman 1972). Northwest of Kungsör, for example, a few larger areas of rocks which were formerly regarded as metasedimentary in character have been reinterpreted as volcanic rocks altered to mica-quartz rock and subsequently metamorphosed.

The stratigraphically lowest units are composed of massive, homogeneous rocks. Two stratigraphically and petrographically distinct levels, which Wikman (1972) subdivided into a lower *sodium leptite etage* and an upper *potassium leptite etage*, occur. The lower unit consists

Fig. 37. Scours and ripples in volcanic metasiltstone in sub-area 10. Photograph: Ingmar Lundström (SGU).

of dark grey, massive, homogeneous, plagioclase- and somewhat quartz-phyric, dacitic volcanic sandstone, which is similar to the rocks in the *Storsjön formation* (Lundström 1983). However, these rocks contain clasts of felsic metavolcanic rocks, metabasic rocks and possibly also metasedimentary rocks and are interbedded with quartzite. The upper unit is also a massive, thick and laterally extensive volcanic sandstone, but is reddish, quartz-phyric, potassium-rich and rhyolitic in composition. Sedimentary intercalations are lacking. Both these units are probably extrusive in origin, and represent pyroclastic mass flows deposited during the intense volcanism and extension stage (Fig. 30).

These rocks are stratigraphically overlain by a several hundred metres thick, stromatolite-bearing crystalline carbonate horizon (Wikman 1972). The marble horizon is in turn stratigraphically overlain by planar-bedded to laminated, feldspar-rich, rhyolitic volcanic siltstones, typical for the deposits of the waning stage (Fig. 30). These rocks were referred to as the *banded leptite etage* in Wikman (1972). Locally, this unit is well exposed and displays both planar graded beds, scours and ripples (Fig. 37). It is inferred that the rocks of the waning stage were deposited under rather tranquil to more agitated conditions. However, planar, non-eroded beds dominate the unit. A transition is recorded from shallow water or subaerial deposition, suggested by quartzite interbeds and stromatolitic carbonates, to deposition under deeper water conditions. The latter is represented by the overlying andalusite-bearing mica schists of the later sedimentary, thermal subsidence stage (Fig. 30).

Sub-area 11. Zinkgruvan

The grade of regional metamorphism in sub-area 11 around Zinkgruvan (Fig. 28) varies between lower and upper amphibolite-facies, permitting some reasonably well-preserved but irregularly distributed areas to be present for volcanological interpretation. Wikström & Karis (1991) described the general geology of the area and Allen et al. (1996) based much of their volcanological synthesis on studies in sub-area 11. Kumpulainen et al. (1996) presented various aspects on the stratigraphic and, particularly, the sedimentary evolution of the area. They informally used the term *Emme group* for the supracrustal succession.

Extensive Svecofennian supracrustal sections have been documented in these studies, ranging from felsic metavolcanic rocks with interbeds of quartzite in the stratigraphically lower parts to metasedimentary rocks in the stratigraphically upper parts of the sequence (Fig. 30). The quartzites, referred to as the *Gryt formation* (Wikström & Karis 1991) or *Närkesberg formation* (Kumpulainen et al. 1996), are commonly cross-bedded and resemble similar lithologies at the stratigraphic top of the *Larsbo formation*.

In the Gryt–Zinkgruvan part of sub-area 11 (Fig. 30), rhyolitic metavolcanic rocks east of Närkesberg have been referred to as the *Igelfors formation* (Wikström & Karis 1991, Kumpulainen et al. 1996). The rocks within this formation are massive and homogeneous over large areas, and contain elongate pumice-like clasts with ragged ends as well as phenoclasts of quartz and feldspar. They are interpreted as pyroclastic flow deposits belonging to the intense volcanism and extension stage (Fig. 30) and individual flow units may be discerned. The flows were probably deposited under subaerial conditions, since some show eroded upper contacts overlain by continental, fluviatile, clast-bearing quartzite. The quartzites and volcanic flow deposits are regularly interbedded on a kilometre scale and are inferred to have shared the same depositional environment. Locally, the clastic metavolcanic rocks grade into more coherent phases, which probably represent subvolcanic intrusions. The latter grade in turn into surrounding metagranitoids (GDG intrusive suite), with which they are probably related.

Homogeneous volcanic rocks, which show a somewhat higher degree of metamorphism, lie structurally and probably also stratigraphically above the *Igelfors formation*. This so-called *Mariedamm volcanic unit* (Wikström & Karis 1991) was probably deposited under subaqueous conditions. Locally, the metavolcanic rocks are interbedded with crystalline carbonate and calc-silicate rocks. The stratigraphic relationship between the *Mariedamm volcanic unit* and the metavolcanic rocks that underlie and host the Zinkgruvan ore deposit is structurally complicated and somewhat ambiguous (Hedström et al. 1989). The footwall of the Zinkgruvan ore consists of a thoroughly recrystallized

and potassium altered metarhyolite of uncertain origin. Wikström & Karis (1991) suggested that it may have formed from reworked volcanic material. The host rock to the ore consists of planar-bedded, volcanic siltstone interbedded with crystalline carbonate rock, typical of the waning volcanic stage (Fig. 30).

In the part of sub-area 11 around Godegård (Fig. 30), rhyolitic to dacitic, syn-eruptive mass flow deposits comprise the lowest part of the stratigraphic pile. They contain monomict, angular lithic clasts as well as weakly welded pumice clasts with ragged ends (Fig. 38) and show no indications of density sorting. They are several kilometres thick and are interpreted as subaerial, caldera-fill successions (Allen et al. 1996) that belong to the intense volcanism and extension stage of the volcanic activity (Fig. 30). These rocks grade stratigraphically downwards into fine-grained metagranitoids of probable subvolcanic origin, which pass transitionally into more deep-seated intrusive rocks. Hence, the juvenile metavolcanic rocks at Godegård resemble the rocks in the *Igelfors formation*, but lack quartzite interbeds at the lower stratigraphic levels.

The juvenile metavolcanic rocks are overlain by fluviatile, post-eruptive volcanogenic metasandstones, which were deposited in a subaerial or shallow subaqeous environment (Fig. 30). These rocks pass abruptly upwards into a thick crystalline carbonate horizon (Fig. 30), which, in turn, is overlain by turbiditic, sandy metasedimentary rocks (Fig. 30) referred to as the *Vintergölen formation* (Kumpulainen et al. 1996). The turbiditic rocks were deposited in connection with a rapid subsidence, and the transition from the juvenile metavolcanic deposits of the intense volcanism stage to the deposits of the sedimentary, thermal subsidence stage was also apparently rapid.

Mafic clasts with concave, chilled outlines occur in the Godegård metavolcanic rocks and possible peperitic contacts against metabasic rocks are also present. Thus, basic volcanism appears to have occurred during deposition of the Godegård metavolcanic rocks (Fig. 30). However, Wikström & Karis (1991) and Kumpulainen et al. (1996) regarded the metabasic rocks as essentially younger than the felsic metavolcanic rocks.

Sub-area 12. Orvar Hill and related areas

In the south-western part of the Bergslagen region (Fig. 28), scattered areas dominated by mafic metavolcanic rocks occur. According to Kumpulainen et al. (1996), the rocks are comparable to the mafic metavolcanic rocks in the Zinkgruvan sub-area and they are either older than or similar in age to the 1.87–1.84 Ga GSDG suite of intrusive rocks. However, no geochronological data are available that help to clarify their

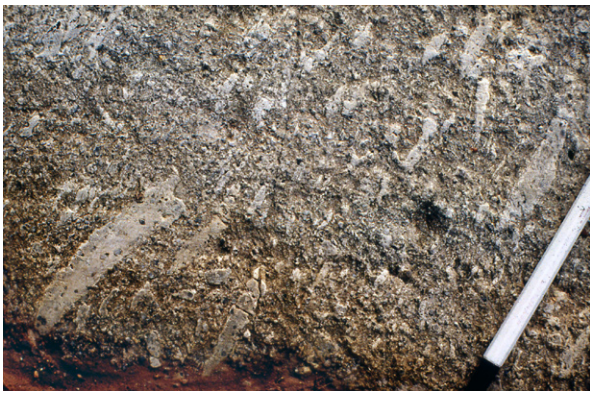

Fig. 38. Pumice clasts with ragged ends at Godegård in sub-area 11. Photograph: Ingmar Lundström (SGU).

stratigraphic position. They are included on the bedrock geological map of the Bergslagen region (Stephens et al. 2007a) together with the Svecofennian volcanic and subvolcanic intrusive rocks (1.91–1.89 Ga).

According to Björklund & Weihed (1997), the so-called Orvar Hill area is a well-preserved, low strain window within the Sveconorwegian orogen. The rocks were metamorphosed under amphibolite-facies conditions and locally display primary structures. The area is dominated by basaltic pillow lava with pillows up to one metre in size. The pillow lavas are interbedded with volcaniclastic material interpreted to have formed as turbidity current deposits. These are in turn overlain by silty to sandy, quartz-bearing metagreywacke. Thus, both coherent and volcaniclastic units indicate a subaqueous depositional environment, and amygdales in the lavas restrict the depositional depth to less than 2000 m. Björklund & Weihed (1997) interpreted the volcaniclastic material to have a subaerial provenance, since, in contrast to the lavas, it is mostly non-spilitic.

The metavolcanic rocks in this area differ from those in the remainder of Bergslagen in having a more primitive source rock, indicated by more primitive Pb isotope compositions (Sundblad 1994). However, the positive ε_{Nd} value (+2.1) calculated for an inferred age of 1.85 Ga (Björklund & Claesson 1992) is compatible with the evolutionary trend defined by the Svecofennian volcanic and younger intrusive rocks on an ε_{Nd} versus age diagram (see section "Sm-Nd analyses of rock suites in the Svecokarelian orogen formed between 1.9 and 1.8 Ga").

Summary

In all sub-areas within the Bergslagen region, the stratigraphically lowermost volcanic rocks belong to the intense volcanism and extension stage (Fig. 30). They consist of more or less juvenile, volcanic mass flows. In

places, individual flow units show normal graded tops from sandy, matrix-supported breccia through sandstone to siltstone. The clasts in sandstone and breccia beds are generally combinations of pumice, crystal fragments and lithic material. In sub-areas 1 and 11, the rocks of the intense volcanism and extension stage formed much thicker successions than in other sub-areas and were interpreted as caldera fill sequences by Allen et al. (1996). In other sub-areas, these rocks presumably represent caldera outflow deposits (e.g. Lipman 1984). Compositionally, the rocks of the intense volcanism stage are dominated by rhyolites, but dacites occur in the easternmost and southernmost sub-areas. Ambient shallow water to subaerial sedimentation in the depositional basin during this stage is locally indicated by intraformational quartzites (sub-areas 1, 10 and 11) and conglomeratic meta-arkose (sub-area 4).

The volcanic rocks of the intense volcanism and extension stage are overlain by bedded to laminated volcanic siltstones to sandstones of the waning volcanic stage (Fig. 30). Intercalations of calcitic to dolomitic crystalline carbonate and calc-silicate rocks are common in this part of the succession. In several sub-areas, at least one thicker (>100 m) crystalline carbonate rock horizon occurs near the stratigraphic top of the sequence in the waning volcanic stage, but, in sub-areas 10 and 11 (Fig. 30), thick crystalline carbonate strata occur immediately on top of the rocks formed during the intense volcanism and extension stage. Compositionally, the volcanic rocks deposited during the waning volcanic stage are rhyolitic to subordinately dacitic. Most iron and base metal mineralizations in Bergslagen are hosted by the lithologies deposited during this stage (see also section "Mineral and bedrock deposits").

From the end of the waning volcanic stage and into the following sedimentary, thermal subsidence stage, a phase of mafic igneous activity occurred. Thus, in sub-areas 2, 3, 6 and 8, mafic lavas and minor intrusions are present at high stratigraphic positions in the rocks of the waning volcanic stage and, in sub-area 1, even in the uppermost slate level included in the sedimentary, thermal subsidence stage. Rocks belonging to the sedimentary stage have also been identified in other sub-areas (Fig. 30). Generally, the rocks belonging to this stage are dominated by volcanogenic slates (see meta-agillite in the previous section); sandstone dominates in sub-areas 3 and 11. The mineralized crystalline carbonate rock horizon at Garpenberg, which lies in the uppermost part of the waning volcanic stage, is overlain by volcanic mass flow rocks (IS2? in Fig. 30) instead of sedimentary rocks. Thus, locally, explosive volcanism also occurred late in the Svecofennian volcanic phase.

Subvolcanic intrusions and cryptodomes intruded the rocks belonging to all three stages in the volcanic evolution. In general, the subvolcanic rocks range from dominantly dacitic to subordinately rhyolitic compositions, but in sub-area 5 and at Grängesberg in sub-area 1, dacitic to andesitic, subvolcanic rocks and dykes occur. According to Allen et al. (1996), the thermal input provided by the intrusion of subvolcanic rocks may be an important factor for the extensive occurrence of metallic mineralization in the strata belonging to the waning volcanic stage. The apatite-bearing iron-rich deposits at Grängesberg (see section "Mineral and bedrock deposits") are at least, in part, hosted by dykes and subvolcanic rocks.

Age of crystallization

Sixteen U-Pb (zircon) ages that date the time of crystallization and contain uncertainties within the range limit adopted in this report are available for the Svecofennian, felsic volcanic and associated subvolcanic intrusive rocks in the Bergslagen region. The locations of the dated samples are shown in Figure 28 and pertinent information concerning the geochronological data is summarized in Table 2. Virtually all the samples analysed are designated as metarhyolite. However, one subvolcanic intrusion from the Sala area with a rhyolitic composition and two amphibolites are also included. Two so-called "meta-tuffites" from the Tunaberg area (Dobbe et al. 1995), which yielded younger ages around 1.87 Ga and 1.84 Ga and were rejected as protolith ages by Lundström et al. (1998), have not been included here. As is evident from Figure 28, the dated samples are relatively unevenly distributed over the project area. The majority of the ages are from the better-preserved, metavolcanic rocks in the central part of the Bergslagen region.

Seven of the sixteen U-Pb (zircon) ages have been obtained in connection with the Bergslagen project (Table 2). This analytical campaign focussed on pyroclastic flow deposits, since such units formed by practically instantaneous and laterally very extensive processes. Hence, they are ideal time markers. The intense volcanism and extension stage produced numerous such units, but during the ensuing waning stage, pyroclastic flow deposition was rare and alternated with ash fall and lava flow emplacement. A more detailed description of these samples as well as the geochronological results is provided in the appendix.

If all the uncertainties in the ages are taken into account and the three ages with uncertainties greater than or equal to 10 Ma are excluded, the range for the timing of crystallization of the Svecofennian volcanic and

Table 2. U-Pb (zircon) ages for the Svecofennian volcanic and subvolcanic intrusive rocks in the Bergslagen region.

Lithology	Method	Age (Ma)	N-S coordinate	E-W coordinate	Reference
Metarhyolite (mass flow, Broddbo)	U-Pb zircon (TIMS)	1906±3	6653405	1542205	Appendix 2, this publication
Metarhyolite (mass flow, Utö)	U-Pb zircon (TIMS)	1904±4	6541400	1647200	Lundström et al., 1998 GFF 120, 315–320
Metarhyolite (Gryt)	U-Pb zircon (TIMS)	1901±18	6530800	1474650	Kumpulainen et al., 1996 Econ. Geol. 91, 1009–1021
Metarhyolite (mass flow, Hällefors)	U-Pb zircon (TIMS)	1897±6	6636190	1428740	Appendix 2, this publication
Metarhyolite (mass flow, Älvlången)	U-Pb zircon (TIMS)	1896±2	6588195	1440645	Appendix 2, this publication
Amphibolite (Fiskbäcken)	U-Pb zircon (SIMS)	1895±5	6681100	1492300	Andersson et al., 2006 Geol. Mag. 143, 679–697
Metarhyolite (ash-fall tuff, Sala)	U-Pb zircon (TIMS)	1894±2	6642500	1542500	Appendix 2, this publication
Metarhyolite (mass flow, Dannemora)	U-Pb zircon (TIMS)	1894±4	6678820	1614300	Appendix 2, this publication
Metarhyolite (Snättbo)	U-Pb zircon (TIMS)	1892±6	6632350	1413340	Welin, 1987 Prec. Res. 35, 95–113
Metaporphyry (subvolcanic intrusion, Sala)	U-Pb zircon (TIMS)	1892^{+5}_{-4}	6647940	1544500	Appendix 2, this publication
Supracrustal rock, volcanic (Borggårde)	U-Pb zircon (SIMS)	1892±7	6681800	1631900	Andersson et al., 2006 Geol. Mag. 143, 679–697
Metarhyolite (mass flow, Hällefors)	U-Pb zircon (TIMS)	1891±4	6629150	1435900	Lundström et al., 1998 GFF 120, 315–320
Metarhyolite (Uppsala)	U-Pb zircon (TIMS)	1891±10	6642800	1596800	Welin, 1987 Prec. Res. 35, 95–113
Metarhyolite (mass flow, Garpenberg)	U-Pb zircon (TIMS)	1891±2 (UI, 4 fractions) 1823±7 ($^{207}Pb/^{206}Pb$ age, 1 fraction)	6687600	1521500	Appendix 2, this publication
Felsic metavolcanic rock (Ramhäll)	U-Pb zircon (SIMS)	1888±12	6666350	1618500	Andersson et al., 2006 Geol. Mag. 143, 679–697
Amphibolite (Rishöjden)	U-Pb zircon (SIMS)	1887±5	6630600	1445900	Andersson et al., 2006 Geol. Mag. 143, 679–697

subvolcanic intrusive rocks in the Bergslagen region lies between 1909 and 1882 Ma (Table 2 and Fig. 39). The age of the pyroclastic flow from Broddbo (sub-area 4) shows that the intense stage of Svecofennian volcanism in the Bergslagen region started at 1906±3 Ma. This is supported by the dating of the pyroclastic flow at Utö in sub-area 9 (1904±4 Ma, Lundström et al. 1998). The stage of intense volcanism was still active approximately ten million years later, according to the age-dating results from Hällefors (sub-area 1, 1897±6 Ma) and Dannemora (sub-area 6, 1894±4 Ma). It ended around 1895 Ma, as indicated by the dating work at Älvlången near Vikern (sub-area 1, 1896±2 Ma) and Sala (sub-area 4, 1894±2 Ma) where units belonging to the waning stage are represented.

Since the rocks belonging to the waning stage at Sala in sub-area 4 are intruded by a subvolcanic intrusion with an age of 1892^{+5}_{-4} Ma, it is inferred that they were deposited prior to this time. Thus, the rock units in the waning volcanic stage, locally including thick stromatolitic carbonate beds, were deposited during a time span of approximately five million years. The stratigraphically uppermost carbonate bed at Garpenberg, belonging to the waning stage of volcanism, was overlain by a pyroclastic flow at 1891±2 Ma. The flow was subsequently intruded by a subvolcanic dacite. The geochronological data presented in this report more or less confirm the results presented by Lundström et al. (1998), who concluded that volcanism started at 1904 and was still active at 1891 Ma.

Inherited zircons with U-Pb ages around 1.94–1.91 Ga are present in two amphibolites that crystallized at c. 1.89 Ga (Andersson et al. 2006 and Table 2). These data indicate the occurrence of a pre-1.91 Ga crust in the Bergslagen region (Andersson et al. 2006) that is only slightly older than the Svecofennian volcanic and subvolcanic intrusive rocks.

Geochemistry

The localities where data bearing on the geochemical composition of Svecofennian volcanic and subvolcanic intrusive rocks have been acquired and used in this report are shown in Figure 40. 153 geochemical analyses

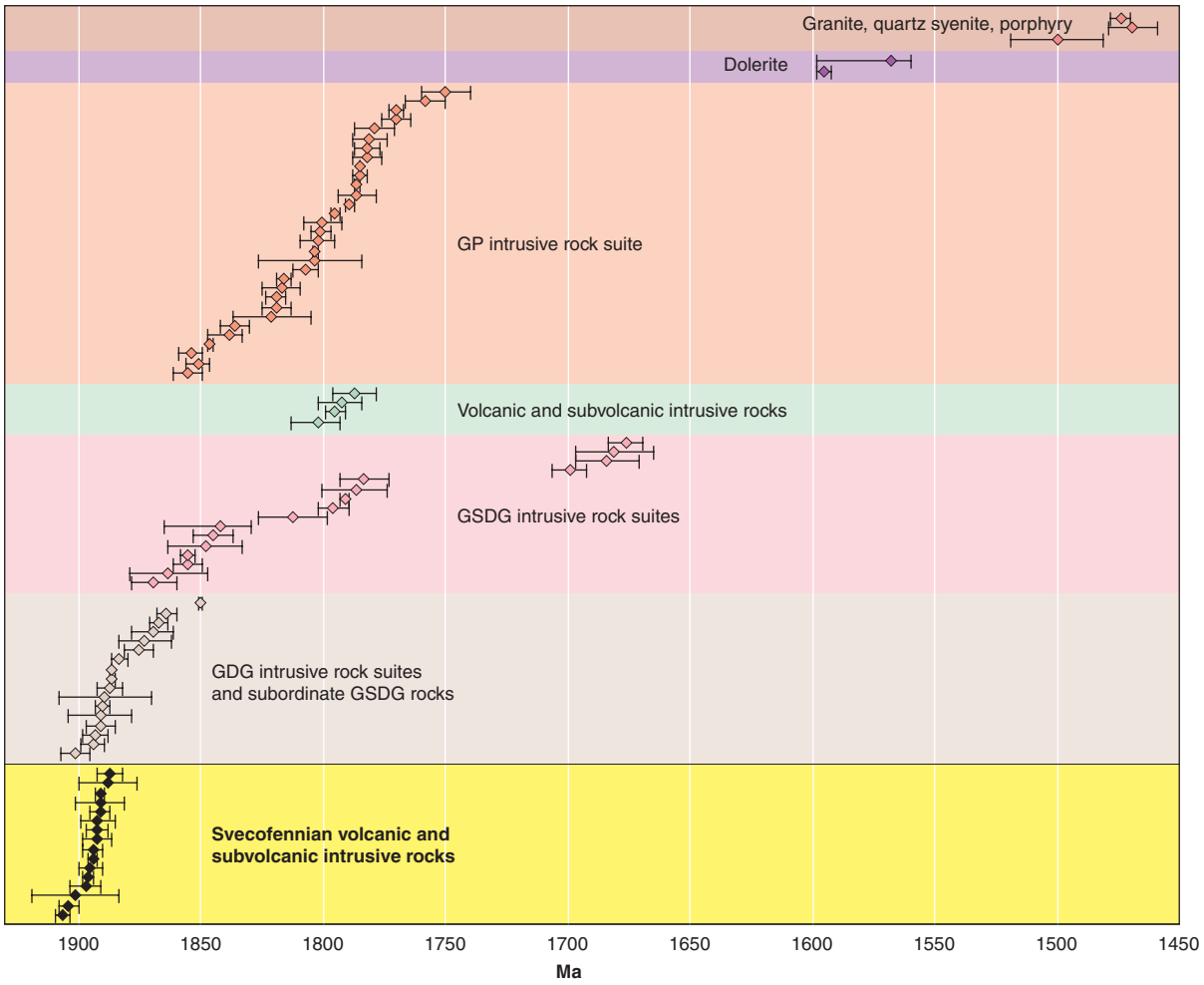

Fig. 39. Summary of U-Pb (zircon) age dates for the Svecofennian volcanic and subvolcanic intrusive rocks in the Bergslagen region. For purposes of comparison, all determinations of the age of crystallization of igneous and meta-igneous rocks in this region, with the exception of a U-Pb (baddeleyite) age from a dolerite in the Falun area (946±1 Ma), are shown and identified according to rock suite(s).

from SGU's bedrock geochemistry database have been used in the compilation work.

The significant alteration that involved a redistribution of the alkali elements sodium and potassium is expressed in the large spread of the analyses in Figure 41a. Several of the analyses lie outside the field in this diagram that shows unaltered volcanic rocks, the so-called igneous spectrum of Hughes (1973). Apparent enrichment in both K_2O and in Na_2O is conspicuous. Even the samples that lie within the igneous spectrum show high total alkali contents.

On the basis of the patterns in the total alkali–SiO_2 diagram for volcanic rocks (Le Bas et al. 1986), where only the samples that lie inside the igneous spectrum of Hughes (1973) have been plotted, and the $Zr/TiO_2 \times 0.0001$ diagram (Winchester & Floyd 1977), where all samples have been plotted, the metavolcanic rocks define a subalkaline trend (Figs. 41b and 41c). The majority of metavolcanic rocks show a rhyolitic or dacitic composition and the subalkaline trend continues through the andesitic, basaltic andesite and basalt fields. The inferred less altered rocks all display a predominantly medium-K or even high-K composition (Fig. 41d).

Representative samples with variable SiO_2 content are enriched in large ion lithophile elements (LILE), such as Ba, Rb, Th and K, relative to high field strength elements (HFSE), such as Zr, Hf, Y and Yb (Fig. 42). Distinctive negative anomalies for Nb and even for Sr, P and Ti are also conspicuous on this spider diagram. This pattern resembles that observed along normal to mature, active continental margins (Brown et al. 1984). Most samples show an enrichment in light rare earth (LREE) relative to heavy rare earth (HREE) elements with a weak, negative Eu anomaly (Fig. 43). However, some samples are also depleted in La, Ce, Nd and Sm, which may be related to alkali alteration. The mobility of rare earth elements in the Svecofennian volcanic rocks was addressed in Baker and de Groot (1983).

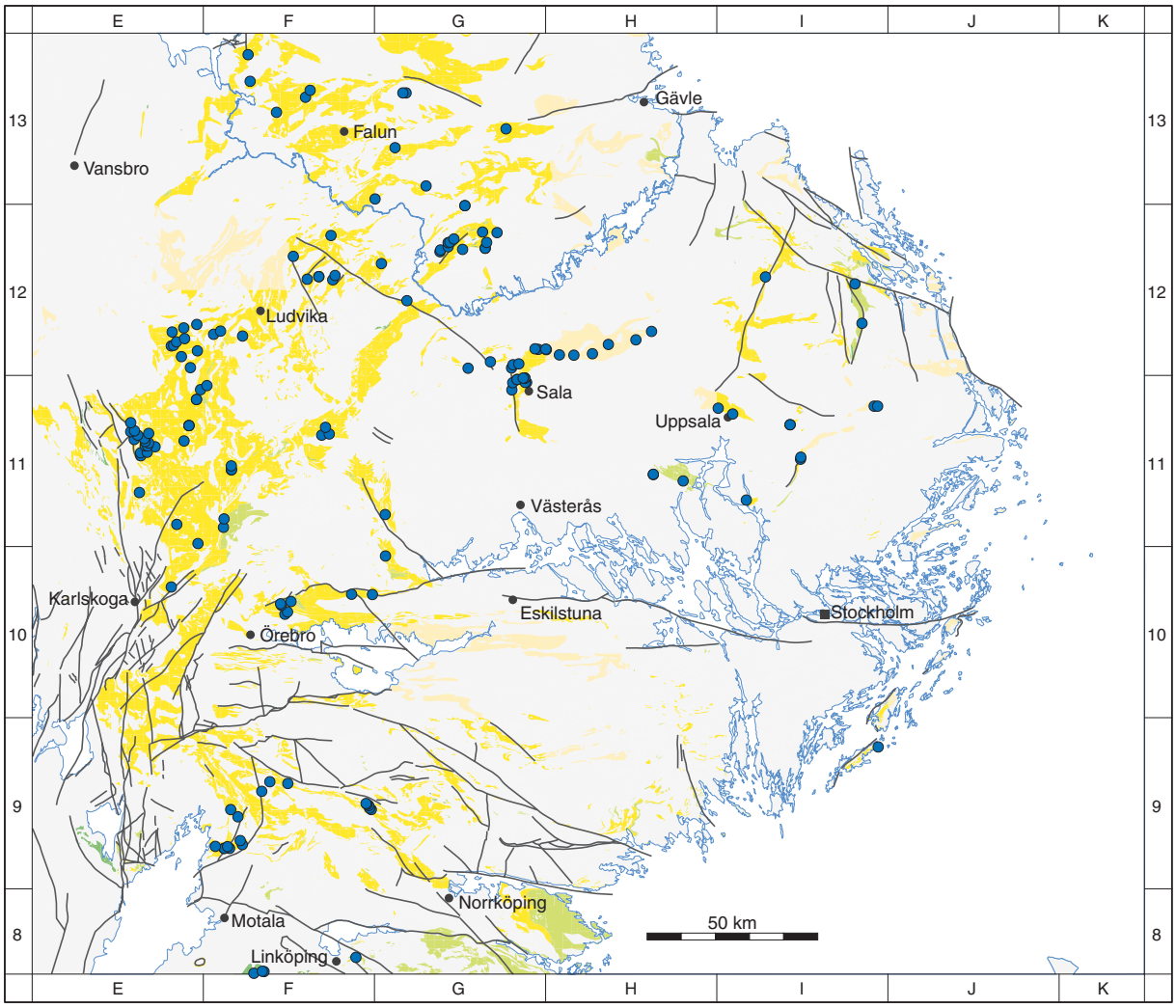

Fig. 40. Location of sample sites for the geochemical analysis of Svecofennian volcanic and subvolcanic intrusive rocks in the Bergslagen region. See Figure 28 for legend to the base geological map.

Mafic metavolcanic rocks from predominantly the eastern part of the Bergslagen region lie inside or immediately adjacent to the fields designated as B and C in the Zr–Ti/100–Y×3 diagram (Fig. 44). Calc-alkaline basalts from active continental margins are included within these two fields (Pearce & Cann 1973).

Petrophysical characteristics and regional geophysical signature

The localities where data bearing on the petrophysical properties of Svecofennian volcanic and subvolcanic intrusive rocks have been acquired and used in this report are shown in Figure 45. Samples from 1359 localities have been analysed, whereas in situ gamma radiation measurements have been carried out at 191 sites. These data have been extracted from SGU's petrophysical database.

Density

The density distribution for the Svecofennian volcanic and subvolcanic intrusive rocks and a comparison with all rocks in the Bergslagen region is shown in Figure 46a. The density values for the Svecofennian rocks are concentrated around 2 660–2 700 kg/m^3, with a mean density of 2 685 kg/m^3. The lower mean density compared with the total population (2 713 kg/m^3), is related to the relatively small number of intermediate and mafic rocks that are present in the analysed samples. This data bias is geologically meaningful, since it reflects the dominant rhyolitic and dacitic compositions of the metavolcanic rocks in the outcrops at the ground surface.

Magnetic susceptibility

The density–susceptibility diagram is shown in Figure 46b. The magnetic susceptibility is shown on a

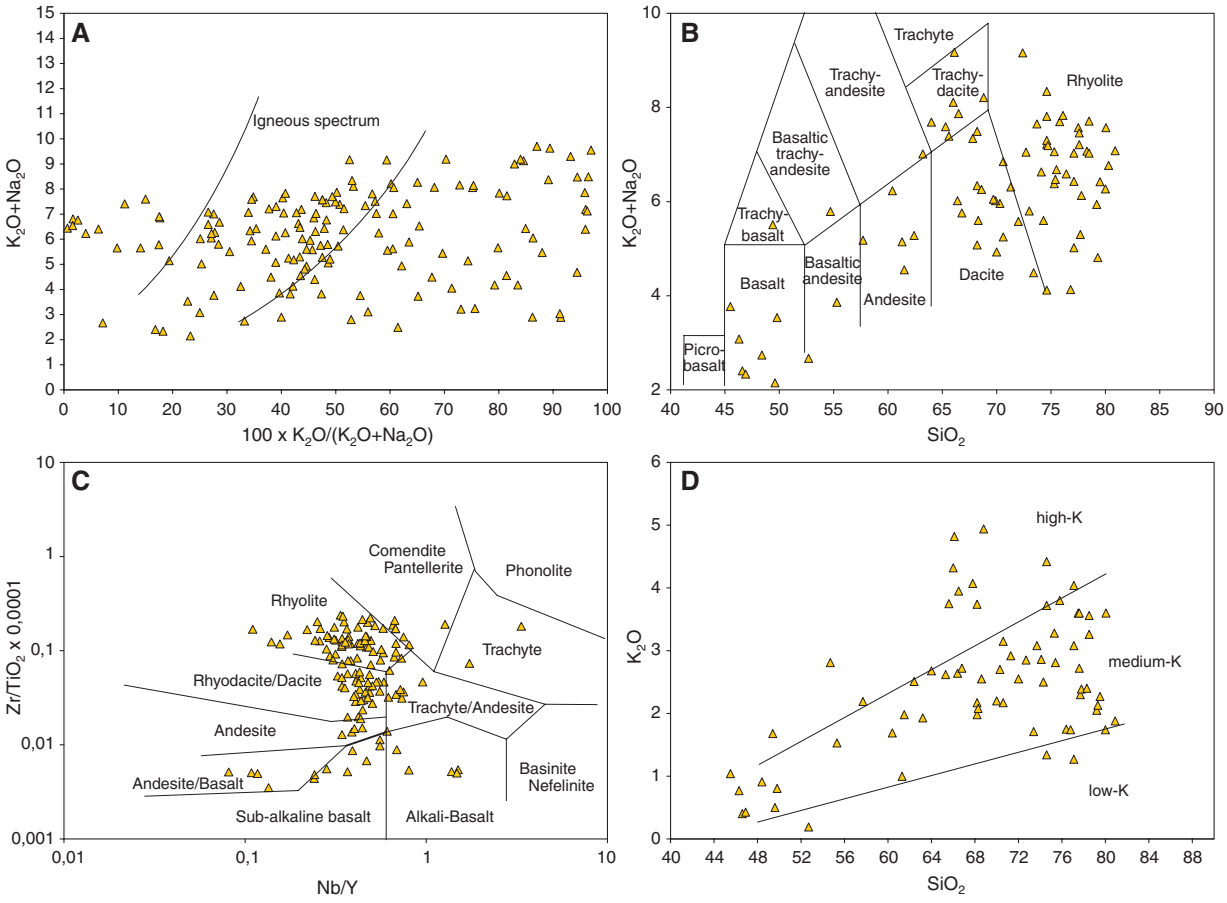

Fig. 41. Geochemical characteristics of the Svecofennian volcanic and subvolcanic intrusive rocks in the Bergslagen region. **A.** Alteration diagram after Hughes (1973). Rock geochemical classification diagrams after **B.** Le Bas et al. (1986), **C.** Winchester & Floyd (1977) and **D.** Peccerillo & Taylor (1976), respectively. Only samples that lie inside the igneous spectrum in A have been plotted in B and D.

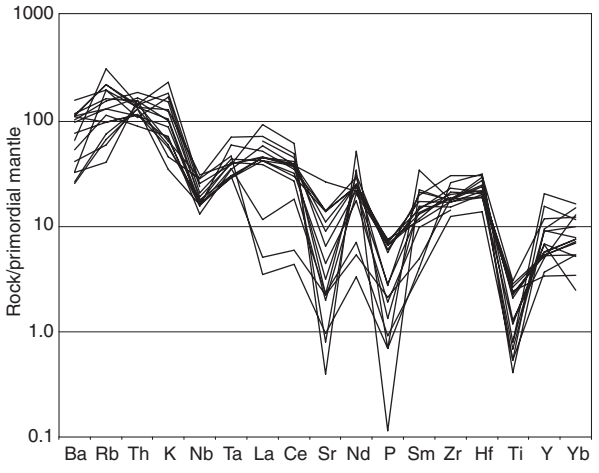

Fig. 42. Rock/primordial mantle spider diagram showing the relationships between large ion lithophile (LILE, e.g. Ba, Rb) and high field strength (HFSE, e.g. Zr, Ti and Y) elements for representative samples of Svecofennian volcanic and subvolcanic intrusive rocks in the Bergslagen region. SiO_2 values for the selected samples span from 66.4 to 80.9%. Primordial mantle values after McDonough et al. (1992).

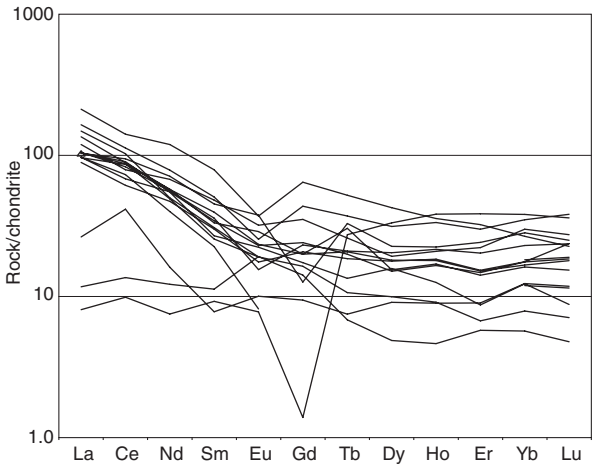

Fig. 43. Rock/chondrite diagram showing the relationships between light rare earth (LREE, e.g. La, Ce) and heavy rare earth (HREE, e.g. Yb, Lu) elements for representative samples of Svecofennian volcanic and subvolcanic intrusive rocks in the Bergslagen region. SiO_2 values for the selected samples span from 66.4 to 80.9%. Chondrite values after Boynton (1984).

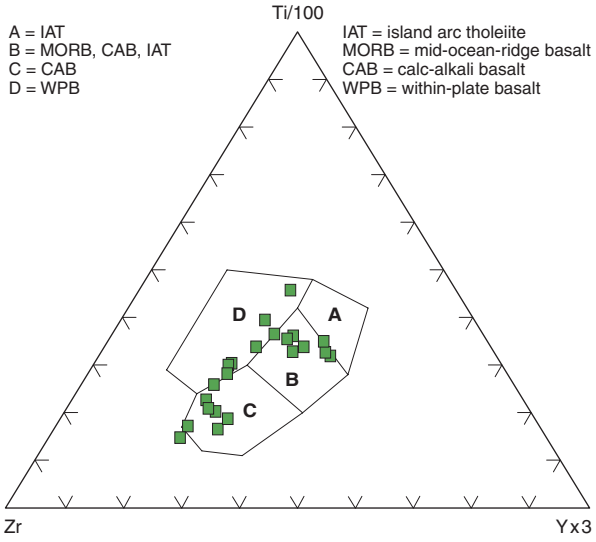

Fig. 44. Distribution of Svecofennian mafic volcanic rocks in the Bergslagen region in the Zr–Ti/100–Y x 3 diagram of Pearce & Cann (1973).

logarithmic scale. The metavolcanic rocks show a large variation in magnetic susceptibility with possible concentrations between 100 and 1 000 as well as 10 000–100 000 × 10^{-6} SI. The magnetite mineralizations in the Bergslagen region are hosted by felsic metavolcanic rocks and most of the samples are collected from the mineralized areas in the western part of Bergslagen (Fig. 45). The strongly mineralized belts around Ludvika and Norberg are clearly seen on the magnetic anomaly map as prominent positive magnetic anomalies (Stephens et al. 2002a). Anomalies up to +35 000 nT have been measured in this region.

Gamma radiation

The gamma radiation characteristics of the Svecofennian volcanic and subvolcanic intrusive rocks are presented in Figure 47. Most of the samples show low concentrations of uranium and thorium, whereas the concentration of potassium is more variable, from 0.3% up to more than 7%.

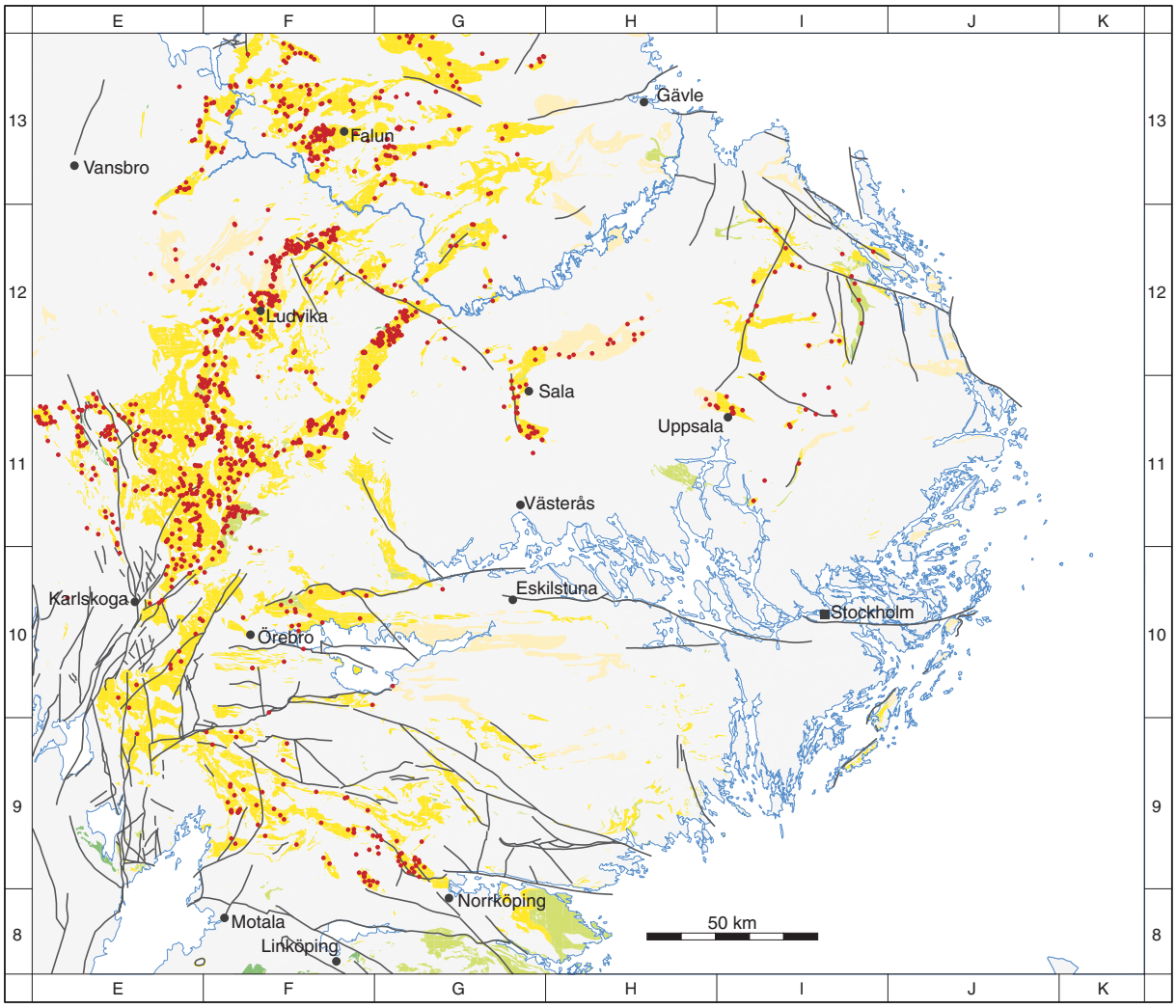

Fig. 45. Location of sample sites of Svecofennian volcanic and subvolcanic intrusive rocks in the Bergslagen region for petrophysical and gamma radiation measurements (red dots). See Figure 28 for legend to the base geological map.

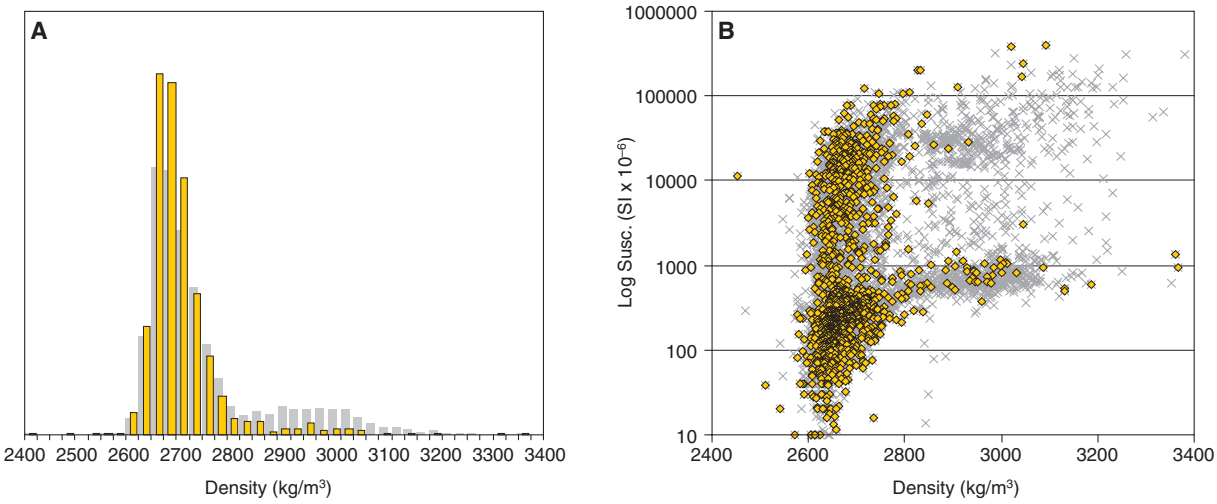

Fig. 46. **A.** Density distribution and **B.** magnetic susceptibility–density diagrams for Svecofennian volcanic and subvolcanic intrusive rocks. For purposes of comparison, all samples from the Bergslagen region are shown in grey.

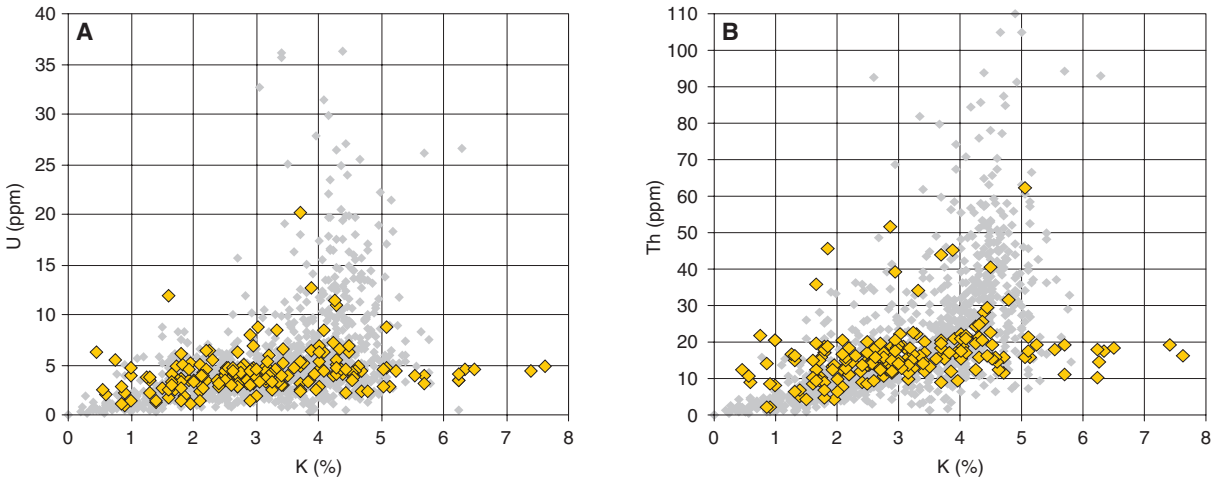

Fig. 47. Concentrations of **A.** uranium versus potassium and **B.** thorium versus potassium for Svecofennian volcanic and subvolcanic intrusive rocks. For purposes of comparison, all samples from the Bergslagen region are shown in grey. The anomalously high values of potassium are related to hydrothermal alteration in the metavolcanic rocks (see also text).

The gamma radiation measurements of potassium in outcrops provide some constraints on the ratio between sodium and potassium in the metavolcanic rocks and the effects of hydrothermal alteration that involves redistribution of the alkali elements (see above). Low concentrations of potassium indicate that the rock is apparently depleted in potassium and enriched in sodium. The opposite is the case for anomalously high concentrations of potassium. This feature has been used to recognize the spatial distribution of areas affected by potassium alteration (see above). One of the largest potassium-enriched anomalies in Sweden occurs north of Zinkgruvan, on map sheet 9E Askersund SV, in the area to the north of Motala. This anomaly can be clearly observed on the published potassium–uranium–thorium composite map (Stephens et al. 2002b) as a pale green shading.

Granitoid-dioritoid-gabbroid (GDG) intrusive rock suites (1.90–1.87 and 1.87–1.85 Ga) and subordinate Granite-syenitoid-dioritoid-gabbroid (GSDG) intrusive rocks (1.88–1.87 Ga)

Rock type, spatial distribution and intrusion–deformation relationships

Rock composition and texture

The Svecofennian supracrustal rocks in the Bergslagen region were intruded by large volumes of quartz-rich magmas that crystallized to plutonic rocks with a composition that ranges from tonalite to granodiorite and granite. Plutonic rocks that are intermediate, mafic and even ultramafic in composition are spatially associated with these quartz-rich rocks and all were

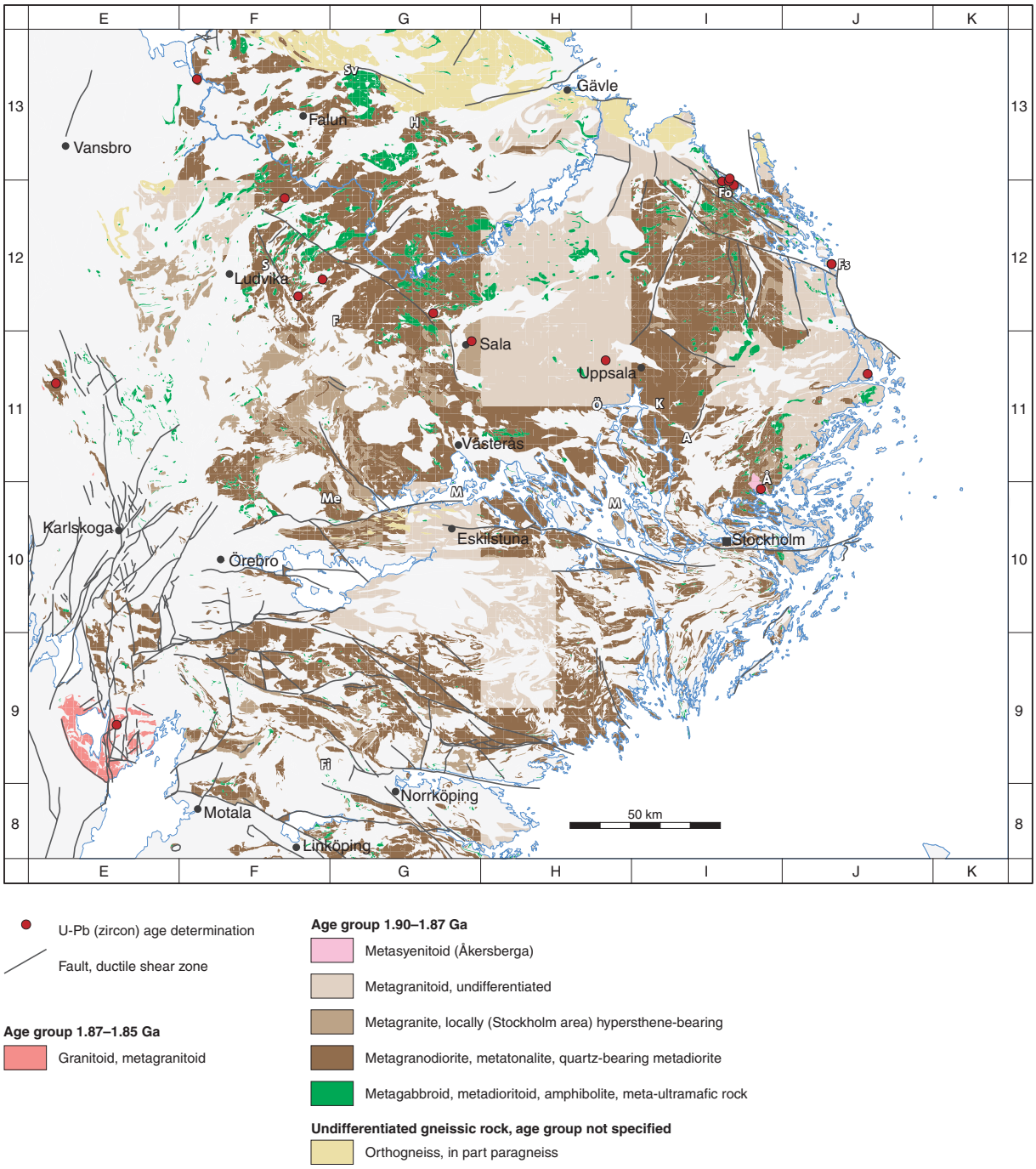

Fig. 48. Distribution of the GDG intrusive rocks at the ground surface in the Bergslagen region. The metasyenitoids in the Åkersberga area, north of Stockholm, which resemble the Granite-syenitoid-dioritoid-gabbroid (GSDG) intrusive rocks (see later text), and the undifferentiated ortho- and paragneisses in the northern part of the region are also included on the map. Furthermore, the location of samples that have been dated using the U-Pb (zircon) technique and the location of place names referred to in the section "Granitoid-dioritoid-gabbroid (GDG) intrusive rock suites (1.90–1.87 and 1.87–1.85 Ga) and subordinate Granite-syenitoid-dioritoid-gabbroid (GSDG) intrusive rocks (1.88–1.87 Ga)" are shown. Å = Åkersberga, A = Arlanda, F = Fagersta, Fi = Finspång, Fs = Fogdösten, Fo = Forsmark, H = Hofors, K = Knivsta, Me = Medåker, M = Mälaren, Ö = Örsundsbro, S = Smedjebacken, Sv = Svärdsjö.

affected by metamorphism, predominantly under amphibolite-facies conditions. Together these rocks form a prominent intrusive rock association, referred to here as the Granitoid-dioritoid-gabbroid or GDG intrusive rocks (Fig. 48).

The U-Pb (zircon) geochronological data (see below) suggest that the bulk of these rocks formed between 1.90 and 1.87 Ga. However, plutonic and hypabyssal GDG rocks with younger ages between 1.87 and 1.85 Ga have been documented in both the north-east-

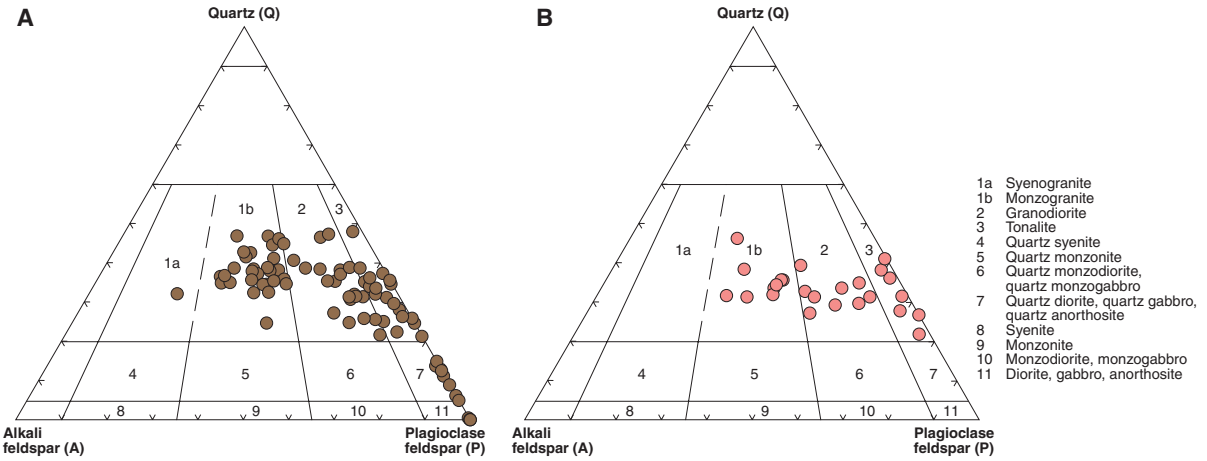

Fig. 49. QAP (F=0) modal classification of analysed surface samples for **A.** the older GDG intrusive rocks (group B of Stephens et al. 2003, 2005) and **B.** the younger GDG intrusive rocks (group C of Stephens et al. 2003, 2005) at Forsmark, in the north-eastern part of the Bergslagen region. These rocks belong to the 1.90–1.87 Ga and 1.87–1.85 Ga suites of GDG rocks in the Bergslagen region, respectively. Granites included in the group D rocks at Forsmark (Stephens et al. 2003, 2005) are also included in Figure 49b. Figures modified after Stephens et al. (2005).

ern and south-western parts of the Bergslagen region. The GDG rocks with an age of 1.85 Ga in the south-western part of the region are sufficiently large to merit attention as a separate rock unit on the geological map (Fig. 48). Thus, two separate age suites of GDG rocks are inferred to be present in the Bergslagen region.

Many of the descriptions to SGU's bedrock maps at local scale (Table 1) contain modal analyses that provide a basis for the assessment of bedrock composition. Based on these analyses, the quartz-rich, felsic rocks in the Bergslagen region have been divided into granitic, granodioritic to granitic, and tonalitic to granodioritic varieties (Stephens et al. 2007a, cf. Fig. 48). In the areas where bedrock mapping at the local scale has not been completed (Fig. 6), no subdivision has been made and the rocks are simply shown as metagranitoids on the bedrock map (Fig. 48). At the time of completion of the bedrock map compilation, no data were available to confidently distinguish felsic intrusive and felsic volcanic rocks in the high-grade metamorphic domain in the north-eastern part of the study area. For this reason, these rocks are simply shown as orthogneisses (Fig. 48). Some paragneisses are also probably present in these areas.

Representative compositional trends are shown on the Streckeisen plot for the so-called group B plutonic rocks and groups C and D hypabyssal rocks at Forsmark (Stephens et al. 2003, 2005), in the north-eastern part of the Bergslagen region (Fig. 49). Field, compositional and high-resolution, geochronological data in this area (Stephens et al. 2003, Hermansson et al. 2007, 2008a) indicate that the rocks in group B belong to the older (1.90–1.87 Ga) suite of GDG rocks and at least the group C rocks belong to the younger (1.87–1.85 Ga) suite of GDG rocks. The similarity in the trends of the modal compositions of the rocks in these two suites and the high content of quartz in all the more evolved samples, i.e. a granitoid trend rather than a syenitoid trend, are conspicuous (Fig. 49).

Enclaves of mafic or intermediate rock are particularly conspicuous in the tonalitic to granodioritic rocks (Fig. 50a) and illustrate the mingling and close temporal relationships between the different melt fractions. Metagranitoids, in particular the granodioritic to granitic varieties, vary in grain size and texture, and porphyritic varieties are also present (Figs. 50b and c). In the southern part of the study area, for example around Finspång, west of Norrköping, there have been difficulties during mapping at the local scale (compare, for example, Wikström 1976 and Wikström & Karis 1991) to distinguish older, porphyritic GDG metagranites from deformed and metamorphosed, porphyritic granites in the younger, so-called Granite-syenitoid-dioritoid-gabbroid or GSDG intrusive rock complex (see later section). The model presented in Wikström & Karis (1991) has been adopted here. This problem can only be resolved with more high-resolution, geochronological data.

Around Åkersberga, immediately north of Stockholm, the felsic plutonic rocks have traditionally been included among the GDG rocks ("gneiss granite" of Stålhös 1969). However, these rocks are porphyritic and vary in composition from quartz monzodiorite to quartz monzonite and granite (Stålhös 1972). Both compositionally and texturally, these rocks resemble the GSDG rocks (see later section) and should be included in the latter. In the same manner as other GDG

Fig. 50. Character of some GDG intrusive rocks and the GSDG intrusive rocks close to Åkersberga, Bergslagen region. **A.** Metatonalite with enclaves that show an intermediate to mafic composition. East of Knivsta (11I Uppsala NV). Photograph: Jan-Olof Arnbom (SGU). **B.** Coarse-grained and unequigranular to porphyritic granite only slightly affected by ductile strain. Örsundsbro (11H Enköping NO). Photograph: Magnus Ripa (SGU). **C.** Porphyritic metagranodiorite or metagranite showing penetrative linear grain-shape fabric. The K-feldspar phenocrysts are also affected by the lineation. South of Medåker (10F Örebro NO). Photograph: Michael Stephens (SGU). **D.** Mafic enclave in porphyritic granite to quartz monzonite close to Åkersberga (10I Stockholm NO). Some of the larger K-feldspar grains in this rock are mantled with plagioclase feldspar and the rock is also strongly lineated (see also photograph of section subparallel to the mineral stretching lineation from the same outcrop in Fig. 51b). View of section at high angle to the mineral stretching lineation. Photograph: Michael Stephens (SGU).

and GSDG rocks, the plutonic rocks around Åkersberga display mingling and mixing relationships with mafic material (Fig. 50d).

Spatial distribution

The GDG intrusive rocks occupy the largest area on the published bedrock geological map of the Bergslagen region (Stephens et al. 2007a). Intermediate, mafic and ultramafic plutonic rocks as well as metagranitoids with a tonalitic to granodioritic composition occur most frequently in the northern part of the region (Fig. 48). These spatial relationships on a regional map scale as well as the mingling relationships on a smaller scale suggest a genetic link between the magma types within this compositional range, possibly by generation of tonalite by partial melting of mafic rock. However, the occurrence of garnet- and fragment-rich metatonalite in the metagreywackes of the *Larsbo formation*, between Fagersta and Smedjebacken, east of Ludvika, opens the possibility that at least these tonalitic rocks formed by partial melting of the host sedimentary rocks. The garnet-rich metatonalite has previously been interpreted as sedimentary in origin in some earlier work (Strömberg & Nisca 1983, cf. Hjelmqvist 1966). Granitic rocks are present throughout the Bergslagen region, but are most conspicuous in the central, western part (Fig. 48).

South of Stockholm, principally in the map area 10I Stockholm SO, hypersthene-bearing granites are present (Stålhös 1969). Besides hypersthene, these granites com-

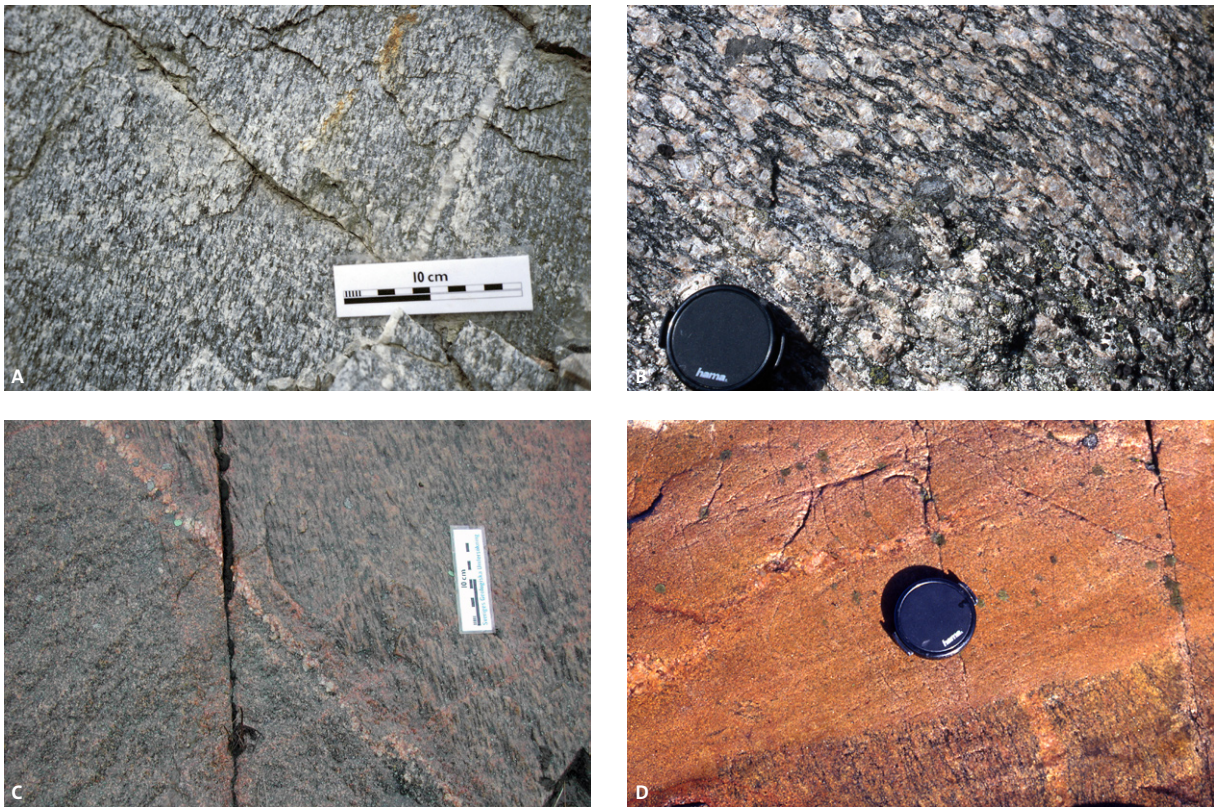

Fig. 51. Intrusion–deformation relationships in some GDG intrusive rocks and the GSDG rocks close to Åkersberga, Bergslagen region. **A.** Penetrative, linear grain-shape fabric in metatonalite (pre-tectonic). Arlanda (11I Uppsala SV). Photograph: Michael Stephens (SGU). **B.** Penetrative, linear grain-shape fabric in porphyritic granite to quartz monzonite, GSDG plutonic rock (pre-tectonic). Åkersberga (10I Stockholm NO). View of section subparallel to the mineral stretching lineation. Photograph: Michael Stephens (SGU). **C.** Minor intrusion of metagranodiorite (group C of Stephens et al 2003, 2005) mildly discordant to penetrative ductile strain in older metagranite (group B of Stephens et al 2003, 2005). The metagranodiorite is inferred to belong to the younger, 1.87–1.85 Ga GDG suite in the Bergslagen region and is only affected by a linear grain-shape fabric (not visible in view here). Forsmark (13I Österlövsta SO). Photograph: Michael Stephens (SGU). **D.** Granite dyke (group D of Stephens et al 2003, 2005) strongly discordant to penetrative ductile strain in older metagranite (group B of Stephens et al 2003, 2005). Note also the occurrence of an earlier generation of pegmatite along the penetrative ductile fabric. Forsmark (13I Österlövsta SO). Photograph: Michael Stephens (SGU).

monly contain perthitic microcline and sporadically also antiperthitic plagioclase (Sundius 1948), indicating that the rocks can be classified as charnockites. Hypersthene is not unique for these granites, but sporadically occurs in other metagranitoids in the Stockholm area (Stålhös 1969). These relationships tentatively indicate that the charnockites are metamorphic in origin, and that low-pressure, granulite-facies metamorphic conditions locally prevailed during the Svecokarelian orogeny in the area south of Stockholm.

Intrusion–deformation relationships

The plutonic GDG rocks in the Bergslagen region (Fig. 51a) and even the subordinate GSDG rocks in the Åkersberga area (Fig. 51b), north of Stockholm, are pre-tectonic in character. Nevertheless, depending on the degree of ductile deformation and metamorphic alteration, these intrusive rocks vary in character from weakly to strongly deformed. In strongly deformed or migmatitic areas, there are often difficulties to distinguish between metagranitoids and rocks of supracrustal origin, especially when the rocks are intimately mixed due to original, sheet-like intrusions of granitoid magma within the supracrustal sequence.

Close to Forsmark, in the north-eastern part of the Bergslagen region, both GDG age suites have been recognized with the help of detailed field investigations (Stephens et al. 2003, 2005) in combination with high-precision geochronological data (Hermansson et al. 2007, 2008a). Granodiorites and tonalites dated at 1.86 Ga (group C rocks in Stephens et al. 2003), which are included in the younger, 1.87–1.85 Ga GDG suite in the Bergslagen region, intruded after ductile deformation and metamorphism had affected the older plutonic rocks dated at 1.89 to 1.87 Ga (Fig. 51c). The latter are included in the older 1.90–1.87 Ga GDG intrusive suite in this region. However, penetrative ductile deformation under lower-grade metamorphic conditions has also affected the younger granodiorites and tonalites. By contrast, even younger fine- to

Table 3. U-Pb (zircon) ages for the GDG intrusive rocks in the Bergslagen region. The age determination from the intrusive rock in the vicinity of Åkersberga (1875±5 Ma), which shows an affinity to the GSDG rocks, is grouped together with the GDG rocks in the table.

Lithology	Method	Age (Ma)	N-S coordinate	E-W coordinate	Reference
Metatonalite (Fogdösten)	U-Pb zircon	1901±6	6672170	1666390	Appendix 2, this publication
Metatonalite, garnet-bearing (Larsbo)	U-Pb zircon (SIMS)	1894±5	6661500	1489500	Andersson, 2004 Unpublished research report, SGU–contract 03–1025/97, Andersson et al., 2004a. GFF 126, 16–17
Quartz-bearing metadiorite (Larsbo)	U-Pb zircon (SIMS)	1893±5	6667110	1497569	Andersson, 2004 Unpublished research report, SGU–contract 03–1025/97, Andersson et al., 2004a. GFF 126, 16–17
Granite (Sala-Vänge)	U-Pb zircon	1891±6	6646600	1546980	Ripa & Persson, 1997 SGU C 830, 57–62
Meta-aplite (Fogdösten)	U-Pb zircon	1891±13	6672170	1666390	Appendix 2, this publication
Granodiorite (Sala)	U-Pb zircon	1890±3	6655920	1534350	Persson, 1993 SGU C 823, 32–35
Granite (Vätö)	U-Pb zircon	1889±19	6635780	1678350	Persson & Persson, 1999 SGU C 831, 91–99
Granite (Horrsjö)	U-Pb zircon	1887±5	6632660	1409140	Högdahl & Jonsson, 2004 GFF 126, 23
Metagabbro (Forsmark)	U-Pb zircon	1886±1	6699652	1630093	Hermansson et al., 2008a Prec. Res. 161, 250–278
Granite (Vänge)	U-Pb zircon	1886	6640300	1591500	Welin et al., 1980 Prec. Res. 13, 87–101
Metatonalite (Forsmark)	U-Pb zircon (SIMS)	1883±3	6698336	1634013	Hermansson et al., 2008a Prec. Res. 161, 250–278
Granite (Åkersberga)	U-Pb zircon	1875±6	6597610	1642960	Persson & Persson, 1997 GFF 119, 91–95
Granite (Svärdsjö)	U-Pb zircon	1873^{+10}_{-11}	6733490	1455880	Åberg et al., 1983b Geol. Fören. Stockh. Förh. 105, 199–203
Granite (Ludvika)	U-Pb zircon	1869^{+9}_{-8}	6694000	1485000	Åberg & Strömberg, 1984 Geol. Fören. Stockh. Förh. 106, 209–213
Metagranite (Forsmark)	U-Pb zircon (SIMS)	1867±4	6699740	1632290	Hermansson et al., 2008a Prec. Res. 161, 250–278
Metagranodiorite (Forsmark)	U-Pb zircon (SIMS)	1864±4	6700532	1632663	Hermansson et al., 2008a Prec. Res. 161, 250–278
Tonalite (Tiveden)	U-Pb zircon	1850±1	6519450	1429300	Wikström, 1996 SGU C 828, 41–47

medium-grained, granite dykes dated at 1.85 Ga (group D rocks in Stephens et al. 2003) are strongly discordant to the ductile deformation and amphibolite-facies metamorphism in the area (Fig. 51d). Further implications of these critical field relationships are addressed in the section "Deformation, metamorphism and mechanism of emplacement of the 1.87–1.84 Ga GSDG suite of intrusive rocks".

Age of crystallization

Seventeen U-Pb (zircon) ages that date the time of crystallization and contain uncertainties within the range adopted in this report are available for samples from the GDG rocks in the Bergslagen region. The locations of the dated samples are shown in Figure 48 and pertinent information concerning the geochronological data is summarized in Table 3. Virtually all the samples analysed are metagranitoids. However, one metagabbro and one quartz-bearing metadiorite have also been dated. As is evident from Figure 48, the dated samples are unevenly distributed over the area. The majority of the ages are from the relatively well-preserved metagranitoids in the central part of the Bergslagen region. Two of the samples were analysed in connection with the Bergslagen project. A more complete description of these two samples and the geochronological results are presented in the appendix.

Bearing in mind the presence of some older inherited zircons in the samples analysed by the SIMS technique (Andersson 2004), care is needed in the interpretation of especially older U-Pb (zircon) ages that have been determined using the conventional TIMS technique when the timing of crystallization is inferred. Furthermore, the previously determined age of 1850^{+8}_{-7} Ma for a metagranite from the Horrsjö area in westernmost Bergslagen (Åberg et al. 1983a) has recently been modified with the help of new analyses to 1887±5 Ma (Högdahl & Jonsson 2004). This exercise raises questionmarks concerning the reliability of the data from, for

example, the metagranites from Svärdsjö and Ludvika that were also acquired over twenty years ago (Åberg et al. 1983b, Åberg & Strömberg 1984). It is noteworthy that these ages were interpreted as minimum ages in these publications.

Fifteen of the seventeen dated metagranitoids and more primitive rocks crystallized during the time period 1.90 to 1.87 Ga and are included in what is referred to here as an older GDG suite (Fig. 52). If all uncertainties in the ages are taken into account, the time range for this age suite lies between 1907 and 1861 Ma. This suite is distinguished on the basis of the pre-tectonic relationship between the intrusive rock and the host bedrock. This observation is conspicuous even for the youngest sample that is present in the Forsmark area (1867±4 Ma).

The rocks that show a granitic composition in the older GDG suite intruded either around 1.89 Ga or during a later period, around 1.87 Ga. The older age is identical to that observed for the enormous volume of Svecofennian volcanic and subvolcanic intrusive rocks with rhyolitic composition that prevail in especially the western part of Bergslagen (see above). The granitic rock that was intruded around 1.87 Ga is similar in age to the sample from Åkersberga, north of Stockholm, where the intrusive rocks represent the earliest occurrence of GSDG rocks in the Bergslagen region (see above). The rocks in the older GDG suite show similar ages as the intrusive rocks in the so-called *Haparanda* (1.89–1.87 Ga) and *Perthite-monzonite* (1.88–1.86 Ga) *suites* in northern Sweden (Bergman et al. 2001).

Two samples of GDG rocks with tonalitic and granodioritic compositions intruded during the time period 1.87 to 1.85 Ga (Fig. 52). If uncertainties are taken into account, a time frame of 1879 to 1849 Ma is apparent. The samples that yielded these ages occur in the marginal, north-eastern and south-western parts of the Bergslagen region, respectively. As indicated above, the sample from Forsmark, in the north-eastern part of

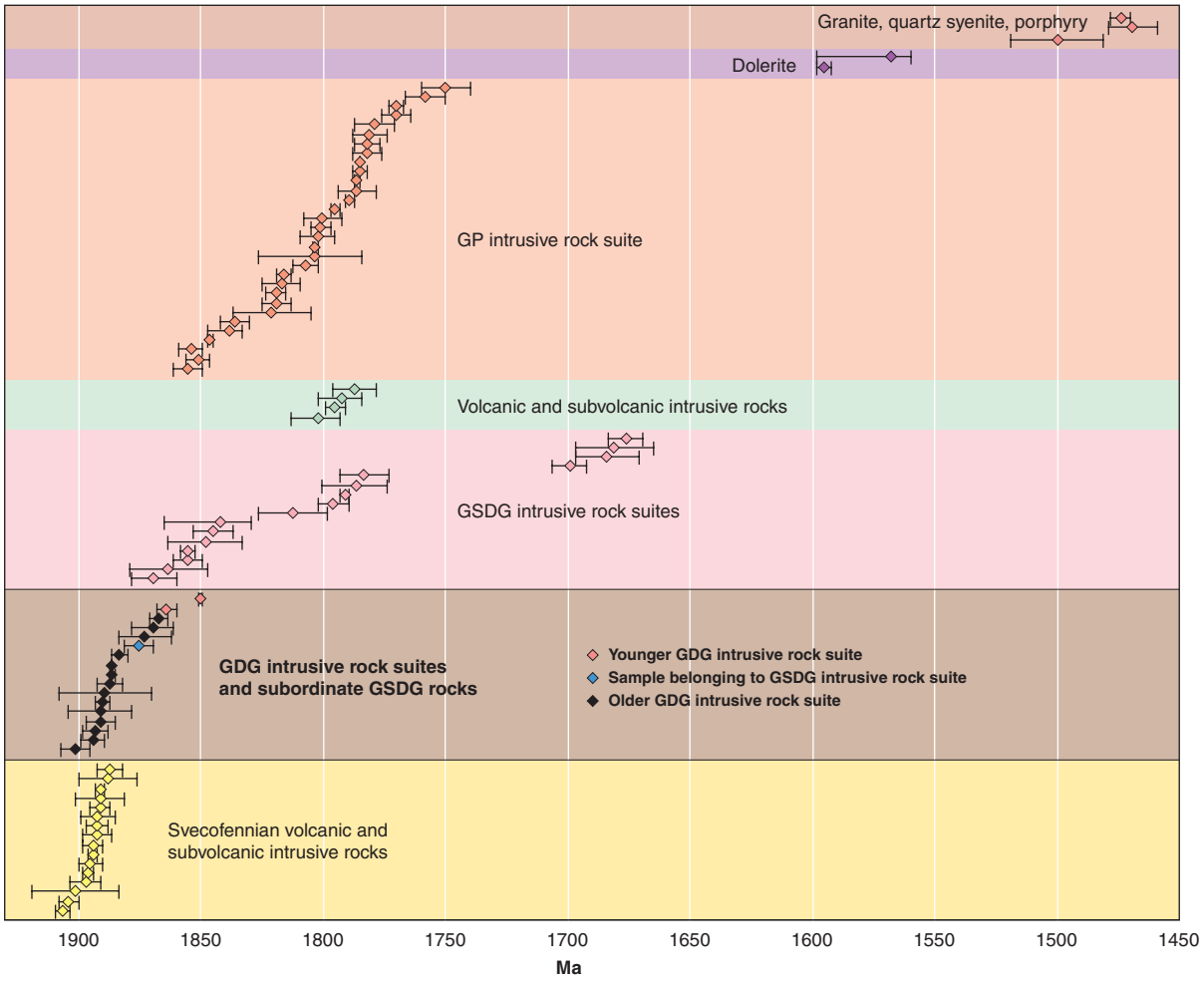

Fig. 52. Summary of U-Pb (zircon) age dates for the GDG rocks in the Bergslagen region. The age determination from the intrusive rock in the vicinity of Åkersberga (1875±5 Ma), which shows an affinity to the GSDG intrusive rocks, is grouped together with the GDG rocks in the figure. For purposes of comparison, all determinations of the age of crystallization of igneous and meta-igneous rocks in the Bergslagen region, with the exception of a U-Pb (baddeleyite) age from a dolerite in the Falun area (946±1 Ma), are shown and identified according to rock suite(s).

the Bergslagen region, intruded after ductile deformation and metamorphism had affected the older plutonic GDG rocks, but prior to later ductile deformation under lower-grade metamorphic conditions.

The ages of the metagranitoids in the younger, 1.87–1.85 Ga GDG suite temporally overlap with the metaigneous rocks immediately north of the Bergslagen region, which consist of metarhyolites and GDG intrusive rocks in the Los area (Delin 1993, 1996, Delin & Persson 1999, Andersson et al. 2004a). However, the igneous rocks to the north of the Bergslagen region are pre-tectonic in character and are commonly affected by high-grade metamorphism, in contrast to the younger GDG rocks in the Bergslagen region. These relationships have contributed to the recognition of separate tectonic domains in the central part of Sweden (see section "Regional tectonic framework").

In summary, it is suggested that two separate age suites of GDG intrusive rocks are present in the Bergslagen region. The pre-tectonic metagranitoids and associated more primitive rocks in the older suite (1.90–1.87 Ga) show the same ages as or are slightly younger than the Svecofennian volcanic and subvolcanic intrusive rocks. Intrusion of metagranite is conspicuous around 1.89 Ga and, together with GSDG rocks, around 1.87 Ga. The rocks that belong to the younger suite (1.87–1.85 Ga) intruded after ductile deformation had already affected the host bedrock and appear to be restricted to the marginal, north-eastern and south-western parts of the Bergslagen region.

Geochemistry

The localities where data bearing on the geochemical composition of GDG intrusive rocks have been acquired and used in this report are shown in Figure 53. 268 geochemical analyses from SGU's bedrock geochemistry database have been used in the compilation work.

The GDG intrusive rocks show a wide range of compositions with I-type characteristics, and a trend that passes from granite through granodiorite and tonalite to quartz diorite and gabbro on a total alkali–SiO_2 diagram for intrusive rocks (Fig. 54a). This trend is confirmed in the Debon & Le Fort (1983) Q–P diagram (Fig. 54b). There is a tendency for some samples to show anomalously high Q (>200) and low P (<100) values on this diagram and, on the basis of a visual inspection, appear to be situated outside the main trend (Fig. 54a). It is inferred that these rocks have been affected by an alteration that involved alkali exchange, including loss of K_2O, and that they show an apparent pseudotonalitic composition. On a more local scale, the same type of alteration was identified (Stephens et al. 2003, 2005) and formed the focus of more detailed investigations (Petersson et al. 2005) in the Forsmark area, in the north-eastern part of the Bergslagen region. The GDG intrusive rocks straddle the boundary between peraluminous and metaluminous compositions in the Maniar & Piccoli (1989) A/NK–CA/CNK diagram (Fig. 54c). They also show a distinctive calc-alkaline to calcic trend (Fig. 54d) in the classification system of Peacock (1931).

Representative analyses of GDG granitoids with different SiO_2 contents show enrichment in large ion lithophile elements (LILE, e.g. Ba, Rb, Th, K) relative to high field strength elements (HFSE, e.g. Zr, Hf, Y, Yb), with a factor difference generally greater than ten (Fig. 55). The samples show consistent trends wih negative anomalies for Nb and Ta, and, particularly at higher SiO_2 values, for even Sr, P and Ti on the McDonough et al. (1992) spider diagram (Fig. 55). The GDG granitoids also show a typical chondrite normalized pattern for rare earth elements in acid rocks, with an enrichment of light rare earth (LREE) relative to heavy rare earth (HREE) elements and a negative Eu anomaly (Fig. 56). The $(La/Yb)_N$ ratios are low in basic to intermediate rocks, whereas there is a larger variation in the acid rocks (Fig. 56). The negative anomalies for both Nb and Ta on the McDonough et al. (1992) plot, as well as the position of the GDG granitoids on the Pearce (1996) Rb–Y+Nb diagram (Fig. 57), indicate the influence of one or more source regions for the GDG granitoids that were affected, at some stage in their history, by subduction-related processes.

Petrophysical characteristics and regional geophysical signature

The localities where data bearing on the petrophysical properties of GDG intrusive rocks have been acquired and used in this report are shown in Figure 58. Samples from 1 971 localities have been analysed, whereas in situ gamma radiation measurements have been carried out at 659 sites. These data have been extracted from SGU's petrophysical database. The GDG intrusive rocks represent the overall largest group of rocks analysed in this study, with around 40% of all the samples.

Density

The density distributions for the metagranitoids and the metamorphosed intermediate, mafic and ultramafic rocks in the GDG rock suites are shown in Figures 59a and 59b, respectively.

The mean density for all the GDG intrusive rocks is 2 842 kg/m^3. The metagranitoids show a mean density of 2 688 kg/m^3 and a variation from 2 560 kg/m^3 for granitic rocks up to 2 800–2 900 kg/m^3 for tonalitic

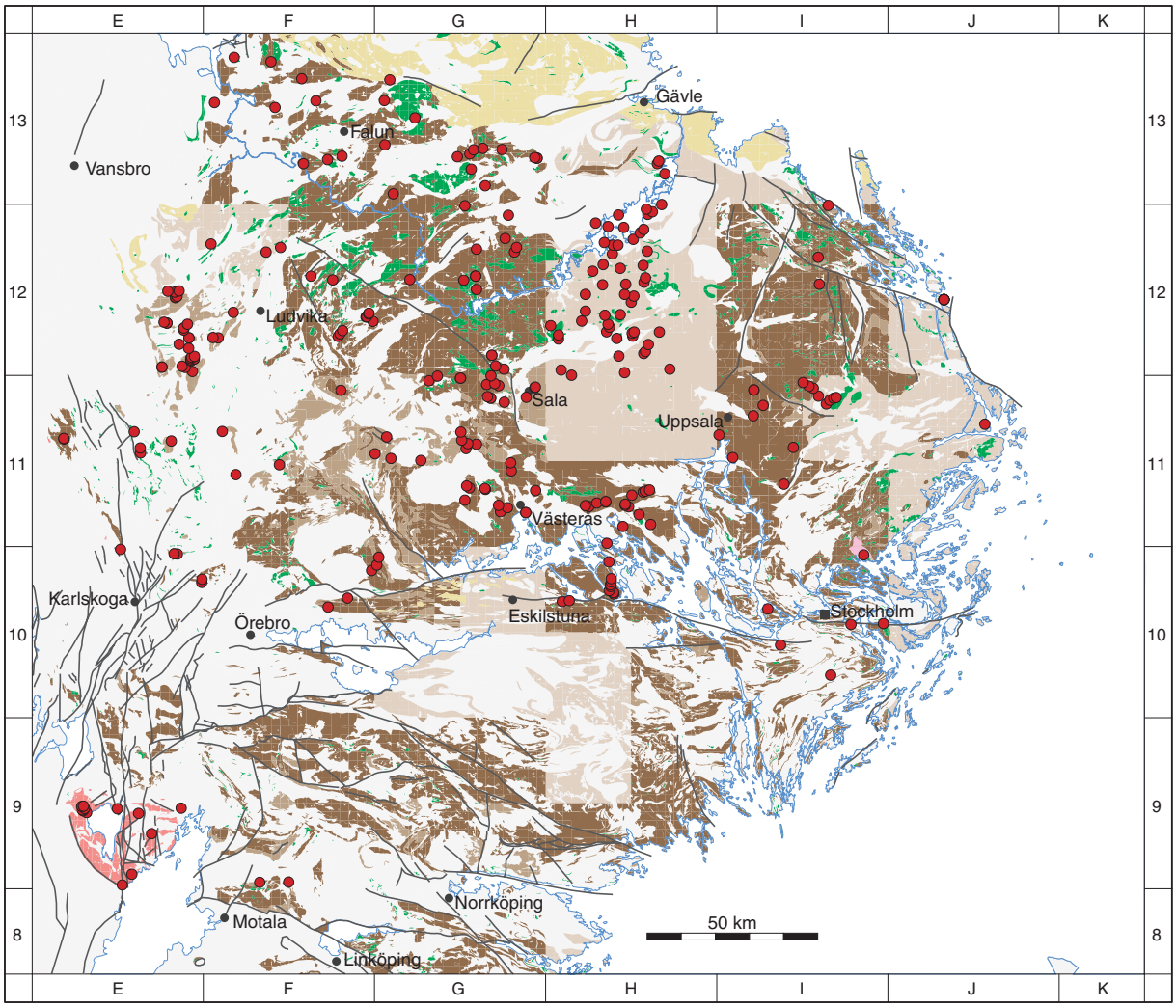

● Sample site for bedrock geochemical analysis

Fig. 53. Location of sample sites for the geochemical analysis of rocks included in the 1.90–1.87 Ga and 1.87–1.85 Ga GDG intrusive rock suites in the Bergslagen region. A sample from the intrusive rock in the vicinity of Åkersberga, which shows an affinity to the GSDG intrusive rocks, is grouped together with the GDG rocks. See Figure 48 for legend to the base geological map.

rocks (Fig. 59a). The intermediate, mafic and ultramafic rocks show a considerably higher mean density of 2 995 kg/m^3, due to their high content of denser minerals such as amphibole, pyroxene and to some extent magnetite. They also show a large variation from around 2 700 kg/m^3 up to greater than 3 400 kg/m^3 (Fig. 59b). Indeed, there are a small number of samples with even higher density than that shown on the diagram. The highest density of 4 080 kg/m^3 occurs in a sample of metagabbro from south of Smedjebacken, east of Ludvika.

Magnetic susceptibility

The density–susceptibility diagrams for the metagranitoids and the metamorphosed intermediate, mafic and ultramafic rocks in the GDG intrusive rock suites are shown in Figures 60a and 60b, respectively, in the same manner as for the density distributions. The magnetic susceptibility is shown on a logarithmic scale.

A large variation in magnetic susceptibility is present in the GDG intrusive rocks. The group covers the whole spectrum from the lowest values of around 10 up to almost 1 000 000 × 10^{-6} SI. The highest magnetic susceptibility values are not shown in Figure 60b, since they correspond to samples with densities larger than 3 400 kg/m^3.

Gamma radiation

The gamma radiation characteristics of the GDG intrusive rocks are shown in Figures 61 and 62. Once again, the metagranitoids and the metamorphosed intermediate, mafic and ultramafic rocks are shown separately. Furthermore, a comparison with all analysed samples is presented.

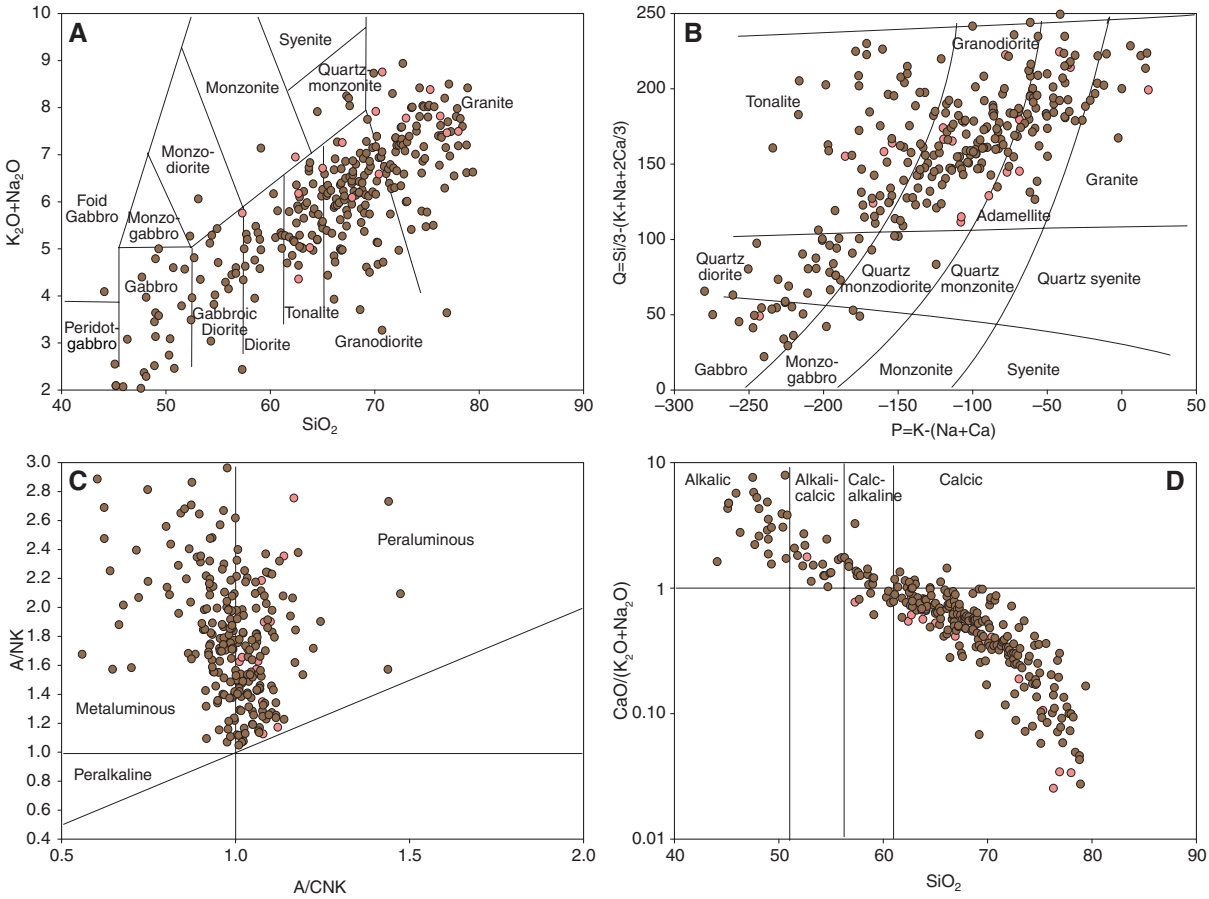

Fig. 54. Geochemical trends of the GDG intrusive rocks in the Bergslagen region. The symbols represent samples from the dominant 1.89–1.87 Ga (brown) and subordinate 1.87–1.85 Ga (pale red) GDG intrusive rock suites. Diagrams after **A.** Middlemost (1994), **B.** Debon & Le Fort (1983), **C.** Maniar & Piccoli (1989) and **D.** Peacock (1931).

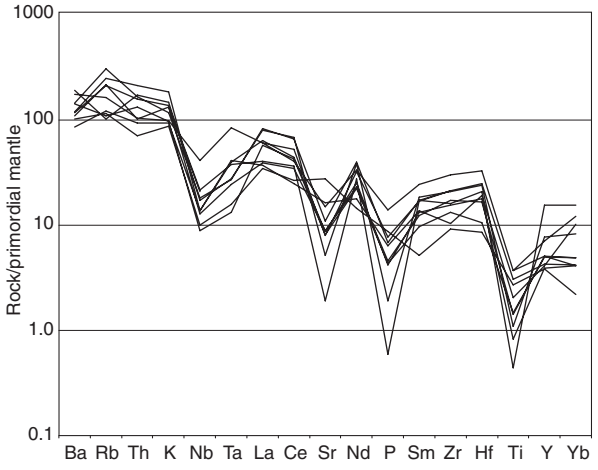

Fig. 55. Rock/primordial mantle spider diagram showing the relationships between large ion lithophile (LILE, e.g. Ba, Rb) and high field strength (HFSE, e.g. Zr, Ti and Y) elements for representative samples of the GDG intrusive rocks in the Bergslagen region. SiO_2 values for the selected samples span from 63.2 to 78.2%. Primordial mantle values after McDonough et al. (1992).

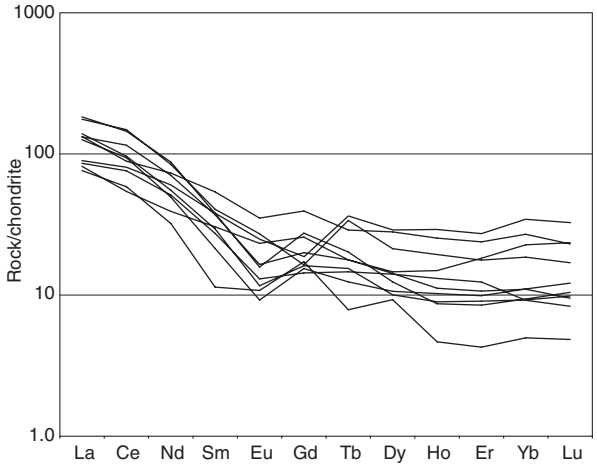

Fig. 56. Rock/chondrites diagram showing the relationships between light rare earth (LREE, e.g. La, Ce) and heavy rare earth (HREE, e.g. Yb, Lu) elements for representative samples of the GDG intrusive rocks in the Bergslagen region. SiO_2 values for the selected samples span from 63.2 to 78.2%. Chondrite values after Boynton (1984).

The metagranitoids generally show low gamma radiation values with uranium concentrations below 10 ppm and thorium concentrations below 40 ppm (Figs. 61a and 62a, respectively). However, in the northern part of the area, north of Falun, a strongly migmatized granitic rock shows an increased gamma radiation. Furthermore, in the area occupied by map sheet 12G Hofors, values of up to 35 ppm for uranium and 130 ppm for thorium have been measured at some locations. As expected, the metamorphosed intermediate, mafic and ultramafic rocks show very low gamma radiation values. The concentrations of uranium and thorium vary between 0–5 ppm and 0–9 ppm, respectively (Figs. 61b and 62b, respectively).

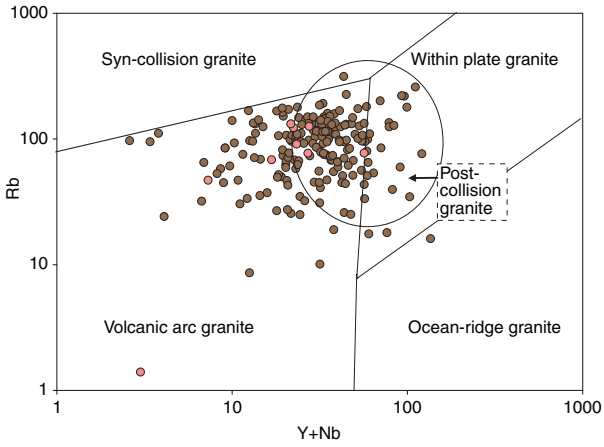

Fig. 57. Tectonic affinity diagram after Pearce (1996) for the GDG intrusive rocks in the Bergslagen region. The symbols represent samples from the dominant 1.89–1.87 Ga (brown) and subordinate 1.87–1.85 Ga (pale red) GDG intrusive rock suites.

Regional geophysical signature

The intermediate, mafic and ultramafic plutons in the northern part of the Bergslagen region correspond to

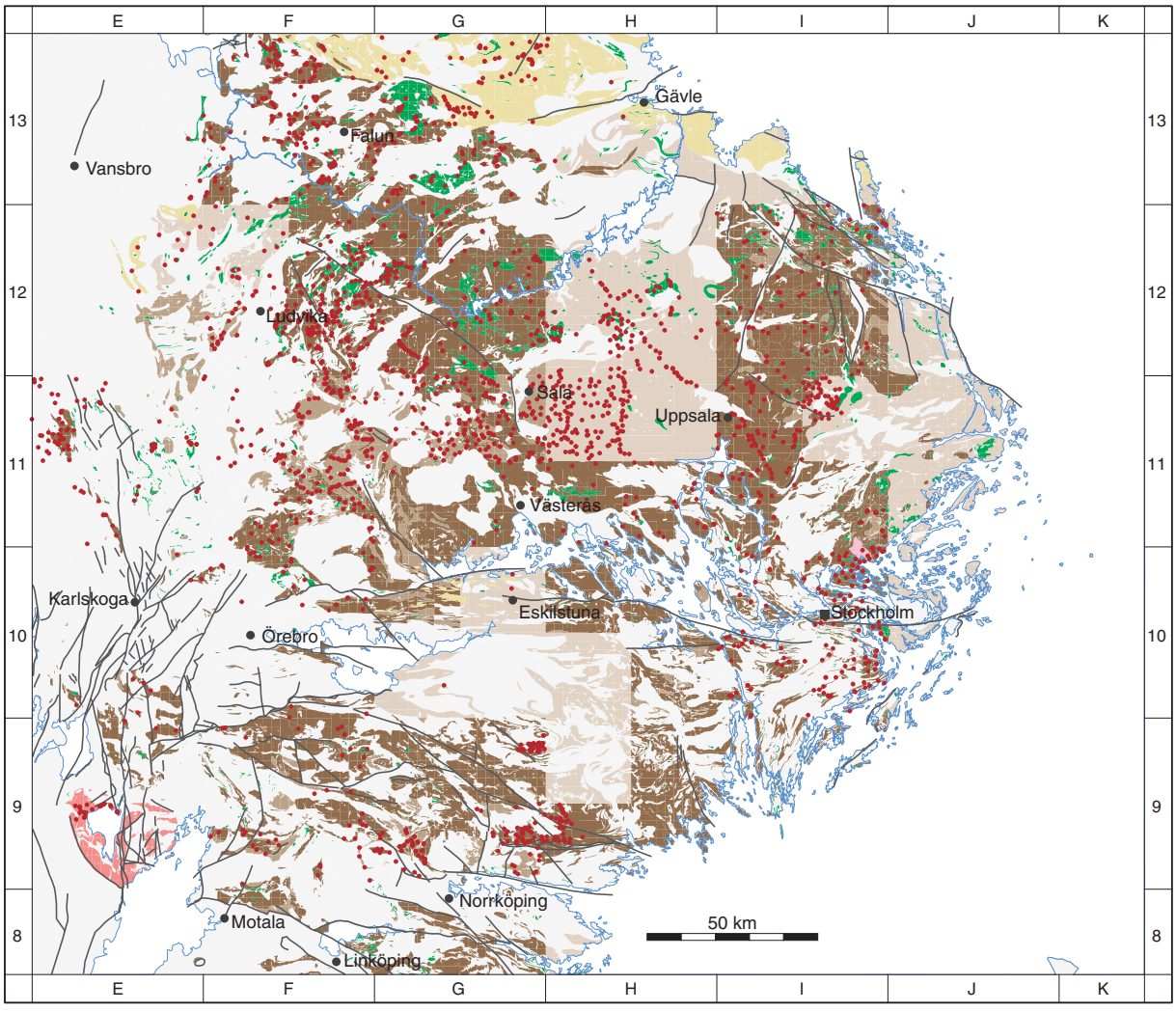

Fig. 58. Location of sample sites of rocks included in the 1.90–1.87 Ga and 1.87–1.85 Ga GDG intrusive rock suites in the Bergslagen region for petrophysical and gamma radiation measurements (red dots). Samples from the intrusive rocks in the vicinity of Åkersberga, which show an affinity to the GSDG suite, are grouped together with the GDG rocks. See Figure 48 for legend to the base geological map.

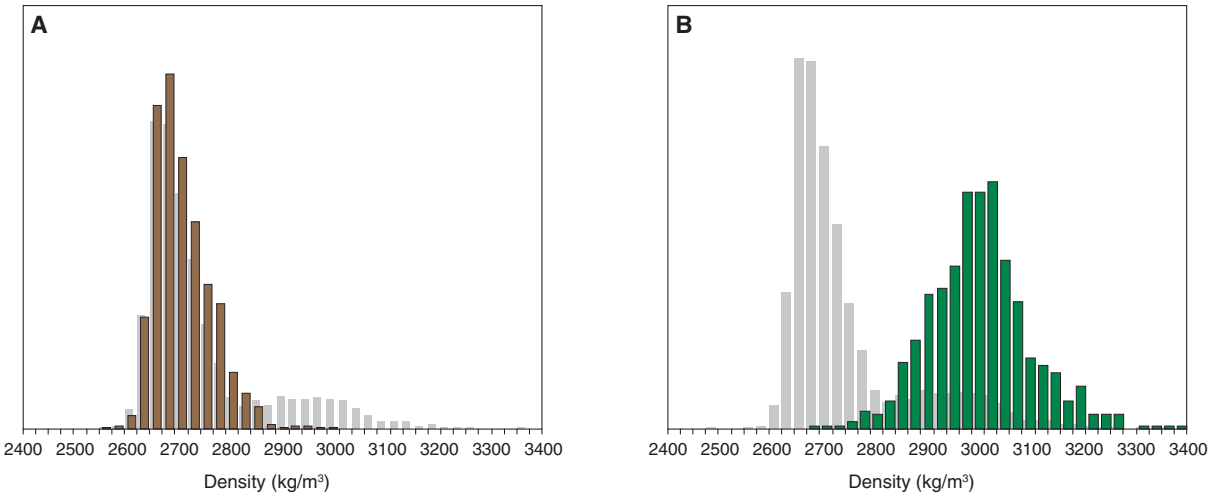

Fig. 59. Density distribution diagrams for GDG intrusive rocks in the Bergslagen region. **A.** Metagranitoid. **B.** Metamorphosed intermediate, mafic and ultramafic rocks. For purposes of comparison, all samples from the Bergslagen region are shown in grey.

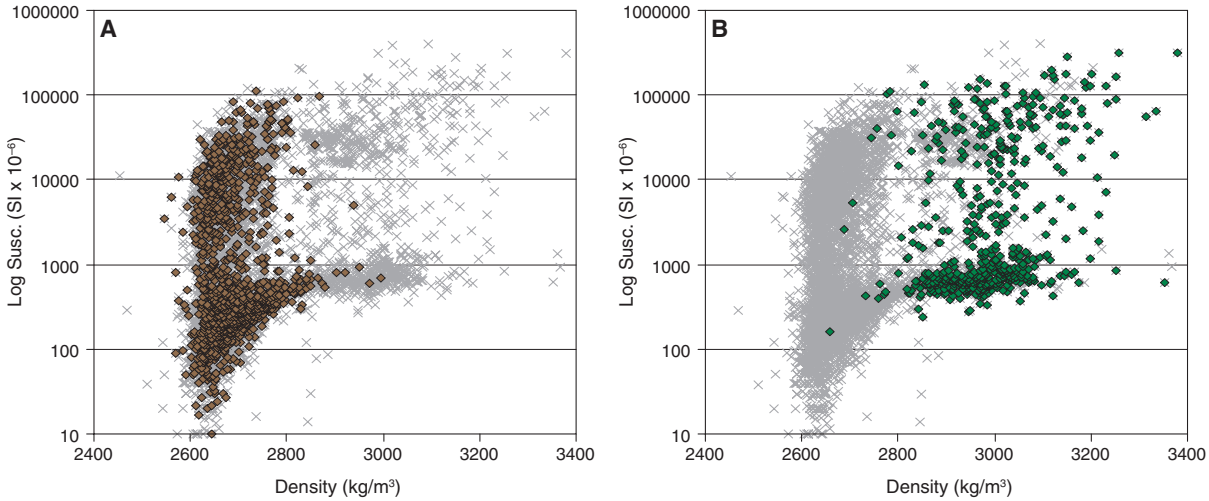

Fig. 60. Magnetic susceptibility–density diagrams for GDG intrusive rocks in the Bergslagen region. **A.** Metagranitoid. **B.** Metamorphosed intermediate, mafic and ultramafic rocks. For purposes of comparison, all samples from the Bergslagen region are shown in grey.

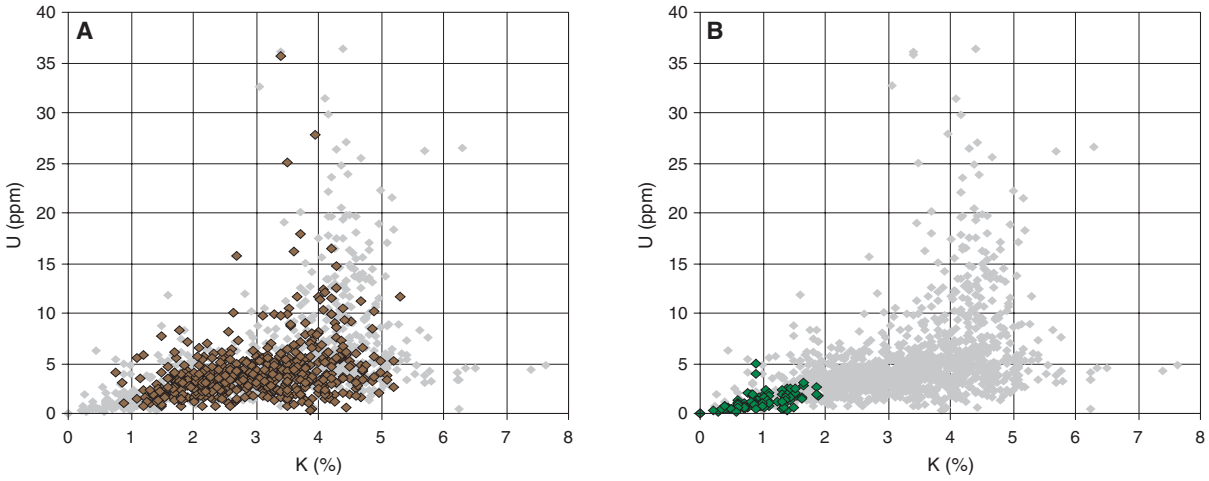

Fig. 61. Concentrations of uranium versus potassium for GDG intrusive rocks in the Bergslagen region. **A.** Metagranitoid. **B.** Metamorphosed intermediate, mafic and ultramafic rocks. For purposes of comparison, all samples from the Bergslagen region are shown in grey.

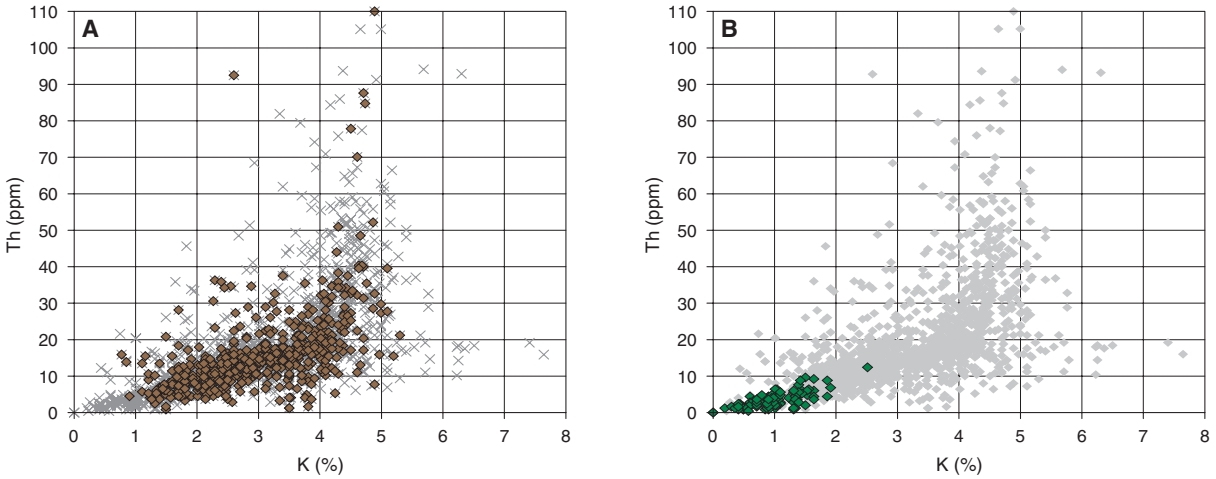

Fig. 62. Concentrations of thorium versus potassium for GDG intrusive rocks in the Bergslagen region. **A.** Metagranitoid. **B.** Metamorphosed intermediate, mafic and ultramafic rocks. For purposes of comparison, all samples from the Bergslagen region are shown in grey.

conspicuous positive gravity anomalies on the Bouguer gravity anomaly map (cf. Figs. 48 and 13, respectively). In agreement with the results of the in situ measurements, the results of the airborne radiometric measurements generally show low gamma radiation values over areas that contain GDG rocks. However, in the northernmost part of the study area, where migmatitic rocks prevail, the bedrock shows an increased gamma radiation, especially related to high thorium contents (Fig. 11). A similar geophysical signature is apparent south of the lake Mälaren, where migmatitic GDG rocks occupy prominent areas (Fig. 11). However, as emphasized earlier, a large part of the thorium anomaly around this lake is caused by a high concentration of thorium in the post-glacial clays and has no direct connection to the character of the bedrock.

Metadolerite

Rock type, spatial distribution and intrusion–deformation relationships

Metadolerite, which commonly occurs as amphibolite, constitutes a significant bedrock component in many parts of the Bergslagen region. Metadolerites are particularly prominent in, for example, the north-eastern part of the region, where they include the so-called *Herräng dykes* (Magnusson 1940). A comprehensive summary of metadolerites and their relation to the deformation in the country rock has been presented by Stålhös (1991). Furthermore, a description of different generations of composite dykes and their relationship to the country rock has been presented by Wikström (1992). Talbot and Sokoutis (1995) completed a structural analysis of metadolerites and their country rocks within the so-called *Singö shear zone* (see later text) in the north-eastern part of the Bergslagen region. The following description of the metadolerites concerns the relationships in this part of the region, where coastal outcrops provide some excellent exposure.

In general, the metadolerites in the north-eastern part of the Bergslagen region display a more or less strongly developed tectonic fabric. According to Stålhös (1991), the majority of the metadolerites are pretectonic in character, and the locally observed discordancy between the structures in the metadolerites and the country rock was interpreted to be apparent and due to the contrast in competency between the rocks. However, different generations of metadolerite exist (see below), and the relationship between their intrusion, the subsequent deformation and metamorphism, and the structural development in the country rock is complex. A key question concerns whether the metadolerites and the surrounding rocks, usually metagranitoids in the older GDG intrusive rock suite, have suffered a mutual structural development, or whether the country rocks were deformed prior to the intrusion of one or more generations of mafic dykes.

Both concordant and strongly discordant (Fig. 63a) relations between the orientation of the metadolerites and the tectonic foliation in the surrounding metagranitoids were observed during field studies, similar to the relationships described earlier by, for example, Stålhös (1972, p. 115). Furthermore, the orientation of the tectonic foliation in the metadolerites locally deviates from the orientation of the tectonic foliation in the country rock. However, linear mineral fabrics, which over large areas form the dominant structure, show a similar orientation in both the metadolerites and the country rock.

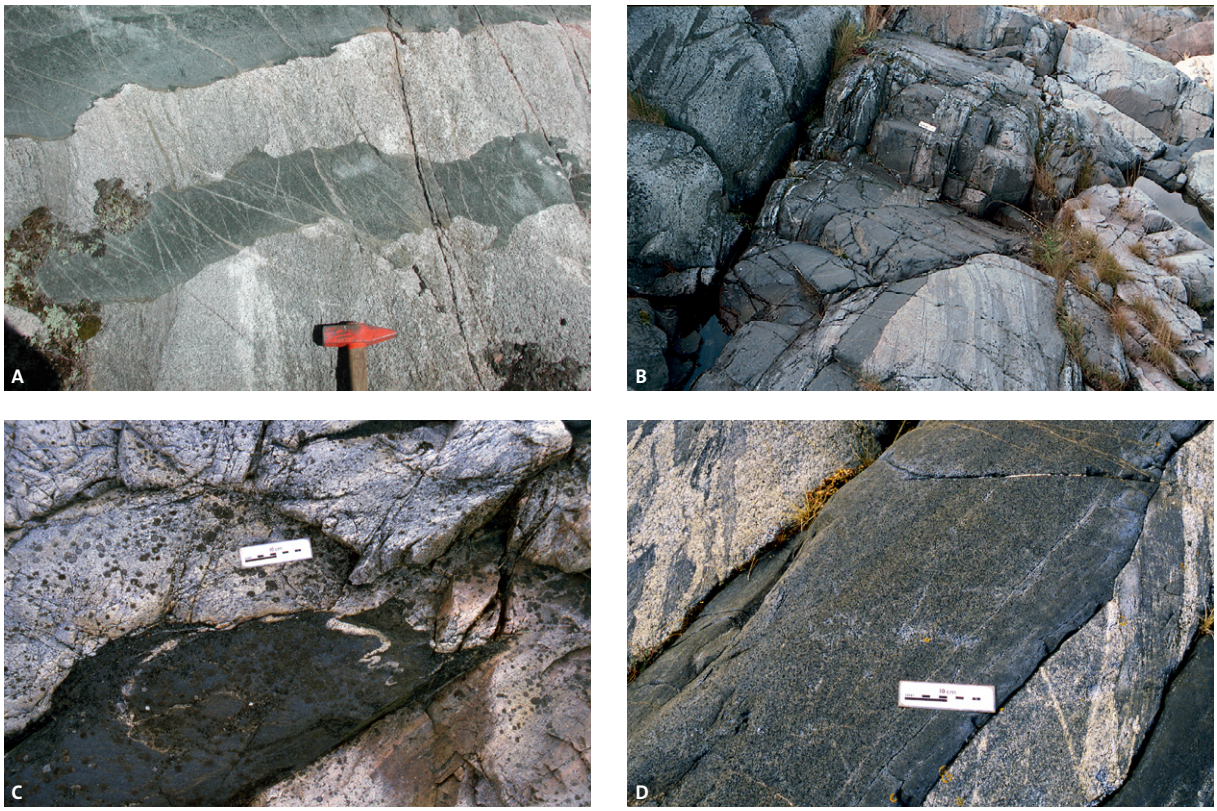

Fig. 63. Relationships between the intrusion of amphibolite (metadolerite) dykes and ductile deformation in the host rock in the north-eastern part of the Bergslagen region. **A.** Foliated metatonalite with flattened enclaves, which is included in the older, 1.90–1.87 Ga GDG intrusive rock suite, intruded by discordant dykes of metadolerite after the development of penetrative ductile strain in the metatonalite. The dykes are also affected by deformation and occur as amphibolite. South of Månkebo (12H Söderfors NO). Photograph: Stefan Bergman (SGU). **B.** Foliated metagranitoid with flattened enclaves of amphibolite, which is included in the older, 1.90–1.87 Ga GDG intrusive rock suite, intruded by different generations of younger metadolerite dykes. These are variably discordant to the ductile strain in the metagranitoid. All rocks are affected by a similar linear grain-shape fabric. View to the west at Fogdösten (12J Grisslehamn NV). Photograph: Michael Stephens (SGU). **C.** Back-veining of aplitic metagranite dated to 1891±13 Ma (see appendix) in equigranular metadolerite. Fogdösten (12J Grisslehamn NV). Photograph: Michael Stephens (SGU). **D.** Metadolerite with hornblende phenocrysts discordant to GDG metagranitoid with flattened enclaves of amphibolite. Fogdösten (12J Grisslehamn NV). Photograph: Michael Stephens (SGU).

On the small island of Fogdösten, the bedrock is dominated by a metagranitoid in which six generations of amphibolite, which are predominantly metadolerite dykes, can be distinguished (Figs. 63b, c and d). These different generations can be distinguished principally on the basis that they display discordant relationships to each other (see, for example, Fig. 63b). They also differ somewhat in mineralogical composition. The oldest generation is intimately mixed with the metagranitoid as enclaves of amphibolite and, for this reason, is inferred to be coeval with the metagranitoid (Figs. 63b and d). The following two generations, one plagioclase-phyric and one equigranular, occur as metadolerite dykes and display mingling relationships (back veining) with a diffusely banded meta-aplite (Fig. 63c). The fourth generation of amphibolite, which also occurs as metadolerite dykes, contains hornblende phenocrysts (Fig. 63d). The two youngest generations form equigranular metadolerite dykes that are inferred to be more or less similar in age.

The host metagranitoid displays a conspicuous, steep to vertical tectonic foliation that strikes west-south-west–east-north-east, and a lineation which is subvertical to vertical. No structural discordancy is present between the metagranitoid and the three oldest generations of amphibolite and metadolerite, the orientations of which are more or less concordant to the foliation in the metagranitoid (Fig. 63b). By contrast, the three youngest generations show a north-west–south-east to west-north-west–east-south-east strike and are discordant to both the orientation of the older dykes and the structures in both the metagranitoid and the older generations of amphibolite and metadolerite (Fig. 63b), i.e. they are inferred to be post-tectonic with respect to these structures. However, even the three youngest generations are affected by ductile deformation and metamorphism. Lundqvist (1959) also described different generations of metadolerites, similar to those on Fogdösten, from a small island c. 1.5 km north-north-west of Fogdösten, also in the north-eastern part of the Bergslagen region.

The oldest metadolerites described by Stålhös (1991) are intimately mixed with the host metagranitoids in the older GDG intrusive rock suite and are more or less synchronous with the metagranitoids. These metadolerites correspond to the first generation of amphibolite on Fogdösten described above. Stålhös (1991) also considered these metadolerites to have acted as feeder dykes to mafic metavolcanic rocks. The composite dykes of Stålhös (1991) correspond to the second and third generations of amphibolite which occur as metadolerite and co-exist with meta-aplite on Fogdösten. The three youngest generations of metadolerite on Fogdösten presumably correspond to the youngest metadolerites described by Stålhös (1991) and the *Herräng dykes* of Magnusson (1940).

Despite being deformed and metamorphosed themselves, the interpretation of the field relationships on Fogdösten and at other localities in the north-eastern part of the Bergslagen region indicates that the younger generations of metadolerite are post-tectonic with respect to the relatively strong deformation in both the older suite of GDG intrusive rocks and the older generations of metadolerite. They mark an important insurgence of mantle-derived material into the crust, following an early phase of ductile deformation and metamorphism. The concept of intraorogenic development, as discussed by Magnusson (1940) and Stålhös (1976, 1991), is clearly of relevance to the tectonic implications provided by these hypabyssal rocks (see also section "Deformation, metamorphism and mechanism of emplacement of the 1.87–1.84 Ga GSDG suite of intrusive rocks").

Age of crystallization

In order to better understand the time relationships between the metagranitoids in the older GDG intrusive rock suite and the second and third generation of amphibolite (metadolerite), the meta-aplite on Fogdösten was sampled for age-determination work (see Appendix). The U-Pb (zircon) age of 1891±13 Ma indicates that the meta-aplite and the co-existing amphibolite (metadolerite) are more or less synchronous with the surrounding 1.90–1.87 Ga GDG igneous activity, in agreement with the interpretation of Stålhös (1991). These older dykes are possibly hypabyssal varieties of the mafic plutonic rocks that belong to the older GDG intrusive rock suite.

Stålhös (1991) speculated that the younger metadolerites intruded around 1.85 Ga. At Forsmark, use of both U-Pb (zircon) and U-Pb (titanite) age determinations has constrained the timing of intrusion of some amphibolite (metadolerite) dykes in this area to between 1871 and 1857 Ma (Hermansson et al. 2008a). These dykes are similar in age to the younger suite of GDG intrusive rocks (group C in Stephens et al. 2003) that also intruded after the initial development of penetrative ductile deformation under amphibolite-facies conditions (see above). For this reason, it is proposed that they are comparable with the three youngest generations of metadolerite on Fogdösten.

Late Svecokarelian Granite-syenitoid-dioritoid-gabbroid (GSDG) intrusive rock suites (1.87–1.84 and 1.81–1.78 Ga)

GSDG intrusive rock suites and the Transscandinavian Igneous Belt

The Bergslagen region is bordered along its southern and western parts by predominantly intrusive rocks that range in composition from gabbroid and dioritoid via syenitoid to granite (Fig. 64). Ultramafic rocks are also present. Together these rocks form a prominent intrusive rock association, referred to here as the Granite-syenitoid-dioritoid-gabbroid or GSDG intrusive rock association. These intrusive rocks are locally associated with synmagmatic volcanic and subvolcanic rocks, and contemporaneous sedimentary rocks (see later text). Isolated plutons of similar rocks are also present in northern areas, for example in the vicinity of Hedesunda (Fig. 64). On the basis of solely their compositional variation, these intrusive rocks are referred to here as GSDG rocks. Such rocks intruded the Svecofennian supracrustal rocks and most of the GDG intrusive rocks. At several places, granitic end-members are difficult to differentiate from the more homogeneous granites in the granite-pegmatite (GP) intrusive suite (see later text).

Based on the intrusion–deformation relationships with respect to the Svecokarelian tectonic evolution, four different suites of GSDG intrusive rocks are present in the Bergslagen region. Different suites of GSDG intrusive rocks are also affected, to variable extent, by Sveconorwegian ductile deformation and metamorphism in the western part of the Bergslagen region.

The oldest rocks with GSDG composition are strongly subordinate and are restricted to the Åkersberga area, north of Stockholm. They are 1.88–1.87 Ga in age and are pre-tectonic with respect to Svecokarelian ductile deformation and metamorphism. These rocks were addressed earlier in this report together with the strongly dominant GDG rocks with which they are closely associated in space and with which they share similar intrusion–deformation relationships.

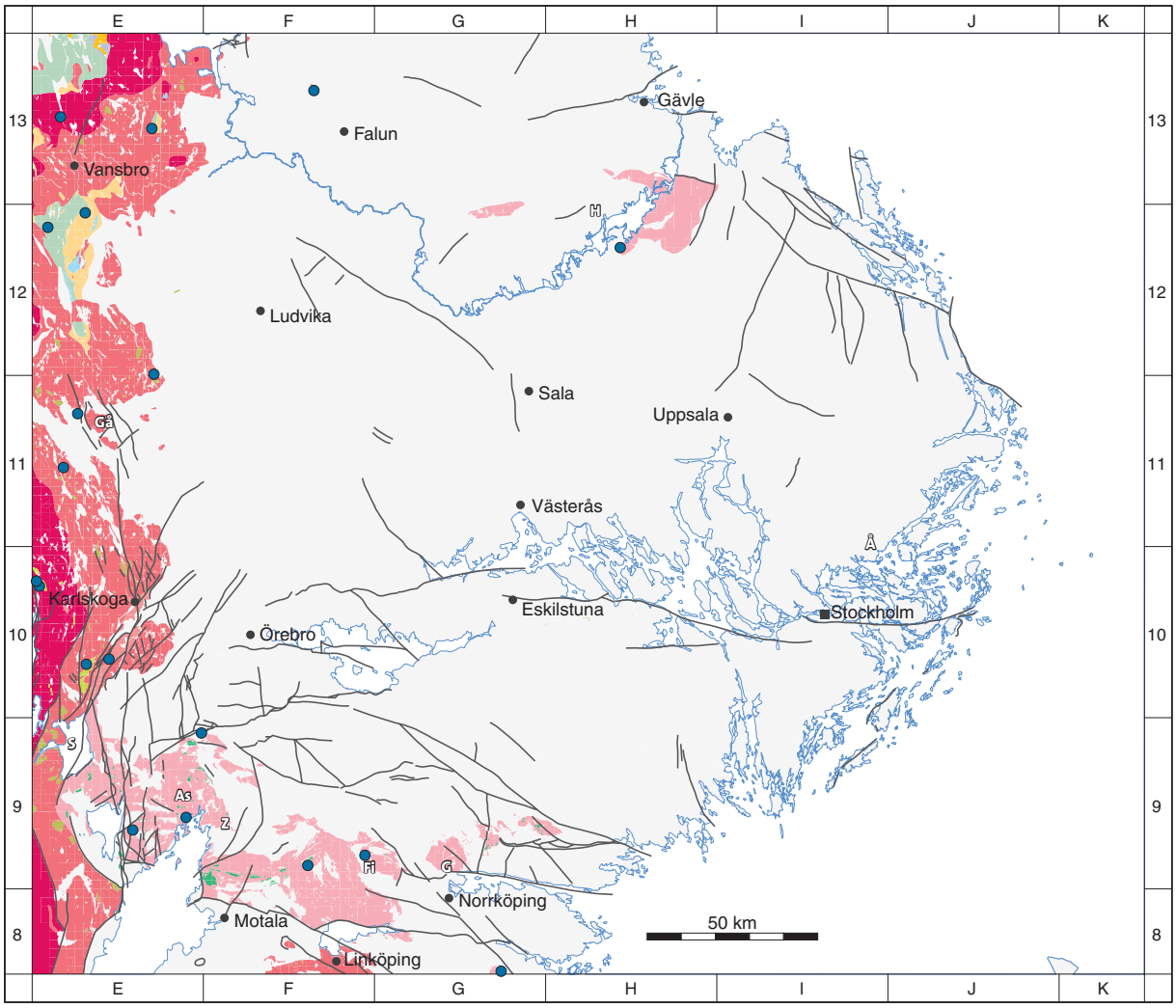

U-Pb (zircon) age determination

Fault, ductile shear zone

Age group 1.70–1.67 Ga

- Granite, syenitoid, quartz monzodiorite and equivalent metamorphic rock
- Gabbroid, dioritoid, ultramafic rock and equivalent metamorphic rock
- Sandstone, argillite
- Rhyolite

Age group 1.81–1.78 Ga

- Granite, syenitoid, quartz monzodiorite and equivalent metamorphic rock
- Metagranite, in part hypersthene-bearing and charnockitic
- Gabbroid, dioritoid, ultramafic rock and equivalent metamorphic rock
- Sandstone, argillite
- Trachyte–trachydacite, basaltic andesite
- Rhyolite

Age group 1.87–1.84 Ga

- Granite, syenitoid, quartz monzodiorite and equivalent metamorphic rock
- Gabbroid, dioritoid, ultramafic rock and equivalent metamorphic rock

Fig. 64. 2-D model at the ground surface in the Bergslagen region for the distribution of different suites of GSDG intrusive rocks that formed around and after 1.87 Ga. Even the post-Svecokarelian, 1.70–1.67 Ga GSDG suite is presented on the map. The supracrustal rocks temporally and spatially associated with the 1.81–1.78 Ga and 1.70–1.67 Ga GSDG suites are also shown. As indicated in the legend to the bedrock map (Stephens et al. 2007a), the labelled areas on the map only indicate the dominate age group in each area. For example, GSDG rocks in the 1.81–1.78 Ga intrusive rock suite are present inside the area marked as age group 1.87–1.84 Ga. The location of samples from the GSDG intrusive rocks and associated porphyries (volcanic and subvolcanic rocks), which have been dated using the U-Pb (zircon, titanite) technique, and the location of place names referred to in the section "Late Svecokarelian Granite-syenitoid-dioritoid-gabbroid (GSDG) intrusive rock suites (1.87-1.84 and 1.81-1.78 Ga)" are also shown. Å = Åkersberga, As = Askersund, Fi = Finspång, Gå = Gåsborn, G = Graversfors, H = Hedesunda, S = Skagern, Z = Zinkgruvan.

Two younger suites of GSDG rocks intruded during later phases of the Svecokarelian orogeny and are referred to here as late Svecokarelian. They are syn- or post-tectonic in character and range in age from 1.87–1.84 Ga and 1.81–1.78 Ga, respectively. These two suites are dominant in the Bergslagen region and are addressed in this section.

The fourth and youngest suite is entirely post-tectonic with respect to this complex, multiphase orogenic system and formed during the time interval 1.70–1.67 Ga. This suite of GSDG intrusive rocks is addressed in a later section in this report.

In the field, there are difficulties to distinguish GSDG intrusive rocks that belong to the different suites. The spatial distribution of different suites or combinations of suites on the geological maps of the Bergslagen region has simply made use of available geochronological data and judgements using published geological maps. Bearing in mind this point, there are considerable uncertainties in the spatial distribution of the different suites or combinations of suites on the maps. The uncertainty in especially the spatial distribution of the 1.87–1.84 Ga and 1.81–1.78 Ga GSDG intrusive rock suites is emphasized in the legends to the maps.

Traditionally, all the GSDG intrusive rocks younger than 1.87 Ga have been included in the so-called *Transscandinavian Igneous Belt* or *TIB* (Patchett et al. 1987, Gorbatschev 2004). The rocks within this belt mainly extend from south-easternmost Sweden via central Sweden (including Bergslagen) to northern Sweden and Norway, and form, in part, the basement to the Caledonian orogenic belt (e.g. Lindström et al. 2000, Gorbatschev 2004). An overview of the *TIB* concept, including its rock types, ages and relationship to surrounding rocks, has recently been presented in a volume edited by Högdahl et al. (2004). The term is generally not used here for four reasons:

- The *TIB* concept neglects rocks of similar composition that formed in the time interval 1.88–1.87 Ga.
- The *TIB* concept takes no account of the fundamentally different relationship that different suites in this group of rocks show to ductile deformation and metamorphism in different orogenic systems.
- The *TIB* concept excludes rocks of similar age and composition but affected by amphibolite-facies metamorphism in the Sveconorwegian orogen.
- There are different opinions in the literature concerning whether GDG rocks younger than 1.87 Ga should or should not be included in the *TIB* concept (compare, for example, Wikström & Karis 1998 and Högdahl et al. 2004).

Rock type, spatial distribution and intrusion–deformation relationships

The 1.87–1.84 Ga GSDG intrusive rock suite mainly occurs in the south-western part of the Bergslagen region, whereas the 1.81–1.78 Ga GSDG suite dominates along its western border (Fig. 68). Close to Askersund, in the south-western part of the region, GSDG intrusive rocks in the older suite are spatially associated with largely contemporaneous GDG rocks (younger, 1.87–1.85 Ga GDG intrusive suite in the previous section). Local names for the GSDG rocks include the *Askersund* and *Gravesfors granites* and the *Finspång augen gneiss massif* for components in the 1.87–1.84 Ga suite and the *Filipstad* and *Järna granites* for components in the 1.81–1.78 Ga suite (e.g. Lindström et al. 2000, Wikström & Andersson 2004, Ahl et al. 2004).

The more primitive rocks in both the late Svecokarelian suites are predominantly gabbroic in composition, including noritic varieties, but dioritic, quartz dioritic and ultramafic compositions are also present (e.g. Ripa 1998, Andersson et al. 2004b). These more primitive rocks are predominantly medium-grained and equigranular to porphyritic. They consist of plagioclase feldspar and hornblende, but olivine and pyroxene locally dominate as mafic phases. In contrast to the granitic end-members, these rocks correspond to conspicuous magnetic maxima on magnetic anomaly maps, which serve to constrain their spatial distribution.

The volumetrically more important felsic rocks are medium- or coarse-grained, and both K-feldspar-phyric (Fig. 65a) and equigranular variants are present. The rocks belonging to the 1.87–1.84 Ga suite are generally coarse-grained, whereas the rocks in the younger 1.81–1.78 Ga suite are medium-grained or medium- to coarse-grained. K-feldspar phenocrysts are locally rimmed by plagioclase feldspar (Fig. 65a). Furthermore, rounded, fine-grained mafic enclaves are conspicuous in these rocks (Fig. 65b) and the older 1.87–1.84 Ga suite is locally intruded by net-veined dykes. The dykes consist of pillowed mafic fragments in a granitic, commonly aplitic matrix (e.g. Wikström & Karis 1991). The field relationships indicate that the more felsic rocks have mingled with gabbroic and noritic rocks and possibly even mixed together to form quartz monzodioritic, monzonitic and quartz monzonitic compositions (Andersson 1997a). Syenitic to quartz syenitic compositions are restricted to the 1.81–1.78 Ga suite with mafic phases that include biotite + hornblende ± pyroxene ± fayalite.

In the Askersund area, the contact to granite that belongs to the 1.87–1.84 Ga GSDG intrusive rock suite is strongly discordant to the gneissic banding in

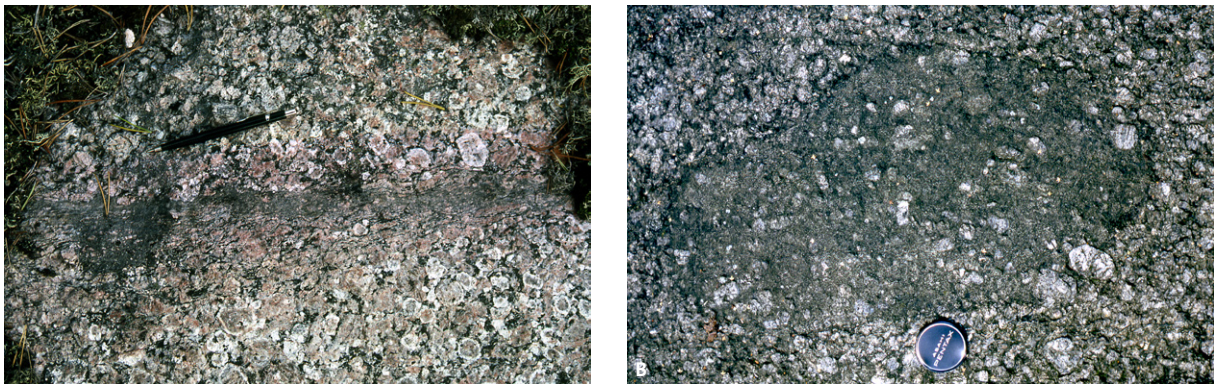

Fig. 65. Character of some GSDG intrusive rocks, Bergslagen region. **A.** Minor ductile shear zone in porphyritic granite with conspicuous mantled texture in the K-feldspar phenocrysts. The granite is inferred to belong to the 1.81–1.78 Ga GSDG intrusive rock suite and the shear zone is inferred to be Sveconorwegian in age (10E Karlskoga NO). Photograph: Michael Stephens (SGU). **B.** Enclave of mafic to intermediate rock in porphyritic granite to quartz monzonite inferred to belong to the 1.81–1.78 Ga intrusive rock suite (10E Karlskoga NO). Photograph: Michael Stephens (SGU).

Fig. 66. Intrusion–deformation relationships in the late Svecokarelian, 1.87–1.84 Ga suite of GSDG intrusive rocks in the Bergslagen region. **A.** Porphyritic, 1.87–1.84 Ga GSDG granite (lower left part of photograph) strongly discordant to banded and foliated supracrustal rocks (upper right part of photograph). View of steep surface to north in road outcrop c. 5 km north-east of Askersund (9F Askersund NV). Photograph: Michael Stephens (SGU). **B.** Porphyritic granite (*Hedesunda granite*) dated to c. 1.87 Ga with flattened enclaves of mafic rock (to the left of the scale marker) and weak grain-shape fabric, intruded by fine-grained granitic dykes (to the right of the scale marker). These relatively well-preserved rocks contrast sharply with the strongly deformed and migmatitic host rocks immediately to the east of the *Hedesunda granite* (13H Gävle SO). Photograph: Michael Stephens (SGU). **C.** Penetratively and strongly foliated metagranite included in the 1.87–1.84 Ga GSDG suite of intrusive rocks, later affected by folding with z-asymmetry. A pegmatite dyke is conspicuous along the axial surface to the post-foliation fold that plunges gently to the east. Approximately 10 km north-east of Zinkgruvan (9F Finspång NV). Photograph: Carl-Henric Wahlgren (SGU). **D.** Coarsely porphyritic granite to quartz monzonite that belongs to the 1.87–1.84 Ga intrusive rock suite. This rock is affected by penetrative foliation that formed under amphibolite-facies metamorphic conditions (parallel to blue pen) and a minor ductile shear zone that strikes east-north-east–west-south-west and shows a dextral component of movement (parallel to black pen). The foliation is inferred to be Svecokarelian in age and the ductile shear zone belongs to the network of minor Sveconorwegian ductile shear zones in the frontal part of the Sveconorwegian orogen (9E Askersund NV). Photograph: Carl-Henric Wahlgren (SGU).

the host Svecofennian supracrustal rocks (Fig. 66a). Furthermore, there is a marked difference in the degree of ductile deformation between the GSDG rocks inside the older phase of the so-called *Hedesunda granite* (Fig. 66b), in the north-eastern part of the Bergslagen region, and the host rocks to this intrusive complex.

It is inferred that the 1.87–1.84 Ga GSDG rocks intruded after ductile deformation under amphibolite-facies metamorphic conditions had affected their host rocks (see also Wikström & Karis 1991, Stephens et al. 2000, Bergman et al. 2004a). However, the margins of this suite, in the southern part of the Bergslagen region, are affected by penetrative ductile strain under amphibolite-facies metamorphic conditions (Wikström & Karis 1991). This deformation produced a grain-shape fabric in the 1.87–1.84 Ga rocks and a folding of this fabric (Figs. 66c and d). Furthermore, it is apparent that ductile strain affected the *Hedesunda granite* either during its intrusion, with the development of a magmatic foliation, or later in the solid state (Bergman et al. 2004a).

In contrast to the older GSDG suite described above, the rocks in the younger 1.81–1.78 Ga GSDG intrusive rock suite are only affected by ductile strain in the western part of the Bergslagen region where the Sveconorwegian tectonic overprint is conspicuous. This strain took the form of discrete shear zones (Fig. 65a). However, west of Skagern, in the south-westernmost part of the region, GSDG intrusive rocks of uncertain age (Wahlgren et al. 2005), but included on the bedrock map in the suite dominated by the 1.81–1.78 Ga GSDG intrusive rocks, are affected by more penetrative ductile deformation under amphibolite-facies conditions. The age of this deformation and metamorphism is also uncertain.

Table 4. Radiometric age data for the different suites of GSDG intrusive rocks, which formed around and after 1.87 Ga, and associated porphyries (volcanic and subvolcanic rocks) in the Bergslagen region. The three principal age suites at 1.87–1.84 Ga (late Svecokarelian), 1.81–1.78 Ga (late Svecokarelian) and 1.70–1.67 Ga (post-Svecokarelian) are distinguished in the table with the help of black lines.

Lithology	Method	Age (Ma)	N-S coordinate	E-W coordinate	Reference
Granite (Hedesunda)	U-Pb zircon	1869±9	6687365	1571830	Bergman et al., 2004a GFF 126, 18–19
Granite (Hedesunda)	U-Pb zircon/ titanite	1863±16	6701180	1595910	Appendix 2, this publication
Metagranite (Finspång)	U-Pb zircon (SIMS)	1855±6	6509750	1497200	Andersson et al., 2006 Geol. Mag. 143, 679–697
Quartz monzonite (Tiveden)	U-Pb zircon	1855±3	6517100	1429350	Wikström, 1996 SGU C 828, 41–47
Granite (Askersund)	U-Pb zircon	1848±15	6520850	1444950	Persson & Wikström, 1993 Geol. Fören. Stockh. Förh. 115, 321–329
Metagranodiorite (Hälla)	U-Pb zircon	1845±8	6475900	1537000	Wikström & Persson, 2002 SGU C 834, 58–61
Metagranite (Askersund)	U-Pb zircon	$1842^{+2\,3}_{-1\,3}$	6545500	1449450	Persson & Wikström, 1993 Geol. Fören. Stockh. Förh. 115, 321–329
Monzodiorite	U-Pb zircon	1812±14	6506820	1480570	Andersson, 1997a SGU Rapp. and medd. 91
Porphyry (Älgberget)	U-Pb zircon	$1802^{+1\,1}_{-9\,1}$	6722200	1435000	Lundqvist & Persson, 1999 GFF 121, 315–330
Granite, locally charnockitic (Degerfors)	U-Pb zircon	1796^{+6}_{-7}	6567100	1422400	Stephens et al., 1993 SGU C 823, 46–59
Porphyry (Lilla Digerliden)	U-Pb zircon	1795±4	6697500	1415500	Lundqvist & Persson, 1999 GFF 121, 315–330
Porphyry (Stora Kullsberget)	U-Pb zircon	$1792^{+1\,0}_{-8\,0}$	6693250	1404550	Lundqvist & Persson, 1999 GFF 121, 315–330
Granite (Hyttsjö)	U-Pb zircon	1791±2	6638860	1413270	Högdahl et al., 2007 GFF 129, 43–54
Porphyry (Bjursås)	U-Pb zircon	1787±9	6733240	1482315	Lundström, Persson & Ahl, 2002b SGU C 834, 43–49
Granite (Järna)	U-Pb zircon	$1786^{+1\,4}_{-1\,2}$	6650320	1435580	Persson and Ripa, 1993 SGU C 823, 41–45
Granite (Filipstad)	U-Pb zircon	1783±10	6623050	1409100	Jarl & Johansson, 1988 Geol. Fören. Stockh. Förh. 110, 21–28
Quartz monzodiorite (Roted)	U-Pb zircon	1699±7	6565550	1415850	Stephens et al., 1993 SGU C 823, 46–59
Metagranite (Hagfors-type)	U-Pb zircon	1684±13	6588400	1402100	Lindh et al., 1994 Lithos 31, 65–79
Granite (Siljan-type)	U-Pb zircon	1681±16	6725550	1408250	Ahl et al., 1999 Prec. Res. 95, 147–166
Metagranite (Filipstad-type)	U-Pb zircon	1676±7	6589900	1401250	Lindh et al., 1994 Lithos 31, 65–79

Age of crystallization

Sixteen U-Pb (zircon and titanite) ages that date the time of crystallization and contain uncertainties within the range adopted in this report are available for the late Svecokarelian, GSDG intrusive rocks and associated volcanic–subvolcanic rocks, referred to as porphyry, in the Bergslagen region. The locations of the dated samples are shown in Figure 64 and information concerning the geochronological data are summarized in Table 4. U-Pb ages for zircons and titanites on one sample from the so-called *Hedesunda granite* were obtained in connection with and following the work with the Bergslagen project. A more complete description of this sample and the geochronological results are presented in the appendix.

The separation of the late Svecokarelian GSDG intrusive rocks into two suites, based on the observed contrast in intrusion–deformation relationships, is confirmed by the geochronological data with age limits of 1.87–1.84 Ga and 1.81–1.78 Ga (Fig. 67). If all the uncertainties in the ages are taken into account, the time range lies between 1879 and 1829 Ma for the older suite, and between 1826 and 1773 Ma for the younger suite (Table 4). The older of these two suites overlaps in age with the younger, subordinate suite of GDG intrusive rocks in the marginal north-eastern and south-western parts of the Bergslagen region (Fig. 67). Thus, intrusive rocks with different composition formed simultaneously in this region.

The metagranite from Finspång, with a crystallization age of 1855±6 Ma, contains older inherited zircons with $^{207}Pb/^{206}Pb$ ages around 2.47–2.45 Ga, 2.03–2.02 Ga and 1.97 Ga (Andersson et al. 2006). These ages are similar to the detrital zircon ages in metasedimentary rocks in the Bergslagen region (see above). The occurrence of these inherited zircons and the peraluminous composition of the rock (Wikström

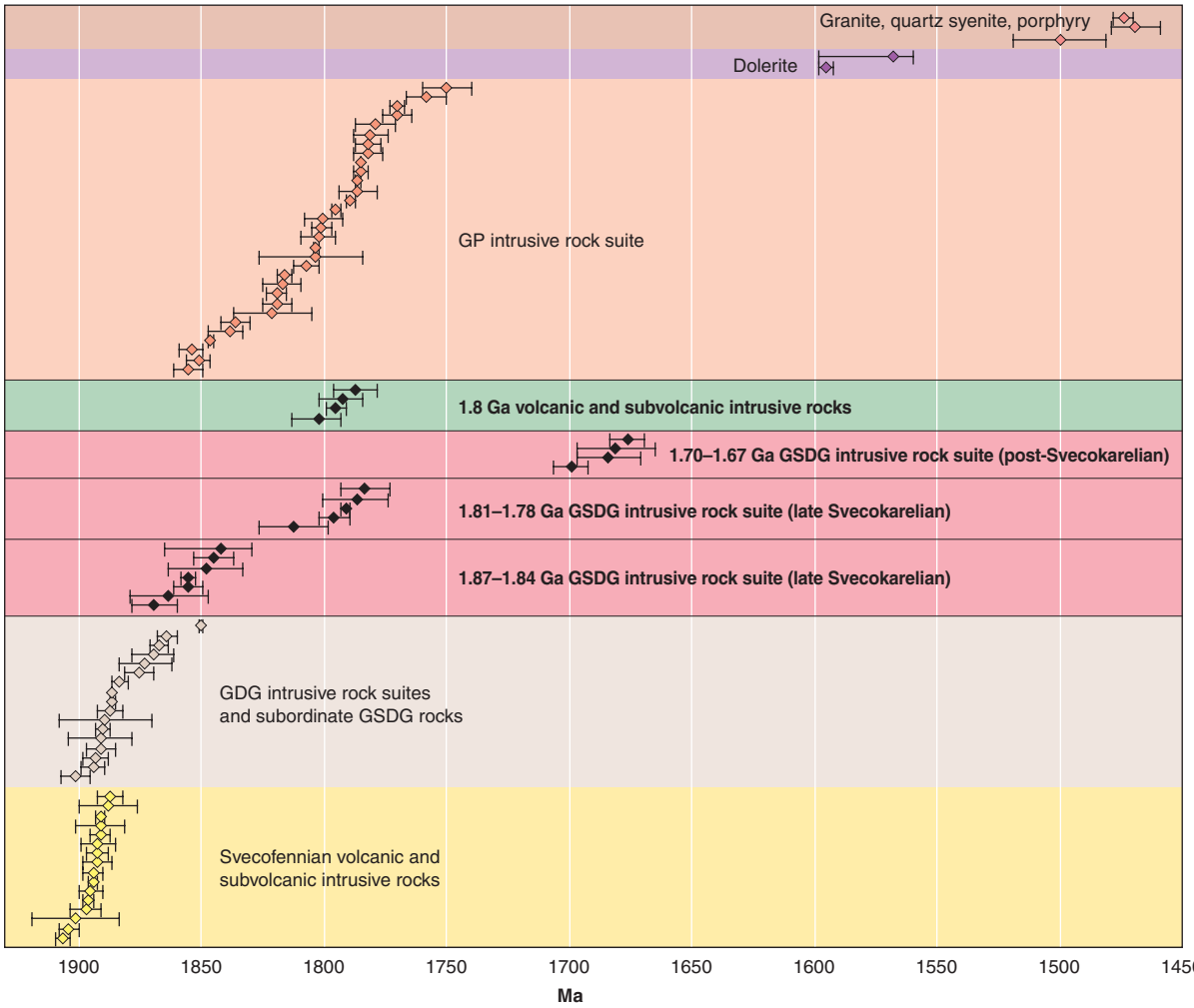

Fig. 67. Summary of U-Pb (zircon, titanite) age dates for the different suites of GSDG intrusive rocks, which formed around and after 1.87 Ga, and associated porphyries (volcanic and subvolcanic rocks) in the Bergslagen region. For purposes of comparison, all determinations of the age of crystallization of igneous and meta-igneous rocks in this region, with the exception of a U-Pb (baddeleyite) age from a dolerite in the Falun area (946±1 Ma), are shown and identified according to rock suite(s).

& Aaro 1986) indicate the contribution of a sedimentary source in the generation of the magma (Wikström & Aaro 1986, Andersson et al. 2006).

Geochemistry

The localities where data bearing on the geochemical composition of GSDG intrusive rocks have been acquired and used in this report are shown in Figure 68. 205 geochemical analyses from SGU's bedrock geochemistry database have been used in the compilation work.

The rocks within the GSDG intrusive rock suites show a wide range of compositions with I-type characteristics. In contrast to the GDG rocks, they show a trend from granite through quartz monzonite and quartz monzodiorite to gabbro in the Debon & Le Fort (1983) Q–P diagram (Fig. 69a). The GSDG intrusive rocks show a predominantly metaluminous composition in the Maniar & Piccoli (1989) A/NK–A/CNK diagram (Fig. 69b). However, at higher SiO_2 contents, they tend to lie in the peraluminous field (Fig. 69b). In sharp contrast to the GDG intrusive rocks, they show an alkali-calcic trend (Fig. 69c) in the classification system of Peacock (1931). The suite shows a shoshonitic character in a $K_2O/Na_2O–SiO_2$ diagram (Fig. 69d) modified after Turner et al. (1996).

Representative analyses of GSDG felsic intrusive rocks, with different SiO_2 contents, show a strong enrichment in large ion lithophile elements (LILE, e.g. Ba, Rb, Th, K) relative to high field strength elements (HFSE, e.g. Zr, Hf, Y, Yb) on the McDonough et al. (1992) spider diagram (Fig. 70). A factor difference greater than 10 is apparent. The samples show

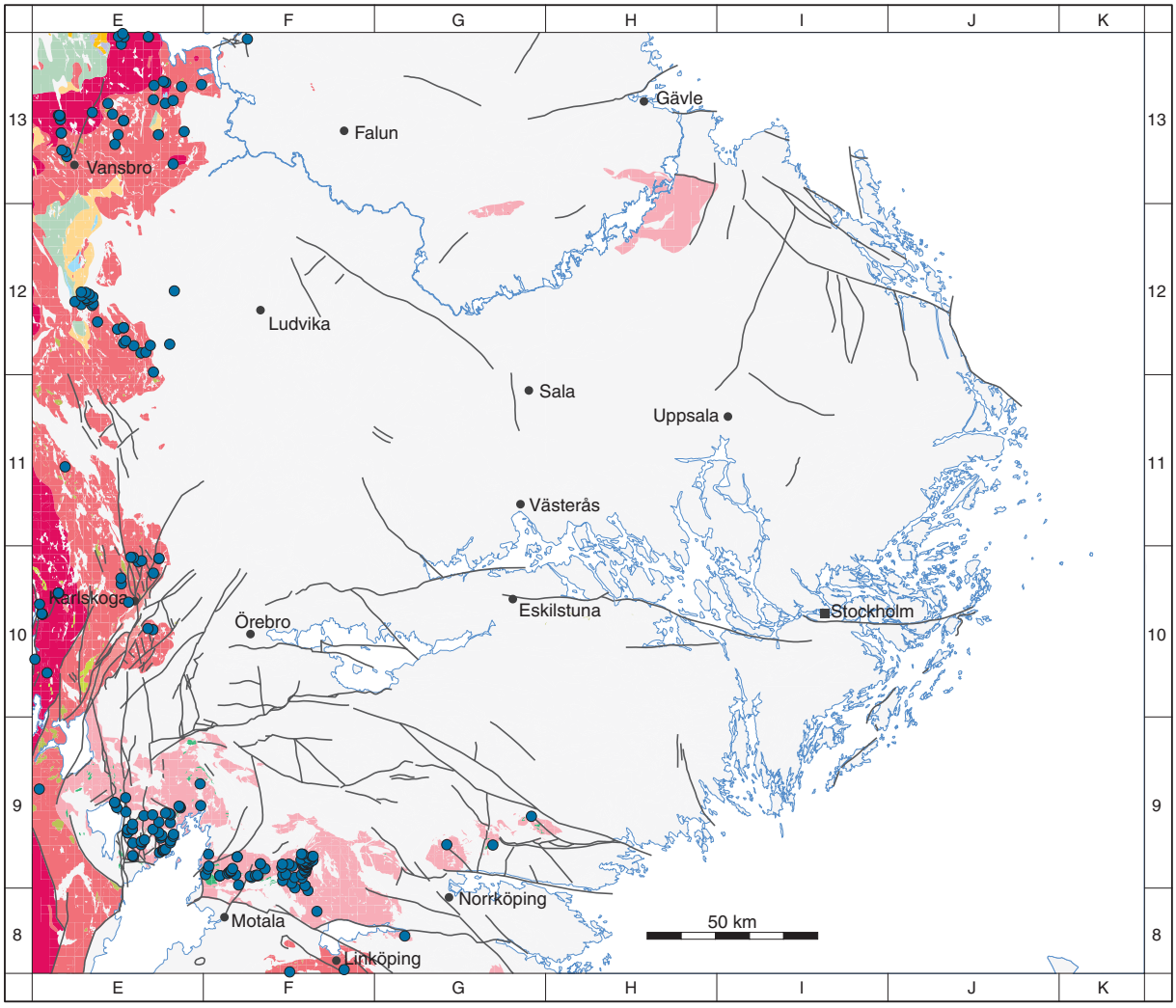

Sample site for bedrock geochemical analysis

Fig. 68. Location of sample sites for the geochemical analysis of the different suites of GSDG intrusive rocks that formed around and after 1.87 Ga in the Bergslagen region. Even the limited number of samples from the post-Svecokarelian, 1.70–1.67 Ga GSDG intrusive rock suite are included on the map. See Figure 64 for legend to the base geological map.

the same trends as the GDG intrusive rocks, with negative anomalies for Nb and Ta, and, particularly at higher SiO_2 contents, negative anomalies even for Sr, P and Ti. A conspicuous feature of the GSDG intrusive rocks is the high content of Ba in rocks with SiO_2 content around 60%. The GSDG rocks show a typical chondrite normalized pattern for rare earth elements in felsic rocks, with an enrichment of light rare earth (LREE) relative to heavy rare earth (HREE) elements and, in many samples, a negative Eu anomaly (Fig. 71). The $(La/Yb)_N$ ratios are variable with a mean value of approximately 10. Although there is considerable overlap, several analyses of GSDG intrusive rocks show higher Rb and Y+Nb contents than the GDG rocks and, consequently, a higher proportion of GSDG analyses lie in the within-plate field on the Pearce (1996) Rb–Y+Nb diagram (Fig. 72).

In the same manner as the GDG intrusive rocks, the negative anomalies for both Nb and Ta on the McDonough et al. (1992) plot (Fig. 70) indicate the influence of one or more source regions for the GSDG rocks that were affected, at some stage in their history, by subduction-related processes. A continental arc setting for the generation of these igneous rocks rather than an inherited signature from previous subduction events has been proposed by Andersson et al. (2004b). The strong enrichment in Ba, Rb, Th and K, and the position of the GSDG intrusive rocks on the Rb–Y+Nb diagram (Fig. 72) are consistent with a more mature continental source region relative to the generally older GDG rocks.

Petrophysical characteristics

The localities where data bearing on the petrophysical properties of late Svecokarelian, 1.87–1.84 Ga and 1.81–1.78 Ga GSDG intrusive rocks have been acquired and used in this report are shown in Figure 73. Samples from 595 localities have been analysed, whereas in situ gamma radiation measurements have been carried out at 58 sites. These data have been extracted from SGU's petrophysical database.

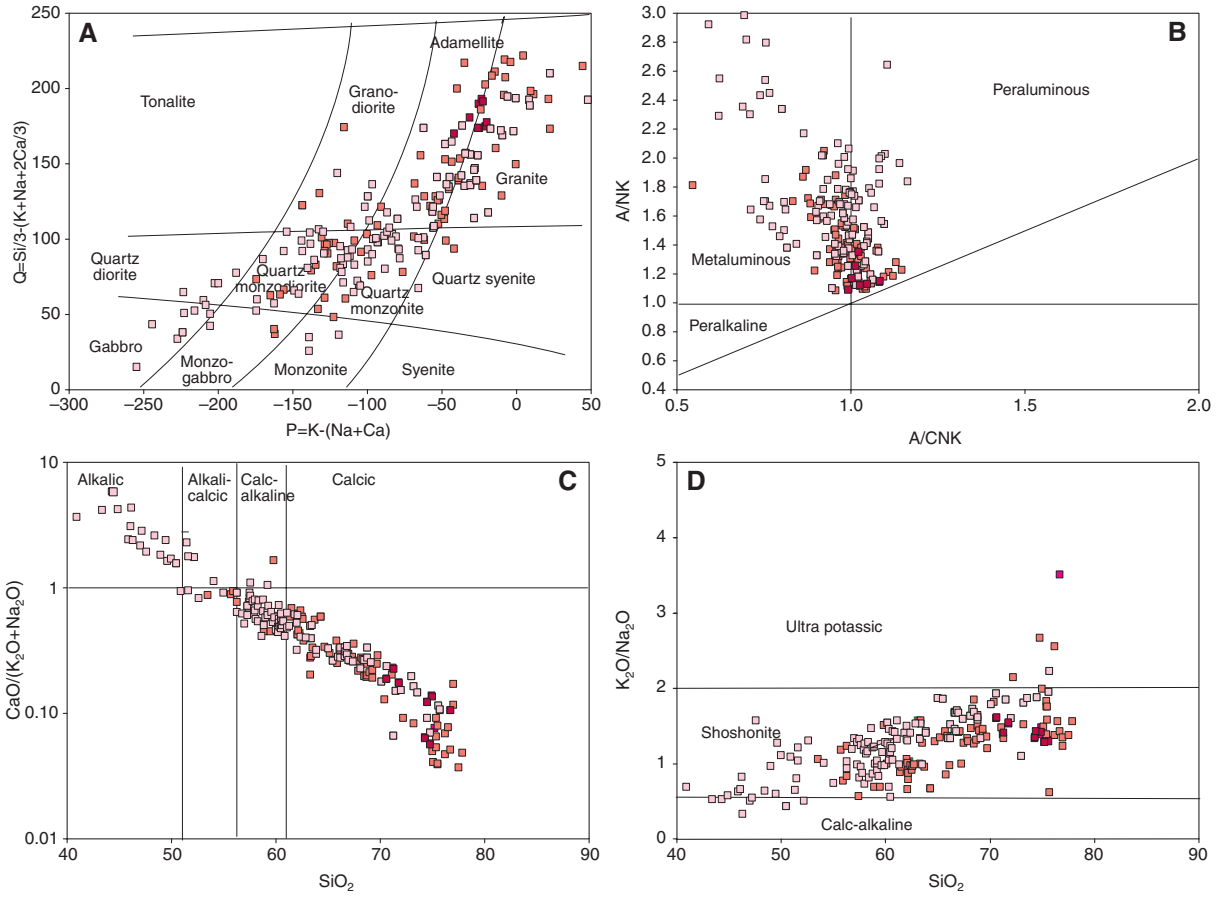

Fig. 69. Geochemical trends for GSDG intrusive rocks that formed around and after 1.87 Ga in the Bergslagen region. The symbols represent samples from the late Svecokarelian, 1.87–1.84 Ga (pink) and 1.81–1.78 Ga (red) GSDG intrusive rock suites. The limited number of samples from the post-Svecokarelian 1.70–1.67 Ga GSDG intrusive rock suite (dark red) are also included on the four diagrams. Diagrams after **A.** Debon & Le Fort (1983), **B.** Maniar & Piccoli (1989), **C.** Peacock (1931) and **D.** Turner et al. (1996).

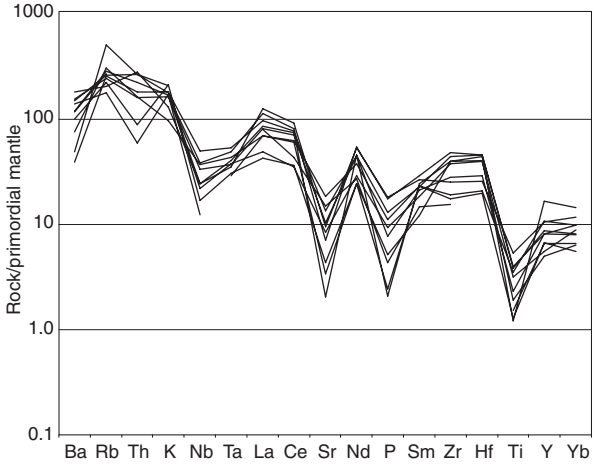

Fig. 70. Rock/primordial mantle spider diagram showing the relationships between large ion lithophile (LILE, e.g. Ba, Rb) and high field strength (HFSE, e.g. Zr, Ti and Y) elements for representative samples of the late Svecokarelian, 1.87–1.84 Ga and 1.81–1.78 Ga GSDG suites of intrusive rocks in the Bergslagen region. SiO_2 values for the selected samples span from 55.0 to 75.6%. Primordial mantle values after McDonough et al. (1992).

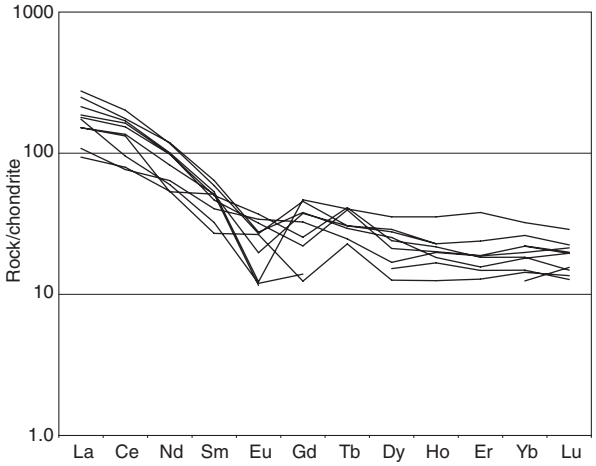

Fig. 71. Rock/chondrites diagram showing the relationships between light rare earth (LREE, e.g. La, Ce) and heavy rare earth (HREE, e.g. Yb, Lu) elements for representative samples of the late Svecokarelian, 1.87–1.84 Ga and 1.81–1.78 Ga GSDG suites of intrusive rocks in the Bergslagen region. SiO_2 values for the selected samples span from 55.0 to 75.6%. Chondrite values after Boynton (1984).

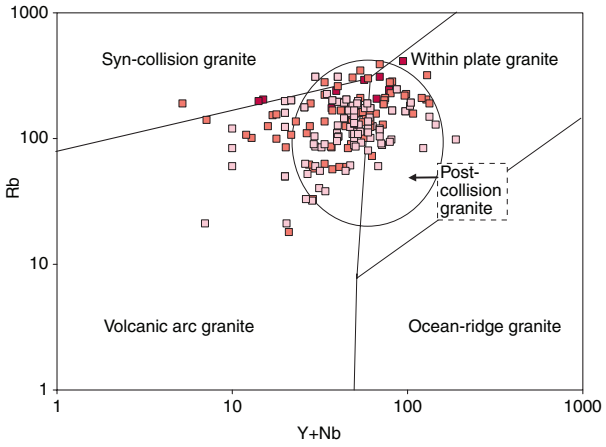

Fig. 72. Tectonic affinity diagram after Pearce (1996) for GSDG intrusive rocks that formed around and after 1.87 Ga in the Bergslagen region. The symbols represent samples from the late Svecokarelian, 1.87–1.84 Ga (pink) and 1.81–1.78 Ga (red) GSDG suites. The limited number of samples from the post-Svecokarelian 1.70–1.67 Ga GSDG intrusive rock suite (dark red) are also included in the figure.

Density

The density distributions for the rocks classified as granite and syenitoid and as dioritoid and gabbroid in the late Svecokarelian, 1.87–1.84 Ga and 1.81–1.78 Ga GSDG suites are shown in Figures 74a and 74b, respectively. The mean density for the granites and syenitoids is 2 689 kg/m^3, with a variation from 2 586 kg/m^3 to 2 882 kg/m^3. By contrast, the dioritoids and gabbroids show a mean density of 2 924 kg/m^3. Only 24 samples were classified as dioritoid–gabbroid rocks. This explains the irregular shape in the histogram in Figure 74b.

Magnetic susceptibility

The density–susceptibility diagram for all late Svecokarelian, 1.87–1.84 Ga and 1.81–1.78 Ga GSDG intrusive rocks is shown in Figure 75. The magnetic susceptibility is shown on a logarithmic scale in this illustration. The magnetic susceptibility shows a large variation. However, it is evident that susceptibility values beneath 50×10^{-6} SI and above $50\,000 \times 10^{-6}$ SI are rare.

Gamma radiation

The gamma radiation characteristics of the rocks in the late Svecokarelian, 1.87–1.84 Ga and 1.81–1.78 Ga GSDG intrusive suites are shown in Figures 76a and 76b. The single gabbroid sample shows a low gamma radiation with low values of uranium, thorium and potassium. Most of the granite–syenitoid rocks show moderate gamma radiation values with uranium concentrations below 7 ppm and thorium concentrations below 25 ppm. Higher thorium concentrations are found in the south-western part of the Bergslagen region in the area of map sheet 9E Askersund. In this area, the so-called *Askersund granite* shows a somewhat increased concentration of thorium.

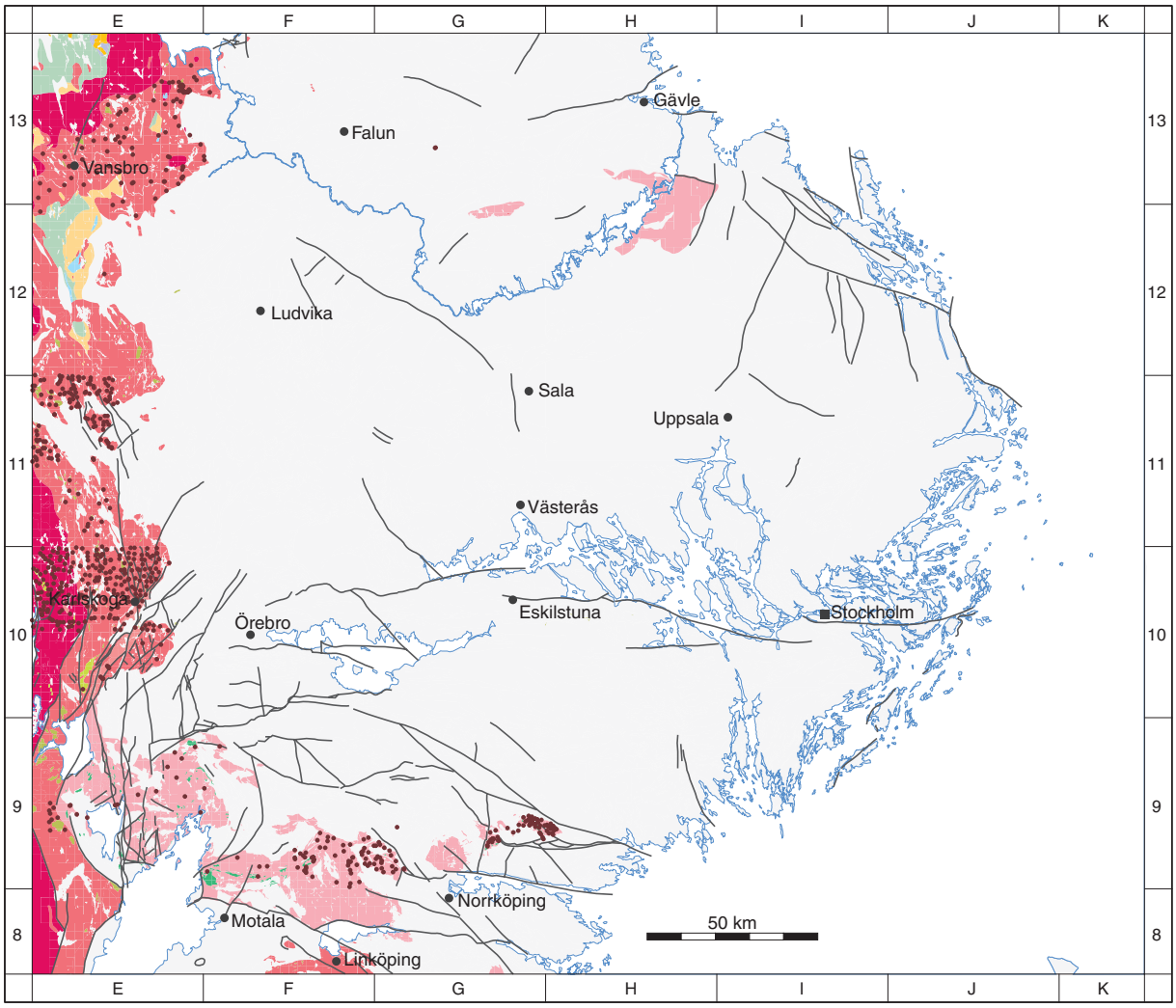

Fig. 73. Location of sample sites of late Svecokarelian, 1.87–1.84 Ga and 1.81–1.78 Ga GSDG intrusive rocks in the Bergslagen region for petrophysical and gamma radiation measurements (brown dots). See Figure 64 for legend to the base geological map.

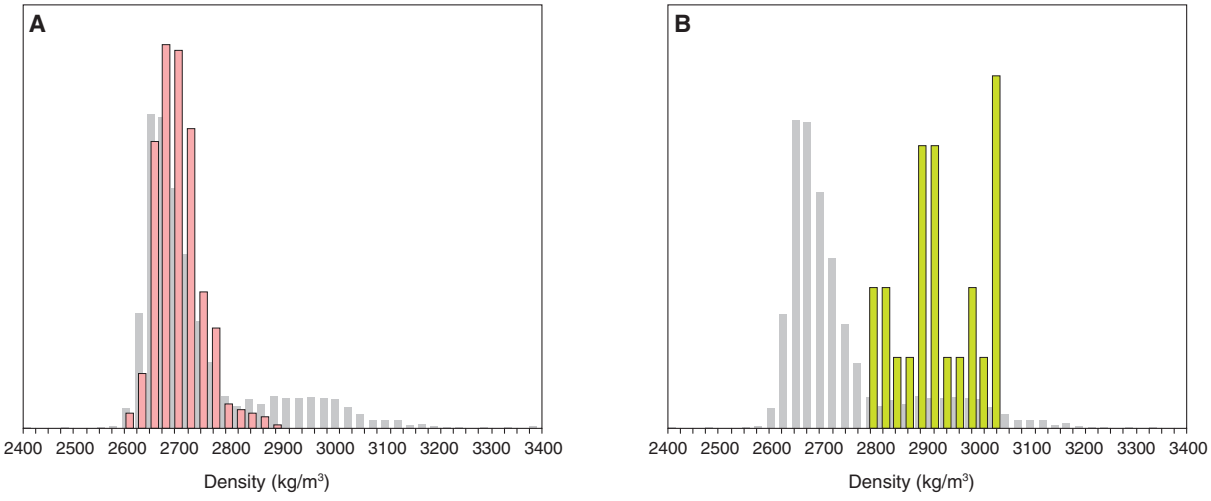

Fig. 74. Density distribution diagrams for the late Svecokarelian, 1.87–1.84 Ga and 1.81–1.78 Ga GSDG intrusive rocks in the Bergslagen region. **A.** Granites and syenitoids. **B.** Dioritoids and gabbroids. For purposes of comparison, all samples from the Bergslagen region are shown in grey.

Gravity anomalies, gravity modelling and inferred 3-D shape of some GSDG intrusive rocks

As indicated above, the late Svecokarelian, 1.87–1.84 Ga and 1.81–1.78 Ga GSDG intrusive rocks are dominated by granites and syenitoids with relatively low density. The large mass deficiency in the western part of the Bergslagen region coincides with the GSDG intrusive rocks that range in age from 1.81–1.78 Ga and 1.70–1.67 Ga (Fig. 77). In the south-western part of the Bergslagen region, especially in map areas 9E Askersund and 9F Finspång, gravity highs coincide with the older GSDG rocks that belong to the 1.87–1.84 Ga intrusive suite. An increased frequency of more mafic rocks at depth may explain the significant mass excess.

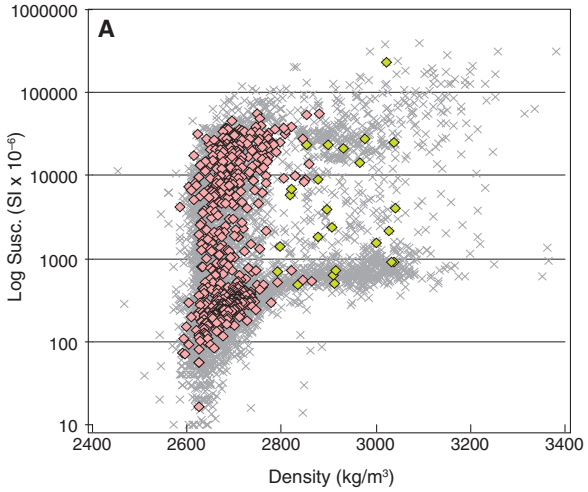

Fig. 75. Magnetic susceptibility–density diagram for the late Svecokarelian, 1.87–1.84 Ga and 1.81–1.78 Ga GSDG intrusive rocks in the Bergslagen region. For purposes of comparison, all samples from the Bergslagen region are shown in grey.

Attempts to understand the 3-D shape of some GSDG intrusions have been carried out, using integrated geophysical and structural geological studies in three separate bodies: the *Graversfors granite* (Wikström et al. 1980) and the *Finspång augen gneiss massif* (Wikström and Aaro, 1986), which outcrop on map sheets 9G Katrineholm SV and 9F Finspång SO, respectively (Fig. 77), and the *Gåsborn granite* (Cruden et al. 1999), which outcrops on map sheet 11E Filipstad NV (Fig. 77).

Graversfors granite

The *Graversfors granite* appears on the surface as a rounded massif c. 10 km in diameter. Lineaments inferred to represent a fault zone that strikes north–south divide the granite into two parts (Fig. 78). The eastern part has been inferred to represent a deeper section than the western half (Wikström et al. 1980). The detailed gravimetric and petrophysical study over the *Graversfors granite* includes gravity measurements at 265 stations and density measurements on samples from 315 locations.

The eastern part of the *Graversfors granite* shows a higher mean density (2 710 kg/m^3) compared with the western part (2 690 kg/m^3). This is consistent with the pattern on the Bouguer gravity anomaly map, where a gravity high is present in the eastern part of the intrusion (Fig. 78). Measurements of the magnetic susceptibility from 280 sites show that the western part has a higher magnetic susceptibility compared with the eastern part. A 3-D model for the shape of the intrusion was constructed based on calculations carried out along three different profiles on the Bouguer gravity anomaly map. A root zone in the eastern part of the intrusion that extends down to 5 km depth and a more limited thickness of 0.5–1 km for the western part of the intrusion has

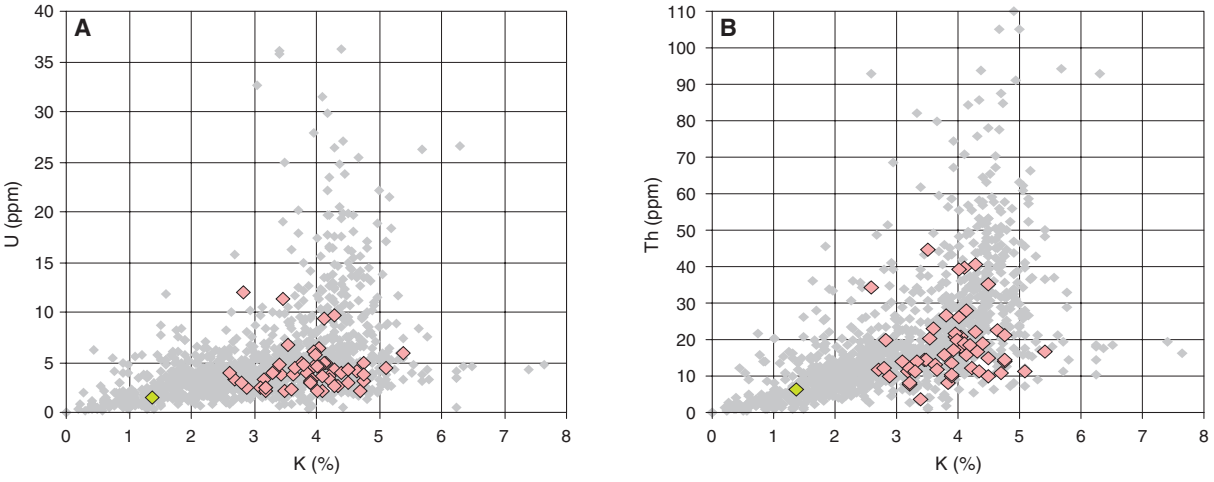

Fig. 76. Concentrations of **A.** uranium versus potassium and **B.** thorium versus potassium for the late Svecokarelian, 1.87–1.84 Ga and 1.81–1.78 Ga GSDG intrusive rocks in the Bergslagen region. For purposes of comparison, all samples from the Bergslagen region are shown in grey.

been inferred in the adopted 3-D model (Wikström et al. 1980). A mushroom-shaped structure inferred to be of diapiric origin was proposed (Wikström et al. 1980). Further discussion of the mechanism of emplacement of the 1.87–1.84 Ga suite of GSDG rocks is provided in the section "Deformation, metamorphism and mechanism of emplacement of the 1.87–1.84 Ga GSDG suite of intrusive rocks".

Finspång augen gneiss massif

A detailed geophysical, geochemical and stuctural investigation of the *Finspång augen gneiss massif* was carried out by Wikström & Aaro (1986). The geophysical study includes a combined interpretation of both gravimetric (Fig. 78) and magnetic data.

Prior to the interpretation, almost 200 new gravity stations were measured mainly along profiles with a point distance of approximately 200 m. The density of 162 samples of the different granites in the area was determined. The data were interpreted along two profiles using 2.5-D forward modelling software. The magnetic data were mainly used to resolve the dips of the contacts between different rock units. The results from the modelling work, based on both gravity and magnetic data, indicate that the *Finspång augen gneiss massif* has a restricted thickness of 3 km.

Gåsborn granite

Cruden et al. (1999) presented a structural geological and geophysical study of the *Gåsborn granite* in the western part of the Bergslagen region (Fig. 79). In particular, a detailed gravity survey was carried out with 555 measurements over the granite and the surrounding bedrock in order to carry out gravity modelling work. The gravity field over the *Gåsborn granite* is asymmetric. A large gravity minimum occurs over the

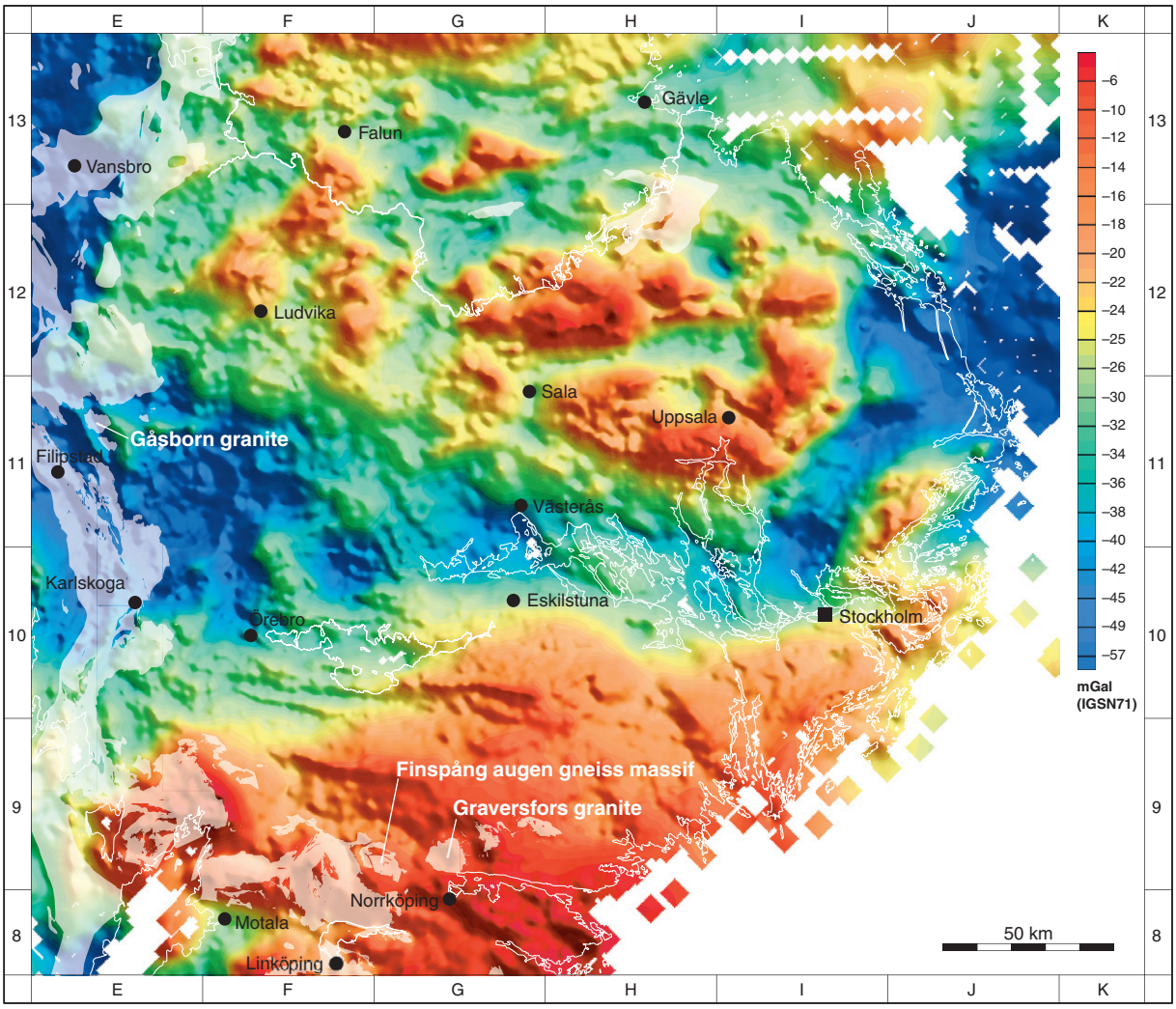

Fig. 77. Bouguer gravity anomaly map over the Bergslagen region. The areas shaded in grey represent the occurrences of late Svecokarelian, 1.87–1.84 Ga and 1.81–1.78 Ga GSDG intrusive rocks. Younger, 1.70–1.67 Ga GSDG rocks are also present further west in the westernmost part of the Bergslagen region (see Stephens et al. 2007a). The three massifs within which detailed geophysical and structural investigations and 3-D modelling work have been carried out are also marked on this map.

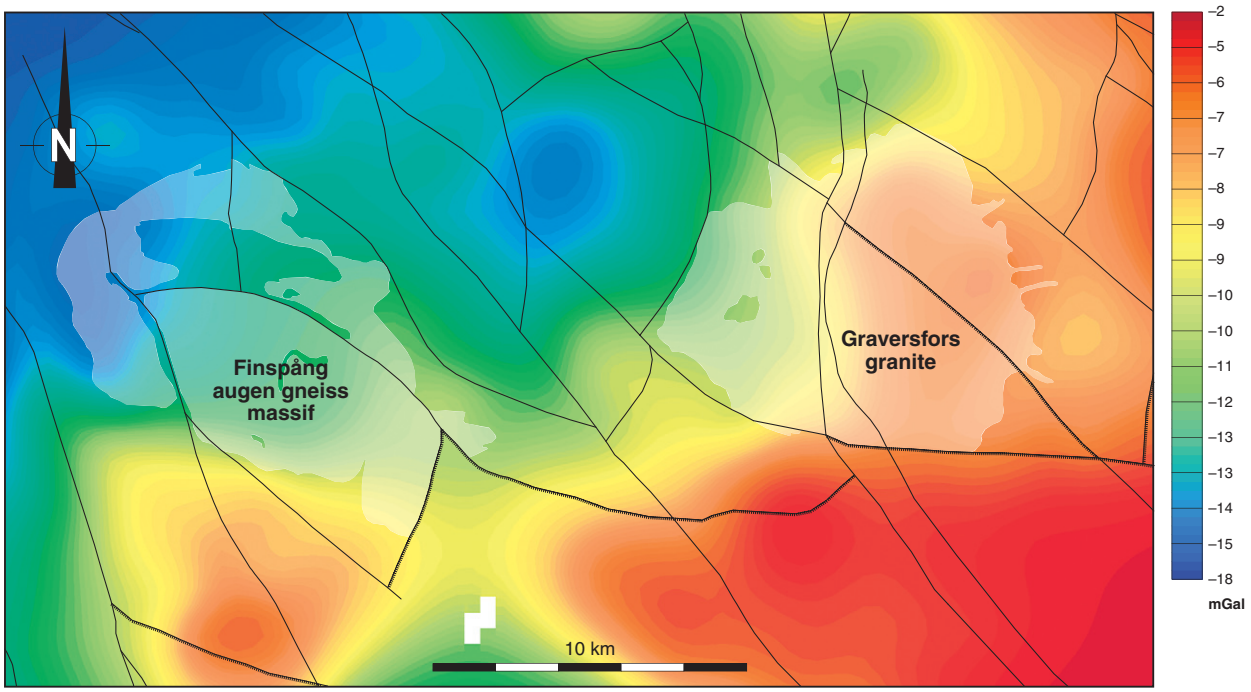

Fig. 78. Bouguer gravity anomaly map over and around the *Graversfors granite* and *Finspång augen gneiss massif* in the southern part of the Bergslagen region (see Fig. 77). Lineaments (thinner lines) and faults (thicker lines) are also shown.

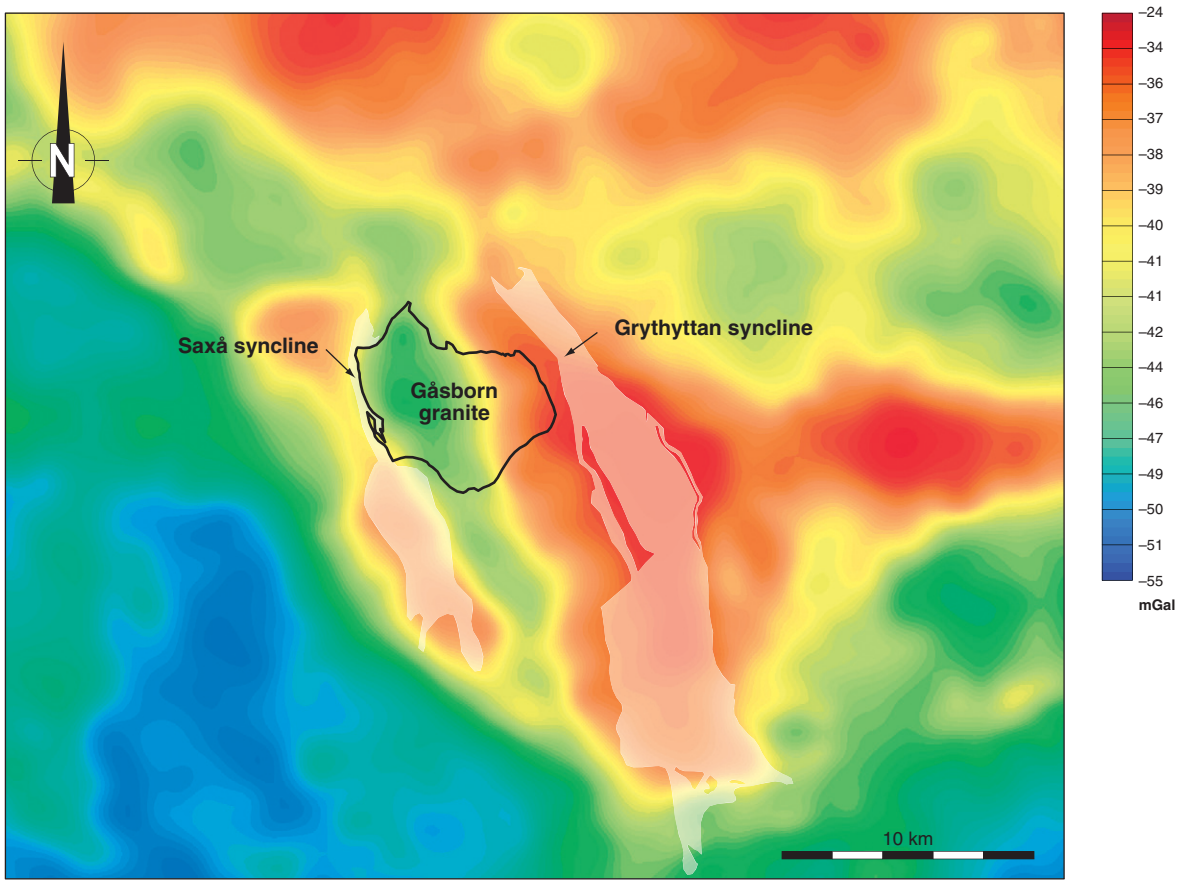

Fig. 79. Bouguer gravity anomaly map over and around the *Gåsborn granite* in the western part of the Bergslagen region (see Fig. 77). Note the large gravity minimum over the western part of the *Gåsborn granite*.

western part of the intrusion (Fig. 79) and the adjacent gravity maxima are spatially associated with metasedimentary rocks in the core of the adjacent *Saxå* and *Grythyttan synclines* (Fig. 79) identified, for example, in Plate 1 in Geijer & Magnusson (1944). The results of gravity modelling work across the major synclinal fold structures in this area were reported earlier in a regional traverse study (Werner et al. 1977).

A 15 km long profile was selected in a west-north-west–east-south-east direction and the gravity data were interpreted using 2.5-D forward modelling software (Cruden et al. 1999). The density used in the calculation for the *Gåsborn granite* was 2 662 kg/m^3 for the western part of the massif and a slightly higher value of 2 671 kg/m^3 for the eastern part. The density of the surrounding bedrock varied from 2 715 to 2 797 kg/m^3.

A good fit to the data was achieved in a model where the western half of the Gåsborn intrusion, corresponding to the main gravity minimum, has a depth of 2–3 km and the eastern half has a depth of only 100–300 m. The deeper western part of the intrusion was interpreted as a root zone with a sill-like body in the east where the emplacement and geometry of the intrusion were affected by a reactivated shear zone in a north-north-west–south-south-east strike direction (Cruden et al. 1999). The metasedimentary rocks were inferred to extend to a depth of 3 km in the synclinal fold structures (Cruden et al. 1999), in good agreement with the earlier interpretation (Werner et al. 1977).

Volcanic, subvolcanic and sedimentary rocks (1.8 Ga)

In the north-western part of the Bergslagen region, the 1.81–1.78 Ga suite of GSDG intrusive rocks is spatially associated with supracrustal rocks (Fig. 64). According to Hjelmqvist (1966), a stratigraphy can be established among the supracrustal rocks, which only locally are affected by ductile strain.

The lowermost unit is a grey to brownish, quartz- and plagioclase-phyric rock. Locally, hornblende also occurs as phenocrysts and the intensity of phenocrysts varies. The lowermost unit consists of both a coherent, subvolcanic facies with flow-banding and a tuffitic facies with clastic sedimentary interbeds. The unit was intruded by the so-called *Venjan porphyrite*, a white to reddish, subvolcanic rock with phenocrysts of plagioclase, K-feldspar, biotite and hornblende. Subsequently, several varieties of porphyry formed. They consist of both tuffitic and subvolcanic facies, show a variety of colours and range from phenocryst-rich to phenocryst-poor with plagioclase, K-feldspar and quartz phenocrysts. The volcanic and subvolcanic rocks vary from rhyolitic to trachytic, trachydacitic, dacitic and basaltic andesitic in composition. Clastic sedimentary rocks, which include quartz arenite, arkose, argillite and conglomerate, are interlayered with and stratigraphically overlie the volcanic units.

The subvolcanic porphyries contain xenoliths of coarser GSDG intrusive rocks that resemble the so-called *Filipstad granite*. West of the Bergslagen region, they also occur as dykes that intrude this GSDG rock (Hjelmqvist 1966). A close temporal relationship between the porphyries and the 1.81–1.78 Ga GSDG suite of intrusive rocks has been inferred. The supracrustal rocks show signs of alteration close to the contact with the so-called *Dala granites*, which belong to the younger 1.70–1.67 Ga GSDG intrusive suite (see later text).

Four U-Pb (zircon) ages in the range 1813 to 1778 Ma are available for the subvolcanic and volcanic porphyries that are spatially associated with the 1.81–1.78 Ga GSDG intrusive suite (Fig. 64 and Table 4). These geochronological data confirm the close temporal relationship between the porphyries and the coarser intrusive rocks (Fig. 67) and all these igneous rocks are inferred to be magmatically related to each other (e.g. Lindström et al. 2000).

Late Svecokarelian Granite-pegmatite (GP) intrusive rock suite (1.85–1.75 Ga)

Rock type, spatial distribution and intrusion–deformation relationships

Granite sensu stricto, as well as associated pegmatite, aplite and granite dykes, veins and lenses, which mainly cross-cut, but are locally conformable with structures in the surrounding country rock, occur in many parts of the Bergslagen region (Fig. 80). On the basis of these field relationships, this Granite-pegmatite or GP intrusive rock suite is inferred to have intruded during the waning stages of the Svecokarelian orogeny as late- or post-tectonic intrusions, i.e. they show the same tectonic relationships as the GSDG rocks formed around and after 1.87 Ga.

The granites in the GP intrusive rock suite are red to grey, vary in grain size from fine- to coarse-grained and are either equigranular (Fig. 81a) or microcline-phyric (Fig. 81b). Fine- to medium-grained, equigranular varieties are commonly referred to in the literature as the *Stockholm-type*, whereas coarsely and finely porphyritic varieties are generally referred to as the *Fellingsbro-type* and *Enkullen-type*, respectively. The so-called *Malingsbo-type* granites contain abundant, more or less assimi-

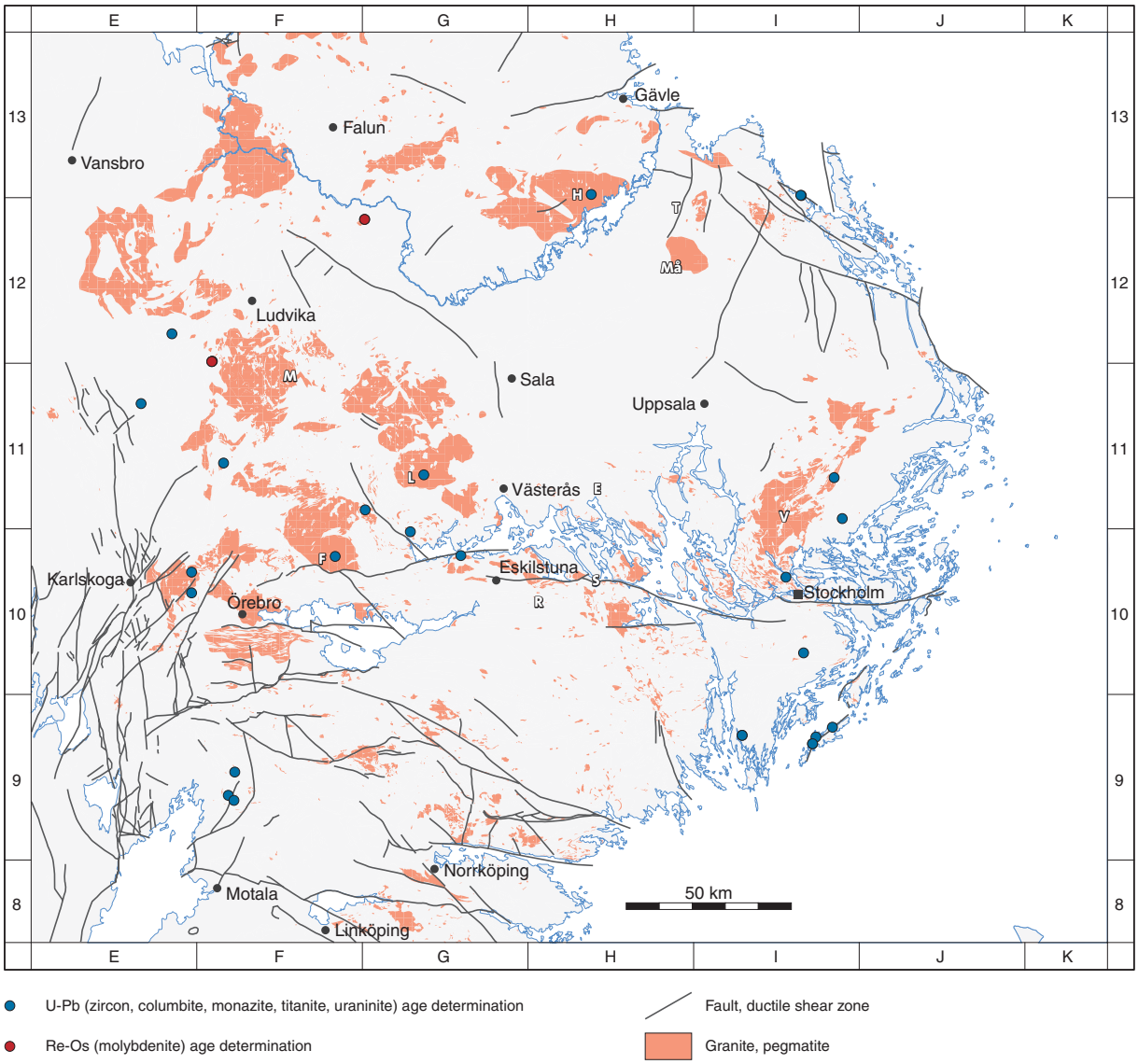

Fig. 80. Distribution of rocks belonging to the late Svecokarelian, 1.85–1.75 Ga GP intrusive suite at the ground surface in the Bergslagen region. The location of samples from this suite of intrusive rocks that have been dated using the U-Pb (zircon, columbite, monazite, titanite, uraninite) and Re-Os (molybdenite) age dating techniques in the Bergslagen region, and the location of place names referred to in the section "Late Svecokarelian Granite-pegmatite (GP) intrusive rock suite (1.85-1.75 Ga)" are also shown. E = Enköping, F = Fellingsbro, H = Hedesunda, L = Lisjö, M = Malingsbo, Må = Månkarbo, R = Ribbingelund, S = Strängnäs, T = Tierp, V = Vallentuna.

lated inclusions (restites) of the country rocks (Fig. 81c), indicative of their source from older crustal material. Furthermore, the larger intrusive bodies are locally associated with dyke swarms that intrude the older country rocks. In places, the country rocks show signs of coarsening and recrystallization in direct contact with the GP intrusive rocks.

In contrast to the GSDG rocks, the rocks in the GP intrusive suite are compositionally quite simple, with high contents of quartz. In general, they also lack enclaves of mafic material. However, scattered occurrences of dolerite are spatially associated with equigranular granite, similar to that referred to as *Stockholm-type*, in the Strängnäs area in the central part of the Bergslagen region (Stålhös & Björk 1983, Stålhös 1984). During field work in connection with the current work, it was concluded that these rocks formed synchronously as composite dykes (Fig. 81d). The dykes are clearly discordant to the high-grade gneissic structure in the country rock. Despite the relatively few documented occurrences, this dolerite-granite association indicates the intrusion of some mantle-derived material at a crustal level where the intrusion of granite dominated.

The pegmatites included in the GP intrusive suite form three varieties. One variety shows a simple mineralogy with quartz, feldspar (albite and microcline-perthite) and muscovite (locally also minor biotite and garnet). The other two varieties have relatively more

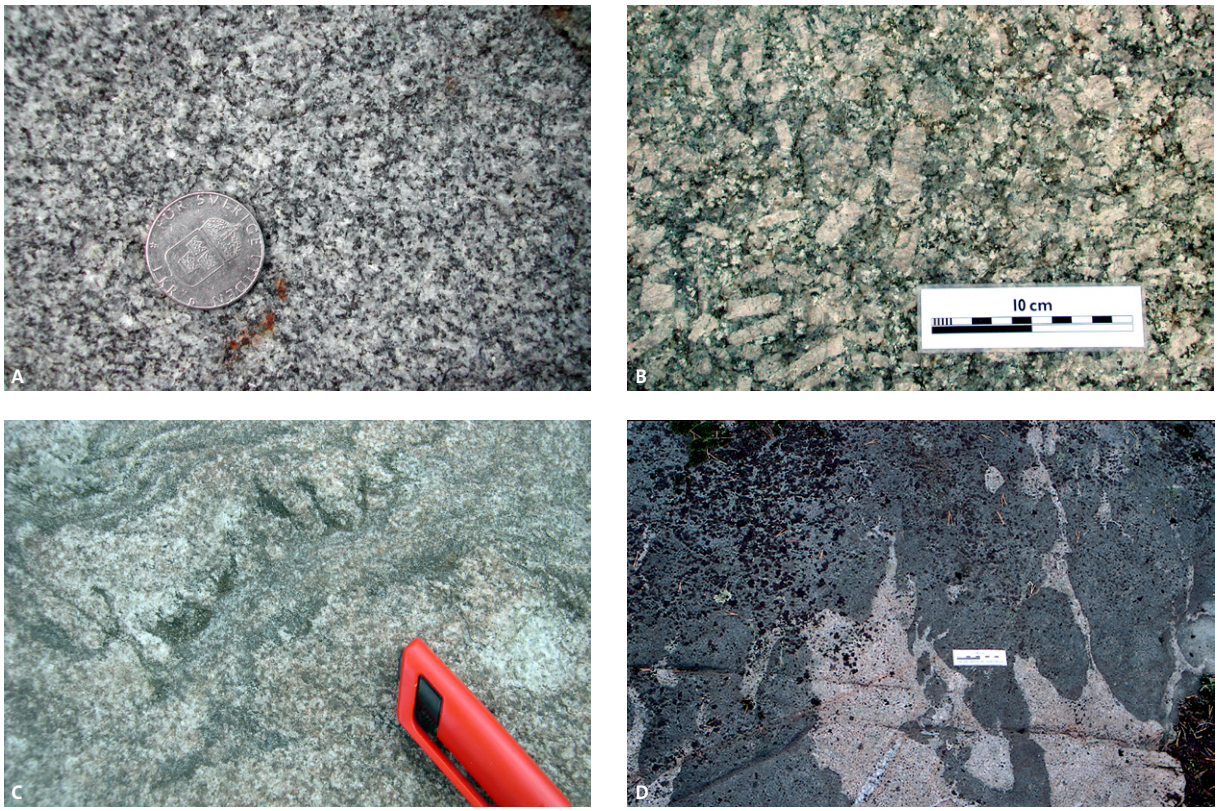

Fig. 81. Character of some rocks in the GP intrusive suite, Bergslagen region. **A.** Grey, equigranular, post-tectonic granite (*Stockholm-type*). E18 roadside exposure, Stockholm (10I Stockholm NV). Photograph: Benno Kathol (SGU). **B.** Post-tectonic porphyritic granite with rectangular K-feldspar phenocrysts. Månkarbo (12H Söderfors NO). Photograph: Stefan Bergman (SGU). **C.** Medium-grained, equigranular and restite-bearing granite in migmatite complex (12E Säfsnäs NV). Photograph: Magnus Ripa (SGU). **D.** Post-tectonic composite dyke with dolerite and grey, equigranular granite of *Stockholm-type*. View of horizontal section to east in outcrop 1 km north-north-west of Ribbingelund (10H Strängnäs NV). Photograph: Michael Stephens (SGU).

complex mineralogies that, in addition to the mineral phases mentioned above, consist of beryl, monazite, topaz, tourmaline and REE minerals. The mineralogically more complex types can be chemically divided into NYF (Nb-Y-F rich) and LCT (Li-Cs-Ta rich) pegmatites (Smeds 1990, 1994). Certain minerals in pegmatite have been exploited as a non-metallic mineral resource in the Bergslagen region (see section "Mineral and bedrock deposits").

Age of crystallization

Thirty-one age determinations that date the time of crystallization and contain uncertainties that lie within the range adopted in this report are available for rock samples from the GP intrusive suite in the Bergslagen region. The locations of the dated samples are shown in Figure 80 and pertinent information bearing on the geochronological data is summarized in Table 5.

The majority of age determinations arise from U-Pb (zircon) data from granitic intrusions (Table 5). However, granites in the GP intrusive suite have also been dated with the help of U-Pb (monazite) and U-Pb (titanite) data (Table 5). Furthermore, U-Pb dating of titanite and uraninite in skarn as well as Re-Os dating of molybdenite in a mineralization has also been carried out (Table 5). The skarn and molybdenite mineralization occurrences are spatially associated with and are inferred to have formed in connection with the intrusion of the granites in the GP suite. U-Pb (zircon) and U-Pb (monazite) ages were determined from one sample of metagranite during the current work (Table 5) and these data are presented and evaluated in more detail in the appendix. Pegmatites in the GP intrusive suite have been dated primarily with the help of the U-Pb (columbite) age dating technique (Table 5).

Difficulties in the interpretation of some of the older U-Pb (zircon) ages due to the inheritance of older zircons have been observed (Romer 1997 and the appendix) and further work is necessary to resolve the significance of this issue in the interpretation of the geochronological data from the GP intrusive suite. For this reason, the geochronological data need to be handled with care. Bearing in mind these remarks, no detailed subdivision

Table 5. Radiometric age data for rocks belonging to the late Svecokarelian, 1.85–1.75 Ga GP intrusive suite in the Bergslagen region.

Lithology	Method	Age (Ma)	N-S coordinate	E-W coordinate	Reference
Granite (Forsmark)	U-Pb zircon (SIMS)/ titanite	1855±6/ 1844±4	6700543	1632654	Hermansson et al., 2007. Prec. Res. 153, 29–45
Pegmatite (Stora Vika)	U-Pb zircon	1854±5	6537500	1614800	Welin & Stålhös, 1986. Geol. Fören. Stockh. Förh. 108, 31–34
Granite (Forsmark)	U-Pb zircon (SIMS)	1851±5	6700655	1632484	Hermansson et al., 2007. Prec. Res. 153, 29–45
Granite (Köping)	U-Pb monazite	1846±1	6599000	1514600	Romer & Öhlander, 1995. GFF 117, 69–74
Metagranite (Haninge)	U-Pb monazite/ zircon	1838^{+9}_{-5}, 1877±5	6562425	1633335	Appendix 2, this publication
Tonalite (Åmmeberg)	U-Pb zircon	1836±6	6519450	1459650	Billström, 1985. Medd. Stockholms Univ. Geol. Inst. 263
Pegmatite (Utö)	U-Pb columbite	1821±16	6540000	1642000	Romer & Smeds, 1994. Prec. Res. 67, 141–158
Pegmatite (Norrö)	U-Pb columbite	1819±6	6535000	1636000	Romer & Smeds, 1994. Prec. Res. 67, 141–158
Pegmatite (Rånö)	U-Pb columbite	1819±4	6537000	1637000	Romer & Smeds, 1994. Prec. Res. 67, 141–158
Skarn (Högberget)	Re-Os molybdenite	1817±8	6650450	1454600	Stein et al., 1996. Abstract, Goldschmidt Conf. 594
Pegmatite (Norrö)	U-Pb columbite	1816±3	6535000	1636000	Romer & Smeds, 1994. Prec. Res. 67, 141–158
Granite (Älvlången)	U-Pb zircon	1807±5	6586840	1448480	Stephens et al., 1993. SGU C 823, 46–59
Granite (Stockholm)	U-Pb zircon	1803^{+23}_{-19}	6585300	1627950	Ivarsson & Johansson, 1995. GFF 117, 67–68
Pegmatite (Reboda)	U-Pb columbite	1802.7±1	6619800	1458200	Romer and Smeds 1997. Prec. Res. 82, 85–99
Granite (Bispberg)	Re-Os molybdenite	1802±7	6693350	1500750	Sundblad et al., 1996. Abstract, 7th Int. Meeting on Rapakivi granites, 72–73
Pegmatite (Kolsva)	U-Pb columbite	1801.1±3.8	6605600	1500900	Romer & Smeds, 1997. Prec. Res. 82, 85–99
Skarn (Högberget)	Re-Os molybdenite	1800±8	6650450	1454605	Sundblad et al., 1996. Abstract, 7th Int. Meeting on Rapakivi granites, 73–74
Pegmatite (Gruvdalen)	U-Pb columbite	1795±2	6603000	1645000	Romer & Smeds, 1994. Prec. Res. 67, 141–158
Skarn (Yxsjöberg)	U-Pb titanite	1789±2	6658850	1442570	Romer & Öhlander, 1994. GFF 116, 161–166
Granite (Kilsbergen)	U-Pb zircon	1786±8	6580560	1448480	Stephens et al., 1993. SGU C 823, 46–59
Pegmatite (Skrumpetorp)	U-Pb columbite	1786.4±1	6517900	1461300	Romer & Smeds, 1997. Prec. Res. 82, 85–99
Pegmatite (Stora Vika)	U-Pb columbite	1785±3	6537500	1614800	Romer & Smeds, 1997. Prec. Res. 82, 85–99
Skarn (Håkanstorp)	U-Pb uraninite	1785	6526400	1461600	Welin, 1961. Geol. Fören. Stockh. Förh. 83, 129–143
Granite (Fellingsbro)	U-Pb zircon	1782±6	6591530	1491870	Patchett et al., 1987. Prec. Res. 35, 145–160
Granite (Hedesunda)	U-Pb zircon/titanite	1782±5	6700920	1569210	Persson & Persson, 1997. GFF 119, 91–95
Granite (Bispberg)	Re-Os molybdenite	1781±7	6693350	1500755	Sundblad et al., 1996. Abstract, 7th Int. Meeting on Rapakivi granites, 73–74
Granite (Vallentuna)	U-Pb zircon	1779±8	6615400	1642500	Öhlander & Romer, 1996. GFF 118, 217–225
Granite (Lisjö)	U-Pb zircon	1770±6	6616250	1518650	Öhlander & Romer, 1996. GFF 118, 217–225
Granite (Lisjö-type)	U-Pb zircon	1769.7±3.4	6591800	1529800	Öhlander & Romer, 1996. GFF 118, 217–225
Granite (Skålhöjden)	U-Pb zircon	1758±8	6637700	1433240	Sundblad et al., 1993. Prec. Res. 64, 319–335
Granite (Högberget)	U-Pb zircon	1750±10	6650500	1454750	Bergman et al., 1995. GFF 117, 87–95

into different age groups is proposed and the ages for the granites and pegmatites in the GP intrusive suite fall in the time intervals 1861 Ma to 1740 Ma and 1837 to 1782 Ma, respectively, when uncertainties in ages are accounted for (Fig. 82). Nevertheless, it can be noted that, if one analysis of a pegmatite from Utö in the Stockholm archipelago (1821±16 Ma) with a large uncertainty in age is removed from the data set, all the ages for granites and pegmatites lie in two distinct groups. These two groups show ranges between 1861 and 1830 Ma and 1825 and 1740 Ma, reminiscent of the ages of the late Svecokarelian, 1.87–1.84 and 1.81–1.78 Ga GSDG intrusive rock suites (Fig. 82).

Geochemistry

The localities where data bearing on the geochemical composition of rocks in the GP intrusive suite have been acquired and used in this report are shown in Figure 83. 237 geochemical analyses from SGU's bedrock geochemistry database have been used in the compilation work.

The silica content is consistently high in the rocks that belong to the GP suite with an average of 72.4 wt %. For this reason and in contrast to both the GDG and GSDG intrusive rocks, the analyses are strongly concentrated in the adamellite and granite fields in a

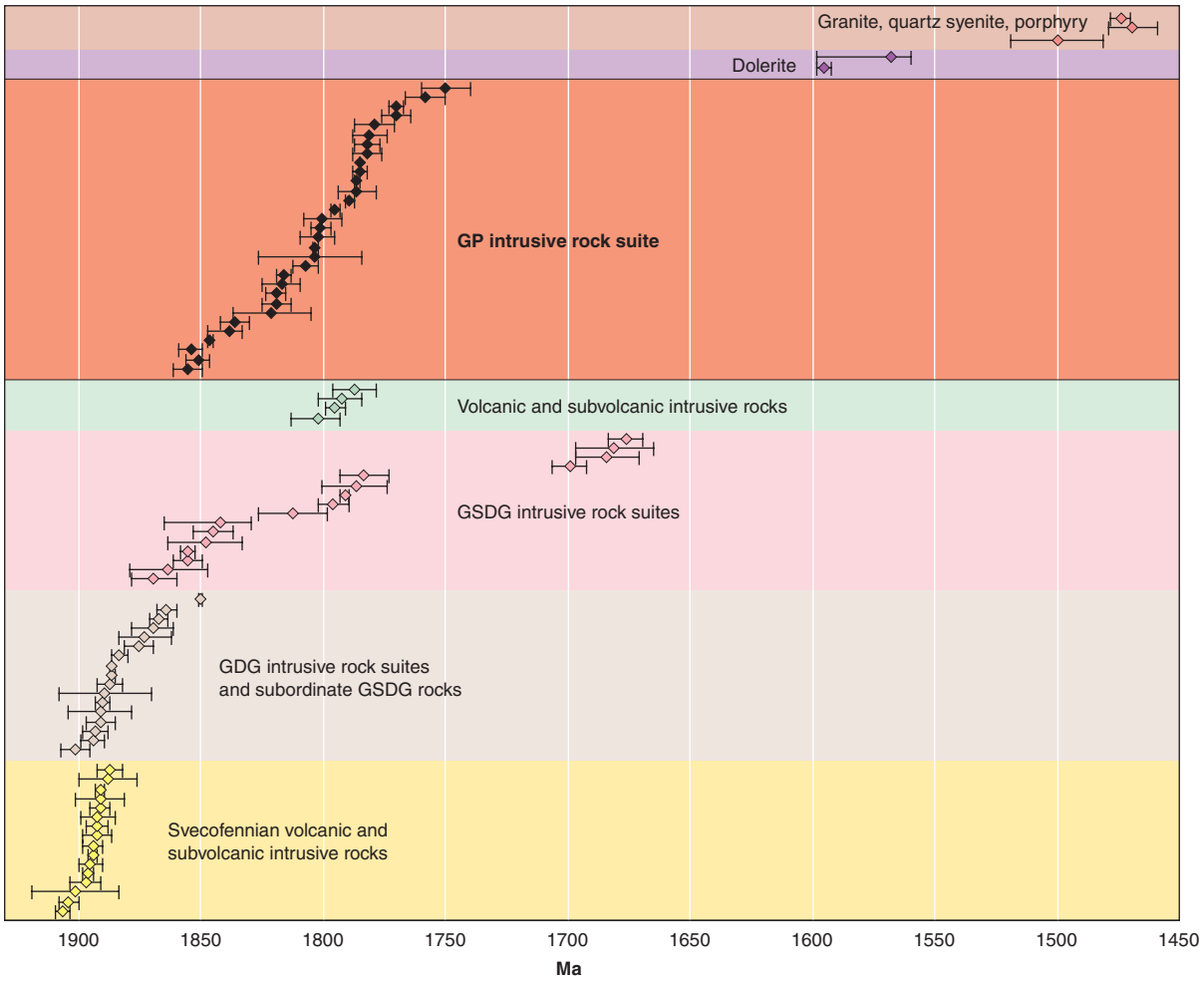

Fig. 82. Summary of U-Pb (zircon, monazite, columbite, titanite, uraninite) and Re-Os (molybdenite) age dates for the rocks belonging to the GP intrusive suite in the Bergslagen region. For purposes of comparison, all determinations of the age of crystallization of igneous and meta-igneous rocks in this region, with the exception of a U-Pb (baddeleyite) age from a dolerite in the Falun area (946±1 Ma), are shown and identified according to rock suite(s).

Debon & Le Fort (1983) Q–P diagram (Fig. 84a). The rocks in the GP intrusive suite show a predominantly peraluminous composition in the Maniar & Piccoli (1989) A/NK–A/CNK diagram (Fig. 84b). Since less evolved compositions are absent, it is difficult to assess the compositional trend in the Peacock (1931) classification system (Fig. 84c). The analyses are concentrated in the shoshonitic field in a $K_2O/Na_2O–SiO_2$ diagram (Fig. 84d) modified after Turner et al (1996), identical to the most evolved GSDG intrusive rocks.

Representative analyses of GP intrusive rocks show a strong enrichment in large ion lithophile elements (LILE, e.g. Ba, Rb, Th, K) relative to high field strength elements (HFSE, e.g. Zr, Hf, Y, Yb) on the McDonough et al. (1992) spider diagram (Fig. 85). As for the GDG and GSDG intrusive rocks, a factor difference greater than 10 is apparent. The samples show the same trends as especially the GSDG rocks, with negative anomalies for Nb and Ta, as well as sharp, negative anomalies for Sr, P and Ti (Fig. 85), consistent with the evolved character of the GP rocks. Representative analyses of GP intrusive rocks show a distinctive enrichment of light rare earth (LREE) relative to heavy rare earth (HREE) elements and a sharp negative Eu anomaly (Fig. 86). The $(La/Yb)_N$ ratios are somewhat variable with a mean value of approximately 10.

The analyses show a restricted range of high Rb values compared with the GDG and GSDG intrusive rocks, in accordance with their consistently evolved character. However, there is a wider spread in the Y+Nb values compared with the analyses in the other intrusive rock suites. For these reasons, the analyses spread out over the fields of volcanic arc and within plate granites on the Pearce (1996) Rb–Y+Nb diagram (Fig. 87).

The GP rocks are geochemically distinguishable from the GDG and GSDG intrusive rocks on the basis of their consistent, evolved character and the stronger tendency to a peraluminous composition. However, several

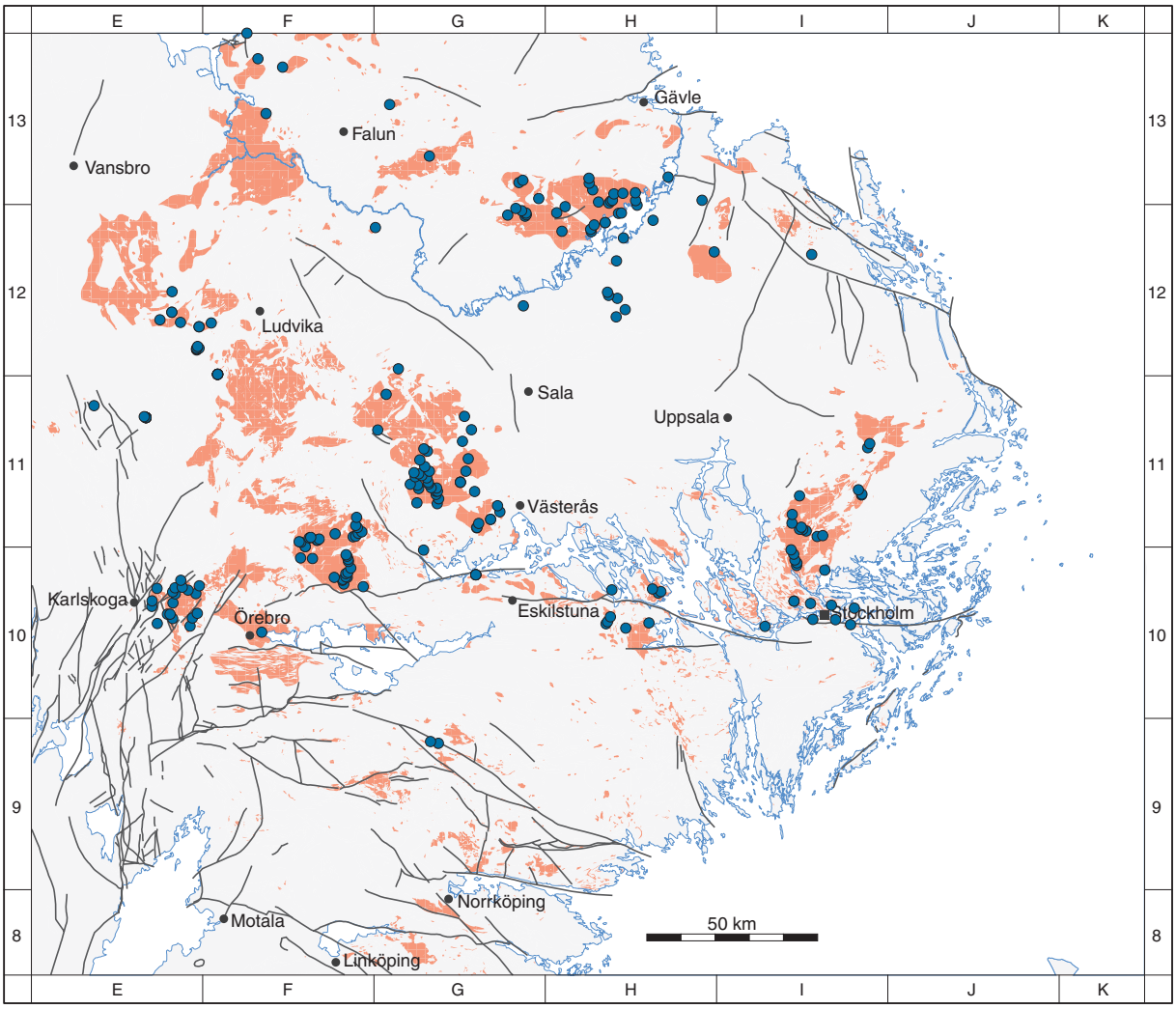

● Sample site for bedrock geochemical analysis

Fig. 83. Location of sample sites for the geochemical analysis of rocks included in the late Svecokarelian, 1.85–1.75 Ga GP intrusive suite in the Bergslagen region. See Figure 80 for legend to the base geological map.

trace element characteristics resemble those observed in especially the GSDG rocks. It is inferred that these rocks were derived from a mature continental environment that was affected, at one or more periods during its geological history, by subduction-related processes.

Petrophysical characteristics

The localities where data bearing on the petrophysical properties of rocks in the GP intrusive suite have been acquired and used in this report are shown in Figure 88. Samples from 514 localities have been analysed, whereas in situ gamma radiation measurements have been carried out at 228 sites. As for the other intrusive suites, these data have been extracted from SGU's petrophysical database. Petrophysically, the rocks in the GP intrusive suite differ significantly from other rock suites in the Bergslagen region. This difference is consistent with their more evolved character as described above.

Density

In agreement with their generally homogeneous granitic composition, the rocks in the GP intrusive suite show a lower density compared with the rocks in the other igneous suites. The mean density of these rocks is 2 650 kg/m^3 (Fig. 89a) compared with a mean density of 2 713 kg/m^3 for the total population. However, the range in density of the felsic rocks is from 2 540 to 2 750 kg/m^3 and a higher density tail is present in the density distribution diagram (Fig. 89a). Thus, the density values permit the detection of some samples that show densities higher than that encountered in granite sensu stricto.

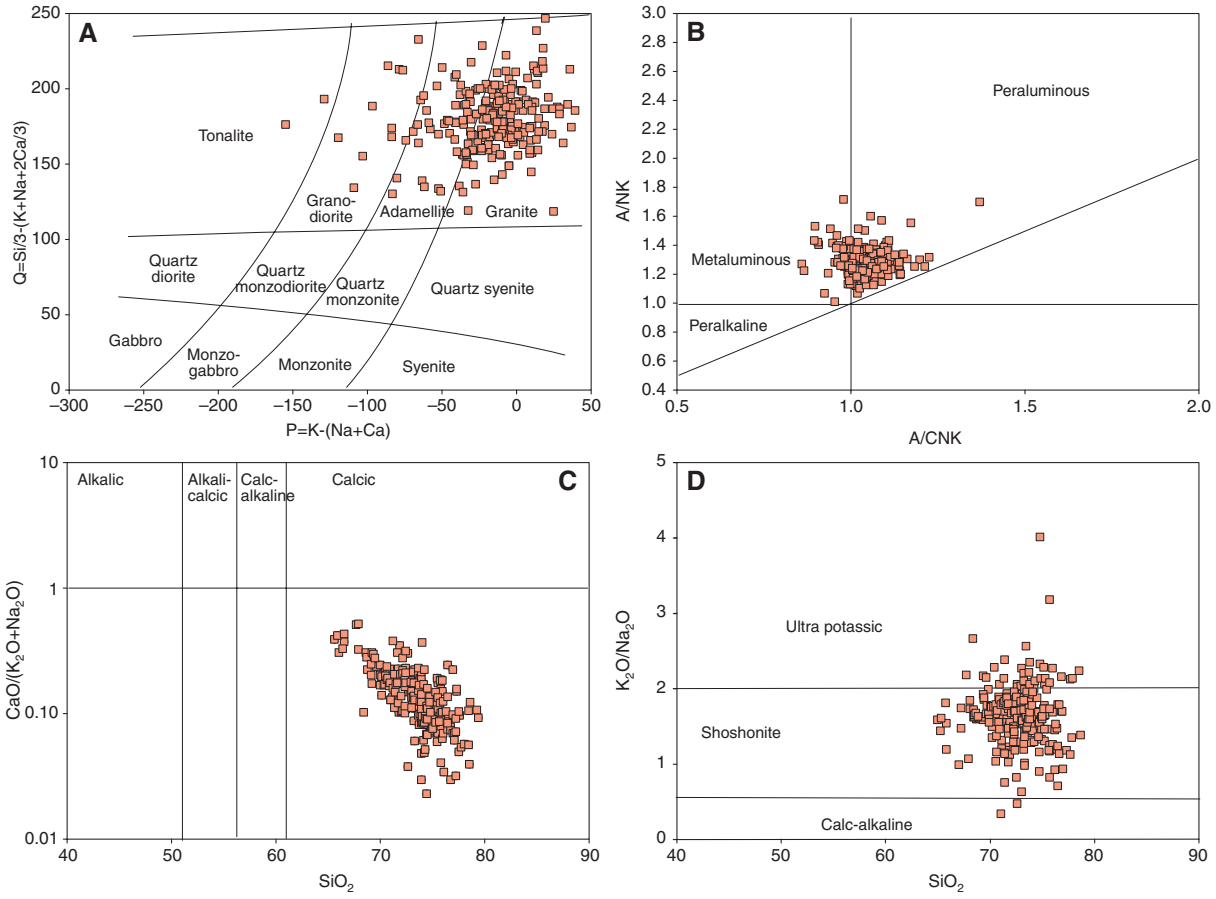

Fig. 84. Geochemical trends for rocks belonging to the late Svecokarelian, 1.85–1.75 Ga GP intrusive suite in the Bergslagen region. Diagrams after **A.** Debon & Le Fort (1983), **B.** Maniar & Piccoli (1989), **C.** Peacock (1931) and **D.** Turner et al. (1996).

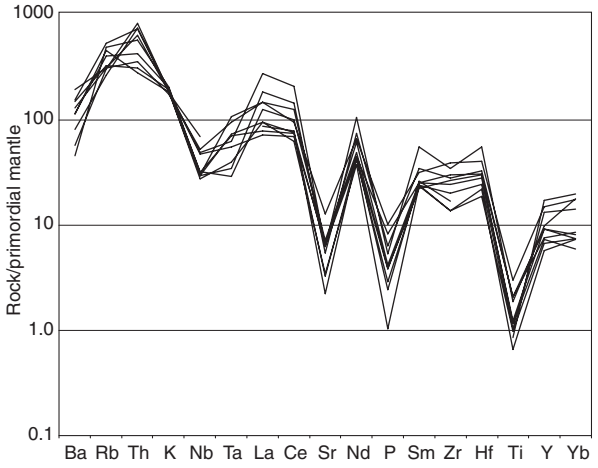

Fig. 85. Rock/primordial mantle spider diagram showing the relationships between large ion lithophile (LILE, e.g. Ba, Rb) and high field strength (HFSE, e.g. Zr, Ti and Y) elements for representative samples of rocks belonging to the late Svecokarelian, 1.85–1.75 Ga GP intrusive suite in the Bergslagen region. SiO_2 values for the selected samples span from 68.8 to 75.2%. Primordial mantle values after McDonough et al. (1992).

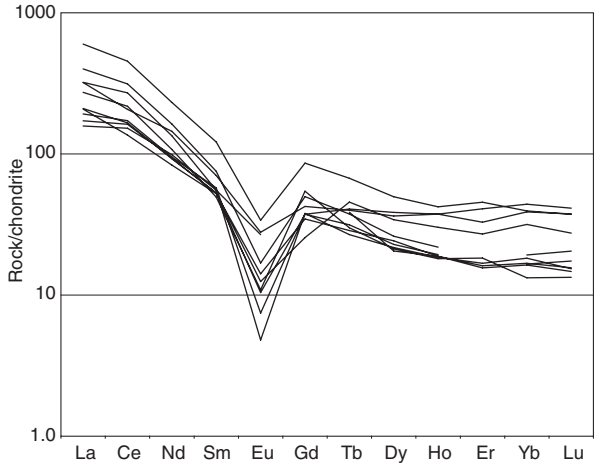

Fig. 86. Rock/chondrites diagram showing the relationships between light rare earth (LREE, e.g. La, Ce) and heavy rare earth (HREE, e.g. Yb, Lu) elements for representative samples of rocks belonging to the late Svecokarelian, 1.85–1.75 Ga GP intrusive suite in the Bergslagen region. SiO_2 values for the selected samples span from 68.8 to 75.2%. Chondrite values after Boynton (1984).

Magnetic susceptibility

The GP intrusive rocks show a large spread in magnetic susceptibility, although values in the highest range (>100 000 × 10^{-6} SI) are lacking (Fig. 89b).

Gamma radiation

The rocks in the GP intrusive suite are characterized by a higher gamma radiation related to generally higher concentrations of particularly uranium and thorium compared with other igneous suites in the Bergslagen region (Fig. 90). In accordance with the granitic composition, the concentration of potassium varies predominantly from around 3% up to 5.8%, despite a group of samples in the northern part of the region that shows concentrations beneath 3%. The concentration of uranium varies from 1.3 up to 48 ppm with a mean concentration of 9.2 ppm (Fig. 90a). This can be compared with a mean value of 4.9 ppm for all the igneous rocks in the region. Furthermore, the concentration of thorium varies from 5.7 up to 160 ppm with a mean concentration of 30.9 ppm

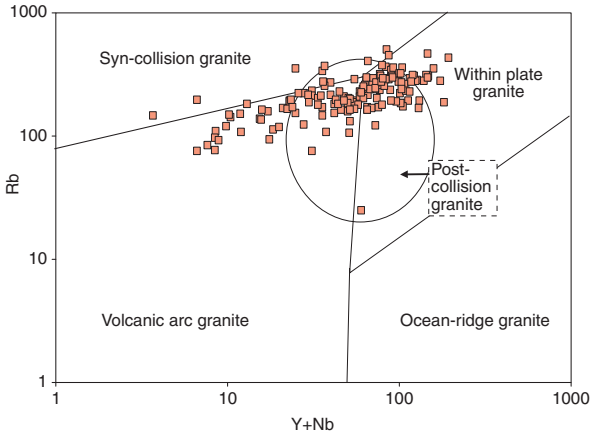

Fig. 87. Tectonic affinity diagram after Pearce (1996) for rocks belonging to the late Svecokarelian, 1.85–1.75 Ga GP intrusive suite in the Bergslagen region.

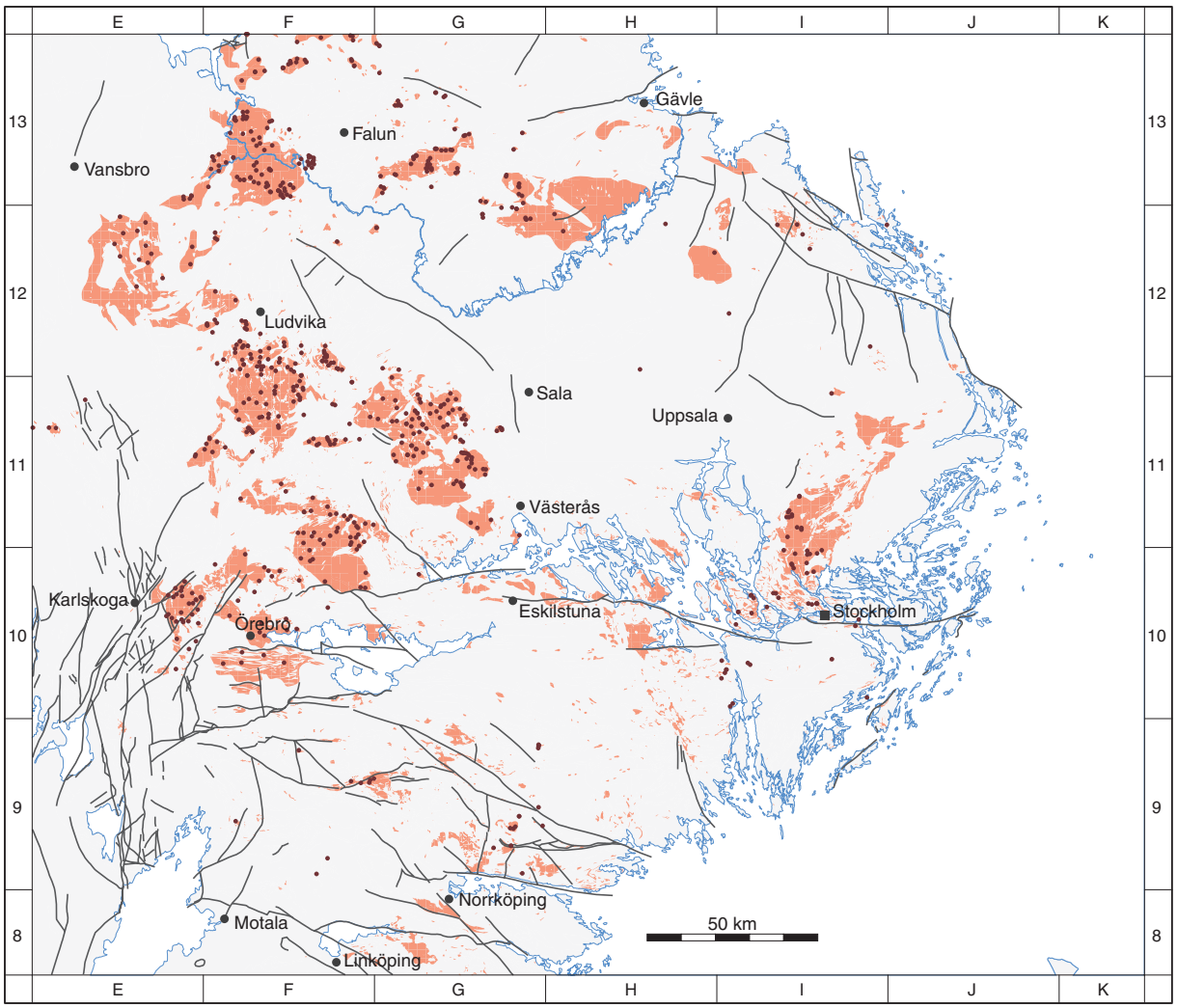

Fig. 88. Location of sample sites of rocks included in the late Svecokarelian, 1.85–1.75 Ga GP intrusive suite in the Bergslagen region for petrophysical and gamma radiation measurements (brown dots). See Figure 80 for legend to the base geological map.

(Fig. 90b), compared with a mean value of 17.5 ppm for the whole population.

Regional geophysical signature

Relative to all the other rock suites, the GP intrusive rocks yield more conspicuous regional geophysical signatures, not least in the gravity and airborne radiometric data. This attribute can be related to the homogeneous, more evolved character of these granitic rocks. A summary of some important geophysical features is provided below.

Gravity anomalies

As a consequence of their low density, the rocks in the GP intrusive suite give rise to low gravity anomalies on the Bouguer gravity anomaly map (Fig. 91). For example, a conspicuous gravity low is apparent in the area occupied by the homogeneous, porphyritic granite to the north-east of Månkarbo in the north-eastern part of the Bergslagen region (Fig. 92). On a regional scale, the large negative gravity anomaly in the central part of the Bergslagen region, extending from the area north of Örebro in the west to Stockholm and north-eastwards to Vallentuna (Fig. 91) coincides approximately with the surface distribution of many of the granites in the GP intrusive suite (e.g. the so-called *Malingsbo*, *Fellingsbro*, *Lisjö*, *Stockholm* and *Vallentuna granites*, cf. Fig. 80). This important anomaly has been referred to as the *Central Swedish Gravity Low* (Werner et al. 1977) and has attracted much attention in the context of 3-D gravity modelling work. It is referred to here as the *CSGL anomaly* (Fig. 91).

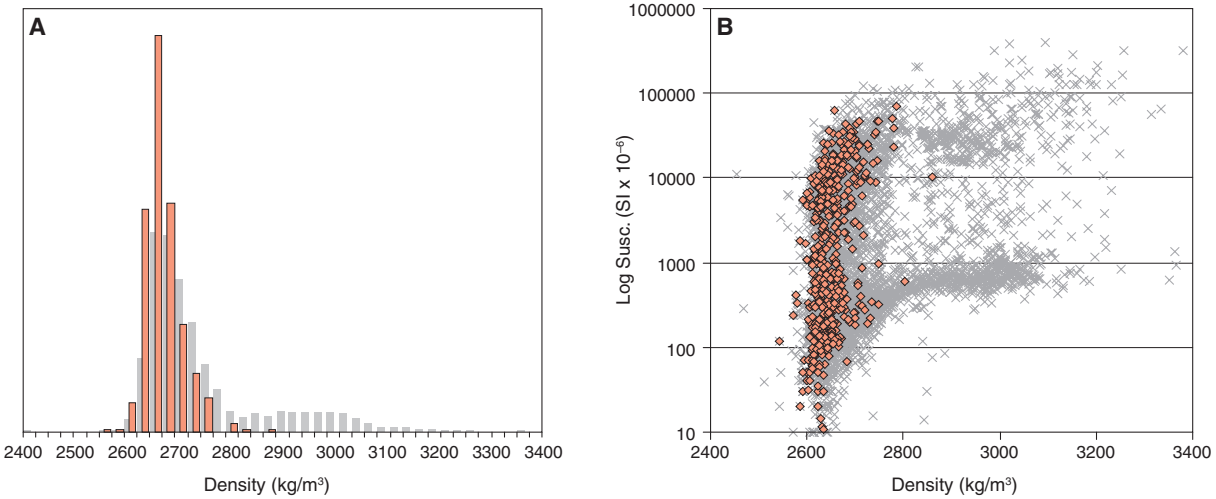

Fig. 89. **A.** Density distribution and **B.** magnetic susceptibility–density diagrams for rock samples from the late Svecokarelian, 1.85–1.75 Ga GP intrusive suite. For purposes of comparison, all samples from the Bergslagen region are shown in grey.

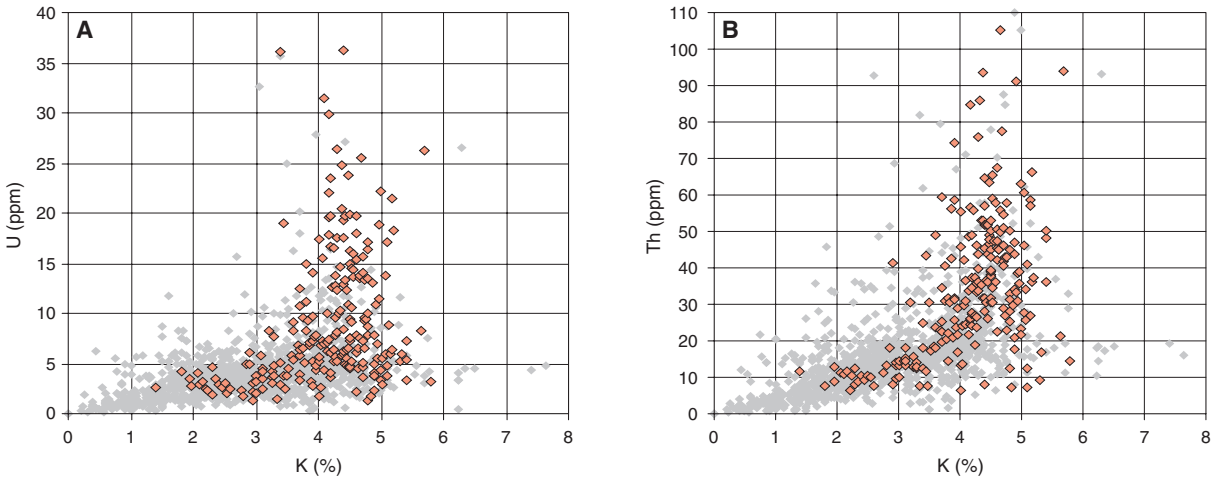

Fig. 90. Concentrations of **A.** uranium versus potassium and **B.** thorium versus potassium for rocks in the late Svecokarelian, 1.85–1.75 Ga GP intrusive suite in the Bergslagen region. For purposes of comparison, all samples from the Bergslagen region are shown in grey. Note the more frequent occurrence of rocks with uranium and thorium anomalies in the GP suite compared with that in the other rock suites in the Bergslagen region.

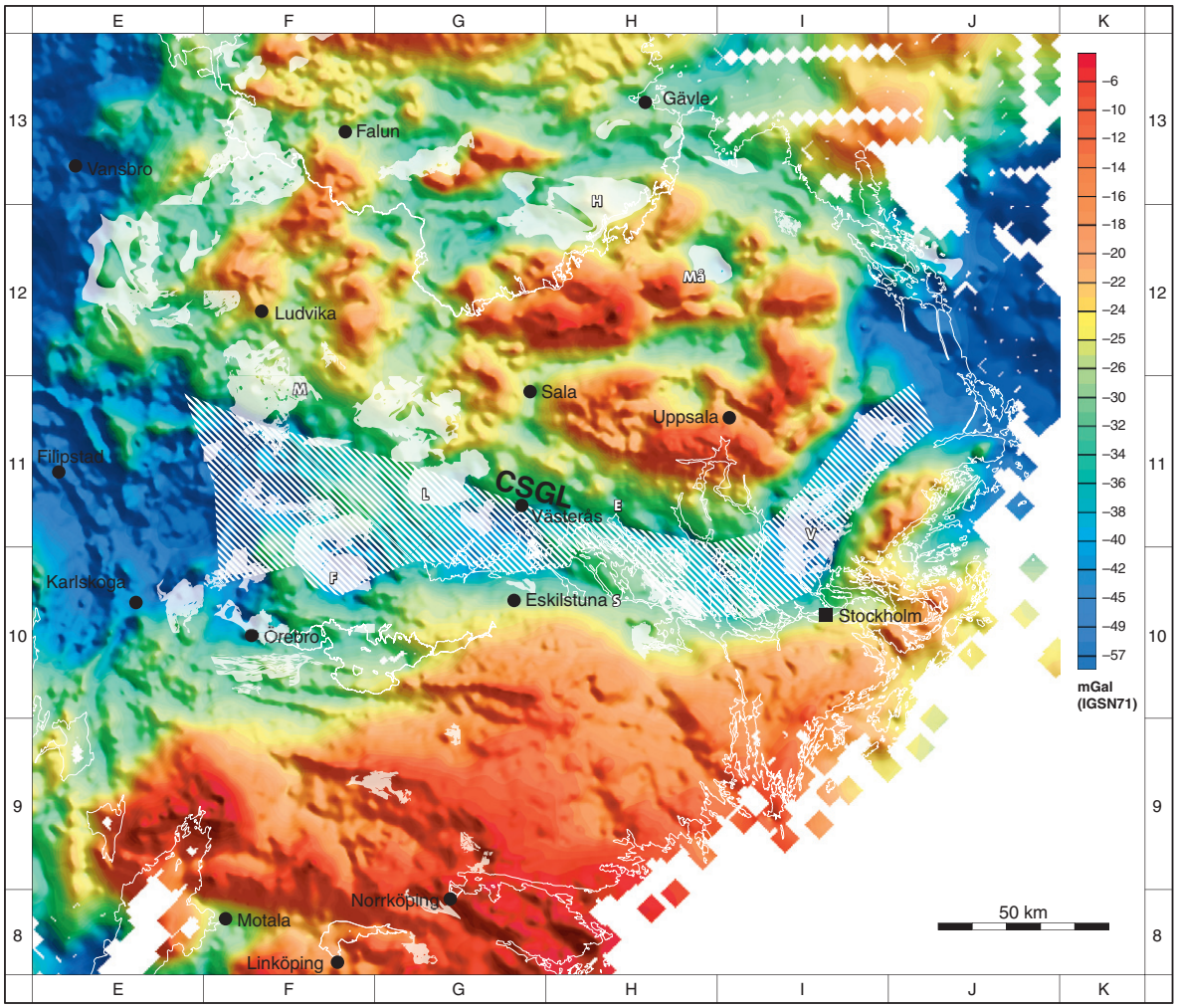

Fig. 91. Bouguer gravity anomaly map over the Bergslagen region. The major negative anomaly *Central Swedish Gravity Low (CSGL)* is shown (diagonal white lines) together with intrusive rocks included in the late Svecokarelian, 1.85–1.75 Ga GP suite (grey shade). E = Enköping, F = Fellingsbro, H = Hedesunda, L = Lisjö, M = Malingsbo, Må = Månkarbo, S = Strängnäs, V = Vallentuna.

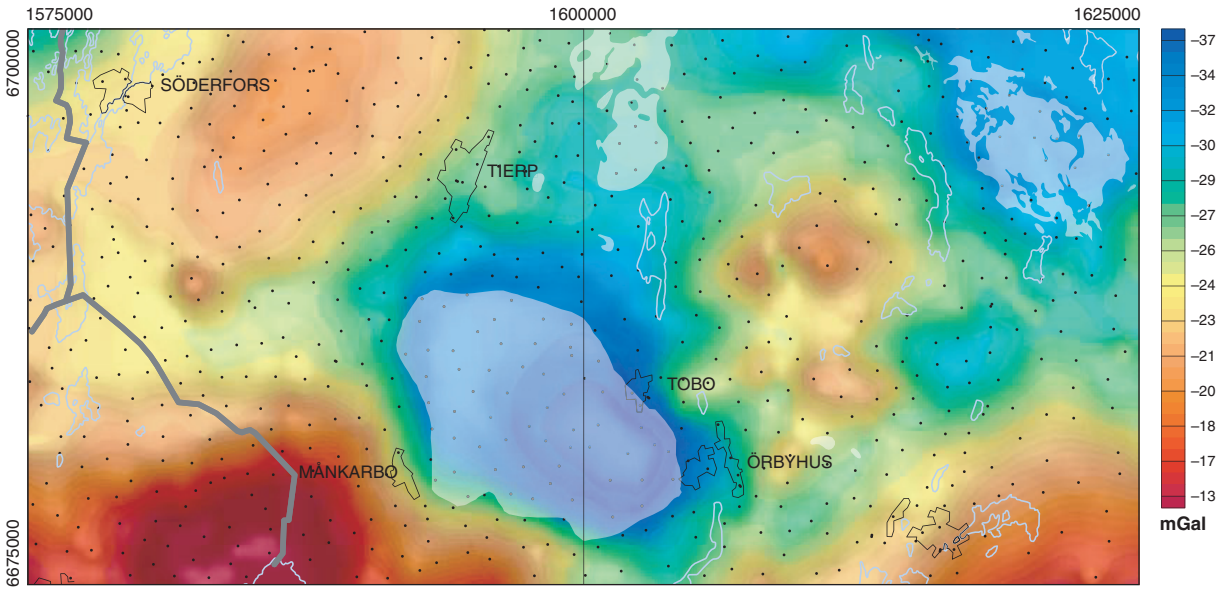

Fig. 92. Gravity anomaly map around Tierp in the north-eastern part of the Bergslagen region. Note the gravity minimum north-east of Månkarbo that corresponds to a homogeneous porphyritic granite included in the late Svecokarelian, 1.85–1.75 Ga GP intrusive suite (grey shade). The positive gravity anomaly south-west of Månkarbo corresponds to major intrusions of intermediate to mafic rocks (see section on GDG intrusive rocks). Measurement points are shown with black dots.

Anomalies in the airborne magnetic data

Several granite intrusions that belong to the GP intrusive suite are visible on the magnetic anomaly map as rounded anomalies with a magnetic pattern that differs from the surrounding bedrock. In the central part of the Bergslagen region, west of Västerås, the granites with the local names *Lisjö*, *Fellingsbro* and *Malingsbo* show a somewhat higher magnetization and different magnetic pattern than the surrounding bedrock (Fig. 93). For example, the *Lisjö granite* is characterized by a high magnetic boundary zone in the south-western part of the intrusion.

The *Hedesunda granite* in the north-eastern part of the Bergslagen region, south of Gävle, shows a complex magnetic pattern with variable high and low magnetization that clearly differs from the surrounding bedrock (Fig. 93). The compilation work indicates that this complex body consists of two major components that formed at 1.87 Ga and 1.78 Ga, belonging to the late Svecokarelian, 1.87–1.84 Ga GSDG (see earlier) and 1.85–1.75 Ga GP intrusive suites, respectively (see also Figs. 64 and 80). The homogeneous, porphyritic granite intrusion south-east of the *Hedesunda granite* close to Månkarbo shows up as a homogeneous, low-magnetic anomaly that is distinctive from the surrounding GDG intrusive rocks (Fig. 93).

Anomalies in the airborne radiometric data

The high concentrations of particularly uranium and thorium are also reflected in the airborne radiometric measurements. On the potassium-uranium-thorium composite map (Stephens et al. 2002b), most of the GP granite intrusions (cf. Fig. 80) appear as well-defined pink areas related to the higher contents of uranium and thorium in these granites. The generally higher content of thorium in the GP rocks is illustrated in Figure 94. Examples include the *Malingsbo*, *Fellingsbro*, *Lisjö*, *Stockholm* and *Vallentuna granites* in the central

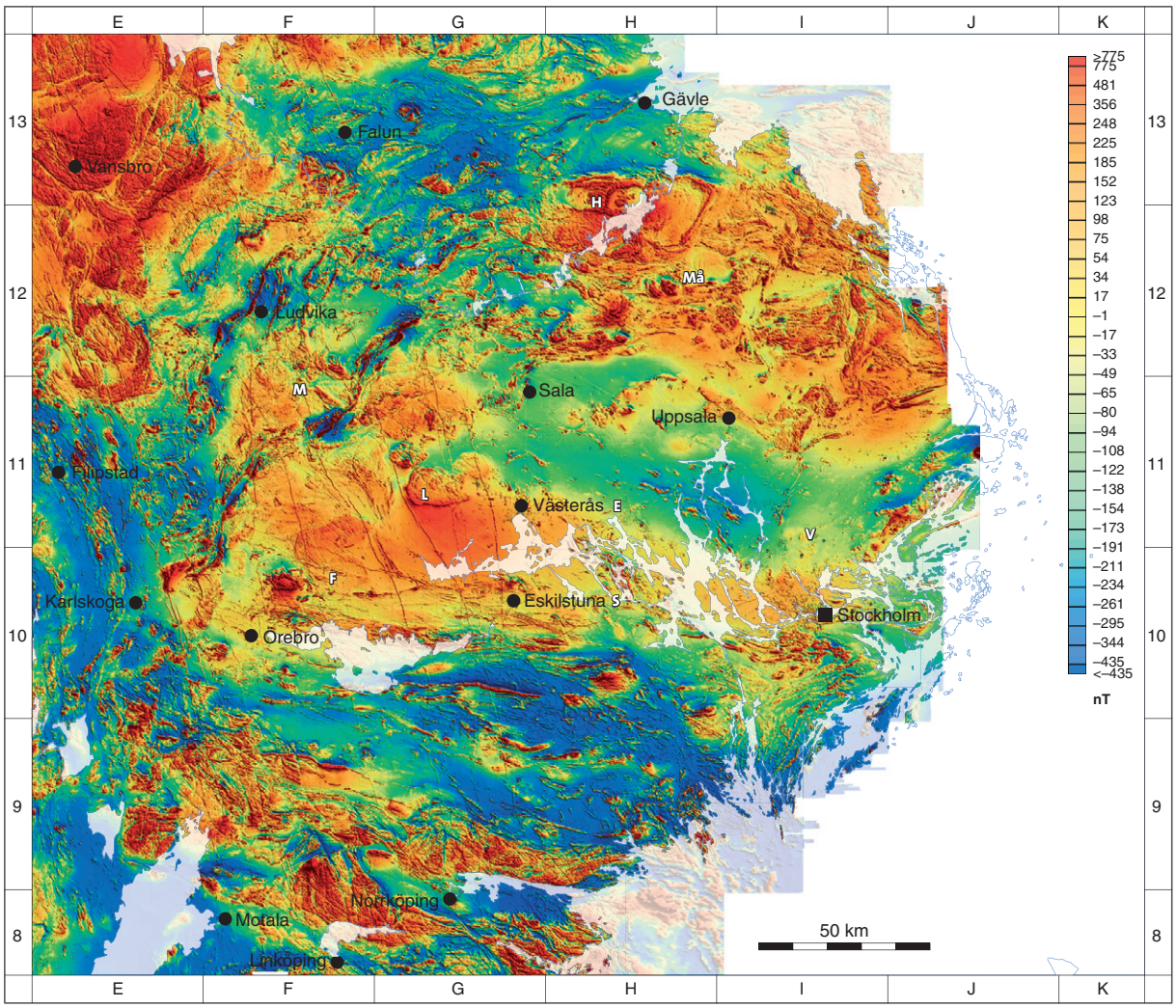

Fig. 93. Magnetic anomaly map over the Bergslagen region inferred from airborne magnetic data, with examples of magnetic anomalies related to the occurrence of rocks belonging to the late Svecokarelian, 1.85–1.75 Ga GP intrusive suite (see also Fig. 91).

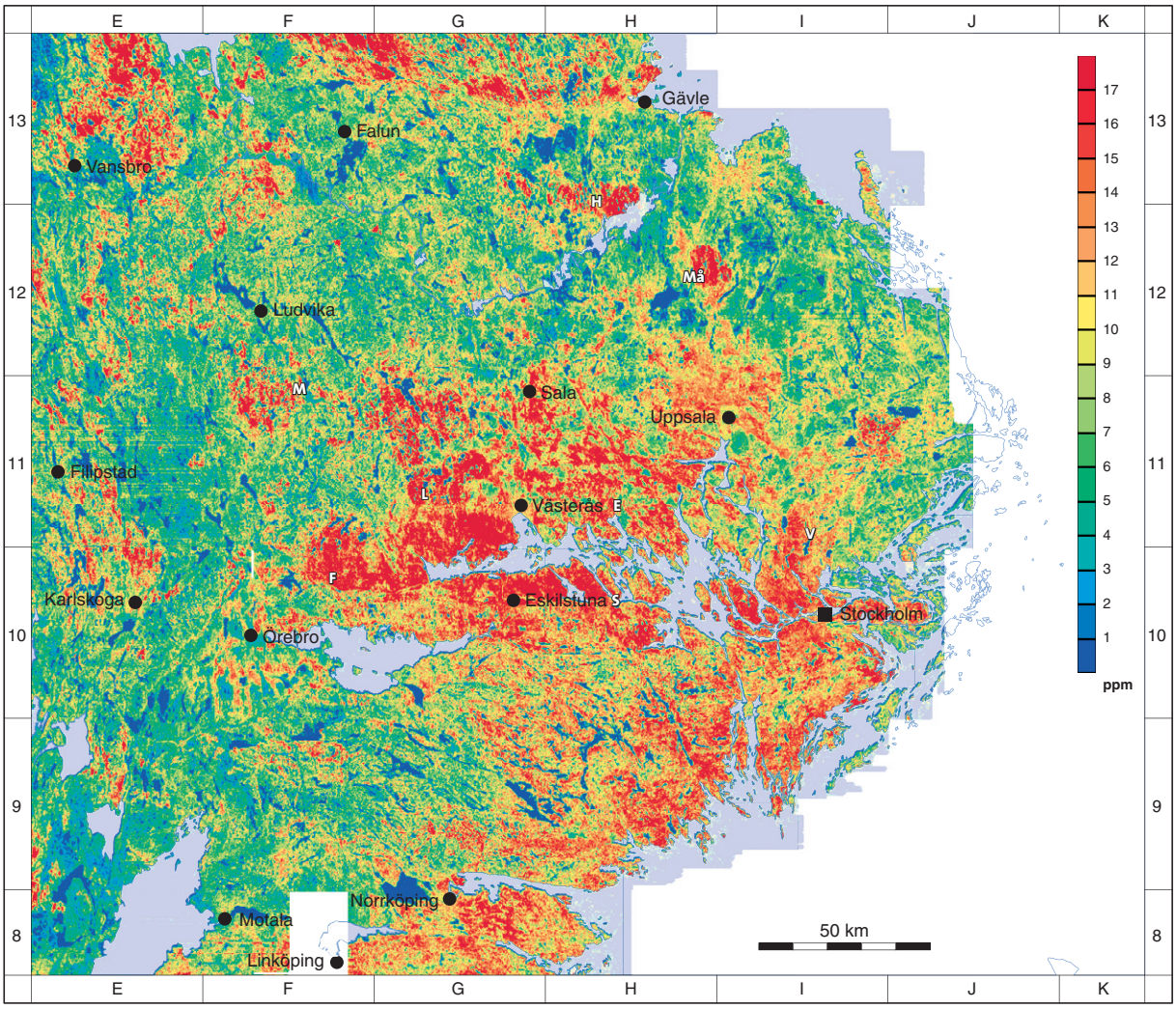

Fig. 94. Radiometric map over the Bergslagen region inferred from airborne data. The map displays the spatial distribution of thorium in the uppermost part of the bedrock and in the Quaternary cover. Examples of thorium anomalies related to the occurrence of rocks belonging to the late Svecokarelian, 1.85–1.75 Ga GP intrusive suite are indicated (see also Fig. 91).

part of the Bergslagen province, parts of the *Hedesunda granite* and the homogeneous, porphyritic granite intrusion south-east of the *Hedesunda granite* in the vicinity of Månkarbo (Fig. 94). Such features can be used to provide some support to the classification of some of the granite bodies in the region as belonging to the GP suite.

Gravity modelling and 3-D shape of granites in the GP intrusive rock suite

Several geophysical studies have been carried out in order to explain the origin of the regional *CSGL anomaly* in the central part of the Bergslagen region and to model the spatial distribution of the rocks belonging to the GP intrusive suite at depth. Stephanson (1975) carried out a simple model calculation along a 50 km profile in a north-west–south-east direction across the Vallentuna granite along the eastern part of the *CSGL anomaly* (Fig. 91). Rock density data along the profile showed that the Vallentuna granite and the surrounding bedrock had mean densities of 2 630 kg/m^3 and 2 680 kg/m^3, respectively, i.e. they show a density contrast of 50 kg/m^3 (density of granite is lower than the density of the surrounding bedrock). The size of the inferred anomaly was almost 20 mGal and the spatial distribution of the granite at depth was interpreted by the modelling of three rectangular prisms. This modelling work indicated that the Vallentuna granite formed a ridge with a depth extent of c. 18 km in its deepest, central part.

A second gravity modelling study along the *CSGL anomaly* was completed by Werner et al. (1977). These authors explained the negative gravity anomaly of 20 mGal as a large granite ridge with lower density than the surrounding bedrock. They showed that the

depth extent of the granite ridge was c. 15 km along a selected profile in a north–south direction across the anomaly. A density contrast of 50 kg/m^3 was used in the modelling work based on rock density data from a large number of samples in the area, i.e. the same contrast as that used by Stephansson (1975).

A more extensive investigation of several granite intrusions along the *CSGL anomaly* was subsequently completed in a series of studies by Zuber (1986), Öhlander & Zuber (1988) and Zuber & Öhlander (1991). They combined both geophysical and geochemical data to interpret the origin and structure of the *CSGL anomaly* as well as the granites inferred to be related to the gravity low. Gravity data were acquired along three north–south profiles that transect the anomaly. The lengths of the profiles vary from c. 50 to 70 km. From west to east, the profiles transect the *Fellingsbro granite*, the *Lisjö granite*, and the area from south of Strängnäs to north of Enköping that is dominated by migmatitic rocks at the ground surface (Fig. 91). A 2.5-D forward modelling software was used in the interpretation of the gravity data.

The *Fellingsbro granite* was interpreted as an asymmetric body with a depth extent of 15 to 20 km in its southern part (Zuber 1986). In the inferred model, the thickness of this body decreases rapidly towards the central part of the massif and the granite was inferred to be no thicker than 1 to 2 km in its northern part. The size of the inferred anomaly was c. 11 mGal and a density contrast of 60 kg/m^3 was used in the modelling work.

The second, c. 60 km long profile transects the so-called *Lisjö granite massif* (Fig. 91). Öhlander & Zuber (1988) concluded that this massif, as exposed at the ground surface, cannot explain the large negative gravity anomaly that occurs mainly to the south of the granite. A deep-seated, 40–50 km wide granite ridge (cf. Werner et al. 1977) at a depth between 20 and 40 km was inferred to explain the *CSGL anomaly* in this area. The granites exposed at the ground surface and included here in the GP intrusive suite (e.g. the *Lisjö granite*) were interpreted to be sheet-like bodies that are less than 5 km thick, with "root zones" that are connected at depth with the deep-seated granite ridge. Based mainly on rock density data from the area close to the profile, a density contrast that varies from 25 to 55 kg/m^3 was used for the modelling of the granite bodies close to or at the ground surface, whereas a density contrast for the deep granite ridge was inferred to be 35 kg/m^3 (density of granite is lower than the density of the surrounding bedrock).

A similar model was presented by Zuber & Öhlander (1991) for the easternmost, c. 70 km long profile in the Strängnäs–Enköping area (Fig. 91). On the basis of this modelling work, these authors concluded that the wide negative gravity anomaly of c. 17 mGal was caused partly by 2 to 8 km thick dyke-like bodies with a depth extent of c. 20 km and partly by an underlying, major c. 50 km wide granite ridge at a depth between 20 and 40 km. The density constrasts used in the modelling work were 50 and 100 kg/m^3 (density of granite is lower than the density of the surrounding bedrock). The larger density contrasts along this profile are related to the higher densities measured in the surrounding GDG intrusive rocks (metatonalites and metagranodiorites) in the eastern part of the Bergslagen region. Zuber & Öhlander (1990) speculated that the major granite ridge may have formed when "tensional fracture zones" were generated in the continental crust as a result of a collision between a magmatic arc to the west and older continental crustal material to the east.

Concluding remarks

In the earlier work by Stephansson (1975) and Werner et. al. (1977), a granite ridge that extended downwards to a depth of 15 to 18 km was inferred to explain the major *CSGL anomaly*. It needs to be kept in mind that only simple modelling tools were available for the interpretation of gravity data when this pioneering work was carried out.

In the later work by Zuber (1986), Öhlander & Zuber (1988) and Zuber & Öhlander (1991), software was used that permitted more sophisticated modelling work. The main result of these studies was that the *CSGL anomaly* is related to a major granite ridge at much greater depth (Fig. 95). Furthermore, these authors speculated that the granite ridge was formed in connection with extensional deformation and that the granites exposed at the ground surface were emplaced at a higher crustal level relative to the ridge but are connected to the ridge by extensional structures. Although the model presented by these authors fits the measured data, there are some ambiguities in the interpretation of the gravity data and there exists no unique solution to the problem, i.e. the model presented by these authors is one of several possible interpretations.

The gravity database at SGU now contains more than 36 000 data points and the petrophysical database more than 9 000 density measurements in the Bergslagen region. Furthermore, 3-D modelling software is currently available for the interpretation of gravity data. Consequently, there are now excellent possibilities to improve the interpretation of the *CSGL anomaly* and the 3-D distribution of the granitic bodies included in the GP intrusive rock suite that are spatially related to this major anomaly. Furthermore, integration with

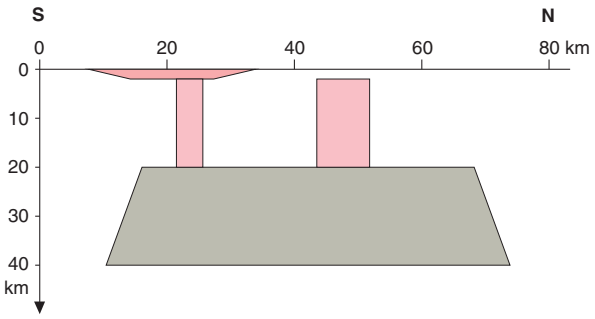

Fig. 95. Schematic 2-D model (Zuber & Öhlander 1991) for the distribution of granites at depth that are coupled to the anomaly referred to as the *Central Swedish Gravity Low (CSGL).* An inferred deeper granitic ridge (grey) is connected to thin, sheet-like bodies (sills) of late Svecokarelian, 1.85–1.75 Ga GP intrusive rocks close to and at the ground surface (red) by steeply dipping, dyke-like granitic bodies (pink).

other geophysical information, e.g. the results from seismic profiling and electromagnetic measurements, as well as structural geological data would naturally provide tighter constraints on the modelling work.

Sm-Nd analyses of rock suites in the Svecokarelian orogen formed between 1.9 and 1.8 Ga

With the help of the significant number of new age determinations that have emerged following the original acquisition of the Sm-Nd data, new ages for the timing of deposition or crystallization of these rocks, referred to here as $T_{age/BP}$, have been used in the data evaluation during the Bergslagen project. All other data, including the rock name or place name for the analysed sample, have been compiled without modification from the source publications (see also section "Data input").

The Sm-Nd isotope data are described in the text that follows according to each of the four main groups of rocks in Bergslagen (see text earlier): the Svecofennian sedimentary rocks, the Svecofennian volcanic and subvolcanic intrusive rocks, the GDG intrusive rock suites and the younger, combined GSDG and GP intrusive rocks. The fourth group includes the rocks belonging to the so-called *TIB*. The data are summarized for each rock suite in Tables 6–9. The geological significance of the data is subsequently evaluated with the help of a compilation in an ε_{Nd}–$T_{age/BP}$ (Ma) diagram (Fig. 96).

Svecofennian sedimentary rocks

Sm-Nd isotope data for twelve samples of Svecofennian sedimentary rocks in the Bergslagen region have been acquired. Assuming a $T_{age/BP}$ of 1900 Ma, eleven of these samples yield an average ε_{Nd} value of –2.28 with a range from –1.12 to –3.24 and an average T_{DM} value of 2347 Ma (Table 6). One sample with an anomalous ε_{Nd} value of 0.98 (NERK 94004 in Table 6) was excluded from the statistical analysis.

Svecofennian volcanic and subvolcanic intrusive rocks (1.91–1.89 Ga)

The analysis of fourty samples of Svecofennian volcanic and subvolcanic intrusive rocks yield an average ε_{Nd} value of 1.15, a range from +3.96 to –2.60 and an average T_{DM} value of 2225 Ma (Table 7). Calculations have beeen carried out assuming a $T_{age/BP}$ of 1900 Ma for these rocks. The Sm-Nd isotope data from the metavolcanic rocks at Orvar Hill in sub-area 12 (Fig. 28) were not included due to the uncertainty in the age of these rocks. A positive ε_{Nd} value of +2.1 has

Table 6. Sm-Nd isotope data and ε_{Nd} values for the Svecofennian sedimentary rocks in the Bergslagen region. $T_{age/BP}$ is the depositional age adopted here for these rocks and used in the calculation of ε_{Nd} values. $T_{age/publ.}$ is the assumed age in the source publications. T_{DM} calculated according to DePaolo (1981). Data from (1) Patchett et al. (1987), (2) Kumpulainen et al. (1996) and (3) Andersson (1997a).

Sample	Rock or place (ref.)	Sm	Nd	$^{147}Sm/^{144}Nd$	$^{143}Nd/^{144}Nd$	T_{age}/BP	$T_{age}/publ.$	T_{CHUR}	T_{DM}	$\varepsilon_{Nd(T)}$
NERK 94004	Vintergölen (2)	6.66	34.70	0.1164	0.511684	1900	1900	1806	2119	+0.98
SW-40	Black slate (1)	6.71	35.20	0.1152	0.511562	1900	1860	2006	2284	–1.12
NERK 93002	Vintergölen (2)	5.27	29.90	0.1066	0.511441	1900	1900	2018	2272	–1.38
NERK 93001	Närkesberg (2)	5.04	28.50	0.1072	0.511424	1900	1900	2059	2309	–1.85
124/89	Paragneiss (3)	8.97	51.44	0.1054	0.511394	1900	1800	2069	2314	–2.01
NERK 92017	Närkesberg (2)	4.29	24.00	0.1084	0.511422	1900	1900			–2.19
NERK 92020	Nerkesberg (2)	7.29	43.75	0.1012	0.511312	1900	1900	2107	2337	–2.57
NERK 94002	Vintergölen (2)	4.14	23.70	0.1058	0.511369	1900	1900	2120	2358	–2.60
NERK 92018	Närkesberg (2)	2.16	10.80	0.1214	0.511563	1900	1900	2167	2440	–2.62
KS 9203	Närkesberg (2)	4.99	29.70	0.1016	0.511313	1900	1900	2116	2346	–2.66
NERK 92021	Närkesberg (2)	4.53	24.60	0.1118	0.511433	1900	1900	2155	2403	–2.81
SW-33	Schist (1)	7.94	44.86	0.1070	0.511351	1900	1860	2178	2412	–3.24

been calculated for an inferred age of 1.85 Ga (Björklund & Claesson 1992).

GDG intrusive rock suites (1.90–1.87 Ga and 1.87–1.85 Ga)

The analysis of twenty-three samples of intrusive rocks that belong to the two age suites of GDG intrusive rocks have provided Sm-Nd isotope data in the Bergslagen region. One sample, a fine-grained enclave (8857E in Table 8) with an anomalous ε_{Nd} value of –3.86, has been excluded from the statistical analysis. Calculations on the twenty-two remaining analyses have been carried out assuming a $T_{age/BP}$ of 1880 Ma for the older suite (19 analyses) and 1850 Ma (3 analyses) for the younger suite of GDG rocks, respectively. The samples from the older, GDG intrusive rock suite yield an average ε_{Nd} value of +0.85, a range from +2.37 to –1.17 and an average T_{DM} value of 2215 Ma (Table 8). The samples from the younger, GDG intrusive rock suite yield an average

Table 7. Sm-Nd isotope data and ε_{Nd} values for the Svecofennian volcanic and subvolcanic intrusive rocks (1.91–1.89 Ga) in the Bergslagen region. $T_{age/BP}$ is the crystallization age adopted here for these rocks and used in the calculation of ε_{Nd} values. $T_{age/publ.}$ is the assumed age in the source publications. T_{DM} calculated according to DePaolo (1981). Data from (1) Patchett et al. (1987), (2) Valbracht (1991), (3) Valbracht et al. (1994) and (4) Kumpulainen et al. (1996).

Sample	Rock or place (ref.)	Sm	Nd	$^{147}Sm/^{144}Nd$	$^{143}Nd/^{144}Nd$	T_{age}/BP	T_{age}/publ.	T_{CHUR}	T_{DM}	$\varepsilon_{Nd(T)}$
KS 9213	Mafic volcanic rock (4)	2.02	6.42	0.1899	0.512755	1900	1900			+3.96
Vp33A	Blomberga dike (2)	1.95	9.97	0.1178	0.511808	1900	1880	1600	1952	+3.07
Rr208	Ställdalen sill (2)	6.43	30.08	0.1291	0.511933	1900	1880	1586	1988	+2.75
KS 9216	Zinkgruvan (4)	1.48	4.71	0.1901	0.512665	1900	1900			+2.15
SW-37	Metarhyolite (1)	7.69	39.78	0.1168	0.511747	1900	1860	1696	2028	+2.12
Bj705A	Hjulsjö dike (2)	9.56	42.79	0.1351	0.511971	1900	1880	1647	2068	+2.02
Cad45	Sundsjö sill (2)	4.16	22.23	0.1128	0.511688	1900	1880	1723	2037	+1.93
Vb480B	Rishöjden sill (2)	2.68	15.80	0.1026	0.511552	1900	1880	1755	2036	+1.78
KS 9208	Marketorp (4)	2.59	10.55	0.1477	0.512114	1900	1900	1626	2135	+1.74
SW-38	Rhyolitic tuff (1)	3.49	15.19	0.1389	0.512002	1900	1860	1673	2111	+1.70
KS 9217	Närkesberg (4)	2.45	8.31	0.1786	0.512496	1900	1900	1195	2380	+1.65
Vp132	Korparberget dike (2)	3.50	14.10	0.1500	0.512137	1900	1880	1632	2158	+1.63
Za54-85F	Tallåsberget dike (2)	4.89	17.56	0.1685	0.512367	1900	1880	1462	2275	+1.60
Vb480A	Ekebergshöjden sill (2)	3.36	15.23	0.1336	0.511929	1900	1880	1708	2110	+1.57
Vb350	Bullarmossen (2)	2.00	10.24	0.1179	0.511727	1900	1880	1758	2084	+1.46
Vp346K	Kraftbö dike (2)	4.45	17.13	0.1572	0.512217	1900	1880	1621	2221	+1.43
Vp503	Yxsjö-Gråsberget dike (2)	1.92	8.66	0.1341	0.511928	1900	1880	1724	2125	+1.43
Bj122	Ekebergshöjden dike (2)	7.22	38.18	0.1143	0.511680	1900	1880	1767	2080	+1.42
Hel8446	Sör-Älgen dike (2)	3.25	11.60	0.1691	0.512354	1900	1880	1565	2354	+1.20
Cad15	Sundsjö sill (2)	4.62	24.22	0.1152	0.511680	1900	1880	1787	2099	+1.20
Hw531/1	Saxå dike (2)	1.64	6.34	0.1566	0.512197	1900	1880	1672	2252	+1.18
KS 9204	Mariedamm (4)	3.22	16.20	0.1211	0.511752	1900	1900	1782	2115	+1.16
Bj490A	Hjulsjö dike (2)	3.72	12.93	0.1739	0.512411	1900	1880	1515	2426	+1.14
Bj392	Hjulsjö granite (3)	8.13	36.66	0.1340	0.511911	1900	1880	1763	2156	+1.12
Vp346R1	Kraftbö dike (2)	3.08	11.02	0.1688	0.512341	1900	1880	1619	2384	+1.02
BL-80-120	Mafic rock (1)	2.84	12.08	0.1422	0.512005	1900	1860	1766	2204	+0.95
Vp346R2	Kraftbö dike (2)	3.08	11.57	0.1606	0.512226	1900	1880	1735	2343	+0.77
Hw369	Saxå flow (2)	2.01	8.28	0.1465	0.512045	1900	1880	1796	2257	+0.68
BL-80-117	Mafic rock (1)	3.49	14.54	0.1450	0.512022	1900	1860	1811	2258	+0.60
Hel8445	Sör-Älgen sill (2)	4.56	19.39	0.1422	0.511980	1900	1880	1835	2259	+0.46
Vb64	Vasselsjön dike (2)	5.22	24.49	0.1289	0.511813	1900	1880	1849	2202	+0.45
SW-32	Meta-andesite (1)	7.30	36.83	0.1197	0.511695	1900	1890	1861	2177	+0.39
KS 9201	Gryts bruk rhyolite (4)	14.30	67.50	0.1280	0.511798	1900	1900	1858	2206	+0.37
SW-34	Metadacite (1)	5.32	28.78	0.1116	0.511590	1900	1890	1872	2160	+0.31
KS 9403	Godegård (4)	3.30	20.00	0.1000	0.511437	1900	1900	1887	2144	+0.16
KS 9211	Igelfors (4)	9.28	43.05	0.1305	0.511817	1900	1900	1883	2237	+0.14
Hw734	Saxå dike (2)	2.39	9.97	0.1451	0.511999	1900	1880	1882	2314	+0.12
KS 9202	Godegård (4)	4.85	27.80	0.1054	0.511501	1900	1900	1892	2161	+0.09
Hw89/2	Saxå flow (2)	3.30	13.84	0.1441	0.511962	1900	1880	1953	2364	–0.36
Cab242	Hjulsjö granite (3)	4.77	21.90	0.1315	0.511690	1900	1880	2207	2508	–2.60

ε_{Nd} value of –0.09, a range from +0.34 to –0.80 and an average T_{DM} value of 2136 Ma (Table 8).

Late Svecokarelian GSDG (1.87–1.84 Ga and 1.81–1.78 Ga) and GP (1.85–1.75 Ga) intrusive rock suites

The analysis of fourty-one samples of intrusive rocks that belong to the two age suites of late Svecokarelian, GSDG rocks and the late Svecokarelian, GP rocks in the Bergslagen region have provided Sm-Nd isotope data in the Bergslagen region. One sample (Da471 in Table 9) with an anomalous ε_{Nd} value of +7.63 has been excluded from the statistical analysis. Calculations on the fourty remaining analyses have been carried out assuming a $T_{age/BP}$ of 1850 Ma for the older suite of GSDG intrusive rocks (24 analyses) and 1800 Ma for the younger suite of GSDG intrusive rocks in combination with the GP intrusive rocks (16 analyses), respectively. The samples from the older, GSDG intrusive rock suite yield an average ε_{Nd} value of +0.72, a range from +3.67 to –0.47 and an average T_{DM} value of 2107 Ma (Table 9). The samples from the combined younger, GSDG and GP intrusive rock suites yield an average ε_{Nd} value of +0.76, a range from +2.34 to –0.75 and an average T_{DM} value of 2048 Ma (Table 9). Additional data have recently been reported (Rutanen & Andersson 2009) for some rocks in the 1.87–1.84 Ga and 1.81–1.78 Ga GSDG intrusive suites. These new data were not included in the current evaluation but are similar to the data compiled here.

Geological evaluation

The negative ε_{Nd} values for the Svecofennian sedimentary rocks indicate the influence of a mixed Archaean and Proterozoic detrital source for these clastic rocks (Fig. 96), consistent with the limited U-Pb age determinations of detrital zircons in the region (Claesson et al. 1993, Andersson et al. 2006). It is inferred that the sedimentary detritus was derived from a continental landmass with a prolonged, earlier geological evolution that extended back to Archaean time, with the involvement of probably more than one erosional-depositional cycle. Kumpulainen et al. (1996) suggested an increase of younger juvenile detritus with time in the Zinkgruvan area, in the south-western part of the Bergslagen region, as indicated by a shift from negative to more positive ε_{Nd} values upward through the stratigraphic succession in this area.

The Svecofennian volcanic and subvolcanic intrusive rocks are mildly depleted and follow the same evolutionary trend on the ε_{Nd}–$T_{age/BP}$ (Ma) diagram as the

Table 8. Sm-Nd isotope data and ε_{Nd} values for the two age suites of GDG intrusive rocks in the Bergslagen region. The two age suites are separated in the table by a black line. $T_{age/BP}$ is the crystallization age adopted here for these rocks and used in the calculation of ε_{Nd} values. $T_{age/publ.}$ is the assumed age in the source publications. T_{DM} calculated according to DePaolo (1981). Data from (1) Patchett et al. (1987), (2) Valbracht et al. (1994) and (3) Andersson (1997a).

Sample	Rock or place (ref.)	Sm	Nd	$^{147}Sm/^{144}Nd$	$^{143}Nd/^{144}Nd$	T_{age}/BP	T_{age}/publ.	T_{CHUR}	T_{DM}	$\varepsilon_{Nd(T)}$
Bj1069	Bastfallsh. granite (2)	11.10	64.09	0.1047	0.511621	1880	1880	1681	1978	+2.37
Hel8327	Rällen granite (2)	5.82	28.89	0.1217	0.511827	1880	1880	1645	2004	+2.29
Bj1069A	Bastfallsh. granite (2)	5.24	29.91	0.1059	0.511618	1880	1880	1708	2005	+2.02
Hel8297	Rällen granite (2)	5.05	24.20	0.1262	0.511857	1880	1880	1685	2055	+1.79
SW-26	Diorite (1)	7.09	34.27	0.1251	0.511834	1880	1890	1707	2069	+1.60
Bj246	Hjulsjö granophyre (2)	4.13	22.85	0.1091	0.511634	1880	1880	1743	2043	+1.56
BjH44	Knapphöjden granite (2)	8.46	47.84	0.1092	0.511635	1880	1880	1743	2044	+1.56
BjH37	Storhöjden granite (2)	13.86	56.73	0.1476	0.512099	1880	1880	1669	2168	+1.34
SW-30	Mafic rock (1)	1.19	4.16	0.1730	0.512401	1880	1890	1521	2408	+1.10
Ca1303	Finnån granite (2)	6.06	28.73	0.1275	0.511829	1880	1880	1777	2137	+0.92
Bj468	Hjulsjö granophyre (2)	6.76	36.78	0.1110	0.511616	1880	1880	1813	2108	+0.75
Bj1047	Horrsjö granite (2)	12.26	58.44	0.1268	0.511800	1880	1880	1822	2171	+0.52
SW-29	Rådmansö complex (1)	0.81	3.95	0.1247	0.511768	1880	1890	1837	2175	+0.41
SW-44	Vänge granitoid (1)	4.83	25.57	0.1143	0.511634	1880	1890	1852	2151	+0.30
SW-22	Tonalite (1)	2.51	15.63	0.0970	0.511409	1880	1890	1873	2125	+0.09
SW-28	Rådmansö complex (1)	3.36	17.99	0.1130	0.511594	1880	1890	1895	2184	–0.17
SW-42	Sala granitoid (1)	5.17	26.44	0.1182	0.511648	1880	1890	1916	2218	–0.37
SW-45	Uppsala granitiod (1)	4.34	22.88	0.1147	0.511585	1880	1890	1951	2237	–0.76
WeyGR223	Nybergsfältet granite (2)	2.34	11.46	0.1232	0.511669	1880	1880	2003	2308	–1.17
142:1/89	Tonalite (3)	3.30	17.95	0.1110	0.511612	1850	1800	1820	2114	+0.34
8819	Tonalite (3)	3.59	18.43	0.1177	0.511687	1850	1800	1830	2144	+0.21
8832	Adamellite (3)	7.24	43.93	0.0996	0.511415	1850	1800	1914	2166	–0.80
8857E	Fine-grained enclave (3)	7.14	39.01	0.1107	0.511394	1850	1800	2196	2436	–3.86

plutonic intrusive rocks in the slightly younger GDG, GSDG and GP suites (Fig. 96). The ε_{Nd} value of +2.1 calculated for an inferred age of 1.85 Ga for the meta-volcanic rocks from Orvar Hill in sub-area 12 (Fig. 28) is also compatible with this trend. The consistent ε_{Nd} values imply a homogenous source and the incorpora-

Table 9. Sm-Nd isotope data and ε_{Nd} values for the two age suites of late Svecokarelian, GSDG intrusive rocks and for the late Svecokarelian, GP intrusive rocks in the Bergslagen region. The samples from the 1.87–1.84 Ga GSDG intrusive rock suite are separated from the remaining samples by a black line. $T_{age/BP}$ is the crystallization age adopted here for these rocks and used in the calculation of ε_{Nd} values. $T_{age/publ.}$ is the assumed age in the source publications. T_{DM} calculated according to DePaolo (1981). Data from (1) Patchett et al. (1987), (2) Valbracht et al. (1994) and (3) Andersson (1997a).

Sample	Rock or place (ref.)	Sm	Nd	$^{147}Sm/^{144}Nd$	$^{143}Nd/^{144}Nd$	T_{age}/BP	T_{age}/publ.	T_{CHUR}	T_{DM}	$\varepsilon_{Nd(T)}$
8822	Fine-grained basite (3)	4.60	16.99	0.1635	0.512421	1850	1800	996	1872	+3.67
203	Lherzolite (3)	1.15	5.32	0.1310	0.511973	1850	1800	1540	1960	+2.64
9M	Quartz diorite dyke (3)	5.88	27.61	0.1248	0.511885	1850	1800	1593	1974	+2.39
8859DI	Basite (3)	1.99	9.14	0.1317	0.511934	1850	1800	1647	2051	+1.71
100/89	Gabbro (3)	3.80	22.61	0.1014	0.511564	1850	1800	1714	1997	+1.69
200	Lherzolite (3)	1.82	8.00	0.1378	0.511999	1850	1800	1650	2086	+1.53
8814	Hybrid enclave (3)	20.60	105.00	0.1186	0.511750	1850	1800	1729	2062	+1.23
SW-23	Granitoid (1)	14.93	77.66	0.1277	0.511854	1850	1780	1728	2097	+1.10
8844A	Coarsely porphyritic granite (3)	9.16	51.05	0.1084	0.511615	1850	1800	1761	2057	+1.02
8853A	Coarsely porphyritic granite (3)	7.33	40.24	0.1101	0.511609	1850	1800	1806	2100	+0.49
8843C	Coarsely porphyritic granite (3)	8.84	54.13	0.0987	0.511462	1850	1800	1824	2086	+0.33
8811A	Microgranular enclave (3)	33.64	160.80	0.1264	0.511799	1850	1800	1814	2163	+0.33
8853C	Microgranular enclave (3)	15.54	76.89	0.1222	0.511745	1850	1800	1822	2153	+0.27
8845	Coarsely porphyritic felsic granite (3)	4.88	25.80	0.1144	0.511646	1850	1800	1832	2135	+0.19
8840	Basite slightly hybrid (3)	7.14	32.49	0.1328	0.511868	1850	1800	1832	2206	+0.15
119	Very dark hybrid (3)	8.30	41.04	0.1223	0.511739	1850	1800	1837	2166	+0.13
8859B	Dark hybrid (3)	7.16	35.11	0.1232	0.511744	1850	1800	1849	2179	+0.01
8815	Coarsely porphyritic felsic granite (3)	9.42	51.13	0.1113	0.511595	1850	1800	1856	2146	−0.07
143	Medium-dark hybrid (3)	6.46	32.36	0.1207	0.511709	1850	1800	1858	2178	−0.08
8823	Coarsely porphyritic granite (3)	7.83	40.59	0.1166	0.511659	1850	1800	1858	2164	−0.08
XE	Light hybrid (3)	9.59	50.53	0.1147	0.511633	1850	1800	1863	2162	−0.13
AW9325	Coarsely porphyritic granite (3)	6.50	35.29	0.1113	0.511586	1850	1800	1872	2160	−0.24
SW-72	Hedemora (1)	4.74	22.54	0.1272	0.511769	1850	1890	1900	2237	−0.45
257/93	Coarsely porphyritic granite (3)	7.02	38.42	0.1105	0.511565	1850	1800	1892	2174	−0.47
Da471	Östra Höjden granite (2)	15.49	44.25	0.2116	0.513204	1800	1780			+7.63
Da500	Östra Höjden granite (2)	5.99	16.80	0.2154	0.512979	1800	1780			+2.34
SW-35	Granitoid (1)	7.11	38.62	0.1112	0.511721	1800	1780	1631	1955	+1.87
SW-71	Granitoid (1)	6.67	37.92	0.1062	0.511661	1800	1700	1642	1949	+1.85
SW-36	Malingsbo (1)	8.91	47.29	0.1138	0.511744	1800	1790	1640	1971	+1.72
8511	Quartz monzodiorite (3)	17.52	91.46	0.1158	0.511738	1800	1800	1692	2021	+1.14
8508	Very dark hybrid (3)	18.28	94.85	0.1165	0.511736	1800	1800	1710	2039	+0.93
132b	Dark hybrid (3)	17.30	89.90	0.1163	0.511729	1800	1800	1719	2046	+0.84
11	Coarse hbl-gabbro (3)	3.72	16.86	0.1333	0.511926	1800	1800	1708	2108	+0.76
39	Coarsely porphyritic granite (3)	7.05	35.72	0.1192	0.511754	1800	1800	1734	2069	+0.66
8504	Even-grained felsic granite (3)	8.17	45.43	0.1086	0.511627	1800	1800	1745	2044	+0.63
SW-24	Granite (1)	18.06	118.48	0.0921	0.511423	1800	1790	1766	2021	+0.46
129d	Hybrid and mafic (3)	15.86	82.38	0.1164	0.511695	1800	1800	1785	2102	+0.15
SW-31	Granite (1)	14.68	78.79	0.1126	0.511646	1800	1790	1793	2097	+0.08
1bb	Light hybrid (3)	14.31	72.74	0.1189	0.511715	1800	1800	1803	2126	−0.03
SW-25	North of Stockholm (1)	10.81	62.40	0.1048	0.511521	1800	1790	1847	2121	−0.56
ZaNKop	Granite (2)	6.78	10.95	0.3744	0.514704	1800	1780	1767		−0.75

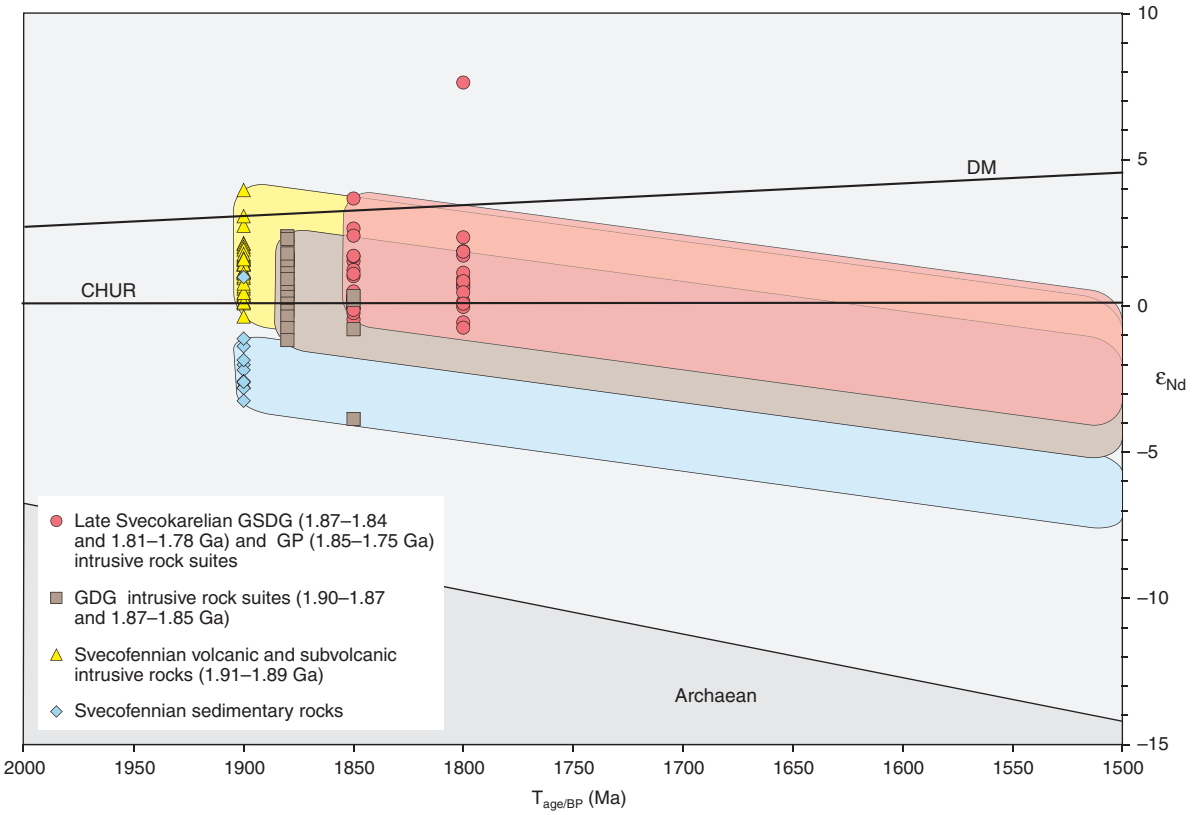

Fig. 96. ε_{Nd}–$T_{age/BP}$ (Ma) diagram for the four main groups of rocks in the Bergslagen region. Data from Patchett et al. (1987), Valbracht (1991), Valbracht et al. (1994), Kumpulainen et al. (1996) and Andersson (1997a). DM is depleted mantle (DePaolo, 1981), CHUR is the chondritic uniform reservoir (DePaolo & Wasserberg, 1976) and Archaean refers to the evolution of the Archaean crust in the Fennoscandian Shield (Andersson 1997a).

tion of relatively juvenile mantle material. There are no indications of an influence from an Archaean crust in any of these volcanic and younger intrusive rocks (Patchett et al. 1987, Andersson 1997a). These features are consistent with models for a juvenile volcanic-arc crust that formed around 2.1–1.9 Ga and probably formed a continental basement to the Bergslagen region (Lahtinen & Huhma 1997 and references therein, Rutanen & Andersson 2009).

ALKALINE INTRUSIVE ROCK OF UNCERTAIN AGE

A single alkaline intrusive rock complex occurs within the Bergslagen region. It is situated close to Almunge, east of Uppsala, on map sheet 11I Uppsala NO (Fig. 97). Detailed geological mapping of this alkaline complex was carried out by Gorbatschev (1960). The complex has also been investigated more recently in connection with SGU's geological mapping programme at the local scale (see, for example, Ripa et al. 2006).

The alkaline intrusive complex is dominated by syenite with subordinate amounts of nepheline syenite and nepheline diorite. The surrounding GDG intrusive rocks show fenitization. Although older K-Ar data suggested a late Palaeoproterozoic or Mesoproterozoic age for the alkaline complex (Gorbatschev 1960), field relationships and the interpretation of new U-Pb (titanite) radiometric age data suggest that the complex is considerably older and similar in age to the surrounding GDG rocks (Ripa et al. 2006).

POST-SVECOKARELIAN ROCKS PARTLY AFFECTED BY SVECONORWEGIAN DEFORMATION AND METAMORPHISM

Granite-syenitoid-dioritoid-gabbroid (GSDG) intrusive rock suite (1.70–1.67 Ga)

The youngest suite of GSDG intrusive rocks in the Bergslagen region, which formed after the Svecokarelian tectonic evolution, forms a mappable rock unit at the ground surface in the north-westernmost part of the region (Fig. 97). Rocks that belong to this suite, possibly together with older GSDG intrusive rocks, are also present in the westernmost part of the Bergslagen region (Fig. 97) where they are affected, to variable extent, by Sveconorwegian deformation under greenschist- or

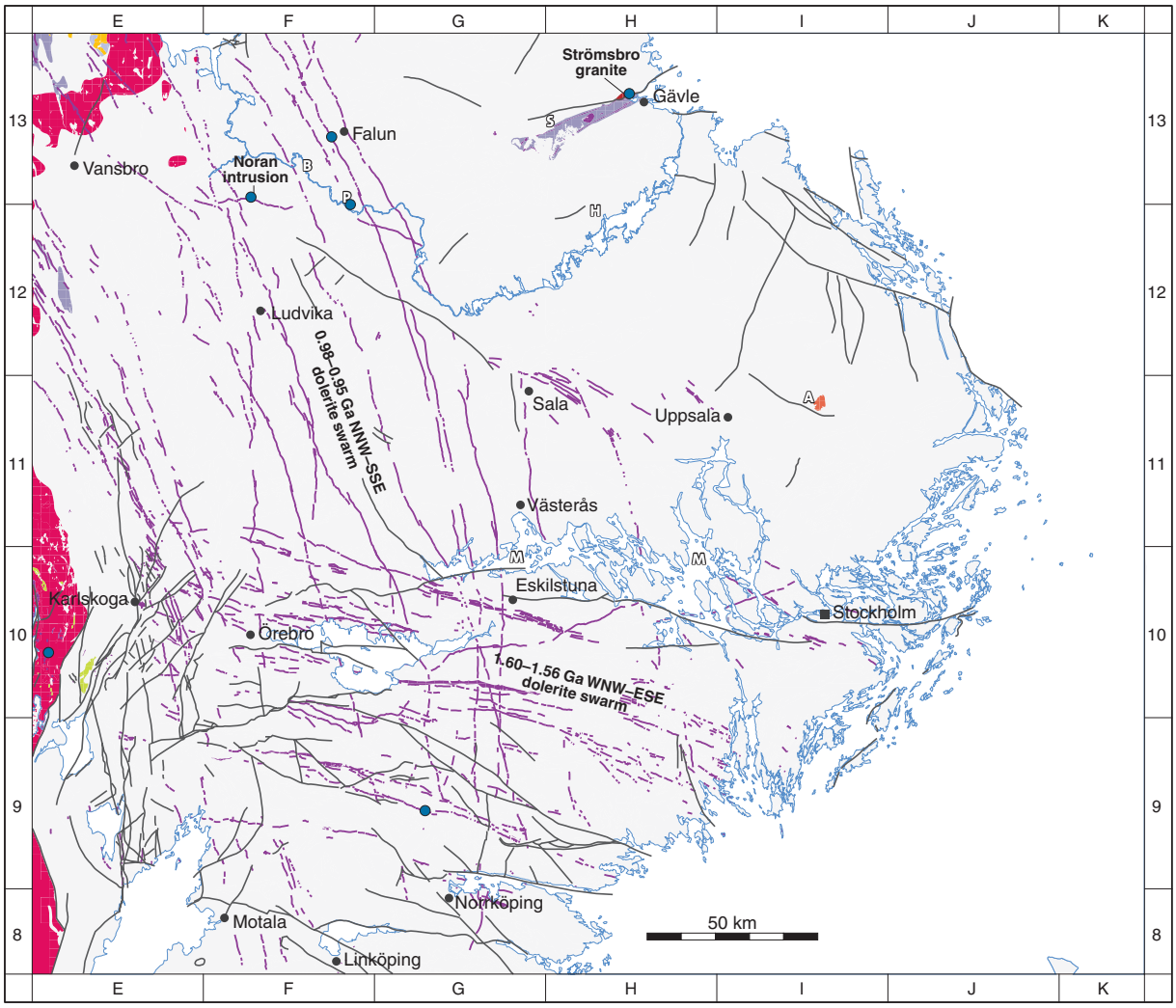

U-Pb (zircon, baddeleyite) age determination

Fault, ductile shear zone

Mesoproterozoic and Neoproterozoic rocks (excluding Neoproterozoic clastic sedimentary rocks)

Dolerite and equivalent metamorphic rock (Mesoproterozoic and Neoproterozoic)

Granite, quartz syenite (Mesoproterozoic)

Sandstone, siltstone, shale (Mesoproterozoic)

GSDG intrusive rocks and associated supacrustal rocks, age group 1.70–1.67 Ga

Granite, syenitoid, quartz monzodiorite and equivalent metamorphic rock

Gabbroid, dioritoid, ultramafic rock and equivalent metamorphic rock

Sandstone, argillite

Rhyolite

Alkaline intrusive complex, uncertain age

Syenite, nepheline syenite, nepheline diorite

Fig. 97. Distribution of post-Svecokarelian, Proterozoic rocks at the ground surface in the Bergslagen region. An alkaline intrusive complex of uncertain age is also shown on the map. Neoproterozoic clastic sedimentary rocks, which formed after the Sveconorwegian orogenic activity, are excluded. They are discussed below together with the Lower Palaeozoic sedimentary cover rocks (see Fig. 99). The location of place names referred to in the sections "Alkaline intrusive complex of uncertain age" and "Post-Svecokarelian rocks partly affected by Sveconorwegian deformation and metamorphism" is also shown. A = Almunge, B = Borlänge, M = Mälaren, P = Pellesberget, S = Sandviken.

amphibolite-facies metamorphic conditions (see text below). The rocks that belong to the post-Svecokarelian GSDG intrusive suite have been described by, for example, Annertz (1984), Lindström et al. (2000) and Ahl et al. (2004). The post-Svecokarelian GSDG intrusive rocks and the older GSDG suites, which formed during the later stages of the Svecokarelian orogeny, are all grouped together in the *Transscandinavian Igneous Belt* (see discussion earlier).

The granites sensu stricto in the north-western part of the Bergslagen region are red or rarely grey, medium- to coarse-grained and generally equigranular (Fig. 98a). They show mineralogical features that are reminiscent of the so-called rapakivi granites, i.e. K-feldspar is orthoclase or a mixture of orthoclase and microcline, plagioclase locally rims K-feldspar phenocrysts and the granites contain fluorite. The post-Svecokarelian GSDG rocks in the westernmost part of the Bergslagen region consist

Fig. 98. Character of some post-Svecokarelian, 1.70–1.67 Ga GSDG intrusive rocks, Bergslagen region. **A.** Coarse-grained, equigranular granite referred to as the *Siljan-type* (13E Vansbro NV). Photograph: Martin Ahl (SGU). **B.** Medium-grained granite to quartz monzonite with weak grain-shape fabric (10E Karlskoga NV). This rock type is generally finely porphyritic. Photograph: Carl-Henric Wahlgren (SGU). **C.** Equigranular granite intruded by dolerite dykes that belong to the 1.60–1.56 dolerite suite (10E Karlskoga SV). Photograph: Carl-Henric Wahlgren (SGU). **D.** Porphyritic granite to quartz monzonite included in the 1.81–1.78 Ga GSDG suite intruded by a dyke of monzodiorite (10E Karlskoga SV). The dyke belongs to the spatially adjacent *Roted massif* that has been dated to 1699±7 Ma. Prograde hypersthene and garnet have been observed in the 1.81–1.78 Ga GSDG rocks inside a thermal contact aureole around the *Roted massif*. Photograph: Carl-Henric Wahlgren (SGU).

of both finely porphyritic (Fig. 98b) and red, medium-grained and equigranular varieties (Fig. 98c). A separate massif *(Roted massif)* consists of grey, medium-grained rocks that range in composition from diorite through quartz monzodiorite to quartz monzonite, but locally even ultramafic varieties are present (Annertz 1984). The massif is rimmed by a thermal contact aureole that shows prograde growth of garnet and hypersthene. This thermal aureole affects the surrounding, older (1.81–1.78 Ga) GSDG intrusive rocks (Fig. 98d).

The rocks included in the post-Svecokarelian, GSDG suite in the Bergslagen region intrude the older, 1.81–1.78 Ga GSDG intrusive rock suite. U-Pb (zircon) age dating results confirm the relative time relationships inferred from the field observations. The post-Svecokarelian GSDG intrusive rocks formed between 1.70 and 1.67 Ga (Table 4 and Fig. 67). If all the uncertainties are taken into account, the time range lies between 1706 and 1665 Ma. The locations of the dated samples are shown in Figure 64.

The rocks in the post-Svecokarelian, 1.70–1.67 Ga GSDG intrusive suite that have been analysed geochemically are granitic in composition (Fig. 69a). They lie within the shoshonitic field in the $K_2O/Na_2O–SiO_2$ diagram (Fig. 69d), similar to that observed for the older, Svecokarelian GSDG intrusive rocks (see earlier section). As for the older GSDG rocks, it is concluded that the 1.70–1.67 Ga suite of GSDG intrusive rocks also formed in a more mature continental source region relative to that represented by the older 1.90–1.87 Ga GDG intrusive rocks.

Volcanic and sedimentary rocks (1.7 Ga)

Supracrustal rocks, which are spatially and genetically associated with the youngest suite of GSDG intrusive rocks, are restricted to the north-westernmost part of the Bergslagen region (Fig. 97). However, north and north-west of this region, in the county of Dalarna, these rocks are common and occupy large areas at the current level of erosion. The rocks have been described by, for example, Hjelmqvist (1966), Lundqvist & Persson (1999) and Nyström (2004). In the same manner as for the older (1.8 Ga), GSDG-related supracrustal

rocks, a crude stratigraphy may be discerned. According to Hjelmqvist (1966), the stratigraphy is valid for the entire area of occurrence, whereas Nyström (2004) claimed that deviations from the proposed succession are common. The character of the 1.7 Ga supracrustal rocks presented here is based on these detailed descriptions.

The basal part of the supracrustal sequence is composed of immature sedimentary rocks including silicified arkose, conglomerate and breccia. Basic to intermediate volcanic rocks (*Dala porphyrites*), which range in composition from basalt and andesite to quartz trachyte and quartz latite, stratigraphically overlie the basal strata. These volcanic rocks contain phenocrysts of plagioclase, orthopyroxene, olivine and hornblende. They mainly formed as lavas, but tuffs, breccias and agglomerates have also been reported. Nevertheless, Nyström (2004) has reinterpreted some breccias and agglomerates as autoclastic lava facies. Clastic sedimentary rocks (*Digerberg sedimentary rocks*), which consist of lithic sandstone and conglomerate, are interlayered with the basic to intermediate volcanic rocks.

Acid volcanic and subvolcanic rocks (*Dala porphyries*), which range in composition from phenocryst-poor rhyolite to phenocryst-rich quartz trachyte, both overlie and intrude the older supracrustal rocks. The phenocrysts in these rocks consist of plagioclase, orthoclase variably intermixed with microcline, mafic minerals and, locally, quartz. The porphyries occur as ignimbritic flow deposits with pumice clasts and as subvolcanic intrusions.

A comparison of the 1.7 Ga volcanic rocks with recent equivalents along the active continental margin in the Andes has been made (Nyström 1982, 2004). In particular, similarities between the basic to intermediate 1.7 Ga volcanic rocks (*Dala porphyrites*) and lavas of the shoshonite series that were formed along the Andean active continental margin at a considerable distance from the trench have been recognized (Nyström 2004). Nyström (2004) proposed deposition during an extensional phase in a subsiding volcano-tectonic graben along a thick, active continental margin.

The supracrustal rocks lack penetrative tectonic structures, but have been affected by burial metamorphism that varies from prehnite-pumpellyite through pumpellyite-actinolite to greenschist facies (Nyström & Levi 1980, Nyström 1983). Bedding in the sedimentary rocks is generally subhorizontal and, only locally, more steeply dipping, and the supracrustal rocks rest unconformably on top of Svecofennian volcanic rocks (1.91–1.89 Ga) and GSDG intrusive rocks that belong to the older, 1.81–1.78 Ga suite. Clasts of granite from the 1.70–1.67 Ga GSDG intrusive suite occur in the sedimentary rocks, but the supracrustal rocks were also intruded by these granites, indicating the occurrence of more than one generation of granite.

No geochronological data are available in the Bergslagen region for the 1.7 Ga suite of supracrustal rocks. However, several U-Pb (zircon) analyses are present in the main outcrop area immediately to the north and north-west of the Bergslagen region. These ages range from 1711^{+7}_{-6} Ma to 1692±6 Ma (Lundqvist & Persson 1999) and confirm the temporal association of these supracrustal rocks with the 1.70–1.67 Ga GSDG intrusive rock suite.

Mesoproterozoic clastic sedimentary rocks

Scattered occurrences of Mesoproterozoic sandstone with subordinate shale and conglomerate, generally referred to as the *Jotnian* (or *Dala*) *sandstone*, are present in the Bergslagen region (Fig. 97). The largest of these occurrences is a partially fault-bounded outlier between Sandviken and Gävle in the north-eastern part of the region. Smaller occurrences are present in the north-westernmost part of Bergslagen where they lie stratigraphically on top of the 1.7 Ga GSDG intrusive rocks and the associated supracrustal rocks. The Mesoproterozoic sedimentary rocks in this part of Bergslagen expand to the north and north-west in the county of Dalarna, where they occupy more than 6 000 km^2 directly beneath the Quaternary overburden. The character of the Mesoproterozoic sedimentary rocks presented here is based on the detailed descriptions of the sandstones in Dalarna (e.g. Hjelmqvist 1966, Andersson et al. 2005). Minor occurrences of Mesoproterozoic sedimentary rocks are also present on some islands in the lake Mälaren, west of Stockholm.

According to Hjelmqvist (1966), the *Jotnian sandstone* in Dalarna has a maximum thickness of c. 800 m. By contrast, Juhlin et al. (1991) estimated a minimum thickness of 1 270 m. It can be stratigraphically divided into lower and upper parts, separated by a basalt unit, the so-called *Öje basalt*. The lower part is dominated by lithic sandstone with variable content of feldspar up to arkosic composition. These sandstones are normally red and medium-grained but locally more coarse-grained. A characteristic feature is the occurrence of reduction spots. The lithic clasts, both sand-sized and coarser in conglomeratic varieties, are dominated by volcanic rocks derived from the underlying 1.7 Ga igneous suite. The upper part of the *Jotnian sandstone* consists of reddish grey sandstone with quartz arenitic to sub-arkosic composition. More fine-grained interbeds of shale and mudstone as well as dolerites occur in both the lower and upper parts of the sandstone. It is only the lower part of

the *Jotnian sandstone* which extends southwards into the north-westernmost part of the Bergslagen region.

The dominantly red colour and the lithic and partly arkosic compositions of the *Jotnian sandstone*, in combination with the presence of cross bedding, desiccation cracks and ripple marks, suggest that the sandstone formed in a continental depositional environment. Pulvertaft (1985) interpreted the lower part of the formation as eolian, whereas Andersson et al. (2005) interpreted the upper part of the formation to be mainly eolian or deltaic.

Mesoproterozoic and Neoproterozoic dolerites and associated rocks (1.60–1.56 Ga, 1.48–1.46 Ga, 1.27–1.26 Ga and 0.98–0.95 Ga)

Dolerites are conspicuous in the Bergslagen region (Fig. 97). They mainly occur as dykes and, only locally, as flat-lying sills or possibly as basaltic lavas. In some places, dolerite and felsic dykes coexist, both as separate intrusions in the same region and as composite intrusions. The dolerites intrude and are inferred to be younger than all the rocks that are 1.7 Ga or older. Field data and radiometric age dating results (see below) suggest that they belong to four, separate Mesoproterozoic and Neoproterozoic igneous suites that formed at 1.60–1.56 Ga, 1.48–1.46 Ga, 1.27–1.26 Ga and 0.98–0.95 Ga. The two suites at 1.60–1.56 Ga and 0.98–0.95 Ga are by far the volumetrically most important in the Bergslagen region (Fig. 97).

Age suite 1.60–1.56 Ga

Dolerite dykes, locally associated with granophyre, that belong to the oldest suite of dykes are prominent in the southern part of the Bergslagen region. In this part of the region, the dykes strike west-north-west to east-south-east (Fig. 97) and intruded subparallel to the strong, Svecokarelian anisotropy in the older crystalline bedrock. They are referred to as the *Breven-Hällefors dolerites* and are, locally, up to 1 km in width at the ground surface. The dolerites consist of plagioclase feldspar, clinopyroxene, olivine, orthopyroxene and stilpnomelane. A U-Pb (baddeleyite) age of 1593±3 Ma (see, for example, Fig. 82) is inferred to date the timing of intrusion (Söderlund et al. 2005). This age occurs in the older part of the 1.6 to 1.5 Ga time range indicated by Rb-Sr mineral isochron data (Patchett 1978).

Dolerites in the oldest suite are also present in the westernmost part of the Bergslagen area (Fig. 97), close to Kristinehamn, where the bedrock is generally strongly affected by Sveconorwegian deformation and metamorphism. The degree of metamorphic alteration in these dolerites is variable and rocks with well-preserved igneous mineralogy and textures, and strongly deformed, garnet-bearing amphibolites are both present. Their occurrence as sheets subparallel to the Sveconorwegian structural trend is inferred to be a result of this later ductile strain, i.e. it does not reflect their primary orientation. The better preserved dolerites mainly consist of plagioclase feldspar, which is impregnated by titanium-rich magnetite, pyroxene, olivine and biotite. Two samples from the oldest suite of dolerites in the western part of and immediately to the west of the Bergslagen region have yielded U-Pb (baddeleyite) ages in the time range 1.60 to 1.56 Ga (Wahlgren et al. 1996, Söderlund et al. 2005; see, for example, Fig. 82).

The time range for the intrusion of the dolerites in the 1.60–1.56 Ga suite overlaps temporally with Rapakivi igneous activity further to the north and east in the Fennoscandian Shield and to Gothian orogenic activity in the south-western part of the shield (see, for example, Koistinen et al. 2001).

Age suite 1.48–1.46 Ga

The hypabyssal intrusions that formed at 1.48 to 1.46 Ga occur in restricted areas of Bergslagen, principally in its north-western and north-eastern parts. In the north-western part, between Ludvika and Borlänge (Hjelmqvist & Lundqvist 1953), these rocks occur as dykes that strike north-east–south-west to north–south, and are referred to as the *Tuna dolerites* and the associated felsic *Gustafs porphyries*. Some of the porphyries occur in close spatial association with a *rapakivi-type* intrusion dated at c. 1.47 Ga (see later text) and locally (Pellesberget, south-east of Borlänge) cross-cut or are intermingled with an intrusion breccia (Lundström et al. 2002a). The dolerites locally contain coarse (<1 cm), greenish-white phenocrysts of plagioclase feldspar and amygdales with calcite (±chlorite). The porphyries contain phenocrysts of fine- to coarse-grained alkali feldspar and fine-grained quartz in variable proportions. In composite dykes, the felsic material generally occupies the central part of the intrusion. Locally, the magmas mixed and intermediate hybrid compositions formed.

U-Pb (zircon) dating of a porphyry dyke inside the Bergslagen region (Lundström et al. 2002b) and U-Pb (baddeleyite) dating of dolerites outside this region, in the north-western part of Dalarna (Söderlund et al. 2005), have yielded identical ages in the time span 1.48 to 1.46 Ga (see, for example, Fig. 82). One of these dolerites has been inferred (Söderlund et al. 2005) to be a feeder dyke to the *Öje basalt* that is intercalated within the *Jotnian sandstone* (see above). These geochrono-

logical data and inferred stratigraphic relationships provide support to the correlation between the *Tuna dolerites* and *Öje basalt* proposed earlier by Hjelmqvist & Lundqvist (1953).

Dolerites, which strike north-north-east–south-south-west and are spatially associated with a *rapakivi-type* granite dated at c. 1.50 Ga (see later text) in the north-eastern part of the Bergslagen area, close to Gävle, have also been inferred to belong to the 1.48 to 1.46 Ga igneous suite (Andersson 1997b). A basaltic sill (Gorbatschev 1967) or lava (Bergman et al. 2004b) is interlayered within clastic sedimentary rocks that have been correlated with the *Jotnian sandstone* (Fig. 97). These rocks occur directly south of and in faulted contact with the *rapakivi-type* granite. The amygdaloidal and locally pillowed character of the basaltic rock supports its interpretation as lava (Bergman et al. 2004b). Its age is uncertain, but, by comparison with the *Öje basalt*, is tentatively included here in the early Mesoproterozoic 1.48–1.46 Ga igneous suite.

The dolerites in the 1.48–1.46 Ga igneous suite are close in age to and partly overlap the Hallandian orogenic event in the south-western part of the Fennoscandian Shield (see, for example, Koistinen et al. 2001).

Age suite 1.27–1.26 Ga

In the Gävle area (Fig. 97), dolerite sills that intrude the *Jotnian sandstone* (Fig. 97) have been correlated with the suite of dolerites referred to as *Åsby-type* (Gorbatschev 1967, Bergman et al. 2004b). The *Åsby dolerites* show an alkali basaltic composition, contain olivine and titanium-rich magnetite, are fine- to normally medium-grained and show an ophitic texture with intergranular pyroxene and olivine between plagioclase laths (see, for example, Lindström et al. 2000). Samples that belong to this dolerite suite from outside the Bergslagen region, in north-western Dalarna, have yielded U-Pb (baddeleyite) ages that fall in the range 1.27 to 1.26 Ga (Söderlund et al. 2005).

Age suite 0.98–0.95 Ga

The youngest suite of dolerites in the Bergslagen region occurs as dykes that strike generally north-north-west–south-south-east. These dykes are prominent in the western half of the Bergslagen region, in the vicinity of the Sveconorwegian orogen (Fig. 97). According to Hjelmqvist (1966), these dolerites locally contain both ortho- and clinopyroxene and quartz; granophyric texture is present in some samples. In the westernmost part of the Bergslagen region, close to the eastern boundary of the area that is affected by Sveconorwegian ductile deformation along discrete shear zones (see section "Later phase of Sveconorwegian deformation and metamorphism"), these dykes are affected by ductile deformation under greenschist-facies metamorphic conditions along such a zone. For this reason, the deformation in the dykes is inferred to be associated with the Sveconorwegian tectonic activity (Wahlgren et al. 1994).

The dolerites define an igneous suite that follows the structural trend of the Sveconorwegian orogen, from Blekinge in the south-easternmost part of Sweden to Dalarna in the central and western part of the country (*Blekinge-Dalarna dolerites* or *BDD*). This suite occurs in the easternmost part of and east of the Sveconorwegian orogen. On the basis of U-Pb (baddeleyite) ages, predominantly outside the Bergslagen region, these dolerites intruded at 0.98 to 0.95 Ga (Söderlund et al. 2005). One sample in the Bergslagen region, close to Falun, yielded a U-Pb (baddeleyite) age of 946±1 Ma (Söderlund et al. 2005).

The swarm of 0.98–0.95 Ga dolerites provides an igneous expression of the extensional deformation in an approximately east–west direction that has been inferred to account for the exhumation of high-pressure rocks in the southern part of the Sveconorwegian orogen (Möller 1998).

Granite (1.50 Ga) and quartz syenite (1.47 Ga)

Two occurrences of Mesoproterozoic, *rapakivi-type* intrusive rocks are present in the Bergslagen region (Fig. 97). The so-called *Strömsbro granite* occurs close to Gävle in the north-eastern part of the region. It is porphyritic with perthitic K-feldspar phenocrysts that lack plagioclase rims, and has been classified as A-type in composition (Andersson 1997b). The so-called *Noran intrusion* occurs south-west of Borlänge in the north-western part of the Bergslagen region and has been described as A-type alkali granite to quartz syenite (Hjelmqvist 1966, Claesson & Kresten 1997; see, for example, Fig. 82). U-Pb (zircon) ages indicate that these rocks intruded at 1500±19 Ma and 1469±10 Ma, respectively (Claesson & Kresten 1997, Andersson 1997b). A spatial and possibly genetic relationship to the 1.48–1.46 Ga dolerite dyke suite (see above) is inferred.

NEOPROTEROZOIC AND LOWER PALAEOZOIC SEDIMENTARY COVER ROCKS

Neoproterozoic clastic sedimentary rocks

Neoproterozoic clastic sedimentary rocks that belong to the *Visingsö Group* occur in the western part of the Bergslagen region, predominantly south of Karlsborg

around the lake Vättern, on a few islands in the northern part of this lake (Wikström & Karis 1993) and north-west of Motala (Fig. 99). However, the *Visingsö Group* has also been observed as far north as around Karlskoga (Wikström & Karis 1997). The *Visingsö Group* was probably deposited during the Cryogenian (Middle Neoproterozoic). The most recent isotopic data (Bonhomme & Welin 1983) suggest an age of 706±14 Ma for the entire formation.

Geijer et al. (1951) estimated the thickness of the *Visingsö Group* to more than 1000 m (Fig. 100) and proposed a division into *Lower, Middle* and *Upper units*. These have been treated as formations by some workers (Wikström & Karis 1993, cf. Persson et al. 1985). The *Lower Visingsö unit* is a fluvial deposit (Wikman et al. 1982), composed of white to reddish brown, quartz-rich sandstone deposited on the crystalline basement. It is conformably overlain by a conglomerate bed that belongs to the *Middle Visingsö unit* (Wikman et al. 1982), which is a complex unit with beds of sandstone, siltstone, conglomerate, cross-bedded arkose and breccia. On the basis of lithological characteristics, Wikman et al. (1982) divided the *Middle Visingsö unit* into three mappable sub-units. The contact to the overlying *Upper Visingsö unit* is not clearly defined. The *Upper Visingsö unit* is composed of alternating siltstone and dolomitic limestone. Both the *Middle* and *Upper Visingsö units* are rich in sedimentary structures, such as ripples, desiccation cracks and cross bedding. Stromatolites have also been found in the *Upper Visingsö unit*.

Lower Palaeozoic platformal sedimentary cover rocks

Outliers of clastic sedimentary rocks and limestone, which belong to the Lower Palaeozoic platformal sedimentary cover sequence above the Fennoscandian Shield, occur predominantly in two separate parts of the Bergslagen region, in Östergötland and Närke (Fig. 99). The occurrences in Östergötland are present in the Motala area eastwards as far as the lake Roxen and on the eastern shore of the lake Glan, north-west of Norrköping (Fig. 99). The occurrences in Närke are located in a broadly triangular area east of Kilsbergen towards the lake Hjälmaren, i.e. south of Örebro (Fig. 99). A minor outlier of black shale is also present close to Arboga. In general, the rocks are buried beneath the Quaternary cover and, for this reason, geological information has to a large extent been retrieved from drill core. All these outliers are bounded in part by faults (Fig. 99) that were active during or after the Early Palaeozoic. The successions in these areas are discontinuous and are characterized by stratigraphic gaps (Fig. 100).

Cambrian and Cambrian to Lower Ordovician rocks

Cambrian and Cambrian to Lower Ordovician clastic sedimentary rocks lie unconformably on top of the Palaeoproterozoic crystalline basement rocks. Three lithological units in Östergötland and Närke have been correlated with the established lithostratigraphy (Nielsen & Schovsbo 2006), i.e. the *File Haidar* (Lower Cambrian), *Borgholm* (Lower to Middle Cambrian) and *Alum Shale* (Middle Cambrian to Tremadocian) *Formations* (Fig. 100).

The Lower Cambrian *File Haidar Formation* is mainly composed of quartz-rich sandstone, siltstone and mudstone (Nielsen & Schovsbo 2006). At the base, there is a transgressive conglomerate which can be correlated throughout Sweden. The thickness varies, from 15–18 m in Närke (Lundegårdh & Fromm 1971) to 21–37 m in Östergötland (Fig. 100). The *File Haidar Formation* and the overlying Lower to Middle Cambrian *Borgholm Formation* are separated by an unconformity in the mainland part of Sweden.

The *Borgholm Formation* (Fig. 100) is dominated by siltstone and mudstone interbedded with thin layers of sandstone (Nielsen & Schovsbo 2006). Nielsen & Schovsbo (2006) included the Middle Cambrian glauconitic sandstone (Lundegårdh et al. 1973, Persson et al. 1981) in the *Borgholm Formation*. In Närke, the upper part of the *Borgholm Formation* is missing, whereas it is present in Östergötland. Hence, the thickness varies. In Östergötland, the unit reaches 27 m, whereas in Närke it is approximately 13 m (Nielsen & Schovsbo 2006).

The kerogeneous Middle Cambrian to Tremadocian *Alum Shale Formation* is present in both areas (Fig. 100). Nielsen & Schovsbo (2006) undertook a recent review of this formation, where they restricted the usage of the term to "fine-grained, blackish mudstones/mudshales (with subordinate limestone)". In Östergötland, dark shales belonging to the *Borgholm Formation* interfinger with the lower part of the *Alum Shale Formation*. Thus, there is some difficulty to distinguish between the two formations in this area. The *Alum Shale Formation* is widely recognized for its high content of organic matter and other raw materials, such as uranium and vanadium (Andersson et al. 1985 and see section "Mineral and bedrock deposits"). It is approximately 20 m thick in south-central Sweden (Westergård 1922).

Ordovician rocks

A review of the Ordovician successions in central Sweden has been presented in Ebbestad et al. (2007). In Närke, only the Lower to Middle Ordovician sedimen-

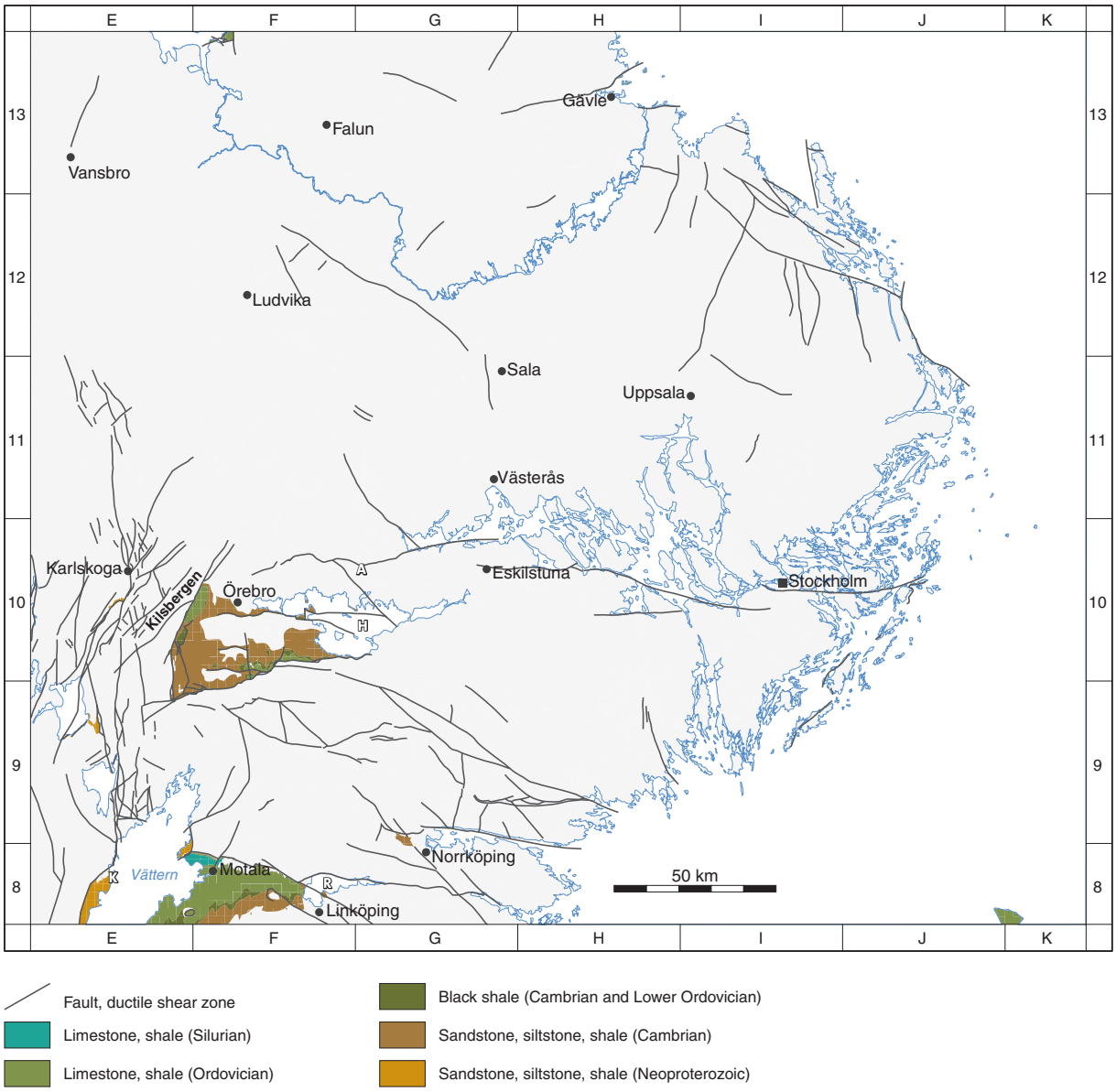

Fig. 99. Distribution of Neoproterozoic and Lower Palaeozoic sedimentary cover rocks at the ground surface in the Bergslagen region. The location of place names referred to in the section "Neoproterozoic and Lower Palaeozoic sedimentary cover rocks" is also shown. A = Arboga, H = Hjälmaren, K = Karlsborg, R = Roxen.

tary rocks are preserved and correlated with the *Latorp Limestone* and the topoformation *Lanna Limestone* (Fig. 100). These rocks are dominated by bedded calcilutitic limestone, mudstone and calcareous mudstone. The lowermost part (2 m) of the limestone succession is rich in glauconite, phosphorite and pyrite (Lundegårdh et al. 1973). Ordovican limestone has also been exploited as a bedrock resource in the Bergslagen region (see section "Mineral and bedrock deposits").

The Ordovician succession in Östergötland (Fig. 100) is more complete compared with that in Närke and is at least 135 m thick in the Motala area (Wikman et al. 1982, Fig. 34). The dominant lithology is bedded, nodular, grey or red limestone with intercalations of mudstone (i.e. *Latorp Limestone*, *Lanna Limestone*, *Segerstad Limestone*, *Skärlöv Formation*, *Seby Limestone*, *Folkeslunda Limestone*, *Furudal Limestone*, *Dalby Limestone*, *Freberga Formation*, *Slandrom Limestone*, *Öglunda Limestone*, *Jonstorp Formation* and *Tommarp Beds*). Other lithologies include bentonite, referred to as the Sandbian *Kinnekulle K-bentonite* (Bergström et al. 1995), and shales that belong either to the Tremadocian *Alum Shale Formation* or the Katian *Fjäcka Shale*. In the Smedsby Gårds drill core, the *Kinnekulle K-bentonite* is 1.4 m thick and the *Fjäcka Shale* is 3–4 m thick.

Silurian rocks

In the Bergslagen region, Silurian rocks are only present in the northern part of the Motala area in Östergötland (Fig. 99). In common with many other Ordovician and Silurian successions, the lower boundary of the Silurian rocks is represented by a significant stratigraphic gap (Fig. 100). The Silurian strata are of Llandovery age, middle to late Rhuddanian to Aeronian according to Bergström & Bergström (1996). There are two main lithologies, nodular limestone (*Motala Formation*) and black shale (*Kallholn Formation*). In the Lindenäs drill core, these strata are up to 37 m in thickness (Wikman et al. 1982). The Silurian strata are faulted (see e.g. Wikman et al. 1982) and, for this reason, their entire thickness is difficult to estimate.

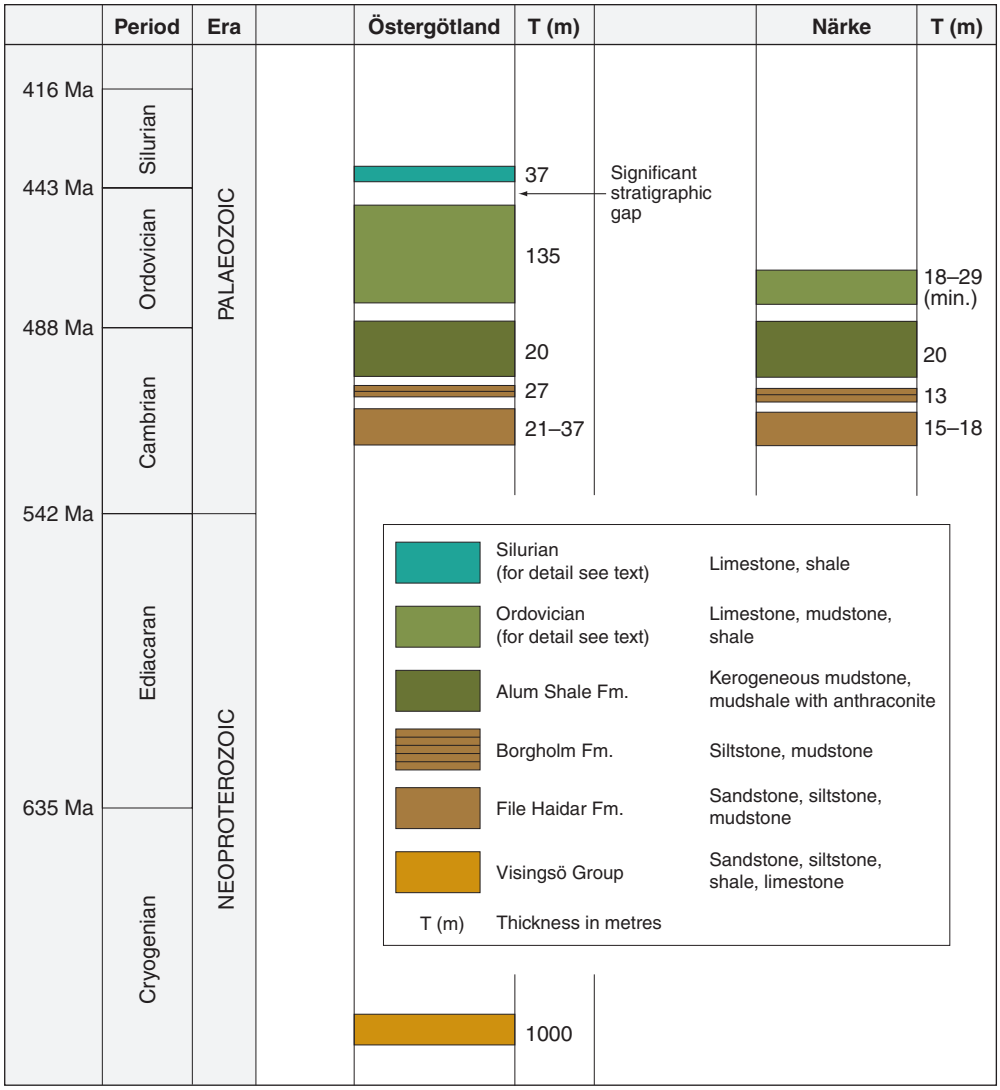

Fig. 100. Schematic stratigraphic sections through the Neoproterozoic and Lower Palaeozoic sedimentary cover rocks in Östergötland (areas around Motala and close to the eastern shore of lake Glan, north-west of Norrköping) and Närke (south of Örebro), Bergslagen region.

Mineral and bedrock deposits

OVERVIEW OF CONTENT

This section addresses the highly variable mineral and bedrock deposits in the Bergslagen region which, from an historical and economic perspective, have been of major significance. It opens with a brief summary of the mining history and the current exploration and mining activities in the region. This is followed by a statement concerning the non-genetic classification of the deposits adopted in this report. This strategy has been deemed to be necessary, since genetic interpretations have tended to follow, in part, trends in the interpretation of mineral deposits in the international literature at the time of the investigations. Nevertheless, comments on genetic aspects are presented for the different groups of deposits in the description. A detailed geological description of the three major groups of deposits forms the main part of this section. These groups comprise metallic mineral deposits, non-metallic mineral deposits and bedrock deposits. Special attention is addressed on the three base metal sulphide deposits that are currently being mined.

Place names referred to in the text that describes each type of mineralization in the Bergslagen region are located in the respective figure that shows the distribution of each type of mineralization at the ground surface in this region. Several local names for mineral deposits or groups of deposits in so-called ore fields are also used in the text below. The reader is referred to the main map on the mineral resources map (Stephens et al. 2007c) for the location of these deposits and ore fields.

SUMMARY OF MINING HISTORY AND CURRENT ACTIVITIES

Mining of metallic ore deposits has a long history in Bergslagen. Mining of copper is documented back to the 13th century and mining of iron to the 14th century. Archaeological data suggest that mining of copper at Falun may have started already c. 500 AD and that blast furnaces for iron production existed at Norberg in the 13th century (Åkerman 1994).

In total, nine major base metal sulphide ore fields with a size larger than 1 million metric tonnes (>1 Mt) in Bergslagen have produced c. 100 Mt of ore until 2005 (Åkerman 1994 and SGU data). The *Falun deposit* (28 Mt) is one of the oldest known sulphide mineralizations in Bergslagen. It was initially referred to as the *Tiskasjöberget* or *Stora Kopparberget deposit*. For a long period, the annual production was approximately 200 000 tonnes at 6% zinc, 2% lead and 0.5% copper (Koark et al. 1986). In addition, silver (50 ppm) and gold (0.4 ppm) were important by-products. Beside metals, the *Falun deposit* has been a major producer of raw material for sulphuric acid and the nationally famous red paint used on wooden houses in Sweden and in the other Nordic countries. Mining ceased during 1992. At the present time, only three base metal sulphide mines are in operation in Bergslagen: the *Garpenberg Zn-Pb-Ag-(Cu-Au) deposit*, the *Zinkgruvan Zn-Pb-Ag deposit* and the minor *Lovisagruvan Zn-Pb deposit* (Fig. 101).

Up to and including 1992, when the iron oxide deposit at Dannemora in the north-eastern part of the Bergslagen region closed, 31 major iron oxide ore fields (>1 Mt) in Bergslagen had together produced c. 420 Mt ore. The largest deposit was the *Grängesberg ore field* with a production of c. 150 Mt between 1500 and 1989. The second largest deposit was the *Dannemora deposit* with a production of c. 24 Mt between 1481 and 1992.

The recent significant increase in world market metal prices and the revised scientific appraisal of the potential relationship between iron oxide and Cu-Au mineralization (e.g. Hitzman et al. 1992) have given rise to a renewed exploration interest in the Bergslagen region. At the current time (October 2008), 40 national and international companies own 338 exploration permits or applications for such permits that cover an area of c. 288 000 ha in the region (Fig. 3). In addition, 34 mining concessions are currently open that cover an area of c. 2 290 ha (Fig. 3). One of these concessions aims to restore mining activity at the iron oxide (±base metal sulphide) deposit in manganese-rich skarn at Dannemora.

CLASSIFICATION OF DEPOSITS

The mineral and bedrock deposits in Bergslagen are classified on both the mineral resource map (Stephens et al. 2007c) and in this report as metallic mineral deposits, non-metallic mineral deposits or bedrock deposits (Fig. 101). The focus in the text that follows here is on the metallic mineral deposits. These deposits are further subdivided according to commodity, host rock and mineralogical characteristics. Thus, the classification is non-genetic in character. The non-metallic mineral deposits are simply subdivided after commodity and comprise, for example, minerals associated with pegmatite, including feldspar, quartz, mica and beryl. Bedrock deposits include only crystalline carbonate rock (marble), limestone and alum shale. Aggregate

and dimension stone deposits have not been included in the compilation.

By far the most common type of metallic mineral deposit in Bergslagen consists of a concentration of iron oxides with variable amounts of manganese in associated skarn and crystalline carbonate rocks (Fig. 101). More than 2 000 deposits are known, most of which are small and, since the middle of the 19th century, without any economic significance. According to Geijer & Magnusson (1944), economically important iron oxide deposits in Bergslagen may be subdivided into the following categories: iron oxide deposits in manganese-poor or manganese-rich skarn and carbonate rocks, quartz-rich iron oxide deposits including banded iron formation (BIF), and apatite-bearing iron oxide deposits. The term "skarn" refers simply to one of the host rocks to the ore minerals and does not have any genetic connotations. This host rock consists of calcium- or magnesium-rich silicate parageneses. In addition, iron oxide deposits associated with high contents of base metal sulphides are also present.

The categories recognized by Geijer & Magnusson (1944) may be considered as end members, and characteristics corresponding to more than one category are locally found in different parts of or along strike in the same deposit. For example, some iron oxide skarn deposits appear to grade into quartz-rich deposits. However, an attempt has been made to classify each deposit into one category on the mineral resources map (Stephens et al. 2007c), in accordance with the above classification system.

Manganese oxide deposits (Fig. 101) comprise both stratiform *Långban-type* deposits associated with iron oxide skarn mineralization and epigenetic deposits associated with fault breccia. Tungsten oxide deposits composed of scheelite and wolframite are also a significant component in the Bergslagen region (Fig. 101).

All sulphide deposits are described under a single heading (Fig. 101). Base metal sulphide deposits are by far the largest group. A subdivision of these deposits based on metal content has generally proven impossible to carry out, due to the lack of detailed grade figures for most of the deposits. However, a dominance of zinc and lead is typical for the base metal sulphide deposits in the Bergslagen region. The mineralogical and textural features are highly variable, which may reflect different origins or different deformational and metamorphic histories. Molybdenum sulphide deposits (*climax-type*), as well as other minor sulphide occurrences (e.g. Ni-Cu-Co deposits), some platinum group element (PGE) deposits and greisen deposits with both oxides and sulphides, are also shown on the map and are described here in the section on sulphide deposits.

METALLIC MINERAL DEPOSITS

Iron, manganese and tungsten oxide deposits

The majority of oxide deposits in the Bergslagen region are dominated by iron and contain variable contents of manganese in associated skarn and crystalline carbonate rocks. Several of these deposits also contain iron sulphides and base metal sulphides. Locally, more exotic metals, including gold, bismuth, uranium, thorium, tungsten and REE, are present in these oxide deposits.

Gold has been noted in anomalous amounts in some iron oxide mineralizations, e.g. the *Malsjöberg* (Löfstrand 1894) and *Nordmark* (Flink 1908) *deposits*. Discoveries of this type of gold occurrence have also been made in the deposits in the *Riddarhyttan ore field* and at the *Boviksgruvan deposit* north-east of Falun (Bergman & Sundblad 1990). Gold is intimately intergrown with bismuth minerals in these deposits (Bergman & Sundblad 1990, Ripa 2001). Locally, uranium and thorium form minor components in the iron oxide skarn deposits but have never had any economic significance. Examples include the *Digerbergsgruvan deposit* in northern Bergslagen and the *Håkanstorp deposit* in the southern part of this region. Tungsten is present in anomalous amounts as a scheelite impregnation in several iron oxide skarn deposits. However, once again, tungsten has never been extracted from these iron oxide deposits. At the *Ceritgruvan deposit* in the *Riddarhyttan ore field* in western Bergslagen and at the *Östra Gyttorpsgruvan deposit* in central Bergslagen, REE-minerals occur together with iron oxide skarn deposits. The different types of iron oxide deposits (including a sulphide-bearing variety) as well as the manganese oxide and tungsten oxide deposits are described in more detail below.

Iron oxide deposits in manganese-poor skarn or crystalline carbonate rock

Iron oxide deposits hosted by manganese-poor skarn or crystalline carbonate rock are the most common type of iron oxide mineralization in Bergslagen (Fig. 102). Such deposits constitute nearly 50% of all known metallic deposits in the region. They are present in all parts of Bergslagen where supracrustal rocks occur. However, they are more frequent in the central and western parts, for example in the Filipstad area, where several ore fields that contain hundreds of minor deposits occur (Fig. 102). The historically most important occurrence is the *Persberg ore field*, the "birthplace" of the skarn concept (Törnebohm 1875). The *Finnshytteberg*, *Nordmark*, *Riddarhyttan*, *Norberg (Åsgruvan)*, *Herräng* and *Kantorp ore fields* (Magnusson 1925, 1929) are also significant occurrences. Iron oxide mineralization in

a manganese-poor host rock dominated by crystalline carbonate rock occurs in several of the typical skarn ore fields. This type of deposit is most common in the *Tuna-Hästberg ore field* south-west of Borlänge, in several deposits in the area between Fagersta and Norberg, and in some deposits in the *Hofors ore field* (Geijer & Magnusson 1944).

The deposits are generally thin (10–50 m) but can be laterally extensive. They are essentially stratiform and concordant with the host 1.91–1.89 Ga felsic metavol-

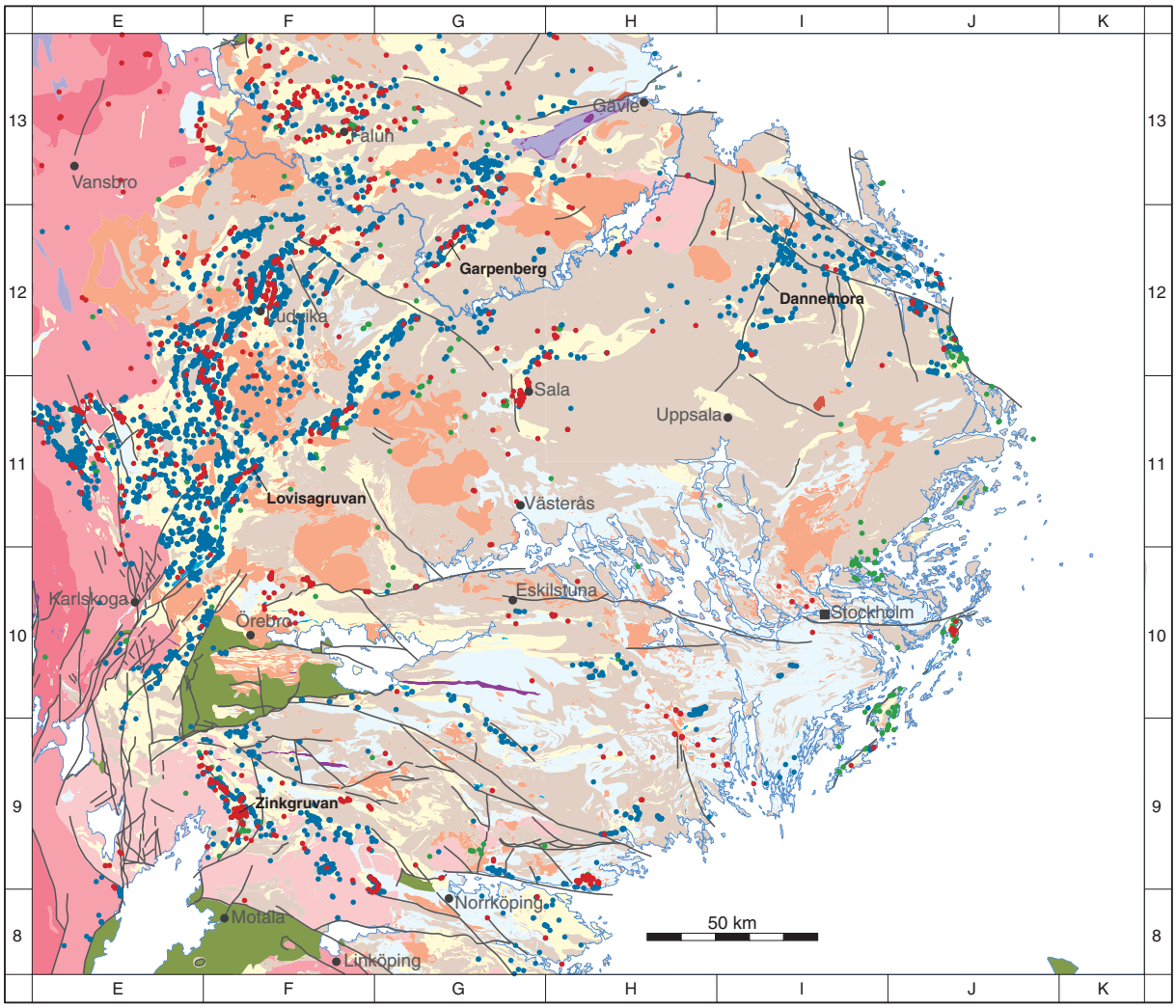

- Iron, manganese and tungsten oxide deposits
- Base metal, iron and other sulphide deposits
- Non-metallic mineral deposit
- Fault, ductile shear zone
- Neoproterozoic and Lower Palaeozoic sedimentary rocks
- Granite, quartz syenite (Mesoproterozoic), alkaline intrusive rock of uncertain age
- Dolerite (Mesoproterozoic)
- Clastic sedimentary rock (Mesoproterozoic)
- GSDG intrusive or meta-intrusive rock suite and associated supracrustal rock (1.70–1.67 Ga)
- GP intrusive rock suite (1.85–1.75 Ga)
- GSDG intrusive or meta-intrusive rock suite and associated supracrustal rock (1.81–1.78 Ga)
- GSDG and subordinate GDG intrusive or meta-intrusive rock suites (1.87–1.84 Ga)
- GDG and subordinate GSDG meta-intrusive rock suites (1.90–1.87 Ga), undifferentiated gneiss
- Svecofennian metavolcanic and subvolcanic meta-intrusive rocks (1.91–1.89 Ga), granofels of uncertain origin
- Crystalline carbonate rock
- Svecofennian clastic metasedimentary rock

GDG = Granitoid–dioritoid–gabbroid
GSDG = Granite–syenitoid–dioritoid–gabbroid
GP = Granite–pegmatite

Fig. 101. Distribution of the two principal types of metallic mineral deposits and the non-metallic mineral deposits in the Bergslagen region. The deposits are presented on a simplified bedrock geological map of the region. The three mines that are currently in production, i.e. the *Garpenberg*, *Zinkgruvan* and *Lovisagruvan base metal sulphide deposits*, and the *Dannemora iron oxide deposit* are identified on the map.

canic rocks (Fig. 102). The iron content is variable along strike and only the richest parts have been mined. The iron content in mined parts is generally between 30 and 50% (Geijer & Magnusson 1944) and the estimated tonnage of most of the individual older deposits is less than 1 Mt. However, when tonnage is calculated for production areas or entire ore fields, which consist of several deposits, 26 sites in the Bergslagen region show a tonnage that lies in the interval 1–10 Mt and a few in the interval greater than 10 Mt, for example the *Riddarhyttan ore field* with c. 15 Mt.

The deposits commonly contain magnetite, actinolite, hedenbergite, andradite garnet and epidote. The manganese-poor skarn parageneses have less than 1% MnO and all the manganese is accommodated in the skarn or carbonate minerals. Magnetite and calc-silicate minerals are irregularly distributed inside the deposits (Fig. 103a), and the volumetric proportion of calc-silicate minerals varies from deposit to deposit and even within individual deposits. Amphibole and garnet are generally the most abundant calc-silicate minerals in the skarn. The quartz content is generally low (<20% SiO_2) in the majority of these iron oxide deposits (Frietsch 1975). However, locally, the quartz content is higher and the deposit grades into quartz-dominated and banded iron formation. One example is the *Striberg deposit* at Nora

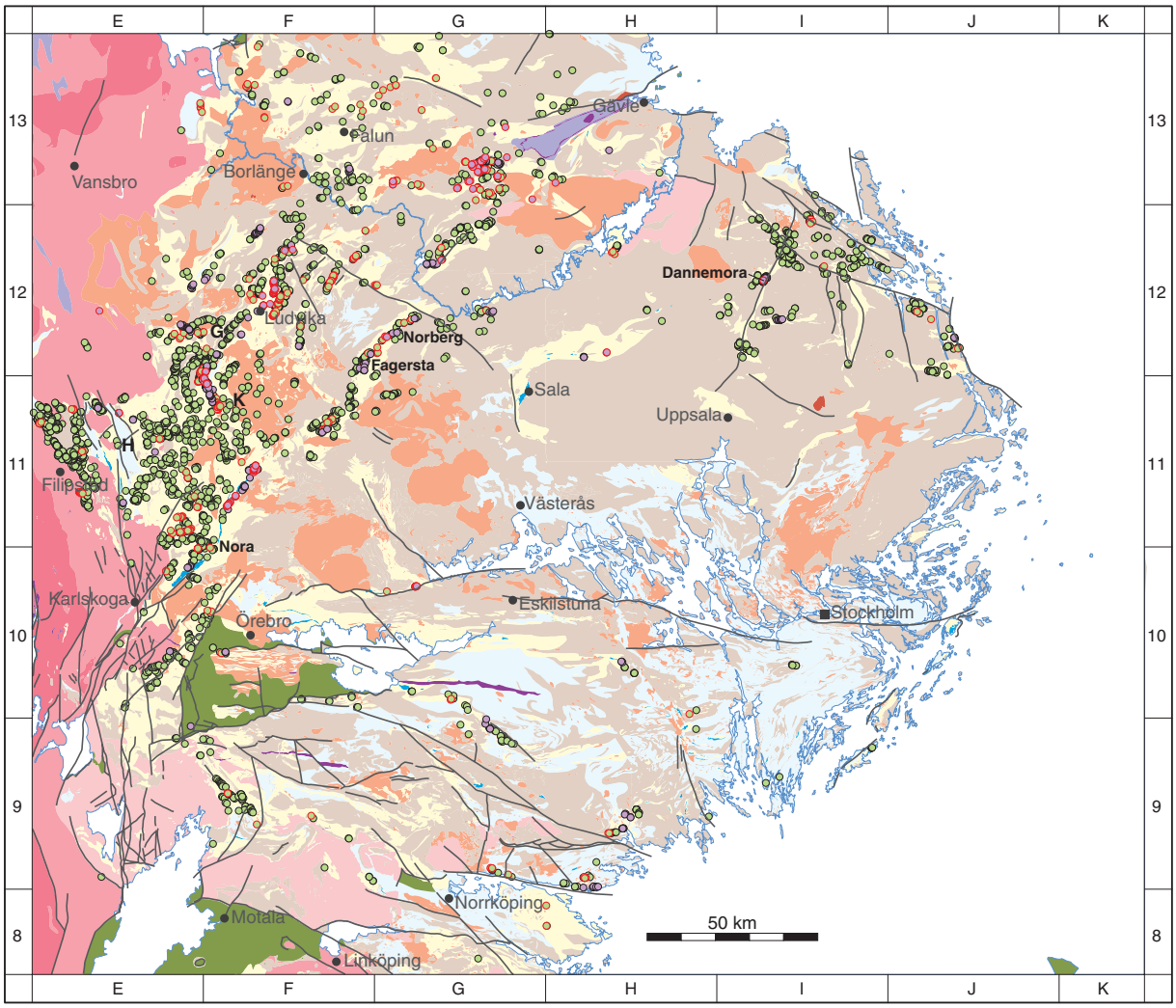

- Iron oxide deposit in manganese-poor (<1% MnO) skarn or crystalline carbonate rock
- Sulphide-disseminated iron oxide deposit in manganese-poor (<1% MnO) skarn or crystalline carbonate rock
- Iron oxide deposit in manganese-rich (>1% MnO) skarn or crystalline carbonate rock
- Sulphide-disseminated iron oxide deposit in manganese-rich (>1% MnO) skarn or crystalline carbonate rock

G = Grängesberg, H = Hällefors, K = Kopparberg

Fig. 102. Distribution of iron oxide deposits hosted by manganese-poor or manganese-rich skarn and crystalline carbonate rock in the Bergslagen region. Similar deposits with conspicuous sulphide dissemination are also shown. The deposits are presented on a simplified bedrock geological map of the region. See Figure 101 for legend to the base geological map. The location of place names referred to in the sections that address the iron oxide deposits hosted by manganese-poor or manganese -rich skarn and crystalline carbonate rock is also shown.

(Geijer & Magnusson 1944). Since skarn-rich layers occur in some banded iron formations in Bergslagen, for example at the *Utö deposit* (Geijer & Magnusson 1944), the classification in some cases is difficult and it is the inferred dominant type which is noted on the mineral resources map (Stephens et al. 2007c).

Some iron oxide mineralizations associated with magnesium-rich silicates are included in the group of iron oxide skarn deposits discussed here. One example is the *Källfallsgruvan deposit* in the *Riddarhyttan ore field* in western Bergslagen, where the host silicate mineral assemblage is dominated by an anthophyllite-cummingtonite-talc paragenesis. They have been interpreted (Magnusson 1973) as iron oxide skarn deposits associated with rocks affected by "magnesium alteration".

Based on the occurrence of a layering in many of the deposits and the overall stratiform appearance, several workers have suggested that the iron oxide deposits associated with skarn or crystalline carbonate rock generally originated as volcanogenic, exhalative-sedimentary deposits (Geijer & Magnusson 1944, Frietsch 1982b). The gradual transitions from banded iron formation to iron oxide skarn deposits and from iron oxide skarn deposits to iron oxide deposits hosted by crystalline carbonate rock provide some support to this hypothesis. However, the origin of these deposits is not fully resolved. The current mineral assemblages were most likely formed in connection with low- or medium-grade regional metamorphism (Magnusson 1973) during the Svecokarelian orogeny. This type of skarn was referred to as "reaction skarn" by Geijer & Magnusson (1944), in contrast to so-called "primary skarns", which are contact metasomatic deposits formed in association with the intrusion of igneous rocks.

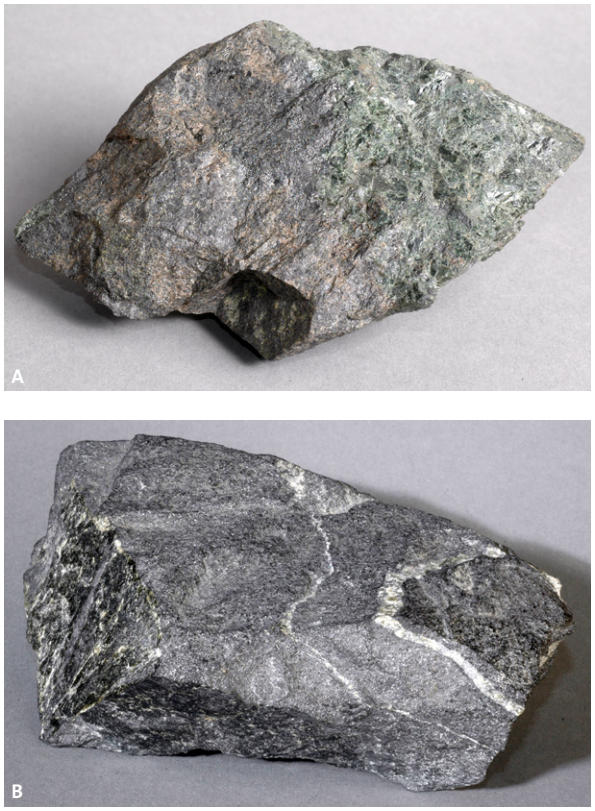

Fig. 103. Iron oxide deposits in manganese-poor and manganese-rich skarn. **A.** Actinolite-garnet-magnetite skarn from the iron oxide deposit in manganese-poor skarn at Persberg, Filipstad area. The specimen is 14 cm wide in a horizontal direction. **B.** Dannemorite-knebelite-magnetite skarn from the iron oxide deposit in manganese-rich skarn at Dannemora. The specimen is 13 cm wide in a horizontal direction. Photographs: Torbjörn Bergman (SGU).

Iron oxide deposits in manganese-rich skarn or crystalline carbonate rock

The regional distribution of iron oxide deposits associated with manganese-rich skarn or crystalline carbonate rock mainly corresponds to that observed for the manganese-poor deposits described above (Fig. 102). However, the former deposits appear to occur more frequently at higher stratigraphic levels and are, to a larger extent, hosted by crystalline carbonate horizons (Magnusson 1973). They are generally stratiform and lens-shaped. The deposits include, for example, the *Dannemora deposit* in north-eastern Bergslagen (Lager 1986, 2001), the *Tuna-Hästberg ore field* in north-western Bergslagen, and the *Bastkärn* and *Stollberg ore fields* in the area between Kopparberg and Grängesberg. All these deposits have an estimated tonnage that is greater than 5 Mt and the largest is the *Dannemora deposit* with a currently estimated tonnage of 53 Mt. Otherwise, most deposits of this type were minor operations with an estimated tonnage that is less than 0.1 Mt. Manganese and iron contents in these deposits are generally c. 2–10% and 30–50%, respectively (Magnusson 1973).

The deposits commonly contain magnetite and manganiferous calc-silicates, including dannemorite, knebelite and spessartine-rich garnet (Fig. 103b), with greater than 1% MnO. The manganese content in magnetite is generally low or very low, and manganese is accommodated in the calc-silicate and carbonate minerals; crystalline carbonate rocks locally contain up to 10% $MnCO_3$. The proportion of manganese-rich carbonate and manganese-bearing silicates is variable. The skarn ore parageneses generally contain minor amounts of graphite (0.5–1.5% C) and disseminations of galena, sphalerite and arsenopyrite (Geijer & Magnusson 1944). Examples of sulphide-rich deposits include the *Dannemora deposit*, the *Stollberg ore field* and the silver-rich deposits at Hällefors (see also below).

Locally, skarn mineralizations rich in both iron and manganese, without or with only minor amounts of

magnetite, occur. These so-called "eulysites" occur high in the stratigraphy, close to the overlying metasedimentary rocks (Frietsch 1982b).

Quartz-rich, iron oxide deposits including banded iron formation

Quartz-rich, iron oxide deposits are distinctly stratiform and locally developed as banded iron formation (BIF). These mineralizations occur mainly in the western part of Bergslagen and several hundred minor deposits of this type occur over a distance of 100 km in the area between Nora and Norberg (Fig. 104). The most prominent deposits of this type that show a tonnage greater than 5 Mt are also present in this part of Bergslagen (e.g. the *Striberg*, *Stripa* and *Strássa deposits*). Quartz-rich, iron oxide deposits also occur in the area north-west of Ludvika (e.g. the *Laxsjö*, *Ikorrbotten* and *Håksbergs ore fields*, see Fig. 104). Single minor occurrences are present in the eastern parts of Bergslagen, for example at the *Utö deposit* in the Stockholm archipelago (Fig. 104). Some mineralizations of this type have been mined since the Middle Ages and some were productive until the second half of the 20th century.

The dominant type of deposit is banded with hematite-rich and quartz-rich layers that are, locally, folded (Fig. 105). This type of iron oxide deposit is also hosted by the Svecofennian, 1.91–1.89 Ga felsic metavolcanic rocks (Fig. 104). Individual hematite-rich and quartz-rich layers are generally 1–10 mm thick and locally thicker. Locally, magnetite is relatively abundant and formed as an alteration product after hematite (Frietsch

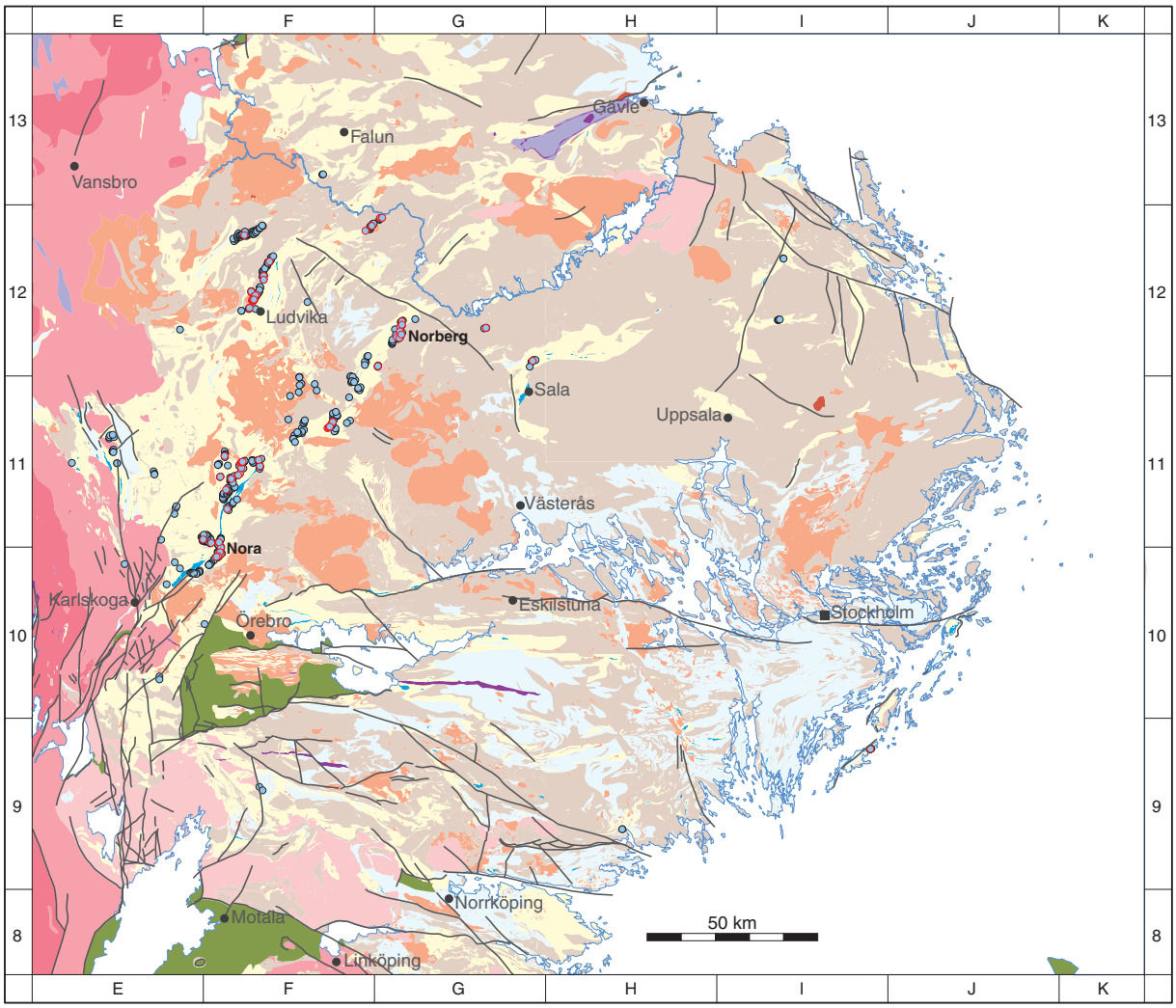

Quartz-rich iron oxide deposit, including banded iron formation (BIF)
Sulphide-disseminated, quartz-rich iron oxide deposit, including banded iron formation (BIF)

Fig 104. Distribution of quartz-rich, iron oxide deposits, including banded iron formation, in the Bergslagen region. Similar deposits with conspicuous sulphide dissemination are also shown. The deposits are presented on a simplified bedrock geological map of the region. See Figure 101 for legend to the base geological map. The location of place names referred to in the section entitled "Quartz-rich, iron oxide deposits, including banded iron formation" is also shown.

1975). The iron content is generally between 30 and 55%. However, some deposits that lack a distinct banding contain up to 60% iron including, for example, individual deposits in the *Bispberg ore field* (Magnusson 1973). SiO_2 contents vary between 18 and 28%, whereas phosphorous and manganese contents are generally low, less than 0.03% and less than 0.2%, respectively. Impregnation of sulphides is common in some occurrences and the sulphur content lies in the range 0.001–0.1% (Frietsch 1975).

The presence of dark red layers of jasper with a fine dissemination of hematite in quartz is typical for the quartz-rich, iron oxide deposits (Fig. 105a, b). Layers of skarn, with the calc-silicate minerals actinolite, pyroxene and epidote, occur in some banded iron formations. As indicated above, transitional varieties between skarn and quartz-rich, iron oxide deposits are developed. Examples include the *Grönvåld* and *Högban ore fields* approximately 10 km north of Nora (Magnusson 1970). According to Geijer & Magnusson (1944), the deposits in these ore fields are thin, fine-grained and relatively rich hematite ores, with a local diffuse banding. They alternate with layers of amphibole-pyroxene skarn with magnetite or hematite, weak hematite-quartz mineralizations, felsic metavolcanic rock and crystalline carbonate rock. These deposits are included in the quartz-rich, iron oxide group on the mineral resources map (Stephens et al. 2007c).

Fig. 105. Quartz-rich, iron oxide deposits including banded iron formation. **A.** Typical jasper-hematite layered banded iron formation sample from Pershyttefältet in the Nora area. **B.** Banded iron formation from the Striberg deposit. The specimen is 16 cm wide in a horizontal direction. Photographs: Torbjörn Bergman (SGU).

Apatite-bearing, iron oxide deposits

Apatite-bearing, iron oxide deposits in Bergslagen are geographically restricted to the Ludvika area in the western part of the region (Fig. 106). Major deposits include the *Grängesberg*, *Blötberget*, *Fredmundsberg*, *Lekomberg* and *Idkerberget ore fields*. This type of iron oxide mineralization has produced more than 40% of all the iron in Bergslagen, despite a limited number of deposits (Geijer & Magnusson 1944, Åkerman 1994). The largest and most well-known ore field is the *Grängesberg ore field*, which was mined between 1858 and 1989 with a total production of 150 Mt containing 40–63% iron (Åkerman 1994). The phosphorous content lies between 0.5 and 1.3%.

The deposits are hosted by the Svecofennian, 1.91–1.89 Ga felsic metavolcanic rocks and generally form lens-shaped bodies. Their stratigraphic position is not clear, but they appear to occur at a lower stratigraphic level than the skarn iron oxide and BIF deposits (Magnusson 1973, Back 1993, Allen et al. 1996). Mineralogically, the apatite-bearing iron ores consist of magnetite and hematite accompanied by apatite and small amounts of quartz and calc-silicate minerals (Frietsch 1975 and Fig. 107). The latter include actinolite and less abundantly epidote, chlorite and garnet. Magnesium-rich silicates are also present in the *Blötberget deposit*.

According to Magnusson (1970), the apatite-bearing, iron oxide deposits inject into, but are more or less coeval with their felsic metavolcanic host rocks. The epigenetic origin was questioned by Back (1993), who suggested a syngenetic origin for at least the *Grängesberg deposit*. A sedimentary origin combined with later remobilization into the metavolcanic rocks had been suggested earlier by Landergren (1948). Allen et al. (1996) emphasized the spatial relationship between this type of mineralization and porphyritic, dacitic subvolcanic intrusions and dykes at the *Grängesberg deposit*. According to these authors, the field relationships favour an igneous hydrothermal origin.

Iron oxide deposits, undifferentiated

Some of the iron oxide mineral deposits in Bergslagen have not been classified in accordance with the groups described above (Fig. 108). In most cases, these mineralizations show the characteristics of both skarn and

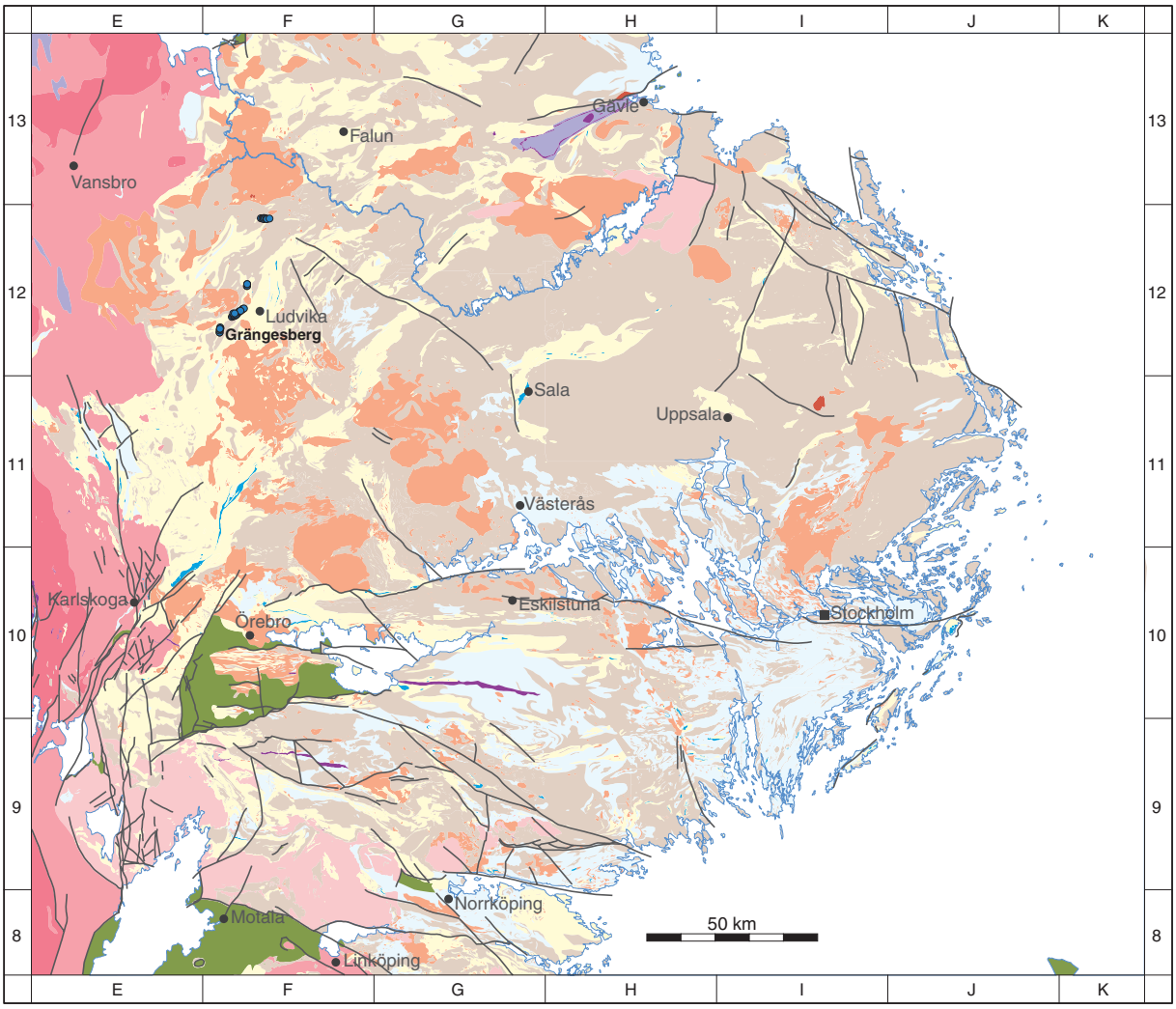

Fig. 106. Distribution of apatite-bearing, iron oxide deposits in the Bergslagen region. The deposits are presented on a simplified bedrock geological map of the region. See Figure 101 for legend to the base geological map. The location of the closed mine at Grängesberg is shown.

Fig. 107. Apatite-bearing magnetite ore from the Grängesberg deposit. The specimen is 8 cm wide in a horizontal direction. Photograph: Torbjörn Bergman (SGU).

quartz-rich, iron oxide deposits and it has proven difficult to classify the deposit according to the scheme adopted here. In some cases, the available information on the deposit is insufficient to permit a classification.

Sulphide dissemination in iron oxide deposits

Several iron oxide deposits in Bergslagen contain, to variable extent, iron and base metal sulphides (see Figs. 102, 104 and 108) and some of these deposits have had a mining history for both iron oxides and base metals. Conspicuous examples include the *Dannemora deposit* and the deposits in the *Stollberg ore field*. The *Dannemora deposit* was mined for silver during the Middle Ages and for zinc and lead from 1890 to 1920 (Tegengren et al. 1924). The *Stollberg ore field* was also mined for silver during the Middle Ages and has later been a major producer of zinc, lead and silver (Magnusson 1973). Indeed, the *Stollberg ore field* is an example of an iron oxide, manganese-rich skarn mineralization in

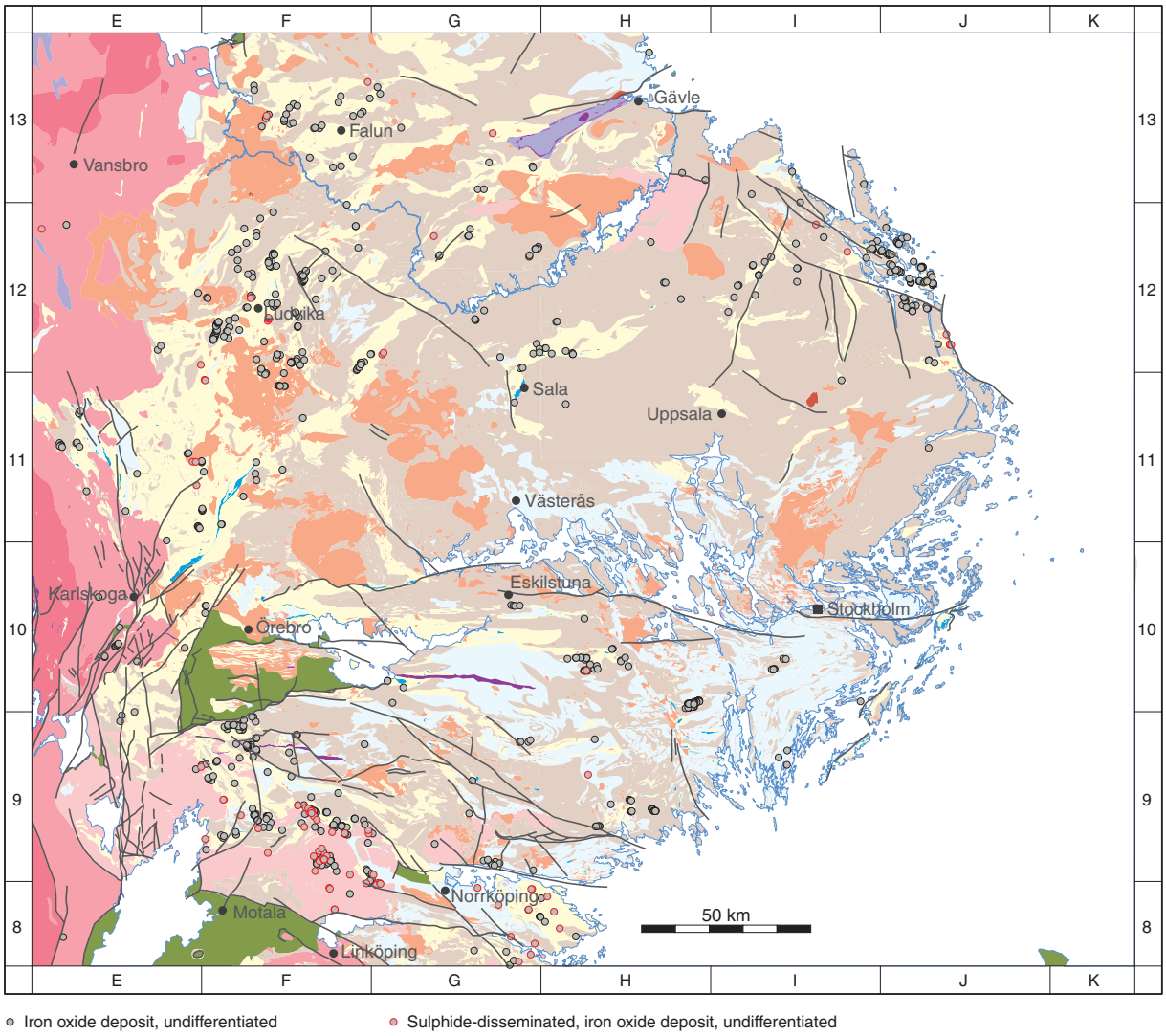

Fig. 108. Distribution of undifferentiated, iron oxide deposits in the Bergslagen region. Similar deposits with conspicuous sulphide dissemination are also shown. The deposits are presented on a simplified bedrock geological map of the region. See Figure 101 for legend to the base geological map.

which disseminated sulphides grade into semi-massive to massive occurrences (Ripa 1996).

In the SGU mineral and bedrock resource database (BERGDB_MDEP), the deposits in this group are classified both as iron oxide and sulphide deposits. On the mineral resources map (Stephens et al. 2007c), they are classified according to type of iron oxide deposit and the iron oxide symbol is enclosed in a red circle in order to emphasize the conspicuous sulphide content.

Manganese oxide deposits

Manganese oxide deposits in Bergslagen (Fig. 109) can be divided into two types:

- Stratiform manganese oxide deposits spatially associated with iron oxide deposits in manganese-poor skarn or crystalline carbonate rock.
- Epigenetic deposits hosted by breccia.

Examples of the former are mainly situated in the Filipstad area (Fig. 109) and include, for example, the *Långban*, *Jakobsbergsgruvan*, *Pajsberg-Harstigen* and *Sjögruvan deposits*. The most famous of these deposits is at Långban and this type of mineralization is generally referred to as the *Långban-type* (Geijer & Magnusson 1944).

The manganese oxide ores of *Långban-type* are hosted by crystalline dolomite and skarn. The ore minerals are hausmannite and braunite, which are irregularly distributed but, locally, arranged in bands (Magnusson 1930, Sandström & Holtstam 1999 and Fig. 110a). Associated skarn minerals are manganese-rich and occur along the contacts between crystalline carbonate

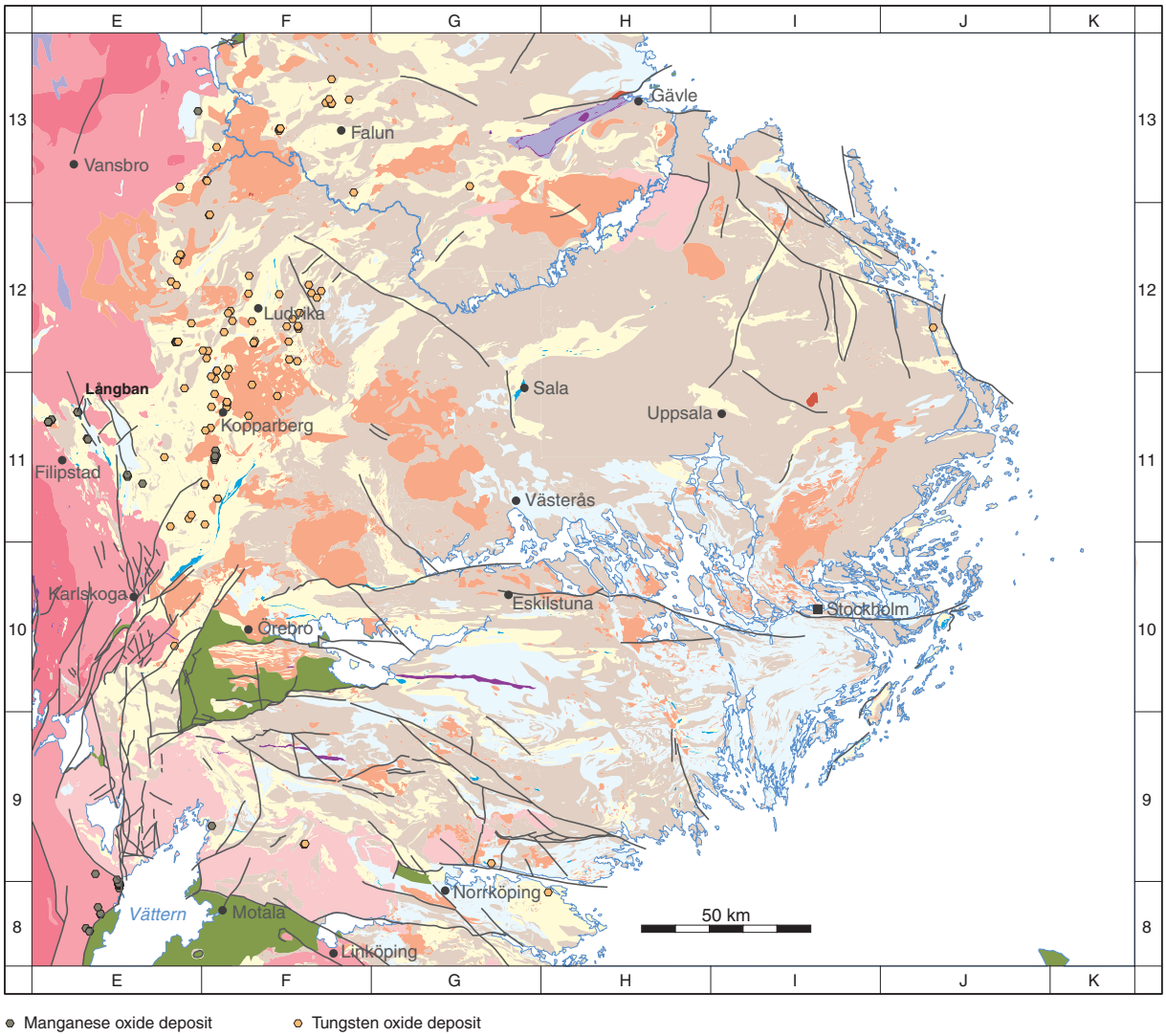

Fig. 109. Distribution of manganese and tungsten oxide deposits in the Bergslagen region. The deposits are presented on a simplified bedrock geological map of the region. See Figure 101 for legend to the base geological map. The location of place names referred to in the sections that address manganese and tungsten oxide deposits is also shown.

rock and the manganese oxide mineralization. These include manganiferous diopside, rhodonite, bustamite, manganiferous olivine and spessartine-rich garnet, as well as manganiferous varieties of phlogopite and richterite (Sandström & Holtstam 1999). In addition, the *Långban deposit* is famous for its abundance of rare lead, antimony and barium minerals. These occur as fissure and fracture fillings, which most likely formed in connection with hydrothermal processes during later brittle deformation (Sandström & Holtstam 1999), and it has been speculated that they formed in connection with Sveconorwegian tectonothermal activity (Jonsson 2004). The association that consists of native lead, barite and calcite in veins is typical for the *Långban deposit* (Jonsson 2004).

The genesis of the manganese-dominated parts of the *Långban deposit* has attracted considerable attention. Sedimentary (Sjögren 1891), metasomatic reaction (Geijer 1926, Magnusson 1930) and exhalative-sedimentary (Boström et al. 1979, Åberg & Charalampides 1986, 1988, Jonsson 2004) origins have all been suggested.

Occurrences of epigenetic, manganese oxide deposits hosted by breccia include, for example, the *Bölet deposit* (Fig. 110b), which consists of several minor mineralizations on the western side of lake Vättern (Tegengren et al. 1924), and a minor deposit north-east of Vättern (Wikström & Karis 1991).

Tungsten oxide deposits

Tungsten oxide deposits in Bergslagen (Fig. 109) can be divided into two major groups (Hübner 1971, Ohlsson 1979):

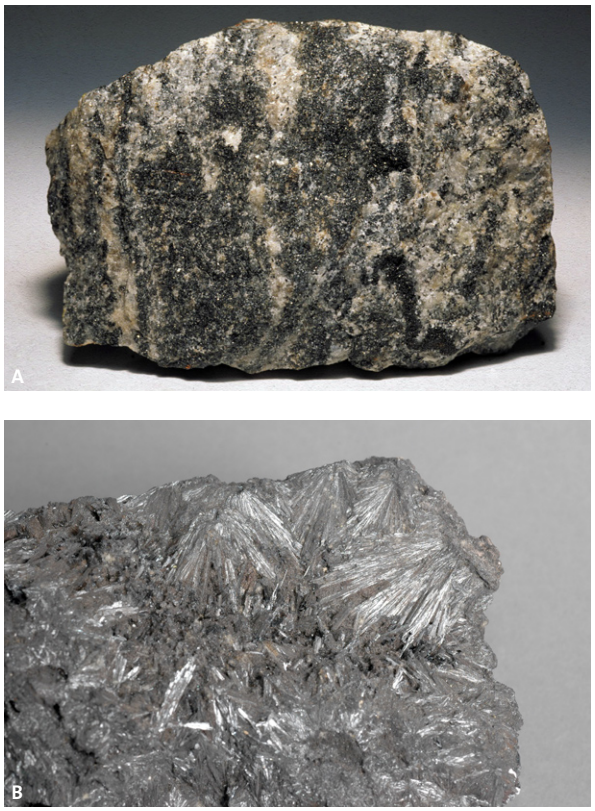

Fig. 110. Manganese oxide deposits. **A.** Slightly banded dolomitic marble impregnated by hausmannite ($Mn^{+2}Mn^{+3}{}_2O_4$) at the Långban deposit. The specimen is 12x8 cm in size. Photograph: Erik Jonsson (SGU), sample NRM31128, copyright Naturhistoriska riksmuseet. **B.** Manganite (MnO(OH)) from the Bölet deposit. The specimen is 8 cm wide in a horizontal direction. Photograph: Torbjörn Bergman (SGU).

- Contact metasomatic tungsten skarn deposits with scheelite.
- Tungsten deposits in quartz veins with wolframite and scheelite.

The tungsten skarn mineralizations are mainly located in the western part of Bergslagen and comprise approximately 20 deposits in the area between Kopparberg and Ludvika (Fig. 109). The majority of these deposits are minor occurrences or prospects and only a few have been mined, for example the *Yxsjöberg*, *Sandudden*, *Wigström (Högfors)* and *Elgfall deposits* (Ohlsson 1979). The most prominent occurrence is the *Yxsjöberg deposit*, with an estimated tonnage of 5 Mt containing 0.3–0.4% tungsten. It was mined until 1989 and was then the largest tungsten deposit in Scandinavia (Ohlsson 1979). The *Elgfall* and *Wigström* (Andersson 1986, Bergman 1994) *deposits* (both less than 0.2 Mt) were mined during two short periods (1970–1971 and 1978–1981, respectively) as satellite bodies to the *Yxsjöberg deposit*.

All known deposits are hosted by the Svecofennian, 1.91–1.89 Ga felsic metavolcanic rocks and crystalline carbonate rocks. The mineralizations are mostly concordant or subparallel to bedding in the supracrustal rocks. Crystalline carbonate rock is generally found as remnants in the skarn but is, in places, completely replaced by skarn. Scheelite, generally with a significant component of powellite, is the only economically important tungsten mineral (Ohlsson 1979). The skarn assemblages consist of grossularite-andradite garnet, hedenbergite-diopside pyroxene and hornblende (Fig. 111a). Scapolite, vesuvianite and wollastonite are important constituents in some deposits, for example at the *Wigström* and *Elgfall deposits* (Ohlsson 1979, Bergman 1994). Fluorite is common in many deposits and a strong positive correlation between fluorine and tungsten contents is noted in the *Yxsjöberg deposit* (Ohlsson 1979), where fluorite was extracted as a by-product.

Molybdenite is a common feature in the tungsten skarn deposits and, in many places, for example in the *Hörken deposit* (Hübner 1971), scheelite and molybdenite occur in approximately equal proportions. Some of these deposits have been registered as molybdenum deposits on the mineral resources map (Stephens et al. 2007c). In general, other sulphide minerals are only present in subordinate amounts. An exception is the *Yxsjöberg deposit*, where significant amounts of pyrrhotite and chalcopyrite are present. Indeed, this mine opened its production as a copper mine. In the *Wigström deposit*, sphalerite is common together with pyrrhotite and molybdenite (Bergman 1994). Minor amounts of gold have been noted in some tungsten skarn deposits.

Several authors have suggested that the tungsten skarn deposits formed from hydrothermal fluids generated in connection with the intrusion of igneous rocks, implying a contact metasomatic origin (Lindroth 1922, Hellingwerf & Baker 1985, Romer & Öhlander 1994, Bergman et al. 1995, Sundblad et al. 1996). In general, the GP granites (see section "Character, spatial distribution, geochronology, geochemical signature, petrophysical characteristics and regional geophysical signature of rock units") have been proposed as responsible for the formation of these deposits (e.g. the minor, so-called *Pingstaberg granite* in the western part of Bergslagen). By contrast, Hellingwerf & Baker (1985) and Hellingwerf et al. (1987) proposed a genetic link to the GDG intrusive rocks (see same section as that referred to above). Furthermore, Plimer (1980) suggested an exhalative-sedimentary origin for the W-Mo mineralizations. However, well-constrained age data on titanite from skarn at the *Yxsjöberg deposit* (Romer & Öhlander 1994) and Re-Os age determinations on molybdenite from the *Wigström deposit* (Sundblad et al. 1996) show that at least these deposits are related to the granites in the GP intrusive suite.

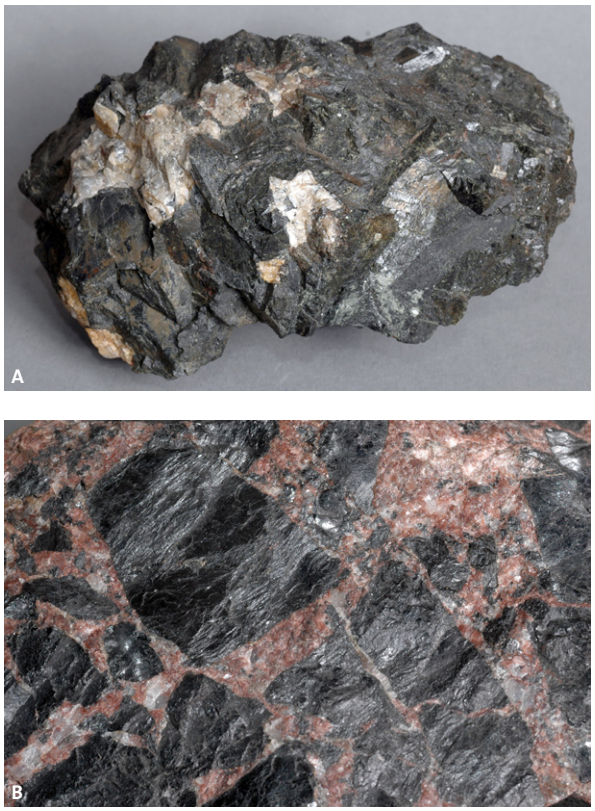

Fig. 111. Tungsten oxide deposits. **A.** Pyroxene-hornblende-scheelite skarn from the Yxsjöberg tungsten skarn deposit. The specimen is 10 cm wide in a horizontal direction. **B.** Wolframite breccia from the tungsten deposit hosted by quartz veins at Baggetorp. The photograph is 10 cm wide in a horizontal direction. Photographs Torbjörn Bergman (SGU).

Tungsten deposits hosted by quartz veins are rare in Bergslagen and most are minor occurrences, for example the *Tyfors deposit* (Ohlsson 1979). The only occurrence that has been mined is the *Baggetorp deposit* (Fig. 111b) in the southern part of the Bergslagen region (Hübner 1971, Gavelin 1985). This mineralization was discovered in 1940 and mined between 1944 and 1958. It is hosted by quartz veins that cross-cut older anatectic veining in a migmatitic gneiss (Gavelin 1985). The main ore minerals are wolframite and scheelite, and wolframite is replaced and locally rimmed by scheelite. Molybdenite as well as pyrite, chalcopyrite and bismuth minerals are also present (Gavelin 1985). It has been suggested that the *Baggetorp deposit* is genetically related to shear zones that formed prior to the intrusion of the 1.81–1.78 Ga suite of GSDG rocks (Gavelin 1985).

Base metal, iron and other sulphide deposits

The current compilation comprises more than 1 000 mineral deposits characterized as sulphide deposits. They are, with some exceptions, iron and base metal sulphide deposits, hosted by the Svecofennian (1.91–1.89 Ga), mainly felsic metavolcanic rocks and intercalated crystalline carbonate rocks (Fig. 112).

Zn-Pb-Ag-(Fe-Cu-Co-Au) sulphide deposits

The base metal sulphide deposits in Bergslagen (Fig. 112) have traditionally been divided into two types on the basis of their character of occurrence, metal content and host rock. No distinction has been made between these two types on the mineral resources map (Stephens et al. 2007c) and in Figure 112. Furthermore, all base metal sulphide deposits are shown with the same symbol, independent of host rock, type of alteration or minor variations in zinc, lead and copper content.

Stratiform, sheet-like, Zn-Pb-Ag-rich and Fe-Cu-poor deposits comprise the first type and include, for example, the operating mine at the *Zinkgruvan deposit* (Hedström et al. 1989 and Fig. 113a). They have been referred to as the *Åmmeberg-type* (Geijer 1917, Magnusson 1953) and as "stratiform ash-siltstone-hosted Zn-Pb-Ag sulphide deposits (*SAS-type*)" (Allen et al. 1996). In general, they are hosted by rhyolitic ash-siltstone metavolcanic rocks in the Svecofennian volcanic and subvolcanic intrusive suite (1.91–1.89 Ga). Crystalline carbonate rock, calc-silicate rock (skarn) and siliceous chemical sediment beds are also present. The footwall lithologies generally show conspicuous potassium and silicon alteration, and subordinate "magnesium alteration" (Henriques 1964, Hedström et al. 1989).

Irregular, multi-lens and podiform, stratabound, massive and disseminated Zn-Pb-Ag-Cu deposits (Fig. 113b) comprise the second type and include, for example, the *Sala deposit* and the operating mine at the *Garpenberg deposit* (Allen et al. 2003), as well as more massive, pyritic Cu-Zn-Pb-Ag-Au ores, for example at the *Falun deposit* (Koark 1962 and Fig. 113b). This type of deposit was referred to as the *Falun-type* by Geijer (1917) and as "stratabound, volcanic-associated, limestone-skarn Zn-Pb-Ag-(Cu-Au) sulphide deposits (*SVALS-type*)" by Allen et al. (1996). The deposits in this group are generally hosted by felsic metavolcanic rocks interbedded with crystalline carbonate rock (1.91–1.89 Ga) and are closely associated with magnesium-rich calc-silicate rock (skarn) and intense footwall magnesium±iron alteration.

The sizes of the base metal sulphide deposits in Bergslagen are relatively small and estimated tonnages based on production figures or exploration drilling are generally less than 1 Mt. Exceptions are the *Falun* (28 Mt), *Zinkgruvan* (43 Mt), *Garpenberg Odalfält* (16 Mt), *Garpenberg Norra* (17 Mt), *Sala* (2 Mt) and

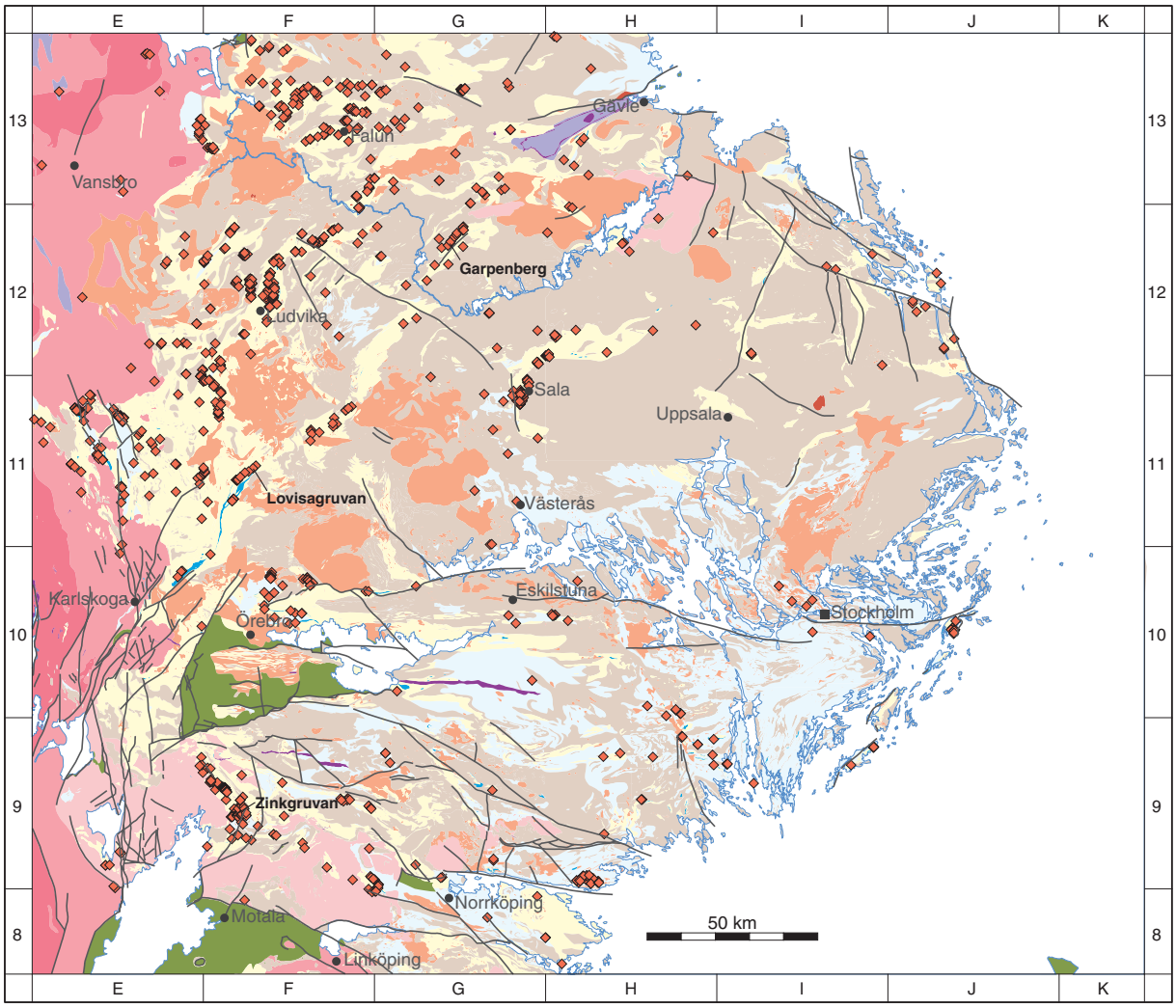

◆ Base metal sulphide deposit

Fig. 112. Distribution of base metal sulphide deposits in the Bergslagen region. The deposits are presented on a simplified bedrock geological map of the region. See Figure 101 for legend to the base geological map. The three mines that are currently in production, i.e. the *Garpenberg*, *Zinkgruvan* and *Lovisagruvan deposits*, belong to the base metal sulphide group and are identified on the map.

Saxberget (6 Mt) *deposits*. The figures for the operating mines have been updated compared with those presented in the table on the mineral resources map (Stephens et al. 2007c). A typical feature of the base metal sulphide deposits in Bergslagen is a relatively high content of zinc. The base metal contents are on average 4.5% zinc, 2.5% lead and 0.5% copper (Frietsch 1986). Ore minerals are pyrite, pyrrhotite, sphalerite, variably argentiferous galena and chalcopyrite.

Silver has varied in significance in most of the base metal deposits in Bergslagen, from a major commodity to an important by-product. Silver contents generally vary between 30 ppm and c. 1 500 ppm. Historically, the most important silver producers in Bergslagen have been the *Falun*, *Sala*, *Hällefors* (c. 1 500 ppm), *Guldsmedshyttan*, *Kaveltorp* and *Lövåsen deposits* (SGU 1999).

Gold has never been an important commodity in any of the base metal deposits in Bergslagen. However, at, for example, the *Falun*, *Garpenberg* and *Saxberget* deposits, it has formed a significant by-product. Gold contents are generally less than 1 ppm, which is comparable to the contents of this metal in base metal sulphide deposits around the world. However, higher grades of gold (2–3 ppm, Geijer 1917) occur in quartz veins (Fig. 114) that are spatially associated with the base metal sulphide ore at the *Falun deposit* (Nordenström 1882, Gavelin 1989, Åberg & Fallick 1993). Otherwise, gold-bearing quartz veins have only been reported from a few localities in Bergslagen and all are minor prospects (Hammergren et al. 1987). The presence of gold in different types of mineral deposits in Bergslagen has been described in Gaál &

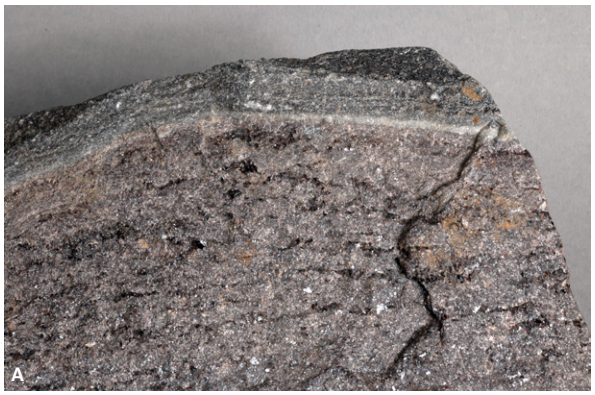

Fig. 113. Two types of base metal sulphide deposits in the Bergslagen region. **A.** Layered sphalerite-dominated *SAS-type* ore (Allen et al. 1996) from the Zinkgruvan deposit. The photograph is 12 cm wide in a horizontal direction. **B.** Semi-massive, chalcopyrite-pyrite *SVALS-type* ore (Allen et al. 1996) from the Falun deposit. The specimen is 13 cm wide in a horizontal direction. Photographs Torbjörn Bergman (SGU).

Fig. 114. Native gold in quartz vein from the Falun base metal sulphide deposit. The specimen was collected by A.E. Törnebohm in 1898 and is archived at SGU. The photograph is 6 cm wide in a horizontal direction. Photograph: Torbjörn Bergman (SGU).

Sundblad (1990), Bergman & Sundblad (1990) and Ripa (2001).

Cobalt is locally present and has been extracted as an economic by-product in some copper-rich base metal sulphide deposits in Bergslagen. These deposits are also hosted by crystalline carbonate rock (marble) and felsic metavolcanic rock, for example the *Tunaberg* (Johansson 1919) and *Vena deposits* in southern Bergslagen.

A variety of models have been presented for the origin of base metal sulphide deposits in the Bergslagen region that span different modes of thinking over more than 100 years. Törnebohm (1893) suggested that the sulphide deposits in the Bergslagen region were syngenetic or slightly epigenetic in character and that the sulphides had precipitated from "hot springs" related to diorites included here in the suite of intrusive rocks referred to as GDG (see section "Character, spatial distribution, geochronology, geochemical signature, petrophysical characteristics and regional geophysical signature of rock units"). Based mainly on detailed studies of the *Falun deposit* and influenced by Eskola (1914), Geijer (1917) argued that the sulphide deposits in Bergslagen, which are spatially associated with "magnesium alteration", were related to ore-forming fluids from granites also included here in the GDG intrusive suite. By contrast, Tegengren et al. (1924) suggested that the anomalous compositions of the volcanic rocks in the Bergslagen region, i.e. the sodium-, potassium- and magnesium-rich varieties, together with the ores, were related to primary magmatic differentiation. Oen et al. (1982), Baker (1985) and Hellingwerf (1986) emphasized a genetic link between hydrothermal alteration, mineralization, subvolcanic intrusive rocks and a rift tectonic setting.

In generally more recent literature, the base metal sulphide deposits are considered to be either synvolcanic, seafloor exhalative (Koark 1962, Vivallo & Rickard 1990, Allen et al. 1996) or synvolcanic, sub-seafloor replacement (Allen et al. 1996, 2003) deposits. According to Allen et al. (1996), both mechanisms of ore formation are relevant for base metal sulphide deposits in the region and are applicable to the deposits identified as *SAS-type* and *SVALS-type*, respectively. More detailed summaries concerning the origin of the mineralization at the operating mines at the *Garpenberg*, *Zinkgruvan* and *Lovisagruvan deposits* are provided below.

Molybdenum sulphide deposits

Molybdenum sulphide deposits in Bergslagen (Fig. 115), which can be classified as *climax-type* deposits, are all minor (<0.1 Mt) and have never had any significant economic importance. Nevertheless, most of these deposits were mined during the 2nd world war. No mining has been carried out after this period. The mineralizations are generally hosted by the granites and pegmatites that belong to the GP suite of intrusive rocks and include, for

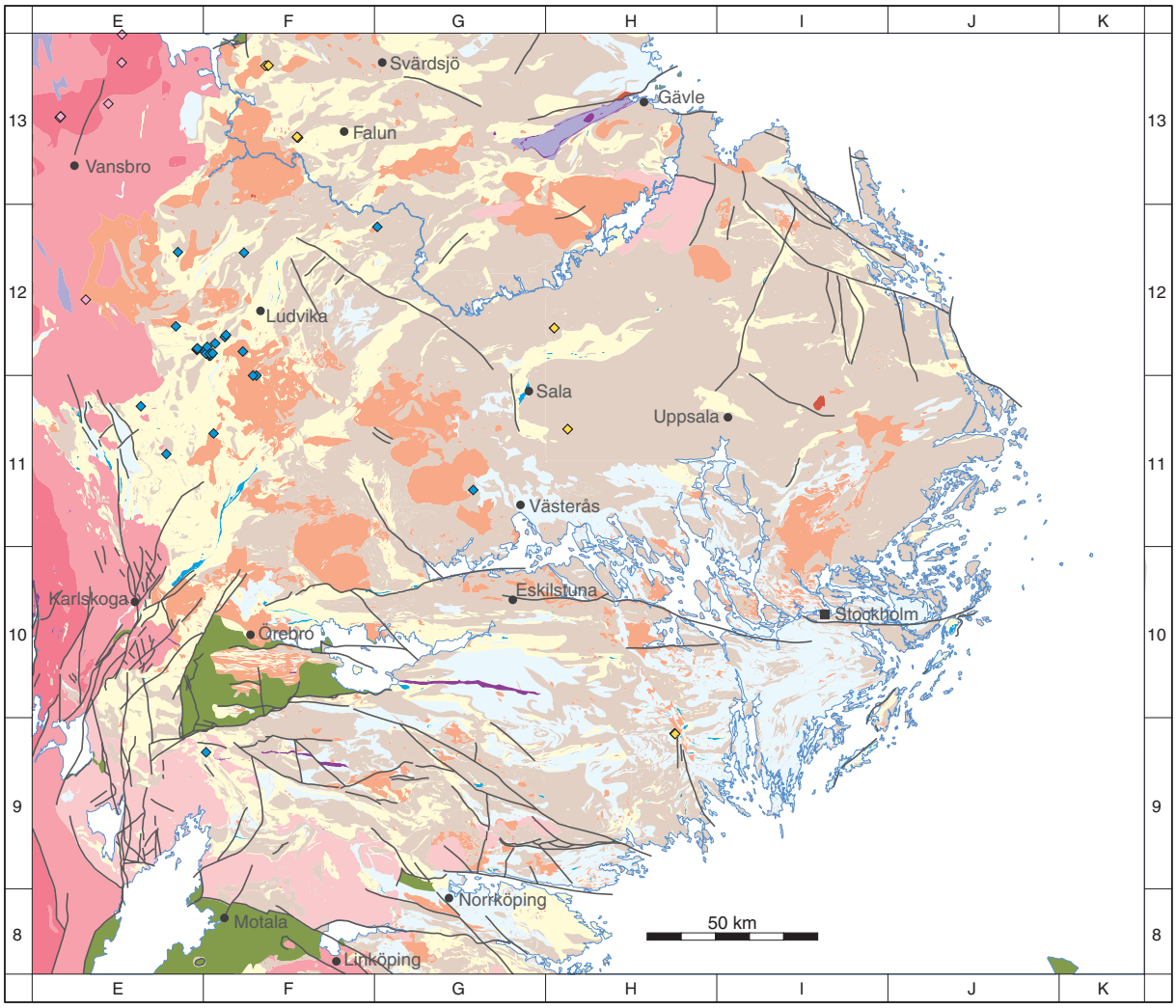

Fig. 115. Distribution of subordinate mineral deposits (molybdenum sulphide, Ni-Cu sulphide and greisen deposits) in the Bergslagen region. The deposits are presented on a simplified bedrock geological map of the region. See Figure 101 for legend to the base geological map. The location of place names referred to in the sections that address these types of deposit is also shown.

example the *Bispbergsklack* (Fig. 116), *Pingstaberg* and *Uddgruvan deposits*. The total production from Swedish deposits is c. 0.2 Mt of MoS_2, of which more than 50% originates from the *Uddgruvan deposit* that is a quartz-rich, pegmatite deposit (Hübner 1971). Molybdenum locally occurs as a minor constituent in base metal, iron oxide and tungsten deposits (see previous text).

Ni-Cu sulphide deposits and PGE deposits

Nickel is locally present as an economically significant component in some copper-rich, base metal sulphide deposits that are hosted by gabbro (Fig. 115). The largest deposits in Sweden are the *Slättberg* and *Kuså deposits* in the northern part of the Bergslagen region (Löfstrand 1903, Grip 1961). Other deposits of this type are the

Fig. 116. Molybdenite from the Bispbergsklack deposit in granite belonging to the GP suite of intrusive rocks. The specimen is 7 cm wide in a horizontal direction. Photograph: Torbjörn Bergman (SGU).

Frustuna deposit in southern Bergslagen and the *Ekedal* and *Gaddbo deposits* in the central part of the region.

Platinum group elements (PGE) have never been mined in Bergslagen, and only one prospect, the *Flinten deposit* in the Svärdsjö area in the northern part of the region, is present. This deposit is hosted by a layered gabbro (Filén 2001), within which sulphide-bearing parts with anomalous amounts of PGE and gold occur. Analysed samples contain up to 0.2 ppm palladium, 0.13 ppm platinum and 1.8 ppm gold (Filén 2001).

Greisen Sn (±Zn-Pb-Cu-Mo-W-Ag-Au-Be) deposits with oxides and sulphides

Greisen-type vein deposits hosted by the 1.70–1.67 Ga suite of GSDG intrusive rocks (see section "Character, spatial distribution, geochronology, geochemical signature, petrophysical characteristics and regional geophysical signature of rock units") occur in the northwesternmost part of the Bergslagen region (Fig. 115). They are economically insignificant and have never been mined. However, two occurrences have been in focus for exploration activity, the *Van* and *Stora Flaten deposits* (Ohlsson 1980, Bromley-Challenor 1984). The *greisen-type* vein deposits are centimetre to metre thick, dark alteration zones (Fig. 117) that are rich in quartz, mica (including Li-rich mica) and chlorite. They contain variable amounts of metal-bearing oxides and sulphides, including cassiterite, galena, sphalerite, chalcopyrite, arsenopyrite and pyrite. In general, fluorite and topaz are also present in small amounts as well as molybdenite, wolframite and scheelite (Ahl & Sundblad 1996).

Operating base metal sulphide mines

At the current time, there are operating mines that are extracting metallic minerals at three separate deposits in the Bergslagen region – the *Garpenberg*, *Zinkgruvan* and *Lovisagruvan* deposits. All these deposits are base metal sulphide deposits. In general, each deposit consists of more than one ore body. Short descriptions of these three deposits are provided in the following text.

Fig. 117. Greisen alteration zone at Stora Flaten in granite belonging to the 1.70–1.67 Ga GSDG suite of intrusive rocks. Photograph: Martin Ahl (SGU).

Garpenberg deposit

Prior to 2004, there were two operating mines at the *Garpenberg deposit* referred to as *Garpenberg Odalfält* and *Garpenberg Norra*. During 2004, these two mines were connected by underground workings 2.5 km in length at the 800–900 m sub-surface level. Although separate main frames remain, they can be regarded as one larger mine.

Mining history

The mine referred to as *Garpenberg Odalfält* is the oldest mine in Sweden that is still in operation. Chemical analyses of sediments from a lake at Garpenberg show a sudden and marked increase in heavy metal concentrations at a particular stratigraphic level. This anomaly was dated using the carbon isotope technique to the 8th or 9th century and interpreted to reflect the commencement of local metal extraction (Qvarfort 1981). According to Boliden AB, the company which presently owns and operates the mine at Garpenberg, and Tegengren et al. (1924), mining started in the 13th or 14th century. However, the oldest written documentation of operations is dated at 1486 AD (Tegengren et al. 1924). Through medieval times and during the 16th to 19th centuries, mining at Garpenberg focussed on copper and to some extent on lead and silver. Since the 20th century, zinc has been the main product.

In 1957, Boliden AB bought the *Garpenberg Odalfält* mine. Exploration in the immediate vicinity of this mine led to the opening of the *Garpenberg Norra* mine in 1972. Subsequently, a third occurrence referred to as the *Lappberget ore body* has come into production and two other occurrences, referred to as the *Kvarnberget* and *Dammsjön ore bodies*, are currently under evaluation. The metal production at the *Garpenberg deposit* during 2006 was c. 1.2 Mt of complex ore from which c. 5% zinc, 0.05% copper, 1.8% lead, 0.2 ppm gold and 0.01% silver was extracted (www.boliden.se). The proven reserves amount to 12.2 Mt with similar grades.

Geological setting and relationship to structural features

The Garpenberg area and base metal sulphide deposit are described in Christofferson et al. (1986). A bedrock geological map of the Garpenberg area is shown in Figure 118 and the detailed stratigraphy at *Garpen-*

berg Norra is described in Allen et al. (2003). Although primary rock terms are generally used in the text that follows, it needs to be kept in mind that the rocks described below have been affected by metamorphism under amphibolite-facies conditions.

The overall footwall lithology at *Garpenberg Norra*, which represents the regional ambient sedimentation, is massive or bedded rhyolitic ash-siltstone. It contains interlayers of coarser-grained volcaniclastic material, basaltic lava and rhyolitic to dacitic pumice breccia to sandstone. The footwall rocks are locally epidote skarn-altered in an irregular patchy manner or along certain horizons. Furthermore, beds of variably skarn-altered and dolomitized stromatolitic limestone are interlayered in the upper part of the footwall volcanic rocks. Although the mineralizations at Garpenberg are predominantly remobilized along secondary structures (see below), it is inferred that the contact zone to the uppermost carbonate bed initially hosted the mineralizations. The footwall volcanic rocks are variably silicified and altered to phlogopite-cordierite-bearing assemblages in their upper parts, i.e. "magnesium alteration", as described earlier in this report, is prevalent. The mineralized horizon is overlain by volcanic breccia to conglomerate and sandstone with rhyolitic to basaltic composition. Subvolcanic, mainly dacitic intrusions occur throughout the stratigraphy.

Allen et al. (2003) interpreted the supracrustal rocks at Garpenberg as a rhyolitic–dacitic caldera complex, where the footwall lithologies represent pre-caldera volcanism, the mineralized limestone a hiatus in the volcanic activity and the hanging wall succession caldera-

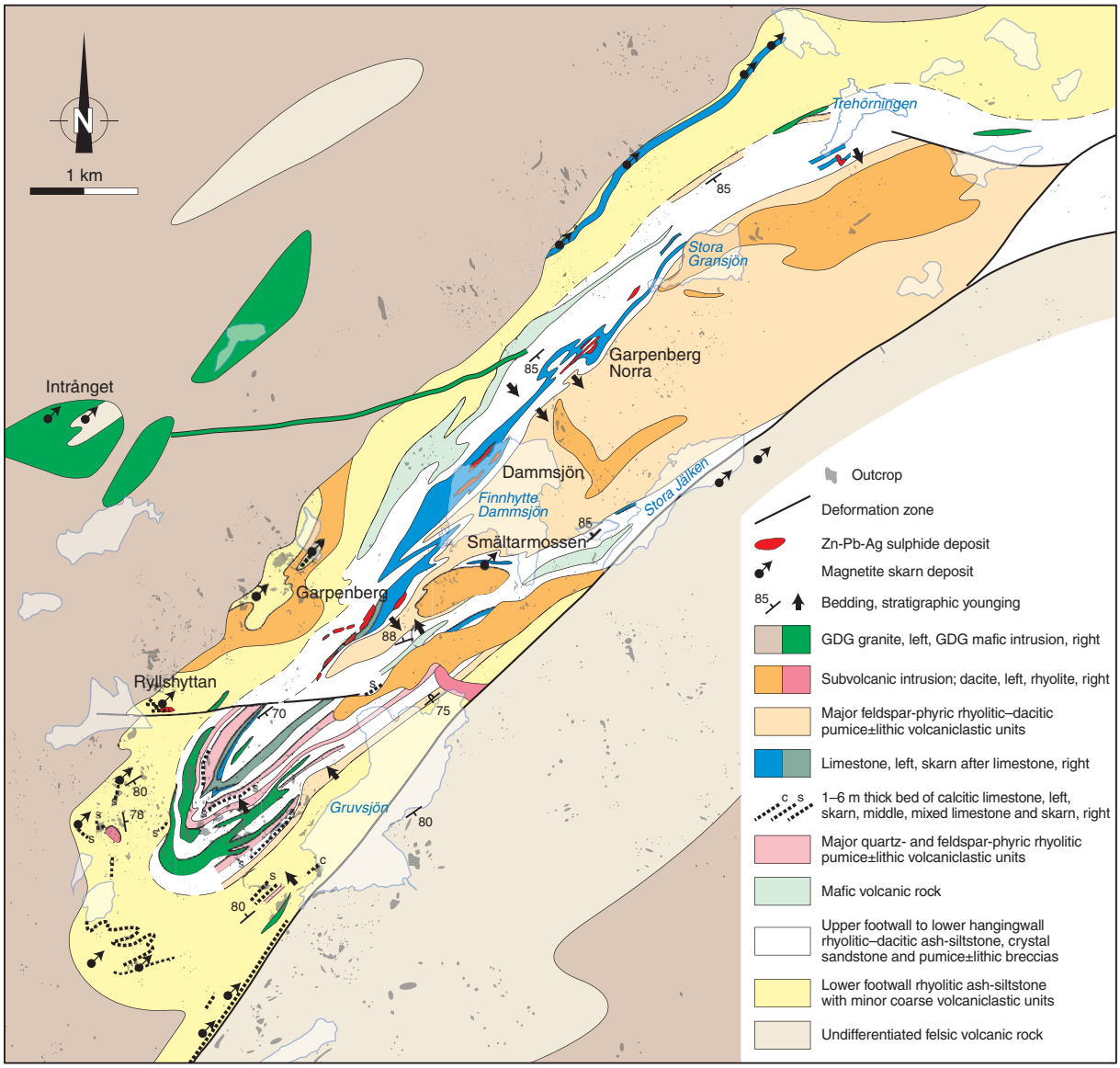

Fig. 118. Bedrock geological map of the Garpenberg area (modified after Allen et al. 2003). All rocks have been metamorphosed under amphibolite-facies conditions.

fill volcanism. A pyroclastic mass flow in the hanging wall has been dated at 1891±2 Ma (see appendix).

The rocks at Garpenberg occur on the north-western limb of a regional, second generation, synclinal fold structure. This structure trends north-east–south-west (Fig. 118) and displays a complex pattern of parasitic folds and later ductile shear zones and faults (Allen et al. 2003). The parasitic folds vary in plunge and form a series of arches and cones, separated by irregular synforms (see also folds in the northern structural domain described in the section "Deformation, metamorphism and mechanism of emplacement of the 1.87–1.84 Ga GSDG suite of intrusive rocks"). The structures have a fundamental influence on the present distribution of mineralizations. Economic ore bodies occur as: a) remobilized ore in veins along late shear zones in the footwall; b) skarn ore in limestone, especially around crests of parasitic anticlines, and even more so if these folds are intersected by shear zones; c) remobilized ore in veins and in crests of parasitic anticlines in the hanging wall; and d) impregnation ore in quartz-skarn rocks at the base of the main limestone unit (Allen et al. 2003).

Ore characteristics

The mineralizations at the *Garpenberg deposit* are of two main types:

- Fluorite-bearing chalcopyrite ore associated with silicified or mica-altered volcanic rocks.
- Sphalerite-argentiferous galena±chalcopyrite ore associated with skarn (Fig. 119), dolomitized limestone or silicified or mica-altered volcanic rocks (Magnusson 1973).

The mineralizations are only locally significantly pyrite- or pyrrhotite-bearing.

Genetic considerations

A classical volcanic massive sulphide (VMS) model for the *Garpenberg deposit* was presented by Vivallo (1985). He interpreted the copper-bearing mineralization at Garpenberg as related to sub-surface replacement and the mineralization dominated by zinc, lead and copper as exhalative chemical sediment deposited on a palaeo-seafloor. By contrast, Allen et al. (2003) argued that the mineralizations at the *Garpenberg deposit* formed through sub-seafloor stratabound replacement within the caldera structure described above. They envisaged that hot, metal-bearing solutions penetrated the volcanic succession, locally in a semi-conformable manner, and that the stromatolitic limestone acted as a barrier and chemically reactive trap which caused precipitation of metal sulphides and skarn formation.

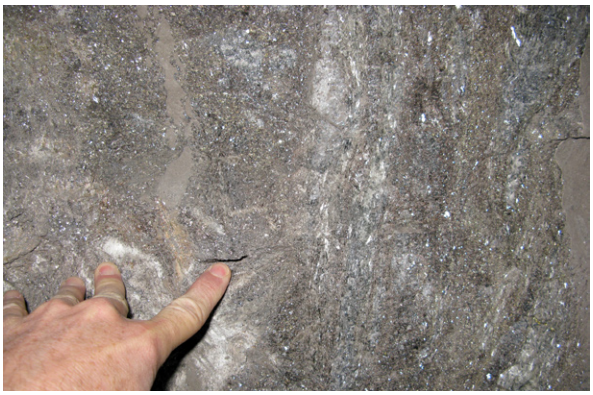

Fig. 119. Sphalerite-tremolite skarn from the Lappberget ore body at Garpenberg. Photograph: Rodney Allen (Boliden AB).

Allen et al. (2003) did not explain the origin of the solutions, but Allen et al. (1996) suggested a regional convective hydrothermal system with a possible magmatic fluid contribution from subvolcanic intrusions for the sulphide deposits in the Bergslagen region in general. Subsequently, the *Garpenberg deposit* and surrounding rocks were affected, to variable extent, by ductile deformation and amphibolite-facies metamorphism.

Zinkgruvan deposit

In older literature, the *Zinkgruvan deposit* is referred to as the *Åmmeberg deposit*, after which the *Åmmeberg-type* sulphide deposits in Bergslagen are named (Geijer 1917). The deposit occurs within the so-called *Åmmeberg ore field* (e.g. Tegengren et al. 1924).

Mining history

According to Tegengren et al. (1924), the presence of secondary zinc minerals (galmeja) in the *Åmmeberg ore field* was known and considered for its potential in the production of brass already in the 16th century. However, documentation of mining, initially of silver, dates back to the 18th century. In the first decades of the 19th century, mining focussed on silver, lead and copper, but changed to zinc in 1849 (Tegengren et al. 1924). In 1857, the *Zinkgruvan deposit* was bought by Vieille-Montagne (incorporated in Union Minière in 1993), and this company owned and operated the mine until 1995. Between 1995 and 2000, the mine was owned and operated by North Ltd., between 2000 and 2004 by Rio Tinto and since 2004 by the Lundin Mining Corporation.

At the current time, the primary metals in production are zinc, lead and silver. Production of copper is planned to start in 2010 (L. Malmström, personal communication 2007). The metal production at the *Zinkgruvan deposit* during 2006 was c. 0.8 Mt with

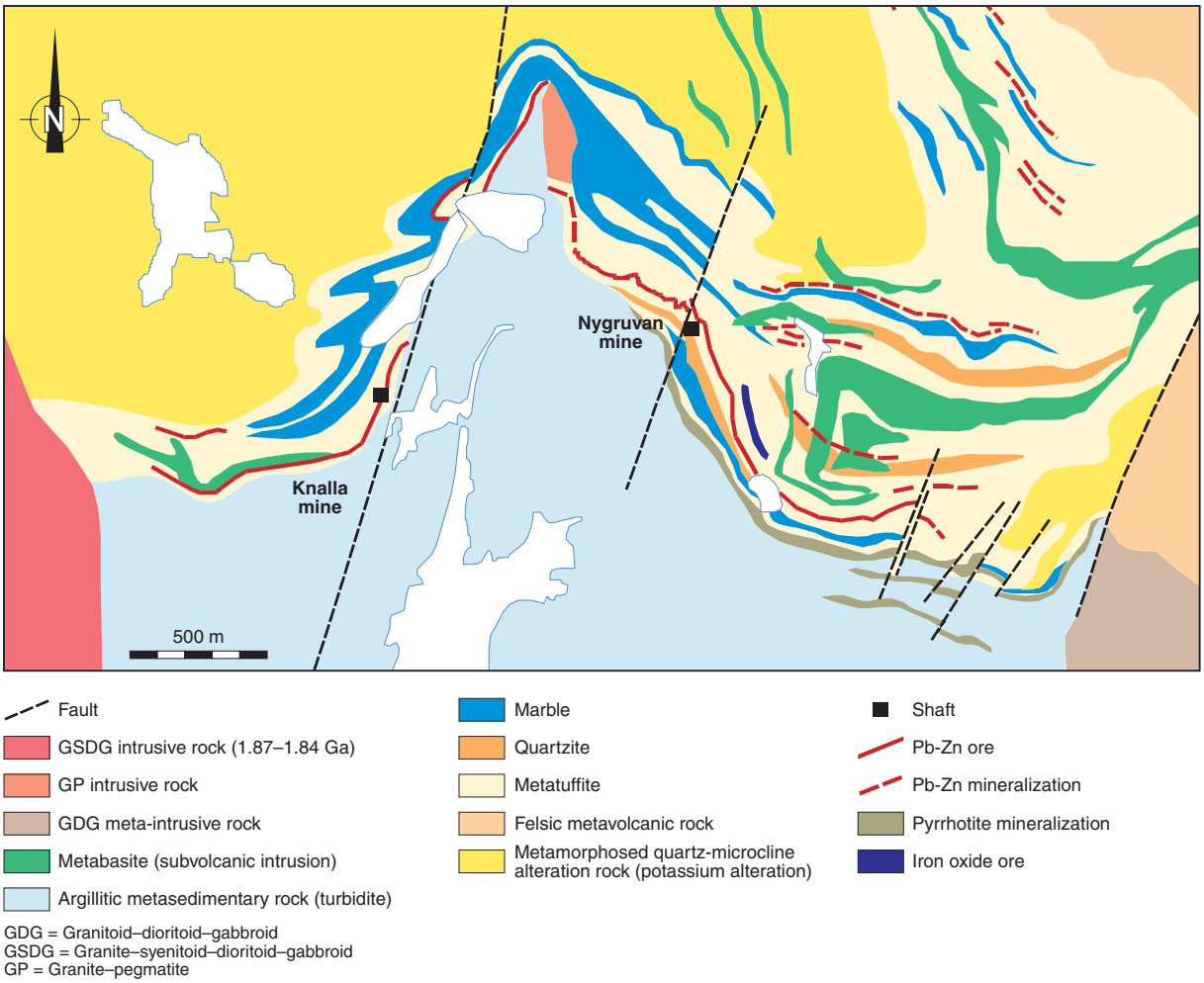

Fig. 120. Bedrock geological map of the Zinkgruvan area (L. Malmström, personal communication 2009).

a grade of 10.3% zinc, 4.6% lead and 93 ppm silver (www.lundinmining.com). Reserves are 8.6 Mt with a grade of 9.7% zinc, 4.9% lead and 100 ppm silver, whereas resources are 9.6 Mt with a grade of 10.4% zinc, 5.1% lead and 95 ppm silver as well as 3.7 Mt with 2.9% copper and 31 ppm gold (L. Malmström, personal communication 2007).

Geological setting

The Zinkgruvan area and base metal sulphide deposit are described in Hedström & Wikström (1986). A bedrock geological map of the Zinkgruvan area is shown in Figure 120. Hedström et al. (1989) and Kumpulainen et al. (1996) described the host rocks and a c. 10 km thick volcano-sedimentary succession, informally referred to as the *Emme group*, which forms the country rock to the *Zinkgruvan deposit*.

Kumpulainen et al. (1996) subdivided the stratigraphy in the *Emme group* into four parts. The lowermost part consists of felsic volcanic rocks and subvolcanic rhyolite intrusions dated at 1901±18 Ma. The lowermost volcanic rocks grade upwards into homogeneous and medium-grained arkoses derived from a continental source, which in turn are overlain once again by felsic volcanic rocks. The latter are locally strongly hydrothermally altered (mainly potassium alteration, Hedström et al. 1989) and form the host rock to the Zn-Pb-Ag ore bodies at the *Zinkgruvan deposit*. The host volcanic rocks contain intercalations of carbonate rock that host the copper-rich mineralizations at the *Zinkgruvan deposit* and were intruded by mafic subvolcanic rocks. The uppermost part of the *Emme group* consists of sandy to muddy turbidites. All the rocks described above have been affected by upper amphibolite-facies metamorphism and the inferred turbidites occur as migmatitic paragneisses, whereas the underlying rocks are relatively better-preserved sillimanite-bearing gneisses. The carbonate rocks occur as marble.

The *Zinkgruvan deposit,* with an overall east–west strike, is divided into two segments by a fault that strikes north-north-east–south-south-west. On the western side of this fault, overturned, isoclinally folded and

north-dipping rock units strike east–west and north-east–south-west, whereas on the eastern side the units strike north-west–south-east and east–west (Fig. 120).

Ore characteristics

According to Hedström et al. (1989), the stratiform, tabular-shaped, massive Zn-Pb-Ag ore bodies at the *Zinkgruvan deposit* form one or two (mainly in the eastern part) subparallel, 5 to 25 m thick layers, which extend along strike for c. 5 km, dip to the north and extend at least 1 300 m at depth. The dip varies along strike from 0 to 80° in the western part and from 60 to 80° in the eastern part. Sphalerite and galena occur with minor amounts of calc-silicates. In the western part of the deposit, the Zn-Pb-Ag ores are underlain by a stockwork-style copper mineralization of chalcopyrite, pyrrhotite and sphalerite as veins and disseminations in crystalline carbonate rock.

Genetic considerations

The first genetical view of the *Zinkgruvan deposit* was presented by Johansson (1910) who favoured a syngenetic origin. This idea was challenged by Magnusson (1950) who maintained that the ores were deposited from fluids that formed in association with the regional metamorphic event which caused migmatization of, for example, the overlying turbidites. Henriques (1964) and Hedström et al. (1989) again suggested a syngenetic origin for the ores and interpreted them to be distal exhalative in character. On the basis of a lead isotope study, Sundblad (1994) showed that the ore-forming fluids at the *Zinkgruvan deposit* had a different source than those at, for example, the *Falun deposit*. The composition of the ore lead at the *Zinkgruvan deposit* indicates an input from a primitive, tholeiitic basalt source in contrast to the calc-alkaline felsic volcanic source rock at the *Falun deposit*.

Lovisagruvan deposit

Mining history and ore characteristics

The *Lovisagruvan deposit* was discovered in 1985 by a joint venture between LKAB and BP Minerals Ltd in connection with exploration around the nearby *Håkansboda deposit* (Cu-Co-As-Bi-Au). However, these companies considered that the deposit was too small for economic mining. During 1989, ownership of the deposit was taken over by John Berge and the deposit was mined during the 1990's but only intermittently due to the low prices for zinc. Since 2004, the deposit has been owned and operated by Lovisagruvan AB. Compared with the *Garpenberg* and *Zinkgruvan deposit*s, the mining of the *Lovisagruvan deposit* is an example of small-scale enterprise using innovative mining techniques.

The *Lovisagruvan deposit* mainly consists of a steeply dipping tabular body of massive sphalerite and galena. The ore horizon is thin, only 0.8 m, but very rich, with 22% zinc, 14% lead and "some" silver (www.lovisagruvan.se). The deposit has been investigated by drilling down to 300 m beneath the ground surface. Initially, the size of the ore body was estimated to 400 000 tonnes; later work has confirmed a further c. 40 000 tonnes. During 2006, c. 17 000 tonnes of ore with a grade of c. 11% zinc and 8% lead were produced and transported to Garpenberg for concentration (www.lovisagruvan.se). The company goal is to produce c. 40 000 tonnes of ore at comparable grades per year. In order to mine the narrow ore body, c. 100% wall rock must be excavated along with the ore and this accounts for the significantly lower production grades mentioned above.

Geological setting

The *Lovisagruvan deposit* is situated in the Guldsmedshyttan area in the central part of the Bergslagen region (Fig. 121). No detailed geological data from the deposit are available. Modern work that describes the geology of the Guldsmedshyttan area is presented in Lundström (1983), Carlon & Bleeker (1988) and Carlon & Bjurstedt (1990). The following description is compiled from these publications.

The lower part of the stratigraphy in the *Guldsmedshyttan syncline* (see, for example, Plate 1 in Geijer & Magnusson 1944 and Fig. 121) consists of massive, plagioclase- and quartz-phyric, fine-grained meta-igneous rocks of the *Storsjön formation* (Lundström 1983). Most of the rocks in this formation were subsequently interpreted as subvolcanic intrusions (Lundström 1995). The upper part of the stratigraphy consists of bedded, felsic metavolcanic rocks of the *Usken formation* (Lundström 1983). These rocks are locally affected by "magnesium alteration" and contain interbeds of variably skarn-altered and mineralized crystalline carbonate rock. The *Lovisagruvan deposit* occurs in the upper part of the stratigraphy (Fig. 121).

The *Guldsmedshyttan syncline* (Fig. 121) is steeply inclined, doubly plunging and isoclinal with an axial surface trace that strikes north-east–south-west and a sense of vergence (overturning) to the north-west (Lundström 1983). It was inferred (Lundström 1983) to be a first generation fold structure (cf. text in section below entitled "Deformation, metamorphism and mechanism of emplacement of the 1.87–1.84 Ga GSDG suite of intrusive rocks"). The structures related to this deformation phase were refolded and reoriented

during a later phase of folding with subvertical axial surfaces that strike north-west–south-east (Fig. 121). The bedrock at Guldsmedshyttan contains abundant cordierite and sillimanite, and the rocks are inferred to have been affected by amphibolite-facies metamorphism (Carlon & Bleeker 1988).

Genetic considerations

Since no modern work has directly addressed the *Lovisagruvan deposit*, information bearing on the origin of this deposit is lacking. Nevertheless, Carlon & Bjurstedt (1990) maintained that some mineralizations, including the *Lovisagruvan deposit*, in the *Guldsmeds-*

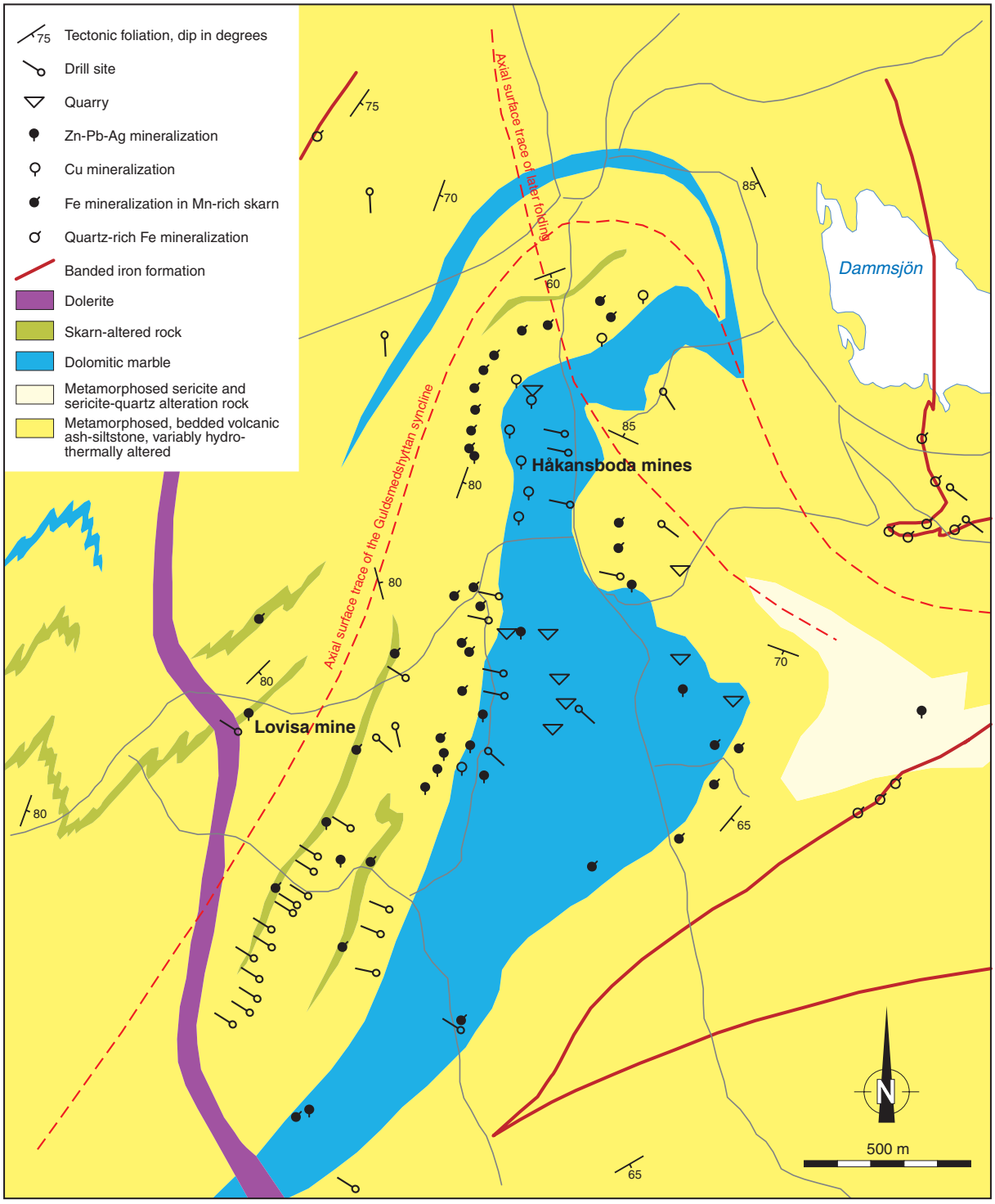

Fig. 121. Bedrock geological map of the Guldsmedshyttan area (modified after Carlon & Bjurstedt 1990).

hyttan syncline are stratabound and stratiform exhalites. The mineralizations were described as displaying a spectrum of syngenetic to epigenetic phenomena, from fine-grained, thinly banded, laminated stratiform sulphides, to strongly deformed laminae with interference structures between different generations of foliation, remobilized stratabound veinlets, piercement structures, breccia pockets and clastic ball-ores (Carlon & Bjurstedt 1990).

NON-METALLIC MINERAL DEPOSITS

In comparison with the metallic mineral deposits in Berslagen, the non-metallic equivalents have been and remain of considerably less economic significance over historical time. Non-metallic mineral deposits are dominated by the occurrence of economically important minerals, particularly feldspar in more than 100 pegmatite deposits (Fig. 122), as well as a few minor deposits or exploration prospects that contain graphite or wollastonite (Fig. 122). Fluorite and talc also occur.

Minerals in pegmatite

Quartz-feldspar-mica deposits in pegmatite are mainly located in the Stockholm archipelago and in the central part of Bergslagen (Sundius 1952, Fig. 122). The largest deposits are the *Forshammar* and *Kolsva deposits* in the central part of the Bergslagen region that have been exploited for their feldspar content. The *Forshammar deposit* (Fig. 122) is still in production and is the major producer of feldspar concentrate in Sweden.

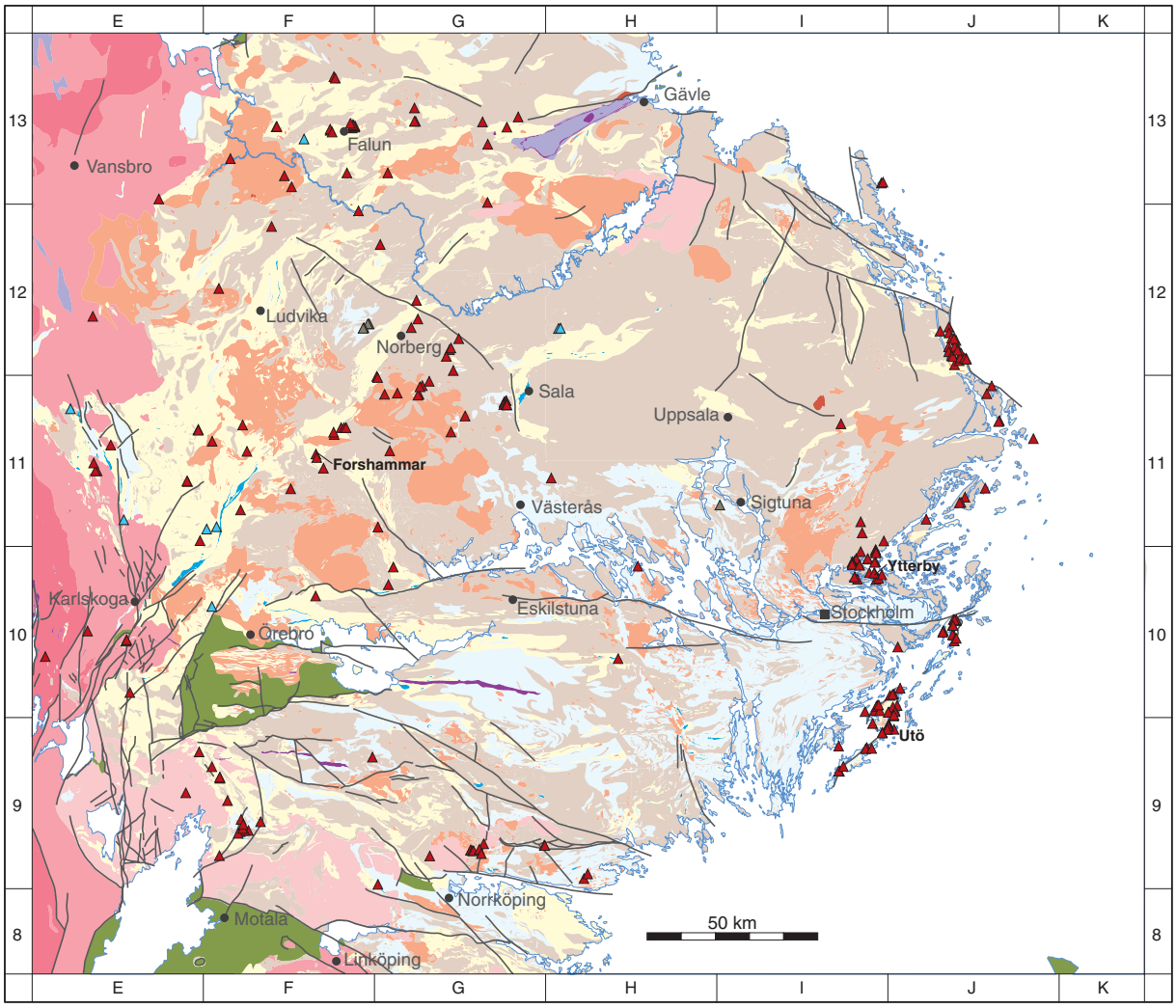

Fig. 122. Distribution of non-metallic mineral deposits in the Bergslagen region. These deposits include various minerals in pegmatite, graphite and wollastonite. The deposits are presented on a simplified bedrock geological map of the region. See Figure 101 for legend to the base geological map. The location of place names referred to in the section entitled "Non-metallic mineral deposits" is also shown.

Most of the deposits in the Stockholm archipelago were mined during the late 19th to middle 20th centuries (Stålhös 1969).

Rare earth element (REE)-bearing minerals locally occur in some pegmatites, for example at Ytterby 20 km north-east of Stockholm (Fig. 122). Beryl is also locally present but has never been of any economic significance. Lithium-bearing pegmatites occur in one of the iron oxide mineral deposits on the island of Utö in the Stockholm archipelago (Fig. 122, *Nyköpingsgruvan*). These pegmatites cross-cut the iron oxide mineralization at this deposit but have never been mined. Lithium occurs in spodumene, lepidolite and petalite (Sundius 1952, Smeds & Cerny 1989). The metal lithium was extracted for the first time in 1817 from a sample of spodumene from Utö (Holmquist 1904).

Graphite

Graphite has been mined at a few localities in Bergslagen (Fig. 122). It is generally hosted by paragneiss and pegmatitic rocks, for example at the *Skälsta deposit*, west of Sigtuna, and in the *Skrammelfall* and *Gilltjärn deposits*, west of Norberg. The *Skälsta deposit* was mined during 1935 to 1942 (Lundegårdh 1971) and the *Skrammelfall* and *Gilltjärn deposits* were mined intermittently from the beginning of the 19th century up to 1920.

Wollastonite

Wollastonite has never been exploited in the Bergslagen region. However, significant exploration prospects are present at the *Banmossen deposit,* 20 km north-north-east of Sala, and at the *Frösvidal deposit*, c. 14 km north-west of Örebro (Fig. 122).

BEDROCK DEPOSITS

The present description of bedrock deposits is restricted to crystalline carbonate rock (marble), limestone and alum shale deposits. Other dimension stone and aggregate deposits are not included in the current compilation. However, many of these deposits are present in the SGU mineral and bedrock resource database (BERGDB_MDEP).

Crystalline carbonate rock (calcite marble, dolomite marble) and limestone

Deposits of crystalline carbonate rock occur throughout Bergslagen (Fig. 123) and both dolomite-rich and calcite-rich varieties have been quarried. More than 400 deposits are included in the SGU mineral and bedrock resource database (BERGDB_MDEP). However, most of these deposits are abandoned at the current time. Some of them were quarried for greenish-coloured, skarn-altered crystalline carbonate rock. The largest and most well-known occurrences are the *Brännlyckan* and *Kolmården deposits* in the southern part of the Bergslagen region, where crystalline carbonate rock was quarried for dimension stone and frequently used as floor tiles and facings on buildings. However, most deposits were quarried for agricultural purposes and as the raw material for Portland cement and concrete.

Resources of limestone are geographically restricted to the occurrences of Ordovician limestone in the Lower Palaeozoic cover sedimentary rocks in the central and south-western parts of Bergslagen (Fig. 123). The largest occurrences are the *Kvarntorp* and *Hynneberg deposits*.

Alum shale

Cambrian to Lower Ordovician black shale has been quarried at a few places in the central and south-western parts of Bergslagen (Fig. 123) for use as a source of fuel in the production of cement as well as a source of oil and alum. For this reason, the stratigraphic unit in the Lower Palaeozoic succession is generally referred to as the *Alum Shale Formation*. Locally, the Cambrian to Lower Ordovician alum shale also shows high contents of uranium and vanadium (Andersson et al. 1985). The largest occurrence is the *Kvarntorp deposit*, situated 5 km south-east of Kumla. It was quarried from 1940 to 1967 with a total extraction of 50 Mt of alum shale (Lundegårdh 1971). The second largest occurrence is the *Hynneberg deposit (Yxhult),* situated further east in the same area. Other occurrences include the *Latorp deposit*, west of Örebro, and the *Knivinge* and *Pålstorp deposits*, north-west of Linköping.

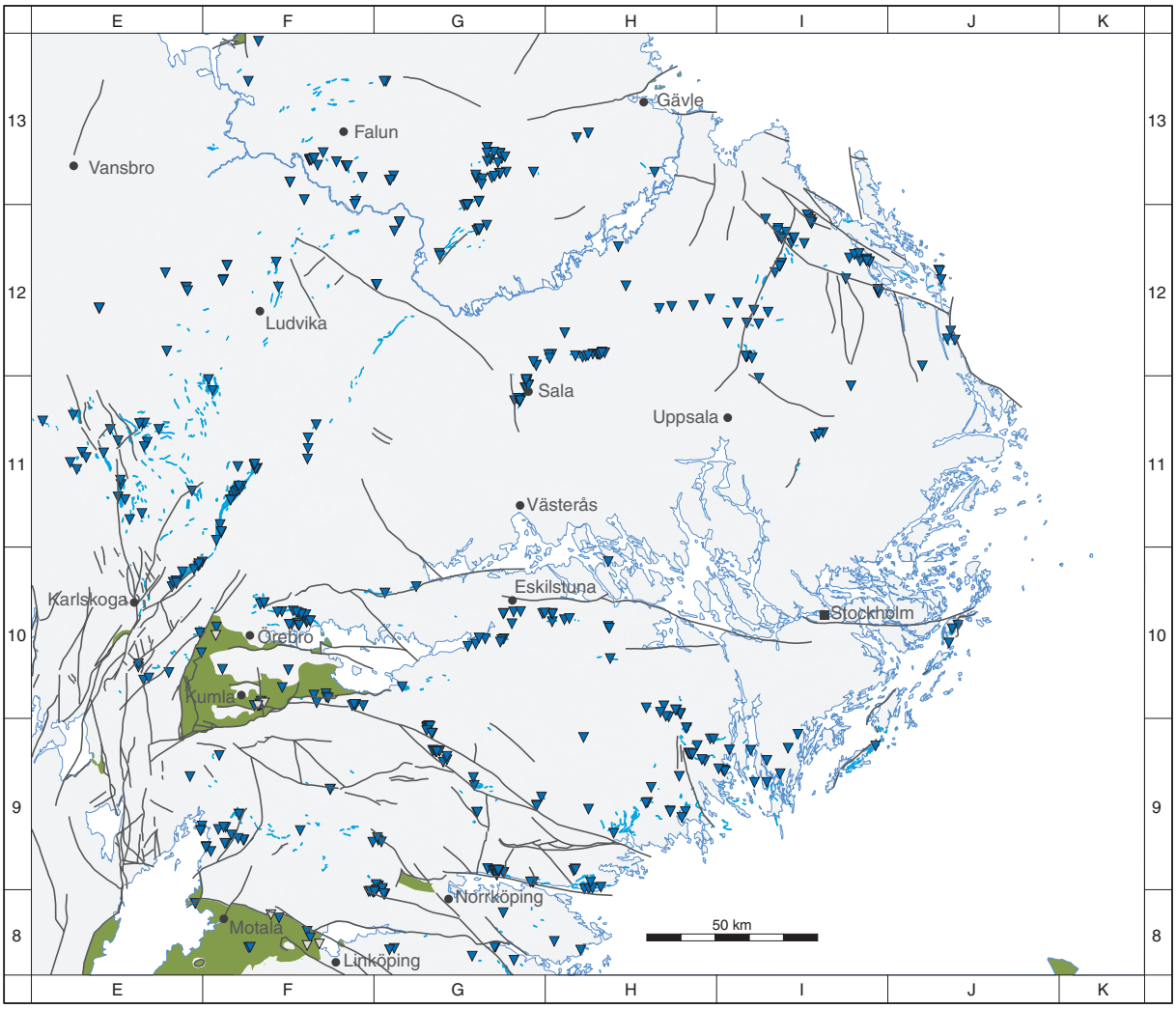

Crystalline carbonate rock (calcite marble, dolomite marble), limestone

Alum shale

Neoproterozoic and Lower Palaeozoic sedimentary rocks

Crystalline carbonate rock (calcite marble, dolomite marble), in part with stromatolites, left, ditto as <250 m wide horizon, right

Fig. 123. Distribution of bedrock deposits in the Bergslagen region, including crystalline carbonate rock (marble), limestone and alum shale. The deposits are presented on a simplified bedrock geological map of the region. This map shows the occurrence of crystalline carbonate rock and Neoproterozoic and Lower Palaeozoic sedimentary rocks, including alum shale and limestone, in the region. The location of place names referred to in the section entitled “Bedrock deposits” is also shown.

Deformation, metamorphism and mechanism of emplacement of the 1.87–1.84 Ga GSDG suite of intrusive rocks

OVERVIEW OF CONTENT

This section addresses firstly the ductile deformation in the bedrock. The multiphase ductile deformation in four structural domains, referred to here as the northern, central, southern and western structural domains, is described separately for each domain. These domains have been defined primarily on the basis of differences in the style and orientation of the ductile strain in the bedrock. To some extent, these differences correspond to differences in the grade of metamorphism as well as to differences in the timing of the deformation. The timing of ductile deformation in the bedrock, as inferred from the protolith ages of rocks that show distinctive relative age relationships with respect to the ductile deformation, are summarized under the respective structural domain.

The text on the ductile deformation in the bedrock is followed by an evaluation of the metamorphism in the Bergslagen region. This is justified since it appears that the peak of metamorphism followed establishment of penetrative fabric development in the bedrock. The distribution of key metamorphic minerals that have a bearing on the variation in the grade of regional metamorphism are described initially. A compilation of the pressure-temperature (P-T) data that provide some quantitative constraints on the metamorphic conditions in the region and a summary of the regional variation in metamorphic grade follow. The latter has given rise to the identification of four Svecokarelian metamorphic domains, referred to here as the northern migmatitic, central low-grade, central medium-grade and southern migmatitic metamorphic domains. Three of these domains are overprinted in western parts by Sveconorwegian metamorphism. Furthermore, contact metamorphism related to a 1.7 Ga intrusive body has also been identified. It is important to keep in mind that the spatial distributions of the structural domains referred to above and the major metamorphic domains are similar but are not fully compatible with each other.

An evaluation of especially U-Pb (zircon, monazite, titanite) and ^{40}Ar-^{39}Ar (hornblende, biotite) geochronological data that constrain the timing of metamorphism or the timing of later cooling events beneath a particular temperature follows. The timing of ductile deformation in the bedrock in relation to the timing of metamorphic and early cooling events is discussed. Some ^{40}Ar-^{39}Ar (white mica) ages from the western part of the region, which is overprinted by the Sveconorwegian orogenic development, as well as (U-Th)/He (apatite) and apatite fission track data from the Forsmark area, in the north-eastern part of the Berslagen region, are also addressed. The geochronological data are compiled and evaluated separately for the central medium-grade and the southern migmatitic metamorphic domains. This part of the section concludes with the presentation of a possible mechanism for the establishment of the peak of metamorphism in the region.

A review of the current model for the mechanism of emplacement of the 1.87–1.84 Ga GSDG intrusive rocks in the southern structural domain is presented. This review takes note of key structural and metamorphic information presented earlier in this section as well as the results of geophysical modelling work discussed in the section entitled "Character, spatial distribution, geochronology, geochemical signature, petrophysical characteristics and regional geophysical signature of rock units".

The section concludes with some comments on the trends of possible or confirmed fracture zones in the bedrock and their relationship to the post-Svecokarelian tectonic units in the region, as well as a summary of recently acquired data bearing on the character, timing and kinematic signature of brittle deformation in the Forsmark area in the north-eastern part of the region. In general, the brittle deformation in the Bergslagen region is very poorly understood.

Place names referred to in the text that describes the ductile deformation, metamorphism and brittle deformation in the bedrock are located in the respective figure that presents an overview of each of these features in the Bergslagen region.

DUCTILE DEFORMATION UNDER AMPHIBOLITE- OR GREENSCHIST-FACIES METAMORPHIC CONDITIONS

Multiphase deformation and structural sequence

Older studies in the Bergslagen region, for example in Geijer & Magnusson (1944), suggested that much of the deformation in the bedrock occurred synchronously with the emplacement of what is referred to here as the 1.90–1.87 Ga suite of GDG intrusive rocks. Deformation in connection with the emplacement of what is referred to here as the GP intrusive rocks was also inferred locally. Later deformation gave rise to faulting.

A pioneering synthesis of the ductile structural evolution in the region around the lake Mälaren was presented in Stålhös (1976), following detailed geological mapping of the bedrock in this part of Bergslagen (see Table 1). This synthesis identified the presence of multiphase ductile deformation in the region. In particular, Stålhös (1976) recognized that the intrusion of a swarm of metadolerites occurred between two separate phases of regional folding, referred to as F_1 and F_2, and these dykes defined an intra-orogenic stage. Stålhös (1976) continued to assign at least the F_1 folding to the intrusion of the 1.90–1.87 Ga suite of GDG intrusive rocks, i.e. these rocks were syntectonic in character.

Later modifications emphasized firstly the pre-tectonic rather than the syntectonic character of the 1.90–1.87 Ga suite of GDG intrusive rocks (Stålhös 1981), i.e. both phases of folding occurred in the solid state after intrusion of these rocks. Secondly, Wikström (1979) and Stålhös (1981) concluded that the two phases of folding (F_1 and F_2) took place under high-temperature metamorphic conditions and were probably closely connected in time. The second of these modifications apparently reduced somewhat the tectonic significance of the metadolerites.

Although detailed work has recently described the presence of possibly three fold phases at some localities in the Bergslagen region (Persson & Sjöström 2002, 2003, Talbot 2008), the terminology adopted by Stålhös (1976, 1981) for the regional, multiphase ductile deformation is maintained here for four reasons:

- The field studies carried out in the Bergslagen region in the context of this project (see section "Acquisition of new data and data interpretation – methodological aspects") have confirmed the development of a regional planar and linear grain-shape fabric in the bedrock (D_1). This development was followed by folding of at least the planar grain-shape fabric that was coupled with a continued development of a linear grain-shape fabric (D_2). An important new development in the region, addressed by several workers during the last 15 years (see later text), is the identification of ductile high-strain belts or more restricted zones.
- Detailed work in connection with the operation of the Garpenberg base metal sulphide deposit (see section "Mineral and bedrock deposits") has confirmed the D_1–D_2 ductile structural evolution on the scale of mining activity (R. Allen & E. Lundstam, personal communication 1998).
- The evidence for an earlier generation of folding (pre-D_1 according to the terminology in this report) has emerged either from the study of a ductile high-strain belt (Persson & Sjöström 2002) or from an interpretation of the patterns of the contacts between metavolcanic and GDG intrusive rocks (Persson & Sjöström 2003). Neither of these lines of evidence is judged to be sufficiently strong to motivate, at this stage, the application of a three-stage regional folding model to the whole Bergslagen region. For example, the evolution of ductile deformation along high-strain belts or zones may differ somewhat from that in the volumetrically more significant bedrock between such structures. The D_3 structures recognized by Talbot (2008) are conjugate kink bands and chevron folds that formed under low-temperature conditions.
- The two later phases of deformation recognized in Persson & Sjöström (2002, 2003) form the most significant structures and can be correlated confidently with the F_1 and F_2 phases of Stålhös (1976, 1981).

Bearing in mind that different parts of the Bergslagen region were affected by multiphase ductile deformation at different times (see later text), the sequence of deformation in each of the four structural domains is described separately for each domain.

Structural trends and definition of structural domains

A form line map, which shows the inferred structural trend of the tectonic foliation in the bedrock at the ground surface, is presented in Figure 124. In the areas affected by greenschist-facies and low to middle amphibolite-facies metamorphism (see later text), the tectonic foliation is a planar grain-shape fabric. In the migmatitic rocks (see later text), the form lines represent the interpolated trend of a gneissic banding (gneissosity) at the ground surface. The measured structural data that form the basis to the construction of the form lines have been extracted primarily from SGU's published Af and Ai bedrock geological maps (Fig. 6 and Table 1). Data have also been extracted from SGU's older published Aa geological maps in some of the areas not covered by the more modern maps (Fig. 6).

In the areas where measurements of structural data are totally lacking, use has been made of magnetic maxima connections that are inferred to represent the trend of the tectonic foliation at the ground surface. These connections have been constructed using the magnetic anomaly map over the Bergslagen region (Fig. 125).

Interpolated form lines and magnetic maxima connections were constructed at the scale 1:250 000. The length and intensity of these features generally reflect the amount of available structural information and, for this reason, provide a guide to the reliability of the

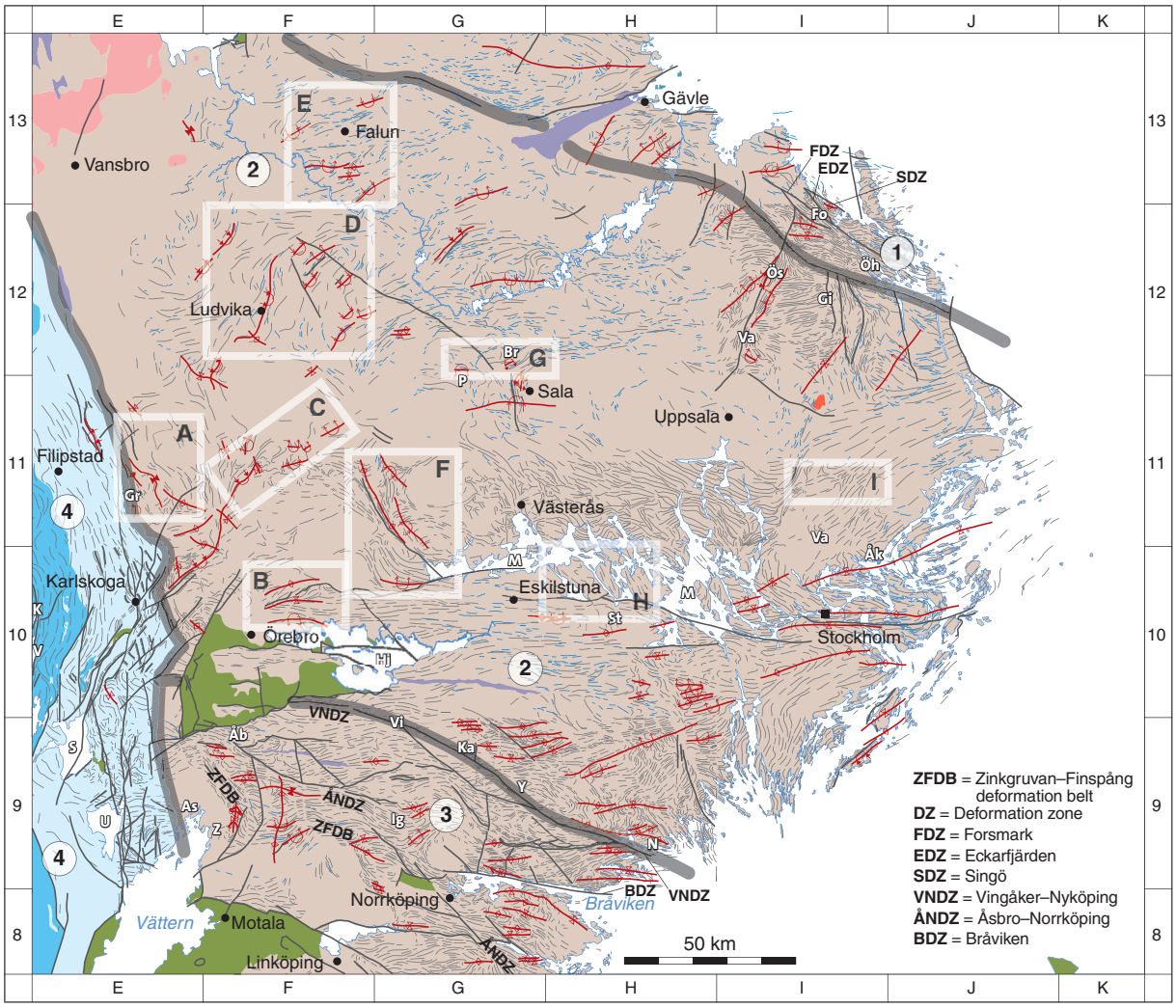

Syncline
Synform
Syncline, overturned
Synform, overturned
Anticline
Antiform
Anticline, overturned
Antiform, overturned
Fault, ductile shear zone
Structural form line for tectonic foliation
Magnetic maxima connection (selected areas)

Boundary to structural domain
1 Northern
2 Central
3 Southern
4 Western

Sedimentary cover rocks
Neoproterozoic and Lower Palaeozoic sedimentary rocks

Sveconorwegian orogen
Palaeoproterozoic (1.7 Ga) and Mesoproterozoic rocks affected, to variable extent, by Sveconorwegian ductile deformation and metamorphism
Palaeoproterozoic rocks (1.9–1.8 Ga) affected, to variable extent, by Sveconorwegian and older ductile deformation and metamorphism

Post-Svecokarelian rocks
Mesoproterozoic rocks
Palaeoproterozoic rocks (1.7 Ga)

Alkaline intrusive rock (uncertain age)
Alkaline intrusive rock (uncertain age)

Svecokarelian orogen
Palaeoproterozoic rocks (1.9–1.8 Ga) affected, to variable extent, by Svecokarelian ductile deformation and metamorphism

Fig. 124. Structural domains and their relationship to form lines for the tectonic foliation, magnetic maxima connections, axial surface traces of major, post-foliation folds and deformation zones in the Bergslagen region. The curved part of the U-symbol used in the display of overturned folds points in the direction of dip of the axial surface to the fold. The sense of vergence for such a fold is in the opposite direction. No attention is taken in the figure to different phases of foliation or folding (see text). The map also shows selected sub-areas in the central structural domain where structural field studies were completed in the context of the Bergslagen project. Sub-area A = Grythyttan–Älvestorp–Hällefors, sub-area B = Glanshammar–Rinkeby, sub-area C = Riddarhyttan–Guldsmedshyttan, sub-area D = Ställdalen–Ludvika–Smedjebacken–Säter, sub-area E = Borlänge–Falun–Bjursås–Sågmyra, sub-area F = Kungsör–Kolsva, sub-area G = Broddbo–Prästhyttan, sub-area H = Eskilstuna–Strängnäs–Nykvarn, sub-area I = Arlanda–Kårsta. Furthermore, the location of place names referred to in the section "Ductile deformation under amphibolite- or greenschist-facies metamorphic conditions" is shown on the map. Åk = Åkersberga, Åb = Åsbro, As = Askersund, Br = Broddbo, Fo = Forsmark, Gi = Gimo, Gr = Grythyttan, Hj = Hjälmaren, Ig = Igelfors, Ka = Katrineholm, K = Kristinehamn, M = Mälaren, N = Nyköping, Ös = Österbybruk, Öh = Östhammar, P = Prästhyttan, S = Skagern, St = Strängnäs, U = Unden, V = Vänern, Va = Vattholma, Vi = Vingåker, Y = Yyngaren, Z = Zinkgruvan.

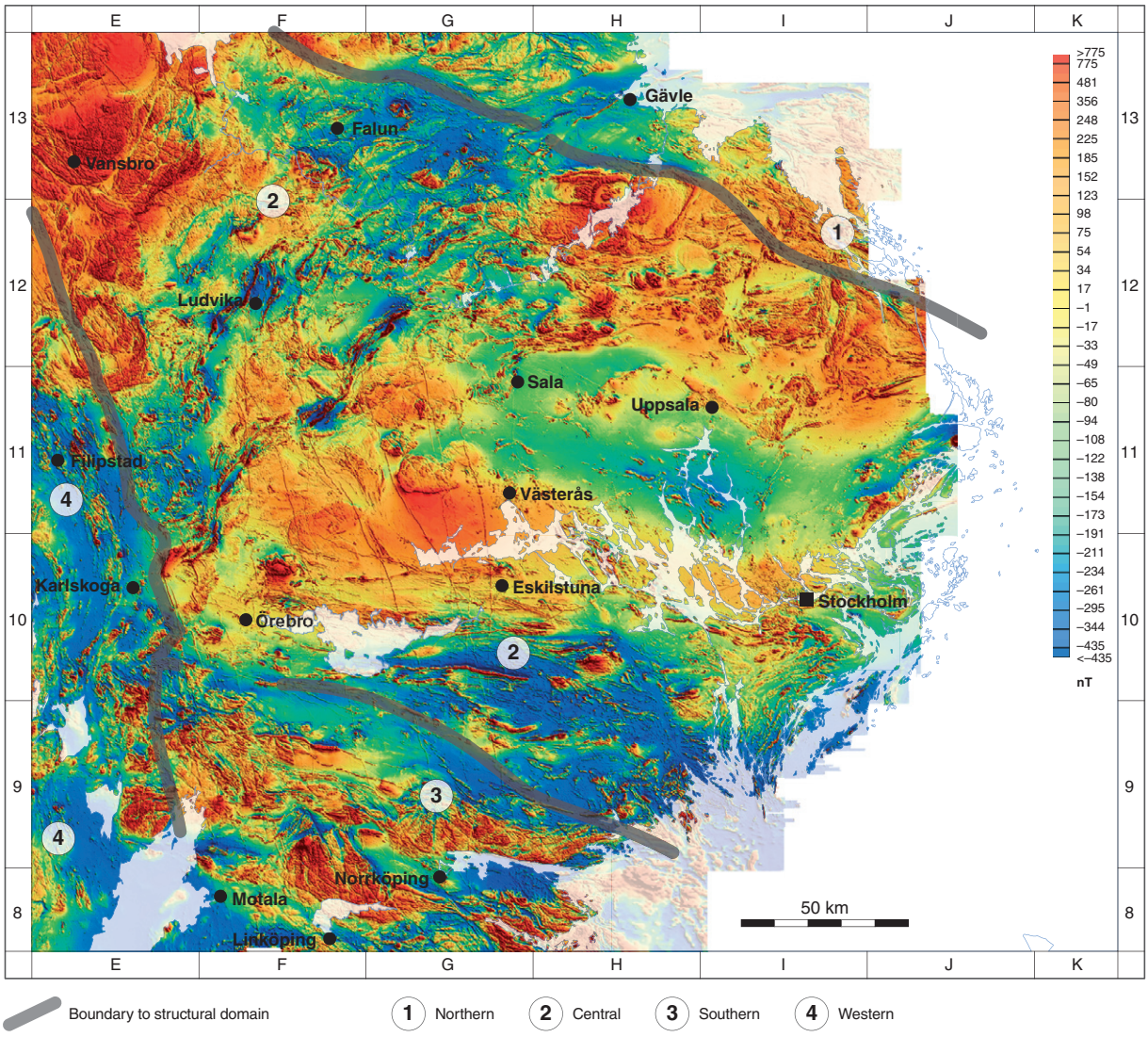

Fig. 125. Structural domains and their relationship to the magnetic anomaly map over the Bergslagen region inferred from airborne magnetic data.

linear interpolations that have been drawn on the map. The traces of the form lines and magnetic maxima connections have been used to construct the inferred axial surface traces of major folds and the extension along the ground surface of some deformation zones in the bedrock (Fig. 124). Together these structural features provide a basis for the division of the Bergslagen region into four structural domains (Figs. 124 and 125). A short summary of the important structural features in each domain is provided below. This is followed by a more detailed description of the character and timing of deformation in each of the structural domains based on investigations in specific parts of each domain.

Northern structural domain

The northern structural domain (Figs. 124 and 125) is well-constrained around Forsmark and Östhammar in its easternmost part, where it corresponds to tectonic domain 2 in the larger-scale perspective (see section "Regional tectonic framework" and Fig. 5). In this area, the domain contains a network of steeply dipping structural belts with high ductile strain that formed under amphibolite-facies metamorphic conditions and strike west-north-west–east-south-east (Stephens et al. 2007d). These belts anastomose around sub-domains where the tectonic foliation strikes east-north-east–west-south-west to north-east–south-west or is affected by major folding (Stephens et al. 2007d). The folds show axial surface traces that strike east–west to west-north-west–east-south-east and are upright or overturned to the north.

The structural belts with high ductile strain contain more discrete, steeply dipping high-strain zones with similar strike as the broader structural belts. Ductile and later brittle deformation took place under lower-grade metamorphic conditions along these zones (Talbot &

Sokoutis 1995, Bergman et al. 1996a, 1999c, Persson & Sjöström 2003, Stephens et al. 2007d, 2008a, b). The penetrative ductile grain-shape fabric and the high-strain belts around Forsmark and Östhammar formed between 1.87 and 1.86 Ga (Hermansson et al. 2008a). The more discrete high-strain zones were active after 1.85 Ga (Hermansson et al. 2008b).

The boundaries and internal character of the northern structural domain are far more uncertain in the generally less well-exposed bedrock further to the west, around and west of Gävle. Furthermore, no investigations were carried out in this area in the context of the Bergslagen project. The bedrock in this area was included in tectonic domains 1 and 2 in the larger-scale perspective (see section "Regional tectonic framework" and Fig. 5). North of Gävle, there is evidence for penetrative ductile deformation and high-grade metamorphism after 1.85 Ga (S. Bergman, personal communication 2009), typical of tectonic domain 1. Furthermore, ductile high-strain zones that enclose lozenge-shaped tectonic lenses, similar to the structural style around Forsmark and Östhammar in tectonic domain 2, have recently been described in the approximately 25 km wide so-called *Gävle-Rättvik Zone* around and west of Gävle (Högdahl et al. 2009). The area included in this "zone" lies on both sides of the boundary between the northern and central structural domains in this report (cf. Figure 2 in Högdahl et al. 2009 and Figs. 124 and 125).

Central structural domain

The central structural domain (Figs. 124 and 125) is dominated by different generations of major folding with variable axial surface trace orientations and, in general, constrictional ductile strain. It corresponds to tectonic domain 3 in the larger-scale perspective (see "Regional tectonic framework" and Fig. 5). In the major part of the domain, the folds show axial surfaces with east–west to north-east–south-west strike, are overturned with a vergence to the north to north-west and deform the planar tectonic fabric in the rocks. However, in western areas, these axial surface traces are refolded by more open, upright folds with axial surfaces that strike north-west–south-east to north-north-west–south-south-east. In westernmost areas (including the western structural domain), all fold structures show a north-north-west–south-south-east axial surface orientation.

Broad ductile high-strain belts are prominent around Eskilstuna, where the tectonic foliation displays a consistent east–west strike, and in the archipelago south-east of Stockholm, where the tectonic foliation strikes north-north-east–south-south-west. Both these regionally important structures formed under amphibolite-facies metamorphic conditions and the latter is folded by major structures with axial surfaces that strike north-east–south-west to east–west. It has been inferred that the regional ductile grain-shape fabric in the central structural domain formed between 1.88 and 1.86 Ga (Hermansson et al. 2008a).

Southern structural domain

In a structural sense, the southern structural domain (Figs. 124 and 125), which corresponds more or less entirely to tectonic domain 4 in the larger-scale perspective (see "Regional tectonic framework" and Fig. 5), strongly resembles the northern domain. It consists of structural belts that formed under amphibolite-facies metamorphic conditions and more discrete zones that formed under lower-grade conditions, all of which strike west-north-west–east-south-east (Stephens & Wahlgren 1996, Bergman et al. 1996b). These features can be followed for several tens of kilometres and anastomose around sub-domains where the tectonic foliation strikes east-north-east–west-south-west or is affected by major upright to overturned folding with axial surfaces that strike east–west to north-east–south-west. The overturned structures verge north to north-west. Younger, more open and upright folds, with axial surface traces that strike approximately north–south, are present in the western part of this domain.

Although there is evidence for amphibolite-facies deformation and metamorphism prior to 1.85 Ga in the southern domain (for example, Wikström & Karis 1991), there is also a strong influence of deformation after 1.85 Ga as well as amphibolite- and even granulite-facies metamorphism at one or more times between 1.85 Ga and 1.78 Ga (Andersson et al. 2006). Thus, the tectonic evolution of the southern structural domain differs from that in the central structural domain and in the easternmost part of the northern structural domain around Forsmark and Östhammar. However, it resembles the tectonic evolution in the area north of Gävle in the northern domain.

Western structural domain

There is a complex interference of pre-Sveconorwegian and Sveconorwegian structures in the western structural domain (Figs. 124 and 125), which forms the frontal, easternmost part of the Sveconorwegian orogen in the larger-scale perspective (see "Regional tectonic framework" and Fig. 5). In the eastern part of the domain, the Sveconorwegian deformational overprint developed

under greenschist-facies metamorphic conditions and is not penetrative in character (Wahlgren et al. 1994). A ductile grain-shape fabric and discrete, ductile high-strain zones that strike predominantly north-east–south-west or north–south are conspicuous. Rocks affected by Svecokarelian deformation or deformation of uncertain age, both of which developed under higher-grade metamorphic conditions, or more or less undeformed bedrock are sandwiched between the bedrock segments affected by Sveconorwegian deformation. In the western part of the domain, the Sveconorwegian tectonic overprint is more penetrative in character, formed under amphibolite-facies metamorphic conditions and strikes more consistently in an approximately north–south direction (Wahlgren et al. 1994).

Northern structural domain around Forsmark and Östhammar: Penetrative deformation under amphibolite-facies metamorphic conditions between 1.87 and 1.86 Ga

The character of the bedrock structures in the area around Forsmark and Östhammar in the easternmost part of the northern structural domain is based on a compilation of results from several studies:

- Bedrock mapping at the local scale of 1:50 000 in the area around Östhammar (Stålhös 1991).
- Structural analysis of the so-called *Singö shear zone* in the easternmost part of the domain (Talbot & Sokoutis 1995).
- Desk-top studies of geological and geophysical data and some field work in the areas around Östhammar, Tierp and Älvkarleby (Bergman et al. 1996a, 1999c, 2000).
- Detailed structural field studies and acquisition of anisotropy of magnetic susceptibility (AMS) data around the Forsmark nuclear power plant (Stephens et al. 2003, 2007d, 2008a, b, Isaksson et al. 2004, SKB 2005, 2008).
- An evaluation of ductile shearing and folding in the north-eastern part of the Bergslagen region (Persson & Sjöström 2003).
- Structural field studies carried out in the context of the Bergslagen project (see Fig. 18).

Much attention is addressed below on the data and the data interpretation in the Forsmark area for two reasons. Firstly, this area has been a focus for detailed structural studies both at the surface and at depth along cored boreholes (Stephens et al. 2003, 2007d, 2008a, b, SKB 2008). Anisotropy of magnetic susceptibility measurements have also been acquired and interpreted (Isaksson et al. 2004, SKB 2005). Secondly, different types of geochronological data have been generated that constrain the timing of deformation, metamorphism and cooling in this part of the domain (Hermansson et al. 2007, 2008a, 2008b, Söderlund et al. 2008, in press, Stephens & Wahlgren 2008).

The northern structural domain in the area around Forsmark and Östhammar is several tens of kilometres wide. It is characterized by a general structural grain that trends west-north-west–east-south-east to north-west–south-east, as revealed, for example, in the magnetic anomaly map (Fig. 126). Steeply dipping, high-strain belts with west-north-west–east-south-east to north-west–south-east strike are inferred to anastomose around tectonic lenses, in which the bedrock is folded, more variable in orientation and, in general, affected by lower ductile strain (Stephens et al. 2007d and Fig. 127).

Tectonic fabric, ductile high-strain belts and folding of the planar structures

The ductile fabric (D_{1N} = first phase of deformation $\{D_1\}$ in the northern $\{_N\}$ structural domain) inside both the tectonic lenses and high-strain belts around Forsmark formed under amphibolite-facies metamorphic conditions (e.g. Stålhös 1991, Stephens et al. 2003) and was subsequently affected by folding (D_{2N}) at different scales. A 3-D model for the bedrock structure in the Forsmark area (Stephens et al 2007d) is shown in Figure 128.

Ductile structures at Forsmark include a planar grain-shape fabric (tectonic foliation), a tectonic banding, a linear grain-shape fabric, which is inferred to correspond to the direction of stretching (mineral stretching lineation), and minor fold axes. There is a strong variation in the intensity of development of especially the planar D_{1N} structures that gave rise to a distinctive structural anisotropy in the bedrock, i.e. the division into tectonic lenses and high-strain belts.

The penetrative D_{1N} grain-shape fabric in the older (1.89 to 1.87 Ga) GDG metagranitoids is defined by oriented grains of biotite and elongate aggregates of recrystallized feldspar and quartz (Fig. 129a). Deformation under amphibolite-facies metamorphic conditions is indicated both by the recrystallization of feldspar in these metagranitoids and by the mineral assemblage in the spatially associated mafic to intermediate rocks consisting of hornblende, plagioclase feldspar, biotite and, locally, quartz (Fig. 129b). The lack of intracrystalline deformation suggests that the metamorphism peaked after the ductile strain had affected the bedrock. The grain-shape fabric in the younger (1.86 Ga) GDG metagranitoids is a linear structure that formed under lower

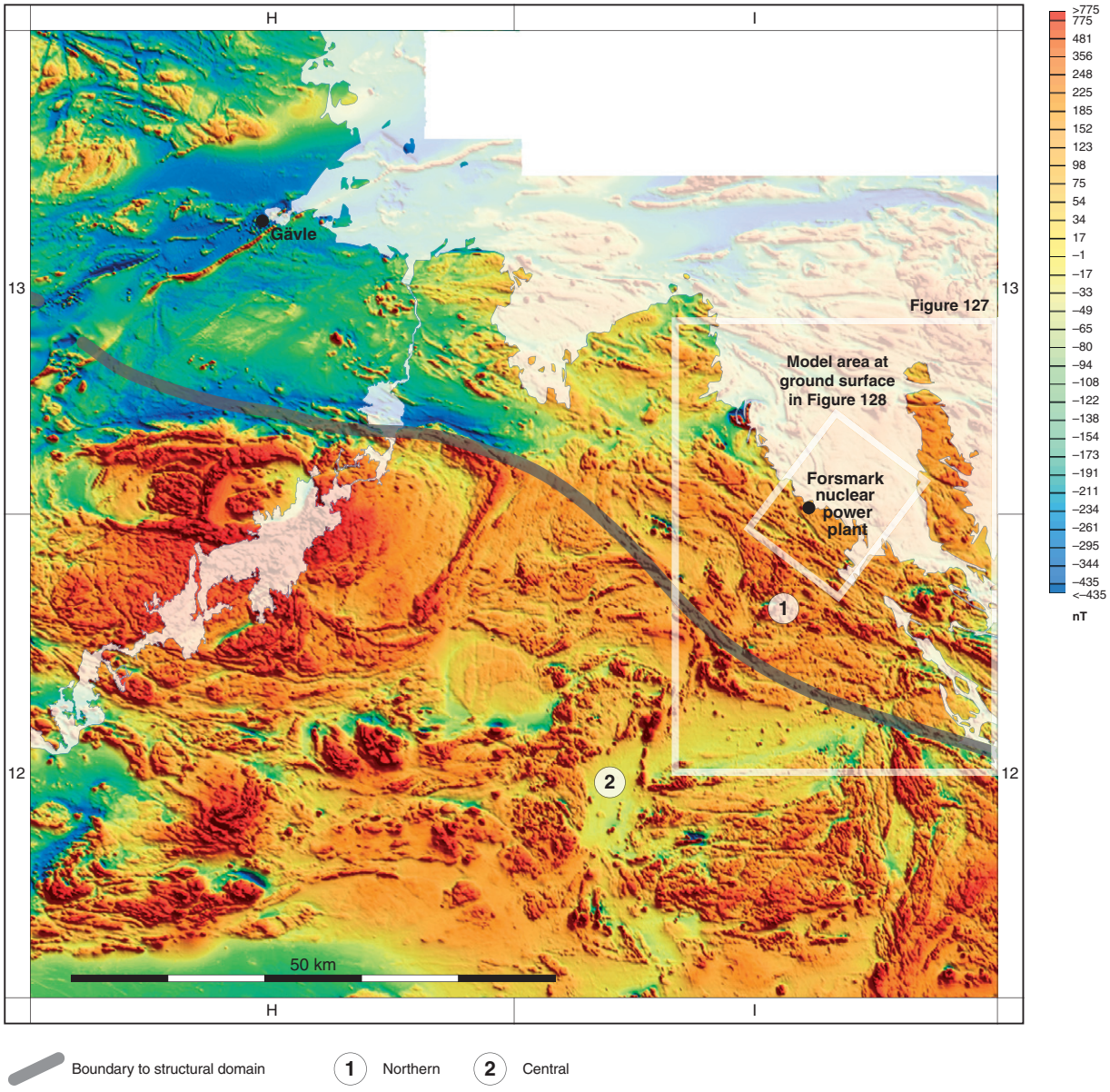

Fig. 126. Magnetic anomaly map over the north-eastern part of the Bergslagen region inferred from airborne magnetic data. Note the general, west-north-west–east-south-east to north-west–south-east, structural grain in the bedrock in the northern structural domain, which anastomoses around bedrock segments with more varied structural grain commonly related to major folding. These major structural features are inferred to represent ductile high-strain belts and tectonic lenses with lower ductile strain, respectively (see, for example, Bergman et al. 1996a, 1999c and Figure 127). The outlined areas are shown in Figures 127 and 128.

amphibolite-facies metamorphic conditions (Fig. 129c). The limited ductile strain in the youngest (1.85 Ga) granitic dykes inside the tectonic lenses formed under greenschist-facies metamorphic conditions (Fig. 129d).

Inside the tectonic lenses, a linear grain-shape fabric is dominant (LS-tectonites) and D_{2N} folding is prominent, i.e. the ductile strain is prolate in character. On a larger scale, the boundaries between different rock units as well as a D_{1N} ductile high-strain belt are affected by the folding. On a smaller scale, folding of the D_{1N} penetrative planar grain-shape fabric (Figs. 130a and 130b), with an inferred fold axis that plunges moderately to the south-east (Fig. 131), is indicated from the outcrop data inside one such lens. AMS data from surface samples provide an independent assessment of the inferred geometry of the major folding inside this lens (Fig. 131). Both the mineral stretching lineation (Fig. 131) and the measured fold axes (Fig. 131) plunge with variable inclination to the south-east.

The orientation of linear structures at Forsmark is in good agreement with that presented by Stålhös (1991, Fig. 63) from a much larger area around Östhammar (map-sheet 12E Östhammar NO). It is apparent that the fold axes are subparallel to the stretching direc-

tion in the bedrock in at least this part of the northern structural domain. Evidence for folding of the mineral stretching lineation is lacking. It is inferred that the linear grain-shape fabric is a combined D_{1N} and D_{2N} structure that was established prior to but continued to develop during the D_{2N} folding.

Outside the tectonic lenses at Forsmark, strongly deformed rocks that are apparently simpler from a structural viewpoint define amphibolite-facies, D_{1N} high-strain belts. The rocks inside these belts show both planar and linear grain-shape fabrics (SL-tectonites) as well as tectonically banded rocks in compositionally less homogeneous segments (BSL-tectonites or mylonitic striped gneisses). AMS data provide independent evidence for the higher degree of ductile strain outside the tectonic lenses and the more oblate character of this strain. The planar grain-shape fabric commonly dips steeply to the south-west and the mineral stretching lineation and minor D_{2N} folds plunge with variable inclination to the south-east (Fig. 131). A major difference between the ductile structures outside and within (see above) the tectonic lenses is the more consistent orientation of the steeply dipping, planar grain-shape fabric in the former (Fig. 131).

Limited kinematic data indicate a component of dextral strike-slip deformation along the high-strain belts on different flanks of the D_{2N} fold structures (Fig. 132a). These data are consistent with the few kinematic observations and inferences drawn in other

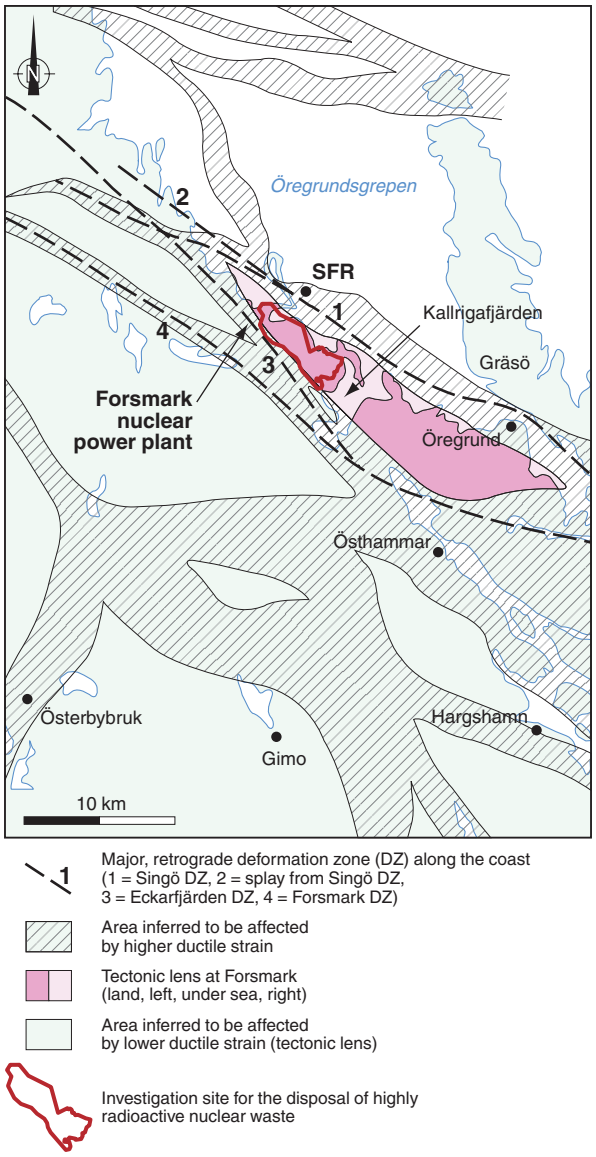

Fig. 127. Inferred high-strain belts and tectonic lenses in the Östhammar area in the north-eastern part of the Bergslagen region. Confirmation of these structures has taken place in connection with the detailed surface mapping and drill core investigations within and around the investigation site for the disposal of highly radioactive nuclear waste, close to the Forsmark nuclear power plant. Only a selected number of regional deformation zones with both ductile and brittle deformation are shown on the map. The character of these zones has been established with the help of various surface and drill core geological and geophysical data at Forsmark (Stephens et al. 2007d, 2008a, b, SKB 2008). Figure modified slightly after Stephens et al. (2007d).

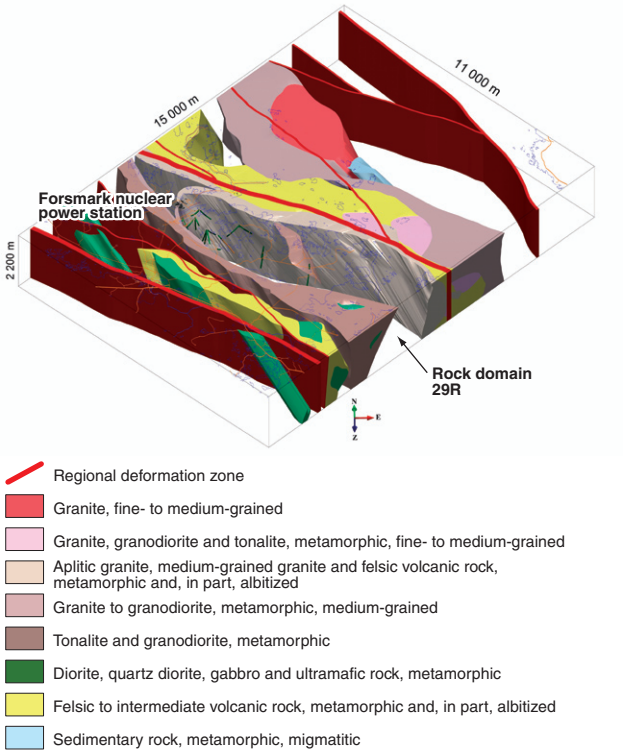

Fig. 128. 3-D model for bedrock units and regionally important deformation zones at Forsmark inside the northern structural domain (after Stephens et al. 2007d). The north-western part of the rock domain labelled 29R, which is dominated by a 1.87 Ga metagranite and is intersected by most of the boreholes, has been selected as a potential site for the repository of highly radioactive nuclear waste. Note the broad belts that contain rocks with steep dip and west-north-west–east-south-east to north-west–south-east strike and more discrete, steeply dipping regional deformation zones. The tectonic lenses between these belts contain fold structures that plunge steeply to gently to the south-east.

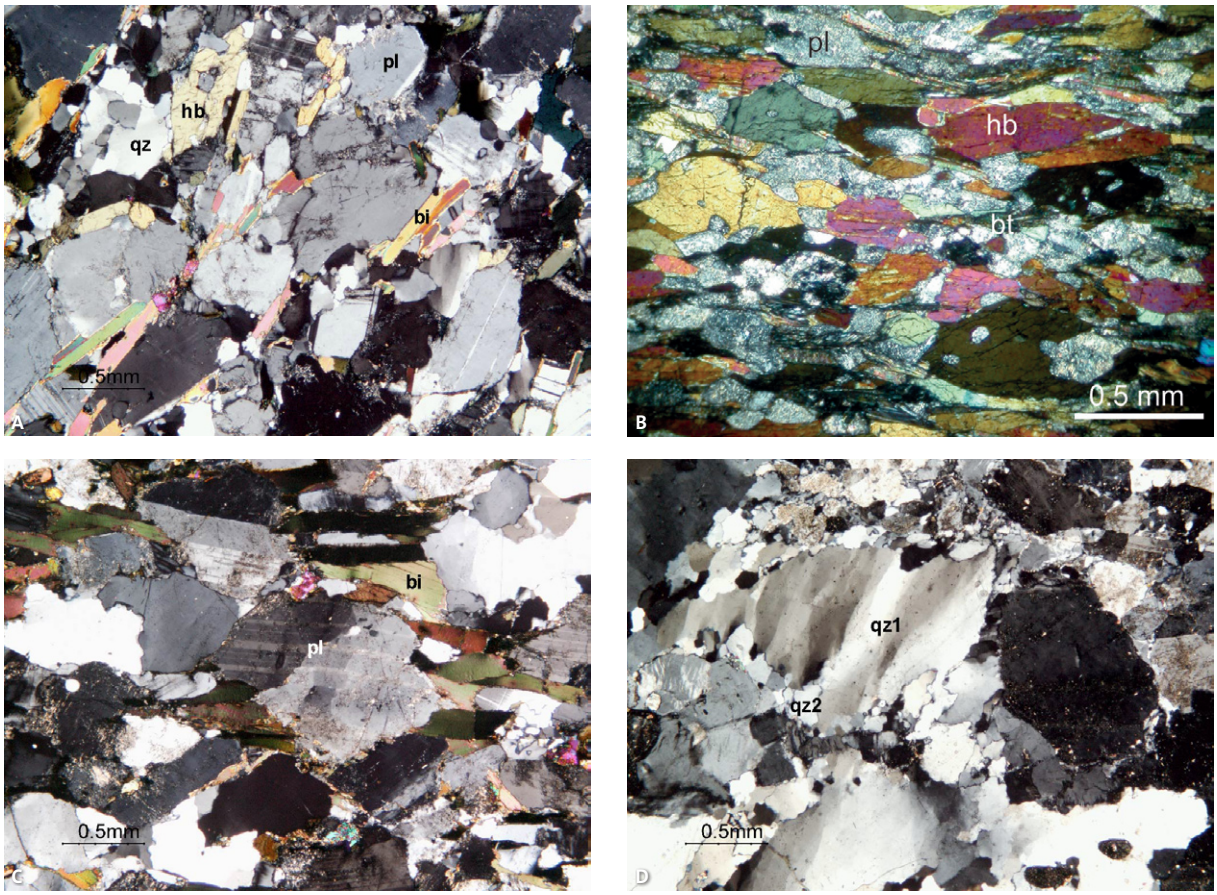

Fig. 129. Photomicrographs of representative samples showing the microstructural developments in the different suites of meta-igneous rocks at the Forsmark site, northern structural domain. **A.** Planar grain-shape fabric in metagranodiorite that belongs to the older, 1.90–1.87 Ga GDG intrusive rock suite in the Bergslagen region. The fabric is defined by oriented grains of biotite (bi) and hornblende (hb) as well as oriented aggregates of totally recrystallized plagioclase feldspar (pl) and quartz (qz). Penetrative ductile deformation under amphibolite-facies conditions with continued metamorphism after deformation is inferred. Photograph: Sven Lundqvist and Michael Stephens (SGU). **B.** Amphibolite that has yielded a ^{40}Ar-^{39}Ar (hornblende) age of 1805±3 Ma. The sample was taken in a ductile high-strain belt close to the *Forsmark deformation zone*. The grain-shape fabric is defined by oriented hornblende (hb), biotite (bt) and plagioclase feldspar (pl). Penetrative ductile deformation under amphibolite-facies conditions is inferred. Photograph: Tobias Hermansson (Boliden AB). **C.** Linear grain-shape fabric in metagranodiorite dated to 1.86 Ga that belongs to the younger, 1.87–1.85 Ga GDG intrusive rock suite in the Bergslagen region. The fabric is defined by oriented grains of biotite (bi), quartz and feldspar. The twinned, plagioclase feldspar grain in the central part of the picture (pl) shows a weak development of subgrains and limited recrystallization. Ductile deformation under lower amphibolite-facies conditions is inferred. Photograph: Sven Lundqvist and Michael Stephens (SGU). **D.** Leucocratic granite dated to 1.85 Ga that shows elongate subgrains in relics of large, old quartz grains (qz1). These grains are surrounded by small, dynamically recrystallized, new grains of quartz (qz2) in a core-and-mantle structure. Deformation under greenschist-facies conditions is inferred. Photograph: Sven Lundqvist and Michael Stephens (SGU).

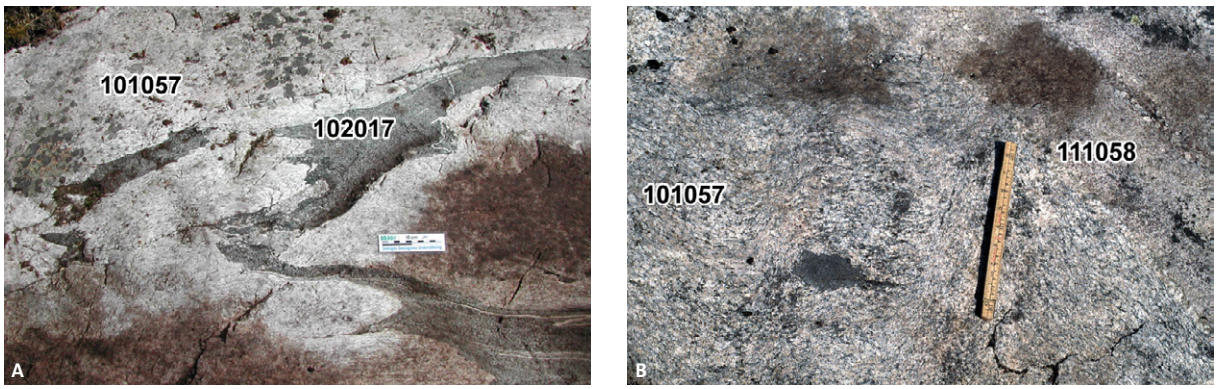

Fig. 130. Character of the bedrock inside a tectonic lens at Forsmark, northern structural domain. **A.** The rock contact between metagranite (code 101057) and an amphibolite dyke (code 102017) as well as the planar grain-shape fabric (D_{1N}) in the metagranite are affected by D_{2N} folding. Photograph: Michael Stephens (SGU). **B.** Folded tectonic foliation with minor ductile shear zone development in 1.87 Ga metagranite that belongs to the older, 1.90–1.87 Ga GDG intrusive rock suite in the Bergslagen region (code 101057). The tectonic fabric is markedly discordant to a younger granite dyke (code 111058) that belongs to a group of igneous rocks at the site (group D) dated at 1.85 Ga. Photograph: Michael Stephens (SGU).

parts of the northern structural domain, both during earlier studies (Talbot & Sokoutis 1995, Bergman et al. 1999c) and during the Bergslagen project (Fig. 132b). The mylonitic striped gneisses at Forsmark are deformed by minor D_{2N} folds (Fig. 132c) that are inferred to be parasitic and related to larger-

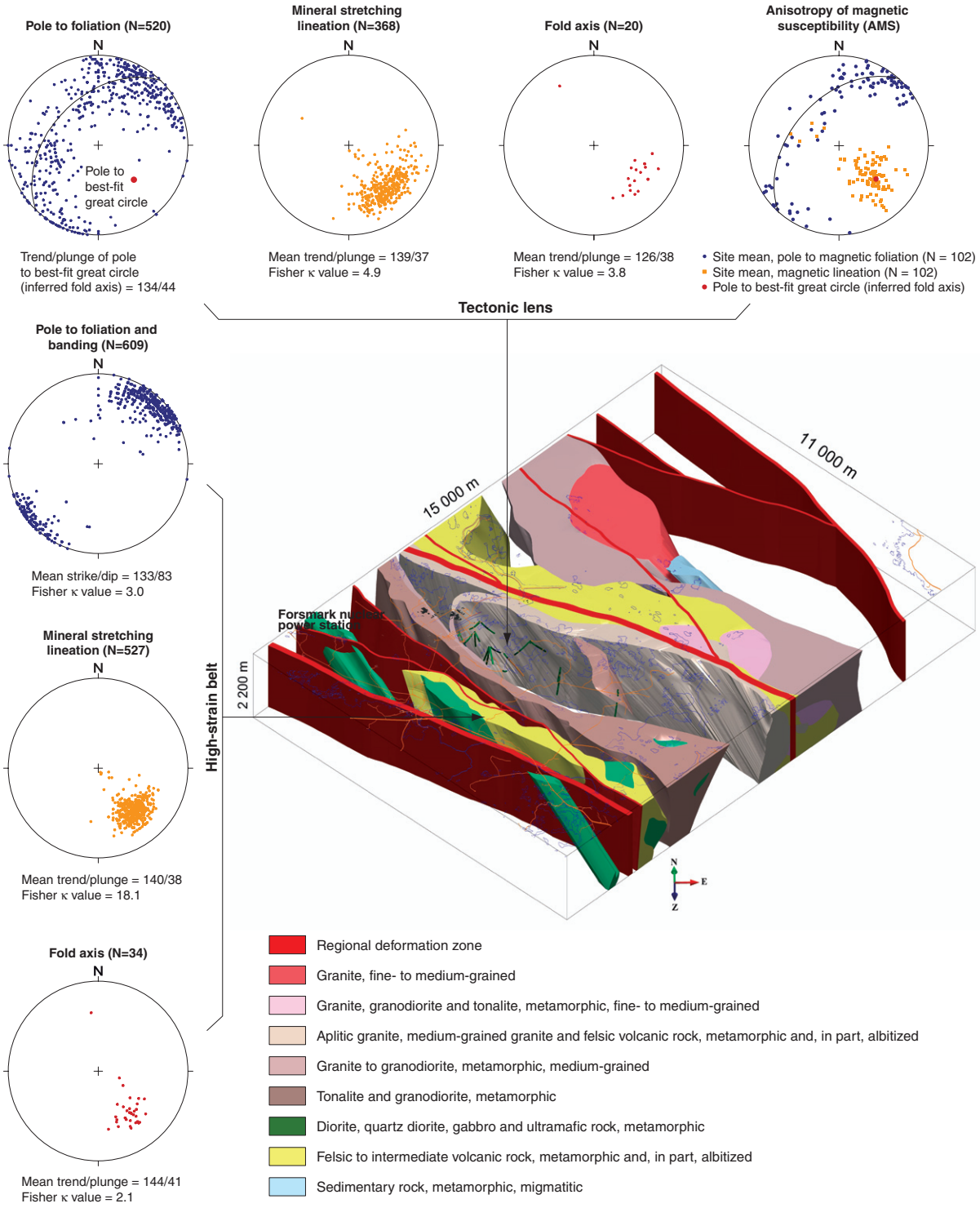

Fig. 131. Orientation of structures inside the tectonic lens situated predominantly to the south-east of the nuclear power plant at Forsmark and along the ductile high-strain belt to the south-west of this lens, northern structural domain. All structures have been plotted on the lower hemisphere of an equal-area stereographic projection. Planar structures have been plotted as poles to planes. The majority of anisotropy of magnetic susceptibility (AMS) data come from the tectonic lens. Note how the inferred fold axis from the AMS data is in excellent agreement with the inferred fold axis from the folded planar grain-shape fabric data. Structural data from Stephens et al. (2003). AMS data from Isaksson et al. (2004).

scale fold structures. Locally, eye-shaped sheath folds are present (Fig. 132d).

Retrogressive ductile high-strain zones

In connection with or after the D_{2N} phase, the ductile high-strain segments developed a more focussed, zone-like character at Forsmark (Fig. 127). Examples of such zones include the regionally important *Singö*, *Eckarfjärden* and *Forsmark deformation zones* (Stephens et al. 2007d, 2008a, b, SKB 2008), all of which are shown in the 3-D model for the bedrock structure at Forsmark (Fig. 128). This strain gave rise to the development of retrograde, protomylonitic or mylonitic structures along the ductile high-strain belts with west-north-west–east-south-east or north-west–south-east strike (Fig. 133a). The ^{40}Ar-^{39}Ar (hornblende) data indicate deformation under low amphibolite- or greenschist-facies metamorphic conditions (see later text). At Forsmark, limited kinematic data also indicate a dextral strike-slip component of deformation at this stage in the deformational history (Fig. 133b).

Field and geochronological constraints on the timing of Svecokarelian ductile deformation

Summaries of the intrusion–deformation field relationships for the two different suites of GDG intrusive rocks in the Forsmark area and the metadolerites in northern Uppland, both of which lie within the northern structural domain, were provided earlier in this report (see, for example, Figs. 51 and 63). Such relationships for the metadolerites are also addressed in the appendix.

The critical field relationships at Forsmark have provided a firm basis for constraining the timing of Svecokarelian D_{1N} deformation in the northern structural domain, using the U-Pb (zircon) protolith ages of rocks that crystallized at different times during the tectonic evolution. Three samples from the older, 1.90–1.87 Ga suite of GDG intrusive rocks, which show a pre-tectonic

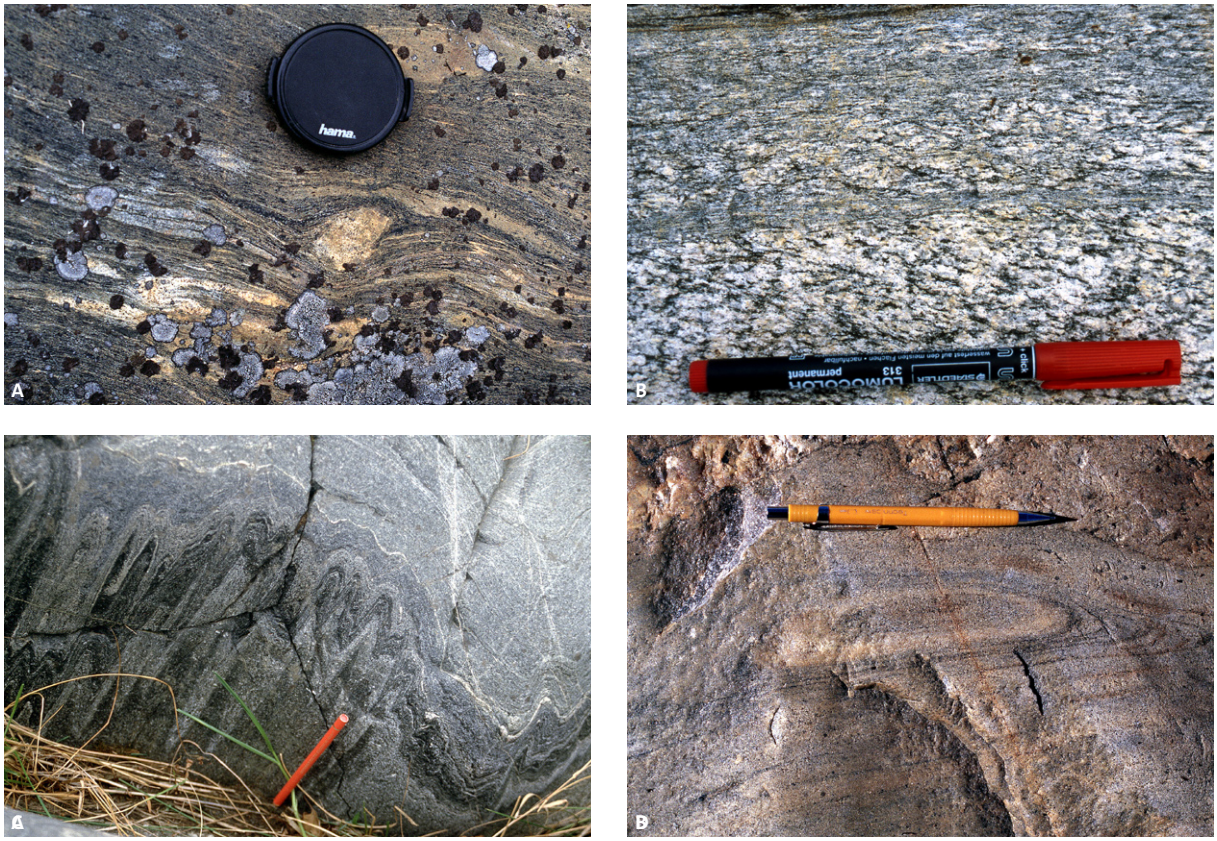

Fig. 132. Character of the bedrock inside ductile high-strain belts in the northern structural domain at Forsmark and close to Östhammar. **A.** Winged porphyroclast (δ-type) in D_{1N} mylonitic gneiss at Forsmark, belonging to the older, 1.90–1.87 Ga GDG intrusive rock suite in the Bergslagen region (mylonitic gneissic fabric using right-hand-rule method = 140°/90°). A component of dextral strike-slip displacement is inferred along the steeply dipping, mylonitic gneissic fabric. **B.** C′-type shear bands and combined CS fabric in protomylonitic tonalite at Östhammar, belonging to the older, 1.90–1.87 Ga GDG intrusive rock suite in the Bergslagen region. A component of dextral strike-slip displacement is inferred (CS protomylonitic fabric using right-hand-rule method = 100°/70°, mineral stretching lineation = 140°/65°). **C.** D_{2N} folding of the highly-strained GDG rocks shown in Figure 132a with s-asymmetry. D_{2N} fold axis = 140°/60°. **D.** Eye-shaped, sheath fold in fine-grained, banded orthogneiss at Forsmark. Photographs: Michael Stephens (SGU).

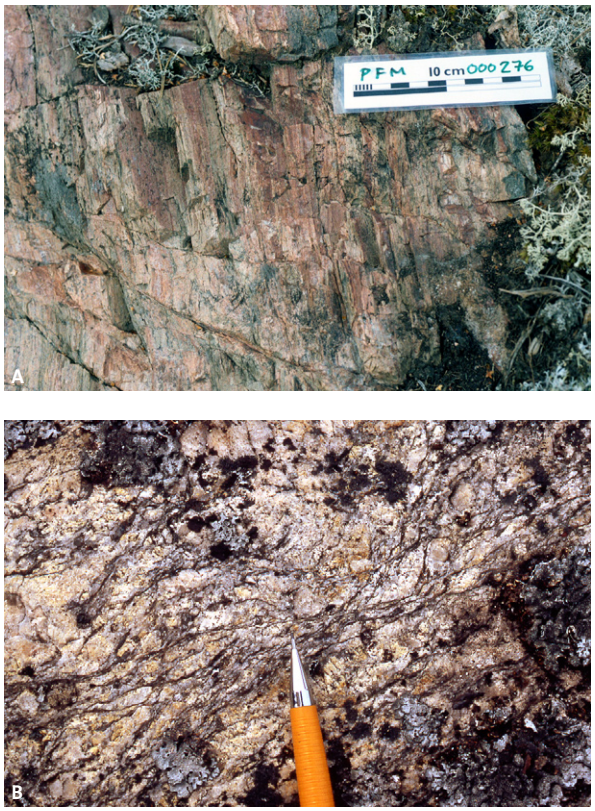

Fig. 133. Post-D_{2N}, retrograde, high ductile strain along deformation zones at Forsmark, northern structural domain. **A.** Mylonite along the *Eckarfjärden deformation zone*. Note also the intense hematite- and epidote-rich alteration. Photograph: Torbjörn Bergman (SGU). **B.** C′-type shear bands in protomylonitic pegmatite indicate a dextral strike-slip component of displacement. This field observation point occurs along the steeply dipping high-strain belt that hosts the *Singö deformation zone* and various splays, with west-north-west–east-south-east and north-west–south-east strike, respectively. Photograph: Michael Stephens (SGU).

relationship to the penetrative deformation under amphibolite-facies metamorphic conditions, have been analysed (Hermansson et al. 2008a). Furthermore, an age from the younger, 1.87–1.85 Ga suite of GDG intrusive rocks and two ages from even younger granite dykes, which show a syn- or post-tectonic relationship to the penetrative ductile strain and were affected by a lower grade of metamorphism, have been acquired (Hermansson et al. 2007, 2008a). The U-Pb (zircon) data have been complemented with age data from other isotope systems that constrain the timing of the later cooling history (see later text).

The geochronological data indicate that the D_{1N} ductile deformation in the Forsmark area initiated between 1.87 and 1.86 Ga. The development of broad belts with higher ductile strain, which strike west-north-west–east-south-east and north-west–south-east and surround tectonic lenses with generally lower ductile strain, also occurred around 1.86 Ga. The amphibolite dykes and the GDG intrusive rocks that belong to the younger suite intruded during the waning stages of and after the development of the penetrative, D_{1N} ductile strain in the area, prior to 1.85 Ga. These rocks were only affected by prolate strain. Regional folding of the variably intense, planar grain-shape fabric also occurred after intrusion of the amphibolite dykes, i.e. after 1.87 to 1.86 Ga. The minimum age of the D_{2N} folding during the Svecokarelian tectonic evolution is not constrained.

Ductile strain along the retrogressive shear zones after 1.85 Ga in the northern structural domain made use of the already established anisotropy in the bedrock. For this reason, these regionally important deformation zones followed but were focussed along a more restricted part of the steep, high-strain belts that strike west-north-west–east-south-east and north-west–south-east. This principle of progressively focussed strain continued when these zones were subsequently reactived in the brittle régime (see later text). It is apparent that the bedrock anisotropy that was established in the high-temperature ductile régime at around 1.86 Ga played an important role in the development of subsequent deformation under lower-grade conditions. The change from ductile to brittle deformation occurred around 1.7 Ga (see later text).

Conceptual model for D_{2N} folding in the Forsmark area

The D_{2N} folds in the Forsmark area show three important characteristics:

- an eye-shaped pattern on the ground surface at different scales,
- an absence of mesoscopic structures that can explain this pattern by fold interference (type 1 in Ramsay & Huber 1988) and
- a fold axis orientation that is subparallel to the stretching lineation.

Overall, the ductile structures in this part of the northern structural domain are characteristic of regions where high-temperature ductile strain with variable intensity, stretching, folding and retrogressive ductile strain were intimately related during strong, progressive, non-coaxial deformation. It is assumed that the D_{2N} folding developed initially with a normal cylindrical shape. It is not known whether the folding formed as a result of the simple shear deformation along the high-strain belts in the area (transtensional or transpressional deformation) or in connection with shortening across these belts (transpressional deformation). This matter is addressed further in the section entitled "Tec-

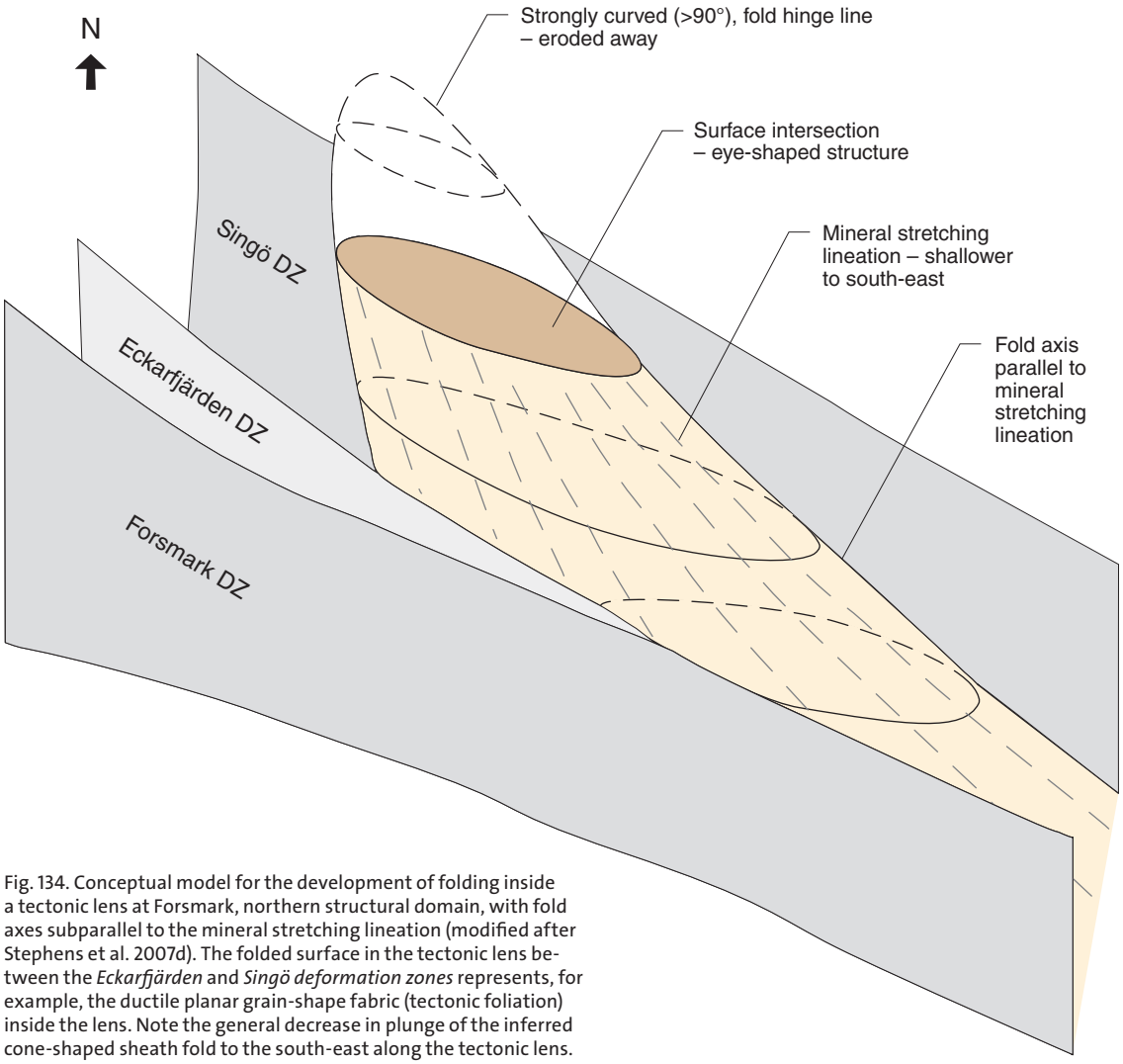

Fig. 134. Conceptual model for the development of folding inside a tectonic lens at Forsmark, northern structural domain, with fold axes subparallel to the mineral stretching lineation (modified after Stephens et al. 2007d). The folded surface in the tectonic lens between the *Eckarfjärden* and *Singö deformation zones* represents, for example, the ductile planar grain-shape fabric (tectonic foliation) inside the lens. Note the general decrease in plunge of the inferred cone-shaped sheath fold to the south-east along the tectonic lens.

tonic model for Svecokarelian orogenic activity in the Bergslagen region". However, it is suggested that the D_{2N} folds were progressively drawn out, to a variable extent, in the stretching direction into cone-shaped structures, i.e. sheath folds, so that their orientation ultimately followed the stretching lineation.

A conceptual geometric model for a major sheath fold inside the tectonic lens to the south-east of the nuclear power plant at Forsmark is presented in Figure 134. An important geometric component is the predicted eye-shaped pattern of the boundaries between rock units in 2-D sections at the ground surface. It is suggested that this model is applicable to other parts of the Bergslagen region where the ductile strain is high, where major eye-shaped structures are present on the bedrock geological map and where there is no evidence for fold interference with formation of dome and basin structures (type 1 in Ramsay & Huber 1988).

Central structural domain: Major folding, constrictional strain and ductile high-strain zones or belts

One of the major aims of the field studies carried out in the context of the Bergslagen project was to provide a better understanding of the relationship between different generations of planar structures, including primary bedding, and the folding in the bedrock in the central structural domain. Focus in the field work was placed on those parts of the domain that contain rock units rich in phyllosilicates, i.e. the Svecofennian sedimentary rocks and the Svecofennian volcanic rocks that show an increased effect of the hydrothermal alteration referred to as "magnesium alteration" (see earlier). However, the structural development in the spatially associated and volumetrically more important, volcanic and GDG intrusive rocks, which are rich in quartz and

feldspar, was also addressed. The relationship between mesoscopic planar and linear structures and large-scale folding was studied in several sub-areas (Fig. 124).

Folding of an early, planar grain-shape fabric (S_{1C} = first phase of planar fabric development $\{S_1\}$ in the central $\{_C\}$ structural domain) in the bedrock, referred to here as folding during D_{2C} (second phase of deformation $\{D_2\}$ in the the central $\{_C\}$ structural domain), is a prominent geological feature in the central structural domain. The folding is apparent on different scales, not least on a larger-scale, as inferred from an inspection of the form line (Fig. 124) and magnetic anomaly (Fig. 125) maps, as well as the spatial distribution of the boundary between the central medium-grade and southern migmatitic domains (see text below). The occurrence of regional-scale folding is inferred. Bearing in mind the trend of associated linear structures (see below), this regional folding consists of the following five components (Figs. 124 and 125):

- a complexly folded but essentially antiformal hinge in sub-area E around Falun,
- a complexly folded limb with north-east–south-west strike in sub-area D, north-east of Ludvika,
- a synformal hinge in, for example, the Sala area, south of sub-area G,
- a highly-strained deformation belt with E–W strike along a fold limb in the Eskilstuna–Örebro area (including sub-area H), and
- a major, antiformal hinge south-west of Stockholm.

On a mesoscopic scale, the D_{2C} deformation commonly gave rise to a transposition of the earlier planar structures (bedding and S_{1C}) into an S_{2C} planar structure, particularly on the major limb components recognized above. It was also associated with the development of a linear grain-shape fabric, especially in the mica-poor rocks, indicative of widespread prolate or constrictional strain. The strong influence of D_{2C} folding and lineation development has generally inhibited a better understanding of the older D_{1C} strain in the bedrock. For this reason, there are few remnants of major structures that can be confidently related to the early, planar grain-shape fabric (S_{1C}).

A more detailed description of the structures in the central structural domain is provided below.

Early-stage folding and stratigraphic inversion (D_{1C})

Sub-areas A and B, east of Filipstad and north-east of Örebro, respectively (Figs. 124 and 125), were studied in the context of the Bergslagen project with focus on possible early-stage D_{1C} major folds. The low-grade rocks (see section on metamorphism below) in sub-area A belong to both the central and western structural domains (Figs. 124 and 125). Sub-area B is situated in the south-western part of the central structural domain (Figs. 124 and 125).

The stratigraphically youngest metasedimentary rocks in sub-area A (Sundius 1923, Lundström 1995) are preserved in the core of major synclines inferred to form the first generation of Svecokarelian ductile structures in the region (Lundström 1995). These folds plunge gently along axial surface traces that strike north-north-west–south-south-east and dip steeply westwards. In the context of the Bergslagen project, mesoscopic structures in the low-grade, bedded metasandstone and meta-argillite (slate) have been studied south of Grythyttan. A simple bedding-cleavage relationship, with a first generation slaty cleavage (S_{1C}) at a high angle to bedding (S_0), is present (Fig. 135a). The intersection of these structures defines a fold axis orientation that plunges gently to the south-east. These field data confirm the occurrence of D_{1C} folding in these low-grade rocks.

The distribution of different rock units on the ground surface as well as the magnetic anomaly pattern indicate major fold structures in sub-area B with axial surfaces that strike east–west (Figs. 124 and 125). However, different structural and especially stratigraphic models have been presented for these rocks (Gorbatschev 1969, 1972, Wikman 1972, 1973). Both these workers indicate that the major, east-plunging synform, referred to as the *Käglan synform* (Gorbatschev 1969, 1972) or *Listre synform* (Wikman 1972), was formed after development of the tectonic planar grain-shape fabric in the rocks, i.e. the fold corresponds to a D_{2C} structure in this report. The difference between the structural interpretations and, as a consequence, the stratigraphic models for the area concerns the interpretation of the major fold structure further south, to the east of Örebro, referred to as the *Glanshammar antiform* (Gorbatschev 1969) or *Rinkaby syncline* (Wikman 1972).

Andalusite-bearing metasedimentary rocks are present in the core of the *Glanshammar antiform* (Fig. 135b). In the model presented by Gorbatschev (1969, 1972), these metasedimentary rocks are inferred to be older than metavolcanic rocks and are not the stratigraphic equivalents to the metasedimentary rocks in sub-area A, east of Filipstad. By contrast, Wikman (1972) concluded that the major fold to the east of Örebro did not belong to the same generation of folding as the *Käglan (Listre) synform* to the north, but belonged to an earlier phase (D_{1C} in this report) with an original gentle north–south trend. Wikman (1972) concluded that this fold was synclinal in character and that the

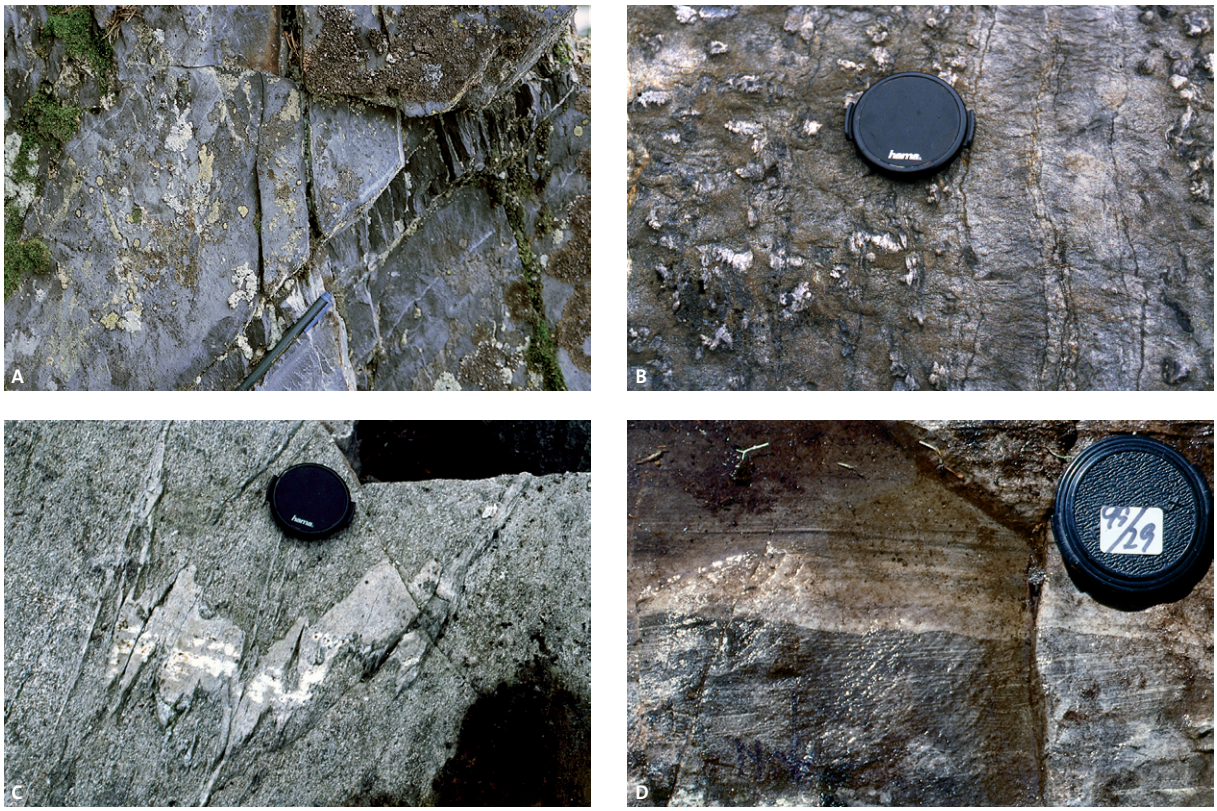

Fig. 135. Mesoscopic structures and way-up determination in sub-areas A and B (see Fig. 124), central structural domain. **A.** High angle between bedding and S_{1C} in bedded, fine-grained metasandstone and meta-argillite. Bedding dips moderately to the north-east and S_{1C} dips steeply to the south-west. The intersection lineation between these two surfaces plunges gently to the south-east. View of vertical surface to the south-east (11E Filipstad SO). Photograph: Michael Stephens (SGU). **B.** Bedding surfaces defined by andalusite-rich (beneath the camera lens cover) and andalusite-poor (to the right of the cover) sandy beds that are subparallel to the S_{2C} fabric in the rock (276°/90° using right-hand-rule method). The andalusite porophroblasts are folded and cleaved. View of horizontal surface to the east in the core of the *Glanshammar antiform* (10F Örebro NV). Photograph: Michael Stephens (SGU). **C.** Mesoscopic D_{2C} folding in a felsic metavolcanic rock. The fold axis plunges moderately to the east. View of horizontal surface to the west in the core of the *Käglan (Listre) synform* (10F Örebro NV). Photograph: Michael Stephens (SGU). **D.** Laminated volcanic metasiltstone with cross bedding that indicates right-way-up to the south (upwards in the photograph). View of horizontal surface to the south on the fold flank between the *Käglan (Listre) synform* and *Glanshammar antiform* (10F Örebro NV). Photograph: Ingmar Lundström (SGU).

andalusite-bearing metasedimentary rocks in the core of this structure form the stratigraphically youngest rocks in the area. For this reason, they were inferred to be stratigraphically equivalent to the metasedimentary rocks in sub-area A.

Field work in connection with the Bergslagen project has confirmed that the *Käglan (Listre) synform* is a D_{2C} structure. Both mesoscopic F_{2C} folds (Fig. 135c) and the mineral stretching lineation in the area show a moderate to steep plunge to the east. Way-up structures that indicate right-way-up to the south (Fig. 135d), as well as z-shaped F_{2C} folds with a weakly developed axial surface cleavage with east-north-east–west-south-west strike, are both present on the fold flank between the *Käglan (Listre) synform* and the *Glanshammar antiform*. The andalusite porphyroblasts in the metasedimentary rocks in the core of the *Glanshammar antiform* are also deformed (Fig. 135b). Mesoscopic folds plunge moderately to steeply to the east-south-east, similar to that in the *Käglan (Listre) synform*. No evidence for folded, gently dipping D_{1C} structures was observed.

It is concluded that the andalusite-bearing metasedimentary rocks are situated in the core of a D_{2C} antiformal structure and that all the fold structures belong to the same generation, as indicated by Gorbatschev (1969, 1972). However, the way-up determinations on the fold flank between the *Käglan (Listre) synform* and the *Glanshammar antiform* indicate an inversion of the stratigraphy prior to the D_{2C} deformation. This interpretation suggests that the andalusite-bearing metasedimentary rocks form the youngest part of the sequence, in agreement with the conclusions on the stratigraphy drawn by Wikman (1972). However, the *Glanshammar antiform* is an antiformal syncline and use of the term *Rinkaby syncline* is not recommended.

Major folding (D_{2C}) of the planar tectonic fabric

Field studies in several sub-areas in the central structural domain, in both the medium-grade rocks and the high-grade, migmatitic rocks immediately to the south, have established the regional significance of D_{2C} folding on different scales. These sub-domains are treated separately below.

Major folding (D_{2C}) of the planar tectonic fabric in medium-grade rocks

Large-scale D_{2C} folds with axial surfaces that strike north-east–south-west are prominent in the medium-grade rocks in sub-areas C–E, from south of Ludvika to Falun (Figs. 124 and 125). The D_{2C} folds show an s-asymmetry with short and long limbs that strike approximately north-west–south-east and north-east–south-west, respectively. Minor folds and crenulation of the S_{1C} planar grain-shape fabric, an axial surface cleavage (S_{2C}) that is markedly discordant to S_{1C} (and bedding), and an intersection lineation between the two planar structures are conspicuous in the more phyllosilicate-rich rocks in the fold hinges and short limbs of the larger-scale folds. By contrast, a strong S_{2C} foliation, which commonly transposes the S_{1C} planar fabric, is present in the long limbs with north-east–south-west strike (Fig. 136a). It is commonly difficult to distinguish the two generations of foliation on the long limbs, which essentially correspond to D_{2C} ductile high-strain zones formed during the folding phase.

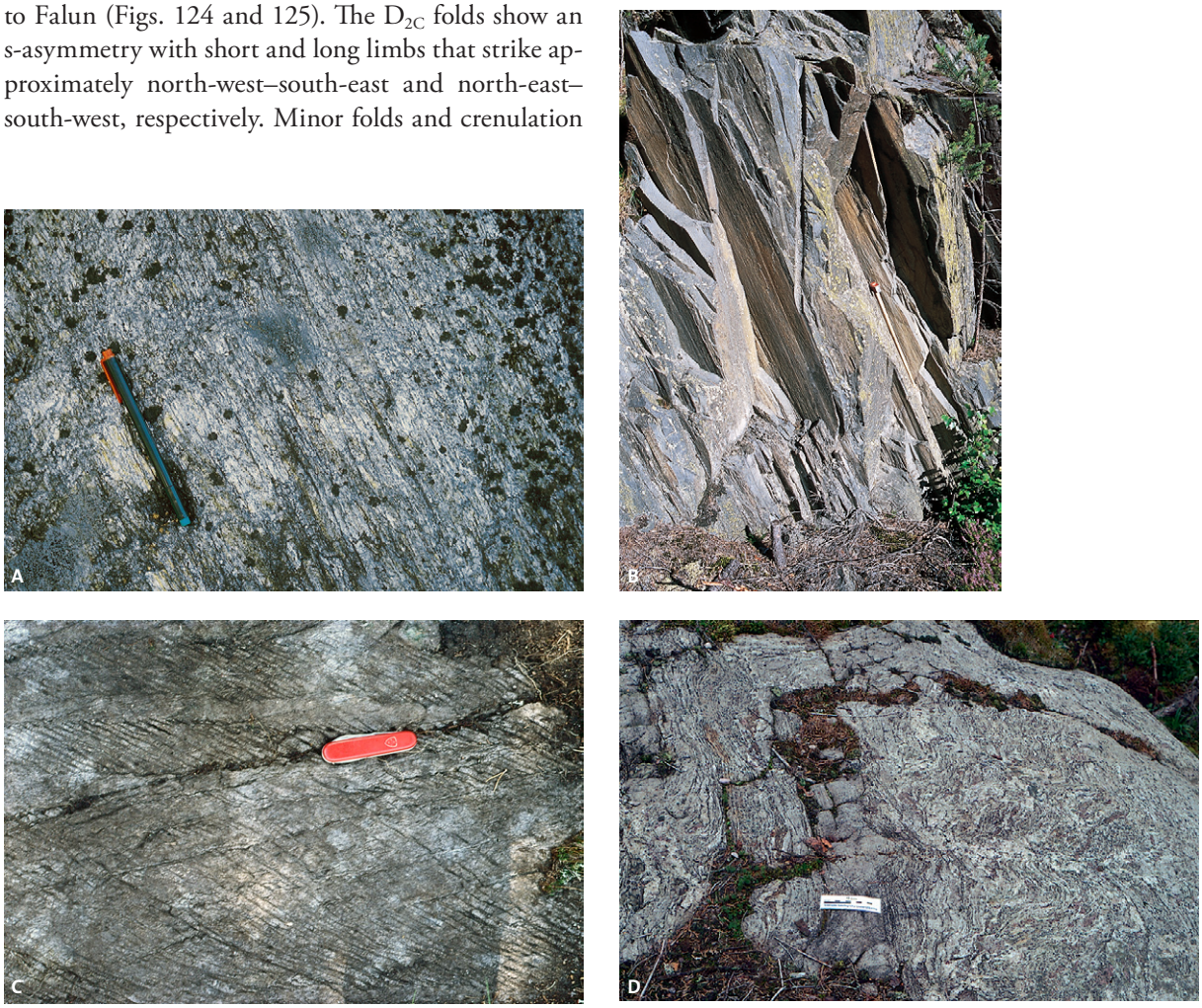

Fig. 136. D_{2C} mesoscopic structures in the central structural domain. The observations shown in A, B and C come from the medium-grade rocks in the northern part of the domain. By contrast, the observation shown in D comes from the high-grade rocks further south in this domain. **A.** Strongly developed S_{2C} foliation that has more or less completely transposed the older S_{1C} planar grain-shape fabric in a metagreywacke and meta-argillite sequence. The rocks strike north-east–south-west. View of vertical surface on the steeply dipping long limb of a major D_{2C} fold with s-asymmetry (12F Ludvika NO). Photograph: Michael Stephens (SGU). **B.** Strongly lineated, mica-poor felsic metavolcanic rock. The mineral lineation plunges steeply to the south-south-west and is subparallel to the axis of a mesoscopic fold with s-asymmetry that deforms both bedding and S_{1C}. View of vertical surface to the south (11F Lindesberg NO). Photograph: Michael Stephens (SGU). **C.** Bedded volcanogenic metagreywacke belonging to the *Larsbo formation* where the S_{2C} foliation (top left to bottom right in photograph) is strongly discordant to bedding and the S_{1C} planar grain-shape fabric (parallel to pocket knife). View of horizontal surface to the north (12G Avesta SO). Photograph: Michael Stephens (SGU). **D.** Migmatitic paragneiss with argillitic and sandy layers. Note the weaker development of leucosome in the sandy layers (e.g. beneath the scale marker) and the occurrence of pegmatitic leucosome along the axial surface of the mesoscopic D_{2C} folds that deform an older leucosome. View of horizontal surface to the north-west (10H Strängnäs SO). Photograph: Carl-Henric Wahlgren (SGU).

Fold axes show a moderate to steep plunge in an easterly direction (Fig. 137a). Mica-poor, metamorphosed volcanic and GDG intrusive rocks in these sub-areas are predominantly L-tectonites (Fig. 136b). The lineation shows a strong variation in plunge in predominantly the south-eastern quadrant on a stereographic projection (Fig. 137b). D_{1C} folds with gently plunging fold axes in a north-west–south-east direction, similar to those observed in the sub-area A east of Filipstad, have not been observed in sub-areas C–E.

D_{2C} folds, on different scales, also dominate the structure of the medium-grade rocks inside sub-areas F and G, west of Västerås and north of Sala, respectively (Figs. 124 and 125). In the former, the S_{2C} foliation strikes north-west–south-east, dips steeply and is locally discordant to both primary bedding and the S_{1C} fabric. However, these older structures are more commonly transposed into the S_{2C} foliation (see also above).

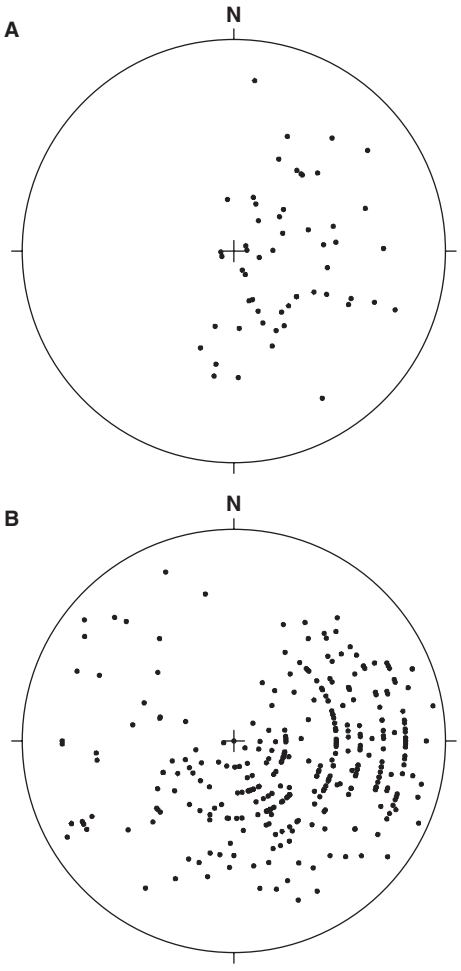

Fig. 137. Orientation of linear structures in sub-areas C, D and E (see Fig. 124), central structural domain. **A.** Minor fold axes (N = 55). **B.** Mineral stretching lineation (N = 326). All structures have been plotted on the lower hemisphere of an equal-area stereographic projection and have been compiled from the data set shown on the metamorphic, structural and isotope age map (Stephens et al. 2007b).

The intersection lineation between S_{1C} and S_{2C} and the D_{2C} fold axes generally plunge steeply to the south. As in other places, the mica-poor rocks are lineated and it was not possible to determine whether the mineral lineation formed during D_{1C}, D_{2C} or both these structural generations.

The dominant planar structure in sub-area G north of Sala is a foliation with an approximately east–west strike that forms an axial surface structure to D_{2C} folds. In the hinge of larger-scale structures, the S_{2C} foliation is distinctly discordant to the bedding and the S_{1C} planar grain-shape fabric (Fig. 136c, cf. Fig. 136a). Minor fold axes plunge moderately to the east (Prästhyttan) or moderately to steeply with more variable trend (Broddbo). Sub-area G is dominated by a major D_{2C} anticline with variable fold axis orientation.

Major folding (D_{2C}) of the planar tectonic fabric in high-grade, migmatitic rocks

Inspection of the form line (Fig. 124) and magnetic anomaly (Fig. 125) maps, in combination with field studies in the high-grade, migmatitic rocks in sub-areas H and I, east of Eskilstuna and north of Stockholm, respectively (Figs. 124 and 125), indicate once again the regional significance of D_{2C} structures on different scales. On the mesoscopic scale, these structures fold, for example, relics of bedding in migmatitic paragneiss as well as the gneissosity in these rocks (Fig. 136d). A pegmatitic leucosome is locally present along the axial surface trace of the D_{2C} folds (Fig. 136d). High-grade metamorphic conditions prevailed during both the development of the gneissic structure and the subsequent folding of this structure. Both the D_{2C} fold axes and mineral stretching lineation in sub-area H plunge gently to moderately in an approximately easterly direction (see Fig. 27 in Stålhös 1984).

3-D shape of the Guldsmedshyttan syncline using gravity modelling

Gravity data have been acquired along several profiles that transect the important ore-bearing belt from Nora in the south-west to Norberg in the north-east in the regional traverse study in Bergslagen (Werner et al. 1977, see also the section "Character, spatial distribution, geochronology, geochemical signature, petrophysical characteristics and regional geophysical signature of rock units"). This belt is dominated by iron oxide deposits (see section "Mineral and bedrock deposits"). The data were used to carry out gravity modelling work that provides, amongst other features, some constraints on the 3-D shape of the D_{2C} *Guldsmedshyttan syncline* in this part of the Bergslagen region (Werner et al. 1977). All profiles were measured with a point distance

of c. 100 m and the length of the profiles varies from 10 to 20 km (Fig. 138).

The metasedimentary rocks in the area between Nora and Norberg, including crystalline carbonate rock (marble), define a bedrock component with a higher density compared with the surrounding Svecofennian, 1.91–1.89 Ga felsic volcanic and subvolcanic intrusive rocks and GDG intrusive rocks. The density of marble used in the interpretation of the profiles varies from 2 780 to 2 890 kg/m^3 compared with the felsic metavolcanic rocks with a density of 2 660 kg/m^3. Even the metavolcanic rocks with intercalations of iron oxide deposits show a higher density and a value ranging from 2 730 to 2 990 kg/m^3 was used for these rocks in the modelling work.

Four profiles transect the *Guldsmedshyttan syncline* (see Plate 1 in Geijer & Magnusson 1944, Lundström 1983 and the section entitled "Mineral and bedrock deposits") on map-sheet 11F Lindesberg SV in the southern part of the study area. The positive gravity anomalies along the profiles are to a large extent caused by marble and only to a minor extent by metallic mineral deposits. The gravity modelling work indicates that the depth to the base of the marble unit in the major fold structure increases from 250 m along the southernmost profile (Siggebohyttan, see Fig. 138) up to 1.5 to 2.5 km along the profiles further north (Mårdshyttan and Storå, see Fig. 138).

Gravity modelling work along the five profiles further to the north, from Riddarhyttan to Norberg, shows that the gravity anomalies are mainly caused by a unit composed of metallic mineral deposits with higher density than the surrounding bedrock. Generally the ore-bearing unit produces a positive anomaly of 1–3 mGal.

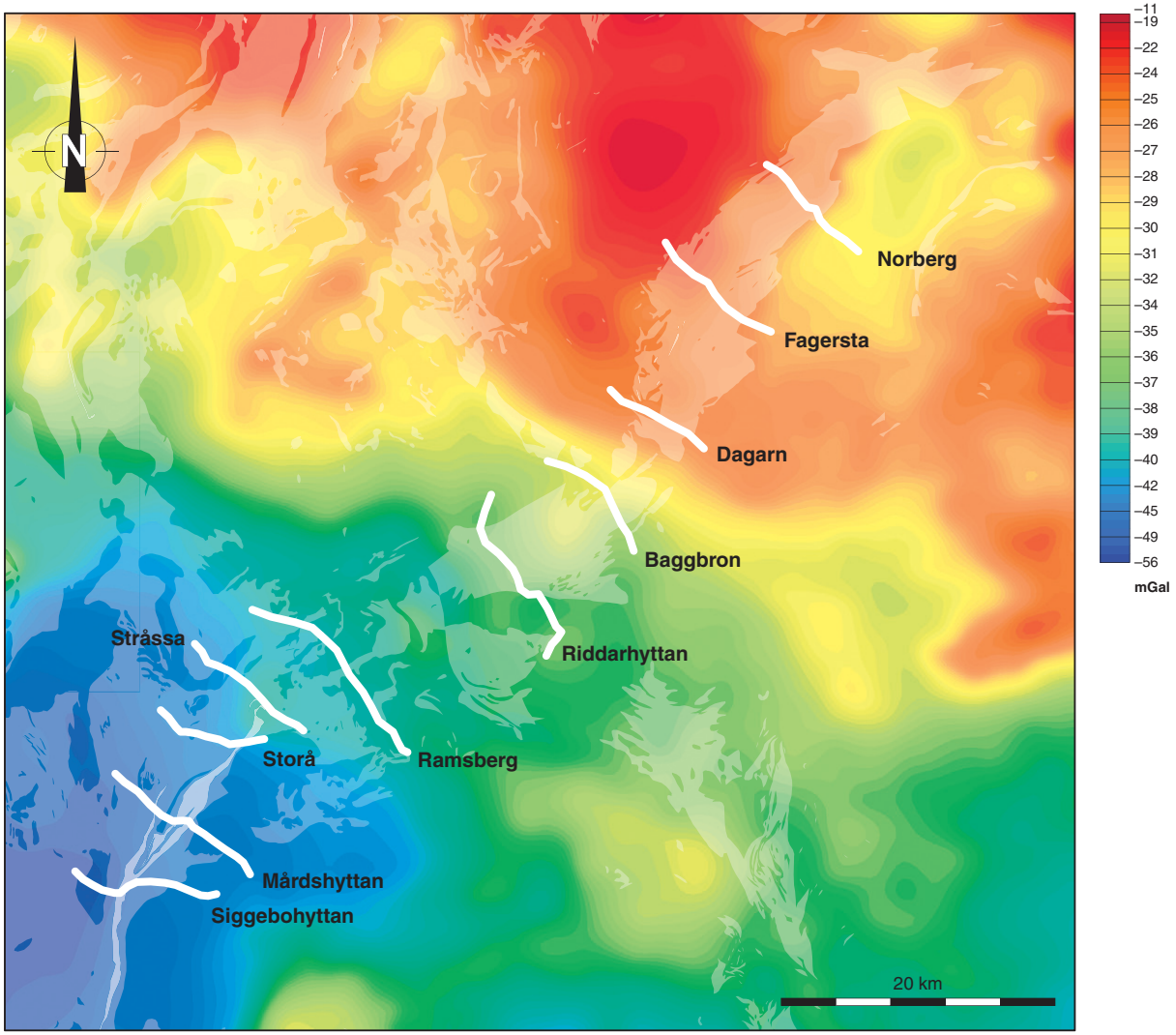

Fig. 138. Bouguer gravity anomaly map over the strongly mineralized area south-east of Norberg, central structural domain. The D_{2C} *Guldsmedshyttan syncline* (Plate 1 in Geijer and Magnusson 1944, Lundström 1983) is situated in the south-western part of this area. The pale white shade indicates the surface distribution of felsic metavolcanic and subvolcanic meta-intrusive rocks (1.91–1.89 Ga). The stronger white shade shows the surface distribution of crystalline carbonate rock, mainly in the hinge of the *Guldsmedshyttan syncline*. The gravity profiles discussed in the text are named and shown with white lines.

The depth of this unit also varies considerably along the profiles, with a greatest depth of 1.5 to 2.5 km along profiles Baggbron and Norberg (see Fig. 138).

Late-stage regional open folds and crenulation structure (D_{3C})

The trends of structural form lines especially in the western part of the central structural domain indicate that this area contains large-scale, open and upright folds with axial surfaces that strike north-west–south-east to north-north-west–south-south-east (Fig. 124). These structures deform the axial surface traces of the D_{2C} regional folds described above (e.g. south-west of Ludvika). Furthermore, the later folding that deforms the axial surface trace of the D_{2C} *Guldsmedshyttan syncline* (Fig. 121) is attributed to this late-stage, regional folding. In several of the sub-areas where field studies have been completed (sub-areas A, F and H) and in the bedrock east of Karlskoga, a late crenulation structure with similar axial surface orientation occurs in phyllosilicate-rich rocks without any or with only a weak development of a new axial surface cleavage (Fig. 139a). Locally, it is apparent that this crenulation structure deforms the D_{2C} intersection lineation (Fig. 139b). All these observations suggest that the central structural domain is affected by a D_{3C} phase of deformation.

Fig. 139. D_{3C} crenulation structures in the central structural domain. **A.** Crenulation of a complex tectonic foliation in a felsic metavolcanic rock, with the development of a non-penetrative, steeply dipping axial surface foliation (S_{3C}) that strikes north-north-west–south-south-east. The intersection lineation between the two foliations is subvertical. View of horizontal surface (10E Karlskoga NO). Photograph: Michael Stephens. **B.** Steeply plunging crenulation lineation (L_{3C}) that is strongly discordant to an older L_{2C} lineation. The L_{2C} lineation is oriented parallel to the pen and plunges moderately to steeply to the south-south-west. View of vertical surface to the east (11G Eskilstuna SV). Photograph: Michael Stephens (SGU).

Ductile high-strain belts or zones

Ductile high-strain belt established prior to D_{2C} folding in the Stockholm archipelago

Tectonically banded rocks, referred to as the *Ornö banded series* by Sundius (1939), define a ductile high-strain belt that extends for at least 80 km in a south-west–north-east direction within the archipelago south-east of Stockholm. This high-strain belt corresponds to a break in metamorphic grade between high-grade rocks to the north-west and rocks that are better-preserved and affected by metamorphism under medium-grade conditions to the south-east (see later text). The ductile high-strain character of this belt was recognized and described in Persson & Sjöström (2002), and the summary presented below is based on the results reported in this work. This high-strain belt continues to the south-west into the *Utö shear zone* on the island of Utö (Talbot 2008).

The *Ornö banded series* contains intrafolial and rootless folds, sheath folds and mylonitic rock in the form of striped gneisses. All these structures formed under high-temperature metamorphic conditions but, as noted in other areas of Bergslagen (e.g. northern structural domain), the high ductile strain occurred prior to the peak of metamorphism. In the Stockholm area, this peak is marked by the development of migmatitic rocks. A mineral stretching lineation and an intersection lineation, which both plunge to the north-east, are inferred to be related to the intrafolial and rootless folds within the shear fabric in the *Ornö banded series*. This fabric was subsequently refolded by large-scale structures that are parasitic to the major folds referred to as D_{2C} structures in this report (F_3 in Persson & Sjöström 2002, see comments earlier). A pegmatitic neosome locally formed along the spaced axial surface foliation to these later folds (cf. Fig. 136d). The *Ornö banded series* was also affected by retrograde ductile strain following the peak of metamorphism.

As at Forsmark, in the northern structural domain, the use of kinematic indicators is restricted on account of the strong static recrystallization shown by the rocks and the interference with later folding of the high-strain ductile fabric. Sinistral and north-west-side-up shear

dominates in the most intensely deformed parts of the *Ornö banded series* (Persson & Sjöström 2002). Shear along the long limbs of the later, large-scale folds with s-asymmetry is sinistral in character, whereas, along the short limbs of these structures, early stage sinistral and south-side-up shear is overprinted by dextral shear related to the folding (Persson & Sjöström 2002).

Possible ductile high-strain belt and ductile retrograde zones east of Eskilstuna

East of Eskilstuna in sub-area H, the form lines and magnetic maxima connections show a consistent east–west trend (Figs. 124 and 125). This structural trend extends several kilometres across the strike of the contacts between rock units and several tens of kilometres in this strike direction. Inspection of the trends of such structures to the east and west of sub-area H shows that the ductile strain in the bedrock south of Stockholm and north-east of Örebro, respectively, was absorbed by major D_{2C} folding of a penetrative S_{1C} tectonic fabric. On the basis of this regional analysis, a broad ductile high-strain belt in sub-area H has been inferred to be present on the northern flank of a large-scale, D_{2C} antiform with easterly plunge (Antal et al. 1998b).

Close to Strängnäs, within the inferred high-strain belt, retrograde ductile high-strain zones, up to c. 100 m wide, are present in the migmatitic gneisses. Grain-size reduction and transposition of the migmatitic structures into a mylonitic foliation (Fig. 140), in part with the development of a mylonitic banding, have been observed along these zones. The retrograde structures strike west-north-west–east-south-east, are either vertical or dip steeply to the north and contain a moderately to steeply plunging stretching lineation. Some evidence for a dextral strike-slip component of shear is present (Fig. 140) which is consistent with the location of these structures on the northern flank of the major D_{2C} antiform. The mylonitic structures are also deformed by folds that plunge gently to the west and show both z- and s-asymmetries.

Fig. 140. Transposed and retrograded migmatitic structure along a ductile high-strain zone with west-north-west–east-south-east strike in sub-area H close to Strängnäs, central structural domain. A component of dextral strike-slip displacement is inferred along this high-strain zone. View of horizontal surface to the south (10H Strängnäs NV). Photograph: Michael Stephens (SGU).

More detailed work is needed to resolve:

- the structural significance of the deformation with east–west trend, and
- the relationship between the structures in this inferred high-strain belt, the regional D_{1C} and D_{2C} structures discussed above and the younger, post-1.85 Ga ductile deformation that is prominent in the southern structural domain (see later text).

Ductile high-strain zones along flanks of D_{2C} folds

North-east of Uppsala, the contacts between rock units as well as the steeply dipping S_{1C} planar fabric generally strike east-north-east–west-south-west but are rotated locally into approximately north–south or north-north-east–south-south-west directions by major D_{2C} folds (Fig. 124) with steep fold axes (Stålhös 1991). Ductile high-strain zones with later reactivation in the brittle régime (see also below) have been inferred to be present along the short flanks of these fold structures (Bergman et al. 1996a, 1999c). The occurrence of mylonites along both a zone with north–south strike to the east of Gimo and a zone with north-north-east–south-south-west strike between Vattholma and Österbybruk (Stålhös 1991), in combination with the occurrence of cohesive fault breccias along the latter (Stålhös 1991), provided support to this interpretation.

A subsequent structural study along and in the vicinity of these two zones confirmed the steep plunge of the major D_{2C} fold axes and the occurrence of ductile high-strain zones along their short flanks (Persson & Sjöström 2003). This study also provided new kinematic data along the zones that were referred to as the *Gimo (GZ)* and *Österbybruk–Skyttorp (ÖSZ) Zones*, respectively (Persson & Sjöström 2003). Hydrothermal fluid flow in connection with later brittle and brittle-ductile deformation along the *ÖSZ* has also been described (Engström & Skelton 2002).

Striped gneisses and a composite CS fabric with stable hornblende and biotite indicate ductile deformation under amphibolite-facies conditions along the *GZ*, whereas microstructures and chlorite-bearing shear bands indicate upper greenschist-facies conditions for the ductile deformation along the *ÖSZ* (Persson & Sjöström 2003). The two zones share east-side-up displacement, commonly with a sinistral strike-slip component, whereas the *ÖSZ* possibly had an older(?), west-side-up sense of movement (Persson & Sjöström

2003). The possibly older movement along the *ÖSZ* was inferred to have occurred prior to the D_{2C} folding in connection with dextral strike-slip and south-west-side-up shear further north (Persson & Sjöström 2003), inside what is referred to here as the northern structural domain. The later, east-side-up and sinistral displacement along the *ÖSZ* occurred during the later stages of the D_{2C} folding (Persson & Sjöström 2003). All these structures, including the D_{2C} folds with their steep fold axes, were inferred to be related to progressive, bulk dextral strike-slip movement along the steep structures with west-north-west–east-south-east strike in the northern structural domain (Persson & Sjöström 2003).

Field and geochronological constraints on the timing of Svecokarelian ductile deformation

A compilation and evaluation of the quality of radiometric age data that constrain the timing of crystallization of igneous rocks that formed between 1.91 and 1.84 Ga has recently been completed for the central structural domain (Hermansson et al. 2008a). One of the purposes of this work was to constrain the timing of Svecokarelian ductile deformation in this part of the Bergslagen region. The ductile deformation under scrutiny concerns what has been referred to above as the D_{1C} fabric development, in particular the planar grain-shape fabric development. The timing of the later D_{2C} folding and the D_{3C} structures (see above) is not constrained by the radiometric age data.

Penetrative D_{1C} ductile deformation, of variable intensity and under amphibolite-facies metamorphic conditions, is constrained to the time interval between 1.88 and 1.86 Ga (Hermansson et al. 2008a). The establishment of this time span is based on the critical, intrusion–deformation relationships for two dated samples from the pre-tectonic GSDG intrusive rocks in the Åkersberga area (1875±6 Ma), close to Stockholm, and the older phase of intrusive rocks in the *Hedesunda granite* (1869±9 Ma), in the northern part of the domain, that are included in the 1.87–1.84 Ga GSDG intrusive rock suite (see especially Figs. 51b and 66b). The GSDG rocks at Åkersberga are affected by a penetrative, linear grain-shape fabric. By contrast, the older intrusive rocks in the *Hedesunda granite* were emplaced after penetrative ductile deformation of the country rock but were affected by ductile strain either during their emplacement, with the development of an igneous grain-shape fabric, or later in the solid state (Bergman et al. 2004a). The underlying assumption in this analysis is that the ductile grain-shape fabric in the GSDG rocks at Åkersberga belongs to the same generation of structures as the penetrative grain-shape fabric in the country rocks to the *Hedesunda granite*.

The establishment of a 1.88–1.86 Ga time span for the penetrative D_{1C} ductile deformation is consistent with the U-Pb (columbite) ages of pegmatites in the archipelago, south-east of Stockholm, that indicate a minimum age of 1.82 Ga for the high-T ductile strain along the *Ornö banded series* (Persson & Sjöström 2002). However, these pegmatites are themselves affected by retrograde ductile deformation after 1.82 Ga with the development of a stretching lineation and shear structures (Persson & Sjöström 2002).

The relationships described above are similar to those described in the Forsmark area in the northern structural domain. Furthermore, Persson & Sjöström (2002) suggested that the high-strain belt with north-east–south-west strike and with sinistral and north-west-side-up kinematic signature, south-east of Stockholm (*Ornö banded series*) in the central structural domain, and a high-strain belt with west-north-west–east-south-east strike and with dextral and south-west-side-up kinematic signature in the northern structural domain are conjugate structures on a regional scale. It is concluded that the central structural domain and at least the easternmost part of the northern structural domain, around Forsmark and Östhammar, share a similar tectonic history.

Southern structural domain: Two separate phases of Svecokarelian deformation under amphibolite-facies metamorphic conditions

Ductile high-strain belts or zones, intermediate sub-domains and regional folding of the planar tectonic fabric

In the area south of a line that extends approximately from Örebro in the north-west to Nyköping in the south-east, the structural form lines for the tectonic foliation define a family of bedrock corridors or sub-domains approximately 10–25 km wide, bounded by narrower bedrock strips where the foliation is steeply dipping and strikes west-north-west–east-south-east to north-west–south-east (Fig. 124). Within the intermediate sub-domains, the form lines trend east–west and, in easternmost areas, even north-east–south-west (Fig. 124). They rotate smoothly into a regular, west-north-west–east-south-east to north-west–south-east trend along the narrower bedrock strips (Fig. 124). The latter are inferred to represent a belt or more discrete zones of enhanced ductile strain along which body shape change involving intense attenuation of

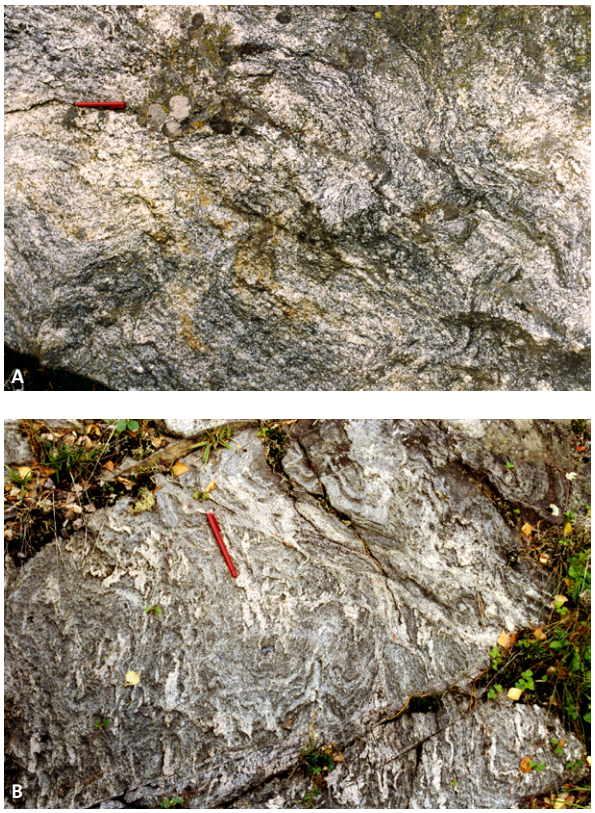

Fig. 141. Examples of high-grade ductile structures inside the sub-domains between inferred ductile high-strain zones, southern structural domain. **A.** Diatexitic migmatite with folded (D_{2c}) gneissosity (9H Nyköping SV). Photograph: Michael Stephens (SGU). **B.** Migmatitic veining in inferred supracrustal rock west of the Graversfors granite affected by D_{2c} folding (9G Katrineholm SV). Photograph: Michael Stephens (SGU).

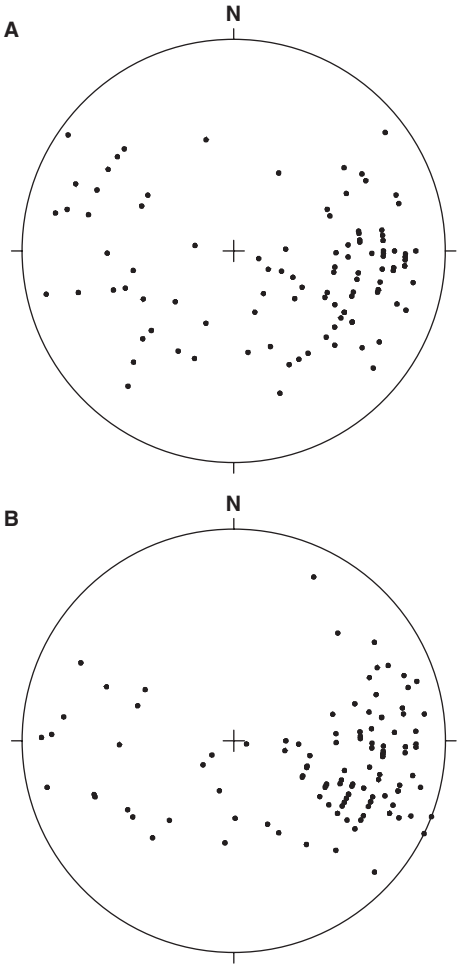

Fig. 142. Orientation of linear structures in the southern structural domain. a) Minor fold axes (N = 105). b) Mineral stretching lineation (N = 114). All structures have been plotted on the lower hemisphere of an equal-area stereographic projection and have been compiled from the data set shown on the metamorphic, structural and isotope age map (Stephens et al. 2007b).

rock units has occurred, whereas the intermediate sub-domains are dominated by older ductile structures. The intermediate sub-domains are structurally equivalent to the tectonic lenses identified in the northern structural domain.

The older mesoscopic structures (D_{1S} = first phase of deformation {D_1} in the southern {$_S$} structural domain) in the sub-domains between the inferred zones consist of a gneissosity, associated with extensive migmatization in the bedrock (Fig. 141), or a variably developed, commonly diffuse planar or linear grain-shape fabric. All these structures formed under amphibolite-facies metamorphic conditions.

Mesoscopic folds (D_{2S}) that deform the D_{1S} foliation are common within the sub-domains (Fig. 141). In especially the south-eastern part of the Bergslagen region, around Nyköping and east of Norrköping, major D_{2S} folds are prominent on a map scale between inferred zones (Fig. 124). These structures plunge gently to moderately to the east (Lundström 1974, Wikström 1975, 1979) along axial surface traces that trend approximately east–west. In general, minor folds and the mineral stretching lineation in the southern structural domain plunge gently to moderately to the east and south-east (Fig. 142). Relative to the central structural domain, there appears to be a lower frequency of steeply plunging linear structures (cf. Fig. 137). In the area between Zinkgruvan and Åsbro (Fig. 124), the structural form-line pattern is irregular (Fig. 124) and all rocks, including a satellite body to the 1.87–1.84 Ga GSDG suite of intrusive rocks, are folded by major, post-foliation folds. These structures also plunge gently to moderately, both eastwards and westwards, along axial surface traces with east–west strike and show a distinctive z-asymmetry (Wikström & Karis 1991).

Within a broad belt that extends approximately 5–10 km across strike on both sides of the boundary between the 1.87–1.84 Ga GSDG suite of intrusive rocks to the south and the older supracrustal and GDG in-

trusive rocks to the north, the structural form lines display a regional west-north-west–east-north-east trend (Fig. 124). In essence, the form lines are parallel to the contact between the different rock units. Isoclinal folds within this belt deform the contacts between the different lithologies, and display axial surface traces which also trend parallel to the trend of the belt.

The structural features in the broad structural belt with west-north-west–east-north-east strike described above are strongly reminiscent of the structural anisotropy in the ductile high-strain belts in the northern structural domain around Forsmark and Östhammar. It is also inferred to be a belt of enhanced ductile strain and is referred to here as the *Zinkgruvan–Finspång deformation belt* or *ZFDB* (Fig. 124). Since both the planar and linear tectonic fabrics in the *ZFDB* (S_{DB} and L_{DB}, respectively) and later folding (F_{DB}) affected the 1.87–1.84 Ga GSDG intrusive rocks and, consequently, formed after the emplacement of these rocks (see also below), all these structures are treated separately and referred to collectively as D_{DB}.

Several more discrete, ductile high-strain zones have been recognized in the southern structural domain (*Vingåker–Nyköping deformation zone {VNDZ}, Åsbro–Norrköping deformation zone {ÅNDZ}* and *Bråviken deformation zone {BDZ}* on Figure 124). The planar (S_{DZ}) and linear (L_{DZ}) structures within these ductile deformation zones are defined by a combination of reoriented older structures and a later retrogressive fabric that was established during the deformation along a particular zone (see below). The zones themselves are not rotated by the D_{2S} fold structures but are located along the limbs of these folds, i.e. they formed either in connection with or after this folding in a similar manner as the retrogressive ductile high-strain zones in the northern structural domain. However, small-scale folds deform the mylonitic fabric along the zones (F_{DZ}). All the planar and linear structures along the zones are referred to collectively as D_{DZ}.

Open folds with axial surface traces that trend approximately north–south and with broad fold wavelengths of 10 km or more (Fig. 124) define the youngest ductile structural feature in the southern structural domain. These open folds are reminiscent of the D_{3C} structures in the central structural domain.

The following text focuses attention on the characteristics of the three examples of the inferred ductile high-strain zones in the southern structural domain referred to above, i.e. the *VNDZ*, *ÅNDZ* and *BDZ* (Fig. 124). A more detailed structural analysis of the sub-domains between the ductile high-strain zones and the *ZFDB* was not carried out in the scope of the current work. The reader is referred to the relevant 1:50 000 bedrock geological map descriptions (see Table 1) for further information on these crustal segments.

Vingåker–Nyköping deformation zone

The *Vingåker–Nyköping deformation zone (VNDZ*) can be traced in a west-north-west–east-south-east strike direction from south-west of the lake Hjälmaren, where it is covered by fault-bounded Cambro-Ordovician rocks (Fig. 124), to east of Vingåker where it bifurcates into two separate, northern and southern branches. These branches merge together again at the lake Yngaren (Fig. 124) to define a tectonic lens approximately 50 km long and up to 6 km wide which is apparently little affected by *VNDZ* deformation. The zone continues south-eastwards to Nyköping (Fig. 124). Deformation linked to the *VNDZ* affected a variety of lithologies, including Svecofennian volcanic and subvolcanic intrusive rocks, the older suite of GDG intrusive rocks, and younger granites and pegmatites that belong to the GP intrusive suite. The deformation zone is estimated to be approximately 200–300 m thick.

Previous work near the lake Yngaren (Lundström 1974, Wikström 1983) and west of Katrineholm (Wikström 1983) recognized mylonites along a tectonic zone (Lundström 1974) or prominent topographic lineaments (Wikström 1983) that lie along the *VNDZ* as defined above. These features were inferred to be related to fracture zones or faults suggesting deformation in the brittle régime. However, both authors speculated that these zones had been active at an earlier stage (>1 Ga). The *VNDZ* displays no linear low-magnetic anomaly, as is often observed along younger, brittle deformation zones, and the only possible evidence for movement in the brittle régime is an apparent sinistral strike-slip displacement of a 0.98–0.95 Ga dolerite dyke with north-north-west–south-south-east strike along the southern shore of Yngaren (Wikström 1983).

Apart from the occurrence of mylonites and topographic lineaments, the *VNDZ* can be recognized by the smooth rotation of older, D_{1S} planar structures, which formed under amphibolite-facies metamorphic conditions, into the zone (Fig. 124). Outside the *VNDZ* and within the internal tectonic lens, these structures strike more or less east–west, oblique to the zone. High-magnetic anomalies, related to an increased content of magnetite in, for example, metasedimentary rocks or mafic sheets within felsic metavolcanic rocks, are also oriented along and thereby characterize the zone. In the Nyköping area, a high-magnetic anomaly related to a magnetite-rich, iron mineralization with east-north-east–west-south-west strike direction rotates smoothly into the *VNDZ* and may well account

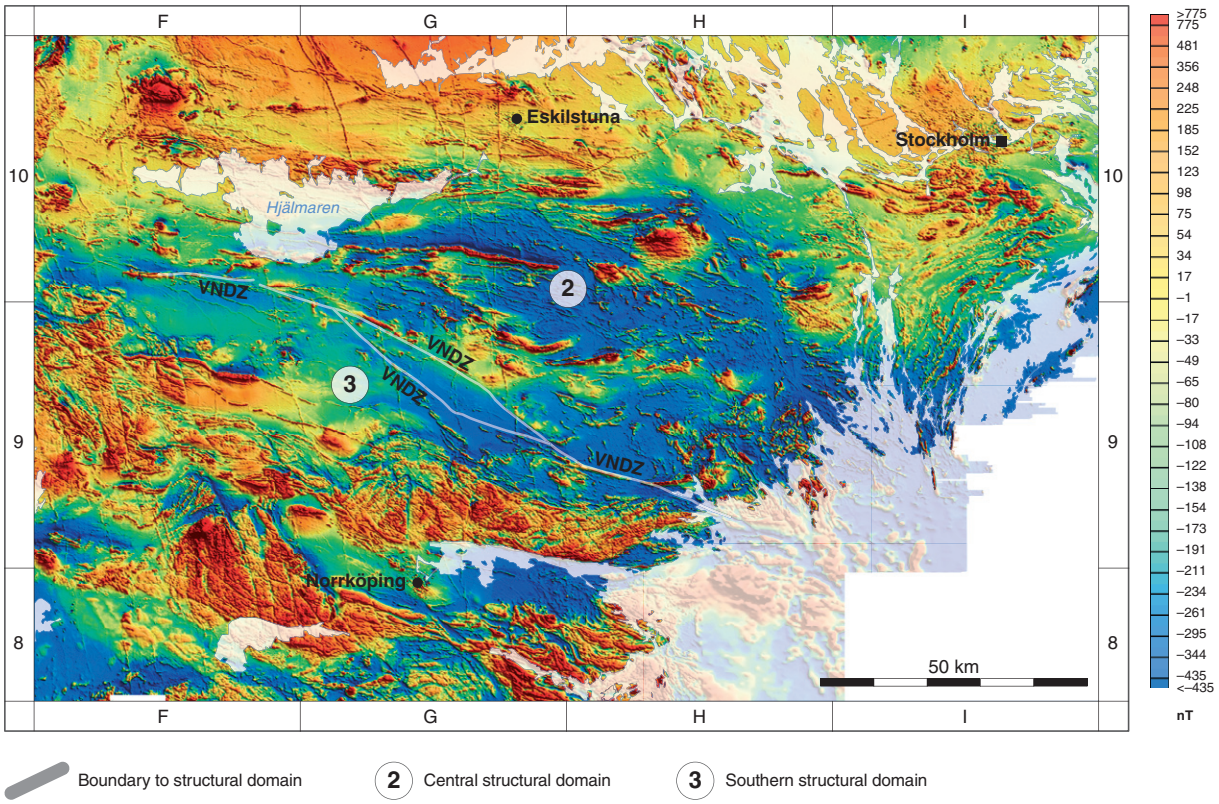

Fig. 143. Southern structural domain in the context of the magnetic anomaly map inferred from airborne magnetic data over the south-eastern part of the Bergslagen region. VDNZ = Vingåker–Nyköping deformation zone.

for the high-magnetic anomaly along the zone in this area (Fig. 143).

The smooth rotation of both pre-*VNDZ*, planar structures and high-magnetic anomalies into the zone is consistent with ductile strain and an important component of dextral strike-slip movement along the zone. West of Vingåker, the *VNDZ* also corresponds to a metamorphic break. Migmatitic GDG intrusive rocks and felsic metavolcanic rocks north of the deformation zone are separated by the *VNDZ* from non-migmatitic, GDG intrusive rocks and metasedimentary rocks to the south (see also later text).

Character, orientation and kinematic signature – deformation under greenschist-facies metamorphic conditions

Meso- and microstructures along the *VNDZ* have been studied at 19 field observation points (cf. Figs. 18 and 124). Structures related to ductile deformation along the zone include a protomylonitic or mylonitic foliation (S_{DZ}), a mineral stretching lineation (L_{DZ}) on the S_{DZ} surfaces and a variety of folds and fold axis lineations, most of which deform the S_{DZ} (F_{DZ}). The microstructures are described below according to rock type.

The S_{DZ} in the felsic metavolcanic rocks is characterized by ribbons of quartz, bands of K-feldspar±biotite retrogressed to chlorite, bands of K-feldspar+plagioclase feldspar+quartz+epidote+hornblende retrogressed to actinolite or tremolite, bands of quartz+epidote, or oriented white mica locally intergrown with chlorite. Orthoamphibole porphyroblasts are also aligned in the intense SL-fabric in these rocks.

Biotite retrogressed to white mica defines the S_{DZ} in the predominantly semi-pelitic metasedimentary rocks (Fig. 144a). A slightly positive magnetic lineament in mica schist along the western part of the *VNDZ*, south of the lake Hjälmaren (Fig. 143), may be related to the abundant post-S_{DZ} growth of metamorphic magnetite porphyroblasts (Fig. 144a).

The S_{DZ} in the older suite of GDG intrusive rocks is defined by ribbons of quartz, flattened feldspar porphyroclasts, or discontinuous sheets of oriented phyllosilicates with abundant white mica and chlorite locally retrogressive after biotite. In strongly mylonitic varieties, felsic bands and lenses, consisting of recrystallized, fine-grained aggregates of quartz and feldspar, alternate with phyllosilicate sheets. Twinned plagioclase feldspar porphyroclasts display bend or kink structures and fracturing (Fig. 144b). Some of these fractures are infilled with chlorite, and recrystallization of feldspar is restricted to the rims of the porphyroclasts. Transitions into less deformed and more well-preserved protoliths

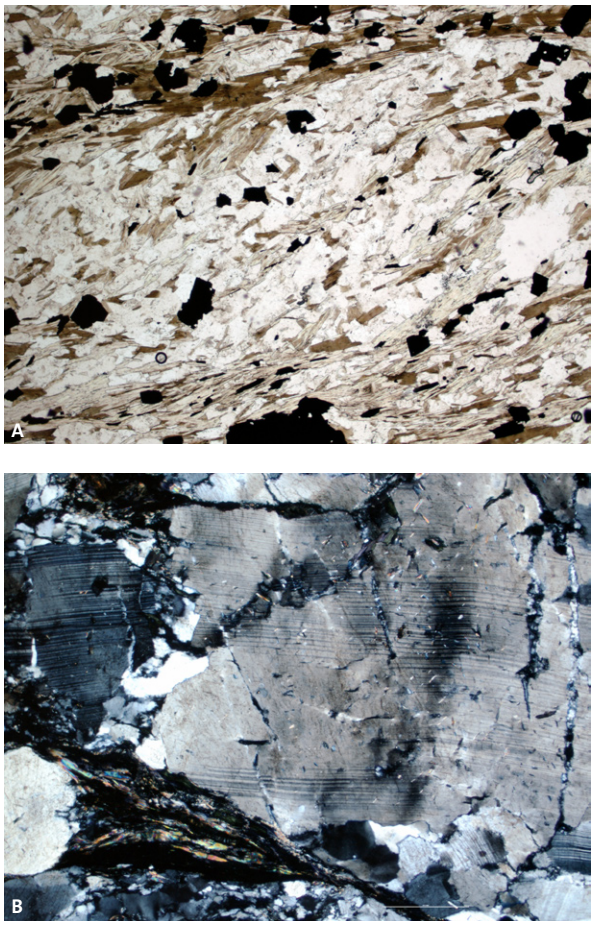

Fig. 144. Representative samples showing the microstructural developments in rocks along the *Vingåker–Nyköping deformation zone (VNDZ)*, southern structural domain. **A.** Biotite retrogressed to white mica along a foliation between shear bands and even along the shear bands (10F Örebro SO). The shear bands trend from bottom left to top right in the photograph. The spatial relationship between the foliation and the shear bands indicates a south-side-up, dip-slip component of movement at this locality. Magnetite porphyroblasts (black) grew statically after development of the retrogressed fabric. The photograph is 3.4 mm wide in a horizontal direction. Photograph: Sven Lundqvist and Michael Stephens (SGU). **B.** Brittle deformation with kinking and fracturing of twinning in plagioclase feldspar porphyroclast in metagranodiorite or metatonalite (9G Katrineholm NV). Chlorite, white mica and titanite are present along the shear band in the lower part of the photograph. Ribbons of quartz are also present in this thin-section. The photograph is 3.4 mm wide in a horizontal direction. Photograph: Sven Lundqvist and Michael Stephens (SGU).

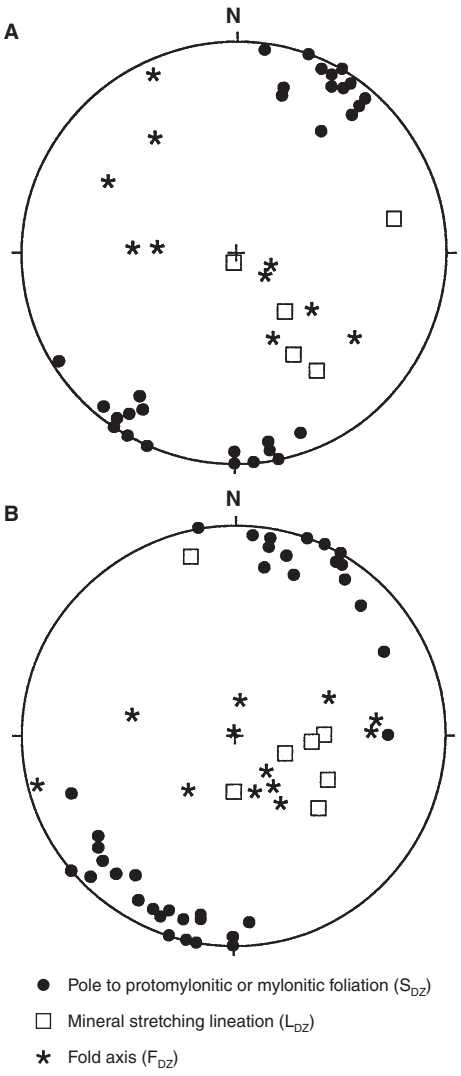

Fig. 145. Orientation of structures measured in different suites of meta-igneous rocks along ductile high-strain zones in the southern structural domain. All structures have been plotted on the lower hemisphere of an equal-area stereographic projection. **A.** *Vingåker–Nyköping deformation zone (VNDZ)*. **B.** *Åsbro–Norrköping* and *Bråviken deformation zones* (*ÅNDZ* and *BDZ*, respectively).

as well as mineralogical features (e.g. content of K-feldspar) suggest that several lenses of metasedimentary rocks marked on published geological maps along the *VNDZ* are highly deformed, more or less phyllonitic metagranitoids.

Since white mica and chlorite define S_{DZ} in the various protoliths along the *VNDZ*, this foliation is inferred to have developed under greenschist-facies metamorphic conditions. The presence of quartz ribbons and the common brittle behaviour of feldspar during the shear deformation are also consistent with movement along the *VNDZ* under low-grade conditions. The older deformation developed under amphibolite-facies conditions and is preserved in the rocks surrounding the deformation zone. White mica and chlorite are retrogressive after biotite. Furthermore, the retrogression of hornblende to actinolite or tremolite is also inferred to be related to the shear deformation along the *VNDZ*. Although virtually all minerals are oriented in the intense fabric along the *VNDZ*, metamorphic minerals such as biotite and amphibole may have crystallized prior to rather than during the deformation along this shear zone.

The S_{DZ} strikes west-north-west–east-south-east and is subvertical, whereas the L_{DZ} shows a variable, moderate to steep plunge to the south-east (Fig. 145a). Folds and intersection lineations (F_{DZ}) also display a highly

variable orientation within the mean S_{DZ} surface orientation (Fig. 145a). 11 of the 19 field observation points yielded kinematic indicators (Table 10). These indicators are based on the rotation of an older fabric into the S_{DZ} or on the relationships inside what is inferred to be a composite S_{DZ} fabric with foliation (S) and shear band (C or C′) components (e.g. Berthé et al. 1979, Platt & Vissers 1980, White et al. 1980, Hanmer & Passchier 1991). With the exception of one locality, more or less horizontal outcrop surfaces yielded a consistent dextral strike-slip sense of shear (Fig. 146a). The dip-slip component is unequivocally south-side-up (Figs. 144a and 146b). The kinematic field data indicate oblique, dextral south-side-up sense of shear along the *VNDZ*.

Åsbro–Norrköping and Bråviken deformation zones

The *Åsbro–Norrköping deformation zone (ÅNDZ*) has been traced in a west-north-west–east-south-east direction from Åsbro, which lies directly south of the outlier of Cambro-Ordovician rocks south-west of the lake Hjälmaren, to Igelfors where it apparently changes strike to a more north-west–south-east direction (Fig. 124). North-west of Norrköping, the deformation divides into three separate branches (Fig. 124). The northern branch strikes approximately east–west along the northern shore of Bråviken (*Bråviken deformation zone, BDZ*) and the two southern branches (*ÅNDZ*) strike north-west–south-east in the area to the south-east of Norrköping (Fig. 124). Bifurcation of the western branch is apparent south-east of Söderköping, south of the Bergslagen project area, and this principal branch of the deformation zone continues south-eastwards to the eastern coast of Sweden (Valdemarsvik).

Ductile deformation associated with the *ÅNDZ* and the *BDZ* affected a variety of lithologies. These include the Svecofennian volcanic and subvolcanic intrusive rocks, the older suite of GDG intrusive rocks, the 1.87–1.84 Ga GSDG suite of intrusive rocks and the granites and pegmatites that belong to the GP intrusive suite. Between Åsbro and Igelfors, the *ÅNDZ* is estimated to be several hundred metres thick. A similar thickness estimate is apparent for each of the three branches recognized close to Norrköping. Markedly thicker, intensely planar-foliated rocks with north-west–south-east and west-north-west–east-south-east strike (see also Wikström 1976) are inferred to have formed in connection with the shear deformation north-west of Norrköping, where the three branches converge and also interfere with the deformation along the *ZFDB*.

Previous work, which was carried out in connection with bedrock mapping at the local scale 1:50 000, recognized mylonites along tectonic zones (Kornfält 1975, Wikström 1975, 1976) and prominent topographic lineaments (Wikström & Karis 1991) that correspond to the *ÅNDZ*, as defined here. As for the *VNDZ*, these

Table 10. Kinematic data along the *Vingåker–Nyköping deformation zone (VNDZ).* The field observation points are tabulated in geographic order from south-east to north-west.

Field ID	N-S coordinate	E-W coordinate	Field data	Microstructural data
92-79	6519650	1552250	Dextral strike-slip component (shear bands). Strain gradient.	No data.
91-36	6525900	1538300	Sinistral strike-slip component (shear bands). Folds with s- and z-asymmetry.	No data.
91-37	6526400	1535900	Dextral strike-slip component (σ porphyroclasts).	No data.
92-58	6535900	1530800	Dextral strike-slip component (shear bands). Folding of hydrothermal quartz veins. Strain gradient.	South-side-up dip-slip component (shear bands).
92-55	6533150	1523950	Dextral strike-slip component (folding with z-asymmetry).	No data.
92-56	6532950	1523650	Dextral strike-slip component (shear bands).	South-side-up dip-slip component (shear bands). Retrogressive deformation with biotite altered to white mica, chlorite.
92-49	6545400	1511050	Dextral strike-slip component (shear bands).	Quartz ribbons. Brittle deformation in feldspar.
92-50	6545550	1510800	South-side-up dip-slip component (shear bands and tile structure in feldspar). Strain gradient.	No data.
92-52	6549100	1507850	Dextral strike-slip and south-side-up dip-slip components (shear bands).	No data.
92-84	6552500	1499800	Dextral strike-slip component (shear bands).	South-side-up dip-slip component (shear bands).
92-87	6553400	1485350	Dextral strike-slip component (shear bands).	South-side-up dip-slip component (shear bands). Retrogressive deformation with biotite altered to chlorite.

features were interpreted as fracture zones or faults, thus emphasizing deformation in the brittle régime. Indeed, the lineament with east–west trend along Bråviken has been interpreted as a geologically relatively young (post-Cambrian) fault (Wikström 1976, 1979). Although all these studies as well as Lundström (1974) postulated a long history of movement along these lineaments, based principally on the occurrence of intrusive rocks (GP intrusive rocks, dolerite dykes) either along them or parallel to their strike direction, they did not recognize that the brittle structures followed broader zones of concentrated ductile strain within the Svecokarelian orogen.

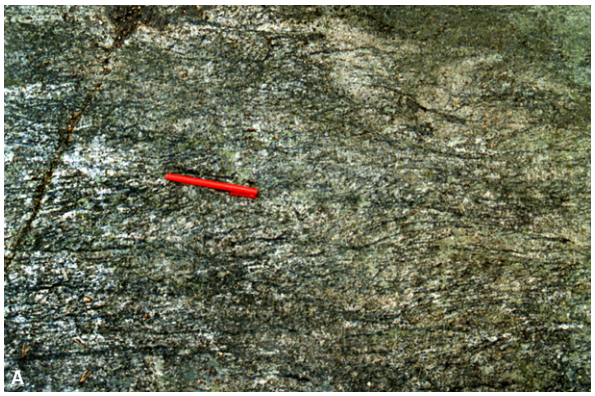

Fig. 146. Kinematic indicators along the *Vingåker–Nyköping deformation zone (VNDZ)*, southern structural domain. **A.** Dextral strike-slip component of movement based on the relationship between a planar grain-shape fabric (S) and C′-type shear bands observed in a more or less horizontal outcrop surface viewed to the north along the *VNDZ* (9G Katrineholm NV). Photograph: Michael Stephens (SGU). **B.** South-side-up, dip-slip component of movement based on the relationship between a planar grain-shape fabric (S) and shear bands (C-type) parallel to the pen, observed in a steeply dipping outcrop section viewed to the west along the *VNDZ* (9G Katrineholm NV). Photograph: Michael Stephens (SGU).

On a megascopic scale, the concentration of ductile deformation along both the *ÅNDZ* and the *BDZ* can be recognized by the smooth rotation of older, Svecokarelian D_{1S} planar structures, which formed under amphibolite-facies metamorphic conditions, into these zones (Fig. 124). Between Åsbro and Igelfors, the form lines of older D_{1S} planar structures between the *ÅNDZ* and the *VNDZ* strike east–west to east-north-east–west-south-west and rotate smoothly into a west-north-west–east-south-east direction as they approach the *ÅNDZ*, in a manner that indicates an apparent dextral strike-slip sense of shear. South-east of Igelfors, the dextral rotation of older structures into the *ÅNDZ* is more conspicuous. This is compatible with the slightly larger angle between the *ÅNDZ* and the older D_{1S} structures. A distinctive contrast in the orientation of linear, high-magnetic anomalies from a north-east–south-west strike direction north of the *ÅNDZ* to north-west–south-east along this zone is also evident in the area north-west of Norrköping (Fig. 143). Between Åsbro and Igelfors and near Norrköping, the *ÅNDZ* also corresponds to breaks in regional metamorphic grade (Kornfält 1975, Wikström & Karis 1991, see below).

The discordance between older D_{1S} planar structures and a younger ductile deformation zone, and the dextral rotation of the older structures into the deformation zone are also well-illustrated along the *BDZ*, east of Norrköping (Fig. 124). Furthermore, a smooth rotation of linear, high-magnetic trails from an east-north-east–west-south-west into a west-north-west–east-south-east direction provides further documentation of the *BDZ* (Fig. 143).

Character, orientation and kinematic signature – deformation under amphibolite- and greenschist-facies metamorphic conditions

Meso- and microstructures along the *ÅNDZ* and *BDZ* have been studied at 30 field observation points (cf. Figs. 18 and 124). The types of structures considered to be linked to deformation along these shear zones are similar to those observed along the *VNDZ*.

The S_{DZ} in inferred supracrustal rocks along the *ÅNDZ* is defined by an intense tectonic banding (Fig. 147a, b) with individual bands rich in biotite, plagioclase feldspar+quartz+biotite, K-feldspar+quartz+biotite, or quartz + feldspar. The quartz and feldspar

Fig. 147. Deformation under different metamorphic conditions along the *Åsbro–Norrköping deformation zone (ÅNDZ),* the *Bråviken deformation zone (BDZ)* and the *Zinkgruvan–Finspång deformation belt (ZFDB),* southern structural domain. **A.** View to the east on steep road section of high-temperature mylonitic banding (striped gneiss) in migmatitic supracrustal rock (*ÅNDZ*, *BDZ* or *ZFDB*, 9G Katrineholm SV). The bending of the planar structures into the highly deformed part in the central part of the outcrop indicates a south-side-up, dip-slip component of movement. High ductile strain under amphibolite-facies metamorphic conditions is inferred. Photograph: Michael Stephens (SGU). **B.** Detailed view of the highly deformed rock shown in Figure 147a (9G Katrineholm SV). Photograph: Michael Stephens (SGU). **C.** View to the west on steep road section of high-temperature mylonitic banding (striped gneiss) in metagranitoid that belongs to the 1.90–1.87 Ga GDG intrusive rock suite with pegmatite veins (*ÅNDZ*). The mylonitic banding developed under amphibolite-facies metamorphic conditions. Note how the pegmatite veins are deformed along the S_{DZ} foliation and contain an internal grain-shape fabric. The S_{DZ} dips steeply to the south-south-west and the internal foliation within the veins is subvertical. The deformation that affected the pegmatite veins is inferred to show a south-side-up, dip-slip component of movement (9F Finspång NV). Photograph: Michael Stephens (SGU). **D.** Biotite retrogressed to chlorite and recrystallized ribbons of quartz along an S_{DZ} fabric (*BDZ*, 9G Katrineholm SV). The photograph is 3.4 mm wide in a horizontal direction. Photograph: Sven Lundqvist and Michael Stephens (SGU).

grains have recrystallized and show apparently little deformation whereas the biotite grains are well-oriented along the S_{DZ}. Local ribbons of recrystallized quartz and porphyroblasts of amphibole (cummingtonite with hornblende rims and brownish hornblende with greenish hornblende rims) are also oriented along the S_{DZ}. In some samples, biotite grains show retrogression to chlorite and white mica, whereas thicker bands with conspicuous grain-size reduction and extensive retrogression of biotite to chlorite are also present.

Fig. 148. Deformation along the *Bråviken deformation zone (BDZ)* in the southern structural domain, inferred to have occurred under greenschist-facies metamorphic conditions. **A.** View to west-northwest showing retrogressed migmatitic paragneiss along ductile high-strain zone structurally beneath contact to metabasic rock to left in photograph (9G Katrineholm SO). Photograph: Michael Stephens (SGU). **B.** Composite foliation–shear band (S–C/C′) fabric in the retrogressed migmatitic paragneiss shown in Figure 148a. A south-side-up, dip-slip component of movement is inferred. The red pen marking is parallel to the C-type shear bands. C′-type shear bands, defined in part by a thin trail of magnetite grains, are present in the lower part of the photograph (9G Katrineholm SO). Photograph: Sven Lundqvist and Michael Stephens (SGU).

Distinctive strain gradients from migmatite into banded mylonitic rocks are apparent along parts of the *BDZ*. A retrogressed (phyllonitic), migmatitic paragneiss along an individual ductile deformation zone within the *BDZ* (Fig. 148a) contains alternating biotite-rich and biotite+quartz+feldspar bands along the S_{DZ} (C surfaces). An oblique, planar grain-shape fabric, defined by oriented biotite grains, is conspicuous in the more quartz+feldspar-rich bands and weakly developed C′-type shear bands are present in the biotite-rich, C-type shear bands (Fig. 148b).

There is considerable variation in the appearance of the S_{DZ} in both the GDG intrusive rocks and the 1.87–1.84 Ga suite of GSDG intrusive rocks along the *ÅNDZ*. One variety shows an intense, mylonitic banding (Fig. 147c) with well-oriented biotite overgrown by titanite and more feldspar-rich bands drawn out into a ribbon-like structure. The quartz and feldspar grains are equigranular and fully recrystallized, and there is no evidence for retrogression to greenschist-facies minerals (chlorite, white mica). The S_{DZ} in a second variety is commonly defined by oriented biotite and quartz as well as variably flattened, feldspar porphyroclasts. Biotite and plagioclase feldspar show retrogression to white mica. A third type shows a distinctive mylonitic banding with bands rich in flattened and fractured feldspar porphyroclasts alternating with sheets rich in chlorite, epidote and titanite, and thin quartz ribbons which display dynamic recrystallization (Fig. 147d). Plagioclase feldspar porphyroclasts are altered to white mica and epidote, and the twinning structure in the feldspar grains is bent and fractured.

Granitic and pegmatitic veins (GP suite) in the GDG intrusive rocks lie parallel or slightly oblique to the S_{DZ} and, as in the supracrustal rocks, display an internal planar grain-shape fabric that bends into the S_{DZ} along the contact to the host metagranitoid (Fig. 147c). Rotation of the veins more or less into the S_{DZ} is inferred.

The association of an intense banding and a biotite planar fabric with equigranular and fully recrystallized quartz and feldspar grains suggests that deformation along the *ÅNDZ* was active under amphibolite-facies metamorphic conditions. The attenuation of GP veins along the segments of the *ÅNDZ* which display deformation under amphibolite-facies metamorphic conditions suggests that this deformation occurred after the peak of metamorphism. Similar deformation is inferred to be present along the *BDZ*. However, the growth of white mica and chlorite after biotite along the S_{DZ}, the style of deformation in plagioclase feldspar and the occurrence of quartz ribbons that display dynamic recrystallization indicate that deformation under retrogressive, greenschist-facies metamorphic conditions has also occurred along both these zones.

The orientation of mesoscopic structural elements along the *ÅNDZ* and *BDZ* (Fig. 145b) is similar to that along the *VNDZ* (cf. Fig. 145a). 11 of the 30 field observation points have yielded kinematic indicators defined by rotation of an older foliation into a mesoscopic ductile shear zone or a composite foliation-shear band (S–C/C′) fabric (Table 11). A combination of dextral strike-slip and south-side-up dip-slip sense of shear is supported by these data irrespective of whether the deformation occurred under amphibolite- or greenschist-facies metamorphic conditions (Figs. 147a, 147c and 148b).

Table 11. Kinematic data along the *Åsbro–Norrköping* and *Bråviken deformation zones* (*ÅNDZ* and *BDZ*, respectively). The field observation points are tabulated in geographic order from south-east to north-west along each zone.

Field ID	N-S coordinate	E-W coordinate	Field data	Microstructural data
Åsbro-Norrköping deformation zone				
92-92	6477000	1538200	South-side-up dip-slip component (shear bands).	No data.
92-102	6485650	1529350	Strain gradient.	Dextral strike-slip component (shear bands and folding). Retrogressive deformation.
92-77	6504900	1508950	No data.	Dextral strike-slip component (shear bands). Quartz ribbons. Retrogressive deformation.
91-51	6506700	1507750	South-side-up dip-slip component (shear bands). Strain gradient. Younger brittle deformation shows south-side-down kinematics.	Amphibolite-facies deformation. Static recrystallization.
91-33	6509050	1507000	South-side-up dip-slip component (shear bands). Folding.	No data.
91-34	6523300	1502850	Dextral strike-slip component (shear bands). Folding of mylonitic foliation.	Retrogressive deformation.
91-40	6523900	1502100	No data.	South-side-up dip-slip component (shear bands). Retrogressive deformation with biotite altered to white mica.
91-29	6535100	1468550	South-side-up dip-slip component (shear bands). Folding of mylonitic foliation.	Amphibolite-facies deformation. Static recrystallization.
91-30	6539100	1463250	Dextral strike-slip component (shear bands).	No data.
91-46	6542600	1452650	No data.	Dextral strike-slip component (shear bands, (σ porphyroclasts). Brittle deformation in feldspar.
Bråviken deformation zone				
92-67	6503100	1545550	South-side-up dip-slip component (shear bands). Strain gradient.	South-side-up dip-slip component (shear bands).

Field and geochronological constraints on the timing of Svecokarelian ductile deformation

The D_{1C} planar grain-shape fabric and gneissic banding in the migmatitic rocks in the central structural domain can be traced southwards into the D_{1S} structures in the bedrock corridors between the ductile high-strain zones in the southern structural domain (Fig. 125), i.e. the D_1 structures in both domains are inferred to be identical. On this basis, it is inferred that the D_{1S} ductile structures also formed around 1.88 to 1.86 Ga (see above). Even the major D_{2C} fold structures in the central structural domain can be traced into the southern domain where, however, they become much tighter. The presence of pre-1.85 Ga ductile deformation, which formed under amphibolite-facies metamorphic conditions, is strongly supported by the intrusion–deformation field relationships and geochronological data from the 1.87–1.84 Ga suite of GSDG intrusive rocks in the Askersund area (see section "Character, spatial distribution, geochronology, geochemical signature, petrophysical characteristics and regional geophysical signature of rock units" and especially Fig. 66a).

The amphibolite-facies deformation along the *ZFDB* as well as the tight folding of the grain-shape fabric immediately north of this belt clearly affected the 1.87–1.84 Ga GSDG suite of intrusive rocks (see above). Ductile deformation under retrograde metamorphic conditions after 1.85 Ga has been demonstrated in the northern structural domain and it is inferred that the retrograde deformation along the zones with west-north-west–east-south-east to north-west–south-east strike in the southern structural domain (*VNDZ*, *ÅNDZ* and *BDZ*) also occurred after 1.85 Ga.

It is concluded that at least two major phases of ductile deformation under amphibolite-facies metamorphic conditions, prior to 1.85 Ga and after 1.85 Ga, are prominent in the southern structural domain. Furthermore, the reduced interlimb angle of the major folds that can be traced from the central into the southern structural domain is related to an increased significance of the post-1.85 Ga deformation to the south in the Bergslagen region. It is speculated that the late open folds with axial surface traces that strike approximately north–south in the southern structural domain can be correlated with the D_{3C} structures in the central structural domain (see above). The intrusion–deformation relationships in the southern domain suggest that this deformational event also occurred after 1.85 Ga.

Western structural domain: Sveconorwegian tectonic overprint

Interference between Sveconorwegian and older ductile structures

In the western structural domain, the broadly west-north-west–east-south-east structural grain in the Svecokarelian orogen is overprinted by structures which strike approximately north–south (Fig. 124). The latter is related to the Sveconorwegian tectonic overprinting in this domain (Wahlgren et al. 1994, Page et al. 1996, Söderlund et al. 1999).

Once again it is vital to emphasize that not necessarily all the structures that lie in the north–south orientation were formed during the younger tectonic event. Structures formed during older events may have been simply rotated into the younger structural grain. This point is important to keep in mind when considering the north–south trend of major Svecokarelian fold structures with their associated gravity maxima in the Filipstad area (*Saxå* and *Grythyttan synclines* on Figure 79). Furthermore, large areas affected by penetrative, Svecokarelian deformation and amphibolite-facies metamorphism are present north-east of Karlskoga and east of lake Skagern in the western structural domain. Tectonic lenses sandwiched between the inferred Sveconorwegian structures with north–south trend are also present in the GSDG rocks in the westernmost part of the domain (Fig. 124). These lenses contain an older west-north-west–east-south-east structural grain, inferred to be Svecokarelian or younger in age, or consist of more or less undeformed bedrock that is 1.8 Ga or younger.

Bearing in mind these considerations, there is some difficulty to constrain in space the eastern boundary of the Sveconorwegian orogen in the Bergslagen region. The attempt shown in Figure 124, for example, simply uses the inferred eastern limit of significant ductile high-strain zones that bear the kinematic and metamorphic signatures of Sveconorwegian tectonics. The eastern boundary of penetrative Sveconorwegian deformation under amphibolite-facies metamorphic conditions occurs further to the west, for example close to Kristinehamn (Fig. 124, see also below). This boundary corresponds to the eastern limit of gneissic metaigneous rocks which have been generally referred to in the literature as the *Southwest Scandinavian Domain* (e.g. Gaál & Gorbatschev 1987).

In the western structural domain, intrusive rocks belonging to the 1.87–1.84 Ga, 1.81–1.78 Ga and 1.70–1.67 Ga GSDG intrusive rock suites (see section "Character, spatial distribution, geochronology, geochemical signature, petrophysical characteristics and regional geophysical signature of rock units") dominate the bedrock. Svecofennian supracrustal rocks, different suites of GDG intrusive rocks and rocks belonging to the GP intrusive suite are also present. Furthermore, younger dolerites that belong to both the 1.60–1.56 Ga and 0.98–0.95 Ga suites (see same section referred to above) are conspicuous. Penetrative, Svecokarelian deformation that occurred under greenschist- or amphibolite-facies metamorphic conditions affected the rocks older than 1.8 Ga. However, all rock units are affected by later, non-penetrative or penetrative deformation under greenschist- or amphibolite-facies metamorphic conditions, respectively, that is inferred to be Sveconorwegian in age (see also below). There remains considerable uncertainty concerning the timing of amphibolite-facies deformation with west-north-west–east-south-east trend in the rocks immediately west and south-west of Skagern (Fig. 124). The bedrock in this area has been included in the GSDG suite dominated by 1.81–1.78 Ga intrusive rocks and the amphibolite-facies deformation is either Sveconorwegian (Wahlgren et al. 2005, Stephens et al. 2007b) or older.

Regional tectonic framework of the Sveconorwegian orogen

The structural framework for the Sveconorwegian orogen in Sweden was initially established by Berthelsen (1980) with the introduction of informal tectonostratigraphic units from east to west across the orogen, the *Eastern segment*, the *Medium segment* and the *Östfold slab*. The continuation of the *Eastern segment* east of Kristinehamn into the western part of the Bergslagen region was proposed in this pioneer work. New structural geological, geochronological and reflection seismic data from the north-eastern part of the Sveconorwegian orogen, partly including the western structural domain in the Bergslagen region (Fig. 124), were presented in, for example, Wahlgren et al. (1994), Page et al. (1996), Stephens et al. (1996), Söderlund et al. (1999) and Juhlin et al. (2000). The text that follows provides a brief overview of the results in these studies, with attention addressed on the structures related to the Sveconorwegian overprint. These data confirmed the broad structural framework envisaged by Berthelsen (1980), but the kinematic data motivated some revision of Berthelsen's work (see below).

Earlier phase of Sveconorwegian deformation and metamorphism

The Sveconorwegian ductile strain inside the western structural domain consists of a grain-shape fabric with

Fig. 149. Kinematic indicators along the Karlskoga–Kristinehamn transect in the western structural domain. **A.** Composite fabric between foliation and shear bands (probably C′-type) in protomylonitic, porphyritic granite to quartz monzonite that belongs to the 1.81–1.78 Ga suite of GSDG intrusive rocks (10E Karlskoga NO). The view is to the south-east in a steep face. The dip-slip sense of movement is west-side-up. Photograph: Michael Stephens (SGU). **B.** Tiling structure in K-feldspar phenocrysts in similar rock as that shown in Figure 149a (10E Karlskoga NO). The view is once again to the south-east in a steep face and the dip-slip movement is west-side-up. Photograph: Michael Stephens (SGU). **C.** Composite fabric between foliation and shear bands (probably C-type) in protomylonitic, porphyritic granite to quartz monzonite that belongs to the 1.70–1.67 Ga suite of GSDG intrusive rocks (10E Karlskoga SV). The view is to the north in a steep face. The dip-slip sense of movement is west-side-up. Photograph: Carl-Henric Wahlgren (SGU). **D.** Fold with z-asymmetry in 1.70–1.67 Ga suite of GSDG intrusive rocks immediately north of Kristinehamn (10E Karlskoga NV). View of vertical surface to the north. The fold vergence indicates a west-side-up sense of movement. Photograph: Carl-Henric Wahlgren (SGU).

both planar and linear components. The planar grain-shape fabric varies in strike from north-west–south-east in the northern part of the domain to north–south and, locally, north-east–south-west in the area between Karlskoga and the lake Skagern (Fig. 124). It once again shows a north–south or north-west–south-east strike south of Skagern (Fig. 124).

There is distinctive variation in the intensity of the Sveconorwegian ductile strain at different scales. On a regional scale, the ductile strain varies from spaced to semi-penetrative to penetrative from east to west across the western structural domain. This strain gradient is prominent along the Karlskoga–Kristinehamn transect, where the Sveconorwegian orogen shows its widest extension in the western structural domain, and corresponds to a change in the syn-deformational metamorphic conditions from greenschist facies in the east to amphibolite facies further west (Wahlgren et al. 1994 and see below). As a result of this variation, mappable tectonic lenses, where the bedrock is not affected

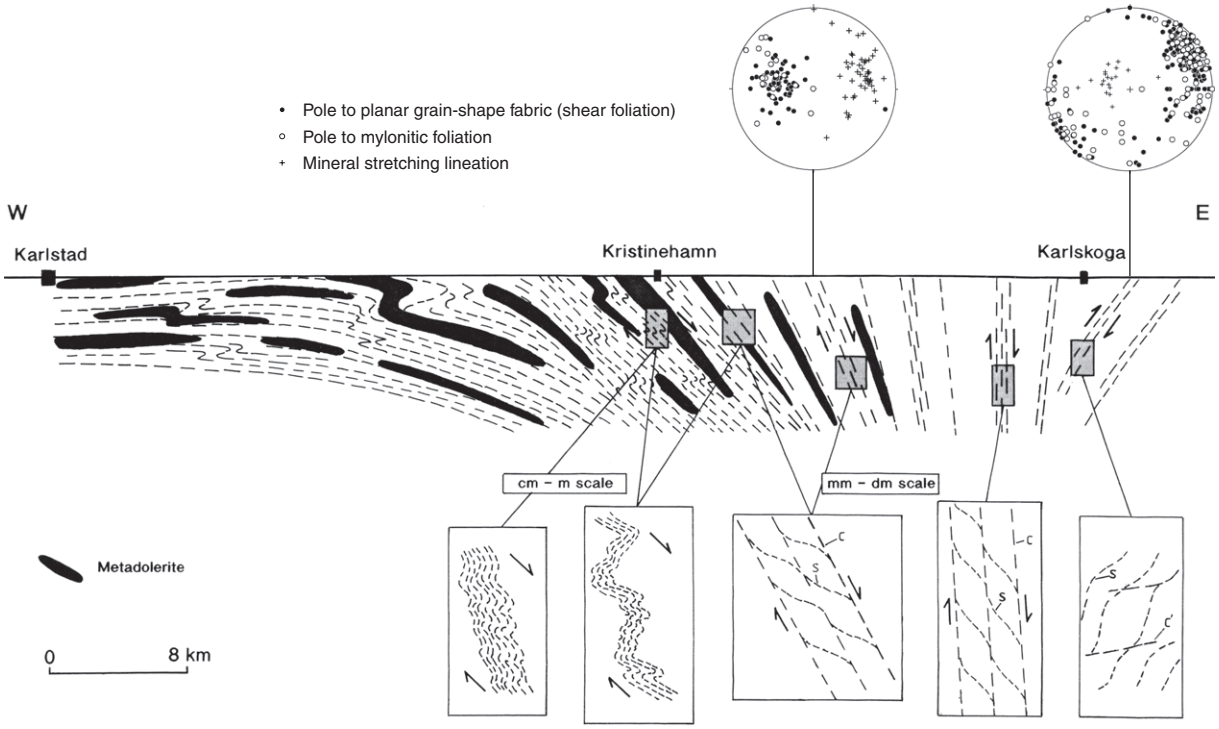

Fig. 150. Schematic structural section across the eastern part of the Sveconorwegian orogen, from Karlskoga in the east to Kristinehamn in the west, in the western structural domain, and further west to Karlstad (after Wahlgren et al. (1994). Horizontal and vertical scales are identical. The flat-lying structures west of Kristinehamn are also apparent down to depths of 5 to 6 km in seismic reflection profile studies (Dahl-Jensen et al. 1991, Dyrelius et al. 1992). Structural orientation data from east of Kristinehamn and north-east of Karlskoga after Wahlgren et al. (1994).

by Sveconorwegian deformation, become less frequent in westernmost areas.

There is also a significant variation in the intensity of Sveconorwegian ductile strain on a local scale with the development of ductile high-strain zones with evidence for shear displacement (Fig. 149). Composite planar fabrics (CS and C′S), winged porphyroclasts (σ- and less commonly δ-type), tiling structure and rotation of older structures indicate that dip-slip movement predominates with a west-side-up sense of shear (Fig. 149a–c). Asymmetric folding of the planar and linear grain-shape fabrics becomes conspicuous in westernmost areas, where the strain is penetrative in character, and the vergence of these folds is also consistent with a west-side-up sense of movement (Fig. 149d).

Along a west to east transect immediately north and north-east of the lake Vänern, between Karlstad to the west of the Bergslagen region and Karlskoga to the east inside this region, the shear foliation constitutes a strongly asymmetric fan-like structure (Wahlgren et al. 1994 and Fig. 150). In the penetratively deformed area between Karlstad and west of Kristinehamn, the ductile structures are subhorizontal. In the Kristinehamn area, the shear foliation dips gently to moderately to the east, is subvertical further to the east and dips steeply to the west in the easternmost frontal part of the orogen around Karlskoga (Fig. 150). An integrated evaluation of the structural orientation and kinematic data indicates apparent extensional and apparent compressional ductile shear deformation from west to east across the domain (Figs. 149 and 150). The fan-like configuration of the shear foliation in the western structural domain has been verified in a 17 km long reflection seismic profile from the eastern shore of lake Vänern, south of Kristinehamn, and eastwards (Juhlin et al. 2000).

The broad-scale structural geometry in the western structural domain is similar to that envisaged by Berthelsen (1980). However, the established west-side-up sense of displacement across the entire frontal part of the orogen, does not support thrusting to the west along the east-dipping shear zones in the western part of the area as suggested by Berthelsen (1980). The structures here show apparent extensional shear strain (see Wahlgren et al. 1994).

Later phase of Sveconorwegian deformation and metamorphism

The significant change in strike direction of the regional ductile structures in the Karlskoga–Skagern area (Fig. 124) is a result of a younger phase of Sveconorwegian deformation along a high-strain belt. This belt

contains a high frequency of steeply dipping, ductile high-strain zones that were active under greenschist-facies metamorphic conditions, are steeply dipping with north-east–south-west strike and show a dextral strike-slip component of movement (Fig. 151a).

Such structures are also conspicuous between the lakes Skagern and Vättern, in the vicinity of the lake Unden (Fig. 151b). In this area, there is close spatial and temporal relationship between steeply dipping or subvertical ductile high-strain zones that strike north-east–south-west and show a dextral strike-slip component of movement, a subordinate set that strikes north-west–south-east to west-north-west–east-south-east and shows a sinistral strike slip component of movement and a third set that is more significant east of Unden (Wikström & Karis 1998), strikes north–south and shows west-side-up and predominantly reverse movement (Wahlgren et al. 2005).

These relationships have been explained to be the result of shortening in an approximately east–west direction (Wahlgren et al. 2005). The zones that strike north-east–south-west and north-west–south-east to west-north-west–east-south-east and show significant strike-slip movement have been inferred to form a conjugate set (Wahlgren et al. 2005) and to have behaved as lateral ramp structures in close orientation to the bulk shortening direction. In contrast, the structures that strike north–south, which are oriented at a much higher angle to the bulk shortening direction, have absorbed the ductile strain by predominantly dip-slip (reverse) movement as a frontal ramp structure.

One of the conclusions of the work carried out by Wahlgren et al. (1994) was to question the usage of the term *Protogine Zone* (Gorbatschev 1980) for the high-strain zones along what was, prior to this paper, inferred to be the frontal part of the Sveconorwegian orogen. In particular, it was shown that the so-called *Protogine Zone* in the Kristinehamn area simply corresponds to the changeover to penetratively deformed GSDG intrusive rocks *within* the eastern part of the orogen. The eastern boundary of the orogen was extended some 40 km further to the east. It was proposed that the term *Sveconorwegian Frontal Deformation Zone (SFDZ)* should be used for the complex network of steeply dipping, ductile and brittle deformation zones with north–south strike south of the lake Vättern (see Fig. 4) and it was inferred that this complex strain belt continued northward into the late Sveconorwegian structures in the Karlskoga–Skagern area. However, there is a strong possibility that the structures referred to as the *Protogine Zone* south of Vättern represent a complex mixture of structures that belong to both the earlier and later phases of Sveconorwegian deformation north of this lake as well as even pre-Sveconorwegian structures.

Fig. 151. Later phase of Sveconorwegian deformation under greenschist-facies metamorphic conditions in the western structural domain. **A.** Deflection of an older protomylonitic shear foliation in porphyritic granite to quartz monzonite (1.81–1.78 Ga GSDG intrusive rock suite) into a younger, ductile high-strain zone that strikes north-east–south-west. The latter is included in the *Sveconorwegian Frontal Deformation Zone (SFDZ)* as defined in Wahlgren et al. (1994). The view is on a top face and a dextral strike-slip component of movement along the younger shear zone is inferred. Photograph: Michael Stephens (SGU). **B.** Dextral deflection of an older, penetrative foliation in coarsely porphyritic granite to quartz monzonite (1.87–1.84 Ga GSDG intrusive rock suite) into a younger, vertical ductile high-strain zone that strikes north-east–south-west. The latter is included in the *Sveconorwegian Frontal Deformation Zone (SFDZ)* as defined in Wahlgren et al. (1994). Photograph: Carl-Henric Wahlgren (SGU).

Field and geochronological constraints on the timing of Sveconorwegian ductile deformation

Rb-Sr metamorphic mineral ages around 0.9 Ga from the area close to Filipstad (Verschure et al. 1987) provided the first indications of a Sveconorwegian tectonic overprint in the Bergslagen region. However, the earlier phase of post-Svecokarelian deformation in the western structural domain, with variable grain-shape fabric development related to non-coaxial ductile strain under greenschist- and amphibolite-facies metamorphic conditions, is only poorly constrained by the protolith

ages of the rocks affected by this phase. Such data in the area suggest that this deformation and metamorphism occurred between the intrusion of dolerites at 1.60–1.56 Ga and the deposition of Neoproterozoic clastic sedimentary rocks (see section "Character, spatial distribution, geochronology, geochemical signature, petrophysical characteristics and regional geophysical signature of rock units"). The relative time relationship between the early phase of post-Svecokarelian deformation and metamorphism and the 0.98–0.95 Ga suite of dolerites is not constrained.

U-Pb ages between 0.98 and 0.95 Ga (uncertainties included) for metamorphic titanites in metagranite in the penetratively deformed rocks north of the lake Vänern (Söderlund et al. 1999) provided firmer constraints on the timing of the regional, grain-shape fabric development. The preservation of igneous titanites, which display U-Pb ages similar to U-Pb (zircon) ages around 1.7 Ga for the metagranites, indicate that no major tectonic event had affected the *Eastern segment* in the area north of Vänern, from the time of emplacement of these 1.7 Ga GSDG rocks until the late Sveconorwegian tectonic overprinting (Söderlund et al. 1999). ^{40}Ar-^{39}Ar hornblende ages in the range 1009–965 Ma are present in the same area (Page et al. 1996) but some uncertainties remain concerning especially the older ^{40}Ar-^{39}Ar hornblende ages due to difficulties with excess argon.

The zones that are included in the younger *SFDZ* structural complex deform the 0.98–0.95 Ga suite of dolerites with north-north-west–south-south-east strike, east of Karlskoga, and retrograde these rocks locally to greenschist [see section "Mesoproterozoic and Neoproterozoic dolerites and associated rocks (1.60–1.56 Ga, 1.48–1.46 Ga, 1.27–1.26 Ga and 0.98–0.95 Ga)"]. ^{40}Ar-^{39}Ar (white mica) ages in the time range 936 to 900 Ma (uncertainties included) have been interpreted to date the later phase of Sveconorwegian deformation along the *SFDZ* (Page et al. 1996).

Structural model for Sveconorwegian ductile deformation

Notwithstanding the consistent kinematic data, there remains uncertainy concerning whether the earlier phase of Sveconorwegian deformation including grain-shape fabric development was related to the build-up of an imbricate thrust stack in a compressional tectonic setting or to regional east–west extension (Wahlgren et al. 1994). Both models were proposed in Wahlgren et al. (1994) and these authors favoured the compressional model. Evidence for regional east–west extension is provided by the intrusion of the 0.98–0.95 Ga dolerites in a north–south direction along the Sveconorwegian orogen. Furthermore, Möller (1998) has suggested that extension was a main cause for the decompression and exhumation of high-pressure rocks in the southern part of the orogen.

On the basis of kinematic data and geological time constraints, Wahlgren et al. (1994) concluded that the later phase of Sveconorwegian deformation along the *SFDZ* in the Karlskoga–Skagern area was compressional in character. It is important to emphasize again that the deformation along the *SFDZ* affected the dolerites in the 0.98–0.95 Ga suite and, for this reason, occurred after the regional east–west extension. Wahlgren et al. (1994) suggested that the deformation along the *SFDZ* accounted for a rotation of the earlier Sveconorwegian structures and the establishment of their fan-like configuration in the area between Karlskoga and Kristinehamn. Alternatively, the fan-like structure formed as a result of the rotation of the early Sveconorwegian structures in connection with exhumation of the deeper crustal segments in the southern part of the Sveconorwegian orogen. In this alternative, the fan-like structure was established prior to the later phase of deformation along the *SFDZ*.

METAMORPHISM

Input data and limitations – a short overview

The quartz- and feldspar-rich character of the dominant lithologies in the Bergslagen region seriously hinders the use of mineral parageneses for the establishment of the grade of metamorphism in this region. However, the metamorphic minerals in mafic rocks, the metamorphic minerals in especially the more pelitic facies in metasedimentary rocks and the onset of anatectic melting in the bedrock provide some control on the regional variation in the grade of metamorphism in the region. Several pressure-temperature (P-T) determinations have also been carried out that provide quantitative constraints on the metamorphic conditions. Finally, direct geochronological constraints on the timing of metamorphism using U-Pb (zircon, monazite, titanite) ages and subsequent cooling using ^{40}Ar-^{39}Ar (hornblende, biotite, white mica), (U-Th)/He (apatite) and apatite fission track ages are also available.

As indicated below, the effects of two major phases of metamorphism associated with Svecokarelian and Sveconorwegian tectonic activity as well as more local contact metamorphism around 1.7 Ga are preserved in different parts of the Bergslagen region. Furthermore, Svecokarelian tectonic activity between 1.9 Ga and 1.8 Ga involved different phases of ductile deformation and metamorphism.

Critical data that document the detailed overprinting relationships between the different phases of Svecokarelian metamorphic mineral growth are lacking. This statement is also relevant where it concerns the relationship between, for example, the aluminosilicates andalusite and sillimanite. Furthermore, there is also relatively little published information that specifically addresses the detailed relationships between deformation and metamorphism. Notwithstanding these limitations, inspection of map descriptions (Table 1) and local detailed work in, for example, the northern and central structural domains (see above) indicate that many of the rocks show a static recrystallization with strain-free grains. It is inferred that the metamorphic peak was established after penetrative ductile deformation had already affected the bedrock. As indicated above, folding on different scales followed the establishment of the metamorphic peak.

Distribution of key metamorphic minerals

The documentation of metamorphic minerals is available in the various detailed map descriptions in the Bergslagen region (see Table 1). Chlorite, albite and epidote are present in the fine-grained mafic rocks in the Grythyttan area and this assemblage indicates greenschist-facies metamorphic conditions, lower than that observed elsewhere in the Bergslagen region. The finer-grained mafic rocks in the remaining part of the Bergslagen region affected by the Svecokarelian orogeny (Fig. 5) are dominated by the metamorphic minerals hornblende, plagioclase feldspar and biotite, i.e. these rocks occur as amphibolite and the metamorphism occurred under amphibolite-facies or higher-grade conditions. Garnet-bearing amphibolite is locally present in Mesoproterozoic mafic rocks in the westernmost part of the region, where the metamorphic mineral assemblage was established during the Sveconorwegian orogeny (Fig. 5).

The metamorphic minerals andalusite, cordierite, garnet and sillimanite are sporadically present in the central and the coastal, south-easternmost parts of the Bergslagen region (Fig. 152). The sporadic occurrence of these minerals is related in part to the limited occurrence of rocks with suitable composition. These areas are also characterized by the absence of migmatitic structures (Fig. 152) and the common occurrence of muscovite in stable association with quartz. These data indicate metamorphism under lower or middle amphibolite facies. In contrast, cordierite, garnet, sillimanite (and very rarely staurolite) are conspicuous in the southern and northernmost parts of the region (Fig. 152). Migmatitic structures are also common in these areas, especially in the south-eastern (Norrköping–Västerås–Stockholm–Nyköping area) and northernmost parts (Fig. 152). Furthermore, muscovite and quartz were unstable and broke down to give K-feldspar, sillimanite and fluid. Metamorphism under upper amphibolite or higher-grade conditions is inferred. The absence of kyanite and other higher-pressure minerals is a characteristic metamorphic feature of the Bergslagen region.

Hypersthene is a relatively uncommon mineral in the Bergslagen region. However, it has been documented in some isolated occurrences of charnockitic GDG rocks in the area between Västerhaninge and Stockholm (Fig. 153) and in charnockitic 1.8 Ga GSDG rocks close to Karlskoga (Fig. 153). Hypersthene and garnet as well as cordierite, garnet, sillimanite and andalusite are also locally present in inferred contact aureoles to the 1.87–1.84 Ga (e.g. Nygården), 1.81–1.78 Ga (Karlskoga) and 1.70–1.67 Ga (south-west of Karlskoga) suites of GSDG intrusive rocks (Fig. 153 and see text below). Metamorphism under granulite-facies conditions in these areas is inferred.

Pressure-temperature (P-T) determinations

Pertinent information bearing on the fifty pressure-temperature (P-T) determinations in the Bergslagen region is summarized in Table 12 and a statistical analysis of these data is presented in Figure 154. In this analysis, the data from the central part of the region, where the bedrock is affected by Svecokarelian lower or middle amphibolite-facies metamorphism, are separated from the data in the southern part of the region, where the rocks are commonly affected by Svecokarelian migmatization (Fig. 152). These two areas are included in separate metamorphic domains that are referred to here as the central medium-grade and southern migmatitic metamorphic domains, respectively (see below).

Some of the samples in the bedrock in the southern migmatitic metamorphic domain (Fig. 154) have been taken from gneissic rocks that lack any distinctive spatial relationship at the ground surface to younger intrusive rocks. Examples include the samples from the Flen and Nyköping areas and have been inferred to represent the regional metamorphism (Andersson 1997c, Sjöström & Bergman 1998). However, several of the samples in this Svecokarelian high-grade metamorphic domain have been taken in the close vicinity of either the 1.87–1.84 Ga or the 1.81–1.78 Ga GSDG intrusive suites, and their metamorphic mineral parageneses are inferred to have formed during contact metamorphism. Examples include the granofelsic rocks in the Nygården and Karlskoga areas, respectively (Andersson et al. 1992, Wikström & Larsson 1993, Andersson 1997c).

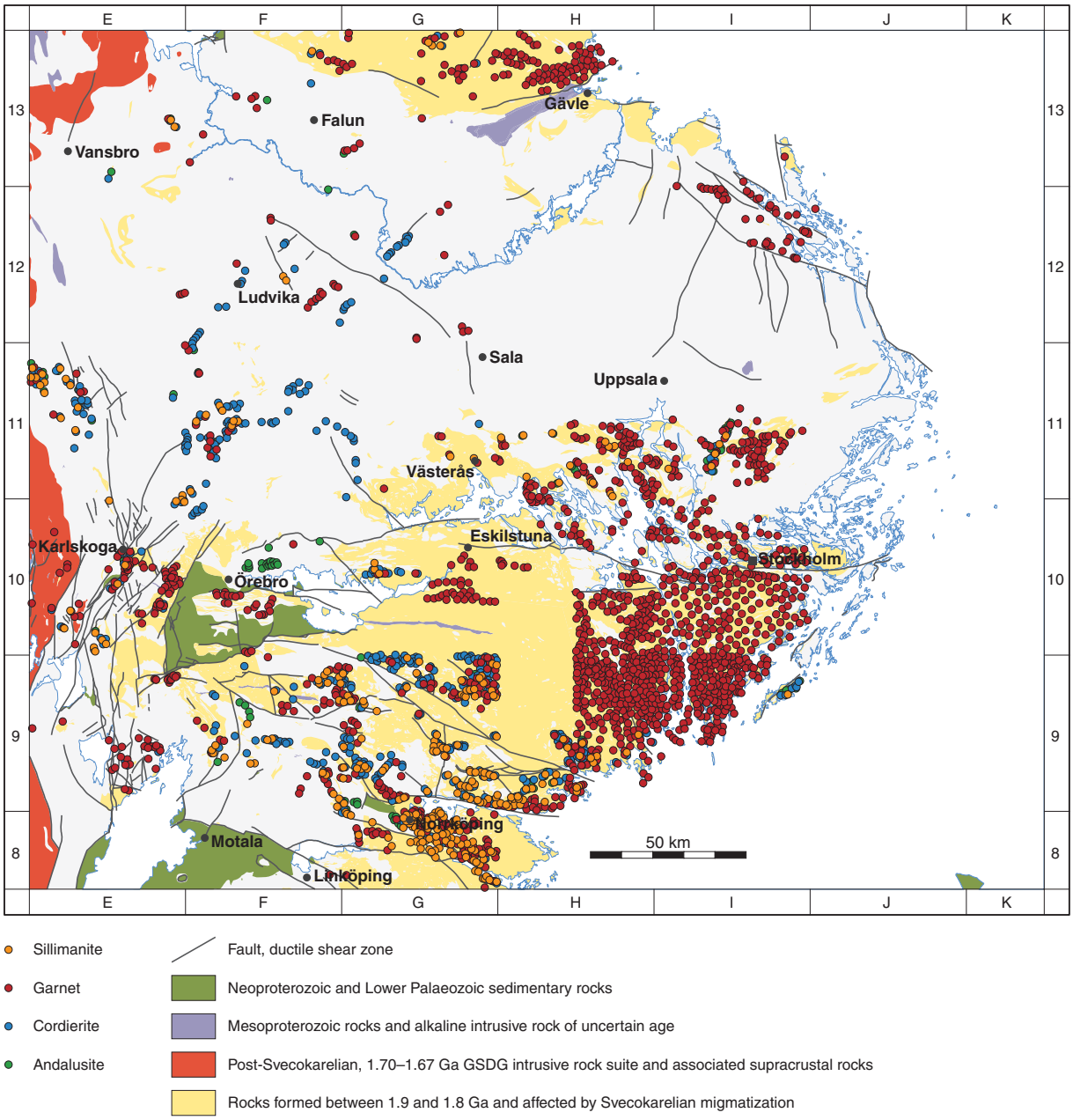

Fig. 152. Occurrence of andalusite, cordierite, garnet, sillimanite and rocks with migmatitic structure in the Bergslagen region. The absence of key minerals in some areas reflects the absence of data and data description rather than true differences in the frequency of occurrence of these minerals (see also Fig. 6).

Bearing in mind these considerations, it is apparent that the P-T data from the southern migmatitic domain represent different metamorphic events, both regional and contact, and complementary U-Pb (monazite) geochronological data provide support to this statement (see later text). By contrast, the samples from the central medium-grade metamorphic domain (Fig. 154) have been considered to be entirely representative of the regional metamorphism (Sjöström & Bergman 1998). However, as indicated below, it is possible that a rigid distinction between so-called regional and contact (sensu lato) metamorphism in the Bergslagen region is unnecessary and actually misleading.

In both the central medium-grade and southern migmatitic metamorphic domains, the majority of pressure determinations lie between 4 and 6 kbar. However, the variation in the pressure values is higher in the samples from the central part of the Bergslagen region and values in the range 3–10 kbar have been obtained in relatively resticted areas around both Arlanda and Östhammar. It is also noteworthy that there is a high variation in pressure values, in the range 2–7 kbar, in

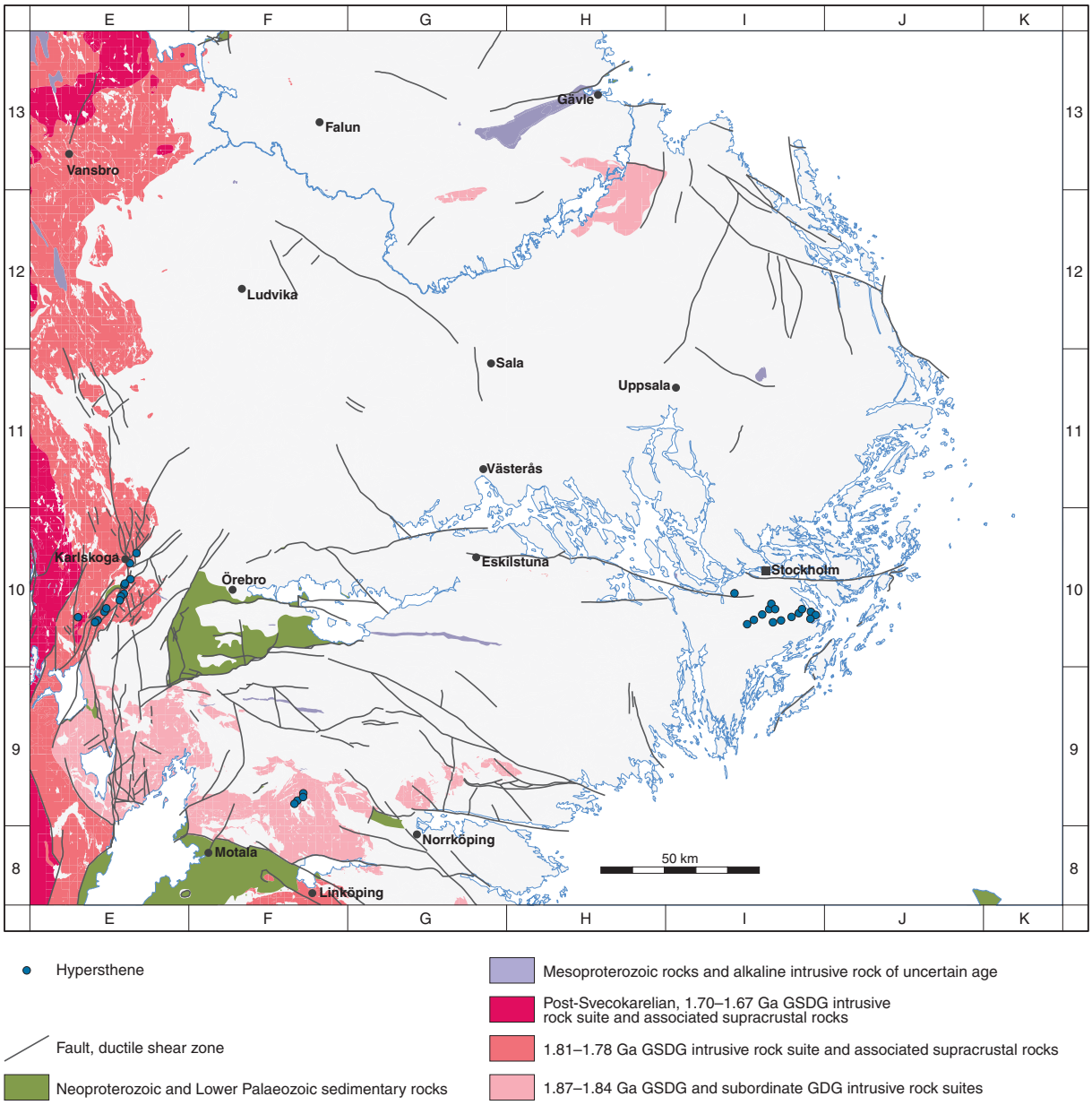

Fig. 153. Occurrence of hypersthene in the Bergslagen region. The different suites of GSDG intrusive rocks are included on this map.

the regionally metamorphosed gneissic rocks from the Flen and Nyköping areas, in the southern migmatitic domain. It has not been resolved whether the more extreme, higher values in both parts of the Bergslagen region reflect true variations in metamorphic pressures or methodological problems in the analytical work.

Most of the temperature determinations in the southern migmatitic metamorphic domain fall in the range 600–800 °C, with three analyses above 800 °C. The mean and standard deviation values in this part of the region are 681 °C and 92 °C, respectively. These results indicate amphibolite- to locally granulite-facies metamorphism and are consistent with the common occurrence of migmatitic rocks in this part of the region. By contrast, the more limited temperature data from the central medium-grade domain fall in the range 500–700 °C, with a mean value of 591 °C and a standard deviation of 64 °C. These data are fully consistent with an inferred lower degree of amphibolite-facies metamorphism in this area relative to that observed in the southern part of the region.

In summary, the P-T data suggest metamorphism under low pressure conditions, in general at depths close to or shallower than c. 20 km. The P-T data also indicate a variable grade of metamorphism from lower amphibolite- to locally granulite-facies conditions

Table 12. Pressure-temperature (P-T) data in the Bergslagen region. Data from (1) Sjöström & Bergman (1998), (2) Andersson et al. (1992), (3) Wikström & Larsson (1993) and (4) Andersson (1997c).

Area	Lithology	N-S coordinate	E-W coordinate	P (kbar)	T (°C)	Reference
Central medium-grade metamorphic domain						
Arlanda	Metasandstone	6611050	1619000	4.36	579	1
Arlanda	Metasandstone	6611200	1619550	4.7	573	1
Arlanda	Mica schist	6617100	1616550	4.16	564	1
Arlanda	Mica schist	6614550	1619950	3.02	541	1
Arlanda	Mica schist	6609800	1616950	4.63	625	1
Arlanda	Metasandstone	6628770	1627610	10.3	690	1
Östhammar	Metasandstone	6698400	1629850	4.73	490	1
Östhammar	Metagreywacke	6681700	1636000	3.04	543	1
Östhammar	Metagreywacke	6676800	1645350	3.65	529	1
Östhammar	Metagabbro	6701400	1628700	8.65	698	1
Östhammar	Metatonalite	6692750	1651800	10.4	665	1
Östhammar	Metasandstone	6709350	1641950	6.69	653	1
Östhammar	Mica schist	6685350	1648450	5.47	578	1
Östhammar	Meta-andesite/dacite	6676800	1645850	4.32	551	1
Southern migmatitic metamorphic domain						
Karlskoga	Granofels	6577080	1431480	5.2	683	2
Karlskoga	Granofels	6577000	1431700	6	763	2
Karlskoga	Granofels	6577940	1431180	5.5	735	2
Karlskoga	Granofels	6578060	1431140	5	718	2
Karlskoga	Granofels	6578500	1431600	5.1	693	2
Svenshyttan	Orthogneiss	6574400	1446750	2.9	551	3
Svenshyttan	Orthogneiss	6574700	1445500	3.9	620	3
Svenshyttan	Orthogneiss	6574700	1445600	3.5	577	3
Kinkhyttan	Granofels	6566100	1442000	4.6	663	3
Kinkhyttan	Granofels	6566000	1442000	5.4	738	3
Nygården	Granofels	6542150	1440100	4.3	589	3
Nygården	Granofels	6542000	1440600	4.7	665	3
Nygården	Granofels	6542000	1440600	4.6	609	3
Nygården	Granofels	6541770	1445230	5.6	740	4
Nygården	Granofels	6542050	1445570	5.6	770	4
Nygården	Metagranite	6543300	1446240	7.1	795	4
Nygården	Granofels	6542830	1446920	6.4	925	4
Tiveden	Paragneiss	6506900	1430700	5.5	660	4
Tiveden	Paragneiss	6519250	1442000	5.9	675	4
Tiveden	Paragneiss	6520900	1440750	5.5	780	4
Tiveden	Paragneiss	6520650	1436900	5.6	695	4
Tiveden	Paragneiss	6520100	1438100	4.2	730	4
Tiveden	Paragneiss	6517200	1429350	6.4	700	4
Tiveden	Paragneiss	6514900	1432250	5.5	765	4
Tiveden	Paragneiss	6514650	1430850	2.3	515	4
Graversfors	Granofels	6511050	1519150	5.4	805	4
Finspång	Metagranite	6511850	1495950	5	720	4
Finspång	Paragneiss	6511050	1489000	5.1	680	4
Finspång	Paragneiss	6510100	1494550	6.2	830	4
Flen	Orthogneiss	6549000	1546850	2.8	585	4
Nyköping	Paragneiss	6514500	1576900	6	655	4
Nyköping	Metabasite	6514500	1576900	7.1	630	4
Nyköping	Paragneiss	6504000	1574700	1.89	546	1
Nyköping	Paragneiss	6520500	1574900	2.43	585	1
Nyköping	Paragneiss	6514300	1574200	2.16	550	1
Nyköping	Paragneiss	6513000	1574650	2.64	581	1

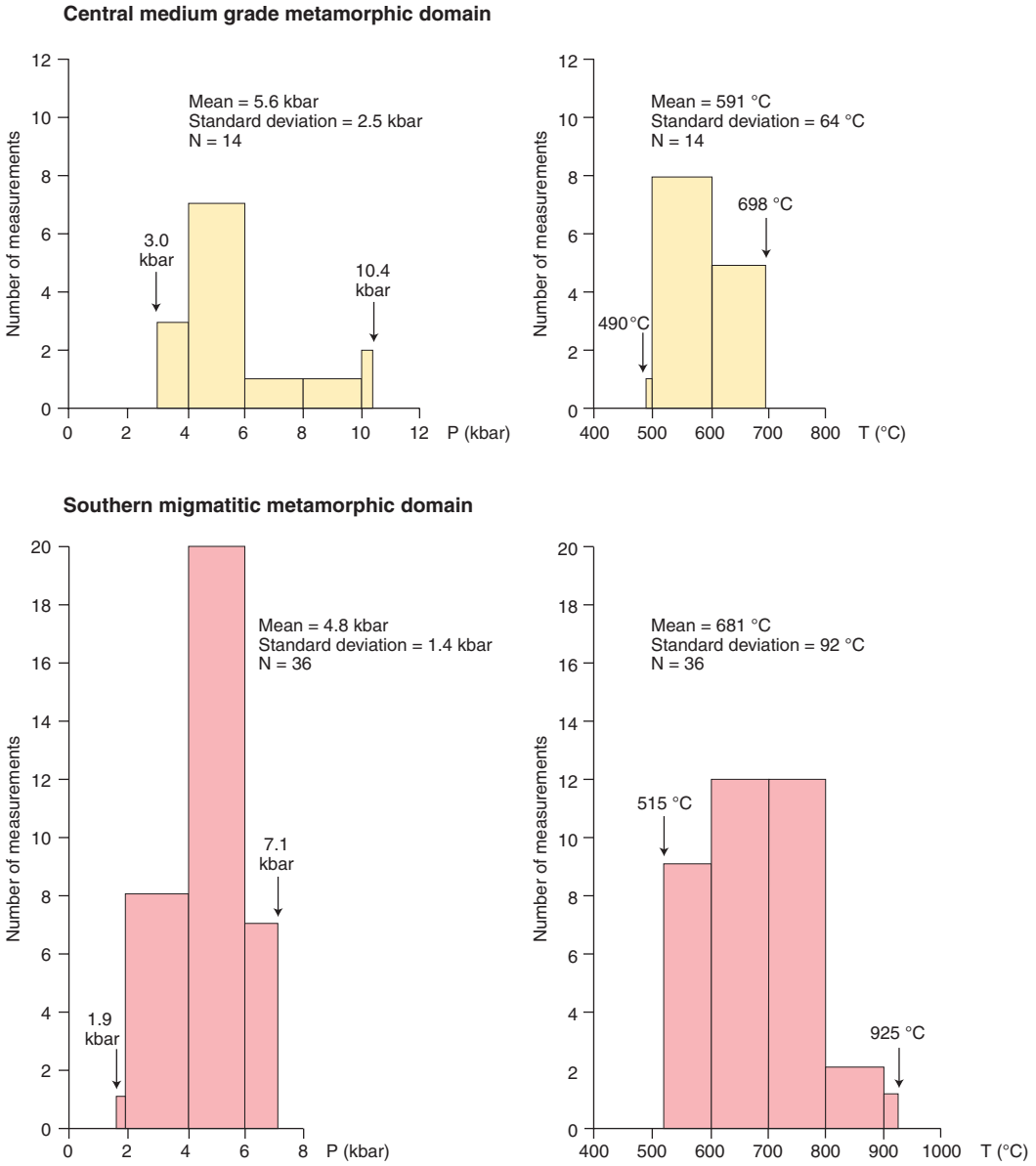

Fig. 154. Histograms, mean values and standard deviation values for the pressure and temperature conditions during metamorphism in the central medium-grade and southern migmatitic metamorphic domains in the Bergslagen region. Analyses that provide maximum and minimum values are also indicated.

and are consistent with the field evidence for abundant anatectic melting in especially the southern part of the region.

Spatial variation in metamorphic grade and definition of metamorphic domains

An attempt has been made on the metamorphic, structural and isotope age map (Stephens et al. 2007b) to distinguish areas with different grades of regional metamorphism in relation to the two main orogenic events in the region, the Svecokarelian and Sveconorwegian events (Fig. 5). The definition of these metamorphic domains is based on the occurrence of key metamorphic mineral assemblages and the quantitative pressure-temperature determinations. A minor thermal contact aureole, which was established at 1.7 Ga, is also shown on the map. The effects of Svecokarelian metamorphism dominate inside the Bergslagen region. The metamorphic grade during this tectonic phase varied from greenschist to granulite facies and gave rise to large areas affected by migmatization, especially in the southern and northernmost parts of the region (Fig. 155). However, some of the late- or post-tectonic GSDG and GP intrusive rocks that formed around and after 1.85 Ga as well as the 1.8 Ga supracrustal rocks are either non-metamorphic or are affected solely by subgreenschist- or locally greenschist-facies metamorphism (Fig. 155).

A summary of the Svecokarelian and Sveconorwegian metamorphic domains as well as the 1.7 Ga thermal contact aureole is provided below. There are insufficient data at the current time to define more explicitly the areas affected by the different pulses of Svecokarelian metamorphism between 1.9 Ga and 1.8 Ga, as discussed in the following section.

Svecokarelian metamorphic domains formed between 1.9 and 1.8 Ga

Four Svecokarelian metamorphic domains have been identified in the Bergslagen region (domains 1 to 4 in Fig. 155). The occurrence of chlorite, albite and epidote in mafic rocks, Mg-rich chlorite and muscovite in the Svecofennian volcanic rocks affected by "magnesium alteration", and the very fine-grained, compact and well-preserved character of the Svecofennian felsic volcanic rocks provide the basis for the definion of a restricted area affected by Svecokarelian greenschist-facies regional metamorphism in the western part of the Bergslagen region (central low-grade metamorphic domain in Fig. 155).

By contrast, the presence of hornblende and plagioclase feldspar in mafic rocks, the occurrence of, for example, cordierite, phlogopite and amphibole in the Svecofennian volcanic rocks affected by "magnesium alteration", and the coarser-grained, recrystallized character of the Svecofennian felsic volcanic rocks provide the basis for the definition of a large area in the central part of the region that is affected by lower or middle amphibolite-facies metamorphic conditions (central medium-grade metamorphic domain in Fig. 155). The occurrence of garnet and andalusite in this part of the Bergslagen region is consistent with this evaluation. However, as indicated earlier, further work is needed to more fully understand the timing relationship between the aluminosilicates andalusite and sillimanite in this domain.

The presence of K-feldspar, sillimanite, cordierite and neosome provides the basis for the recognition of migmatitic, amphibolite- or even granulite-facies rocks in the southern and northernmost parts of the region (southern and northern migmatitic metamorphic domains in Fig. 155). Garnet is also a common metamorphic mineral in these two areas. The few occurrences of granulite-facies rocks have been recognized on the basis of the pressure-temperature determinations or by the presence of hypersthene (±garnet). The current data suggest that these occurrences are spatially highly restricted (Fig. 155). The broader regional significance of granulite-facies metamorphism in the southern part of the Bergslagen region requires further investigation.

The boundary between the southern migmatitic and central medium-grade domains is not concordant with the boundaries between the mappable bedrock units (compare, for example, the bedrock and metamorphic geological maps in Figures 19 and 155, respectively, in the Västerås–Örebro area). Furthermore, in a similar manner to that observed on outcrop scale (see, for example, Fig. 136d), the boundary between the southern migmatitic and central medium-grade domains is folded by major D_{2C} folding in the central structural domain (see also above).

Contact metamorphism at 1.7 Ga

A thermal contact aureole that contains a prograde growth of hypersthene and garnet is apparent along the western side of a major diorite to quartz-bearing monzodiorite pluton, south-west of Karlskoga in the western part of the Bergslagen region (Fig. 155). Age-dating work has established that this body belongs to the 1.70–1.67 Ga GSDG intrusive rock suite (Stephens et al. 1993). For this reason, it is inferred that this contact metamorphism is also 1.7 Ga in age.

Sveconorwegian metamorphic domains formed between 1.0 and 0.9 Ga

The most conspicuous feature of the western part of the Bergslagen region is the regional overprint by greenschist- and, in westernmost areas, even amphibolite-facies metamorphism, which is inferred to be Sveconorwegian in age (Fig. 155). However, as pointed out earlier, there remains considerable uncertainty concerning the timing of amphibolite-facies metamorphism in the GSDG intrusive rocks immediately west and south-west of Skagern (Fig. 155). As for the Svecokarelian metamorphism, the metamorphic mineral assemblages in the mafic rocks and the absence or presence of recrystallization of feldspar in the dominant felsic rocks have provided the basis for the recognition of areas with different grades of Sveconorwegian metamorphism.

Integrated evaluation of the timing of Svecokarelian ductile deformation, metamorphism and cooling

This section focuses attention on data that provide constraints on the timing of Svecokarelian metamorphism, using the U-Pb (zircon, monazite, titanite) technique, and the timing of cooling of the bedrock beneath the closing temperature for argon isotopic mobility in hornblende and biotite, using the ^{40}Ar-^{39}Ar technique. All these data provide information on the geological evolu-

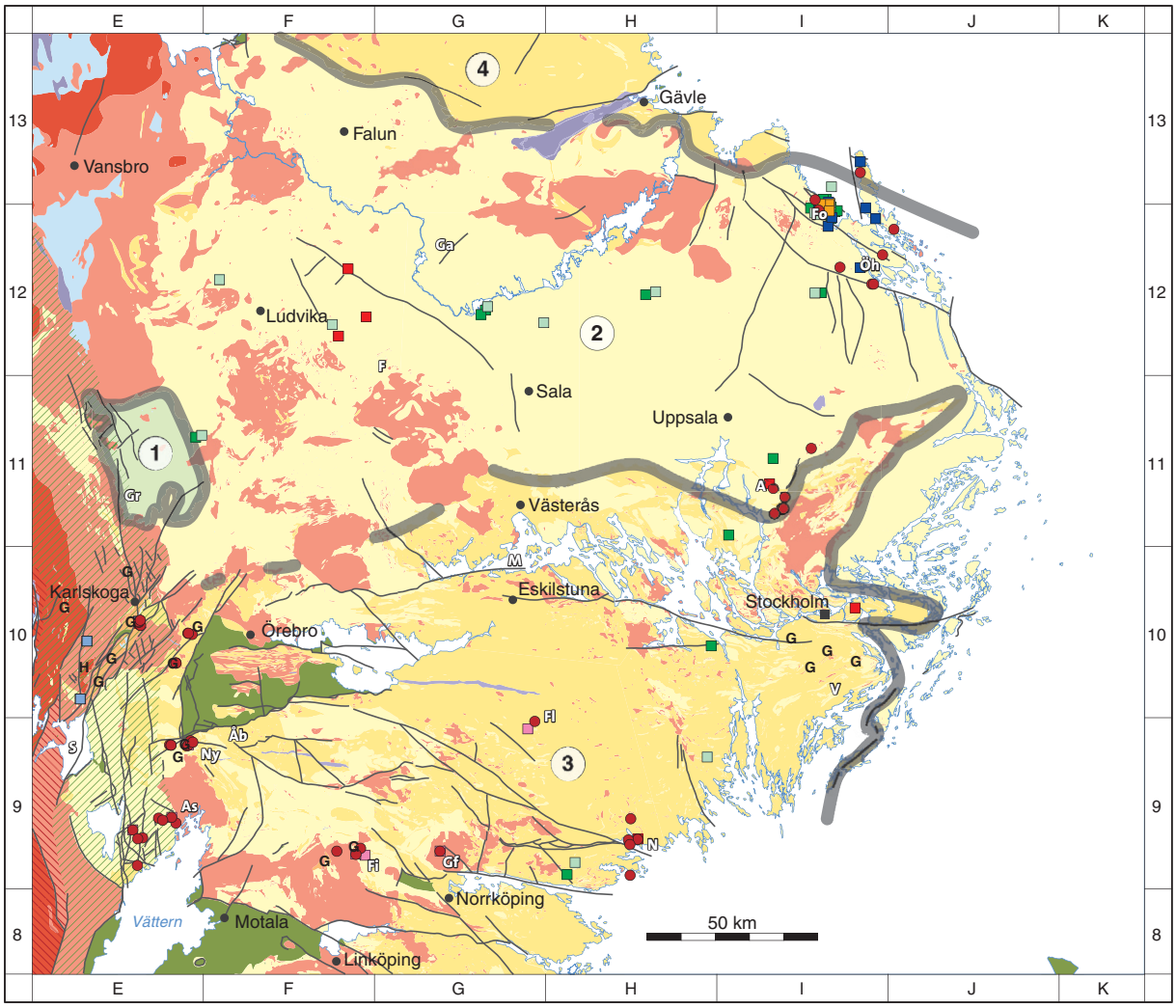

Boundary to Svecokarelian metamorphic domain

1 Central low-grade

2 Central medium-grade

3 Southern migmatitic

4 Northern migmatitic

- Sample site for P-T determination
- U-Pb (zircon or zircon and monazite) age determination
- U-Pb (monazite) age determination
- U-Pb (titanite) age determination (Forsmark area)
- ^{40}Ar-^{39}Ar (hornblende) age determination
- ^{40}Ar-^{39}Ar (biotite) age determination
- ^{40}Ar-^{39}Ar (white mica) age determination
- (U–Th)/He (apatite) age determination (Forsmark area)

Fault, ductile shear zone

Neoproterozoic and Lower Palaeozoic sedimentary rocks (non-metamorphic)

Sveconorwegian tectonic overprint (1.0–0.9 Ga)

Greenschist facies (non-penetrative deformation)

Amphibolite facies (penetrative deformation), amphibolite-facies metamorphism and deformation directly west and south-west of Skagern either Sveconorwegian or older

Post-Svecokarelian, Mesoproterozoic rocks and alkaline intrusive rock of uncertain age

Non-metamorphic or subgreenschist facies

Post-Svecokarelian, Palaeoproterozoic (1.7 Ga) rocks and associated contact metamorphism (1.7 Ga)

Post-Svecokarelian, 1.70–1.67 Ga GSDG intrusive rock suite and associated supracrustal rocks (non-metamorphic or subgreenschist facies)

H Contact metamorphism, granulite facies

Svecokarelian metamorphism (1.9–1.8 Ga) which affects, to variable extent, Palaeoproterozoic (1.9–1.8 Ga) rocks

Non-metamorphic, subgreenschist facies or greenschist facies

Greenschist facies

Amphibolite facies

Amphibolite facies, migmatitic

G Granulite facies, partly migmatitic

Fig. 155. Regional variation in the grade of metamorphism in the Bergslagen region. Deformation zones, sample sites for the determination of pressure-temperature (P-T) conditions and sample sites for age data bearing on the timing of metamorphism and cooling are also shown on the map. For purposes of clarity, the different types of deformation zone (fault, ductile shear zone) have not been distinguished and lineaments have not been shown on the map. In addition, only the thicker dykes or sills, which are Mesoproterozoic in age, are shown. Neoproterozoic dykes have not been displayed. Furthermore, the location of place names referred to in the section "Metamorphism" is shown on the map. A = Arlanda, Åb = Åsbro, As = Askersund, F = Fagersta, Fi = Finspång, Fl = Flen, Fo = Forsmark, Ga = Garpenberg, Gf = Graversfors, Gr = Grythyttan, Ny = Nygården, N = Nyköping, S = Skagern, Öh = Östhammar, V = Västerhaninge. See also Tables 12, 13 and 14.

tion of the Bergslagen region from the period the bedrock was affected by Svecokarelian metamorphism to the time when the bedrock entered structural levels where it was able to respond to deformation in a more brittle manner. These data are also integrated with those presented earlier bearing on the timing of ductile deformation in the Bergslagen region. Some ^{40}Ar-^{39}Ar (white mica) ages from the western part of the region, which is overprinted by the Sveconorwegian orogenic development, as well as (U-Th)/He (apatite) and apatite fission track data from the Forsmark area, in the north-eastern part of the Bergslagen region, are also addressed. Due to significant differences in their tectonic evolution, the data from the central medium-grade and southern migmatitic metamorphic domains are evaluated separately.

Central medium-grade metamorphic domain

Table 13 lists key components of the data bearing on the timing of metamorphism and the cooling history of the bedrock now exposed at the ground surface in the central medium-grade metamorphic domain, down to temperatures of c. 300 °C. The data are illustrated in Figure 156.

The occurrence of a garnet-rich, anatectic metatonalite that intruded metasedimentary rocks belonging to the *Larsbo formation* in the area to the northwest of Fagersta at 1894±5 Ma (see section "Character, spatial distribution, geochronology, geochemical signature, petrophysical characteristics and regional geophysical signature of rock units" and Table 3) is the oldest record of a thermal metamorphic event in the Bergslagen region (Andersson 2004, Andersson et al. 2004a). At the current state of knowledge, this occurrence is unique in the Bergslagen region and its regional significance is not resolved. It is suggested here that the generation of this anatectic melt represents a local contact metamorphic event that is related to the intrusion of abundant dioritic, gabbroic and tonalitic GDG rocks in a sedimentary rock sequence.

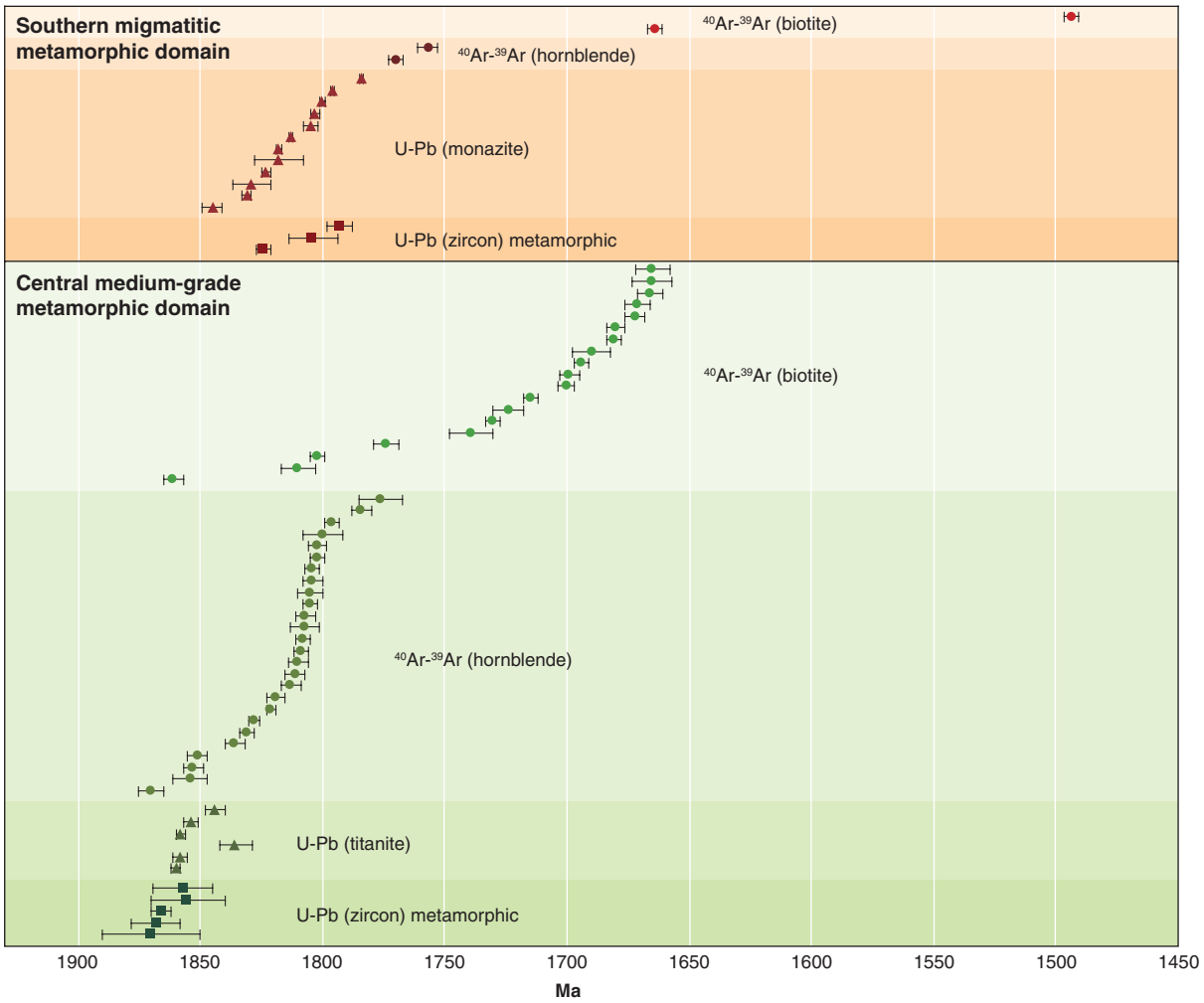

Fig. 156. Summary of age dates bearing on the timing of metamorphism and cooling in the central medium-grade and southern migmatitic metamorphic domains in the Bergslagen region. Three ^{40}Ar-^{39}Ar (white mica) ages from the easternmost part of the Sveconorwegian orogen in the western structural domain, which fall in the range 936 to 900 Ma, are not included in the figure.

Table 13. Radiometric age data bearing on the timing of metamorphism and cooling of the bedrock in the central medium-grade metamorphic domain in the Bergslagen region. Data from (1) Andersson et al. (2006), (2) Andersson (2004) and Andersson et al. (2004b), (3) Hermansson et al. (2008a), (4) Page et al. (2007), (5) Hermansson et al. (2008b), (6) Söderlund et al. (in press).

Lithology	Method	Age (Ma)	N-S coordinate	E-W coordinate	Reference
Amphibolite (Fiskbäcken)	U-Pb zircon (SIMS)	1870±20	6681100	1492300	1
Metatonalite, garnet-bearing (Larsbo)	U-Pb zircon SIMS	1868±10	6661500	1489500	2
Metasedimentary rock (Odensala)	U-Pb zircon SIMS	1866±4	6618300	1615450	1
Quartz-bearing metadiorite (Larsbo)	U-Pb zircon SIMS	1855±15, 1857±12	6667110	1497569	2
Amphibolite (Forsmark)	U-Pb titanite	Olive-brown titanite: 1860±2, 1858±3. Pale brown or brown titanite: 1840±2 to 1832±3 ($^{207}Pb/^{206}Pb$ ages)	6699917	1632853	3
Amphibolite (Forsmark)	U-Pb titanite	1858±2 (UI age)	6699971	1630334	3
Amphibolite (Forsmark)	U-Pb titanite	1854±3 (UI age)	6698019	1632862	3
Amphibolite (E–W transect, Sala–Forsmark)	^{40}Ar-^{39}Ar hornblende	1870±5	6673569	1579200	4
Amphibolite (Forsmark)	^{40}Ar-^{39}Ar hornblende	1854±7. Forced plateau	6695914	1633344	5
Metadiorite (E–W transect, NE of Uppsala)	^{40}Ar-^{39}Ar hornblende	1853±4	6674143	1630469	4
Amphibolite (N–S transect, SE of Uppsala)	^{40}Ar-^{39}Ar hornblende	1851±4	6625755	1616424	4
Metadiorite (E–W transect, NE of Uppsala)	^{40}Ar-^{39}Ar hornblende	1836±4	6674057	1628699	4
Amphibolite (Forsmark)	^{40}Ar-^{39}Ar hornblende	1831±3. Forced plateau	6697859	1634625	5
Amphibolite (Forsmark)	^{40}Ar-^{39}Ar hornblende	1828±2	6699743	1632308	5
Amphibolite (Forsmark)	^{40}Ar-^{39}Ar hornblende	1821±2	6699917	1632853	5
Amphibolite (Forsmark)	^{40}Ar-^{39}Ar hornblende	1819±4	6698164	1635212	5
Amphibolite (E–W transect, Ludvika–Filipstad)	^{40}Ar-^{39}Ar hornblende	1813±4	6632458	1449514	4
Metagabbro (N-S transect, NW of Stockholm)	^{40}Ar-^{39}Ar hornblende	1811±4	6603309	1603462	4
Amphibolite (Forsmark)	^{40}Ar-^{39}Ar hornblende	1810±4	6701132	1630850	5
Metagabbro (Forsmark)	^{40}Ar-^{39}Ar hornblende	1809±3	6699652	1630093	5
Amphibolite (Forsmark)	^{40}Ar-^{39}Ar hornblende	1808±3	6697733	1631685	5
Amphibolite (Forsmark)	^{40}Ar-^{39}Ar hornblende	1807±6. Forced plateau	6701391	1632043	5
Amphibolite (Forsmark)	^{40}Ar-^{39}Ar hornblende	1807±4	6699213	1633390	5
Amphibolite (Forsmark)	^{40}Ar-^{39}Ar hornblende	1805±3	6698839	1627369	5
Metagabbro (E–W transect, Ludvika–Filipstad)	^{40}Ar-^{39}Ar hornblende	1805±5	6631979	1447801	4

U-Pb (zircon) SIMS ages (Fig. 156) in the range 1.87 to 1.86 Ga (1890 to 1840 Ma if all uncertainties are taken into consideration), which have been interpreted as metamorphic ages, have been acquired from four, widely spaced localities in the central part of the Bergslagen region (Andersson 2004, Andersson et al. 2004a, 2006). If the most precise determination from the metasedimentary rock between Uppsala and Stockholm is adopted (Andersson et al. 2006), then the timing of the peak of metamorphism in the central medium-grade domain is constrained between 1870 and 1862 Ma. The $^{207}Pb/^{206}Pb$ age of 1823±7 Ma for a zircon fraction in a felsic metavolcanic rock sample from Garpenberg (see the appendix and Table 2) also indicates the effects of a younger geological event after the crystallization of the rock at 1891±2 Ma. However, a precise age for the timing of this event cannot be determined from these data.

The U-Pb (zircon) SIMS metamorphic ages (Fig. 156) overlap in age with the more precise timing of penetrative deformation under amphibolite-facies metamorphic conditions (see text above and Fig. 156) between 1880 and 1860 Ma (uncertainties included) in the central structural domain (Bergman et al. 2004a, Hermansson et al. 2008a) and with the even more precise estimate of the timing of penetrative ductile deformation between 1871 and 1860 Ma (uncertainties included) in the easternmost part of the northern structural domain (Hermansson et al. 2007, 2008a). On the basis of all these data, it is inferred that significant ductile deformation, with the development of the tectonic fabric in the bedrock, as well as the regional metamorphism occurred between 1.87 and 1.86 Ga inside the central medium-grade metamorphic domain.

This conclusion is consistent with and, thereby, supported by the ages from other isotope systems in this metamorphic domain (Fig. 156). These include U-Pb (titanite) ages that are 1.86 Ga or younger (Hermansson et al. 2008a), ^{40}Ar-^{39}Ar (hornblende) ages that, with one exception, are 1.85 Ga or younger (Page et al. 2007,

Table 13. Continued.

Lithology	Method	Age (Ma)	N-S coordinate	E-W coordinate	Reference
Amphibolite (Forsmark)	^{40}Ar-^{39}Ar hornblende	1804±4	6700172	1633052	5
Amphibolite (Forsmark)	^{40}Ar-^{39}Ar hornblende	1804±3	6698361	1633262	5
Amphibolite (Forsmark)	^{40}Ar-^{39}Ar hornblende	1802±3	6699506	1631340	5
Amphibolite (Forsmark)	^{40}Ar-^{39}Ar hornblende	1802±4	6701419	1631060	5
Metagabbro (E–W transect, NW of Sala)	^{40}Ar-^{39}Ar hornblende	1800±8. Forced plateau	6669045	1532369	4
Amphibolite (Forsmark)	^{40}Ar-^{39}Ar hornblende	1796±3	6700651	1632580	5
Amphibolite (E–W transect, NW of Ludvika)	^{40}Ar-^{39}Ar hornblende	1784±4. Forced plateau	6677969	1454687	4
Metagabbro (E–W transect, NW of Sala)	^{40}Ar-^{39}Ar hornblende	1776±9	6667790	1531128	4
Metagranite (E–W transect, Sala–Forsmark)	^{40}Ar-^{39}Ar biotite	1861±4. Forced plateau	6674429	1582133	4
Metatonalite (E–W transect, north of Sala)	^{40}Ar-^{39}Ar biotite	1810±7. Forced plateau	6665379	1549469	4
Metatonalite (E–W transect, NE of Uppsala)	^{40}Ar-^{39}Ar biotite	1802±3	6674050	1628678	4
Metagranite (E–W transect, NW of Ludvika)	^{40}Ar-^{39}Ar biotite	1774±5	6677969	1454687	4
Metagranite to metagranodiorite (E–W transect, NW of Sala)	^{40}Ar-^{39}Ar biotite	1739±9. Forced plateau	6670083	1533076	4
Metagranite (Forsmark)	^{40}Ar-^{39}Ar biotite	1730±3	6697447	1628558	6
Metatonalite (E–W transect, SE of Ludvika)	^{40}Ar-^{39}Ar biotite	1724±6	6664857	1487650	4
Amphibolite (Forsmark)	^{40}Ar-^{39}Ar biotite	1715±3	6700172	1633052	6
Metatonalite (Forsmark)	^{40}Ar-^{39}Ar biotite	1700±4	6698352	1629723	6
Metagranodiorite (Forsmark)	^{40}Ar-^{39}Ar biotite	1699±4	6693523	1632499	6
Felsic metavolcanic rock (E–W transect, Ludvika–Filipstad)	^{40}Ar-^{39}Ar biotite	1694±3	6632469	1449524	4
Metagranodiorite (Forsmark)	^{40}Ar-^{39}Ar biotite	1690±8. Forced plateau	6697474	1629821	6
Metagranite (Forsmark)	^{40}Ar-^{39}Ar biotite	1681±3	6698781	1630655	6
Metagranite (Forsmark)	^{40}Ar-^{39}Ar biotite	1680±4. Forced plateau	6699740	1632290	6
Metagranodiorite (Forsmark)	^{40}Ar-^{39}Ar biotite	1672±4	6700532	1632663	6
Metagranite (Forsmark)	^{40}Ar-^{39}Ar biotite	1671±5	6699088	1629974	6
Metagranite (Forsmark)	^{40}Ar-^{39}Ar biotite	1666±5	6698910	1631010	6
Metagranodiorite (Forsmark)	^{40}Ar-^{39}Ar biotite	1665±8. Forced plateau	6696945	1630110	6
Metagranite (Forsmark)	^{40}Ar-^{39}Ar biotite	1665±7. Forced plateau	6705094	1633496	6

Hermansson et al. 2008b), and ^{40}Ar-^{39}Ar (biotite) ages that, with one exception, are 1.81 Ga or younger (Page et al. 2007, Söderlund et al. in press).

The U-Pb (titanite) ages in amphibolite from the Forsmark area in the northern structural domain (Fig. 156) have been derived from at least two different generations of optically distinct titanite and indicate a multi-stage tectonothermal evolution that succeeded the formation of the mafic precursors to these rocks at 1.87 to 1.86 Ga (Hermansson et al. 2008a and see section "Character, spatial distribution, geochronology, geochemical signature, petrophysical characteristics and regional geophysical signature of rock units"). The older ages between 1.86 and 1.85 Ga (uncertainties included), partly from olive-brown titanites, have been interpreted to date a metamorphic event or cooling through the titanite closure temperature (500–700 °C) after a metamorphic event (Hermansson et al. 2008a). The youngest age of 1832±3 Ma for a pale brown or brown fraction of titanites reflects a younger tectonothermal event around or after 1.83 Ga (Hermansson et al. 2008a). The spread in ages for the younger fraction of titanites between 1.84 and 1.83 Ga has been interpreted as due to mixing between the two age groups that are related to the different tectonothermal events (Hermansson et al. 2008a). It cannot be excluded that even the youngest age of 1832±3 Ma is a mixing age between the event at 1.86 Ga and a post-1.83 Ga event.

The ^{40}Ar-^{39}Ar (hornblende) age data from the Forsmark area in the northern structural domain show a wide variation in ages (1854±7 to 1796±3 Ma, see Table 13 and Fig. 156) in a highly restricted area. Hermansson et al. (2008b) identified a spatial relationship between the distribution of these ages and major structural features – tectonic lenses and high-strain belts – in the bedrock in the Forsmark area. In particular, they noted that temperatures above the closing temperature for the ^{40}Ar-^{39}Ar (hornblende) isotope system at c. 500 °C were maintained along the steeply dipping, high-strain belts in the area (see earlier text)

down to 1.8 Ga. This observation was inferred to be due to post-1.85 Ga ductile deformation under retrograde lower amphibolite- to upper greenschist-facies metamorphic conditions along more discrete zones within the high-strain belts (Hermansson et al. 2008b). The structural control on the variation in ages at Forsmark emphasizes the need for care in the interpretation of the similar variation in the ^{40}Ar-^{39}Ar (hornblende) age data (1870±5 to 1776±9 Ma, see Table 13 and Fig. 156) that is present, over a much larger area, in the central structural domain (Page et al. 2007).

The range in ^{40}Ar-^{39}Ar (biotite) ages from the Forsmark area in the northern structural domain (1730±3 to 1665±7 Ma, see Table 13 and Fig. 156) is younger than the range observed from the data in the central structural domain (1810±7 to 1694±3 Ma, see Table 13 and Fig. 156). The anomalously high ^{40}Ar-^{39}Ar (biotite) forced plateau age at 1861±4 Ma from the area between Sala and Forsmark has been ignored in this evaluation. It is inferred that the bedrock at the current level of erosion cooled beneath the closing temperature for the ^{40}Ar-^{39}Ar (biotite) isotope system at c. 300 °C, at different times in different parts of the central medium-grained metamorphic domain, i.e. around 1.8 Ga to the south and around 1.7 Ga further north. Thus, the time when this bedrock was able to respond to tectonic activity in a more brittle manner, under subgreenschist-facies conditions (pumpelleyite-prehnite sub-facies), was probably older in the southern part of this metamorphic domain. Once again, detailed investigations at Forsmark have shown that the wide variation in ages in this restricted area is structurally controlled and related, at least partly, to faulting after establishment of the sub-Cambrian unconformity (Söderlund et al. in press).

Apatite from different fault blocks at the surface and at different depths in boreholes have been analysed for (U-Th)/He age determination in the Forsmark area in the northern structural domain (Söderlund et al. 2008). Following correction for loss of helium due to ejection of α-particles, such analyses are perceived to provide an estimate of when the bedrock cooled below c. 70 °C (Farley 2000). After the exclusion of some highly anomalous old ages, the (U-Th)/He apatite ages in, for example, borehole KFM01A, corrected for loss of helium, range from 467±32 (c. 100 m depth) to 186±13 Ma (c. 1000 m depth), i.e. from Mid Ordovician to Early Jurassic. The corresponding uncorrected ages lie between 271±19 Ma and 97±7 Ma, i.e. from Early Permian to Late Cretaceous.

Apatite fission track ages, derived from different laboratories, are also available from the north-eastern part of the Bergslagen region, including the Forsmark area (Larson et al. 1999, Cederbom et al. 2000, Söderlund et al. 2008). However, there are inconsistencies between the (U-Th)/He and fission track ages for the apatites as well as between older and more recent apatite fission track ages (Söderlund et al. 2008). The difficulties in the interpretation of all these ages have been addressed in Söderlund et al. (2008) and Stephens & Wahlgren (2008). Notwithstanding these difficulties, it is apparent that the data indicate the presence of a substantial sedimentary cover on top of the crystalline basement rocks in the north-eastern part of the Bergslagen region during much of the Phanerozoic. Further work with these data and the acquisition of new apatite fission track data are ongoing.

Southern migmatitic metamorphic domain

Table 14 lists key components of the data bearing on the timing of metamorphism and the cooling history of the bedrock now exposed at the ground surface in the southern migmatitic metamorphic domain, down to temperatures of c. 300 °C. The data are also illustrated in Figure 156.

U-Pb (zircon) SIMS ages of 1804±10 and 1793±5 (Fig. 156), which have been interpreted as metamorphic ages, have been acquired from two, widely spaced localities in the eastern and western parts, respectively, of the southern migmatitic metamorphic domain (Andersson et al. 2006). Bearing in mind the uncertainties provided, these ages are identical to the U-Pb (monazite) ages from the same localities (Andersson 1997c, see Table 14). All these data are considered to date with confidence the timing of at least one major metamorphic event between 1814 and 1788 Ma in this domain.

The U-Pb (monazite) ages in the southern migmatitic metamorphic domain (Fig. 156) vary considerably from 1.85 to 1.78 Ga (1849 to 1783 Ma if all uncertainties are taken into consideration). The oldest age at 1845±4 Ma has been related to a thermal event caused by the intrusion of a norite belonging to the 1.87–1.84 Ga GSDG intrusive suite (Andersson 1997c). Deformation and so-called "elevated thermal activity" at 1.83 to 1.82 Ga as well as "regional peak metamorphism and migmatite formation" at 1.80 to 1.79 Ga have also been suggested (Andersson et al. 2006). A U-Pb (zircon) age of 1824±3 Ma and a U-Pb (monazite) age of 1803±2 Ma have also been interpreted to date separate thermal events in a 1.89 Ga GDG orbicular metagranite in the Stockholm region (Persson et al. 2002). Thus, the possible influence of at least three metamorphic events in the complex, southern migmatitic metamorphic domain is apparent. The significant variation in the U-Pb (monazite) ages over the whole range from

1.85 to 1.78 Ga remains an enigma and provokes an alternative explanation.

In the alternative explanation, the southern migmatitic domain was affected by metamorphism in connection with the intrusion of the 1.87–1.84 Ga GSDG suite of intrusive rocks. The peak of this metamorphic event, with the development of migmatites, closely followed penetrative, pre-1.85 Ga deformation in the bedrock (see above). The tectonic development is reminiscent of the episode of ductile deformation and metamorphism between 1.87 and 1.86 Ga further north in the Bergslagen region (see above). Later deformation in the southern migmatitic domain affected the rocks in the 1.87–1.84 Ga GSDG intrusive suite along ductile high-strain belts or zones, and reworked the pre-1.85 Ga structures in the older bedrock. A second metamorphic event, which at its peak was of sufficient grade and regional significance to give rise to metamorphic U-Pb (zircon) ages over a wide area, to reset U-Pb (monazite) ages and to form migmatite, occurred in connection with intrusion of the younger, 1.81–1.78 Ga GSDG rock suite. Thus, the span in U-Pb (monazite) ages from 1.85 to 1.78 Ga is simply due to the variable effects of the younger metamorphic event around 1.8 Ga on its older precursor at or prior to 1.85 Ga. The inheritance of igneous crystallization components in the U-Pb (zircon) age for the orbicular metagranite from the Stockholm region may explain the 1824±3 U-Pb (zircon) age and, thereby, also remove the need for separate thermal events as proposed by Persson et al. (2002).

Relative to the central medium-grade metamorphic domain, there are few ^{40}Ar-^{39}Ar ages (Page et al. 1996, 2007) in the southern migmatitic domain (Fig. 156). Nevertheless, ^{40}Ar-^{39}Ar (hornblende) ages older than 1.78 Ga and ^{40}Ar-^{39}Ar (biotite) ages older than 1.67 Ga are lacking in the southern migmatitic domain and are consistent with the more complex, high-grade metamorphic evolution that is apparent in this domain as late as 1.80 to 1.79 Ga. The Sveconorwegian reworking in the western structural domain is apparent in the ^{40}Ar-^{39}Ar (white mica) ages in the range 936 to 900 Ma (uncertainties included).

Concluding statement

More than one event of regional heating at mid-crustal levels, which resulted in low-pressure and high-temperature metamorphism, is present in the Bergslagen region. In the central medium-grade metamorphic domain, the peak of metamorphism is constrained between 1.88 and 1.86 Ga, in its northern part between 1.87 and 1.86 Ga. Subsequent events were retrogressive in character. Although there is evidence for an early thermal event at or prior to 1.85 Ga in the southern migmatitic metamorphic domain, there is a significantly different, post-1.85 Ga thermal history in this

Table 14. Radiometric age data bearing on the timing of metamorphism and cooling in the southern migmatitic metamorphic domain in the Bergslagen region. Data from (1) Persson et al. (2002), (2) Andersson et al. (2006), (3) Andersson (1997c), (4) Page et al. (2007), (5) Page et al. (1996).

Lithology	Method	Age (Ma)	N-S coordinate	E-W coordinate	Reference
Orbicular metagranite (Orminge)	U-Pb zircon/monazite	1824±3 / 1803±2	6582070	1640390	1
Grt-cord-sill gneiss (Nyköping)	U-Pb zircon (SIMS)/monazite	1804±10 / 1805±3	6514500	1576900	2 / 3
Grt-cord gneiss (Karlskoga)	U-Pb zircon (SIMS)/monazite	1793±5 / 1796±1	6577600	1431350	2 / 3
Grt-cord gneiss (Nygården)	U-Pb monazite	1845±4	6542050	1445570	3
Metagranite (Finspång)	U-Pb monazite	1831±2, 1823±2	6509750	1497200	2
Hornfels xenolith (Graversfors)	U-Pb monazite	1829±8	6511050	1519150	3
Cord-sill gneiss (Flen)	U-Pb monazite	1818±10	6546700	1544750	3
Paragneiss (Tiveden)	U-Pb monazite	1818±1	6520900	1440750	3
Paragneiss (Finspång)	U-Pb monazite	1813±1	6510100	1494550	3
Grt-cumm gneiss (Tiveden)	U-Pb monazite	1800±1	6517200	1429350	3
Grt-cumm gneiss (Tiveden)	U-Pb monazite	1784±1	6517200	1429350	3
Amphibolite (N–S transect, SW Stockholm)	^{40}Ar-^{39}Ar hornblende	1770±3	6570961	1598346	4
Amphibolite (N–S transect, NE Norrköping)	^{40}Ar-^{39}Ar hornblende	1757±4	6504124	1556283	4
Metagranite (N–S transect, Stockholm–Norrköping)	^{40}Ar-^{39}Ar biotite	1664±3	6538460	1597192	4
Metgranite (N–S transect, NE Norrköping)	^{40}Ar-^{39}Ar biotite	1494±3	6507705	1558578	4
Metagranite (Björneborg)	^{40}Ar-^{39}Ar white mica	930±6	6572400	1416000	5
Phyllonite (Karlskoga)	^{40}Ar-^{39}Ar white mica	918±8	6578150	1431050	5
Metagranite (Skagern)	^{40}Ar-^{39}Ar white mica	905±5	6555500	1414050	5

domain. This post-1.85 Ga history involved either separate major thermal events at 1.83–1.82 Ga and 1.80–1.79 Ga (hypothesis 1) or, alternatively, a single, major thermal event around 1.8 Ga that disturbed older U-Pb (monazite) ages at or prior to 1.85 Ga and, thereby, gave rise to a spectrum of mixing ages between 1.85 and 1.78 Ga (hypothesis 2).

It is considered likely that the older, metamorphic event in the southern migmatitic domain at or prior to 1.85 Ga is identical to the 1.88 (1.87)–1.86 Ga event preserved in the central medium-grade domain. This metamorphic event is referred to as the M_1 event. The younger, 1.8 Ga metamorphic event (or events) in the Bergslagen region is less extensive. It is referred to here as M_2. However, the northern boundary of the M_2 1.8 Ga metamorphism in the southern part of the region is not established. For this reason, the relative importance of the 1.88 (1.87)–1.86 Ga event and the 1.8 Ga metamorphic event (or events) in the northern part of the region is poorly understood.

Peak metamorphism related to two major phases of mafic underplating

The high-grade amphibolite- and granulite-facies metamorphic rocks in the southern part of the Bergslagen region occur in a part of the Fennoscandian Shield where there is a distinctive gradient in crustal thickness (Fig. 157). In this part of the shield, the crust increases in thickness from values less than 46 km in the central part of the Bergslagen region to values greater than 50 km in the southernmost part of this region. However, a low surface relief and isostatic balance have characterized the whole shield area for a long period

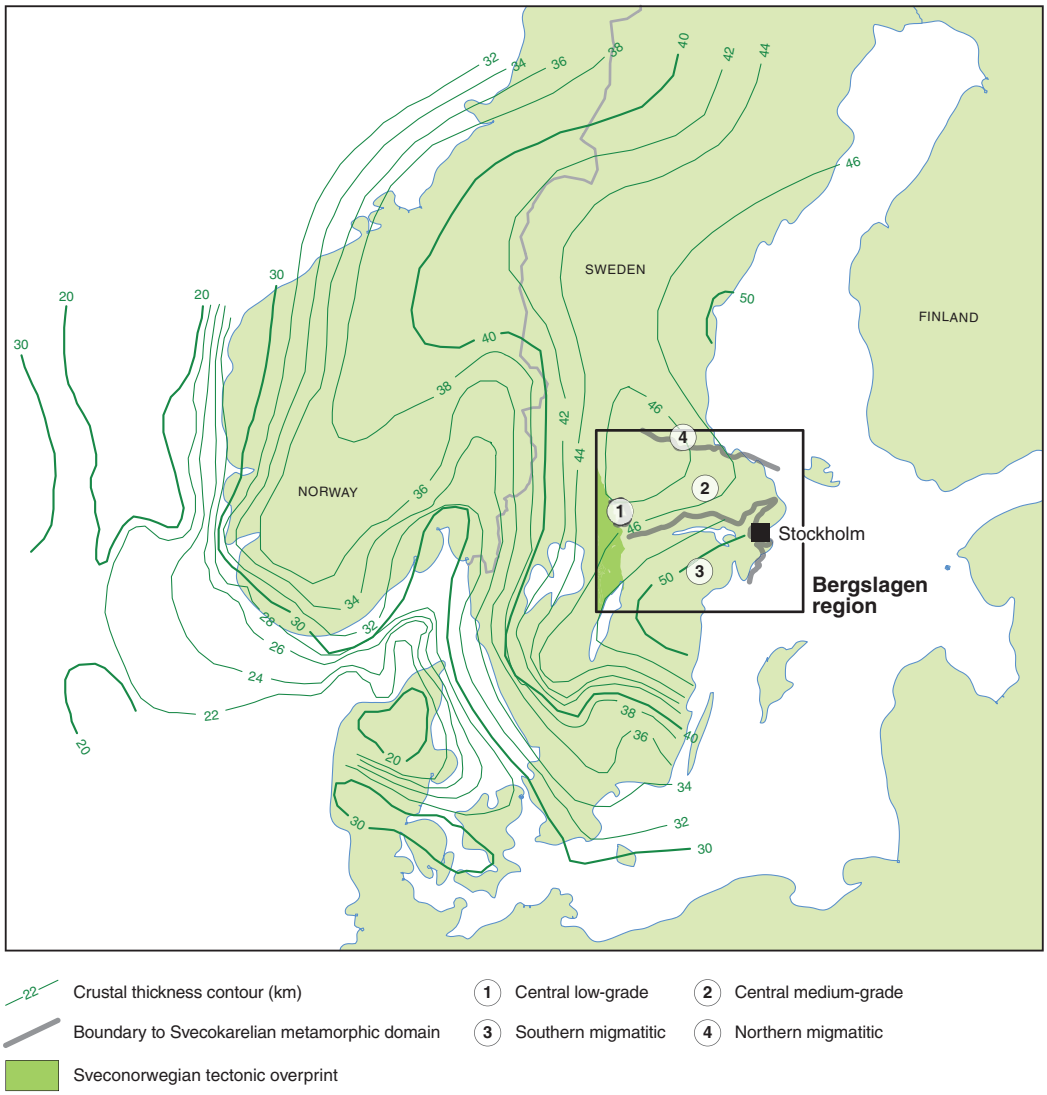

Fig. 157. Variation in crustal thickness in northern Europe (after Kinck et al. 1993) and its relationship to the variation in the grade of Svecokarelian metamorphism under low-pressure conditions in the Bergslagen region.

of time, at least prior to the establishment of the sub-Cambrian unconformity.

A thick crust in stable isostatic balance over a long period of time can be explained by abundant sheets of high-density, mafic and intermediate igneous material in the crust, i.e. by mafic underplating. Similar conclusions were also made by Sjöström & Bergman (1998) for the whole area occupied by tectonic domains 1 to 4 in the central part of Sweden (see Fig. 5). In this context, it is important to note that the southward increase in grade of metamorphism and the positive gradient in crustal thickness to the south in the Bergslagen region both correspond to the occurrence of a diffuse, regional gravity maximum on the Bouguer gravity anomaly map, indicative of a distinctive excess of mass at depth in the crust (Fig. 158).

The consistency in the spatial occurrence of these three features – increase in grade of metamorphism, increase in crustal thickness and mass excess at depth – provides support to the hypothesis that the Svecokarelian, peak high-grade metamorphism at relatively shallow pressures in the southern part of the Bergslagen region, with formation of migmatites, is related to mafic underplating at or prior to 1.85 Ga and around 1.8 Ga, i.e. the metamorphism is steered by the thermal input from the injection of hot, mafic

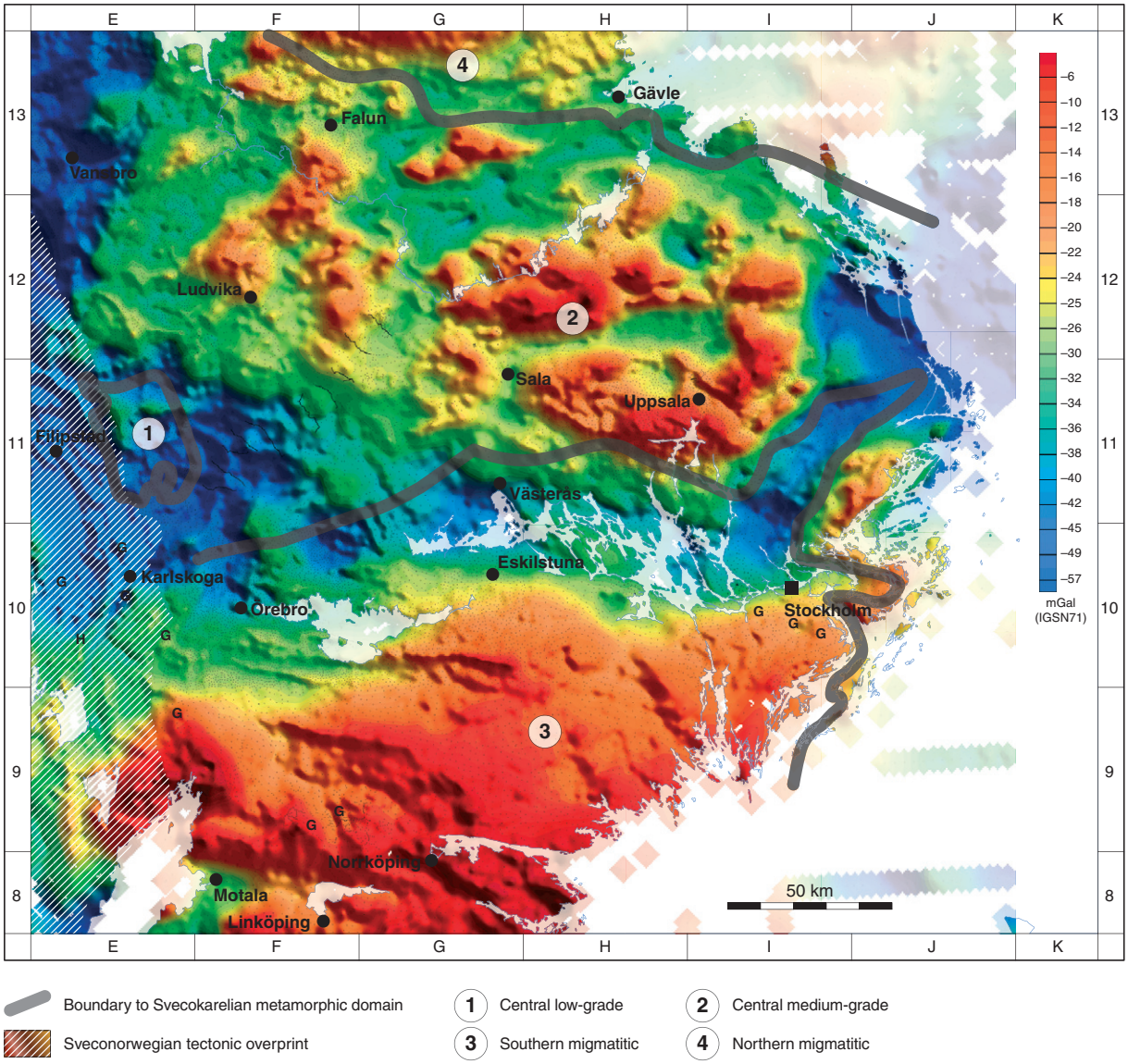

Fig. 158. Bouguer gravity anomaly map and its relationship to the variation in the grade of Svecokarelian metamorphism under low-pressure conditions in the Bergslagen region.The diffuse gravity maximum in the southern part of the region indicates an excess of mass at depth in the crust. The more distinct gravity maxima in the central part of the region indicate several occurrences of excess mass closer to the ground surface, consistent with the increased frequency of metamorphosed dioritic, gabbroic and ultramafic GDG rocks at the ground surface in this part of the Bergslagen region (see bedrock geological map in Stephens et al. 2007a).

igneous material during these two time intervals. The geochronological data evaluated above and in the section entitled "Character, spatial distribution, geochronology, geochemical signature, petrophysical characteristics and regional geophysical signature of rock units" support the concept that there is a close temporal relationship between peak metamorphism and the intrusion of magma belonging to the 1.87–1.84 (1.85) Ga (GSDG and subordinate GDG) and 1.81–1.78 Ga (GSDG) rock suites. The dominant felsic component in each of these suites as well as the granites in the GP intrusive suite are simply a further manifestation of the mafic underplating that took place at levels in the crust deeper than that exposed at the current ground surface.

MECHANISM OF EMPLACEMENT OF THE 1.87–1.84 Ga GSDG SUITE OF INTRUSIVE ROCKS IN THE SOUTHERN STRUCTURAL DOMAIN

Various sets of data from intrusive rocks are required before models for their emplacement can be discussed with any degree of confidence. These include depth of emplacement, 3-D shape, nature and kinematic signature of fabric development, both within and outside an individual intrusion, and relationship to ductile high-strain belts or zones. Many of these data are available for the 1.87–1.84 Ga GSDG rocks in the southern structural domain and, for this reason, the mechanism of emplacement of these rocks is addressed here.

Depth of emplacement

Pressure-temperature (P-T) determinations from xenoliths within the 1.87–1.84 Ga suite of intrusive rocks or from country rock samples in direct contact with these intrusive rocks have yielded temperatures of 589 to 830 °C (locally >900 °C) and pressures of 4.3 to 7.1 kbar (Wikström & Larsson 1993, Andersson 1997c and Table 12). Assuming that the metamorphism is related to the intrusion of the 1.87–1.84 Ga GSDG suite, as indicated by the U-Pb (monazite) ages that vary between 1845±4 to 1823±2 Ma (Andersson 1997c, Andersson et al. 2006 and Table 14), it can be inferred that the emplacement of these intrusions occurred at depths around 20 km, i.e. at crustal levels conspicuously beneath the brittle upper crust. It is necessary to keep in mind that current crustal thickness in the Fennoscandian Shield in this part of Sweden is greater than 50 km. Thus, at the time of emplacement of the 1.87–1.84 Ga suite of GSDG intrusive rocks, the crust was probably greater than 70 km thick.

3-D shape

Gravity data have been acquired and modelling work completed across the 1.87–1.84 Ga GSDG intrusive rocks in the Graversfors (Wikström et al. 1980) and Finspång (Wikström & Aaro 1986) areas in order to constrain the 3-D shape of these intrusive bodies (see section "Character, spatial distribution, geochronology, geochemical signature, petrophysical characteristics and regional geophysical signature of rock units"). These studies demonstrated the laccolithic character of the intrusions. Furthermore, the *Graversfors granite* consists of a deeply-protruding, inferred root zone linked at higher crustal levels to a flat-lying, sheet-like body which is exposed at the ground surface (Wikström et al. 1980). The root zone of the *Graversfors granite* is situated in the eastern part of the massif.

Structural relationships

Analysis of data pertaining to fabric development both within and immediately adjacent to younger intrusive rocks has been presented for the marginal part of the 1.87–1.84 Ga GSDG intrusive rocks in the Graversfors area (Wikström et al. 1980) and in the area which extends north-westwards from Finspång to Askersund and Åsbro (Wikström & Aaro 1986). The relationship between the contact to the surrounding country rocks and the fabric development in the country rocks has also been addressed in these studies.

The *Graversfors granite* displays a discordant relationship to the planar grain-shape fabric in the country rocks along its eastern margin and a concordant relationship elsewhere. The analysis presented here for the southern structural domain indicates that this massif is located within a network of steeply dipping, ductile high-strain belts or zones which strike west-north-west–east-south-east to north-west–south-east (Fig. 124). Both the conspicuous change in degree of concordancy across the massif and the asymmetry of the 3-D geometry of the intrusion inferred from gravity data track the stretching direction associated with the ductile strain.

The *Finspång augen gneiss massif*, situated c. 12 km to the west of the *Graversfors granite* and west of the rocks affected by strong ductile strain between the two massifs (Fig. 124), forms an isolated elliptical lozenge of granite and metagranite with north-west–south-east strike. It displays a strong, moderately to steeply inclined planar grain-shape fabric throughout the massif, with the notable exception of the south-eastern part. The amphibolite-facies fabric in the metagranite is concordant to both the contact with

the country rocks and to the grain-shape fabric within the latter.

Emplacement model

Models for the emplacement of major intrusions in the Earth's crust (see, for example, reviews in Castro 1987, Hutton 1988, 1996) have invoked the following mechanisms:

- Uplift of the Earth's free surface related to excess magma pressure and development of cone sheets, ring dykes and cauldron subsidence in central igneous complexes.
- Large-scale stoping controlled by fracture propagation under high magma pressure.
- Forceful emplacement related to diapirism or in situ inflation at the site of emplacement, so-called ballooning.
- Emplacement within the space created during the development of regionally significant structures, particularly those formed in tectonic régimes dominated by strike-slip displacement including both transtensional and transpressional settings.

The occurrence of cauldron subsidence and stoping is well-established but these mechanisms are either restricted to or act most effectively at high crustal levels where the country rocks deform in the brittle régime, i.e. down to a few kilometres from the Earth's free ground surface. Furthermore, other arguments (see, for example, Castro 1987) suggest that stoping plays a relatively minor role in magma ascent and emplacement.

Quantitative estimates of the depth of emplacement of the 1.87–1.84 Ga GSDG suite of intrusive rocks in the southern structural domain, in combination with the field relationships in this area, argue strongly against an emplacement mechanism by simple uplift of the Earth's free surface or by large-scale stoping. Attention in earlier literature has focussed instead on magma transfer from deeper crustal levels and forceful emplacement at shallower levels by diapirism (Wikström et al. 1980, Wikström & Aaro 1986, Wikström 1987). The complementary effect of ballooning, in connection with the intrusion of younger pulses of magma in the 1.87–1.84 Ga GSDG suite, was invoked to explain the development of the marginal planar grain-shape fabric in this suite (Wikström 1984), but was rejected in a later synthesis (Wikström 1991). Diapiric emplacement in a tectonic régime with broadly north–south compression and east–west extension was also proposed in this later synthesis. Thus, the influence of both the vertical rise of magma due to buoyancy and a tectonic stress field comprise the current emplacement model for the 1.87–1.84 Ga GSDG suite of intrusive rocks.

Features that have been used as key arguments for the involvement of a diapiric mechanism of emplacement include:

- The contrasting contact relationships on different sides of the *Gravers fors granite.*
- The inferred geometry of the northern, marginal part of the 1.87–1.84 Ga GSDG suite of intrusive rocks around and west of Finspång (see, for example, schematic profiles in Fig. 1 in Wikström & Aaro 1986 and in Fig. 3 in Wikström 1991).

The discordant contact relationships on the eastern side of the *Gravers fors granite* were inferred to represent the deeper, vertical stem of a diapir and the concordant relationships on, for example, the western side were suggested to form part of the shallower, relatively flat-lying roof of the diapir (Wikström et al. 1980). A younger fault that strikes north–south across the intrusion was inferred to display major dip-slip movement (east-side-up) and to have tectonically juxtaposed these contrasting structural sub-domains. The similarity of the geometry of the northern, marginal part of the 1.87–1.84 Ga GSDG suite of intrusive rocks to model analogues of diapir structures (e.g. Ramberg 1981) was also proposed (e.g. Wikström & Aaro 1986). In particular, rim synformal lobes and associated "armpit" antiforms, diagnostic of the roofs of mushroom-shaped, diapiric structures, were both inferred to be present in this area.

It is maintained here that neither of these features are unequivocably diagnostic of a mechanism of emplacement related to diapirism. Alternative explanations for the structural and geometrical features described above are possible. For this reason, questionmarks concerning the significance of diapirism in the emplacement of the 1.87–1.84 Ga GSDG suite of intrusive rocks are raised.

Preservation of a pre-intrusive, D_{1S} tectonic fabric (see description of southern structural domain) in a pressure shadow in the country rocks on the eastern side of the *Gravers fors granite*, close to the feeder conduit, can explain the discordant contact relationships in this area. By contrast, more intensive, post-intrusive deformation in the country rocks elsewhere around the intrusion can account for the concordant contact relationships in these areas. This alternative explanation for the contrasting structural sub-domains on both sides of the *Gravers fors granite* gains some support, when it is kept in mind that detailed mapping on the eastern side of the intrusion (Wikström 1979) has documented

no features that can be expected in the stem of a diapir (Ramberg 1981), such as ductile shear zones subparallel to the contact to the granite with a steep lineation and ubiquitous, pluton-up kinematic indicators.

The schematic profiles across the northern, marginal part of the 1.87–1.84 Ga GSDG suite of intrusive rocks, around and west of Finspång (Wikström & Aaro 1986, Wikström 1991), are not a unique solution to the geometry of the contact relationships along this margin. The profiles link isolated bodies of such rocks to the north, via inferred antiformal structures above the ground surface, to the main massif further to the south. Alternative solutions, whereby the isolated bodies represent satellite bodies, like the *Gravers fors granite*, that are not in any way linked to the main massif or are bodies which attach themselves at depth to the main massif, via a narrow feeder conduit, are also possible. In the case of the *Finspång augen gneiss massif*, this conduit would have protruded downwards, as in the *Gravers fors granite*, on the south-eastern side of the massif.

The considerations raised above open the possibility that the mechanism of emplacement of the 1.87–1.84 Ga GSDG suite of intrusive rocks in the southern structural domain at mid-crustal levels was controlled solely by the space created in connection with significant dextral strike-slip movement along west-north-west–east-south-east structures in the Bergslagen region at this time. In short, the emplacement mechanism is simply related to the tectonic régime at this stage in the geological evolution. As developed further in the section "Tectonic model for the Svecokarelian tectonic activity in the Bergslagen region", this period is inferred to herald a changeover from transpressional to transtensional deformation. A transtensional régime would naturally be a highly effective mechanism to create the space needed for injection of voluminous sheets of magma into the middle crust and, as indicated above, account for the peak in metamorphism.

BRITTLE DEFORMATION UNDER SUBGREENSCHIST-FACIES METAMORPHIC CONDITIONS

As indicated above, the ^{40}Ar-^{39}Ar (hornblende, biotite) cooling ages indicate that the bedrock in the Bergslagen region cooled into the subgreenschist-facies metamorphic realm and was able to respond to deformation in the brittle régime some time between 1.8 and 1.7 Ga. Such conditions developed initially in the central part of the region. There are unfortunately few data bearing on the character, timing and kinematic signature of brittle deformation in the region. Apart from Forsmark in the north-eastern part, where SKB have recently completed detailed investigations to locate a site for the possible disposal of highly radioactive nuclear waste, relatively little is known about the structural development in the Bergslagen region from c. 1.7 Ga to the Quaternary period, i.e. throughout nearly 1 700 million years of Earth history. No detailed field characterization of lineaments or faults was carried out in the context of the Bergslagen project.

A summary of the structural trends of lineaments and faults, and their relationship to the post-Svecokarelian tectonic units in the region is provided below. The latter provides some stratigraphic constraints on the timing of brittle deformation in the region. Finally, key information in the north-eastern part of the Bergslagen region, predominantly from Forsmark, that is relevant to the brittle evolution of the bedrock is presented.

Structural trends of lineaments and faults

The distribution at the ground surface of deformation zones that contain evidence for faulting along their length and lineaments, which possibly also represent faults, are shown in Figure 159. The methodology used to define lineaments based on airborne magnetic, airborne electromagnetic VLF and topographic data is presented in the section entitled "Acquisition of new data and data interpretation – methodological aspects". No statistical analysis of the size, orientation and kinematic signature of lineaments and faults in the Bergslagen region has been carried out in the context of the present study. Some aspects of the spatial distribution of different orientation sets, based on a simple inspection of the lineament and fault map (Fig. 159), is presented below.

Lineaments and faults that trend west-north-west–east-south-east or north-west–south-east dominate in the north-easternmost part of the Bergslagen region (Fig. 159). This trend is identical to that shown by the ductile high-strain belts or zones in the area (see northern structural domain above) and the occurrence of both ductile and brittle deformation along some zones is apparent (Fig. 159). Furthermore, detailed drilling investigations in the Forsmark area (Stephens et al. 2007d, SKB 2008) confirm the reactivation of older ductile structures in the brittle régime in this area.

Lineaments and faults that trend north-west–south-east or west-north-west–east-south-east comprise a strongly conspicuous structural component in the bedrock between Norrköping and Eskilstuna in the south-eastern part of the Bergslagen region (Fig. 159). The occurrence of some of these structures along older ductile zones (Fig. 159) indicates once again the reactivation of older structures in the brittle régime. The bedrock

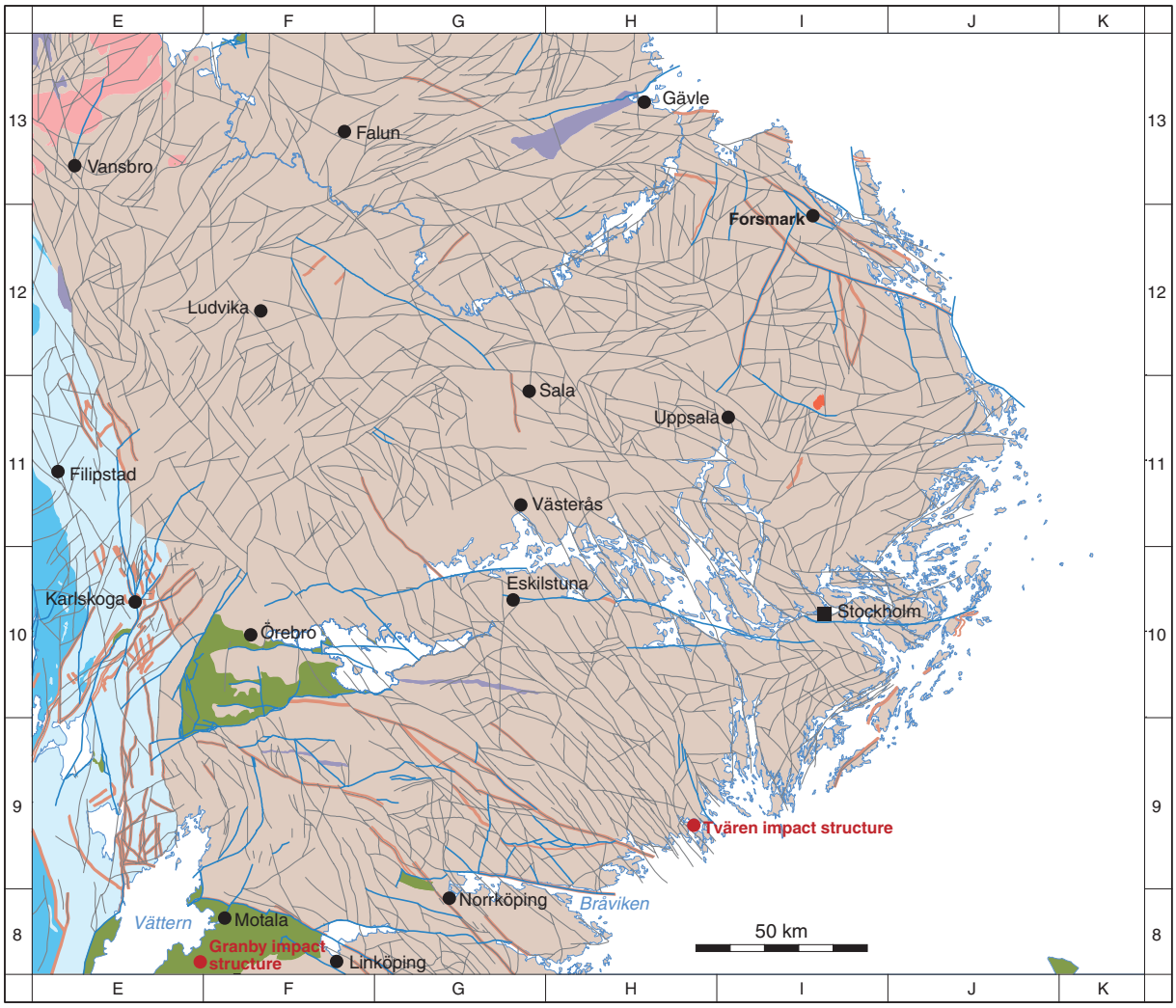

Fault

Ductile shear zone

Lineament indicated by geophysical or topographic data (possible fault)

Sedimentary cover rocks

Neoproterozoic and Lower Palaeozoic sedimentary rocks

Sveconorwegian orogen

Palaeoproterozoic (1.7 Ga) and Mesoproterozoic rocks affected, to variable extent, by Sveconorwegian ductile deformation and metamorphism

Palaeoproterozoic rocks (1.9–1.8 Ga) affected, to variable extent, by Sveconorwegian and older ductile deformation and metamorphism

Post-Svecokarelian rocks

Mesoproterozoic rocks

Palaeoproterozoic rocks (1.7 Ga)

Alkaline intrusive rock (uncertain age)

Alkaline intrusive rock (uncertain age)

Svecokarelian orogen

Palaeoproterozoic rocks (1.9–1.8 Ga) affected, to variable extent, by Svecokarelian ductile deformation and metamorphism

Fig. 159. Traces of lineaments and faults, and their relationship to ductile shear zones and the major tectonic units at the ground surface in the Bergslagen region. The location of place names referred to in the section "Brittle deformation under subgreenschist-facies metamorphic conditions" is shown on the map.

to the north of the major fault along Bråviken, east of Norrköping, that strikes west-north-west–east-south-east, was uplifted relative to the bedrock south of Bråviken following the development of the sub-Cambrian unconformity (see also below). This uplifted block, in predominantly the county of Södermanland, is conspicuous as far north as the major system of faults that strike east–west in the Eskilstuna–Stockholm area. This system of faults with east–west strike shows a north-side-down sense of movement that also occurred after the development of the sub-Cambrian unconformity.

The influence of the ancient Svecokarelian structural anisotropy (ductile high-strain zones, boundaries between rock units) on the orientation of lineaments and faults is also apparent in the north-western and eastern parts of the Bergslagen region (cf. Figs. 19 and 159). Lineaments with a north-east–south-west trend are common in the north-western part of the region, where-

as north of Stockholm, in the eastern part of the region, lineaments and faults oriented north-north-west–south-south-east or north-north-east–south-south-west are conspicuous.

A similar relationship between the orientation of lineaments and faults and the orientation of Sveconorwegian ductile structures in the area that corresponds to the western structural domain is also apparent (Fig. 159). A dominance of structures with an approximately north–south trend (Fig. 159) and the reactivation of Sveconorwegian ductile structures in the brittle régime is inferred.

Stratigraphic constraints on the timing of brittle deformation

The occurrence of different suites of igneous and sedimentary rocks that are 1.7 Ga or younger as well as Neoproterozoic and Lower Palaeozoic sedimentary cover rocks in the Bergslagen region (Fig. 159) provides some stratigraphic constraints on the timing of brittle deformation. The maximum age of the deformation is constrained by the age of the faulted rocks. In particular, Silurian or younger faulting is inferred in the area around the lake Vättern in the south-western part of the Bergslagen region (cf. Figs. 99 and 159). However, zones with a brittle component of deformation that are located along the boundaries between rocks affected by Svecokarelian tectonic activity and rocks that are post-Svecokarelian in age may have been established earlier in the ductile régime. In such cases, the brittle deformation would have given rise to reactivated structures in the older rocks on one side of the boundary and newly formed brittle structures in the younger rocks on the other.

Disturbances in the sub-Cambrian unconformity, which marks a conspicuous exhumed denudation surface that formed prior to 545 Ma, also provide constraints on the timing of faulting after the establishment of this major discontinuity (Lidmar-Bergström 1993, 1994). This surface is exposed at the current level of erosion in a large part of the Bergslagen region. Conspicuous examples of faulting that disturbed the sub-Cambrian unconformity occur in the county of Uppsala in the north-eastern part of the Bergslagen region (Bergman et al. 1996a, 1999c, Söderlund et al. in press), in the Eskilstuna–Stockholm area (Lidmar-Bergström 1994) and along Bråviken in the south-eastern part of the Bergslagen region (Bergman et al. 1996b)

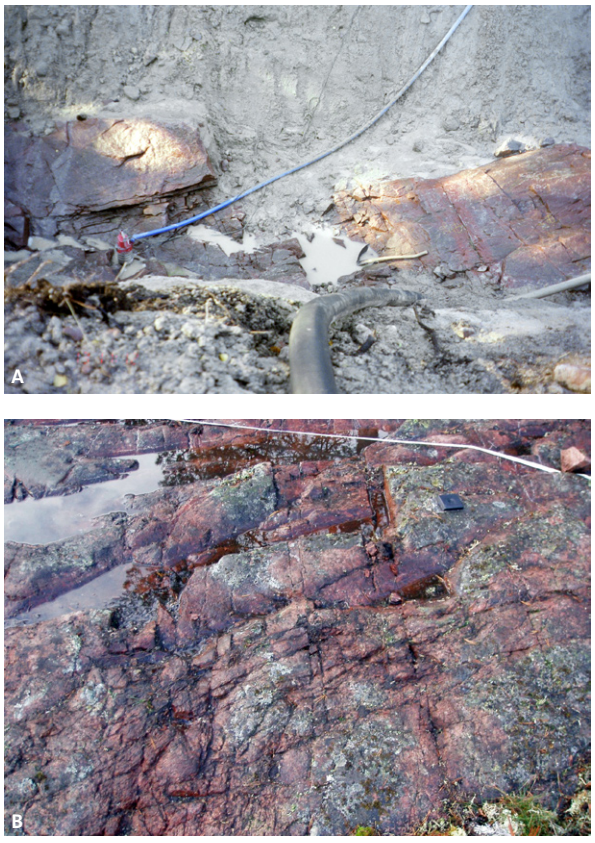

Fig. 160. Fracturing and wall rock alteration (red-staining) along exposed lineaments classified as magnetic minima at Forsmark in the north-eastern part of the Bergslagen region. **A.** Excavation site AFM001243 (Cronquist et al. 2005). **B.** Excavation site LFM001027 (Petersson et al. 2007). The identification codes refer to areal (AFM) and linear (LFM) SKB data sets at Forsmark.

Character, timing and kinematic signature of brittle deformation in the Forsmark area in the north-eastern part of the Bergslagen region

Geological significance of lineaments

The geological character of some lineaments defined by magnetic minima has been determined at Forsmark with the help of excavation work at the ground surface and drilling (see overview in Stephens et al. 2007d, p. 104–111). Investigations of lineaments with east-north-east–west-south-west or north-north-east–south-south-west trends confirmed that these structures represent steeply dipping fracture zones (Fig. 160). These zones are associated with wall rock hydrothermal alteration in the bedrock. This alteration consists of an intense hematite dissemination and is optically visible as red staining (Fig. 160). However, one excavation of a lineament, c. 1.2 km in length and with a north–south trend, revealed that the lineament is related to a swarm of dykes of granite and pegmatite with low magnetic susceptibility. In this case, the lineament was not unequivocably related to a fracture zone. This result illustrates the care that needs to be

taken in the interpretation of the geological significance of lineaments, even those defined by magnetic minima.

Gently dipping fracture zones and groundwater

High-resolution seismic reflection data have been acquired at the ground surface at the Forsmark site (see overview in Stephens et al. 2007d, p. 111–116). The seismic reflection data in combination with drilling work has demonstrated the occurrence of gently dipping (<30°) fracture zones (Juhlin & Stephens 2006). Such zones are not easy to detect using the standard airborne geophysical data acquired by SGU. The identification of gently dipping zones at Forsmark is important, since these structures, which are oriented at a high angle to the minimum prinicipal stress (σ_3) in the upper part of the bedrock in the current stress régime (Glamheden et al. 2007), are the most hydraulically transmissive at the site (Follin 2008). The fracture mineralogy along the gently dipping zones indicates that these structures, like all the other sets of fracture zones at the Forsmark site, formed during Proterozoic time (see also below). Since the gently dipping zones are at a high angle to σ_3 in the current stress régime, the gently dipping fractures in these zones will be most susceptible to dilatational strain and reactivation as joints in this stress régime and, thereby, most susceptible to bear groundwater at the current time.

Fracture minerals – relative and absolute ages

Four different groups of fracture minerals have been identified at Forsmark (see overview in Sandström et al. 2008a). These groups are summarized below in decreasing relative age of formation:

Generation 1 (oldest) minerals consist mainly of epidote, quartz and Fe-rich chlorite. Furthermore, the wall-rock to the fractures that contain this generation of minerals is altered and shows a red staining with fine-grained hematite dissemination. The deformation associated with this generation of minerals varies from brittle-ductile to brittle, in contrast with the deformation during the younger phases (generations 2 to 4) that is entirely brittle in character.

Generation 2 is a sequence of hydrothermal minerals that probably formed over an extended time interval. The absolute time span is not known. The sequence consists of a first phase of hematite-stained adularia (low temperature K-feldspar) and albite, followed by prehnite and calcite, and a later phase of hematite-stained laumontite and calcite. Once again, the wall-rock to the fractures that contain this generation of minerals is altered and shows a red staining with fine-grained hematite dissemination.

Generation 3 minerals are dominated by euhedral quartz, calcite and pyrite, together with subordinate albite, euhedral adularia that lacks hematite staining, corrensite and analcime. Oily asphaltite is also present, predominantly in the upper parts of the boreholes. No red staining is visible in the wall-rock to the fractures.

Generation 4 (youngest) minerals consist of clay minerals and calcite that precipitated as an outermost layer in open fractures. The youngest calcites are found in fractures and fracture zones that are hydraulically conductive at the current time (Sandström & Tullborg 2007).

Five adularia samples from both the generation 2 and generation 3 fracture mineral assemblages and three K-feldspar samples from rock fragments inside fault breccias have been dated with the ^{40}Ar-^{39}Ar method (Sandström et al. 2006a, 2008b). A fracture filling, which includes an assemblage of generation 2 adularia, prehnite, calcite and altered wall rock, has also been dated by the Rb-Sr method (Sandström et al. 2006a). Most samples were taken from steeply dipping fracture zones that strike east-north-east–west-south-west to north-north-east–south-south-west or from rock that was affected by such zones. One of the dated fault breccias was sampled along a composite ductile and brittle deformation zone that strikes north-west–south-east. It should be noted that lineaments and deformation zones with similar orientation are common throughout a large area close to and to the south-east of Gävle, in the north-eastern part of the Bergslagen region (Fig. 159). For this reason, it is considered that the geochronological data from fracture minerals at Forsmark are of regional significance.

^{40}Ar-^{39}Ar dating of generation 2, hematite-stained adularia has yielded consistent ages that range between 1.1 and 1.0 Ga. By contrast, K-feldspar from rock fragments in the fault breccias yielded two different, ^{40}Ar-^{39}Ar ages at 1.4 and 1.1 Ga. These two ages are younger than the ^{40}Ar-^{39}Ar (K-feldspar) ages in the bedrock outside deformation zones (Page et al. 2007) but older than the dated generation 2 adularia along fractures. ^{40}Ar-^{39}Ar dating of a younger generation 3 adularia yielded a well-defined plateau with a Permian age of 277 ± 1 Ma. The Mesoproterozoic ages for generation 2 fracture minerals and fault breccias at Forsmark bear some similarity to U-Pb (pitchblende) and Rb-Sr data from fracture minerals in the northern part of the county of Uppsala (Welin 1964, Wickman et al. 1983). A synthesis of the radiometric age determinations at the Forsmark site, including the ^{40}Ar-^{39}Ar (K-feldspar) ages, and the inferred bedrock geological evolution at this site is shown in Figure 161.

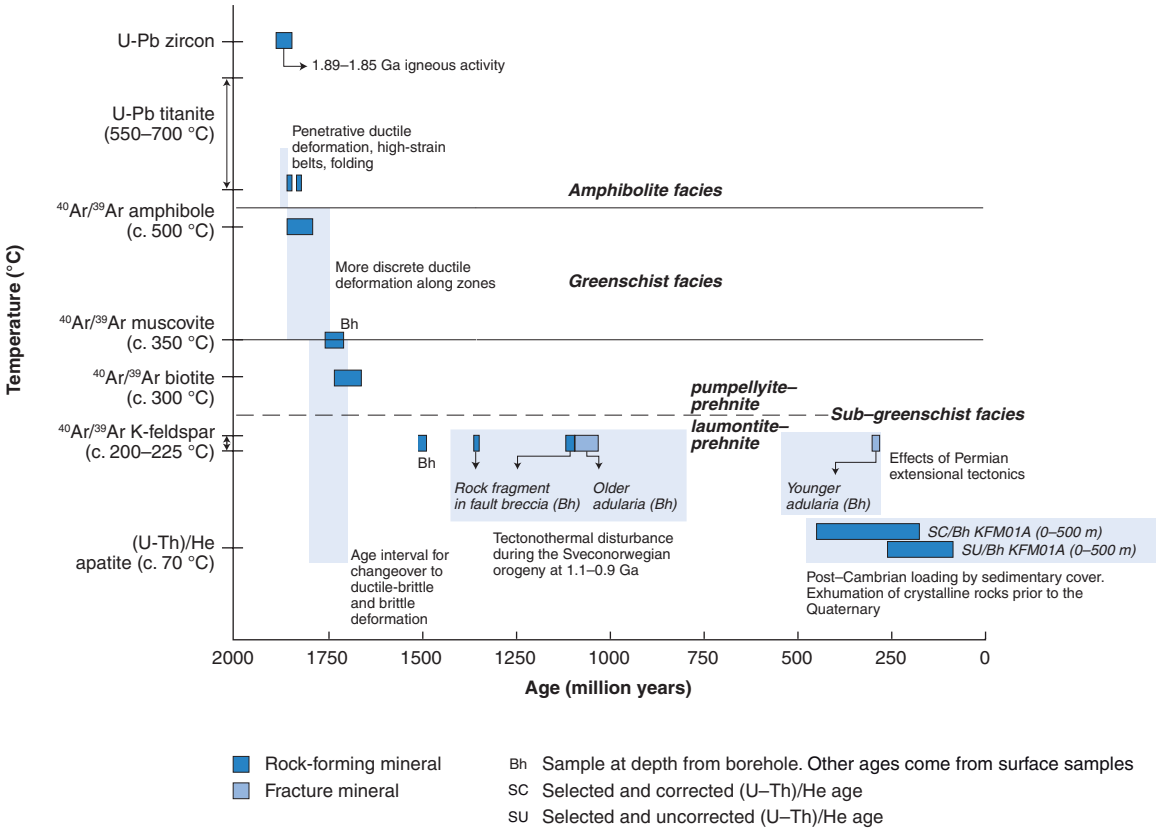

Fig. 161. Summary of radiometric age data and the bedrock geological evolution in the Forsmark area in the north-eastern part of the Bergslagen region (after SKB 2008). Only a selection of (U-Th)/He data from drill hole KFM01A are shown. The procedure adopted concerning the interpretation of all the (U-Th)/He data, both corrected and uncorrected, is discussed in Söderlund et al. (2008) and Stephens and Wahlgren (2008). The ^{40}Ar-^{39}Ar (white mica, K-feldspar) data from boreholes are included in this figure. ^{40}Ar-^{39}Ar (biotite) data from depth in drill holes are not shown. As expected, these data are somewhat younger than the equivalent surface data. Further discussion of the contents of this figure can be found in Stephens and Wahlgren (2008).

The generation 2 adularia and fault breccia ages from Forsmark indicate the importance of Sveconorwegian brittle reactivation in the north-eastern part of the Bergslagen region. However, before any coupling can be made between a mineral age and the actual timing of movement along a brittle structure, it is necessary to know the blocking temperatures for the different minerals within the selected isotope system. If shear or extensional failure along the fracture in combination with fluid flow occurred at temperatures that are lower than the blocking temperature, then the age reflects the time when the fracture mineral crystallized. In such an instance, it is possible to relate the age to the brittle deformational event. If brittle deformation and fluid flow occurred at temperatures above the blocking temperature, then the interpretation of the age is more complicated. An alternative interpretation, which involves a resetting of the isotope system during the brittle event and crystallization of the dated mineral earlier during the geological history, is possible.

The blocking temperature for the ^{40}Ar-^{39}Ar (K-feldspar) isotope system of c. 200–225 °C is close to the boundary of the stability fields for the pumpelleyite-prehnite and laumontite-prehnite subfacies (Fig. 161). For this reason, the ^{40}Ar-^{39}Ar (K-feldspar) isotope system is sensitive for resetting during growth of, for example, laumontite and there is some uncertainty with the interpretation of the ^{40}Ar-^{39}Ar dates for generation 2 adularia at 1.1 to 1.0 Ga (cf., for example, Sandström & Tullborg 2007 and Stephens & Wahlgren 2008). If the ages represent a resetting of this isotope system in connection with a flushing of hot fluids along the fracture zones and the growth of laumontite during a Sveconorwegian reactivation, then at least hematite-stained adularia in the generation 2 mineral paragenesis may be older than 1.1 Ga, i.e. pre-Sveconorwegian. Partial resetting of the ^{40}Ar-^{39}Ar (K-feldspar) isotope system, in response to the influence of hot hydrothermal fluids during a Sveconorwegian event, may also account for the variable ^{40}Ar-^{39}Ar (K-feldspar) ages inside the fault breccias.

Irrespective of which hypothesis is adopted (crystallization age or resetting), the generation 2 adularia data indicate that the the generation 1 minerals (epidote, quartz and Fe-rich chlorite) formed prior to 1.1 Ga,

Fig. 162. Subhorizontal and gently dipping fractures close to the ground surface at Forsmark in the north-eastern part of the Bergslagen region. **A.** Subhorizontal fracture filled with glacial sediment (Quaternary) inferred to be a sheet joint formed in connection with release of stress close to the ground surface. Excavation at the Forsmark nuclear power plant (after Carlsson 1979). **B.** Gently dipping fracture with wide aperture at drill site 5, Forsmark. The impressive aperture along this fracture is also inferred to have formed in connection with the release of stress close to the ground surface. Several fractures with this orientation at drill site 5 are filled with glacial sediment (Quaternary).

i.e. they are pre-Sveconorwegian. The corollary follows that the brittle deformation along the different sets of deformation zones at the Forsmark site (see below), all of which contain fractures with generation 1 or generation 2 minerals and hydrothermal alteration with hematite dissemination, initiated between 1.7 and 1.0 Ga.

The Permian adularia has grown on pyrite included in generation 3 and represents a late phase of the generation 3 mineral precipitation (Sandström et al. 2006a). A Palaeozoic age for the generation 3 minerals is supported by the isotopic compositions of the associated minerals calcite, pyrite and oily asphaltite, which all indicate an organic influence in the fluid from which these minerals precipitated (Sandström et al. 2006b, Sandström & Tullborg 2007). In particular, the asphaltite was derived from Cambrian to Lower Ordovician alum shale (Sandström et al. 2006b) that, together with limestone and other clastic sedimentary rocks, covered the crystalline bedrock at Forsmark during much of the Phanerozoic (see above).

The youngest generation of calcite (generation 4) occurs along hydraulically conductive fractures and zones. This mineral may have precipitated over a long period extending to the present. Fluids, which transported glacial sediment, also migrated downwards and filled reactivated fractures or newly formed sheet joints in the near-surface realm at Forsmark during the later part of the Quaternary (Fig. 162). These structures are inferred to have developed due to release of stress during unloading caused by the removal of ice (Carlsson 1979, Leijon 2005, Olofsson et al. 2007).

Kinematic signature of fracture zones

Surface and drill core data bearing on the character and kinematic signature of four sets of fracture zones at Forsmark (steep west-north-west–east-south-east to north-west–south-east, steep east-north-east–west-south-west to north-north-east–south-south-west, steep north-north-west–south-south-east and gently dipping) have been acquired. An overview of the primary data and an evaluation of these data have been presented by Stephens et al. (2008b). Virtually all zones (85%) contain broken fractures, along which shear striae are present (shear fractures). Thus, evidence for displacement along minor faults within fracture zones is apparent.

Polyphase brittle shear deformation is apparent along all the different sets of fracture zones. There is a dominance of compressive, strike-slip deformation and subordinate dip-slip movement along the steeply dipping structures. Reverse dip-slip and subordinate strike-slip senses of movement occurred along the gently dipping zones. The magnitude of both strike-slip and dip-slip displacement along fracture zones is poorly constrained. However, assessment of magnetic and reflection seismic data indicates only minor displacements (Stephens et al. 2007d).

Inferred meteorite impact structures

Circular geological or topographic features at Granby and Tvären in the south-western and south-eastern parts of the Bergslagen region (Fig. 159) have been interpreted as Ordovician meteorite impact structures (Grahn & Nolvak 1993, Lindström et al. 1994). By far the best-documented structure of this type in Sweden, with a diameter of c. 50 km, occurs in the Siljan area, in the central part of Sweden, and formed during the Late Devonian or Early Carboniferous (Wickman 1988, Henkel & Pesonen 1992). The southernmost part of this circular geological and topographic feature borders into the north-westernmost part of the Bergslagen region.

Tectonic model for Svecokarelian orogenic activity in the Bergslagen region

MODEL FOR THE TECTONIC EVOLUTIONARY DEVELOPMENT

Earlier workers proposed different coaxial strain models for the development of ductile structures in the bedrock in the Bergslagen region. Radically different opinions were expressed concerning the bulk horizontal shortening direction to which these structures were assumed to be related. Several workers proposed crustal shortening in a north–south direction (e.g. Magnusson 1936, Lundegårdh 1959, Wikström 1979) or a combination of north–south shortening and east–west extension (Wikström 1991). By contrast, Stålhös (1981, 1984, 1991), for example, envisaged bulk horizontal shortening in an east–west direction that gave rise to both F_1 folding and F_2 cross-folding close to each other during geological time.

Later workers have recognized the occurrence of ductile high-strain zones or broader high-strain belts in the Bergslagen region and the significance of non-coaxial strain in the structural development (see, for example, Talbot & Sokoutis 1995, Stephens et al. 1997d, Persson & Sjöström 2002, 2003, Talbot 2008, Högdahl et al. 2009 and the section "Deformation, metamorphism and mechanism of emplacement of the 1.87–1.84 Ga GSDG suite of intrusive rocks" in this report). In particular, structural data along the high-strain belts that formed prior to the major folding in the northern and central structural domains (general D_1 strain, see below) and the retrogressive ductile high-strain zones in the northern and southern structural domains (D_{DZ}) indicate a significant component of strike-slip shear deformation in the region. The occurrence of both transpressional and transtensional deformation (see, for example, Dewey et al. 1998 for definitions) is proposed below.

Shift from transpressional to transtensional deformation in the northern and central structural domains around 1.86 Ga

The evaluation of ductile structures presented in the section entitled "Deformation, metamorphism and mechanism of emplacement of the 1.87–1.84 Ga GSDG suite of intrusive rocks" indicates that the grain-shape fabric in the easternmost part of the northern structural domain (D_{1N}), in the central structural domain (D_{1C}) and in the bedrock corridors outside younger ductile high-strain zones (or belt) in the southern structural domain (D_{1S}) are identical. The development of this general D_1 fabric, with variable intensity, is constrained between 1.88 and 1.85 Ga in the entire region and more specifically between 1.87 and 1.86 Ga in the Forsmark area in the northern structural domain (Fig. 163). The development of a steeply dipping planar fabric and the variable inclination of the stretching lineation in this fabric suggest development in a transpressive tectonic régime (Fig. 163).

Bulk crustal shortening was absorbed by dextral strike-slip shear deformation along ductile high-strain belts with west-north-west–east-south-east to north-west–south-east strike (northern structural domain), sinistral strike-slip shear along a conjugate ductile high-strain belt with north-east–south-west strike (central structural domain) and shortening across these high-strain belts. Bulk horizontal shortening in an approximately north–south direction in combination with east–west extension is inferred.

The low-P metamorphism in at least the south-eastern part of the northern structural domain and in the central structural domain, in part with the development of migmatites, peaked shortly after D_1 (M_1 in Fig. 163). This development resulted in the common occurrence of recovery and static recrystallization in the bedrock with strain-free grains. In a metallurgical sense, many of the rocks in the Bergslagen region are annealed. It is inferred that the common occurrence of such grains and the establishment of the peak of metamorphism was induced by a passive heating of previously deformed material in what can be referred to as regional contact metamorphism.

As argued earlier, the peak of metamorphism was related to the injection of hot, mafic igneous material into the crust, i.e. by mafic underplating, and that there is a close temporal relationship between the peak of metamorphism and the intrusion of the 1.87–1.84 Ga GSDG and subordinate 1.87–1.85 Ga GDG rock suites (Fig. 163). The intrusion of these igneous rocks after the establishment of D_1 deformation in the bedrock is consistent with this hypothesis. It is suggested that establishment of the metamorphic peak, and not least the migmatization, corresponded to a changeover to a transtensional tectonic régime (Fig. 163).

As indicated in the section entitled "Deformation, metamorphism and mechanism of emplacement of the 1.87–1.84 Ga GSDG suite of intrusive rocks", the changeover to a transtensional tectonic régime would have provided an effective mechanism to create the space needed for the emplacement of major volumes of igneous rock at mid-crustal levels during the 1.87–1.84 Ga time interval. Continued east–west extension and a continued component of dextral strike-slip defor-

mation along the steeply dipping, high-strain belts or zones with west-north-west–east-south-east to north-west–south-east strike are inferred.

Tectonic reworking in the southern structural domain around 1.8 Ga – a renewed transpressional to transtensional shift

The southern structural domain differs from the domains further north by the evidence for more pervasive, post-1.85 Ga tectonic reworking of the older structures discussed above (Fig. 163). This reworking is expressed by:

- Pervasive amphibolite-facies deformation (D_{DB} along the *Zinkgruvan–Finspång deformation belt*) and later z-asymmetric folding further south in the domain.
- Retrogressive deformation along ductile high-strain zones (D_{DZ} along, for example, the *Vingåker–Nyköping deformation zone*) reminiscent of the post-1.85 Ga retrogressive shearing along discrete zones in the northern structural domain.
- One or more events of low-P and high-T metamorphism around 1.8 Ga (M_2), temporally coincident with a new phase of major GSDG intrusive igneous activity.

It is inferred that the steeply dipping planar fabric and the associated linear fabric with highly variable inclination along the retrogressive, ductile high-strain zones in the southern structural domain (D_{DZ}) were formed in connection with transpressive deformation (Fig. 163). Bulk horizontal shortening in an approximately north–south direction would then be required to explain the dextral strike-slip component of deformation along these structures. Bearing in mind the arguments presented in the previous section, the emplacement of the 1.8 Ga GSDG intrusive rocks and the

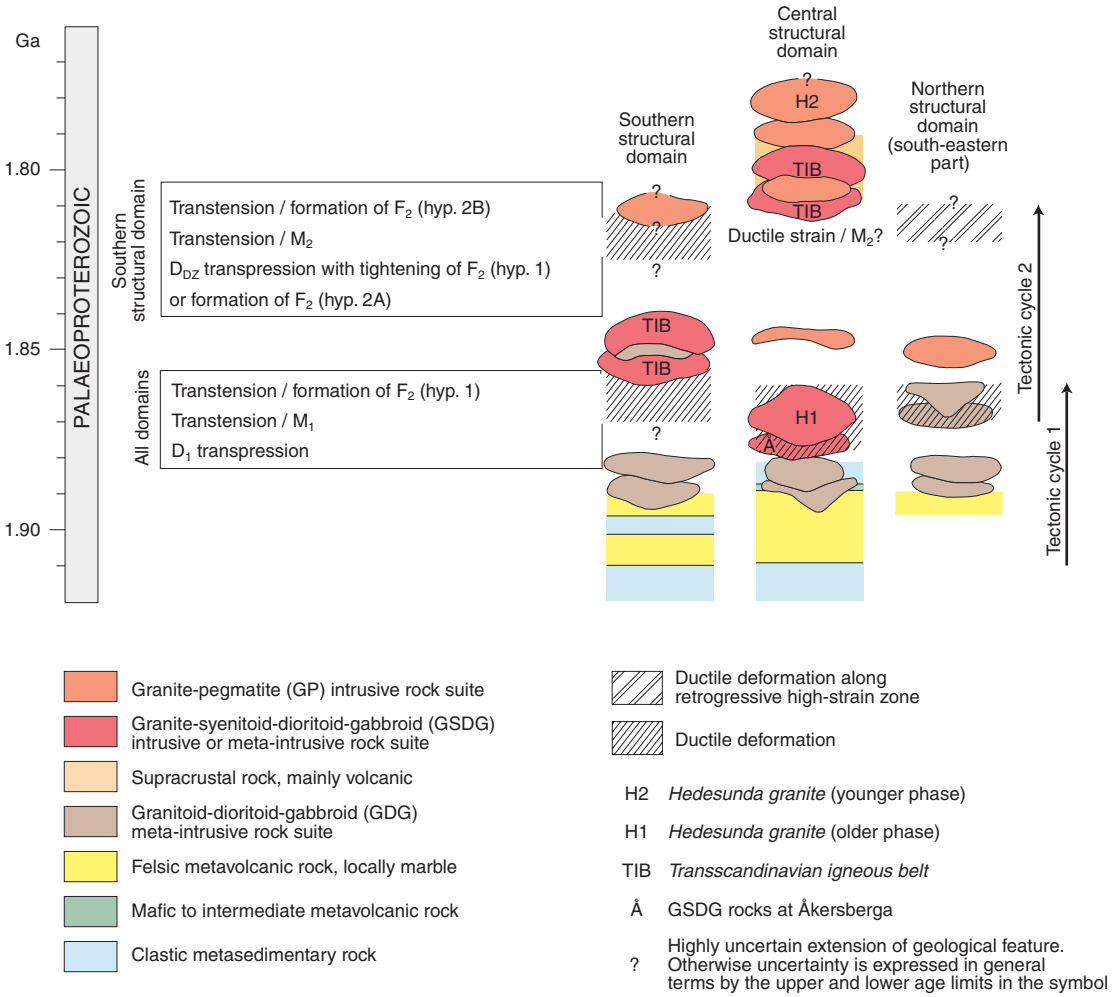

Fig. 163. Simplified sketch that shows the main deformational and metamorphic events, their tectonic setting and their relationship to the stratigraphic model for the time period 1.91–1.78 Ga in the Bergslagen region. D = deformation (general term), F = folding, M = peak metamorphism. See text for further explanation.

peak of the younger phase of metamorphism around 1.8 Ga (see section "Deformation, metamorphism and mechanism of emplacement of the 1.87–1.84 Ga GSDG suite of intrusive rocks") are inferred to have taken place during a renewed phase of transtensional deformation in the crust (Fig. 163).

It appears that the tectonic evolution that occurred around 1.86 Ga repeated itself approximately 50 million years later around 1.8 Ga, and the effects of this reworking are most conspicuous in the southern structural domain. However, the driving mechanism appears to have been similar during these two time intervals. A conceptual mechanism that involved a cyclic tectonic evolution in the region is inferred (Fig. 163). Once again it needs to be emphasized that the northern boundary of the 1.8 Ga metamorphic overprint (M_2 in Fig. 163) in the Bergslagen region is not yet established (see section "Deformation, metamorphism and mechanism of emplacement of the 1.87–1.84 Ga GSDG suite of intrusive rocks").

Regional D_2 folding – mechanism, tectonic setting and timing

Regional-scale folding deformed both the medium-grade, D_1 planar grain-shape fabric in the central structural domain and the D_1 migmatitic gneissic fabric in the southern structural domain. D_1 ductile high-strain belts are also rotated in later folds in the northern and central domains. The axes vary in plunge with a tendency to moderate to steep plunge in the central structural domain and gentle to moderate plunge at least in the high-grade rocks in the southern structural domain. The occurrence of anatectic veins along the axial surface traces to these folds in the high-grade rocks indicate folding, at least locally, under high-grade metamorphic conditions, coupled to one or more, later migmatization events (see earlier text in the section "Integrated evaluation of the timing of Svecokarelian ductile deformation, metamorphism and cooling").

In the major hinge zones in especially the central structural domain, the folds do not show a strong axial surface fabric development but are associated with strong linear fabrics and constrictional strain. However, transposition of older D_1 structures is conspicuous along the flanks of major D_2 folds in this domain, and ductile high-strain zones or belts are commonly developed along these flanks (see earlier text). The folds are markedly tighter in the northern structural domain, where there is evidence for post-1.85 Ga ductile strain along retrograde zones (see earlier text), and in the southern structural domain, where there are both high-strain zones and a broader high-strain belt that affected the 1.87–1.84 Ga GSDG intrusive rocks.

There are major uncertainties concerning the mechanism, tectonic setting and timing of the regional post-D_1 folds. It has been suggested that both the D_1 deformation and the D_2 folding formed as a result of progressive, bulk horizontal shortening in a north–south direction (e.g. Persson & Sjöström 2002). However, if the D_2 folding formed as a result of strike-slip shear deformation rather than by bulk horizontal shortening of the crust, then it is also possible that the D_2 folding developed in a regional-scale, transtensional tectonic régime. The mechanisms for folding of amphibolite- to granulite-facies rocks in an extensional tectonic setting and the difficulties to distinguish such structures from those formed in a compressional régime have been addressed in Harris et al. (2002). A transtensional D_2 tectonic régime in Bergslagen is attractive since it explains the poor development of an axial surface fabric and the continued development of a pronounced linear grain-shape fabric during the D_2 event.

Some hypotheses for the development of the regional D_2 folding that take account of the above considerations and the poor time constraints for their formation are presented in Figure 163. Hypothesis 1 permits the development of these structures in a transtensional régime during the tectonic event around 1.86 Ga with subsequent tightening in the southern structural domain during later 1.8 Ga transpression (Fig. 163). Hypothesis 2 permits the development of the D_2 folding around 1.8 Ga either in a transpressional (hypothesis 2A) or transtensional (hypothesis 2B) tectonic setting. All models contain a strike-slip shear component that can explain fold asymmetry.

CONCEPTUAL DRIVING MECHANISM – MIGRATORY TECTONIC SWITCHING IN AN ACCRETIONARY OROGEN

On the basis of the geochemistry of the Svecofennian 1.91–1.89 Ga metavolcanic rocks, Löfgren (1979) and Loberg (1980) suggested that the Bergslagen region formed as a volcanic arc above a subduction zone. By contrast, Oen et al. (1982), van der Velden et al. (1982) and Oen (1987) proposed a continental rift setting for the western part of the region. Subsequently, Allen et al. (1996) argued for an extensional back-arc setting, along an active continental margin, for the Svecofennian, 1.91–1.89 Ga volcanism and for the deposition of associated iron oxide and Zn-Pb-Ag sulphide deposits in the Bergslagen region. These authors envisaged a cyclic tectonic evolution through "stages of intense magmatism, thermal doming, and crustal extension,

followed by waning extension, waning volcanism, thermal subsidence, reversal from extension to compressional deformation, regional metamorphism, and structural inversion" (p. 979 in Allen et al. 1996).

Both the geochemical character of the igneous rocks in the Bergslagen region (see section "Character, spatial distribution, geochronology, geochemical signature, petrophysical characteristics and regional geophysical signature of rock units") and the close interplay between igneous activity, metamorphism and deformation argue for a convergent plate setting for the 1.9–1.8 Ga tectonic evolution. Furthermore, both Sm-Nd data and U-Pb (zircon) geochronology (see same section as that referred to above) indicate the occurrence of a juvenile, pre-1.91 Ga crust in the region. All these features need to be taken into account when a conceptual model for the geodynamics of the region is discussed.

Hermansson et al. (2008a) recently developed further the cyclic tectonic concept in a continental back-arc setting (Allen et al. 1996), in the context of a complex interplay between igneous activity on the one hand and ductile deformation and metamorphism on the other in separate tectonic cycles. Each cycle extended over approximately 50 million years of geological time. Hermansson et al. (2008a) illustrated the tectonic concept for the older cycle between 1.91 and 1.86 Ga and geochronological data from the Forsmark area in the easternmost part of the northern structural domain were used to constrain the timing of ductile deformation (1.87–1.86 Ga). A description of the concept for the older cycle in Hermansson et al. (2008a), which involved a long period of transtensional tectonics followed by a short period of transpression and a shift back to transtension around 1.86 Ga (see above), is presented below.

Migration of a subduction hinge away from an overriding plate caused continental back-arc extension (Fig. 164). This tectonic scenario is expressed, in particular, by the Svecofennian, 1.91–1.89 Ga bimodal volcanism and the infill by younger clastic sedimentary rocks in agreement with Allen et al. (1996). Major igneous activity continued around 1.89 to 1.87 Ga, within what has been inferred to be a waning extensional tectonic setting (Fig. 164). As a consequence of a change in the migration of the subduction hinge towards the

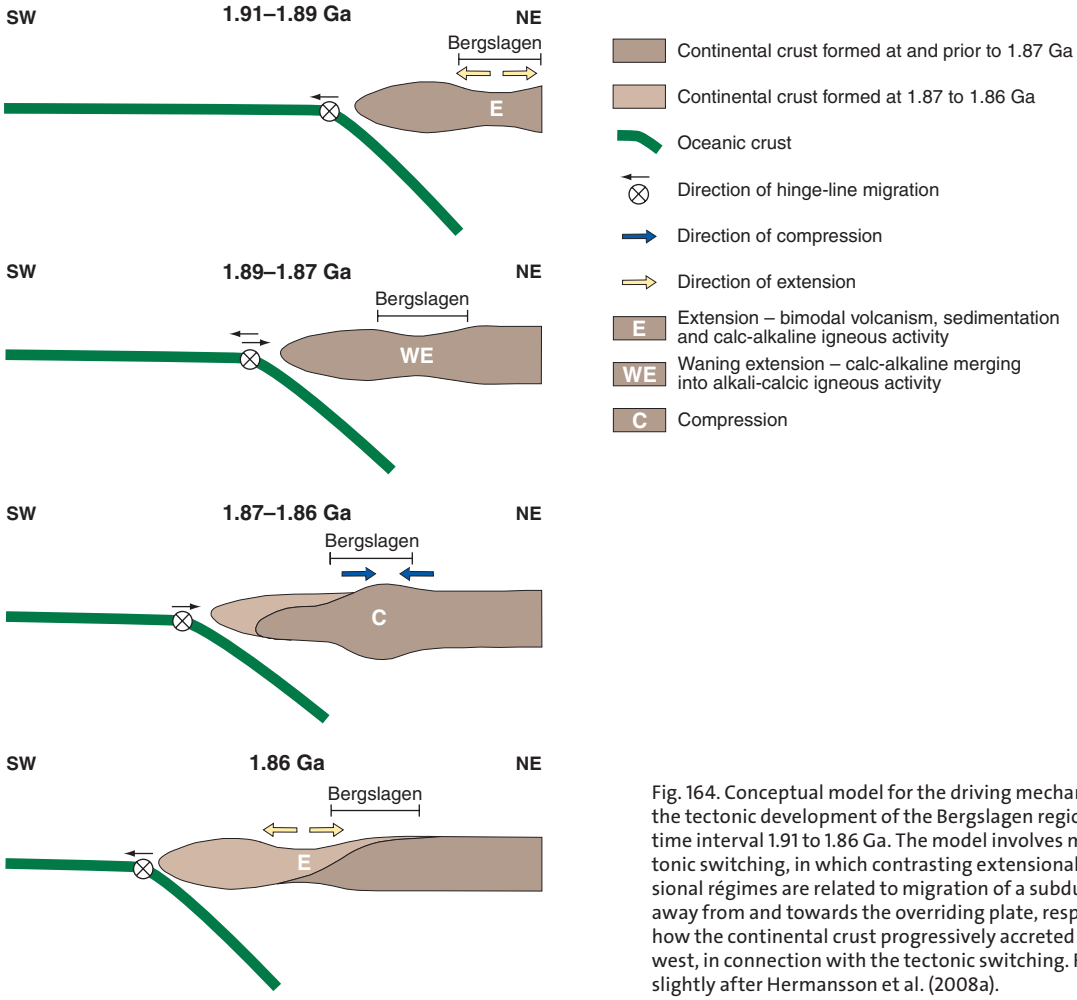

Fig. 164. Conceptual model for the driving mechanism behind the tectonic development of the Bergslagen region during the time interval 1.91 to 1.86 Ga. The model involves migratory tectonic switching, in which contrasting extensional and compressional régimes are related to migration of a subduction hinge away from and towards the overriding plate, respectively. Note how the continental crust progressively accreted to the southwest, in connection with the tectonic switching. Figure modified slightly after Hermansson et al. (2008a).

overriding plate, bulk horizontal shortening of the back-arc region followed in a short time period around 1.87 to 1.86 Ga in a transpressional tectonic régime (Fig. 164). A reversal to migration of the subduction hinge away from the overriding plate caused renewed continental back-arc extension in a transtensional tectonic régime around 1.86 Ga and the initiation of a new tectonic cycle (Fig. 164). This development resulted in a south-westerly migration in the focus of tectonic activity along the active continental margin.

The tectonic model proposed in Hermansson et al. (2008a) involves migration of what has been described as tectonic switching, with rapid changes from extensional to compressional tectonics and the reverse, in the younger accretionary orogenic systems of eastern Australia (Lachlan orogen) and New Zealand (Collins 2002). Bearing in mind the orientation and kinematic signature of the D_1 high-strain belts or zones in the region, approximately northward-directed oblique subduction beneath an active continental margin to the north-east is inferred. The model is also applicable to the second tectonic cycle that ended around 1.8 Ga. However, due to the south-westward migration of the focus of tectonic activity, the effects of this later cycle are suggested to be distinct only in the southern structural domain in the Bergslagen region. The migratory tectonic switching model also takes into account the occurrence of older crust in the Bergslagen region, which formed further to the north-east, possibly during one or more earlier tectonic cycles of similar character.

The migratory tectonic switching model of Hermansson et al. (2008a) highlights the accretionary character of the Svecokarelian orogen, in the manner envisaged on a regional scale by, for example, Hietanen (1975) nearly 35 years ago. It contrasts strongly with current conceptual thinking for the tectonic evolution of the Fennoscandian Shield, including the Bergslagen region. These alternative models involve the removal of oceanic crust and multiple collisions of continental fragments, both with the older continental crust in the north-eastern part of the shield and with each other (see, for example, Nironen 1997, Lahtinen et al. 2008, Talbot 2008).

Key issues for future work

This synthesis of the bedrock geology in the Bergslagen region has identified the need for new data in several areas to better constrain our understanding of the complex geology in this region. Some of the more important issues are summarized below:

- A new appraisal of the origin of the different iron oxide deposits and their relationship to the Zn-Pb-Ag sulphide deposits in the region. A research project financed by Boliden AB, Dannemora Mineral AB, Luleå University of Technology and SGU is currently ongoing.
- A more detailed evaluation of the relative significance of transtensional and transpressional deformation in the Bergslagen region.
- An assessment of the mechanism of formation of the regionally significant D_2 folds that dominate the structural framework of the region and not least the variation in their degree of plunge in different structural domains affected by different grades of metamorphism. This issue is linked strongly to the previous issue.
- Acquisition of detailed microstructural data bearing on the relationships between the different phases of Svecokarelian metamorphic mineral growth and between metamorphism and deformation in the region.
- Acquisition of more geochronological data bearing on the timing of metamorphism in the Bergslagen region, in particular the timing and spatial distribution of the two (or more) phases of Svecokarelian migmatization (M_1 and M_2) in the Svecokarelian orogen and the possibly pre-Sveconorwegian, amphibolite-facies metamorphism inside the Sveconorwegian orogen, in the south-westernmost part of the region. An internal research and development project at SGU has recently been initiated that aims to constrain the timing of migmatization in the eastern part and south of the Bergslagen region.
- Focussed and integrated work bearing on the character, kinematic signature, timing and hydrogeological properties of brittle deformation in the Bergslagen region.

Furthermore, bearing in mind both the wealth of data in the gravity and petrophysical databases at SGU and the developments in 3-D modelling software, there are now excellent possibilities to improve the interpretation of the major gravity anomaly in the central part of the Bergslagen region (*Central Swedish Gravity Low*) and the 3-D geometry of the granitic bodies included in the GP intrusive rock suite that are spatially related to this anomaly.

Description of excursion stops

The stops for a geological excursion in the Bergslagen region, planned over five days, are described below. The excursion has been designed to start and end in Uppsala with overnight stops in Sala, Norberg, Hällefors and Askersund. The description is based on the guide used when the excursion was implemented during 2000 and 2001. However, some of the geological features described may be more difficult to observe at the current time due to the physical deterioration of the quality of the outcrop with time or possibly even to disturbance of the outcrop due to, for example, road construction. The stops are arranged according to different themes that vary in quantity between two and four themes for each day.

The location of the excursion stops are shown in Figure 165 and further assistance with the loca-

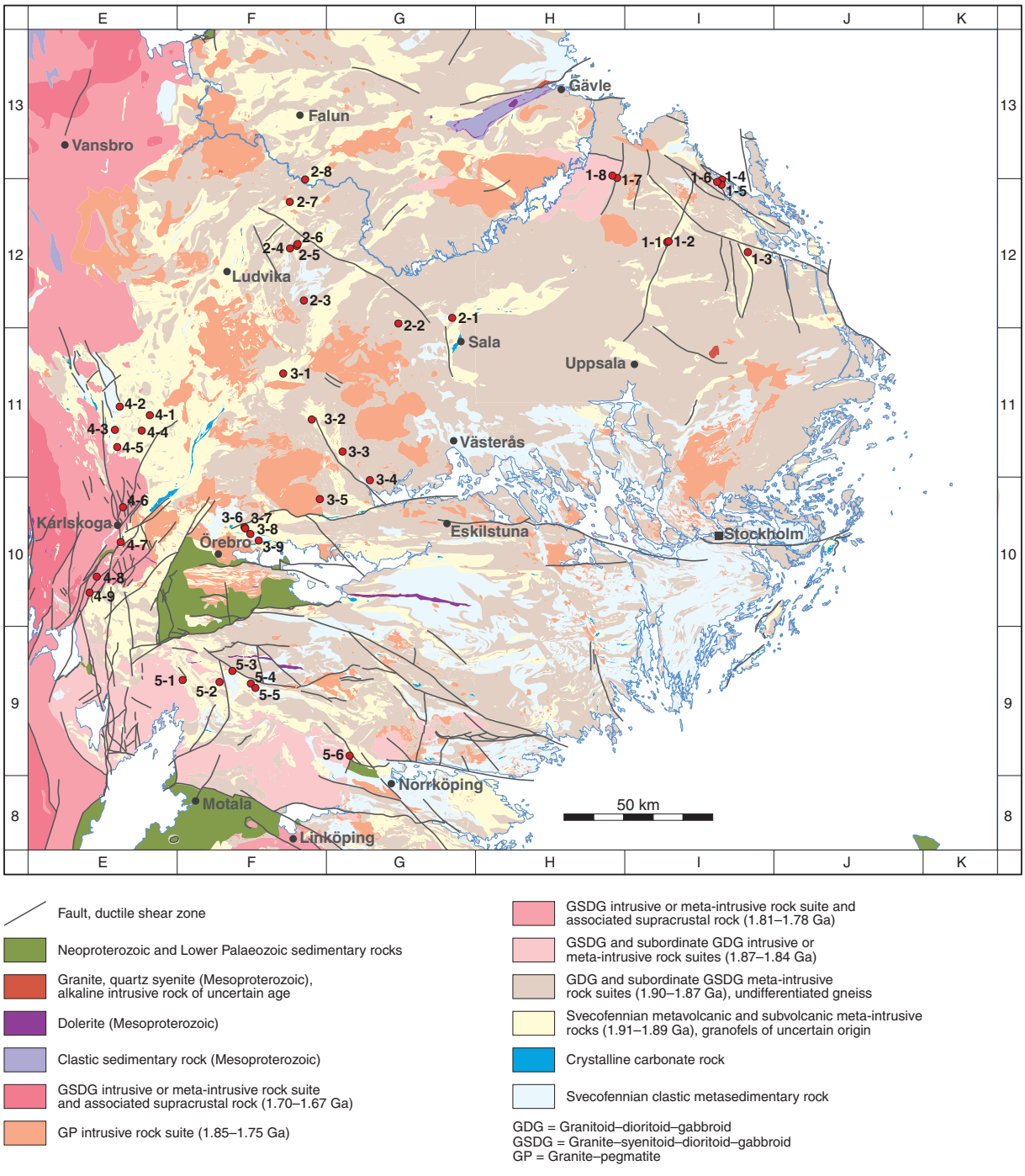

Fig. 165. Location of excursion stops, Bergslagen region.

tion of place names can be found in Figure 28. The information in parentheses after the locality name (e.g. sub-area 6, CSD, CMMD, 12I Östhammar NV, 6678822/1614298) refers to the position of the excursion stop in relation to the different volcanic sub-areas (if relevant), structural domains and metamorphic domains, which were introduced and described in the previous text, and the geographic location of the stop according to topographic map sheet, the square within the map sheet and the coordinates (northing/easting) in the Swedish national grid (RT 90).

The following acronyms are employed: NSD = Northern structural domain, CSD = Central structural domain, SSD = Southern structural domain, WSD = Western structural domain, CLMD = Central low-grade metamorphic domain, CMMD = Central medium-grade metamorphic domain, SMMD = Southern migmatitic metamorphic domain. No excursion stops are included in the northern migmatitic metamorphic domain.

DAY 1

Theme 1: Svecofennian volcanostratigraphy in the Dannemora–Gimo area (sub-areas 6 and 8)

Stop 1-1. Gruvsjön at Dannemora

(sub-area 6, CSD, CMMD, 12I Östhammar NV, 6678822/1614298)

Volcanic metasiltstone with graded beds and accretionary lapilli horizons in contact with a juvenile, rhyolitic pyroclastic mass flow deposit that formed during the intense volcanism and extension stage, according to the general stratigraphic scheme for the Bergslagen region (Allen et al. 1996). The mass flow deposit probably forms the youngest, juvenile volcanic unit in the area and, for this reason, was selected for a U-Pb (zircon) TIMS age determination (1894±4 Ma, see appendix). The tectonic foliation (S_1) is discordant to bedding (S_0), strikes east–west and shows a subvertical dip.

Stop 1-2. Nordschaktets lave at Dannemora

(sub-area 6, CSD, CMMD, 12I Östhammar NV, 6679050/1614750)

Volcanic metasiltstone with beds of crystalline carbonate rock (marble) belonging to the waning volcanic stage, according to the general stratigraphic scheme for the Bergslagen region (Allen et al. 1996). Graded bedding indicates that the rocks young towards the east. The tectonic foliation (S_{1C}) is parallel to bedding (S_0) and this relationship is most prominent in the carbonate-rich beds. D_{2C} deformation is apparent in the form of a discordant spaced cleavage in the volcanic metasiltstone and a crenulation of S_0/S_{1C} in the crystalline carbonate rock. The rocks at this locality belong to the host rock to the *Dannemora iron oxide deposit* and comprise the stratigraphically youngest rocks in the area. The carbonate rocks at Dannemora locally contain stromatolites and pseudomorphs after gypsum and halite, indicating deposition in a shallow water environment with the presence of evaporites (Lager 2001).

Stop 1-3. 100 m south of road 292 between Gimo and Hargshamn

(sub-area 8, CSD, CMMD, 12I Östhammar NO, 6675402/1641245)

Reddish to grey, massive, plagioclase-phyric metavolcanic rock similar to the rocks observed in the *Storsjön formation* in the western part of the Bergslagen region (Lundström 1983). Partly conglomeratic, volcanic metasiltstone that probably represents a pyroclastic mass flow deposit is also present. Clasts inferred to be fragments of pumice occur. The rocks at this stop have been affected by a higher degree of metamorphism relative to that at stops 1-1 and 1-2, and this feature provides some uncertainty in the interpretation of their primary character. The tectonic foliation (S_{1C}) strikes approximately north–south. Conspicuous F_{2C} crenulation of the S_{1C} foliation is apparent in mica-rich parts. The F_{2C} fold axes plunge steeply to the west-north-west and the subvertical, S_{2C} axial surface cleavage shows a west-north-west–east-south-east strike.

Theme 2: Variation in the character and intensity of ductile deformation in metagranitoids belonging to the 1.90–1.87 Ga GDG intrusive suite, Forsmark

Stop 1-4. North-east of Bolundsfjärden

(NSD, CMMD, 12I Östhammar NO, 6699699/1632603)

Pale red, medium-grained, equigranular metagranite with occasional dykes of pegmatite, aplitic granite and amphibolite. A sample of metagranite from an outcrop approximately 300 m to the east has yielded a U-Pb (zircon) SIMS age of 1867±4 Ma (Hermansson et al. 2008a). The metagranite at stop 1-4 shows a weak foliation (S_{1N}) with approximately east–west strike and a conspicuously more intense mineral lineation. The foliation is also folded (F_{2N}). The metagranite at stop 1-4 has been included in the 1.90–1.87 Ga GDG intrusive suite in the Bergslagen region (Stephens et al. 2007a),

on the basis of its age and intrusion–deformation relationships.

Stop 1-4 lies within a tectonic lens that extends from immediately north-west of the Forsmark nuclear power plant in the north-west to Öregrund in the south-east (see Fig. 127). The north-western part of this lens, south-east of the nuclear power plant, has been selected by Svensk Kärnbränslehantering AB (SKB) as the site for the disposal of highly radioactive nuclear waste in Sweden. This tectonic lens is surrounded both to the north-east and to the south-west by ductile high-strain belts that strike west-north-west–east-south-east and dip steeply to the south-south-west. There is also a high concentration of more discrete, complex ductile and brittle deformation zones within the broader high-strain belts, with a similar orientation as the high-strain belts. These include the Singö and Eckarfjärden deformation zones to the north-east and south-west, respectively.

Stop 1-5. South of Bolundsfjärden

(NSD, CMMD, 12I Östhammar NO, 6698012/1632480)

Same metagranite as that observed at stop 1-4 with pegmatite dykes. It is important to compare the character and intensity of ductile deformation at this locality with the ductile strain at stop 1-4. The metagranite at stop 1-5 shows a strongly developed tectonic foliation that strikes west-north-west–east-south-east and dips steeply to the south-south-west. A pegmatite dyke is also affected by the tectonic foliation. Stop 1-5 is situated within the broad belt of high ductile strain to the south-west of the tectonic lens at Forsmark.

Stop 1-6. Outcrop adjacent to drill site 4, Labboskogan

(NSD, CMMD, 12I Östhammar NO, 6698917/1630990)

Strongly banded and foliated metatonalite, amphibolite and fine-grained, felsic meta-igneous rock (metavolcanic rock?) in the same ductile high-strain belt as that observed at stop 1-5. The tectonic banding and foliation in this strongly deformed rock (high-temperature mylonite) strike west-north-west–east-south-east and dip steeply to the south-south-west. A pale red granite dyke is weakly discordant to the tectonic banding. Observations at a limited number of outcrops in the Forsmark area and its surroundings indicate a dextral strike-slip component of deformation along the ductile high-strain belts. The mineral lineation along these belts plunges gently to moderately to the south-east.

Theme 3: High-grade metamorphic rocks immediately east of the *Hedesunda granite* and the older phase of intrusive rocks in the *Hedesunda granite*

Stop 1-7. Road outcrop approximately 1 km north-west of Strömsbergs bruk

(CSD, CMMD, 13H Gävle SO 6700320/1597456)

Grey migmatitic orthogneiss inferred to represent a metagranitoid on the bedrock map of the Berglagen region (Stephens et al. 2007a). Compare the grade of metamorphism here with that observed at especially stops 1-1 and 1-2, approximately 25 km to the south-east. The bedrock at this locality shows a steeply dipping, tectonic banding and foliation that strike north-north-east–south-south-west. These planar structures form an axial surface structure to F_{2C} folds that deform both an older (S_{1C}) planar grain-shape fabric in the orthogneiss and the leucosome veins. Several leucosome veins occur as relic intra-folial structures within S_{2C}. Some bands along S_{2C} are mica-rich and phyllonitic in character. Younger, partly discordant dykes of granite and pegmatite are also present.

The strongly deformed, high-grade rocks at stop 1-7 are situated immediately to the east of the rocks included in the *Hedesunda granite* that show lower ductile strain and are not affected by the high-grade metamorphism (see stop 1-8). The orthogneisses east of the *Hedesunda granite* are also disturbed by a fault that was active after establishment of the sub-Cambrian unconformity (peneplain) in the Bergslagen region.

Stop 1.8. Quarry approximately 2.5 km north-west of Strömsbergs bruk

(CSD, CMMD, 13H Gävle SO, 6701075/1595870)

Coarse-grained, porphyritic granite to quartz monzonite that belongs to the older phase of the so-called *Hedesunda granite*. Mafic enclaves with local xenocrysts of K-feldspar and dykes of fine-grained granite and pegmatite occur within the porphyritic granite to quartz monzonite (Fig. 66b). The porphyritic granite to quartz monzonite shows a distinctive foliation that is defined by an orientation of biotite grains in the groundmass, an orientation of larger phenocrysts of K-feldspar that show little or no internal deformation and flattened enclaves (Fig. 66b). The fine-grained granite and pegmatite dykes are variably discordant to this foliation. A sample of porphyritic granite to quartz monzonite from stop 1-8 has yielded a U-Pb (zircon, titanite) TIMS age of 1863±16 Ma (see Appendix) and the rock has been included in the

1.87–1.84 Ga GSDG intrusive suite in the Bergslagen region (Stephens et al. 2007a).

The results of previous mapping in the area as well as an inspection of the magnetic anomaly map of the Bergslagen region indicate that the eastern marginal part of the *Hedesunda granite* generally shows a distinctive planar fabric. This internal structure bends around the massif and is concordant to both the contact between the *Hedesunda granite* and the adjacent meta-igneous rocks to the east as well as to the tectonic foliation in the adjacent rocks. The foliation in the porphyritic granite to quartz monzonite is inferred to have formed during or shortly after intrusion of this older igneous pulse in the *Hedesunda granite*, under the influence of a regional stress field.

DAY 2

Theme 1: Metavolcanic rocks and stratigraphically underlying metasedimentary rocks in the *Larsbo formation* and its equivalents in the Sala–Fagersta area

Stop 2-1. 4 km east of Broddbo

(sub-area 4, CSD, CMMD, 12G Avesta SO, 6653371/1542226)

Quartzite with cross bedding (see Fig. 23c) occurs close to the road in the northern part of this profile (6653409/1542121). The cross bedding indicates that the rocks young towards the south. The quartzite lies stratigraphically above volcanogenic metagreywacke (Persson 1997) similar to that observed in the type area of the *Larsbo formation* further west in Bergslagen (Hjelmqvist 1938, Strömberg & Nisca 1983) and described below at stop 2-3.

Approximately 100 m south of the road, the quartzite is stratigraphically overlain by a finely bedded volcanic metasiltstone with graded bedding that also indicates younging towards the south. The volcanic metasiltstone is also exposed c. 40 m further to the east where it shows trough bedding and, once again, a younging direction to the south. At several places in the central part of Bergslagen, there is some uncertainty concerning whether such rocks should be classified as metasedimentary or metavolcanic rocks, especially in the areas affected by amphibolite-facies metamorphism. At this locality, the metasiltstone has been classified as volcanic in origin, bearing in mind its mica-poor and feldspar-rich character. This question is also addressed at stops 2-4 to 2-6 (theme 2).

In the western outcrop of the volcanic metasiltstone, the bedding structure is truncated by a mildly discordant, massive, quartz- and plagioclase-phyric metarhyolite which is inferred to represent a pyroclastic mass flow deposit or lava. This rock forms the oldest, juvenile volcanic unit in the several kilometre thick sequence of felsic metavolcanic and subvolcanic meta-intrusive rocks in the Sala area. For this reason, it was selected for a U-Pb (zircon) TIMS age determination (1906±3 Ma, see Appendix). The stratigraphic sequence at stop 2-1 provides evidence for the deposition of quartz-rich sedimentary material in a shallow-water environment prior to the intense volcanism and extension stage at 1.9 Ga, similar to that observed, for example, in sub-areas 2 (Norberg) and 9 (Utö and Ljusterö) elsewhere in the Bergslagen region (see Fig. 28).

The D_{1C} ductile strain at stop 2-1 is represented by a planar grain-shape fabric (S_{1C}) that is parallel to the bedding (S_0). These structures strike east-north-east–west-south-west and are subvertical. The bedrock at this locality is also affected by D_{2C} ductile strain represented by a subvertical spaced cleavage with west-north-west–east-south-east strike. The relationship between S_{1C} and S_{2C} in combination with the way-up determinations suggest that the locality is situated on the southern limb of a D_{2C} anticline with an east–west axial surface trend.

Stop 2-2. Prästhyttan

(CSD, CMMD, 12G Avesta SV, 6651494/1524155)

The southern part of the outcrop area consists of bedded, volcanogenic metagreywacke with alternating sandy and argillitic layers similar to that observed in the *Larsbo formation*. There are some indications of grading that indicate younging to the north. Garnet is locally present. Bedding and an early planar grain-shape fabric (S_0 and S_{1C}, respectively) strike east-north-east–west-south-west and dip steeply in a northerly direction. A more spaced S_{2C} cleavage strikes north-east–south-west and dips steeply to the south-east. Mesoscopic D_{2C} folding of the S_0 and S_{1C} structures show a consistent z-asymmetry and fold axes that plunge moderately towards the east-north-east. The relationship between S_{1C} and S_{2C} in combination with the way-up determination suggest that the locality is situated on the northern limb of a D_{2C} anticline with an east–west axial surface trend (cf. stop 2-1 close to Broddbo).

A grey, lineated metagranitoid that intrudes the metagreywackes is also present in the southern part of the outcrop area. The mineral lineation plunges moderately to the east-north-east, i.e. it shows the same orientation as the D_{2C} fold axes. It is noteworthy how the ductile strain is taken up in different ways in the metagreywacke (SL-tectonite), with its relatively high mica

content and primary structures, and the metagranitoid (L-tectonite). This contrast is a general structural feature in the Bergslagen region. Felsic metavolcanic and meta-intrusive rocks rich in quartz and feldspar are generally lineated, while more mica-rich rocks are generally both foliated and lineated.

The beds of sandy material in the metagreywackes increase in importance northwards in the outcrop area. In the northernmost part of the outcrop area, a cross-bedded, quartz-rich metasandstone is present (Fig. 23c). The cross bedding indicates that the rocks young towards the north (Fig. 23c). The relationships at this stop indicate a gradual change from metagreywackes similar to those observed in the *Larsbo formation* to stratigraphically younger cross-bedded quartzite. This stop complements the relationships between quartzite and metavolcanic rocks observed at stop 2-1.

Stop 2-3. Approximately 2.5 km north-east of Vad inside the type area of the Larsbo formation

(CSD, CMMD, 12F Ludvika SO, 6659233/1492448)

Bedded metagreywacke that belongs to the *Larsbo formation* (Hjelmqvist 1938, Strömberg & Nisca 1983). The bedding is defined by thin, graded units that are only a few centimetres thick (see Fig. 23b) indicating a younging direction to the east-south-east and a possible origin for the metagreywackes as distal turbidites. Bedding and a planar grain-shape fabric (S_0 and S_{1C}, respectively) strike north-north-east–south-south-west and dip steeply to the east-south-east, while the conspicuous S_{2C} foliation, which is represented by a metamorphic banding along the axial surfaces to mesoscopic F_{2C} folds (crenulation cleavage), strikes north-east–south-west to east-north-east–west-south-west and is subvertical. The F_{2C} folds show an s-asymmetry and the S_{1C}-S_{2C} intersection lineation plunges steeply to the north-east. The locality is inferred to be situated on the south-eastern limb of a D_{2C} anticline with north-east–south-west axial surface trend (see also stops 2-1 and 2-2).

Based on the field observations at stops 2-1, 2-2 and 2-3, the following regional stratigraphic relationship is inferred for the oldest rock units exposed in the central structural domain of the Bergslagen region: 1. Volcanogenic metagreywacke deposited as distal turbidites (*Larsbo formation*). 2. Cross-bedded quartzite deposited under shallow-water conditions. 3. Metavolcanic rocks dated to 1.9 Ga belonging to the intense volcanism and extension stage.

Theme 2: Problems with the discrimination of metasedimentary rocks and metamorphosed, resedimented or hydrothermally altered volcanic rocks in sub-area 2. Variation in the character and intensity of ductile deformation in the hinge and on the limb of a major D_{2C} fold

Stop 2-4. Road outcrop at Kybacken

(sub-area 2, CSD, CMMD, 12F Ludvika NO, 6676700/1487845)

Grey, thinly planar-bedded (centimetre-thick layers), probably metavolcanic rock with porphyroclasts of quartz and layers of matrix-supported, polymict metaconglomerate. The metaconglomerate layers are decimetre-thick and consist of strongly elongate pebbles of different felsic metavolcanic rocks in the stretching lineation direction. By contrast, the pebbles are more or less rounded in shape in the plane perpendicular to the stretching lineation. The matrix consists partly of the same type of material as in the finely bedded rock and partly of biotite-rich material that possibly represents a metamorphosed alteration network. Further to the south and structurally beneath the finely bedded rocks with polymict metaconglomerate, a massive felsic rock with angular or rounded megacrysts of quartz is present. The megacrysts are evenly and sparsely (c. 10%) distributed and the rock is inferred to represent a sparsely porphyritic, coherent volcanc rock or subvolcanic intrusion.

Bedding and a planar grain-shape fabric (S_0 and S_{1C}, respectively) are parallel with a north-north-west–south-south-east strike and a moderate dip to the east-north-east. An S_{2C} structure is developed as a spaced cleavage in the northern part of the outcrop but is more penetrative in character in the southern part of the outcrop. The S_{2C} is vertical, strikes east-north-east–west-south-west and is strongly discordant to the S_0 and S_{1C} structures. A D_{2C} crenulation of the S_{1C} surfaces is apparent in the more biotite-rich parts. The crenulation lineation and the stretching direction as observed in the deformed pebbles show the same orientation and plunge moderately to the east-north-east. The structural relationships in the area indicate that stop 2-4 is situated in the hinge of a major F_{2C} synform that plunges to the east-north-east.

Stop 2-5. Rock outcrop west-south-west of Stora Norn

(sub-area 2, CSD, CMMD, 12F Ludvika NO, 6677510/1490120)

Grey, bedded, strongly foliated metavolcanic rock with alternating quartz-feldspar- and mica-rich lay-

ers. It is considered likely that this rock represents a more strongly deformed equivalent to the bedded, felsic metavolcanic rock at stop 2-4.

The strongly developed foliation strikes north-east–south-west, dips steeply to moderately to the south-east and is an S_{2C} structure along which bedding (S_0) and an earlier planar grain-shape fabric (S_{1C}) are more or less completely transposed. Locally, S_{1C} can be observed between the S_{2C} surfaces. The stronger deformation in this outcrop relative to that at stop 2-4 is related to the location of stop 2-5 on the north-western limb of the F_{2C} synform recognized at stop 2-4. This variation in the intensity of D_{2C} ductile strain between the limbs and the hinge of major, predominantly asymmetric F_{2C} structures, represented by the variation in the development of the S_{2C} fabric, has been observed at several places in the Bergslagen region.

Stop 2-6. Road outcrop west of Stora Norn

(sub-area 2, CSD, CMMD, 12F Ludvika NO, 6678103/1490328)

A pale grey, felsic metavolcanic rock that is predominantly equigranular but shows a sparse (<1% in frequency) distribution of feldspar porphyroclasts (<1 mm) occurs as a more than 4 m thick layer within grey, equigranular, thinly planar-bedded (several centimeter thick layers), fine-grained felsic rocks. Some tendency to graded bedding indicates younging in an easterly direction. The planar-bedded rocks are inferred to represent metamorphosed, resedimented volcanic rocks that were possibly affected by some hydrothermal alteration, as inferred at stop 2-4. On map-sheet 12F Ludvika NO (Strömberg 1996), these rocks have been interpreted as sedimentary in origin.

Bedding (S_0) and a planar grain-shape fabric (S_{1C}) show the same orientation with north-north-east–south-south-west strike and a steep dip to the east-south-east. An S_{2C} foliation occurs as a relatively tight, spaced cleavage with a more north–south strike and a more gentle, easterly dip. A D_{2C} crenulation lineation plunges gently to the north-north-east.

Theme 3: Öster Silvberg Zn-Pb-Cu-Fe-(Ag) sulphide deposit in sub-area 2

Stop 2-7. Öster Silvberg

(sub-area 2, CSD, CMMD, 12F Ludvika NO, 6692250/1487750)

Öster Silvberg is probably one of Bergslagens oldest mines that was most productive during the 14th and 15th centuries. The latest mining activity occurred during the later part of the 1st world war during the early part of the 20th century and the mine was finally in production during a short period between 1918 and 1920 (Geijer 1965). The mining activity achieved a maximum annual production of more than 1 tonne of silver. The bulk of the production took place in the so-called Storgruvan in the eastern part of the mine area. The deposit consists predominantly of an impregnation of silver-bearing galena in a fine-grained quartz-rich rock (alteration rock). Sphalerite, pyrrhotite and pyrite form subordinate components. The wall rock consists of mica-rich felsic metavolcanic rock in a larger part of the deposit. A description of this deposit including the wall-rock alteration can be found in Lagerblad et al. (1987).

Theme 4: Post-Svecokarelian, magmatic explosion breccia at Pellesberget

Stop 2-8. Pellesberget (12F Ludvika NO, 6699781/1492922)

Breccia that contains angular fragments of strongly foliated, Svecofennian felsic metavolcanic rock, which vary in size from several centimetres to several metres, forms a significant rock component at this stop. The orientation of the tectonic foliation inside the different fragments is highly variable and there is generally little or no matrix present between the fragments.

An intrusive porphyry belonging to the so-called *Gustafs porphyries* dominates the exposed bedrock in the southern and western parts of stop 2-8. The porphyry occurs together with breccia, particularly on the western side of Pellesberget. At several places, the porphyry intrudes the breccia as discordant dykes and also forms the matrix to the breccia. The matrix porphyry merges into intrusive veins and, at one locality, contains autobrecciated, flow-banded fragments of the same porphyry. The spatial relationship between porphyry dykes and breccia suggests that the latter formed as an explosion breccia during the igneous activity that gave rise to the dykes that belong to the *Gustafs porphyries*. U-Pb (zircon) dating of a porphyry dyke at stop 2-8 has yielded an intrusion age of 1474±4 Ma for these dykes (Lundström et al. 2002b). Bearing in mind the field relationships described above, this age also represents the timing of development of the magmatic explosion breccia at Pellesberget.

DAY 3

Theme 1: Synvolcanic hydrothermal alteration and D_{2C} ductile deformation in the Riddarhyttan area (sub-area 2)

Stop 3-1. Road outcrop 750 m north-west of Bäckegruvan

(sub-area 2, CSD, CMMD, 11F Lindesberg NO, 6634784/1485549)

This stop illustrates the appearance of felsic volcanic rocks following the effects of both strong hydrothermal alteration referred to as "magnesium alteration" and later recrystallization in connection with amphibolite-facies metamorphism. The outcrop is dominated by a grey, quartz-mica alteration rock that consists of the mineral assemblage quartz+biotite+muscovite+cordierite+magnetite±feldspar. The alteration has not completely destroyed the feldspar in the original rock (cf. stop 4-4). Cordierite occurs as pre- or syntectonic porphyroblasts and magnetite as post-tectonic porphyroblasts.

The quartz-mica alteration rock at this stop is dominated structurally by an intense mineral stretching lineation that plunges moderately to the south-west. Elongate porphyroblasts of cordierite clearly define this stretching lineation. Nevertheless, thin bands of mica-rich material show an intense tectonic foliation. It is apparent that the presence or absence of mica determines how the ductile strain is taken up in the rock. The tectonic foliation appears to be a D_{2C} structure that is vertical and strikes north-east–south-west. Relics of an earlier S_{1C} planar grain-shape fabric can be observed locally between the S_{2C} surfaces.

Theme 2: Problems with the discrimination of metasedimentary rocks and metamorphosed, resedimented or hydrothermally altered volcanic rocks in the Kolsva area (sub-area 2). Multiphase deformation in the Kolsva area

Stop 3-2. Skålstugan, approximately 1.7 km west of Karmansbo

(sub-area 2, CSD, CMMD, 11F Lindesberg SO, 6619355/1495076)

Grey, felsic metavolcanic rock with layers dominated by quartz and feldspar alternating with subordinate layers dominated by mica. The degree to which this compositional layering, referred to here as S_0, is a primary bedding structure or alternatively a secondary structure, related to, for example, formation of phyllosilicates by hydrothermal alteration and subsequent ductile strain with the establishment of a metamorphic layering, is open to discussion. The S_0 layering and an S_{1C} planar grain-shape fabric are subparallel in the outcrop and strike north-west–south-east. These surfaces are transposed into a second generation, planar structure that takes the form of a spaced cleavage (S_{2C}) that strikes west-north-west–east-south-east. The intersection lineation between S_{1C} and S_{2C} plunges steeply towards the south-south-east. Folds with s-asymmetry (F_{2C} or F_{3C}) are also present at this stop.

Stop 3-3. Road outcrops 1 km south of Lundbysjön

(sub-area 2, CSD, CMMD, 11G Västerås SV, 6608623/1505409)

Bedded, felsic metavolcanic rock, which consists of more quartz- and feldspar-rich layers alternating with more mica-rich layers, occurs in the south-eastern part of the outcrop area. One of the beds appears to be graded with a younging direction to the west. Crenulation of the mica-rich layers is present. The rocks at this stop have been inferred to be a schistose metagreywacke on the published bedrock geological map of the area at the scale 1:50 000 and in the description to this map (Lundegårdh & Nisca 1978).

The principal exposed surface in the north-western part of the outcrop area is subparallel to bedding (S_0) and a planar grain-shape fabric (S_{1C}). A penetrative fold axis lineation (L_{2C}), which plunges moderately to steeply to the south-south-west, is conspicuous on this surface (see Fig. 139b). This lineation is markedly discordant to and deformed by a later crenulation lineation (L_{3C}) that plunges steeply to the west-north-west (Fig. 139b). The structures observed at stop 3-3 are representative of the structures in the Kolsva–Kungsör–Arboga area.

Theme 3: Granite and pegmatite belonging to the 1.85–1.75 Ga, Granite-pegmatite (GP) intrusive rock suite in the Köping–Fellingsbro area

Stop 3-4. Road outcrop north-west of Lindbacken

(CSD, CMMD, 10G Eskilstuna NV, 6599024/1514586)

Finely medium-grained and partly pegmatitic, leucocratic granite with inclusions rich in quartz, feldspar and mica. Garnet is locally present in the granite (Romer & Öhlander 1995) which is also intruded by a pegmatite dyke. The granite at this stop has yielded a U-Pb (monazite) age of 1846±1 Ma (Romer & Öhlander 1995) in agreement with the oldest U-Pb (monazite) age reported in Andersson (1997c) in the southern part of the Bergslagen region. It is inferred that an important phase of high-grade metamorphism has affected the region prior to or around 1.85 Ga (see also stop 5-1).

Stop 3-5. South of the road immediately to the east of Medåker

(CSD, CMMD, 10F Örebro NO, 6592651/1497797)

Coarsely porphyritic, hornblende-bearing, isotropic granite inside the type area for the intrusive rocks referred to as the *Fellingsbro-type* in the 1.85–1.75 Ga GP intrusive rock suite. K-feldspar phenocrysts show a mantled texture with a rim of plagioclase feldspar. The magnetic susceptibility of this granite is between 800 and 1000×10^{-5} SI. The *Fellingsbro-type* granite in the type area has yielded a U-Pb (zircon) age of 1782±6 Ma (Patchett et al. 1987), similar in age to the compositionally more variable 1.81–1.78 Ga Granite-syenitoid-dioritoid-gabbroid (GSDG) intrusive rock suite further to the west in the Bergslagen region (cf., for example, stop 4-6).

Theme 4: Stratigraphy, hydrothermal alteration and ductile deformation in the Glanshammar–Rinkeby area (sub-area 10). Major, downward-facing D_{2C} folds

Stop 3-6. Outcrops on both sides of the road to the south of the railway intersection, 4 km south-east of Dyltabruk

(sub-area 10, CSD, CMMD, 10F Örebro NV, 6583245/1472578)

An homogeneous, plagioclase-phyric felsic metavolcanic rock occurs in the south-western part of the outcrop area on the western side of the road. This rock belongs to the so-called *sodium leptite etage* of Wikman (1972), which corresponds to the rocks in the *Storsjön formation* (Lundström 1983) in the Lindesberg and Filipstad areas further north in the Bergslagen region, and the intense volcanism and extension stage according to the general stratigraphic scheme for this region (Allen et al. 1996). However, the felsic rock at this outcrop locally contains clasts and is interbedded with quartzite. Both these features indicate the volcanic character of the plagioclase-phyric rock and, in this manner, it differs from the *Storsjön formation* which is dominated by subvolcanic meta-intrusive rocks.

A felsic metavolcanic rock with elongate clasts that are several centimetres thick and several centimetres to more than a decimetre in length comprise the north-eastern part of the outcrop on the eastern side of the road, closest to the railway. The clasts comprise approximately 10% of the rock. They are dominated by mafic and metasedimentary rock fragments with subordinate reddish, felsic, more or less quartz-phyric metavolcanic rock fragments. A felsic rock with cordierite porphyroblasts, which probably represents an hydrothermally altered variety (cf. stop 3-1), occurs in the north-easternmost part of the outcrop in sharp contact with the remaining felsic metavolcanic rocks.

The felsic metavolcanic rocks at stop 3-6 are affected by an intense mineral lineation and folding (see Fig. 135c). The fold axis lineation and the linear grain-shape fabric are parallel to each other and plunge moderately to the east. The outcrop is situated in the hinge of a major D_{2C} synform, referred to as the *Käglan synform* (Gorbatschev 1969), that deforms a planar grain-shape fabric (S_{1C}).

Stop 3-7. Outcrops west of the road, 4.5 km south-east of Dyltabruk

(sub-area 10, CSD, CMMD, 10F Örebro NV, 6582855/1472795)

Red, quartz-phyric, strongly foliated metavolcanic rock which lacks any indication of bedding and within which clasts have not been recognized. The rock is notably homogeneous over an outcrop area that is more than several hundred square metres in areal extent. The rock belongs to the *potassium leptite stage* of Wikman (1972), which contains rocks with up to 7% K_2O. It is inferred to represent a pyroclastic mass flow deposit, which was affected by potassium alteration, and to correspond to the *Vassland* and *Sången formations* in Lundström (1983, 1995) and the intense volcanism and extension stage, according to the general stratigraphic scheme for the Bergslagen region (Allen et al. 1996).

Stop 3-8. Outcrops close to the road at Norrberga

(sub-area 10, CSD, CMMD, 10F Örebro NV, 6580954/1474550)

Laminated volcanic metasiltstone belonging to the *banded leptite stage* of Wikman (1972), which corresponds to the *Usken* and *Älgen formations* in Lundström (1983, 1995) and the waning volcanic stage according to the general stratigraphic scheme for the Bergslagen region (Allen et al. 1996). Graded bedding is present in the eastern outcrop north of the road and cross bedding occurs in an outcrop south of the road (see Fig. 135d). These primary structures indicate a consistent sense of younging to the south. The way-up determinations indicate that the andalusite-bearing mica schists further to the south (see stop 3-9), which occur in the core of a D_{2C} antiform, stratigraphically overlie the metavolcanic rocks. The stratigraphic relationships between the metavolcanic and metasedimentary rocks around stop 3-8 are reminiscent of those in the Grythyttan area in sub-area 1 (see stops 4-1 to 4-5 and cf. stops 2-1 and 2-2).

Stop 3-9. Outcrops close to the road 750 m west of Tåsta

(sub-area 10, CSD, CMMD, 10F Örebro NO, 6578820/1477275 and 6578919/1477275)

Andalusite-bearing, psammitic mica schist that shows a primary bedding structure with alternating andalusite-rich and andalusite-poor, sandy beds (see Fig. 135b). Bedding and the main tectonic foliation strike west-north-west–east-north-east and are subvertical. The main tectonic foliation appears to be an S_{2C} structure that is strongly discordant to a grain-shape fabric defined, for example, by the oriented andalusite porphyroblasts with an approximately north–south strike. The andalusite porphyroblasts in the outcrop to the north of the road are folded by F_{2C} structures and affected by a spaced S_{2C} cleavage (Fig. 135b). The andalusite-bearing mica schist also shows a strong linear fabric that plunges moderately to the east.

The outcrops at stop 3-9 are inferred to be situated in the core of a major D_{2C} antiform that plunges moderately to the east (*Glanshammar antiform* of Gorbatschev 1969). The andalusite porphyroblasts formed prior to the development of D_{2C}. In order to explain the observed stratigraphic and structural relationships at stops 3-8 and 3-9, it is inferred that an inversion of the stratigraphy occurred prior to the development of the F_{2C} folding, i.e. the antiform is a major, downward-facing structure.

DAY 4

Theme 1: Volcanostratigraphy, synvolcanic hydrothermal alteration and D_{1C} deformation in rocks affected by low-grade metamorphism in the Grythyttan area (sub-area 1)

Stop 4-1. Sångesnäs

(sub-area 1, CSD, CLMD, 11E Filipstad SO, 6620800/1440850)

Poorly sorted, massive felsic metavolcanic rock with millimetre- to centimetre-size lithic, crystal and possibly pumice fragments and spherulites, inferred to represent a pyroclastic mass flow deposit. This outcrop belongs to the *Sångesn formation* of Lundström (1995) and is typical of the intense volcanism and extension stage, according to the general stratigraphic scheme for the Bergslagen region (Allen et al. 1996). This locality is situated in the lower part of the volcanostratigraphic sequence in sub-area 1, along strike from the locality referred to as Ekebergshöjden, where a rhyolitic pyroclastic mass flow deposit has yielded a U-Pb (zircon) igneous crystallization age of 1891±4 Ma (Lundström et al. 1998, see also Fig. 30).

Stop 4-2. Hälgsnäsudden–Brevik

(sub-area 1, CSD, CLMD, 11E Filipstad SO, 6623700/1430750)

A type profile can be studied in the outcrops at this stop that extends from volcaniclastic rocks belonging to the waning volcanic stage, according to the general stratigraphic scheme for the Bergslagen region (Allen et al. 1996), in the north-east to slates in the stratigraphically younger, sedimentary thermal subsidence stage, in the same general scheme, in the south-west. The profile is situated close to the road at Brevik and the rocks are well preserved and affected only by low-grade metamorphism.

The outcrops north-east of the road, 300 m north-east of Brevik (6624350/1431500), in the north-eastern part of the profile, consist of volcaniclastic, partly bedded siltstone belonging to the *Sikfors member* in the *Älgen formation* (Lundström 1995) and the waning volcanic stage (Allen et al. 1996). Vitriclastic textures are locally present in this member. A discordant mafic dyke is present in this part of stop 4-2.

The outcrops 500 m south of the farm at Brevik (6623750/1430700) consist of greywacke, conglomerate, siltstone and graphitic mudstone belonging to the *Hälgsnäs member* in the *Torrvarpen formation* (Lundström 1995). Cross bedding, load casts and various erosion structures (e.g. trough bedding) indicate a rather unstable depositional environment for the clastic rocks at this locality (see Figs. 34, 35 and 36 in Lundström 1995).

The outcrops along the road, 1 km south of the farm at Brevik (6623450/1430700), in the south-western part of the profile, consist of graphite-bearing, black, thinly bedded slate belonging to the *Grythyttan member* in the *Torrvarpen formation* (Lundström 1995). Fine cross bedding is locally present in this member (see Fig. 40a in Lundström 1995).

Stop 4-3. Outcrop close to the road at Sandnäsudden

(sub-area 1, CSD, CLMD, 11E Filipstad SO, 6615850/1429150)

This outcrop demonstrates how different types of synvolcanic hydrothermal alteration (see section "Hydrothermal alteration" in the description of the Svecofennian volcanic and subvolcanic intrusive rocks) have successively affected a volcaniclastic rock that is situated at a relatively high level in the volcanostratigraphy,

probably equivalent to that observed in the first part of stop 4-2. The outcrop also shows how the different types of alteration appear in a bedrock affected later by greenschist-facies regional metamorphism.

Volcanic siltstone belonging to the *Älgen formation* (Lundström 1995) shows ovoidal structures (see Fig. 71 in Lundström 1995). The ovoids consist of a potassium-rich core that represents a relic of an early-stage potassium alteration. Such alteration is commonly present in the upper part of the volcanostratigraphy in the Bergslagen region and is solely present in a larger area to the west of stop 4-3. The rims of the ovoids are sodium-rich and indicate a later sodium alteration in the volcanic rocks at this locality. The ovoids occur in a matrix dominated by quartz and biotite that is inferred to have formed during even later "magnesium alteration". The younger sodium and "magnesium" alterations appear to be spatially associated with intrusive metabasic rocks in the Grythyttan area and it is possible that the intrusion of these rocks provided the heat necessary to drive the younger hydrothermal system that produced the sodium and "magnesium" alterations.

Stop 4-4. Kottbo

(sub-area 1, CSD, CLMD, 11E Filipstad SO, 6615650/1438070)

This outcrop demonstrates the appearance of intense "magnesium alteration" in an inferred volcanic rock that is situated at a relatively low level in the volcanostratigraphy in the *Sångenformation*, probably equivalent to that observed in stop 4-1, and that was affected later by greenschist-facies regional metamorphism (cf. stop 3-1). The rock at this locality consists of quartz and mica, and its primary character has been totally destroyed by the intense hydrothermal alteration. The quartz-mica rock has a pseudoconglomeratic appearance (see Figs. 63 and 64 in Lundström 1995). The composition of the apparent pebbles and matrix are identical. The only difference between these two components is the massive character of the apparent pebbles and the more foliated character of the apparent matrix.

Stop 4-5. St. Sirsjön

(sub-area 1, CSD, CLMD, 11E Filipstad SO, 6610100/1429850)

Bedded, fine-grained metasandstone and meta-argillite belonging to the *Torrvarpen formation* lie stratigraphically above the metavolcanic rocks in the Grythyttan area (Lundström 1995). Since volcanic metasiltstone with beds of carbonate rock is present immediately to the west of this locality, it is inferred that the bedrock at stop 4-5 represents approximately the same stratigraphic level as that observed in the final part of stop 4-2.

The low degree of ductile strain at this locality compared with that at many other localities is worth noting. A high angle between bedding (S_0) and a slaty cleavage (S_{1C}), which dip moderately to the north-east and steeply towards the south-west, respectively, is apparent (see Fig. 135a). The intersection between these two planar structures plunges gently to the south-east. The outcrop is inferred to lie on the western limb of a D_{1C} syncline, the axis of which is represented by this intersection lineation.

Theme 2: Intrusive rocks belonging to the 1.81–1.78 Ga Granite-syenitoid-dioritoid-gabbroid (GSDG) suite, granulite-facies metamorphism at 1.8 Ga and Sveconorwegian deformation under greenschist-facies metamorphic conditions between 1.0 and 0.9 Ga

Stop 4-6. Small outcrop close to minor road at Lersjötorp

(WSD, CMMD, 10E Karlskoga NO, 6589960/1431840)

Protomylonitic, porphyritic granite to quartz monzonite which is inferred to belong to the 1.81–1.78 Ga GSDG intrusive suite. The same type of rock yielded a U-Pb (zircon) igneous crystallization age of 1783±10 Ma in the Filipstad area north-west of stop 4-6 (Jarl & Johansson 1988). The rock at stop 4-6 is affected by a C′S composite planar fabric that strikes north-north-west–south-south-east and dips steeply to the west, and a steeply dipping mineral lineation. A study of the composite planar structures in a steep joint surface at a high angle to these structures indicates a west-side-up, i.e. reverse dip-slip, sense of ductile shear strain (see Fig. 149a). This type of spaced ductile shear deformation is common in the Karlskoga area and is inferred to be Sveconorwegian in age (see section "Western structural domain: Sveconorwegian tectonic overprint").

Stop 4-7. Immetorp along the road E18 immediately east of Karlskoga

(WSD, SMMD, 10E Karlskoga NO, 6578260/1431080)

Garnet-cordierite fels, which formed during low-pressure, granulite-facies metamorphic conditions (Andersson et al. 1992), passes to the north-west along the road into a strongly deformed phyllonite that formed under retrograde, greenschist-facies metamorphic conditions. Note especially how the garnet porphyroblasts are af-

fected by the later retrograde deformation. The change from the isotropic fels into the phyllonite occurs over a few metres and is not exposed. The phyllonite contains a composite C′S fabric as well as a mineral stretching lineation. The main tectonic fabric in the phyllonite dips moderately to the west-north-west, the C′ shear bands dip more gently towards the west-north-west and the stretching lineation plunges down the dip of the main tectonic fabric. The structural relationships at this locality indicate a west-side-up, i.e. reverse dip-slip, sense of ductile shear strain.

Stop 4-7 lies within a broad structural belt in the Karlskoga–Skagern area where there is an interference between ductile shear zones that strike both north–south and north-east–south-west (Fig. 124). Locally, in this area, it is apparent that the north-east–south-west zones, included in the *Sveconorwegian Frontal Deformation Zone* (Wahlgren et al. 1994), are younger than and rotate the north–south structures.

A sample of garnet-cordierite fels east of Karlskoga has yielded U-Pb (monazite) and U-Pb (zircon) ages of 1796±1 Ma and 1793±5 Ma, respectively (Andersson 1997c, Andersson et al. 2006), while white mica along the foliation in the phyllonite has yielded a ^{40}Ar-^{39}Ar age of 918±8 Ma (Page et al. 1996). These geochronological data are inferred to indicate low-pressure, granulite-facies metamorphism in connection with the intrusion of the 1.81–1.78 Ga suite of GSDG rocks followed by late Sveconorwegian deformation and retrograde metamorphism.

Stop 4-8. 1.5 km south-south-east of Degerfors
(WSD, SMMD, 10E Karlskoga SV, 6566660/1422990)

Generally reddish grey to greyish red, medium-grained and equigranular granite that is partly affected by an alteration to charnockite. The charnockite occurs as a greenish grey to brownish grey rock and hypersthene has formed from the breakdown of biotite. The charnockite is identical geochemically to the granite that is unaffected by the charnockitization. Both less altered and more altered charnockitic rocks are present at stop 4-8. A sample of granite from a locality c. 500 m closer to Degerfors has yielded a U-Pb (zircon) age of 1796^{+6}_{-7} Ma. The field relationships in the Karlskoga area indicate that the equigranular granite affected by charnockitization is structurally older than the porphyritic, GSDG rocks that dominate in this area and have been included in the 1.81–1.78 Ga GSDG intrusive suite. However, the U-Pb (zircon) ages for these different rocks are similar.

Stop 4-9. Outcrop along minor road at Korpekärret approximately 5 km south of Degerfors
(WSD, SMMD, 10E Karlskoga SV, 6561339/1420638)

Subvertical, ductile shear zone that strikes north-north-east–south-south-west along the contact between partly charnockitic granite, similar to that observed at stop 4-8, to the west along the road, and a porphyritic granite to quartz monzonite included in the 1.81–1.78 Ga GSDG intrusive suite to the east. The increase in ductile shear strain in especially the porphyritic GSDG rock towards the contact between the two rock units is particularly apparent at this stop. This feature is expressed by both the increased intensity in the grain-shape fabric in the rock and the increased flattening of mafic enclaves in the porphyritic granite to quartz monzonite.

The ductile shear zone is approximately 100 m wide and can be followed approximately 20 km along the contact between these two rock units in the Degerfors area. It is characterized kinematically by a west-side-up sense of shear. The ductile shear zone is inferred to be Sveconorwegian in age and is situated inside the structural belt in the Karlskoga–Skagern area where the Sveconorwegian structures strike north-east–south-west (*Sveconorwegian Frontal Deformation Zone* in Wahlgren et al. 1994).

DAY 5

Theme 1: Multiphase, Svecokarelian deformation and metamorphism (pre- and post-1.85 Ga)

Stop 5-1. Outcrop along road 50, approximately 4 km north-north-west of Åmmeberg
(SSD, SMMD, 9F Finspång NV, 6532055/1451782)

Supracrustal rock inferred to represent a metamorphosed felsic volcanic rock affected by "skarn alteration", in which the grain-shape fabric and banding are strongly discordant to an isotropic granite included in the *Askersund granite* (see Fig. 66a). The foliation in the inferred supracrustal rocks is also weakly folded. The *Askersund granite* has yielded U-Pb (zircon) ages of 1848±15 Ma and 1842^{+23}_{-13} Ma (Persson & Wikström 1993) and has been included in the 1.87–1.84 Ga GSDG intrusive suite in the Bergslagen region. The structural relationships at this stop in combination with the geochronological data suggest that the ductile strain under amphibolite-facies metamorphic conditions in the supracrustal rock is older than c. 1.85 Ga (see also stop 3-4).

Stop 5-2. Knutstorp, approximately 10 km north-east of Zinkgruvan

(SSD, SMMD, 9F Finspång NV, 6531392/1464209)

Strongly deformed and metamorphosed, porphyritic granite included in the *Askersund granite* that has the appearance of an augen gneiss. The gneissosity is folded by structures that show a z-asymmetry and plunge gently to the east along fold axial surfaces that strike approximately east–west (Fig. 66c). Both folded pegmatite and pegmatite along the axial surfaces to the post-foliation folds (Fig. 66c) are present. Note the significance of the fold asymmetry for the apparent structural discordance on the top surface of the outcrop. This discordance is related to the sharp break between gently dipping, short limbs and steeply dipping, long limbs in the fold structure.

The structural relationships at this stop in combination with the geochronological data in the region (see stop 5-1) suggest that the development of the gneissic foliation and the later folding at this stop occurred after c. 1.85 Ga (cf. stop 5-1). The bedrock geological mapping in this area (Wikström & Karis 1991) indicates that the *Askersund granite* defines a major, post-gneissosity fold structure with z-asymmetry, consistent with a component of dextral strike-slip ductile deformation during the development of the fold structures in this region.

Theme 2: High-temperature mylonite in veined metagranitoid along the *Åsbro–Norrköping deformation zone (ÅNDZ)*

Stop 5-3. Road outcrop approximately 200 m west of Hjärtsjön

(SSD, SMMD, 9F Finspång NV, 6535070/1468540)

Grey, strongly deformed, veined metagranitoid which can be described as a striped gneiss that represents a high-temperature mylonite (see Fig. 147c). Folding of a planar grain-shape fabric is apparent in the form of intra-folial structures within the main tectonic foliation in the metagranitoid (S_{DZ}). The main foliation is inferred to be at least a second generation structure and strikes west-north-west–east-south-east with a steep dip to the south-south-east. The mineral stretching lineation plunges moderately to the south-east and is not so strongly developed. Mildly discordant pegmatites are present but these rocks are also affected by the ductile deformation. However, the grain-shape fabric in such pegmatites is discordant to the main foliation in the metagranitoid and is subvertical (Fig. 147c). The ductile deformation is inferred to show a south-side-up, dip-slip component of movement. Bearing in mind the orientation of the mineral lineation, a dextral strike-slip component of movement is also inferred.

Theme 3: Subvolcanic meta-intrusive rock and supracrustal rocks south of the *ÅNDZ* (sub-area 11 Gryt–Zinkgruvan)

Stop 5-4. Road outcrop 1.5 km north-east of Gryts bruk

(sub-area 11 Gryt–Zinkgruvan, SSD, SMMD, 9F Finspång SV, 6530823/1474657)

Stop 5-4 consists of a strongly recrystallized and defomed metarhyolite that has yielded a U-Pb (zircon) age of 1901±18 Ma (Kumpulainen et al. 1996). The rock lacks a clastic texture and contains partly euhedral phenocrysts of quartz that are evenly distributed throughout the rock. It resembles a rhyolitic, subvolcanic intrusive rock in the vicinity and is inferred to represent a metamorphosed, intrusive rhyolite in the *Igelfors formation* (Wikström & Karis 1991, Kumpulainen et al. 1996). The *Igelfors formation* is dominated by rhyolitic, pyroclastic mass flow deposits that formed during the intense volcanism and extension stage, according to the general stratigraphic scheme for the Bergslagen region (Allen et al. 1996).

The tectonic foliation in the rock strikes west-north-west–east-north-east to east–west with a vertical to steep southerly dip. The mineral stretching lineation plunges steeply along the foliation. Metadolerites and small bodies of mafic rock with a dioritic or gabbroic composition are present in a quarry in the vicinity. The rocks are affected by inhomogeneous ductile shear deformation. This is most conspicuous in the mafic to intermediate rocks. Distinctive shear bands in these rocks indicate a dextral strike-slip component of ductile deformation. Centimetre-scale folds with z-asymmetry are also present.

Stop 5-5. Outcrops 4 km south-west of Hjortkvarn

(sub-area 11 Gryt–Zinkgruvan, SSD, SMMD, 9F Finspång NO, 6529380/1476195)

A metamorphosed debris flow belonging to the lower part of the *Närkesberg formation* (Kumpulainen et al. 1996) is present in the eastern outcrop at stop 5-5 (6529380/1476195). Angular clasts that contain broken grains and pumice-like fragments are situated within an immature, sandy matrix. The clasts are considered to have been derived from the rhyolitic mass flow deposits in the underlying *Igelfors formation* (Wikström & Karis 1991, Kumpulainen et al. 1996). A layer of similar felsic metavolcanic rock is present in the metasedimentary rocks at this stop.

Felsic metavolcanic rocks and a thin layer of more quartz-rich, cross-bedded metasandstone, which resembles the quartzites in the upper part of the *Närkesberg formation*, is present in the western outcrop at stop 5-5 (6629475/1476087). In the Gryt–Zinkgruvan part of sub-area 11, cross-bedded quartzite is interlayered with felsic metavolcanic rocks that belong to the intense volcanism and extension stage, according to the general stratigraphic scheme for the Bergslagen region (Allen et al. 1996).

Theme 4: Variation in the intensity of ductile deformation in a migmatitic supracrustal rock

Stop 5-6. Outcrop along road 51 between Finspång and Norrköping

(SSD, SMMD, 9G Katrineholm SV, 6506692/1507761)

Stop 5-6 occurs in a structurally complex area, northwest of Norrköping, where the three branches of the *ÅNDZ* converge and interfere with the deformation along the *Zinkgruvan–Finspång deformation belt* (see section "Southern structural domain: Two separate phases of Svecokarelian deformation under amphibolite-facies metamorphic conditions").

The outcrop is dominated by grey, migmatitic gneiss that belongs to a rock unit inferred to have been originally volcanic in origin (Wikström & Karis 1991). Note the significant variation in ductile deformation within the outcrop. Sections with leucosome veins that are either irregularly oriented or folded pass transitionally into sections, with variable thickness, where the rock is affected by an intense planar grain-shape fabric and tectonic banding, i.e. the rock is converted to a striped gneiss that represents a high-temperature mylonite (see Figs. 147a and b). The foliation and tectonic banding in the high-strain sections strike west-north-west–east-south-east and dip steeply in a northerly direction. The rotation of the older gneissic structure into the ductile high-strain sections indicates a south-side-up, dip-slip component of movement (Fig. 147a). The high-strain sections formed under amphibolite-facies metamorphic conditions following development of the leucosome veins.

A concentration of brittle deformation with the development of calcite-cemented fault breccia is present in the eastern part of stop 5-6. This deformation is possibly coupled to the faulting that borders the outlier of Cambrian sandstone close to lake Glan to the south-east of stop 5-6.

Errata and some clarification to the geological maps

The following four errata have been detected in the printed geological maps. Furthermore, a clarification is provided for a symbol on one of these maps:

ERRATA

1. The way-up determination shown at the coordinates 6679000/1612100 in the Swedish National Grid (12I Östhammar NO) on the bedrock geological map, the metamorphic, structural and isotope age map and the mineral resources map (Stephens et al. 2007a, b, c) should be directed to the east-south-east and not to the west-north-west.

2. The coordinates of the apatite-bearing, iron oxide deposit referred to as *Risbergsfältet* (deposit number 218) in the table of larger metallic mineral deposits on the mineral resources map (Stephens et al. 2007c) should be 6663400/1455100 and not as shown on the map. The deposit is also incorrectly located on the inset map that shows the distribution of larger metallic mineral deposits. The deposit is situated south-west of Ludvika, close to Grängesberg, and not as shown on the inset map. The separate minor deposit between Fagersta and Avesta on the main map, also referred to as *Risbergsfältet*, is an iron oxide deposit in manganese-poor (<1% MnO) skarn or crystalline carbonate rock and not an apatite-bearing, iron oxide deposit.

3. The areas mapped as granofels on map-sheets 9E Askersund NO, 10E Karlskoga SO and 10E Karlskoga NO should be marked with a yellow rather than a pale blue colour on both the inset maps on the mineral resources map (Stephens et al. 2007c), i.e. they should be grouped together with the Svecofennian metavolcanic rocks rather than the Svecofennian metasedimentary rocks, in the same manner as that carried out in the main map (Stephens et al. 2007c).

4. The coordinates of the age determination (1469±10 Ma) in the *Noran intrusion* (13F Falun SV) on the metamorphic, structural and isotope age map (Stephens et al. 2007b) should be 6702000/1464000 and not as shown on the map.

CLARIFICATION

The curved part of the U-symbol used in the display of overturned folds on the inset map to the metamorphic, structural and isotope age map (Stephens et al. 2007b) points in the direction of dip of the axial surface to the fold. The sense of vergence for such a fold is in the opposite direction.

References

Åberg, A. & Fallick, A.E., 1993: A fluid inclusion and light element stable isotope study of the gold-bearing quartz vein system, Falun, Sweden. *Mineralium Deposita 28*, 324–333.

Åberg, G. & Strömberg, A.G.B., 1984: Radiometric dating of Svecokarelian metarhyolites and prekinematic granitoids from Bergslagen, south central Sweden. *Geologiska Föreningens i Stockholm Förhandlingar 106*, 209–213.

Åberg, G. & Charalampides, G., 1986: New lead isotope data from the Långban mineralization, central Sweden. *Geologiska Föreningens i Stockholm Förhandlingar 108*, 243–250

Åberg, G. & Charalampides, G., 1988: Evolution of the mineral deposits from Långban, Sweden, as recorded from strontium isotope data. *Geologiska Föreningens i Stockholm Förhandlingar 110*, 329–334.

Åberg, G., Bollmark, B., Björk, L. & Wiklander, U., 1983a: Radiometric dating of the Horrsjö granite, south central Sweden. *Geologiska Föreningens i Stockholm Förhandlingar 105*, 78–71.

Åberg, G., Levi, B. & Fredriksson, G., 1983b: Zircon ages of metavolcanic and synorogenic granitic rocks from the Svärdsjö and Yxsjöberg areas, south central Sweden. *Geologiska Föreningens i Stockholm Förhandlingar 105*, 199–203.

Ahl, M. & Sundblad, K., 1996: Metallogeny of the TIB. *In* M. Ahl, U.B. Andersson, T. Lundqvist & K. Sundblad (eds.): Rapakivi granites and related rocks in central Sweden. *Sveriges geologiska undersökning Ca 87*, 29–32.

Ahl, M., Andersson, U.B., Lundqvist, T. & Sundblad, K. (eds.), 1997: Rapakivi granites and related rocks in central Sweden. *Sveriges geologiska undersökning Ca 87*, 99 pp.

Ahl, M., Sundblad, K. & Schöberg, H., 1999: Geology, geochemistry, age and geotectonic evolution of the Dala granites, central Sweden. *Precambrian Research 95*, 147–166.

Ahl, M., Bergman, S., Bergström, U., Eliasson, T., Ripa, M. & Weihed, P., 2001: Geochemical classification of the plutonic rocks in central and northern Sweden. *Sveriges geologiska undersökning Rapporter och meddelanden 106*, 82 pp.

Ahl, M., Andersson, U.B., Lundqvist, T. & Sundblad, K., 2004: The Dala granitoids. *In* K. Högdahl, U.B. Andersson & O. Eklund (eds.): The Transscandinavian Igneous Belt (TIB) in Sweden: a review of its character and evolution. *Geological Survey of Finland Special Paper 37*, 70–74.

Åkerman, C., 1994: Ores and mineral deposits. *In* C. Fredén (ed.): Geology. *National Atlas of Sweden*, 55–66.

Allen, R., Bull, S., Ripa, M. & Jonsson, R., 2003: Regional stratigraphy, basin evolution, and the setting of stratabound Zn-Pb-Cu-Ag-Au deposits in Bergslagen, Sweden. *Sveriges geologiska undersökning unpublished report 03-1203/99*, 78 pp.

Allen, R.L., Lundström, I., Ripa, M., Simeonov, A. & Christofferson, H., 1996: Facies analysis of a 1.9 Ga, continental margin, back-arc, felsic caldera province with diverse Zn-Pb-Ag-(Cu-Au) sulfide and iron oxide deposits, Bergslagen region, Sweden. *Economic Geology 91*, 979–1008.

Ambros, M., l983a: Beskrivning till berggrundskartan Lindesberg NO. *Sveriges geologiska undersökning Af 141*, 75 pp.

Ambros, M., 1983b: The Precambrian stratigraphy of the Norberg area, central Sweden. *Geologiska Föreningens i Stockholm Förhandlingar 105*, 383–384.

Ambros, M., l988: Beskrivning till berggrundskartorna Avesta NV och SV. *Sveriges geologiska undersökning Af 152, 153*, 84 pp.

Andersson, A., Dahlman, B., Gee, D.G. & Snäll, S., 1985: The Scandinavian alum shales. *Sveriges geologiska undersökning Ca 56*, 50 pp.

Andersson, D., Kübler, L. & Mellqvist, C., 2005: Fulufjället. *In* H. Delin (ed.): Berggrundsgeologisk undersökning. Sammanfattning av pågående verksamhet 2004. *Sveriges geologiska undersökning Rapporter och meddelanden 120*, 164–178.

Andersson, L.G., 1986: The Wigström tungsten deposit. *In* I. Lundström & H. Papunen, (eds.): Mineral deposits of southwestern Finland and the Bergslagen province, Sweden. 7th IAGOD symposium and Nordkalott project meeting, excursion guide No. 3. *Sveriges geologiska undersökning Ca 61*, 41.

Andersson, U.B., 1991: Granitoid episodes and mafic-felsic magma interaction in the Svecofennian of the Fennoscandian Shield, with main emphasis on the ≈ 1.8 Ga plutonics. *In* I. Haapala & K.C. Condie (eds.): Precambrian granitoids – petrogenesis, geochemistry and metallogeny. *Precambrian Research 51*, 127–139.

Andersson, U.B., 1997a: Petrogenesis of some Proterozoic granitoid suites and associated basic rocks in Sweden (geochemistry and isotope geology). *Sveriges geologiska undersökning Rapporter och meddelanden 91*, 216 pp.

Andersson, U.B., 1997b: The Sub-Jotnian Strömsbo granite complex at Gävle, Sweden. *GFF 119*, 159–167.

Andersson, U.B., 1997c: The late Svecofennian, high-grade contact and regional metamorphism in south-western Bergslagen (central southern Sweden). *Sveriges geologiska undersökning unpublished report 03-819/93*, 36 pp.

Andersson, U.B., 2004: Age and P-T paths of metamorphism in the Bergslagen region. *Sveriges geologiska undersökning unpublished report 03-1025/97 (summary and appendices).*

Andersson, U.B., Larsson, L. & Wikström, A., 1992: Charnockites, pyroxene granulites and garnet-cordierite gneisses at a boundary between Early Svecofennian rocks and Småland-Värmland granitoids, Karlskoga, southern Sweden. *Geologiska Föreningens i Stockholm Förhandlingar 114*, 1–15.

Andersson, U.B., Högdahl, K., Sjöström, H. & Bergman, S., 2004a: Magmatic, detrital and metamorphic ages in metamorphic rocks from south-central Sweden. *Abstract 26th Nordic geological winter meeting, GFF 126*, 16–17.

Andersson, U.B., Eklund, O. & Claeson, D.T., 2004b: Geochemical character of mafic-hybrid magmatism in the Småland-Värmland Belt. *In* K. Högdahl, U.B. Andersson & O. Eklund (eds.): The Transscandinavian Igneous Belt (TIB) in Sweden: a review of its character and evolution. *Geological Survey of Finland Special Paper 37*, 9–15.

Andersson, U.B., Högdahl, K., Sjöström, H. & Bergman, S., 2006: Multistage growth and reworking of the Palaeoproterozoic crust in the Bergslagen area, southern Sweden: evidence from U-Pb geochronology. *Geological Magazine 143*, 679–697.

Annertz, K., 1984: *En petrografisk karakteristik av en sent postorogen mafisk intrusion i östra Värmland*. Unpublished thesis, University of Lund, Lund, Sweden, 21 pp.

Antal, I., Bergman, S., Fredén, C., Gierup, J., Johansson, R., Stephens, M. & Thunholm, B., 1998a: Översiktsstudie av Gävleborgs län: Geologiska förutsättningar. *Svensk Kärnbränslehantering AB R-98-34*, 49 pp.

Antal, I., Bergman, T., Johansson, R., Persson, C., Stephens, M., Thunholm, B. & Åsman, M., 1998b: Översiktsstudie av Södermanlands län: Geologiska förutsättningar. *Svensk Kärnbränslehantering AB R-98-28*, 49 pp.

Antal, I., Bergman, T., Johansson, R., Persson, C., Stephens, M., Thunholm, B. & Åsman, M., 1998c: Översiktsstudie av Stockholms län: Geologiska förutsättningar. *Svensk Kärnbränslehantering AB R-98-30*, 47 pp.

Antal, I., Bergman, T., Gierup, J., Johansson, R., Lindén, A., Stephens, M. & Thunholm, B., 1998d: Översiktsstudie av Östergötlands län: Geologiska förutsättningar. *Svensk Kärnbränslehantering AB R-98-26*, 50 pp.

Antal, I., Bergman, S., Gierup, J., Johansson, R., Persson, C., Stephens, M. & Thunholm, B., 1998e: Översiktsstudie av Uppsala län: Geologiska förutsättningar. *Svensk Kärnbränslehantering AB R-98-32*, 49 pp.

Antal, I., Berglund, J., Eliasson, T., Gierup, J., Hilldén, A., Johansson, R., Stephens, M, Stølen, L.K. & Thunholm, B., 1999: Översiktsstudie av västra Götalands län: Geologiska förutsättningar. *Svensk Kärnbränslehantering AB R-99-33*, 57 pp.

Arnbom, J.-O., 1999: Beskrivning till berggrundskartan 11G Västerås SO. *Sveriges geologiska undersökning Af 204*, 46 pp.

Arnbom, J.-O. & Persson L., 2002: Beskrivning till berggrundskartan 11I Uppsala NV. *Sveriges geologiska undersökning Af 210*, 49 pp.

Back, F., 1993: Sammanfattning av de mellansvenska P-malmernas geologi, kvantitativa och kvalitativa egenskaper. *Sveriges geologiska undersökning unpublished report BRAP 93073*.

Baker, J.H., 1985: The petrology and geochemistry of 1.8–1.9 Ga granitic magmatism and related sub-seafloor hydrothermal alteration and ore-forming processes. W. Bergslagen, Sweden. *Ph.D. thesis, University of Amsterdam, Amsterdam, Holland, GUA Papers of Geology Series 1, No. 21*, 204 pp.

Baker, J.H. & de Groot, P.A., l983: Proterozoic seawater – felsic volcanics interaction W. Bergslagen, Sweden. Evidence for high REE mobility and implications for 1.8 Ga seawater compositions. *Contributions to Mineralogy and Petrology 82*, 119–130.

Baker, J.H., Andersson, L.-G. & Marinou, A., 1988: Geochemical variations in a Proterozoic hydrothermal mafic breccia dyke related to Ni-Cu-Fe skarn mineralization at Annehill, Bergslagen, Sweden. *Geologie en Mijnbouw 67*, 363–378.

Bergman, S., Isaksson, H., Johansson, R., Lindén, A., Persson, C. & Stephens, M., 1996a: Förstudie Östhammar. Jordarter, bergarter och deformationszoner. *Svensk Kärnbränslehantering AB PR D-96-016*, 81 pp.

Bergman, S., Kübler, L. & Martinsson, O., 2001: Description of regional geological and geophysical maps of northern Norrbotten county (east of the Caledonian orogen). *Sveriges geologiska undersökning Ba 56*, 110 pp.

Bergman, S., Persson, P.-O., Delin, H., Stephens, M.B. & Bergman, T., 2004a: Age and significance of the Hedesunda granite and related rocks, south-central Sweden. *Abstract 26th Nordic geological winter meeting, GFF 126*, 18–19.

Bergman, S., Delin, H. & Söderman, J., 2004b: Lokala kartor 1:50 000, Svealand. *In* H. Delin (ed.): Berggrundsgeologisk undersökning. Sammanfattning av pågående verksamhet 2003. *Sveriges geologiska undersökning Rapporter och meddelanden 116*, 20–32.

Bergman, T., 1994: The Wigström deposit western Bergslagen Sweden: A contact metasomatic tungsten skarn deposit related to a late Svecofennian granite. *Abstract 21st Nordic geological winter meeting, Tekniska Högskolan i Luleå,* 21.

Bergman, T. & Sundblad, K., 1990: A preliminary overview of gold-bearing skarn mineralizations in Bergslagen, south-central Sweden. *Geologiska Föreningens i Stockholm Förhandlingar 112*, 173–174.

Bergman, T., Schöberg, H. & Sundblad, K., 1995: Geochemistry, age and origin of the Högberget granite, western Bergslagen, Sweden. *GFF 117*, 87–96.

Bergman, T., Isaksson, H., Johansson, R., Lindén, A., Persson, C. & Stephens, M., 1996b: Förstudie Nyköping. Jordarter, bergarter och deformationszoner. *Svensk Kärnbränslehantering AB PR D-96-013*, 82 pp.

Bergman, T., Fredén, C., Gierup, J., Johansson, R., Kübler, L., Stephens, M., Stølen, L.K. & Thunholm, B., 1999a: Översiktsstudie av Örebro län: Geologiska förutsättningar. *Svensk Kärnbränslehantering AB R-99-23*, 49 pp.

Bergman, T., Gierup, J., Johansson, R., Kübler, L., Lindén, A., Stephens, M., Stølen, L.K. & Thunholm, B., 1999b: Översiktsstudie av Västmanlands län: Geologiska förutsättningar. *Svensk Kärnbränslehantering AB R-99-31*, 48 pp.

Bergman, T., Isaksson, H., Johansson, R., Lindén, A.H., Lindroos, H., Rudmark, L. & Stephens, M., 1999c: Förstudie Tierp. Jordarter, bergarter och deformationszoner. *Svensk Kärnbränslehantering AB R-99-53*, 119 pp.

Bergman, T., Isaksson, H., Johansson, R., Lindén, A.H., Lindroos, H., Rudmark, L. & Stephens, M., 2000: Förstudie Älvkarleby. Jordarter, bergarter och deformationszoner. *Svensk Kärnbränslehantering AB R-00-04*, 103 pp.

Bergström, S.M. & Bergström J., 1996: The Ordovician-Silurian boundary successions in Östergötland and Västergötland, S. Sweden. *GFF 118*, 25–42.

Bergström, S.M., Huff, W.D., Kolata, D.R. & Bauert, H., 1995: Nomenclature, stratigraphy, chemical fingerprinting, and areal distribution of some Middle Ordovician K-bentonites in Baltoscandia. *GFF 117*, 1–14.

Berthé, D., Choukroune, P. & Jegouzo, P., 1979: Orthogneiss, mylonite and non-coaxial deformation of granites: the example of the South Armorican shear zone. *Journal of Structural Geology 1*, 31–42.

Berthelsen, A., 1980: Towards a palinspastic tectonic analysis of the Baltic shield. *In* J. Cogné & M. Slansky (eds.): Geology of Europe from Precambrian to Post-Hercynian sedimentary basins. *International Geological Congress Colloquium C6 Paris*, 5–21.

Beyer, M., 1954: Berggrunden inom leptitområdet mellan Harg och Hargshamn i norra Uppland. *Geologiska Föreningens i Stockholm Förhandlingar 76*, 183–214.

Billström, K., 1985: Isotopic studies of two early Proterozoic sulphide ores in the Bergslagen district, south-central Sweden. *Ph.D. thesis, University of Stockholm, Sweden, Meddelanden från Stockholms Universitets Geologiska Institution 263*, 141 pp.

Billström, K., Åberg, G. & Öhlander, B., 1988: Isotopic and geochemical data of the Pingstaberg Mo-bearing granite in Bergslagen, south central Sweden. *Geologie en Mijnbouw 67*, 255–263.

Bingen, B., Andersson, J., Söderlund, U. & Möller, C., 2008: The Mesoproterozoic in the Nordic countries. *Episodes 31*, 29–34.

Björk, L., 1986: Beskrivning till berggrundskartan Filipstad NV. *Sveriges geologiska undersökning Af 147*, 110 pp.

Björklund, L. & Claesson, S., 1992: Geochemical character and preliminary Sm-Nd data on basic metavolcanic rocks in the Tivedon area, south Sweden. *Geologiska Föreningens i Stockholm Förhandlingar 114*, 340–341.

Björklund, L. & Weihed, P., 1997: Geochemistry and tectonic setting of the Orvar Hill mafic volcanic rocks of the Tiveden area, south-central Sweden. *GFF 119*, 123–126.

Bonhomme, M.G. & Welin, E., 1983: Rb-Sr and K-Ar isotopic data on shale and siltstone from the Visingsö group, Lake Vättern basin, Sweden. *Geologiska Föreningens i Stockholm Förhandlingar 105*, 363–366.

Boström, K., Rydell, H. & Joensuu, O., 1979: Långban – An exhalative sedimentary deposit? *Economic Geology 74*, 1102–1011.

Boynton, W.V., 1984. Cosmochemistry of rare earth elements: meteorite studies. *In* P. Henderson (ed.): *Rare earth element geochemistry*. Elsevier, Amsterdam, 63–114.

Bromley-Challenor, M., 1984: *A tin bearing greisen occurrence in central Sweden*. Unpublished thesis, University of Uppsala, Uppsala, Sweden.

Bromley-Challenor, M.D., l988: The Falun supracrustal belt. Part I: primary geochemical characteristics of Proterozoic metavolcanics and granites. *Geologie en Mijnbouw 67*, 239–253.

Brown, G.C., Thorpe, R.S. & Webb, P.C., 1984: The geochemical characteristics of granitoids in constrast-

ing arcs and comments on magma sources. *Journal of the Geological Society of London 141*, 413–426.

Bruun, Å., Nilsson, C.-A., Sundberg, A., Wik, N.-G. & Wikström, A., 1995: Malmer, industriella mineral och bergarter i Östergötlands län. *Sveriges geologiska undersökning Rapporter och meddelanden 80*, 340 pp.

Carlon, C.J. & Bleeker, W., 1988: The geology and structural setting of the Håkansboda Cu-Co-As-Sb-Bi-Au deposit and associated Pb-Zn-Cu-Ag-Sb mineralization, Bergslagen, central Sweden. *Geologie en Mijnbouw 67*, 279–292.

Carlon, C.J. & Bjurstedt, S., 1990: Stratabound and stratiform sulphide mineralization in the evolution of the Guldsmedshyttan Syncline, Bergslagen, south-central Sweden. *Geologiska Föreningens i Stockholm Förhandlingar 112*, 176–177.

Carlsson, A., 1979: *Characteristic features of a superficial rock mass in southern central Sweden. Horizontal and subhorizontal fractures and filling material*. Ph.D. thesis, University of Uppsala, Uppsala, Sweden (Striae 11), 79 pp.

Castro, A., 1987: On granitoid emplacement and related structures. A review. *Geologische Rundschau 76*, 101–124.

Cederbom, C., Larson, S.Å., Tullborg, E.-L. & Stiberg, J.-P., 2000: Fission track thermochronology applied to Phanerozoic thermotectonic events in central and southern Sweden. *Tectonophysics 316*, 153–167.

Christofferson, H., Lundström, I. & Vivallo, W., 1986: The Garpenberg area and zinc-lead-copper deposit. *In* I. Lundström & H. Papunen (eds.): Mineral deposits of southwestern Finland and the Bergslagen province, Sweden. 7th IAGOD symposium and Nordkalott project meeting, excursion guide No. 3. *Sveriges geologiska undersökning Ca 61*, 30–32.

Claesson, S. & Kresten, P., 1997: The anorogenic Noran intrusion – a Mesoproterozoic rapakivi massif in south-central Sweden. *GFF 119*, 115–122.

Claesson, S., Huhmaa, H., Kinny, P.D. & Williams, I.S., 1993: Svecofennian detrital zircon ages – implications for the Precambrian evolution of the Baltic Shield. *Precambrian Research 64*, 109–130.

Collins, W.J., 2002: Hot orogens, tectonic switching, and creation of continental crust. *Geology 30*, 535–538.

Cronquist, T., Forssberg, O., Maersk Hansen, L., Jonsson, A., Koyi, S., Leiner, P., Petersson, J., Skogsmo, G. & Vestgård, J., 2005: Forsmark site investigation. Detailed fracture mapping of two trenches at Forsmark. *Svensk Kärnbränslehantering AB P-04-88*, 32 pp.

Cruden, A.R., Sjöström, H. & Aaro, S., 1999: Structure and geophysics of the Gåsborn granite, central Sweden: an example of fracture-fed asymmetric pluton emplacement. *In* A. Castro, C. Fernandez & J.L. Vigneresse (eds): Understanding granites. Integrating new and classical techniques. *Geological Society of London Special Publications 168*, 141–160.

Dahl-Jensen, T., Dyrelius, D. & Palm, H., 1991: Deep crustal seismic reflection profiling across two major tectonic zones in southern Sweden. *Tectonophysics 195*, 209–240.

Debon, F. & Le Fort, P., 1983: A chemical-mineralogical classification of common plutonic rocks and associations. *Transactions of Royal Society of Edinburgh: Earth Sciences 73*, 135–149.

de Groot, P.A., 1990: A model for the formation of potassic and sodic alteration phases during hydrothermal processes: application of thermodynamic models to natural systems. *Geologiska Föreningens i Stockholm Förhandlingar 112*, 180–183.

de Groot, P.A. & Baker, J.H., 1992: High element mobility in 1.9–1.86 Ga hydrothermal alteration zones, Bergslagen, central Sweden: relationships with exhalative Fe-ore mineralizations. *Precambrian Research 54*, 109–130.

Delin, H., 1993: The radiometric age of the Ljusdal granodiorite of central Sweden. *In* T. Lundquist (ed.): Radiometric dating results. *Sveriges geologiska undersökning C 823*, 13–16.

Delin, H., 1996: U-Pb zircon ages of granitoids in the Kårböle region, central Sweden. *In* T. Lundquist (ed.): Radiometric dating results 2. *Sveriges geologiska undersökning C 828*, 6–14.

Delin, H. & Persson, P.-O., 1999: U-Pb zircon ages of three Palaeoproterozoic igneous rocks in the Loos-Hamra area, central Sweden. *In* T. Lundquist (ed.): Radiometric dating results 4. *Sveriges geologiska undersökning C 831*, 20–31.

DePaolo, D.J., 1981, Neodymium isotopes in the Colorado Front Range and crust-mantle evolution in the Proterozoic. *Nature 291*, 193–196.

DePaolo, D.J. & Wasserberg, G.J., 1976: Nd isotopic variations and petrogenetic models. *Geophysical Research Letters 3*, 249–252.

Dewey J.F., Holdsworth, R.E. & Strachan, R.A., 1998: Transpression and transtension zones. *In* R.E. Holdsworth, R.A. Strachan & J.F. Dewey (eds.): Continental tranpressional and transtensional tectonics. *Geological Society London Special Publications 135*, 1–14.

Dobbe, R.T.M., Oen, I.S. & Verdurmen, E.A.T., 1995: U-Pb ages of metatuffites and older granite from the Tunaberg area, SE Bergslagen, Sweden. *Geologie en Mijnbouw 74*, 129–136.

Dyrelius, D., Dahl-Jensen, T. & Palm, H., 1992: A reflection seismic profile across the Protogine Zone.

Geologiska Föreningens i Stockholm Förhandlingar 114, 342–343.

Ebbestad, J.O.R, Wickström, L.M. & Högström, A.E.S., 2007: WOGOGOB 2007. Field guide and abstracts. *Sveriges geologiska undersökning Rapporter och meddelanden 128*, 110 pp.

Engström, A.V. & Skelton, A., 2002: Hydrothermal minerals, fluid flow and brittle/semi-brittle deformation: A comparison between the Skyttorp–Vattholma Fault Zone (SVFZ), south-central Sweden and the Iberia Abyssal Plain (ODP leg 173, Hole 1067). *GFF 124*, 229.

Eskola, P., 1914: On the petrology of the Orijärvi region in southwestern Finland. *Bulletin de la Commission Geologique de Finlande 40*, 277 pp.

Farley, K.A., 2000: Helium diffusion from apatite: general behaviour as illustrated by Durango flourapatite. *Journal of Geophysical Research 105*, 2903–2914.

Filén, B., 2001: Swedish layered intrusions anomalous in PGE-Au. *In* P. Weihed (ed.): Economic geology research. Vol 1. 1999–2000. *Sveriges geologiska undersökning C 833*, 33–45.

Flink, G., 1908: Bidrag till Sveriges mineralogi. *Arkiv för kemi, mineralogi och geologi 3:11*, 4–6.

Follin, S., 2008: Bedrock hydrogeology Forsmark. Site descriptive modelling, SDM-Site Forsmark. *Svensk Kärnbränslehantering AB R-08-95*, 163 pp.

Fredén, C., Gierup, J., Johansson, J., Stephens, M., Stølen, L.K., Thunholm, B. & Wahlgren, C.-H., 1999: Översiktsstudie av Värmlands län: Geologiska förutsättningar. *Svensk Kärnbränslehantering AB R-99-21*, 53 pp.

Frietsch, R., 1975: Brief outline of the metallic mineral resources of Sweden. *Sveriges geologiska undersökning C 718*, 64 pp.

Frietsch, R., 1982a: Alkali metasomatism in the ore-bearing metavolcanics of central Sweden. *Sveriges geologiska undersökning C 791*, 54 pp.

Frietsch, R., 1982b: A model for the formation of the iron, manganese and sulphide ores of central Sweden. *Geologische Rundschau 71*, 206–192.

Frietsch, R., 1986: Metallogenesis of the Bergslagen province and southwestern Finland: Bergslagen. *In* I. Lundström & H. Papunen (eds.): Mineral deposits of southwestern Finland and the Bergslagen province, Sweden. 7th IAGOD symposium and Nordkalott project meeting, excursion guide No. 3. *Sveriges geologiska undersökning Ca 61*, 11–15.

Gaál, G. & Gorbatschev, R., 1987: An outline of the Precambrian evolution of the Baltic Shield. *Precambrian Research 35*, 15–52.

Gaál, G. & Sundblad, K., 1990: Metallogeny of gold in the Fennoscandian Shield. *Mineralium Deposita 25*, 104–114.

Gavelin, S., 1985: The Baggetorp tungsten deposit, southern Sweden. *Sveriges geologiska undersökning C 810*, 17 pp.

Gavelin, S., 1989: Genesis of the Falun sulphide ores, central Sweden. *Geologiska Föreningens i Stockholm Förhandlingar 111*, 213–227.

Gavelin, S., Lundström, I. & Norström, S., 1976: Svecofennian stratigraphy on Utö, Stockholm archipelago. *Sveriges geologiska undersökning C 719*, 44 pp.

Geijer, P., 1917: Falutraktens berggrund och malmfyndigheter. *Sveriges geologiska undersökning C 275*, 319 pp.

Geijer, P., 1926: Geologiska reseintryck från Nordafrika. *Geologiska Föreningens i Stockholm Förhandlingar 48*, 512–535.

Geijer, P., 1965: Types of sulphide ore and associated wall rock alteration in the Öster Silvberg district, central Sweden. *Sveriges geologiska undersökning C 603*, 32 pp.

Geijer, P. & Magnusson, N.H., 1944: De mellansvenska järnmalmernas geologi. *Sveriges geologiska undersökning Ca 35*, 654 pp.

Geijer, P., Collini B., Munthe H. & Sandegren, R., 1951: Beskrivning till kartbladet Gränna. *Sveriges geologiska undersökning Aa 193*, 100 pp.

Gierup, J., Kübler, L., Lindén, A., Ripa, M., Stephens, M., Stølen, L.K. & Thunholm, B., 1999: Översiktsstudie av Dalarnas län (urbergsdelen): Geologiska förutsättningar. *Svensk Kärnbränslehantering AB R-99-29*, 48 pp.

Glamheden, R., Fredriksson, A., Persson, L., Röshoff, K., Karlsson, J., Bohlin, H., Lindberg, U., Hakami, H., Hakami, E. & Johansson, M., 2007: Rock mechanics Forsmark. Site descriptive modelling Forsmark stage 2.2. *Svensk Kärnbränslehantering AB SKB R-07-31*, 277 pp.

Gorbatschev, R., 1960: On the alkali rocks of Almunge. A preliminary report on a new survey. *Bulletin of the Geological Institution of the University of Uppsala XXXIX*, 69 pp.

Gorbatschev, R., 1967: Petrology of Jotnian rocks in the Gävle area. *Sveriges geologiska undersökning C 621*, 50 pp.

Gorbatschev, R., 1969: A study of Svecofennian supracrustal rocks in central Sweden: lithological association, stratigraphy, and petrology in the northwestern part of the Mälaren-Hjälmaren basin. *Geologiska Föreningens i Stockholm Förhandlingar 91*, 479–535.

Gorbatschev, R., 1972: Beskrivning till berggrundskartan Örebro NO. *Sveriges geologiska undersökning Af 103*, 70 pp.

Gorbatschev, R., 1980: The Precambrian development of southern Sweden. *Geologiska Föreningens i Stockholm Förhandlingar 102*, 392–397.

Gorbatschev, R., 2004: The Transscandinavian Igneous Belt – introduction and background. *In* K. Högdahl, U.B. Andersson & O. Eklund (eds.): The Transscandinavian Igneous Belt (TIB) in Sweden: a review of its character and evolution. *Geological Survey of Finland Special Paper 37*, 9–15.

Gorbatschev, R., Fromm, E. & Kjellström, G., 1976: Beskrivning till berggrundskartan Linköping NO. *Sveriges geologiska undersökning Af 107*, 111 pp.

Grahn, Y. & Nolvak, J., 1993: Chitinozoan dating of Ordovician impact events in Sweden and Estonia. A preliminary note. *Geologiska Föreningens i Stockholm Förhandlingar 115*, 263–264.

Grip, E., 1961: Geology of the nickel deposit at Lainijaur in northern Sweden and summary of other nickel deposits in Sweden. *Sveriges geologiska undersökning C 577*, 79 pp.

Guilbert, J. & Park, C.F. Jr., 1986: *The geology of ore deposits*. Freeman and Company, New York, 985 pp.

Hammergren, P., Sjöblom, B., Thelander, T. & Åkerström, K., 1987: Utvärdering av guldpotentialen inom Östergötland och Norra Småland 1987. *Sveriges geologiska AB prospekteringsrapport 87531*, 57 pp.

Hanmer, S. & Passchier, C.W., 1991: Shear sense indicators: a review. *Geological Survey of Canada Paper 90*, 71 pp.

Harris, L.B., Koyi, H.A. & Fossen, H., 2002: Mechanisms for folding of high-grade rocks in extensional tectonic settings. *Earth-Science Reviews 59*, 163–210.

Hedström, P. & Wikström, A., 1986: The Zinkgruvan (Åmmeberg) zinc-lead deposit. *In* I. Lundström & H. Papunen (eds.): Mineral deposits of southwestern Finland and the Bergslagen province, Sweden. 7th IAGOD symposium and Nordkalott project meeting, excursion guide No. 3. *Sveriges geologiska undersökning Ca 61*, 33–36.

Hedström, P., Simeonov, A. & Malmström, L., 1989: The Zinkgruvan ore deposit, south-central Sweden: A Proterozoic, proximal Zn-Pb-Ag deposit in distal volcanic facies. *Economic Geology 84*, 1235–1261.

Hellingwerf, R.H., 1984: Paragenetic zoning and genesis of Cu-Zn-Fe-Bb-As sulfide skarn ores in a Proterozoic rift basin, Gruvåsen, western Bergslagen, Sweden. *Economic Geology 79*, 696–715.

Hellingwerf, R.H., 1986: Contributions to the geology and ore genesis of western Bergslagen, Sweden. *Ph.D. thesis, University of Amsterdam, Amsterdam, Holland, GUA Papers of Geology Series 1, No. 25*, 260 pp.

Hellingwerf, R.H. & Baker, J.H., 1985: Wall-rock alteration and tungsten and molybdenum mineralizations associated with older granites in western Bergslagen, Sweden. *Economic Geology 80*, 479–487.

Hellingwerf, R.H., Baker, J.H. & van Raaphorst, J.G., 1987: Sulphur isotope data of Proterozoic molybdenites from western Bergslagen, Sweden. *Geologiska Föreningens i Stockholm Förhandlingar 109*, 33–38.

Helmers, H., 1984: Stages of granite intrusion and regional metamorphism in the Proterozoic rocks of western Bergslagen, C. Sweden, as exemplified in the Grängen area. *Neues Jahrbuch für Mineralogie 150*, 307–324.

Henkel, H. & Pesonen, L.J., 1992: Impact craters and craterform structures in Fennoscandia. *Tectonophysics 216*, 31–40.

Henriques, Å., 1964: Geology and ores of the Åmmeberg district (Zinkgruvan) Sweden. *Arkiv för Mineralogi och Geologi 4*, 246 pp.

Hermansson, T., Stephens, M.B., Corfu, F., Andersson, J. & Page, L., 2007. Penetrative ductile deformation and amphibolite-facies metamorphism prior to 1851 Ma in the western part of the Svecofennian orogen, Fennoscandian Shield. *Precambrian Research 153*, 29–45.

Hermansson, T., Stephens, M.B., Corfu, F., Page, L.M. & Andersson, J., 2008a. Migratory tectonic switching, western Svecofennian orogen, central Sweden: Constraints from U/Pb zircon and titanite geochronology. *Precambrian Research 161*, 250–278.

Hermansson, T., Stephens, M.B. & Page, L.M., 2008b: $^{40}Ar/^{39}Ar$ hornblende geochronology from the Forsmark area in central Sweden: Constraints on late Svecofennian cooling, ductile deformation and exhumation. *Precambrian Research 167*, 303–315.

Hietanen, A., 1975: Generation of potassium-poor magmas in the northern Sierra Nevada and the Svecofennian of Finland. *U.S. Geological Survey Journal of Research 3*, 631–645.

Hitzman, M.W., Oreskes, N. & Einaudi, M.T., 1992: Geological characteristics and tectonic setting of Proterozoic iron oxide (Cu-U-Au-REE) deposits. *Precambrian Research 58*, 241–287.

Hjelmqvist, S., 1938: Über Sedimentgesteine in der Leptitformation Mittelschwedens. Die sogenannte "Larsboserie". *Sveriges geologiska undersökning C 413*, 39 pp.

Hjelmqvist, S., 1943: Die natronreiche Randzone des Granitmassivs nördlich von Smedjebacken in Dalarna. Ein beitrag zum Studium der Granitbildung. *Sveriges geologiska undersökning C 453*, 34 pp.

Hjelmqvist, S., 1946: Ett pseudo-agglomerat från trakten av Norberg. *Geologiska Föreningens i Stockholm Förhandlingar 68*, 505–509.

Hjelmqvist, S., 1966: Beskrivning till berggrundskarta över Kopparbergs län. *Sveriges geologiska undersökning Ca 40*, 217 pp.

Hjelmqvist, S. & Lundqvist, G., 1953: Beskrivning till kartbladet Säter. *Sveriges geologiska undersökning Aa 194*, 97 pp.

Hodges, K.V. & Spear, F.S., 1982: Geothermometry, geobarometry and the Al_2SiO_5 triple point at Mt. Moosilauke, New Hampshire. *American Mineralogist 67*, 1118–1134.

Högdahl, K. & Sjöström, H., 2001. Evidence for 1.82 Ga transpressive shearing in a 1.85 Ga granitoid in central Sweden: implications for the regional evolution. *Precambrian Research 105*, 37–56.

Högdahl, K. & Jonsson, E., 2004: The Horrsjö complex in the Bergslagen ore province: a Palaeoproterozoic caldera with a mineralised rim? *GFF 126*, 23.

Högdahl, K., Sjöström, H. & Gromet, L.P., 2001: Character and timing of Svecokarelian, late-orogenic ductile deformation zones in Jämtland, west central Sweden. *GFF 123*, 225–236.

Högdahl, K., Andersson, U.B. & Eklund, O. (eds.), 2004: The Transscandinavian Igneous Belt (TIB) in Sweden: a review of its character and evolution. *Geological Survey of Finland Special Paper 37*, 125 pp.

Högdahl, K., Jonsson, E. & Selbekk, R.S., 2007: Geological relations and U-Pb geochronology of Hyttsjö granites in the Långban-Nordmark area, western Bergslagen, Sweden. *GFF 129*, 43–54.

Högdahl, K., Sjöström, H., Andersson, U.B. & Ahl, M., 2008: Continental margin magmatism and migmatisation in the west-central Fennoscandian Shield. *Lithos 102*, 435–459.

Högdahl, K., Sjöström, H. & Bergman, S., 2009: Ductile shear zones related to crustral shortening and domain boundary evolution in the central Fennoscandian Shield. *Tectonics 28 (TC1003, doi:10.1029/2008TC002277),* 18 pp.

Hoisch, T.D., 1989: A muscovite-biotite geothermometer. *American Mineralogist 74*, 565–572.

Hoisch, T.D., 1990: Empirical calibration of six geobarometers for the mineral assemblage quartz + muscovite + biotite + plagioclase + garnet. *Contributions to Mineralogy and Petrology 104*, 225–234.

Holmquist, P.J., 1904: Utöns bergarter och geologi. *Geologiska Föreningens i Stockholm Förhandlingar 26*, 21–26.

Howell, D.G., 1989: *Tectonics of Suspect Terranes. Mountain building and continental growth*. Topics in the Earth Sciences 3, Chapman & Hall, London and New York, 232 pp.

Hübner, H., 1971: Molybdenum and tungsten occurrences in Sweden. *Sveriges geologiska undersökning Ca 46*, 29 pp.

Hughes, C.J., 1973: Spilites, keratophyres, and the igneous spectrum. *Geological Magazine 109*, 513–527.

Hutton, D.H.W., 1988: Granite emplacement mechanisms and tectonic controls: inferences from deformation studies. *Transactions of the Royal Society of Edinburgh: Earth Sciences 79*, 245–255.

Hutton, D.H.W., 1996: The "space problem" in the emplacement of granite. *Episodes 19*, 114–119.

Isaksson, H., Mattson, H., Thunehed, H. & Keisu M., 2004: Forsmark site investigation. Interpretation of petrophysical surface data. Stage 1 (2002). *Svensk Kärnbränslehantering AB P-03-102*, 81 pp.

Ivarsson, C. & Johansson, Å., 1995: U-Pb zircon dating of Stockholm granite at Frescati. *GFF 117*, 67–68.

Jarl, L.-G. & Johansson, Å., 1988: U-Pb zircon ages of granitoids from the Småland-Värmland granite-porphyry belt, southern and central Sweden. *Geologiska Föreningens i Stockholms Förhandlingar 110*, 21–28.

Johansson, H.E., 1910: The Åmmeberg zinc ore field. *Geologiska Föreningens i Stockholm Förhandlingar 32*, 1051–1078.

Johansson, H.E., 1919: Om Tunabergs kopparmalmsfält. *Sveriges geologiska undersökning C 221*, 19 pp.

Jonsson, E., 2004: *Fissure-hosted mineral formation and metallogenesis in the Långban Fe-Mn-(Ba-As-Pb-Sb…) deposit, Bergslagen, Sweden*. Ph.D. thesis (summary), University of Stockholm, Stockholm, Sweden, 22 pp.

Juhlin, C. & Stephens, M.B., 2006. Gently dipping fracture zones in Paleoproterozoic metagranite, Sweden: Evidence from reflection seismic and cored borehole data and implications for the disposal of nuclear waste. *Journal of Geophysical Research 111, B09302, doi:10.1029/2005JB003887*, 19 pp.

Juhlin, C., Lindgren, J. & Collini, B., 1991: Interpretation of seismic reflection and borehole data from Precambrian rocks in the Dala Sandstone area, central Sweden. *First Break 9*, 24–36.

Juhlin, C., Wahlgren, C.-H. & Stephens, M.B., 2000: Seismic imaging in the frontal part of the Sveconorwegian orogen, south-western Sweden. *Precambrian Research 102*, 135–154.

Kathol, B. & Weihed, P. (eds.), 2005: Description of regional geological and geophysical maps of the Skellefte District and surrounding areas. *Sveriges geologiska undersökning Ba 57*, 197 pp.

Kinck, J.J., Husebye, E.S. & Larsson, F.R., 1993: The Moho depth distribution in Fennoscandia and the regional tectonic evolution from Archean to Permian times. *Precambrian Research 64*, 23–51.

Koark, H.J., 1962: Zur Altersstellung und Entstehung der Sulfiderze vom Typus Falun. *Geologische Rundschau 52*, 123–146.

Koark, H., Kresten, P., Laufeld, S. & Sandvall, J., 1986: *Geology of the Falu Mine*. Sveriges geologiska undersökning, ISBN 91-7158-408-0, 28 pp.

Koistinen, T., Stephens, M.B., Bogatchev, V., Nordgulen, Ø., Wennerström, M. & Korhonen, J. 2001: *Geological map of the Fennoscandian Shield, scale 1:2 000 000*. Geological Surveys of Finland, Norway and Sweden and the North-West Department of Natural Resources of Russia.

Kornfält, K.-A., 1975: Beskrivning till berggrundskartan Örebro SV. *Sveriges geologiska undersökning Af 108*, 54 pp.

Kresten, P., 1986: Geochemistry and tectonic setting of metavolcanics and granitoids from the Falun area, south central Sweden. *Geologiska Föreningens i Stockholm Förhandlingar 107*, 275–285.

Kresten, P. & Aaro, S., 1987a: Bedrock maps 13E Vansbro NO and SO, scale 1:50 000. *Sveriges geologiska undersökning Ai 13*, 14.

Kresten, P. & Aaro, S., 1987b: Bedrock maps 13F Falun NV, SV, NO and SO, scale 1:50 000. *Sveriges geologiska undersökning Ai 15, 16, 17, 18*.

Krogh, T.E., 1973: A low-contamination method for hydrothermal decomposition of zircon and extraction of U and Pb for isotopic age determination. *Geochimica et Cosmochimica Acta 37*, 485–494.

Krogh, T.E., 1982: Improved accuracy of U-Pb (zircon) ages by the creation of more concordant systems using an air abrasion technique. *Geochimica et Cosmochimica Acta 46*, 637–649.

Kumpulainen, R.A., Mansfeld, J., Sundblad, K., Neymark, L. & Bergman, T., 1996: Stratigraphy, age and Sm-Nd isotope systematics of the country rocks to Zn-Pb sulphide deposits, Åmmeberg district, Sweden. *Economic Geology 91*, 1009–1021.

Lager, I., 1986: The Dannemora iron ore deposit. *In* I. Lundström & H. Papunen (eds.): Mineral deposits of southwestern Finland and the Bergslagen province, Sweden. 7th IAGOD symposium and Nordkalott project meeting, excursion guide No. 3. *Sveriges geologiska undersökning Ca 61*, 26–30.

Lager, I., 2001: The geology of the Palaeoproterozoic limestone-hosted Dannemora iron deposit, Sweden. *Sveriges geologiska undersökning Rapporter och meddelanden 107*, 49 pp.

Lagerblad, B., 1988: Evolution and tectonic history of the Bergslagen volcanoplutonic complex, central Sweden. *Geologie en Mijnbouw 67*, l65–l76.

Lagerblad, B. & Gorbatschev, R., 1985: Hydrothermal alteration as a control of regional geochemistry and ore formation in the central Baltic Shield. *Geologische Rundschau 74*, 33–49.

Lagerblad, B., Trägårdh, J., Ripa, M. & Gorbatschev, R., 1987: *Bergslagen excursion guide*. "Proterozoic geochemistry" symposium, IGCP 217, Lund, Sweden, 69 pp.

Lahtinen, R. & Huhma, H., 1997: Isotopic and geochemical constraints on the evolution of the 1.93–1.79 Ga Svecofennian crust and mantle in Finland. *Precambrian Research 82*, 13–34.

Lahtinen, R., Garde, A.A. & Melezhik, V.A., 2008: Paleoproterozoic evolution of Fennoscandia and Greenland. *Episodes 31*, 20–28.

Landergren, S., 1948: On the geochemistry of Swedish iron ores and associated rocks. *Sveriges geologiska undersökning C 496*, 182 pp.

Larson, S.Å., Tullborg, E.-L., Cederbom, C. & Stiberg J.-P., 1999: Sveconorwegian and Caledonian foreland basins in the Baltic Shield revealed by fission-track thermochronology. *Terra Nova 11*, 210–215.

Le Bas, M.J., Le Maitre, R.W., Steckeisen, A. & Zanettin, B., 1986: A chemical classification of volcanic rocks based on the total alkali-silica diagram. *Journal of Petrology 27*, 745–750.

Leijon, B. (ed.), 2005: Forsmark site investigation. Investigations of superficial fracturing and block displacements at drill site 5. *Svensk Kärnbränslehantering AB P-05-199*, 132 pp.

Le Maitre, R.W. (ed.), 2002: *Igneous rocks. A classification and glossary of terms. 2nd edition. Recommendations of the International Union of Geological Sciences Subcommision on the Systematics of Igneous Rocks.* Cambridge University Press, 236 pp.

Lidmar-Bergström, K., 1993: Denudation surfaces and tectonics in the southernmost part of the Baltic Shield. *Precambrian Research 64*, 337–345.

Lidmar-Bergström, K., 1994: Morphology of the bedrock surface. *In* C. Fredén (ed.): Geology. *National Atlas of Sweden*, 44–54.

Lindh, A., Schöberg, H. & Annertz, K., 1994: Disturbed radiometric ages and their bearing on interregional correlations in the SW Baltic Shield. *Lithos 31*, 65–79.

Lindroth, G.T., 1922: Studier över Yxsjöfältets geologi och petrografi. *Geologiska Föreningens i Stockholm Förhandlingar 44*, 20–123.

Lindström, M., Flodén, T., Grahn, Y. & Kathol, B., 1994: Post-impact deposits in Tvären, a marine Middle Ordovician crater south of Stockholm, Sweden. *Geological Magazine 131*, 91–103.

Lindström, M., Lundqvist, J. & Lundqvist, T., 2000: *Sveriges geologi från urtid till nutid, 2nd edition*. Studentlitteratur, Lund, 491 pp.

Lipman, P.W., 1965: Chemical comparison of glassy and crystalline volcanic rocks. *U.S. Geological Survey Bulletin 1201D*, 24 pp.

Lipman. P.W., 1984: The roots of ash flow calderas in western North America: Windows into the tops of granitic batholiths. *Journal of Geophysical Research 89*, 8801–8841.

Loberg, B.E.H., 1980: A Proterozoic subduction zone in southern Sweden. *Earth and Planetary Science Letters 46*, 287–294.

Löfgren, C., 1979: Do leptites represent Precambrian island arc rocks? *Lithos 12*, 159–165.

Löfstrand, G., 1894: Om förekomsten af guld och wismutglans vid Malsjöbergs jernmalmsgrufva. *Geologiska Föreningens i Stockholm Förhandlingar 16*, 71–72.

Löfstrand, G., 1903: Slättbergs och Kuså nickelgruvor. *Geologiska Föreningens i Stockholm Förhandlingar 25*, 103–122.

Ludwig, K.R., 1991a: PBDAT: A computer program for processing Pb-U-Th isotope data. Version 1.20. *U.S. Geological Survey Open File Report 88-542*.

Ludwig, K.R., 1991b: ISOPLOT: A plotting and regression program for radiogenic-isotope data. Version 2.53. *U.S. Geological Survey Open File Report 91*.

Lundegårdh, P.H., 1956: Petrology of the Uppsala region eastern Sweden. *Sveriges geologiska undersökning C 544*, 74 pp.

Lundegårdh, P.H., 1959: Beskrivning till kartbladet Eskilstuna. *Sveriges geologiska undersökning Aa 200*, 56 pp.

Lundegårdh, P.H., 1967: Berggrunden i Gävleborgs län. *Sveriges geologiska undersökning, Ba 22*, 303 pp.

Lundegårdh, P.H., 1971: *Nyttosten i Sverige*. Almqvist and Wiksell förlag AB, 248 pp.

Lundegårdh, P.H., 1974: Beskrivning till berggrundskartan Eskilstuna NV. *Sveriges geologiska undersökning Af 111*, 75 pp.

Lundegårdh, P.H., 1983: Beskrivning till berggrundskartan Lindesberg SO. *Sveriges geologiska undersökning Af 139*, 58 pp.

Lundegårdh, P.H., 1987: Beskrivning till berggrundskartan Filipstad SV. *Sveriges geologiska undersökning Af 157*, 77 pp.

Lundegårdh, P.H., 1995: Beskrivning till berggrundskartan över Värmlands län, östra och mellersta Värmlands berggrund. Fyndigheter av nyttosten och malm i Värmlands län. *Sveriges geologiska undersökning Ba 45:1*, 180 pp.

Lundegårdh, P.H. & Lundqvist, G., 1956: Beskrivning till kartbladet Uppsala. *Sveriges geologiska undersökning Aa 199,* 117 pp.

Lundegårdh, P.H. & Fromm, E., 1971: Beskrivning till berggrundskartan Örebro SV. *Sveriges geologiska undersökning Af 101*, 70 pp.

Lundegårdh, P.H. & Nisca, D., 1978: Beskrivning till berggrundskartan Västerås SV. *Sveriges geologiska undersökning Af 122*, 60 pp.

Lundegårdh, P.H., Hübner, H., Wikman, H., Karis, L. & Magnusson, E., 1972: Beskrivning till berggrundskartan Örebro NV. *Sveriges geologiska undersökning Af 102*, 216 pp.

Lundegårdh, P.H., Karis, L. & Magnusson, E., 1973: Beskrivning till berggrundskartan Örebro SO. *Sveriges geologiska undersökning Af 104*, 76 pp.

Lundqvist, G. & Hjelmqvist, S., 1937: Beskrivning till kartbladet Smedjebacken. *Sveriges geologiska undersökning Aa 181*, 129 pp.

Lundqvist, J., 1994: The deglaciation. *In* C. Fredén (ed.): Geology. *National Atlas of Sweden*, 124–135.

Lundqvist, T., 1959: Berggrunden på Riddarskäret i nordöstra Uppland. *Geologiska Föreningens i Stockholm Förhandlingar 81*, 99–126.

Lundqvist, T., 1962: Det svekofenniska suprakrustalstråket mellan Ljusterö och Rödlöga i Stockholms norra skärgård. *Sveriges geologiska undersökning C 585*, 107 pp.

Lundqvist, T. & Persson, P.-O., 1999: Geochronology of porphyries and related rocks in northern and western Dalarna, south-central Sweden. *GFF 121*, 307–322.

Lundström, I., 1974: Beskrivning till berggrundskartan Nyköping SV. *Sveriges geologiska undersökning Af 109*, 123 pp.

Lundström, I., 1976: Beskrivning till berggrundskartan Nyköping SO. *Sveriges geologiska undersökning Af 114*, 81 pp.

Lundström, I., 1983: Beskrivning till berggrundskartan Lindesberg SV. *Sveriges geologiska undersökning Af 126*, 140 pp.

Lundström, I., l985: Beskrivning till berggrundskartan Lindesberg NV. *Sveriges geologiska undersökning Af 140*, 131 pp.

Lundström, I., 1995: Beskrivning till berggrundskartorna Filipstad SO och NO. *Sveriges geologiska undersökning Af 177*, 185, 218 pp.

Lundström, I., Allen, R.L., Persson, P.-O. & Ripa, M., 1998: Stratigraphies and depositional ages of Svecofennian, Paleoproterozoic metavolcanic rocks in E. Svealand and Bergslagen, south central Sweden. *GFF 120*, 315–320.

Lundström I., Eriksson, G. & Strömberg, A., 2002a: The post-tectonic breccias at Bjursås and Pellesberget as manifestations of post-Svecokarelian volcanism. *Sveriges geologiska undersökning Rapporter och meddelanden 109*, 18 pp.

Lundström, I., Persson, P.-O. & Kübler L., 2002b: Ages of post-tectonic dyke porphyries and breccias in Bergslagen, south-central Sweden. *In* S. Bergman (ed.): Radiometric dating results 5. *Sveriges geologiska undersökning C 834*, 43–49.

Magnusson, N.H., 1925: Persbergs malmtrakt och berggrunden i de centrala delarna av Filipstads bergslag i Värmlands län. *Beskrivningar över mineralfyndigheter 2, Kungliga kommerskollegium and Sveriges geologiska undersökning*, 475 pp.

Magnusson, N.H., 1929: Nordmarks malmtrakt. Geologisk beskrivning. *Sveriges geologiska undersökning Ca 13*, 98 pp.

Magnusson, N.H., 1930: Långbans malmtrakt. *Sveriges geologiska undersökning Ca 23*, 111 pp.

Magnusson, N.H., 1936: Berggrunden inom Kantorps malmtrakt. *Sveriges geologiska undersökning C 401*, 88 pp.

Magnusson, N.H., 1940: Herrängsfältet och dess järnmalmer. *Sveriges geologiska undersökning C 431*, 78 pp.

Magnusson, N.H., 1950: Zinc and lead deposits of central Sweden. *18th International Geological Congress Proceedings F*, 371–379.

Magnusson, N.H., 1953: *Malmgeologi*. Jernkontoret, Stockholm, 439 pp.

Magnusson, N.H., 1970: The origin of the iron ores in central Sweden and the history of their alterations. *Sveriges geologiska undersökning C 643*, 364 pp.

Magnusson, N.H., 1973: *Malm i Sverige 1*. Almqvist & Wiksell Förlag AB, 320 pp.

Maniar, P.D. & Piccoli, P.M., 1989: Tectonic discrimination of granitoids. *Geological Society of America Bulletin 101*, 635–643.

McDonough, W.F., Sun, S.-S., Ringwood, A.E., Jagoutz, E. & Hofmann, A.W., 1992: Potassium, rubidium, and cesium in the Earth and Moon and the evolution of the mantle of the Earth. *Geochimica et Cosmochimica Acta 56*, 1001–1012.

McPhie, J., Doyle, M. & Allen, R.A., 1993: *Volcanic textures*. Centre for Ore Deposits and Exploration Studies, University of Tasmania, Australia, 196 pp.

Middlemost, E.A.K., 1994: Naming materials in the magma/igneous rock system. *Earth-Science Reviews 37*, 215–224.

Möller, C., 1998: Decompressed eclogites in the Sveconorwegian (–Grenvillian) orogen of SW Sweden: petrology and tectonic implications. *Journal of Metamorphic Geology 16*, 641–656.

Nielsen, A.T. & Schovsbo, N.H., 2006: Cambrian to basal Ordovician lithostratigraphy in southern Scandinavia. *Bulletin of the Geological Society of Denmark 53*, 47–92.

Nironen, M., 1997: The Svecofennian orogen: a tectonic model. *Precambrian Research 86*, 21–44.

Nordenström, G., 1882: Fynd av gediget guld i Falu grufva. *Geologiska Föreningens i Stockholm Förhandlingar 6*, 59–69.

Nyström, J.-O., 1982: Post-Svecokarelian Andinotype evolution in central Sweden. *Geologische Rundschau 71*, 141–157.

Nyström, J.-O., 1983: Pumpellyite-bearing rocks in central Sweden and extent of host rock alteration as a control of pumpellyite composition. *Contributions to Mineralogy and Petrology 83*, 159–168.

Nyström, J.-O., 2004: Dala volcanism, sedimentation and structural setting. *In* K. Högdahl, U.B. Andersson & O. Eklund (eds.): The Transscandinavian Igneous Belt (TIB) in Sweden: a review of its character and evolution. *Geological Survey of Finland Special Paper 37*, 58–70.

Nyström, J.-O. & Levi, B., 1980: Pumpellyite-bearing Precambrian rocks and post-Svecokarelian regional metamorphism in central Sweden. *GFF 102*, 37–39.

Oen, I.S., 1987: Rift-related igneous activity and metallogenesis in SW Bergslagen, Sweden. *Precambrian Research 35*, 367–382.

Oen, I.S., Helmers, H., Verschure, R.H. & Wiklander, U., 1982: Ore deposition in a Proterozoic incipient rift zone environment: a tentative model for the Filipstad–Grythyttan–Hjulsjö region, Bergslagen, Sweden. *Geologische Rundschau 71*, 182–194.

Öhlander, B. & Zuber, J., 1988: Genesis of the Fellingsbro-type granites: evidence from gravity measurements and geochemistry. *Geologiska Föreningens i Stockholm Förhandlingar 110*, 39–54.

Öhlander, B. & Romer, R.L., 1996: Zircon ages of granites occurring along the Central Swedish Gravity Low. *GFF 118*, 217–225.

Ohlsson, L.-G., 1979: Tungsten occurrences in Sweden. *Economic Geology 74*, 1012–1034.

Ohlsson, L.-G., 1980: Preliminär översiktlig rapport om arbeten inom Dala-Järnagraniten. *LKAB Prospektering, Grb 189*.

Olofsson, I., Simeonov, A., Stigsson, M., Stephens, M., Follin, S., Nilsson, A.-C., Röshoff, K., Lindberg, U., Lanaro, F., Fredriksson, A. & Persson, L., 2007: Site descriptive modelling Forsmark, stage 2.2. A fracture domain concept as a basis for the statistical modelling of fractures and minor deformation zones, and interdisciplinary coordination. *Svensk Kärnbränslehantering AB R-07-15*, 261 pp.

Page, L.M., Stephens, M.B. & Wahlgren, C.-H., 1996: $^{40}Ar/^{39}Ar$ geochronological constraints on the tectonothermal evolution of the Eastern Segment of the

Sveconorwegian orogen, south-central Sweden. *In* T.S. Brewer (ed.): Precambrian crustal evolution in the North Atlantic region. *Geological Society Special publication 112*, 315–330.

Page, L., Hermansson, T., Söderlund, P. & Stephens, M.B., 2007: Forsmark site investigation. $^{40}Ar/^{39}Ar$ and U-Th/He geochronology: Phase 2. *Svensk Kärnbränslehantering AB P-06-211*, 105 pp.

Patchett, P.J., 1978: Rb/Sr ages of Precambrian dolerites and syenites in southern and central Sweden. *Sveriges geologiska undersökning C 747*, 63 pp.

Patchett, P.J., Gorbatschev, R. & Todt, W., 1987: Origin of continental crust of 1.9–1.7 Ga age. Nd isotopes in the Svecofennian orogenic terrains of Sweden. *Precambrian Research 35*, 145–160.

Peacock, M.A., 1931: Classification of igneous rock series. *Journal of Geology 39*, 65–67.

Pearce, J.A., 1996: Source and settings of granitic rocks. *Episodes 19*, 120–125.

Pearce, J.A. & Cann, J.R., 1973: Tectonic setting of basic volcanic rocks determined by using trace element analyses. *Earth and Planetary Science Letters 19*, 290–300.

Peccerillo, A. & Taylor, S.R., 1976: Geochemistry of Eocene calc-alkaline volcanic rocks from the Kastamonu area, northern Turkey. *Contributions to Mineralogy and Petrology 58*, 63–81.

Pedersen, L.B., Qian, W., Dynesius, L. & Zhang, P., 1994: An airborne tensor VLF system. From concept to realisation. *Geophysical Prospecting 42*, 863–883.

Perchuk, L.L., Aranovich, L.Y., Podleskii, K.K., Lavranteva, I.V., Gerasimov, V.Y., Fedkin, V.V., Kitsul, V.I., Karsakov, L.P. & Berdnikov, N.V., 1985: Precambrian granulites of the Aldan shield, eastern Siberia, USSR. *Journal of Metamorphic Geology 3*, 265–310.

Perkins, D. & Chipera, S.J., 1985: Garnet-orthopyroxene-plagioclase-quartz barometry: Refinement and application to the English river subprovince and Minnesota river valley. *Contributions to Mineralogy and Petrology 89*, 69–80.

Persson, K.S. & Sjöström, H., 2002: Fold and shear accommodated convergence in eastern Bergslagen, central Sweden. *In* K.S. Persson: *Deformation zones in models and nature*. Ph.D. thesis, University of Uppsala, Uppsala, Sweden, 23 pp.

Persson K.S. & Sjöström, H., 2003: Late-orogenic progressive shearing in eastern Bergslagen, central Sweden. *GFF 125*, 23–36.

Persson, L., 1993: U-Pb (zircon) age of the Sala "granite" of south central Sweden. *In* T. Lundqvist (ed.): Radiometric dating results. *Sveriges geologiska undersökning C 823*, 32–35.

Persson, L., 1997: Beskrivning till berggrundskartorna Avesta SO och NO. *Sveriges geologiska undersökning Af 189, 197*, 69 pp.

Persson, L. & Persson, P.-O., 1997: U-Pb datings of the Hedesunda and Åkersberga granites of south-central Sweden. *GFF 119*, 91–95.

Persson, L. & Persson, P.-O., 1999: U-Pb (zircon) age of the Vätö granite, south central Sweden. *In* S. Bergman (ed.): Radiometric dating results 4. *Sveriges geologiska undersökning C 831*, 91–99.

Persson, L. & Stålhös, G., 1991: Beskrivning till provisoriska, översiktliga berggrundskartan Uppsala. *Sveriges geologiska undersökning Ba 47*, 30 pp.

Persson, L., Bruun. Å & Dahlman, B., 1981: Beskrivning till berggrundskartan Linköping SV. *Sveriges geologiska undersökning Af 132*, 150 pp.

Persson, L., Bruun, Å. & Vidal, G., 1985: Beskrivning till berggrundskartan Hjo SO. *Sveriges geologiska undersökning Af 134*, 143 pp.

Persson, L., Persson, P.-O. & Sträng, M., 2002: A new occurrence of orbicular granite in Stockholm, Sweden. *In* S. Bergman (ed.): Radiometric dating results 5. *Sveriges geologiska undersökning C 834*, 50–57.

Persson, P.-O. & Ripa, M., 1993: U-Pb (zircon) dating of a Järna-type granite in western Bergslagen, south-central Sweden. *In* T. Lundqvist (ed.): Radiometric dating results. *Sveriges geologiska undersökning C 823*, 41–45.

Persson, P.-O. & Wikström, A., 1993: A U-Pb dating of the Askersund granite and its marginal augen gneiss. *Geologiska Föreningens i Stockholm Förhandlingar 115*, 321–329.

Petersson, J., Berglund, J., Danielsson, P. & Skogsmo, G., 2005: Forsmark site investigation. Petrographic and geochemical characteristics of bedrock samples from boreholes KFM04A-06A, and a whitened alteration rock. *Svensk Kärnbränslehantering AB P-05-156*, 54 pp.

Petersson, J., Andersson, U.B. & Berglund, J., 2007: Scan line fracture mapping and magnetic susceptibility measurements across two low magnetic lineaments with NNE and NE trend, Forsmark. *In* M.B.Stephens & K. Skagius (eds.): Geology – background complementary studies. Forsmark modelling stage 2.2. *Svensk Kärnbränslehantering AB R-07-56*, 5–15.

Platt, J.P. & Wissers, R.L.M., 1980: Extensional structures in anisotropic rocks. *Journal of Structural Geology 2*, 397–410.

Plimer, I.R., 1980: Exhalative Sn and W deposits associated with mafic volcanism as a precursor to Sn and W deposits associated with granites. *Mineralium Deposita 15*, 275–289.

Pulvertaft, T.C.R., 1985: Paleocurrent directions in the lower Dala sandstone, west central Sweden. *Geologiska Föreningens i Stockholm Förhandlingar 107*, 59–62.

Qvarfort, U., 1981: Sulfidmalmshanteringens början vid Garpenberg och Öster Silvberg. *Järnkontorets forskning serie H 20*, 22 pp.

Ramberg 1981: *Gravity, Deformation and the Earth's Crust. 2nd edition*. Academic Press, London and New York.

Ramsay J.G. & Huber, M.I., 1988: *The techniques of modern structural geology. Volume 2: Folds and fractures*. Academic Press Limited, London, 700 pp.

Rankama, K. & Welin, E., 1972: Subcommision on Precambrian stratigraphy. Joint meeting of the Precambrian stratigraphy groups of Denmark, Finland, Norway and Sweden in Turku, Finland, March 1972. *International Union of Geological Sciences Geological Newsletter 1972-4*, 265–267.

Reche J. & Martinez, F.J., 1996: GPT: an Excel spreadsheet for thermobarometric calculations in metapelitic rocks. *Computers & geosciences 22*, 775–784.

Ripa, M., l988: Geochemistry of wall-rock alteration and of mixed volcanic-exhalative facies at the Proterozoic Stollberg Fe-Pb-Zn-Mn(-Ag)-deposit, Bergslagen, Sweden. *Geologie en Mijnbouw 67*, 443–457.

Ripa, M., 1994: The mineral chemistry of hydrothermally altered and metamorphosed wall-rocks at the Stollberg Fe-Pb-Zn-Mn(-Ag) deposit, Bergslagen, Sweden. *Mineralium Deposita 29*, 180–188.

Ripa, M., 1996: *The Stollberg ore field – petrography, lithogeochemistry, mineral chemistry, and ore formation*. Ph.D. thesis (summary), University of Lund, Lund, Sweden, 23 pp.

Ripa, M., 1998: Beskrivning till berggrundskartan Säfsnäs SO. *Sveriges geologiska undersökning Af 190*, 77 pp.

Ripa, M., 2001: A review of the iron oxide deposits of Bergslagen, Sweden and their connection to Au mineralization. *In* P. Weihed (ed.): Economic geology research Vol. 1, 1999–2000. *Sveriges geologiska undersökning C 833*, 132–136.

Ripa, M. & Persson, P.-O., 1997: The U-Pb age of the Sala-Vänge granite at Sala, south central Sweden. *In* T. Lundqvist (ed.), Radiometric dating results 3. *Sveriges geologiska undersökning C 830*, 57–62.

Ripa, M. & Kübler, L., 2005: Bedrock map 12F Ludvika NV, scale 1:50 000. *Sveriges geologiska undersökning K 30*.

Ripa, M. & Persson, L., 2007: Bedrock map 11H Enköping NO, scale 1:50 000. *Sveriges geologiska undersökning K 85*.

Ripa, M., Kübler, L., Persson, L. & Göransson, M., 2002: Beskrivning till berggrundskartan och bergkvalitetskartan 11G Västerås NO. *Sveriges geologiska undersökning Af 217*, 70 pp.

Ripa, M., Bastani, M., Delin, H. & Persson, L., 2006: Projekt Östra Mälardalen. *In* H. Delin (ed.): Berggrundsgeologisk undersökning. Sammanfattning av pågående verksamhet 2005. *Sveriges geologiska undersökning Rapporter och meddelanden 123*, 68–94.

Romer, R.L., 1997: U-Pb age of rare-element pegmatites at Stora Viker, SE Sweden. *GFF 119*, 291–294.

Romer, R.L. & Öhlander, B., 1994: U-Pb age of the Yxsjöberg tungsten skarn deposit, Sweden. *GFF 116*, 161–166.

Romer, R.L. & Smeds, S.-A., 1994: Implications of U-Pb ages of columbite-tantalites from granitic pegmatites for the Palaeoproterozoic accretion of 1.90–1.85 Ga magmatic arcs to the Baltic Shield. *Precambrian Research 67*, 141–158.

Romer, R.L. & Öhlander, B., 1995: Tectonic implications of an 1846±1 Ma old migmatitic granite in south-central Sweden. *GFF 117*, 69–74.

Romer, R.L. & Smeds, S.-A., 1997: U-Pb columbite chronology of post-kinematic Palaeoproterozoic pegmatites in Sweden. *Precambrian Research 82*, 85–99.

Rutanen, H. & Andersson, U.B., 2009: Mafic plutonic rocks in a continental-arc setting: geochemistry of 1.87–1.78 Ga rocks from south-central Sweden and models of their palaeotectonic setting. *Geological Journal 44*, 241–279.

Sandström, F. & Holtstam, D., 1999: Geology of the Långban deposit. *In* D. Holtstam & E. Jonsson (eds.): *Långban*. The mines, their minerals, geology and explorers. Raster förlag och Naturhistoriska riksmuseet, 29–41.

Sandström, B. & Tullborg, E.-L., 2007: Paleohydrogeological events in Forsmark, central Sweden, recorded by stable isotopes in calcite and pyrite. *In* T.D. Bullen & Y. Wang (eds.): *Water-rock interaction: Proceedings of the 12th International Symposium on Water-Rock Interaction WRI-12*. Taylor and Francis, London, 773–776.

Sandström, B., Page, L. & Tullborg, E.-L., 2006a: Forsmark site investigation. $^{40}Ar/^{39}Ar$ (adularia) and Rb-Sr (adularia, prehnite, calcite) ages of fracture minerals. *Svensk Kärnbränslehantering AB P-06-213*, 31 pp.

Sandström, B., Tullborg, E.-L., de Torres, T. & Ortiz, J.E., 2006b: The occurrence and possible origin of asphaltite in bedrock fractures, Forsmark, central Sweden. *GFF 128*, 233–242.

Sandström, B., Tullborg, E.-L., Smellie, J., MacKenzie, A.B. & Suksi, J., 2008a: Fracture mineralogy of the Forsmark site. SDM-Site Forsmark. *Svensk Kärnbränslehantering AB R-08-102*, 113 pp.

Sandström, B., Page, L. & Tullborg, E.-L. 2008b: Forsmark site investigation. Fracture mineralogy and $^{40}Ar/^{39}Ar$ ages of adularia in fracture filling and K-feldspar in breccia. Data from drill cores KFM01C, KFM01D, KFM02B, KFM04A, KFM06A, KFM06B, KFM07A, KFM08A, KFM08B, KFM08C, KFM08D, KFM09A, KFM09B, KFM10A and KFM11A. *Svensk Kärnbränslehantering AB P-08-14*, 95 pp.

Schermerhorn, L.J.G., 1978: Epigenetic magnesium metasomatism or syngenetic chlorite metamorphism at Falun and Orijärvi. *Institution of Mining and Metallurgy Transactions Section B 87*, B162–B167.

SGU, 1999: Mineralmarknaden. Tema: Silver. *Sveriges geologiska undersökning Periodiska publikationer 1999:4*, 72 pp.

Sjögren, H., 1891: Om de svenska jernmalmslagrens genesis. *Geologiska Föreningens i Stockholm Förhandlingar 13*, 373–435.

Sjöström, H. & Bergman, S., 1998: Svecofennian metamorphic and tectonic evolution of east central Sweden. *Sveriges geologiska undersökning unpublished report 03-854/93:59*, 47 pp.

SKB, 2005: Preliminary site description Forsmark area – version 1.2. *Svensk Kärnbränslehantering AB R-05-18*, 752 pp.

SKB, 2008: Site description of Forsmark at completion of the site investigation phase. SDM-Site Forsmark. *Svensk Kärnbränslehantering AB TR-08-05*, 545 pp.

Smeds, S.-A., 1990: Regional mineral assemblage relationships in Swedish Proterozoic granitic pegmatites and their geological significance. *Geologiska Föreningens i Stockholm Förhandlingar 112*, 227–242.

Smeds, S.-A., 1994: Zoning and fractionation trends of a peraluminous NYF granitic pegmatite field at Falun, south-central Sweden. *GFF 116*, 175–184.

Smeds, S.-A. & Cerny, P., 1989: Pollucite from the Proterozoic petalite-bearing pegmatites of Utö, Stockholm archipelago, Sweden. *Geologiska Föreningens i Stockholm Förhandlingar 111*, 361–372.

Söderlund, P., Juez-Larré, J., Page, L.M., Stuart, F.M. & Andriessen, P.M., 2008: Assessment of discrepant (U-Th)/He and apatite fission-track ages in slowly cooled Precambrian terrains: a case study from SE Sweden. *In* P. Söderlund: ^{40}Ar-^{39}Ar, AFT and (U-Th)/He thermochronologic implications for the low-temperature geological evolution in SE Sweden. *Ph.D. thesis, University of Lund, Lund, Sweden*, 20 pp.

Söderlund, P., Hermansson, T., Page, L.M. & Stephens, M.B., in press: Biotite and muscovite ^{40}Ar-^{39}Ar geochronological constraints on the post-Svecofennian tectonothermal evolution, Forsmark site, central Sweden. *International Journal of Earth Sciences (doi: 10.1007/s00531-008-0346-8),* 17 pp.

Söderlund, U., Jarl, L.-G., Persson, P.-O., Stephens, M.B. & Wahlgren, C.-H., 1999: Protolith ages and timing of deformation in the eastern, marginal part of the Sveconorwegian orogen, southwestern Sweden. *Precambrian Research 94*, 29–48.

Söderlund, U., Isachsen, C., Bylund, G., Heaman, L., Patchett, P.J., Vervoort. J.D. & Andersson, U.B., 2005: U-Pb baddeleyite ages and Hf, Nd isotope chemistry constraining repeated mafic magmatism in the Fennoscandian Shield from 1.6 to 0.9 Ga. *Contributions to Mineralogy and Petrology 150*, 174–194.

Stacey, J.S. & Kramers, J.D., 1975: Approximation of terrestrial lead isotope evolution by a two-stage model. *Earth and Planetary Science Letters 26*, 207–211.

Stålhös, G., 1969: Beskrivning till Stockholmstraktens berggrund. *Sveriges geologiska undersökning Ba 24*, 190 pp.

Stålhös, G., 1972: Beskrivning till berggrundskartbladen Uppsala SV och SO. *Sveriges geologiska undersökning Af 105, 106*, 165 pp.

Stålhös, G., 1974: Beskrivning till berggrundskartbladet Enköping SO. *Sveriges geologiska undersökning Af 110*, 70 pp.

Stålhös, G., 1975: Beskrivning till berggrundskartbladet Nyköping NO. *Sveriges geologiska undersökning Af 115*, 99 pp.

Stålhös, G., 1976: Beskrivning till berggrundskartbladet Enköping SV. *Sveriges geologiska undersökning Af 118*, 45 pp.

Stålhös, G., 1979: Beskrivning till berggrundskartan Nynäshamn NV/SV. *Sveriges geologiska undersökning Af 125*, 106 pp.

Stålhös, G., 1981: A tectonic model for the Svecokarelian folding in east central Sweden. *Geologiska Föreningens i Stockholm Förhandlingar 103*, 33–46.

Stålhös, G., 1982a: Beskrivning till berggrundskartan Nynäshamn NO/SO. Utö med omgivande skärgård. *Sveriges geologiska undersökning Af 138*, 124 pp.

Stålhös, G., 1982b: Beskrivning till berggrundskartan Strängnäs SO. *Sveriges geologiska undersökning Af 142*, 78 pp.

Stålhös, G., 1984: Beskrivning till berggrundskartorna Strängnäs NV och NO. *Sveriges geologiska undersökning Af 144*, 145, 96 pp.

Stålhös, G., 1991: Beskrivning till berggrundskartorna Östhammar NV, NO, SV, SO med sammanfattande översikt av basiska gångar, metamorfos och tektonik i östra Mellansverige. *Sveriges geologiska undersökning Af 161, 166, 169, 172*, 249 pp.

Stålhös, G. & Björk, L., 1983: Interpretation of late Svecokarelian metadiabases associated with eruptive

breccias in south central Sweden. *Geologiska Föreningens i Stockholm Förhandlingar 105*, 321–333.

Steiger, R.H. & Jäger, E., 1977: Convention on the use of decay constants in geo- and cosmochronology. *Earth and Planetary Science Letters 36*, 359–362.

Stephanson, O., 1975: Polydiapirism of granitic rocks in the Svecofennian of central Sweden. *Precambrian Research 2*, 189–214.

Stephens, M.B. & Wahlgren, C.-H., 1996: Post-1.85 Ga tectonic evolution of the Svecokarelian orogen with special reference to central and SE Sweden. *GFF 118*, A26–A27.

Stephens, M.B. & Wahlgren, C.-H., 2008: Bedrock evolution. *In* B. Söderbäck (ed.): Geological evolution, palaeoclimate and historical development of the Forsmark and Laxemar-Simpevarp areas. *Svensk Kärnbränslehantering AB R-08-19*, 25–88.

Stephens, M.B., Wahlgren, C.-H. & Annertz, K., 1993: U-Pb (zircon) dates in two younger suites of Palaeoproterozoic intrusions, Karlskoga area, south-central Sweden. *In* T. Lundqvist (ed.): Radiometric dating results. *Sveriges geologiska undersökning C 823*, 46–54.

Stephens, M.B., Wahlgren, C.-H., Weijermars, R. & Cruden, A.R., 1996: Left-lateral transpressive deformation and its tectonic implications, Sveconorwegian orogen, Baltic Shield, southwestern Sweden. *Precambrian Research 79*, 261–279.

Stephens, M.B., Wahlgren, C.-H. & Weihed, P., 1997: Sweden. *In* E.M. Moores & R.W. Fairbridge (eds.): Encyclopedia of European and Asian Regional Geology. *Encyclopedia of Earth Sciences Series, Chapman & Hall*, 690–704.

Stephens, M.B., Bergman, T., Korja, A., Lundqvist, S., Lundström, I., Mannström, B., Ripa, M. & Wahlgren, C.-H., 1998: Syntes av berggrundsgeologisk och geofysisk information, Bergslagen och omgivande områden. *In* C.-H. Wahlgren (ed.): Regional berggrundsgeologisk undersökning. Sammanfattning av pågående undersökningar 1997. *Sveriges geologiska undersökning Rapporter och meddelanden 97*, 83–87.

Stephens, M.B., Ahl, M., Alm, E., Bergman, T., Finn, K., Lundqvist, S., Lundström, I., Persson, L., Ripa, M., Sjögren, P., Stejskal, V., Thelander, T., Wahlgren, C.-H. & Wikström T., 1999: Syntes av berggrundsgeologisk och geofysisk information, Bergslagen och omgivande områden. *In* C.-H. Wahlgren (ed.): Regional berggrundsgeologisk undersökning. Sammanfattning av pågående undersökningar 1998. *Sveriges geologiska undersökning Rapporter och meddelanden 98*, 105–122.

Stephens, M.B., Ahl, M., Bergman, T., Lundström, I., Persson, L., Ripa, M. & Wahlgren, C.-H., 2000: Syntes av berggrundsgeologisk och geofysisk information, Bergslagen och omgivande områden. *In* H. Delin (ed.): Regional berggrundsgeologisk undersökning. Sammanfattning av pågående undersökningar 1999. *Sveriges geologiska undersökning Rapporter och meddelanden 102*, 78–97.

Stephens, M.B., Ahl, M., Bergman, T., Lundström, I., Persson, L., Ripa, M. & Wahlgren, C.-H., 2001: Syntes av berggrundsgeologisk och geofysisk information, Bergslagen och omgivande områden. *In* H. Delin (ed.): Regional berggrundsgeologisk undersökning. Sammanfattning av pågående undersökningar 2000. *Sveriges geologiska undersökning Rapporter och meddelanden 105*, 63–74.

Stephens, M.B., Ahl, M., Bergman, T., Lundström, I., Persson, L., Ripa, M. & Wahlgren, C.-H., 2002a: Regional geological and geophysical maps of Bergslagen: Magnetic anomaly map. *Sveriges geologiska undersökning Ba 58:4*.

Stephens, M.B., Ahl, M., Bergman, T., Lundström, I., Persson, L., Ripa, M. & Wahlgren, C.-H., 2002b: Regional geological and geophysical maps of Bergslagen: Topographic relief map Bouguer anomaly map, electromagnetic map (VLF), and potassium-uranium-thorium composite map. *Sveriges geologiska undersökning Ba 58:5*.

Stephens, M.B., Lundqvist, S., Ekström, M., Bergman, T. & Andersson, J., 2003: Forsmark site investigation. Bedrock mapping. Rock types, their petrographic and geochemical characteristics, and a structural analysis of the bedrock based on stage 1 (2002) surface data. *Svensk Kärnbränslehantering AB P-03-75*, 133 pp.

Stephens, M.B., Lundqvist, S., Bergman, T. & Ekström, M., 2005: Forsmark site investigation. Bedrock mapping. Petrographic and geochemical characteristics of rock types based on Stage 1 (2002) and Stage 2 (2003) surface data. *Svensk Kärnbränslehantering AB P-04-87*, 151 pp.

Stephens, M.B., Ahl, M., Bergman, T., Lundström, I., Persson, L., Ripa, M. & Wahlgren, C.-H., 2007a: Regional geological and geophysical maps of Bergslagen: Bedrock map. *Sveriges geologiska undersökning Ba 58:1*.

Stephens, M.B., Ahl, M., Bergman, T., Lundström, I., Persson, L., Ripa, M. & Wahlgren, C.-H., 2007b: Regional geological and geophysical maps of Bergslagen: Metamorphic, structural and isotope age map. *Sveriges geologiska undersökning Ba 58:2*.

Stephens, M.B., Ahl, M., Bergman, T., Lundström, I., Persson, L., Ripa, M. & Wahlgren, C.-H., 2007c: Regional geological and geophysical maps of Bergslagen: Mineral resources map. *Sveriges geologiska undersökning Ba 58:3*.

Stephens, M.B., Fox, A., La Pointe, P., Simeonov, A., Isaksson, H., Hermanson, J. & Öhman, J., 2007d: Geology Forsmark. Site descriptive modelling Forsmark stage 2.2. *Svensk Kärnbränslehantering AB R-07-45*, 224 pp.

Stephens, M.B., Bergman, T., Isaksson, H. & Petersson, J., 2008a: Bedrock geology Forsmark. Modelling stage 2.3. Description of the bedrock geological map at the ground surface. *Svensk Kärnbränslehantering AB R-08-128*, 63 pp.

Stephens, M.B., Simeonov, A. & Isaksson, H., 2008b: Bedrock geology Forsmark. Modelling stage 2.3. Implications for and verification of deterministic geological models based on complementary data. *Svensk Kärnbränslehantering AB R-08-64*, 125 pp.

Strömberg, A.G.B., 1996: Bedrock map 12F Ludvika NO, scale 1:50 000. *Sveriges geologiska undersökning Af 174*.

Strömberg, A.G.B. & Nisca, D., 1983: Beskrivning till berggrundskartan Ludvika SO. *Sveriges geologiska undersökning Af 128*, 99 pp.

Sund, R.B., 1957: Nyare undersökningar inom nordöstra Upplands bergrund. *Sveriges geologiska undersökning C 552*, 32 pp.

Sundblad, K., 1994: A genetic reinterpretation of the Falun and Åmmeberg ore types, Bergslagen, Sweden. *Mineralium Deposita 29*, 170–179.

Sundblad, K. & Bergman, T., 1997: "Late Svecofennian" granitoids. *In* M. Ahl, U.B. Andersson, T. Lundqvist & K. Sundblad (eds.): Rapakivi granites and related rocks in central Sweden. *Sveriges geologiska undersökning Ca 87*, 7–15.

Sundblad, K., Ahl, M. & Schöberg, H., 1993: Age and geochemistry of granites associated with Mo-mineralizations in western Bergslagen, Sweden. *Precambrian Research 64*, 319–335.

Sundblad, K., Stein, H., Markey, R.J., Morgan, J.W. & Bergman, T., 1996: Re-Os age and geochemistry of highly evolved granites associated with Mo and W ore deposits in Bergslagen, Sweden. *7th International Symposium on Rapakivi Granites and Related Rocks, abstract volume*, 73–74.

Sundius, N., 1923: Grythyttefältets geologi. *Sveriges geologiska undersökning C 312*, 354 pp.

Sundius, N., 1939: Berggrunden inom sydöstra delen av Stockholms skärgård. *Sveriges geologiska undersökning C 419*, 93 pp.

Sundius, N., 1948: Beskrivning till berggrundskarta över Stockholmstrakten. *Sveriges geologiska undersökning Ba 13*, 98 pp.

Sundius, N., 1952: Kvarts, fältspat och glimmer samt förekomster därav i Sverige. *Sveriges geologiska undersökning C 520*, 231 pp.

Talbot, C.J., 2008: Palaeoproterozoic crustal building in NE Utö, southern Svecofennides, Sweden. *GFF 130*, 49–70.

Talbot, C.J. & Sokoutis, D., 1995: Strain ellipsoids from incompetent dykes: application to volume loss during mylonitization in the Singö gneiss zone, central sweden. *Journal of Structural Geology 17*, 927–948.

Tegengren, F.R. et al., 1924: Sveriges ädlare malmer och bergverk. *Sveriges geologiska undersökning Ca 17*, 406 pp.

Törnebohm, A.E., 1875: Geognostisk beskrifning öfver Persbergets grufvefält. *Sveriges geologiska undersökning C 14*, 21 pp.

Törnebohm, A.E., 1893: Om Falu grufvas geologi. *Geologiska Föreningens i Stockholm Förhandlingar 15*, 609–690.

Trägårdh, J., 1988: Cordierite-mica-quartz schists in a Proterozoic volcanic iron ore-bearing terrain, Riddarhyttan area, Bergslagen, Sweden. *Geologie en Mijnbouw 67*, 397–409.

Trägårdh, J., 1990: Tourmaline-bearing chlorite- and cordierite-rich mica schists in the Bergslagen region, south central Sweden – an example of progressive metamorphism of magnesium-enriched felsic volcanic rocks. *Geologiska Föreningens i Stockholm Förhandlingar 112*, 199–202.

Trägårdh, J., 1991: Metamorphism of magnesium-altered felsic volcanic rocks from Bergslagen, central Sweden. A transition from Mg-chlorite to cordierite-rich rocks. *Ore Geology Reviews 6*, 485–497.

Turner, S., Arnaud, N., Liu, J., Rogers, N., Hawkesworth, C., Harris, N., Kelly, S., van Carlsteren, P. & Deng, W., 1996: Post-collision, shoshonitic volcanism on the Tibetan plateau: implications for convective thinning of the lithosphere and source of ocean island basalts. *Journal of Petrology 47*, 45–71.

Valbracht, P.J., 1991: *The origin of the continental crust of the Baltic shield, as seen through Nd and Sr isotopic variations in 1.89–1.85 Ga old rocks from the western Bergslagen, Sweden*. Ph.D. thesis, University of Amsterdam, Amsterdam, Holland (GUA Papers of Geology Series 1, No. 29), 222 pp.

Valbracht, P.J., Oen, I.S. & Beunk, F.F., 1994: Sm-Nd isotope systematics of 1.9–1.8 Ga granites from western Bergslagen, Sweden: inferences on a 2.1–2.0 Ga crustal precursor. *Chemical Geology 112*, 21–37.

van der Velden, W., Baker, J., de Maesschalck, S. & van Meerten, T., 1982: Bimodal early Proterozoic volcanism in the Grythytte field and associated volcano-plutonic complexes, Bergslagen, Central Sweden. *Geologische Rundschau 71*, 171–181.

Verschure, R.H., Oen, I.S. & Andriessen, P.A.M., 1987: Isotopic age-determinations in Bergslagen,

Sweden: VIII. Sveconorwegian Rb-Sr resetting and anomalous radiogenic argon in the Gothian Trans-Scandinavian Småland-Värmland Granitic Belt and bordering parts of the Svecokarelian Bergslagen region. *Geologie en Mijnbouw 66*, 111–120.

Vivallo, W., 1985: The geology and genesis of the Proterozoic massive sulfide deposit at Garpenberg, central Sweden. *Economic Geology 80*, 17–32.

Vivallo, W. & Rickard, D., 1990: Genesis of an early Proterozoic zinc deposit in high-grade metamorphic terrane, Saxberget, central Sweden. *Economic Geology 85*, 714–736.

Wahlgren, C.-H., Cruden, A.R. & Stephens M.B., 1994: Kinematics of a fan-like structure in the eastern part of the Sveconorwegian orogen, Baltic Shield, south-central Sweden. *Precambrian Research 70*, 67–91.

Wahlgren, C.-H., Heaman, L.M., Kamo, S. & Ingvald, E., 1996: U-Pb baddeleyite dating of dolerite dykes in the eastern part of the Sveconorwegian orogen, south-central Sweden. *Precambrian Research 79*, 227–237.

Wahlgren, C.-H., Bergman, T., Karis, L. & Persson, L., 2005: Bedrock map 9D Mariestad NO & 9E Askersund NV, scale 1:50 000. *Sveriges geologiska undersökning K 40*.

Welin, E., 1961: Uranium mineralization in a skarn iron ore at Håkantorp, county of Örebro, Sweden. *Geologiska Föreningens i Stockholm Förhandlingar 83*, 129–143.

Welin, E., 1964: Uranium disseminations and vein fillings in iron ores of northern Uppland, Central Sweden. *Geologiska Föreningens i Stockholm Förhandlingar 86*, 51–82.

Welin, E., 1987: The depositional evolution of the Svecofennian supracrustal sequence in Finland and Sweden. *Precambrian Research 35*, 95–113.

Welin, E. & Stålhös, G., 1986: Maximum age of the synmetamorphic Svecokarelian fold phases in south central Sweden. *Geologiska Föreningens i Stockholm Förhandlingar 108*, 31–34.

Welin, E., Kähr, A.-M. & Lundegårdh, P.H., 1980: Rb-Sr isotope systematics at amphibolite facies conditions, Uppsala region, eastern Sweden. *Precambrian Research 13*, 87–101.

Werner, S., Aaro, S. & Lagmanson, M., 1977: Gravimeterundersökningar inom Bergslagsgeotraversen. *Styrelsen för Teknisk Utveckling 75-5084*, 61 pp.

Westergård, A.H., 1922: Sveriges Olenidskiffer. *Sveriges geologiska undersökning C 18*, 205 pp.

White, S.H., Burrows, S.E., Carreras, J, Shaw, N.D. & Humphreys, F.J., 1980: On mylonites in ductile shear zones. *Journal of Structural Geology 2*, 175–187.

Wickman, F.E., 1988: Possible impact structures in Sweden. *In* A. Boden & K.G. Eriksson (eds.): *Deep drilling in crystalline bedrock. Volume I: The deep gas drilling in the Siljan impact structure, Sweden and astroblemes*. Springer-Verlag, Berlin, 298–327.

Wickman, F.E., Åberg, G. & Levi, B., 1983: Rb-Sr dating of alteration events in granitoids. *Contributions to Mineralogy and Petrology 83*, 358–362.

Wik, N.-G., Sundberg, A. & Wikström, A., 1999: Malmer, industriella mineral och bergarter i Södermanlands län. *Sveriges geologiska undersökning Rapporter och meddelanden 100*, 199 pp.

Wik, N.-G., Lundqvist, I., Selinus, O., Sivhed, U., Sundberg, A. & Wikström, A., 2002: Malmer, industriella mineral och bergarter i Västra Götalands län, inklusive kommunerna Habo och Mullsjö. *Sveriges geologiska undersökning Rapporter och meddelanden 108*, 231 pp.

Wik, N.-G., Stephens, M.B. & Sundberg, A., 2004: Malmer, industriella mineral och bergarter i Stockholms län. *Sveriges geologiska undersökning Rapporter och meddelanden 117*, 144 pp.

Wik, N.-G., Stephens, M.B. & Sundberg, A., 2006: Malmer, industriella mineral och bergarter i Uppsala län. *Sveriges geologiska undersökning Rapporter och meddelanden 124*, 210 pp.

Wikman, H., 1972: Rinkaby-Väringenområdet. *In* P.H. Lundegårdh, H. Hübner, H. Wikman, L. Karis & E. Magnusson: Beskrivning till berggrundsgeologiska kartbladet Örebro NV. *Sveriges geologiska undersökning Af 102*, 28–114.

Wikman, H., 1973: *Ett svekofenniskt suprakrustalkomplex i Örebroområdet*. Ph.D. thesis, University of Lund, Sweden, 131 pp.

Wikman, H., Bruun, Å. & Dahlman, B., 1980: Beskrivning till berggrundskartan Linköping NV. *Sveriges geologiska undersökning Af 119*, 105 pp.

Wikman, H., Bruun, Å., Dahlman, B. & Vidal, G., 1982: Beskrivning till berggrundskartan Hjo NO. *Sveriges geologiska undersökning Af 120*, 112 pp.

Wikström, A., 1975: Beskrivning till berggrundskartan Norrköping NO. *Sveriges geologiska undersökning Af 112*, 78 pp.

Wikström, A., 1976: Beskrivning till berggrundskartan Katrineholm SV. *Sveriges geologiska undersökning Af 116*, 88 pp.

Wikström, A., 1979: Beskrivning till berggrundskartan Katrineholm SO. *Sveriges geologiska undersökning Af 123*, 101 pp.

Wikström, A., 1983: Beskrivning till berggrundskartan Katrineholm NV och NO. *Sveriges geologiska undersökning Af 131, 137*, 88 pp.

Wikström, A., 1984: A possible relationship between

augen gneisses and postorogenic granites in S.E. Sweden. *Journal of Structural Geology 6*, 409–415.

Wikström, A., 1987: Magmatic diapirism of granites in south-eastern Sweden. *Abstracts of the International Symposium on Granites and Associated Mineralizations (ISGAM), Salvador, Bahia, Brazil,* ***Revista Brasileira de Geosciencias 17***, 456–458.

Wikström, A., 1991: Structural features of some younger granitoids in central Sweden and implications for the tectonic subdivision of granitoids. *Precambrian Research 51*, 151–159.

Wikström, A., 1992: Some composite dikes in Sweden. *Geologiska Föreningens i Stockholm Förhandlingar 114*, 385–394.

Wikström, A., 1996: U-Pb zircon dating of a coarse porphyritic quartz monzonite and an even grained, grey tonalitic gneiss from the Tiveden area, south central Sweden. *In* T. Lundquist (ed.): Radiometric dating results 2. *Sveriges geologiska undersökning C 828*, 41–47.

Wikström, A. & Aaro, S., 1986: The Finnspång augen gneiss massif. Geology, geophysics and relationship to postorogenic granites. *Sveriges geologiska undersökning C 813*, 39 pp.

Wikström, A. & Karis, L., 1991: Beskrivning till berggrundskartorna Finspång NO, SO, NV, SV. *Sveriges geologiska undersökning Af 162, 163, 164, 165*, 216 pp.

Wikström, A. & Karis, L., 1993: Note on the basement-cover relationships of the Visingsö group in the northern part of the Lake Vättern basin, south Sweden. *Geologiska Föreningens i Stockholm Förhandlingar 115*, 311–313.

Wikström, A. & Larsson, L., 1993: Geothermometry of garnet-cordierite rocks in Kilsbergen and northern Tiveden, southern Sweden. *Geologiska Föreningens i Stockholm Förhandlingar 115*, 339–344.

Wikström, A. & Karis, L., 1997: Beskrivning till berggrundskartan Karlskoga SO. *Sveriges geologiska undersökning Af 183*, 112 pp.

Wikström, A. & Karis, L., 1998: Beskrivning till berggrundskartorna Askersund NO och SO. *Sveriges geologiska undersökning Af 186, 195*, 143 pp.

Wikström, A. & Persson, P.-O., 2002: A c. 1845 Ma (”Askersund”) age of the Hälla augen gneiss in south-eastern Östergötland, south-east Sweden. *In* S. Bergman (ed.): Radiometric dating results 5. *Sveriges geologiska undersökning C 834*, 58–61.

Wikström, A. & Andersson, U.B., 2004: Geological features of the Småland-Värmland belt along the Svecofennian margin, part I: from the Loftahammar to the Tiveden-Askersund areas. *In* K. Högdahl, U.B. Andersson & O. Eklund (eds.): The Transscandinavian Igneous Belt (TIB) in Sweden: a review of its character and evolution. *Geological Survey of Finland Special Paper 37*, 22–39.

Wikström, A., Aaro, S. & Lagmansson, M., 1980: The Graverfors and Stavsjö granites. *Sveriges geologiska undersökning C 773*, 48 pp.

Wiman, E., 1930: Studies of some Archean rocks in the neighbourhood of Uppsala, Sweden, and their geological position. *Bulletin of the Geological Institution of the University of Uppsala 23*, 170 pp.

Winchester, J.A. & Floyd, P.A., 1977: Geochemical discrimination of different magma series and their differentiation products using immobile elements. *Chemical Geology 20*, 325–343.

Wolter, H.U. & Seifert, F., l984: Mineralogy and genesis of cordierite-anthophyllite rocks from the sulfide deposit of Falun, Sweden. *Lithos 17*, 147–152.

Zuber, J., 1986: Geological interpretetion of gravity and aeromagnetic surveys over the Fellingsbro-Blixterboda granite. *Geologiska Föreningens i Stockholm Förhandlingar 107*, 203–213.

Zuber, J. & Öhlander, B., 1990: Geophysical and geochemical evidence of Proterozoic collision in the western marginal zone of the Baltic Shield. *Geologische Rundschau 79*, 1–11.

Zuber, J. & Öhlander, B., 1991: Gravimetrical and geochemical studies of 1.8 Ga old granites in the Strängnäs-Enköping area, south central Sweden. *Geologiska Föreningens i Stockholm Förhandlingar 113*, 309–318.

Appendix.
Age determinations using U-Pb analyses of zircon, monazite and titanite

U-Pb age determinations were carried out on eleven samples at ten different sites in the Bergslagen region during 2000 and 2001 in the context of the Bergslagen project. The analyses were completed using the Thermal Ionisation Mass Spectrometry (TIMS) technique on one or more mineral grains at the Laboratory for Isotope Geology, Swedish Museum of Natural History, Stockholm, Sweden. Most of the analyses were carried out on zircon grains, while a few were also carried out on monazite and titanite grains. The ten locations of the analysed samples are shown in Figure 14 in the main text of this report.

The primary focus of the geochronological work was to determine the age of eruption of the felsic metavolcanic rocks, bearing in mind their significance for mineral exploration activities and the limited occurrence of reliable age determinations of these rocks in the region (see review in Lundström et al. 1998). Seven samples of felsic metavolcanic and subvolcanic meta-intrusive rocks from sub-areas 1, 2, 4 and 6 (see the section "Character, spatial distribution, geochronology, geochemical signature, petrophysical characteristics and regional geophysical signature of rock units" in the main text) were analysed. These samples come from the bedrock in the central part of the Bergslagen region that is affected by greenschist- or amphibolite-facies metamorphism without the development of migmatite (central low- and medium-grade metamorphic domains in the section "Deformation, metamorphism and mechanism of emplacement of the 1.87–1.84 Ga GSDG suite of intrusive rocks" in the main text). U-Pb age determinations of four samples from different compositional suites of younger intrusive rocks were also carried out.

The samples are described and the results of the analytical work are presented and interpreted below. All zircon fractions were abraded unless otherwise stated. $^{206}Pb/^{204}Pb$ values were corrected for mass fractionation (0.1% per atomic mass unit) and spike, while ^{206}Pb–^{207}Pb–^{208}Pb values (atom %) were corrected for mass fractionation, spike, blank and common Pb. All analytical uncertainties are provided as 2σ values. Internal textures and structures in the analysed mineral grains were only investigated with the help of optical microscopy. More details on the analytical procedures are described in the section "Acquisition of new data and data interpretation – methodological aspects" in the main text of this report.

The text in this appendix makes use of the format for presentation of radiometric dating results currently employed by the Geological Survey of Sweden and focuses attention on the acquired data and its geological interpretation. The reader is referred to the relevant parts of the sections "Character, spatial distribution, geochronology, geochemical signature, petrophysical characteristics and regional geophysical signature of rock units" and "Deformation, metamorphism and mechanism of emplacement of the 1.87–1.84 Ga GSDG suite of intrusive rocks" in the main text for the broader geological implications of both the geochronological data published outside the Bergslagen project as well as the new data presented in this appendix. Protolith ages are shown on the metamorphic, structural and isotope age map (Stephens et al. 2007b).

FELSIC METAVOLCANIC ROCK, ÄLVLÅNGEN, NORTH-EAST OF KARLSKOGA (SUB-AREA 1)

Rock	Felsic metavolcanic rock, pyroclastic mass flow deposit
Sample number	MBS990102A
Coordinates (RT 90)	6688195/1440645
Map sheet	10E Karlskoga NO
Locality	Älvlången, north-east of Karlskoga
Project	Regional project Bergslagen (code 2412)

The aim of this geochronological study was to determine the age of the waning volcanic stage in sub-area 1 (see Fig. 28 in the main text) of the Svecofennian felsic metavolcanic rocks in the Bergslagen region. The data contribute to a better understanding of the lateral variation in age of the waning stage of volcanic activity in different sub-areas in Bergslagen.

Sample description

Approximately 1 km south-west of the lake Älvlången, north-east of Karlskoga (see Fig. 14 in the main text), a rhyolitic, pyroclastic mass flow deposit was sampled for age determination. The unit is several metres thick and embedded within a sequence of thinly planar-bedded volcanic metasiltstone and marble. The rock contains c. 1% of less than 1 mm size phenoclasts of quartz and K-feldspar and contains visible fiamme. One of the underlying metasiltstone beds contains accretionary lapilli and, for this reason, is inferred to have erupted in a subaerial environment. The dated sample immediately underlies one of the major marble units in the Bergslagen region. On the basis of the geological map of Stephens (1998) and the compilation in Allen et al.

(1996), it is inferred that the sampled unit belongs to the waning volcanic stage in the Svecofennian metavolcanic sequence (see the section "Character, spatial distribution, geochronology, geochemical signature, petrophysical characteristics and regional geophysical signature of rock units" in the main text). The massive, fiamme-bearing structure of the rock indicates that it represents a juvenile volcanic rock. For this reason, a zircon crystallization age should represent the time of emplacement of this metavolcanic rock.

Analytical results and interpretation of geochronological data

Most of the zircon grains are pale brown and small. They are short prismatic (length to width ratio c. 2–3), although more elongate crystals are also present. The zircons are euhedral and have sharp edges and terminations. Generally, only faces with low crystallographic indices are present. Core–rim relations were not detected.

Four zircon fractions were analysed. These were selected primarily on the basis of differences in grain size and general analytical quality related to the frequency of fractures or inclusions in the zircon grains. Fraction 1 is composed of larger crystals than fraction 2, while the zircons in fractions 3 and 4 are of somewhat lower quality.

The analytical results are presented in Table I and a U-Pb concordia diagram is shown in Figure I. Fractions 1 and 4 are markedly discordant and show a somewhat higher uranium content than the more concordant fractions. Nevertheless, the four data points define a discordia line with upper and lower intercept ages at 1896±2 Ma and –1±12 Ma, respectively, and a mean square standard deviation (MSWD) value of 0.35. The upper intercept age is inferred to represent the time of emplacement of this pyroclastic mass flow deposit.

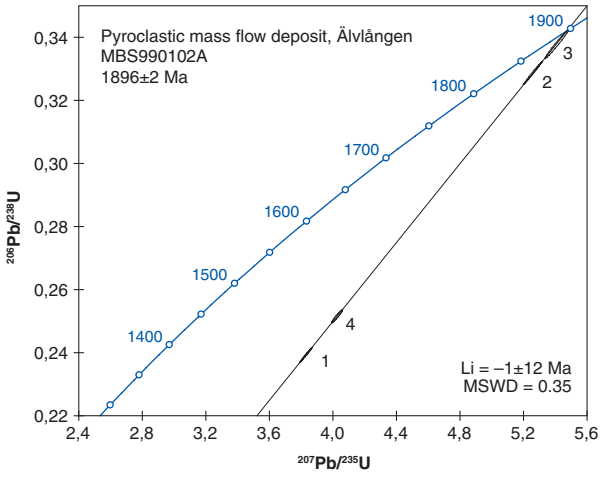

Fig. I. Concordia diagram showing the U-Pb TIMS data for zircons from a pyroclastic mass flow deposit, Älvlången, north-east of Karlskoga (sub-area 1). Li = lower intercept.

FELSIC METAVOLCANIC ROCK, KÄXTJÄRNEN, NORTH-WEST OF HÄLLEFORS (SUB-AREA 1)

Rock	Felsic metavolcanic rock, pyroclastic mass flow deposit
Sample number	OIL000154A
Coordinates (RT 90)	6636190/1428740
Map sheet	11E Filipstad NO
Locality	Käxtjärnen, north-west of Hällefors
Project	Regional project Bergslagen (code 2412)

The aim of this geochronological study was to determine the age of the waning volcanic stage in sub-area 1 (see Fig. 28 in the main text) of the Svecofennian felsic metavolcanic rocks in the Bergslagen region. The data complement the age determination work carried out by Lundström et al. (1998) in the lower part of the metavolcanic unit in the same part of sub-area 1 and, thereby, provide constraints on especially the variation in age of these metavolcanic rocks at different stratigraphic levels.

Sample description

The sample was taken in a small quarry north-west of Käxtjärnen (see Fig. 14 in the main text), which forms a small bay in the lake Norr-Älgen, c. 5 km north of Hällefors. The sample occurs in the part of the Svecofennian metavolcanic sequence that belongs to the waning volcanic stage but the contact to the younger metasedimentary rocks (meta-argillite, volcanogenic metaturbidite) to the west is a fault (Lundström 1995, Allen et al. 1996). The sample is a reddish, very fine-

Table I. U-Pb TIMS isotopic data for zircons from a pyroclastic mass flow deposit, Älvlången, north-east of Karlskoga (sub-area 1).

Fraction	No. of crystals	Weight (µg)	U (ppm)	Pb_{tot} (ppm)	Common Pb (ppm)	$^{206}Pb/^{204}Pb$	^{206}Pb–^{207}Pb–^{208}Pb (atom %)	$^{206}Pb/^{238}U$	$^{207}Pb/^{235}U$	$^{207}Pb/^{206}Pb$ age (Ma)
1	4	5.5	342.7	87.1	0.05	21728	80.4–9.3 –10.3	0.2371±19	3.796±31	1897±2
2	15	8.6	246.4	86.0	0.12	20394	81.0–9.4–9.6	0.3287±30	5.259±49	1896±2
3	12	6.7	297.6	106.6	0.07	29203	81.2–9.4–9.4	0.3379±38	5.410±61	1898±3
4	11	4.9	360.2	96.3	0.06	12268	81.0–9.4–9.6	0.2515±17	4.026±28	1897±4

grained, quartz-phyric, somewhat chlorite-spotted to locally chlorite-brecciated, potassium-rich rhyolite. Colour, phenocryst frequency and form vary substantially on a millimetre scale, giving rise to a fiamme-like structure to the rock. Spherulite-like structures and possible pumice clasts also occur. The rock is inferred to represent a pyroclastic mass flow deposit, although an origin as lava was suggested for a similar rock in the vicinity by Lundström (1995). The juvenile character of the rock suggests that a zircon crystallization age should represent the time of its emplacement.

Analytical results and interpretation of geochronological data

The majority of the zircons are pale brown and a few are nearly colourless. Some grains are clear but most grains are metamict. The zircons are euhedral with sharp edges and terminations. They show a length to width ratio of c. 2–3. Generally, only faces with low crystallographic indices are present. Some grains show internal textural heterogeneities indicative of core–rim relations. These grains were avoided in the analytical work.

Five zircon fractions were analysed. These were selected primarily on the basis of differences in the general analytical quality of the zircon grains related to the frequency of fractures or inclusions. The fractions decrease in quality from fraction 1 (clear crystals without fractures) to fraction 5 (crystals with highest frequency of fractures and inclusions).

The analytical results are presented in Table II and a U-Pb concordia diagram is shown in Figure II. The five data points define a discordia line with upper and lower intercept ages at 1897±6 Ma and 25±120 Ma, respectively, and a MSWD value of 0.5. The upper intercept age is inferred to represent the time of emplacement of this pyroclastic mass flow deposit.

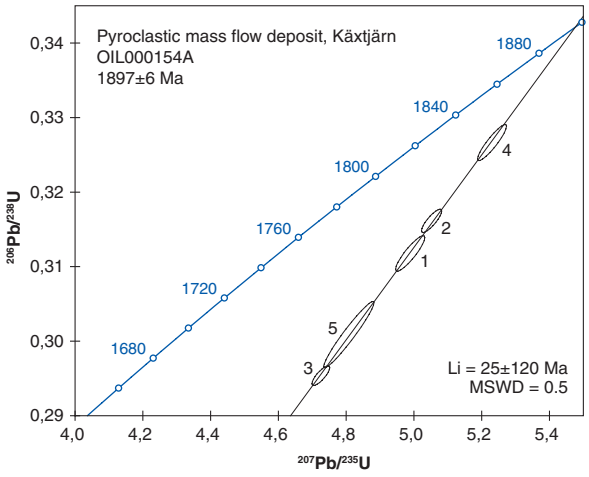

Fig. II. Concordia diagram showing the U-Pb TIMS data for zircons from a pyroclastic mass flow deposit, Käxtjärn, north of Hällefors (sub-area 1). Li = lower intercept.

FELSIC METAVOLCANIC ROCK, GARPENBERG (SUB-AREA 2)

Rock	Felsic metavolcanic rock, pyroclastic mass flow deposit
Sample number	Drill core 162, 51.60–59.50 m, Garpenberg mine
Coordinates (RT 90)	Approximate coordinates 6687600/1521500
Map sheet	12G Avesta NV
Locality	Garpenberg
Project	Regional project Bergslagen (code 2412)

The aim of this geochronological study was to date a younger phase of Svecofennian volcanic activity preserved in the central part of the major syncline at Garpenberg in sub-area 2 (see Fig. 28 in the main text). The data also contribute to a better understanding of the lateral variation in age of the waning stage of volcanic activity in different sub-areas in Bergslagen. They also provide some constraints on the timing of formation of the major base metal sulphide deposit at Garpenberg.

Sample description

With the assistance of personnel from Boliden AB, a sample was taken from drill core 162 at the Garpenberg mine (see Fig. 14 in the main text). The sample comes from the uppermost volcanic unit observed in the central part of the major syncline at Garpenberg (see Fig. 118 in the main text). The sampled rock unit is a c. 450 m thick, juvenile pyroclastic mass flow deposit

Table II. U-Pb TIMS isotopic data for zircons from a pyroclastic mass flow deposit, Käxtjärn, north of Hällefors (sub-area 1).

Fraction	No. of crystals	Weight (µg)	U (ppm)	Pb_{tot} (ppm)	Common Pb (ppm)	$^{206}Pb/^{204}Pb$	^{206}Pb–^{207}Pb–^{208}Pb (atom %)	$^{206}Pb/^{238}U$	$^{207}Pb/^{235}U$	$^{207}Pb/^{206}Pb$ age (Ma)
1	3	4.3	195.4	64.8	0.08	6991	80.9–9.4–9.7	0.3118±19	4.989±35	1896±6
2	5	5.7	210.9	70.9	0.03	11019	81.0–9.4–9.6	0.3161±13	5.052±24	1894±5
3	8	7.5	182.4	57.3	0.25	6303	81.2–9.4–9.4	0.2954±11	4.725±21	1896±5
4	8	6.5	204.6	71.2	0.27	7028	81.0–9.4–9.6	0.3266±20	5.231±35	1898±5
5	4	1.6	264.1	84.2	0.05	2620	80.9–9.4–9.7	0.2996±28	4.786±47	1893±6

with numerous pumice clasts. Lithic clasts occur in the lowest part of this unit, but not in the actual sample chosen for analysis. The sampled rock unit lies stratigraphically above marble and planar-bedded volcanic metasiltstone that host the base metal sulphide deposit at Garpenberg (see Figs. 28 and 118 in the main text). The sampled unit either belongs to the waning volcanic stage in the Bergslagen region or represents a new phase of intense volcanic activity (IS2? in the volcanostratigraphic profile for Garpenberg in Fig. 28 in the main text).

Analytical results and interpretation of geochronological data

The sample contains a rather heterogeneous zircon population. Most zircons are colourless, but metamict zircons are greyish. The length to width ratios vary between c. 1.5 and 4 but considerably longer crystals are also present. Most of the zircons are small, euhedral and contain faces with low-order crystallographic indices.

Five zircon fractions were analysed. These were selected on the basis of differences in grain size (smaller crystals in fractions 4 and 5, larger crystals in fractions 1, 2 and especially 3), and general analytical quality related to the frequency of fractures or inclusions in the zircon grains (no fractures or inclusions in fractions 1 and 3, occurrence of some fractures and inclusions in fractions 2, 4 and especially the complementary zircon fraction 5).

The analytical results are presented in Table III and a U-Pb concordia diagram is shown in Figure III. The complementary zircon fraction 5 is distinctly more discordant than the other fractions but is situated along a well-defined discordia line together with fractions 2, 3 and 4. The line defined by these four fractions intersects the concordia at 1891±2 Ma (upper intercept) and –4±33 Ma (lower intercept) and has a MSWD value of 1.3. The zircons in fraction 1 have a $^{207}Pb/^{206}Pb$ age of 1823±7 Ma and plot to the left of this line. Furthermore, the proportion of ^{208}Pb (thorogenic Pb) in fraction 1 is markedly different from that in the other four fractions. However, these zircons could not be distinguished from the other fractions on the basis of their general appearance (see above). It is considered likely that the crystals in fraction 1 belong to a zircon generation which is younger than that represented in fractions 2 to 5. The timing of emplacement of the pyroclastic mass flow deposit is inferred to be represented by the upper intercept age defined by fractions 2 to 5 and is set at 1891±2 Ma.

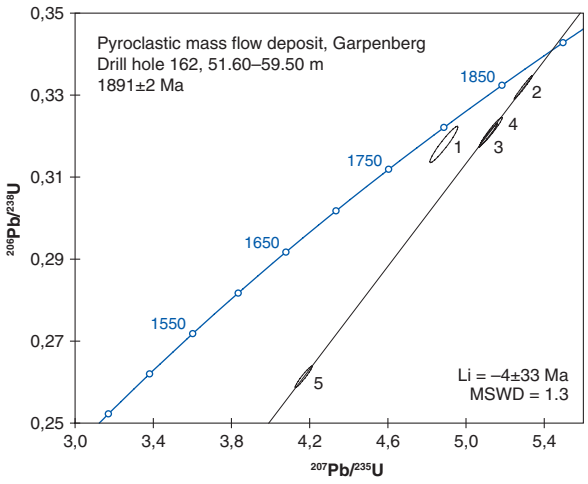

Fig. III. Concordia diagram showing the U-Pb TIMS data for zircons from a pyroclastic mass flow deposit, Garpenberg drill hole 162, 51.60–59.50 m (sub-area 2). Li = lower intercept.

FELSIC METAVOLCANIC ROCK, BRODDBO, NORTH OF SALA (SUB-AREA 4)

Rock	Felsic metavolcanic rock, pyroclastic mass flow deposit or lava
Sample number	OIL991027A
Coordinates (RT 90)	6653405/1542205
Map sheet	12G Avesta SO
Locality	Broddbo, north of Sala
Project	Regional project Bergslagen (code 2412)

The aim of this geochronological study was to determine the age of the Svecofennian felsic metavolcanic rocks close to the stratigraphic base of this rock unit, in an area where the metavolcanic rocks lie stratigraphically on top of quartzite and turbiditic metagreywacke. In this manner, a minimum age for the metasedimen-

Table III. U-Pb TIMS isotopic data for zircons from a pyroclastic mass flow deposit, Garpenberg drill hole 162, 51.60–59.50 m (sub-area 2).

Fraction	No. of crystals	Weight (µg)	U (ppm)	Pb_{tot} (ppm)	Common Pb (ppm)	$^{206}Pb/^{204}Pb$	^{206}Pb–^{207}Pb–^{208}Pb (atom %)	$^{206}Pb/^{238}U$	$^{207}Pb/^{235}U$	$^{207}Pb/^{206}Pb$ age (Ma)
1	2	3.4	167.1	63.7	0.165	3287	72.0–8.0–20.0	0.3180±36	4.886±58	1823±7
2	8	7.6	232.8	81.4	0.067	10556	81.7–9.4–8.9	0.3319±23	5.292±38	1890±2
3	2	8.6	223.7	75.2	0.146	11600	82.1–9.5–8.4	0.3202±24	5.114±39	1893±2
4	5	3.9	263.3	89.4	0.384	5797	81.7–9.5–8.8	0.3212±28	5.128±46	1892±4
5	8	3.8	364.0	101.1	0.029	10861	81.0–9.3–9.7	0.2613±21	4.169±35	1891±4

tary rocks is also defined. The sample is situated in sub-area 4 of the Svecofennian metavolcanic rocks in the Bergslagen region (see Fig. 28 in the main text and stop 2-1 in the excursion guide).

Sample description

A rhyolitic metavolcanic rock was sampled from a horizon situated only c. 10 m stratigraphically above the contact to underlying quartzite in the Broddbo area, north of Sala (see Fig. 14 in the main text). The quartzite lies stratigraphically above turbiditic metagreywacke correlatable with the *Larsbo formation* (see the section "Character, spatial distribution, geochronology, geochemical signature, petrophysical characteristics and regional geophysical signature of rock units" in the main text). The sampled rock is homogeneous and foliated and has a granoblastic texture. Hence, much volcanic textural information has been obliterated. The sample is quartz- and plagioclase-phyric, although the phenocrysts have recrystallized into smaller grains. The frequency of the phenocrysts varies in a lens-like manner suggestive of relict pumice clasts or fiamme. Although the structural and textural information do not permit an unambiguous interpretation of the rock as a pyroclastic mass flow deposit or lava, it is considered to be sufficiently juvenile to permit the inference that a zircon crystallization age represents the time of emplacement of this metavolcanic rock.

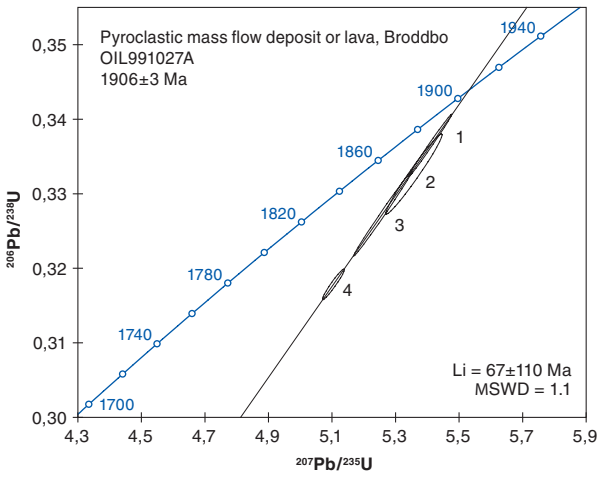

Fig. IV. Concordia diagram showing the U-Pb TIMS data for zircons from a pyroclastic mass flow deposit or lava, Broddbo, north of Sala (sub-area 4). Li = lower intercept.

Analytical results and interpretation of geochronological data

The zircons are colourless or pale yellow. However, many grains are partly red in colour, the red colour generally being localized to patches or fractures. The zircons are euhedral with sharp edges and terminations. The length to width ratio is 3–4. Most crystals have only faces with low-order crystallographic indices. Some rounded grains with abraded terminations, which possibly represent detrital grains, are also present. Zonation and black inclusions are ubiquitous. Many grains contain older cores with a generally rounded outline.

Four zircon fractions were analysed. These were selected on the basis of differences in grain size and the frequency of fractures and inclusions. The zircons in fraction 2 are larger (>74 µm) than the zircons in the other three fractions (<74 µm). Some fractures and inclusions are present in the zircons in fractions 2, 3 and 4.

The analytical results are presented in Table IV and a U-Pb concordia diagram is shown in Figure IV. The zircons are fairly uranium-rich and fractions 1, 3 and 4 show high $^{206}Pb/^{204}Pb$ ratios. The four data points are weakly discordant and define a discordia line which intersects the concordia at 1906±3 Ma (upper intersect) and 67±110 Ma (lower intercept), with a MSWD value of 1.1. The upper intercept age is inferred to represent the time of emplacement of this pyroclastic mass flow deposit or lava.

Table IV. U-Pb TIMS isotopic data for zircons from a pyroclastic mass flow deposit or lava, Broddbo, north of Sala (sub-area 4).

Fraction	No. of crystals	Weight (µg)	U (ppm)	Pb_{tot} (ppm)	Common Pb (ppm)	$^{206}Pb/^{204}Pb$	^{206}Pb–^{207}Pb–^{208}Pb (atom %)	$^{206}Pb/^{238}U$	$^{207}Pb/^{235}U$	$^{207}Pb/^{206}Pb$ age (Ma)
1	15	15.5	435.4	153.7	0.10	38888	82.0–9.6–8.4	0.3365±34	5.409±55	1905±2
2	4	7.8	471.6	164.0	1.94	4182	83.3–9.7–7.0	0.3326±44	5.358±72	1908±5
3	9	7.5	565.8	194.2	0.16	26760	82.1–9.6–8.3	0.3273±46	5.260±75	1904±2
4	7	6.1	379.2	126.6	0.07	19069	82.0–9.5–8.5	0.3179±17	5.104±28	1903±3

FELSIC METAVOLCANIC ROCK, SALA (SUB-AREA 4)

Rock	Felsic metavolcanic rock, pyroclastic ash fall deposit
Sample number	CMR980164A
Coordinates (RT 90)	6642500/1542500
Map sheet	11G Västerås NO
Locality	East of the Finntorpet dolomite quarry, Sala
Project	Regional project Bergslagen (code 2412)

The aim of this geochronological study was to determine the age of the waning volcanic stage in sub-area 4 (see Fig. 28 in the main text) of the Svecofennian felsic metavolcanic rocks in the Bergslagen region. The data contribute to a better understanding of the lateral variation in age of the waning stage of volcanic activity in different sub-areas in Bergslagen.

Sample description

The sample was taken immediately east of the Finntorpet dolomite quarry at Sala (see Fig. 14 in the main text). The rock is an even-grained, rhyolitic metasiltstone, situated stratigraphically immediately beneath an accretionary lapilli-bearing horizon. Although the juvenile character of the dated horizon is not verified with certainty, the associated accretionary lapilli-bearing horizon indicates that active volcanic activity prevailed and the sample is interpreted as belonging to a pyroclastic ash fall deposit. On the basis of these arguments, it is considered likely that a zircon crystallization age dates the eruption and deposition of the rhyolitic metasiltstone.

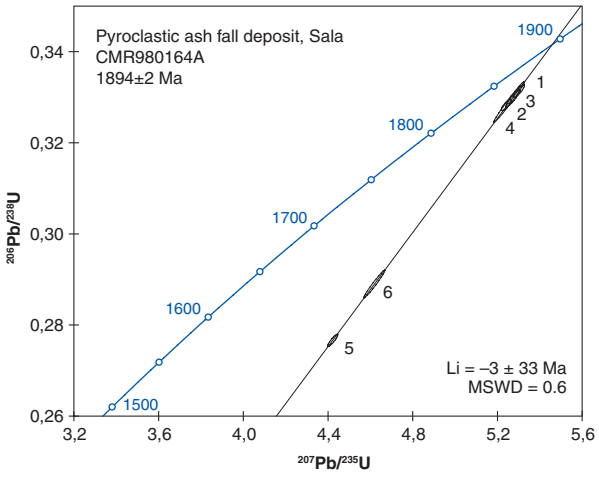

Fig. V. Concordia diagram showing the U-Pb TIMS data for zircons from a pyroclastic ash fall deposit, Sala (sub-area 4). Li = lower intercept.

Analytical results and interpretation of geochronological data

The zircons are colourless to yellowish brown and severely metamict and fractured. They are generally euhedral with sharp edges and pyramids but rounded and anhedral grains are also present. Length to width ratios vary between 1 and 5. Texturally complex, core–rim relations are present in a minority of the zircons. The analysed grains were selected from the colourless and euhedral zircons.

Six zircon fractions were analysed. Fractions 1 to 4 were selected on the basis of differences in the general analytical quality of the zircon grains related to the frequency of fractures or inclusions. The quality of the grains decreases from fraction 1 to fraction 4. The zircons in the complementary fraction 5 are colourless and of good quality, while the zircons in the complementary fraction 6 are colourless and rather metamict.

The analytical results are presented in Table V and a U-Pb concordia diagram is shown in Figure V. The complementary zircon fractions 5 and 6, with variable quality, are distinctly more discordant relative to the other four fractions. However, all six fractions are situated along a well-defined discordia line which intercepts the concordia at 1894±2 Ma (upper intercept) and –3±33 Ma (lower intercept), with a MSWD value of 0.6. The upper intercept age is inferred to represent the igneous crystallization age that coincides with the eruption and depositional age of the pyroclastic ash fall deposit.

Table V. U-Pb TIMS isotopic data for zircons from a pyroclastic ash fall deposit, Sala (sub-area 4).

Fraction	No. of crystals	Weight (µg)	U (ppm)	Pb_{tot} (ppm)	Common Pb (ppm)	$^{206}Pb/^{204}Pb$	^{206}Pb–^{207}Pb–^{208}Pb (atom %)	$^{206}Pb/^{238}U$	$^{207}Pb/^{235}U$	$^{207}Pb/^{206}Pb$ age (Ma)
1	8	8.9	208.5	73.8	0.85	3832	81.4–9.5–9.1	0.3314±11	5.301±22	1896±4
2	5	7.8	226.5	78.0	0.02	11663	82.2–9.5–8.3	0.3290±37	5.255±59	1893±3
3	7	8.4	276.7	97.6	0.40	8535	80.8–9.4–9.8	0.3297±16	5.273±27	1895±4
4	8	15.4	233.9	81.1	0.06	18647	81.5–9.5–9.0	0.3283±10	5.242±19	1892±4
5	6	7.6	212.9	62.8	0.08	10614	80.7–9.4–9.9	0.2766±11	4.422±20	1895±3
6	4	7.6	254.6	77.8	0.04	15422	81.4–9.4–9.2	0.2890±25	4.619±41	1894±3

FELSIC SUBVOLCANIC INTRUSION, SALA (SUB-AREA 4)

Rock	Felsic subvolcanic intrusion
Sample number	CMR940007A
Coordinates (RT 90)	6647940/1544500
Map sheet	11G Västerås NO
Locality	North of Stråbruken, Sala
Project	Regional project Bergslagen (code 2412)

The aim of this geochronological study was to date the igneous crystallization of a porphyritic, felsic subvolcanic intrusion that is surrounded by rocks belonging to the waning volcanic stage at Sala. All these rocks are situated in sub-area 4 (see Fig. 28 in the main text) of the Svecofennian felsic metavolcanic rocks in the Bergslagen region. The data provide constraints on the timing of the later part of the igneous activity that gave rise to the strongly mineralized felsic metavolcanic rocks in the Bergslagen region.

Sample description

North of Stråbruken, close to Sala (see Fig. 14 in the main text), a felsic meta-intrusive rock inferred to be a subvolcanic intrusion was sampled. The rock is isotropic and quartz- or quartz-feldspar-phyric and is included in the so-called *Eklövstorp formation* (Ripa et al. 2002). This body intrudes the metavolcanic rocks that are situated in the upper part of the volcanostratigraphy at Sala and have been included in the waning volcanic stage as defined in Allen et al. (1996).

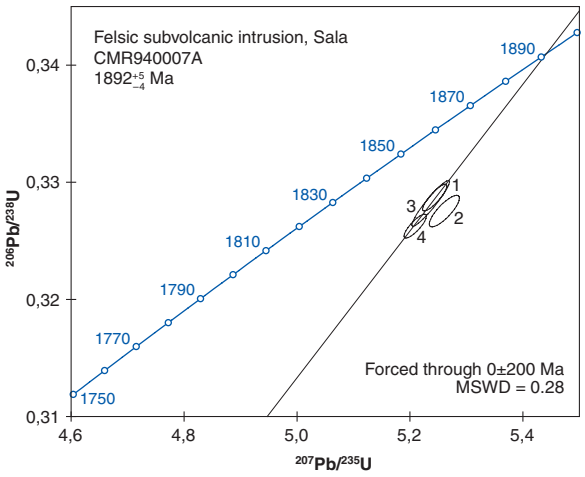

Fig. VI. Concordia diagram showing the U-Pb TIMS data for zircons from a felsic subvolcanic intrusion, Sala (sub-area 4).

Analytical results and interpretation of geochronological data

The zircons are colourless, yellow or partly yellow. Many grains are euhedral with sharp edges and terminations. Length to width ratios are approximately 1.5 to 3, but longer grains are also present. Cores are common in the zircon grains and these show euhedral or less commonly rounded, anhedral boundaries. Most grains are relatively poor in quality and are both fractured and metamict.

Four zircon fractions were analysed. These were selected on the basis of differences in the general analytical quality of the zircon grains related to the frequency of fractures or inclusions. There is a general decrease in quality of these grains from fraction 1 to fraction 4.

The analytical results are presented in Table VI and a U-Pb concordia diagram is shown in Figure VI. All fractions plot closely together in the concordia diagram. The $^{207}Pb/^{206}Pb$ age for fraction 2 is somewhat higher and this fraction plots somewhat to the right of the other three fractions on the concordia digram. It is tentatively inferred that fraction 2 contains older inherited zircon material and, for this reason, data from this fraction were excluded from the age determination.

Since zircon fractions 1, 3 and 4 plot close to each other in the concordia diagram, conforming to a single point, the discordia line was defined assuming a fixed lower intercept. A value of 200±200 Ma was initially chosen. On the basis of this assumption, the upper intercept age is 1896^{+6}_{-5} Ma and the MSWD value for the fitted line is 0.66. If the uncertainty in the lower intercept age is increased to 400 Ma, then the uncertainty in the upper intercept age changes to +13/–8 Ma. An assumed lower intercept of 0±200 Ma yields an upper intercept of 1892^{+5}_{-4} Ma and a MSWD value of 0.28 (Fig. VI). As can be seen, there is relatively little variation in the ages obtained from the different models. Bearing in mind the field relationships described above, the younger age of 1892^{+5}_{-4} Ma, which

Table VI. U-Pb TIMS isotopic data for zircons from a felsic subvolcanic intrusion, Sala (sub-area 4).

Fraction	No. of crystals	Weight (µg)	U (ppm)	Pb_{tot} (ppm)	Common Pb (ppm)	$^{206}Pb/^{204}Pb$	^{206}Pb–^{207}Pb–^{208}Pb (atom %)	$^{206}Pb/^{238}U$	$^{207}Pb/^{235}U$	$^{207}Pb/^{206}Pb$ age (Ma)
1	8	16.9	206.2	72.8	0.61	5123	80.8–9.3–9.9	0.3287±9	5.244±18	1891±3
2	8	14.4	182.0	63.6	0.50	5513	81.3–9.5–9.3	0.3275±11	5.261±22	1903±4
3	6	16.5	240.3	84.4	0.79	4797	81.1–9.4–9.5	0.3282±16	5.237±27	1891±3
4	5	14.4	251.1	87.3	0.51	7464	81.2–9.4–9.4	0.3263±8	5.209±16	1893±3

corresponds to the $^{207}Pb/^{206}Pb$ age, is inferred to represent the igneous crystallization age of the subvolcanic intrusion at Sala.

FELSIC METAVOLCANIC ROCK, DANNEMORA, NORTHERN UPPLAND (SUB-AREA 6)

Rock	Felsic metavolcanic rock, pyroclastic mass flow deposit
Sample number	OIL991076A
Coordinates (RT 90)	6678820/1614300
Map sheet	12I Östhammar NV
Locality	Dannemora mine area, Dannemora, northern Uppland
Project	Regional project Bergslagen (code 2412)

The aim of this geochronological study was to determine the timing of the changeover from the intense volcanism and extension stage to the waning volcanic stage in sub-area 6 (see Fig. 28 in the main text) of the Svecofennian felsic metavolcanic rocks in the Bergslagen region. The data also contribute to a better understanding of the lateral variation in age of the waning stage of volcanic activity in different sub-areas in Bergslagen. They also provide some constraints on the timing of formation of the major iron oxide deposit in manganese-rich skarn or crystalline carbonate rock at Dannemora, which is hosted by the metavolcanic rock and marble deposited during the waning volcanic stage.

Sample description

The uppermost accessible, pyroclastic mass flow deposit at Dannemora was sampled immediately east of the lake Gruvsjön in the Dannemora mine area, northern Uppland (see Fig. 14 in the main text and stop 1-1 in the excursion guide). The sample was taken within a few metres from the contact to a younger, accretionary lapilli-bearing, volcanic metasiltstone. The sampled rock contains c. 10% unevenly distributed quartz phenoclasts that are c. 1 mm in size and are surrounded by a submicroscopic, sericite-rich matrix. The metavolcanic rock has a rhyolitic to dacitic composition. The homogeneous, unbedded structure, the uneven quartz phenoclast distribution and some possible pumice clasts all suggest that this unit was derived from a juvenile, pyroclastic mass flow deposit. For this reason, it is considered that a zircon crystallization age should date emplacement of the mass flow deposit.

Analytical results and interpretation of geochronological data

The zircons are small, colourless and mostly short prismatic, with length to width ratios around 1 to 3. More elongate grains with a length to width ratio around 4 to 5 are also present. Most crystals have faces with low-order crystallographic indices but high-index faces are found on some of the shorter grains. Texturally complex, core–rim relations are generally not visible under the optical microscope.

Five zircon fractions were analysed. These were selected on the basis of differences in grain size and the general analytical quality of the zircon grains related to the frequency of fractures in the grains. The zircons in fractions 1 and 2 are larger than the zircons in fractions 3, 4 and 5. The zircons in fraction 2 are of somewhat poorer quality than the zircons in fraction 1, with an increased frequency of fractures. The zircons in fraction 4 are of good quality, while the frequency of fractures is higher in fraction 5 relative to that in fraction 3.

The analytical results are presented in Table VII and a U-Pb concordia diagram is shown in Figure VII. Fractions 1, 3, 4 and 5 define a discordia with upper and lower intercept ages at 1894±4 Ma and –89±170 Ma, respectively, and a MSWD value of 0.2. Fraction 2 yields a slightly younger $^{207}Pb/^{206}Pb$ age of 1890±2 Ma (Table VII) and plots to the left of the other fractions on the concordia diagram (Fig. VII). The upper intercept age defined by fractions 1, 3, 4 and 5 is inferred to represent the timing of emplacement of this pyroclastic mass flow deposit.

Table VII. U-Pb TIMS isotopic data for zircons from a pyroclastic mass flow deposit, Dannemora (sub-area 6).

Fraction	No. of crystals	Weight (µg)	U (ppm)	Pb_{tot} (ppm)	Common Pb (ppm)	$^{206}Pb/^{204}Pb$	^{206}Pb–^{207}Pb–^{208}Pb (atom %)	$^{206}Pb/^{238}U$	$^{207}Pb/^{235}U$	$^{207}Pb/^{206}Pb$ age (Ma)
1	5	10.2	195.1	67.1	0.97	3194	82.4–9.6–8.0	0.3249±15	5.197±26	1895±4
2	17	31.8	174.5	61.0	0.05	31121	82.2–9.5–8.3	0.3338±21	5.322±34	1890±2
3	40–50	25.8	223.2	78.6	0.03	43380	81.6–9.5–8.9	0.3338±28	5.339±45	1895±2
4	9	9.4	158.1	52.9	0.07	11265	82.5–9.6–7.9	0.3210±16	5.139±27	1897±3
5	14	10.6	200.0	68.6	0.07	15451	82.1–9.5–8.4	0.3268±26	5.230±42	1897±2

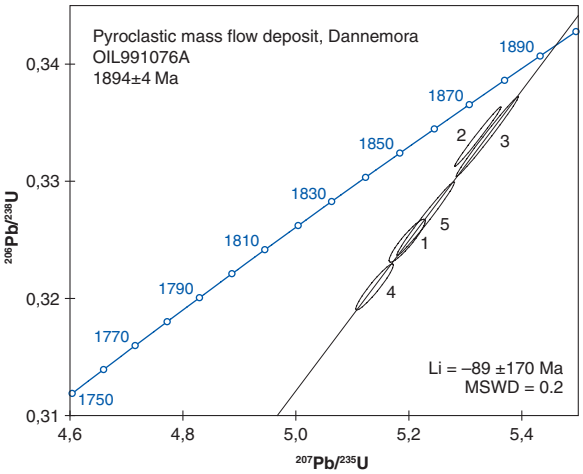

Fig. VII. Concordia diagram showing the U-Pb TIMS data for zircons from a pyroclastic mass flow deposit, Dannemora (sub-area 6). Li = lower intercept.

METAGRANITOID (GDG INTRUSIVE SUITE) AND APLITIC METAGRANITE IN A COMPOSITE DYKE, FOGDÖSTEN, NORTHERN UPPLAND

Rock	Enclave-bearing metagranitoid (GDG intrusive suite)
Sample number	MBS000130G
Coordinates (RT 90)	6672170/1666390
Map sheet	12J Grisslehamn SV
Locality	Fogdösten
Project	Regional project Bergslagen (code 2412)

Rock	Aplitic metagranite in composite dyke
Sample number	MBS000130A
Coordinates (RT 90)	6672170/1666390
Map sheet	12J Grisslehamn SV
Locality	Fogdösten
Project	Regional project Bergslagen (code 2412)

This geochronological study was designed to acquire more data bearing on the timing of emplacement of the Granitoid-dioritoid-gabbroid (GDG) compositional suite of meta-igneous rocks in the north-eastern part of the Bergslagen region and the timing of emplacement of dykes that intrude these GDG rocks. A locality exposing critical field relationships between deformed GDG rocks, metadolerites and composite dykes was selected for this study. The dykes are inferred to belong to the dyke swarm generally referred to as the *Herräng dykes* (Magnusson 1940).

Sample description

On the small island of Fogdösten (see Fig. 14 in the main text), south of Singö, in north-eastern Uppland, the bedrock is dominated by a GDG-type metagranitoid that contains abundant, flattened mafic enclaves

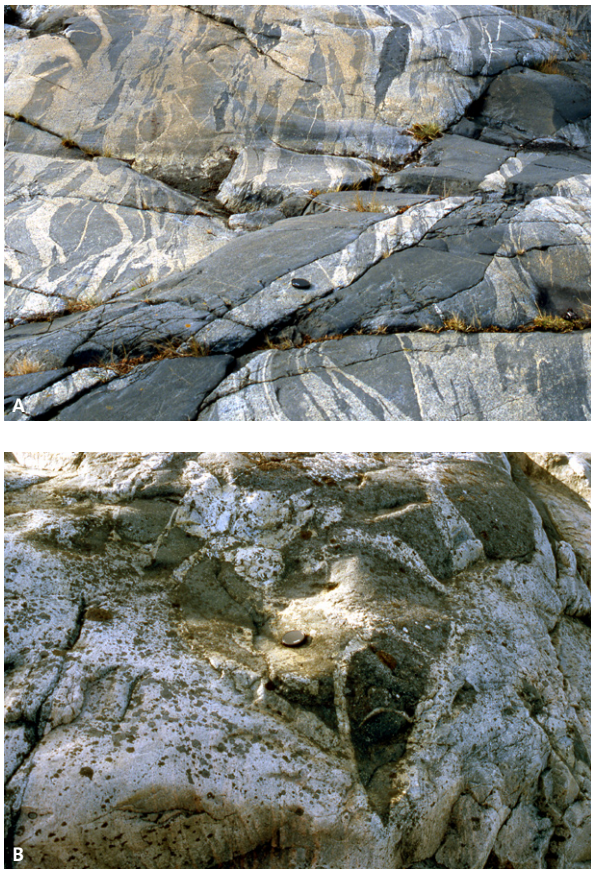

Fig. VIII. Field relationships at Fogdösten, northern Uppland. **A.** Hornblende-phyric metadolerite, inferred to belong to a younger group of *Herräng dykes* (Magnusson 1940) at this locality (see the section "Metadolerite" in the main text), are discordant to the tectonic foliation in a GDG metagranitoid that contains abundant, flattened mafic enclaves. Zircons and monazites from the enclave-bearing, GDG metagranitoid were separated for U-Pb geochronology. **B.** Composite dyke that intrudes the enclave-bearing, GDG metagranitoid. The aplitic metagranite in the composite dyke shows a diffuse banding and is inferred to belong to an older group of *Herräng dykes* at this locality. The ductile strain in this composite dyke is not distinguishable from the ductile strain in the enclave-bearing GDG metagranitoid. Zircons from the aplitic metagranite in the composite dyke were separated for U-Pb geochronology.

(Fig. VIIIa). This rock is intruded by different generations of metadolerite (Fig. VIIIa), including a composite dyke with metadolerite and diffusely banded, aplitic metagranite components (Fig. VIIIb). The enclave-bearing, GDG metagranitoid and the felsic component in the composite dyke were analysed in the geochronological study.

The enclave-bearing, GDG metagranitoid at Fogdösten contains a conspicuous, steep to vertical tectonic foliation that strikes east-north-east–west-south-west, and a subvertical to vertical lineation. No structural discordance is observed between this rock and structurally older generations of deformed metadolerite, including the composite dyke. By contrast, structurally younger metadolerites show a north-west–south-east to

west-north-west–east-south-east strike and are clearly discordant to the structures in both the metagranitod (Fig. VIIIa) and the older dykes. Although the younger metadolerites are also affected by ductile deformation and metamorphism, they are post-tectonic with respect to the relatively strongly developed, ductile deformational fabric in the host GDG metagranitoid and the older metadolerites and composite dyke, as well as to the orientation of the older dykes. A more detailed description of the different generations of dykes is provided in the section "Metadolerite" in the main text of this report, where the variable field relationships between the enclave-bearing metagranitoid and the mafic or composite dykes are also shown (see Figs. 63b, c and d in the main text).

Analytical results and interpretation of geochronological data

Most of the zircons in the enclave-bearing metagranitoid are pale pink, but some are colourless and a few are brownish in colour. Some grains are euhedral in shape but the majority are rounded and some of the latter are markedly rounded. Length to width ratios are approximately 2 to 4, but longer grains are also present. Nearly all zircons are metamict and fractured. Some grains show zoning. Core–rim relationships, with both rounded and euhedral cores, are common. The monazite crystals are yellow-green in colour, small and anhedral. Most grains are fractured. In contrast to all the zircons, the monazite grains were not abraded prior to analysis.

Five zircon fractions and two monazite fractions were analysed. The zircon fractions were selected on the basis of the distinctness of the zoning (more distinct zoning in fractions 3 and 5), the occurrence of core–rim relationships (weak indications in fractions 1 and 4), the frequency of fractures (fraction 4 shows a higher frequency of fractures) and the frequency of inclusions (small inclusions are conspicuous in fraction 2).

The analytical results are presented in Table VIII and a U-Pb concordia diagram that summarizes all the analyses is presented in Figure IX. The five zircon fractions plot along a discordia with upper and lower intercept ages at 1901±6 Ma and 149±120 Ma, respectively, and a MSWD value of 1.3. The upper intercept age has tentatively been shown on the metamorphic, structural and isotopic age map (Stephens et al. 2007b) as the age of intrusion of this GDG metagranitoid and, for this reason, the metagranitoid has been included in the older, 1.90–1.87 Ga GDG intrusive suite (see the section "Character, spatial distribution, geochronology, geochemical signature, petrophysical characteristics and regional geophysical signature of rock units" in the main text). However, the 1901±6 Ma age must be viewed with caution, bearing in mind the character of the zircons and the possibility that some inherited material may be present, i.e. the inferred age may be too old.

$^{207}Pb/^{206}Pb$ ages for the two monazite fractions are younger than the corresponding ages for the zircon

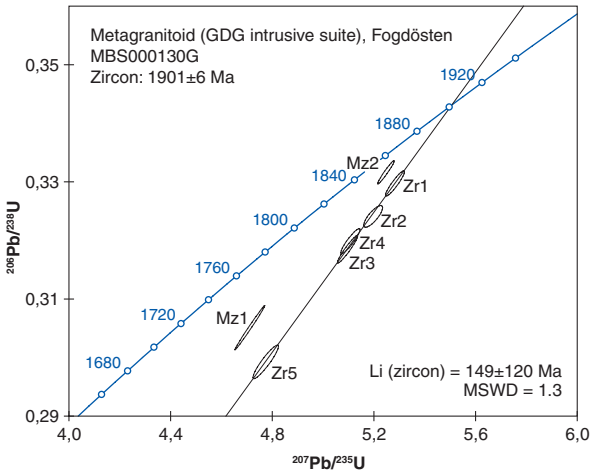

Fig. IX. Concordia diagram showing the U-Pb TIMS data for zircons and monazites from an enclave-bearing metagranitoid in the GDG compositional suite, Fogdösten, northern Uppland. Li = lower intercept.

Table VIII. U-Pb TIMS isotopic data for zircons and monazites from an enclave-bearing metagranitoid in the GDG compositional suite, Fogdösten, northern Uppland.

Fraction	No. of crystals	Weight (µg)	U (ppm)	Pb_{tot} (ppm)	Common Pb (ppm)	$^{206}Pb/^{204}Pb$	^{206}Pb–^{207}Pb–^{208}Pb (atom %)	$^{206}Pb/^{238}U$	$^{207}Pb/^{235}U$	$^{207}Pb/^{206}Pb$ age (Ma)
Zircon										
1	1	5.9	180.6	62.2	0.07	9148	82.5–9.6–7.9	0.3297±18	5.283±30	1899±4
2	3	4.6	148.1	49.9	0.04	6457	82.8–9.6–7.8	0.3241±15	5.197±30	1900±6
3	1	2.9	136.2	44.8	0.13	4184	83.9–9.7–6.4	0.3199±18	5.108±31	1893±4
4	4	3.1	287.5	94.3	0.15	7175	83.6–9.7–6.7	0.3185±19	5.096±32	1896±4
5	3	4.2	234.6	74.6	1.24	2432	82.4–9.5–8.1	0.2993±23	4.774±41	1891±6
Monazite										
1	12	14.2	4456.6	2470.2	1.57	46212	47.6–5.3–47.1	0.3051±31	4.712±48	1832±2
2	1	0.3	11875.8	14752.3	19.11	9046	23.1–2.7–74.2	0.3316±16	5.247±26	1876±2

fractions and are internally inconsistent. Fraction 1 with twelve crystals yields an age of 1832±2 Ma and the single crystal in fraction 2 shows a markedly higher content of uranium and an age of 1876±2 Ma, i.e. closer to the age of intrusion of the enclave-bearing, GDG metagranitoid inferred from the U-Pb (zircon) data. It is inferred that the two monazite fractions represent either different geological events or, more probably, a mix between different geological events. For this reason, no inferences can be drawn from a discordia line between them. It is inferred that the GDG metagranitoid intruded around 1.9 Ga and was affected by a later metamorphic event reflected by the younger monazite fractions. However, a precise age for the timing of this event cannot be determined from the data.

The zircons from the aplitic metagranite in the composite dyke are colourless to grey or brown and all are fractured and metamict. The grains are euhedral and only faces with low crystallographic indices are present.

Four zircon fractions were analysed. These were selected on the basis of differences in grain size and the general analytical quality of the zircons related to the frequency of fractures. For example, radially oriented fractures are present in the outer part of the zircon crystal in fraction 1. Furthermore, the zircons in fractions 3 and 4 are shorter and prismatic in character with length to width ratios of 1 to 2.

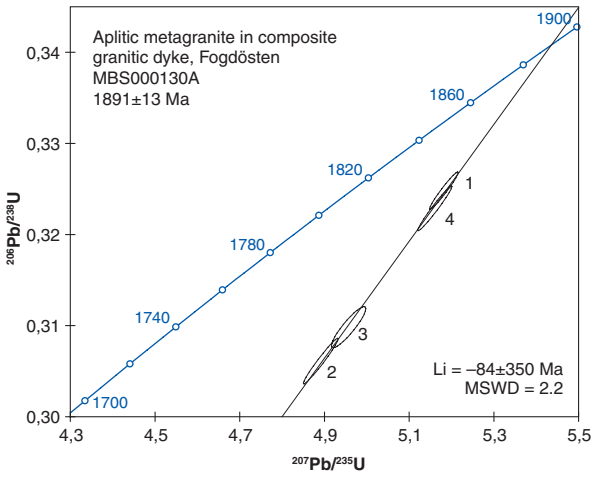

Fig. X. Concordia diagram showing the U-Pb TIMS data for zircons from an aplitic metagranite in a composite dyke, Fogdösten, northern Uppland. Li = lower intercept.

The analytical results are presented in Table IX and a U-Pb concordia diagram is shown in Figure X. Relative to most of the other analyses reported here, the zircons are enriched in uranium. The four fractions define a discordia with upper and lower intercept ages at 1891±13 Ma and –84±350 Ma, respectively, and a MSWD value of 2.2. An estimate of the igneous crystallization age of the composite dyke is provided by the upper intercept age. On the basis of these data, it is inferred that the composite dyke also belongs to the older, 1.90–1.87 Ga GDG intrusive suite.

PORPHYRITIC GRANITE TO QUARTZ MONZONITE (GSDG INTRUSIVE SUITE), NORTH-EAST OF TIERP, NORTHERN UPPLAND

Rock	Porphyritic granite to quartz monzonite (GSDG intrusive suite)
Sample number	MBS000131A
Coordinates (RT 90)	6701181/1595909
Map sheet	13H Gävle SO
Locality	Quarry, north-east of Tierp
Project	Regional project Bergslagen (code 2412)

The aim of this geochronological study was to date a porphyritic granite to quartz monzonite in the so-called *Hedesunda granite*, in the central part of the Bergslagen region, that belongs to the Granite-syenitoid-dioritoid-gabbroid (GSDG) compositional suite of meta-igneous rocks. This igneous body intruded into a bedrock that had already been affected by deformation under amphibolite-facies metamorphic conditions. Locally, migmatitic rocks are spatially associated with the granite (Stephens et al. 2007b). However, the temporal relationship between them is uncertain. The study aimed to date the igneous crystallization of the *Hedesunda granite* and thereby provide some constraints on the timing of deformation and partial melting of the country rock.

Sample description

A coarse-grained, porphyritic granite to quartz monzonite was sampled in a quarry north-east of Tierp (see

Table IX. U-Pb TIMS isotopic data for zircons from an aplitic metagranite in a composite dyke, Fogdösten, northern Uppland.

Fraction	No. of crystals	Weight (µg)	U (ppm)	Pb_{tot} (ppm)	Common Pb (ppm)	$^{206}Pb/^{204}Pb$	^{206}Pb–^{207}Pb–^{208}Pb (atom %)	$^{206}Pb/^{238}U$	$^{207}Pb/^{235}U$	$^{207}Pb/^{206}Pb$ age (Ma)
1	1	3.8	772.1	256.8	0.17	22396	84.1–9.7–6.2	0.3248±17	5.182±28	1891±2
2	5	4.7	568.2	180.6	0.87	7978	83.2–9.7–7.1	0.3061±20	4.891±34	1894±3
3	4	4.5	726.2	234.6	0.59	1518	82.6–9.6–7.8	0.3095±24	4.953±42	1896±6
4	9	3.8	742.4	245.4	0.29	17985	84.1–9.7–6.2	0.3229±20	5.161±33	1894±2

Fig. 14 in the main text and stop 1-8 in the excursion guide). The quarry is situated c. 1.5 km north-west of the contact to migmatitic orthogneiss that shows multiphase ductile deformation. The porphyritic granite to quartz monzonite contains a weak foliation defined by oriented biotite grains, oriented K-feldspar phenocrysts that show little internal deformation and flattened mafic enclaves (see Fig. 66b in the main text). It is intruded by dykes of fine-grained granite and pegmatite (Fig. 66b in the main text) that do not show the internal fabric present in the coarser, porphyritic granite to quartz monzonite.

Analytical results and interpretation of geochronological data

Most of the zircons are metamict and more or less rounded. Only a minority are euhedral with sharp edges. Cores and inclusions are common. However, the three analysed zircon fractions (Table X) are of good analytical quality and devoid of visible cores but show oscillatory zonation. Some fractures are present in fraction 2.

Seven fractions of titanite crystals were analysed (Table X). The colour of the titanite crystals varies from pale to dark brown. All analyses except those of fractions 1 and 3 were carried out on dark crystals. Fractions 1 and 2 were distinguished on the basis of grain size (fraction 2 larger than fracture 1). All recovered titanite grains were anhedral or fragmented.

At an early stage in the geochronological study, only analyses of the three zircon fractions and two titanite fractions (fractions 1 and 2) were available. The $^{207}Pb/^{206}Pb$ ages from these titanites are considerably younger than the $^{207}Pb/^{206}Pb$ ages from the zircons (Table X) and different geological events are represented by these data. The three zircon fractions yielded an upper intercept age of 1868±25 Ma when forced through a lower intercept of 0±400 Ma. The discordia line showed a high MSWD value of 7.4. Due to the high uncertainty in the age, this age was not reported on the metamorphic, structural and isotope age map (Stephens et al. 2007b).

At a later stage in the geochronological study, a complementary set of five more titanite fractions was analysed (fractions 3 to 7 in Table X). The three zircon fractions and the titanite fractions 4, 6 and 7 yielded an upper intercept age of 1863±16 Ma when forced through a lower intercept of 0±400 Ma, with a MSWD value of 3.8 (Fig. XI). As can be seen in Table X, the chemical composition of the younger, titanite crystals in fractions 1, 2 and 3 is different from that of the older, titanite crystals in fractions 4, 5, 6 and 7. In particular, the contents of U and ^{208}Pb (thorogenic lead) is higher in the older titanites. Fraction 5 and possibly also frac-

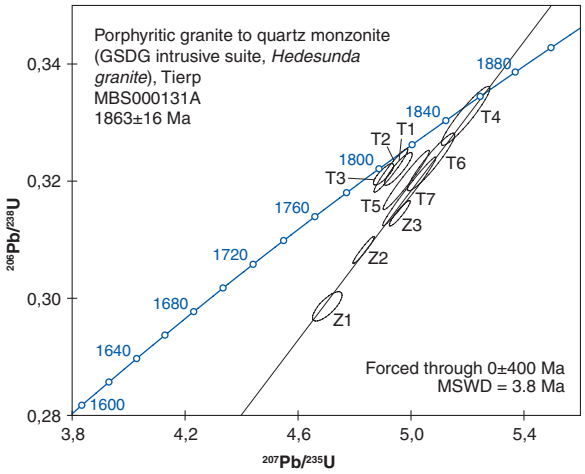

Fig. XI. Concordia diagram showing the U-Pb TIMS data for zircons and titanites from a foliated, porphyritic granite to quartz monzonite in the GSDG compositional suite, north-east of Tierp, northern Uppland.

Table X. U-Pb TIMS isotopic data for zircons and titanites from a foliated, porphyritic granite to quartz monzonite in the GSDG compositional suite, north-east of Tierp, northern Uppland.

Fraction	No. of crystals	Weight (µg)	U (ppm)	Pb_{tot} (ppm)	Common Pb (ppm)	$^{206}Pb/^{204}Pb$	^{206}Pb–^{207}Pb–^{208}Pb (atom %)	$^{206}Pb/^{238}U$	$^{207}Pb/^{235}U$	$^{207}Pb/^{206}Pb$ age (Ma)
Zircon										
1	2	3.3	218.5	72.8	0.61	3251	77.8–8.9–13.3	0.2986±20	4.704±43	1868±11
2	1	3.2	305.9	103.7	0.02	9257	78.3–8.9–12.8	0.3082±19	4.832±31	1859±3
3	2	2.7	305.9	104.7	0.28	5834	79.3–9.1–11.6	0.3145±18	4.960±30	1870±4
Titanite										
1	5	16.3	75.8	25.3	0.80	1398	85.8–9.6–4.6	0.3221±23	4.955±40	1825±7
2	2	23.1	84.7	27.2	0.75	1755	88.4–9.8–1.8	0.3212±15	4.903±29	1811±6
3	9	69.1	90.8	31.7	1.06	1579	82.1–9.1–8.8	0.3218±30	4.929±49	1817±5
4	6	43.9	287.1	137.2	21.23	273	70.7–8.0–21.3	0.3311±41	5.193±70	1860±9
5	6	53.8	231.6	92.0	3.11	1388	72.1–8.1–19.8	0.3215±36	5.003±58	1846±6
6	4	66.6	312.7	136.9	8.85	676	68.0–7.7–24.3	0.3233±40	5.071±68	1861±8
7	4	96.5	256.9	102.4	3.38	1408	71.1–8.1–20.8	0.3183±48	4.994±77	1861±5

tion 1 probably consist of both older and younger material, i.e. they give rise to mixed ages.

The geological implications of these data are threefold:

- The age of 1863±16 Ma is consistent with the U-Pb (zircon) age of 1869±9 Ma for a quartz monzodiorite from the southern part of the *Hedesunda granite* (Bergman et al. 2004). The 1863±16 Ma age is inferred to represent the best estimate of the timing of igneous crystallization of the porphyritic granite to quartz monzonite close to Tierp. Bearing in mind the composition, field character and age of both these dated rocks, it is inferred that they belong to the 1.87–1.84 Ga GSDG intrusive suite in the Bergslagen region. They are considerably older than the U-Pb (zircon, titanite) age of 1782±5 Ma obtained for the igneous crystallization of a granite in the type area close to Hedesunda (Persson & Persson 1997). Clearly, the *Hedesunda granite* consists of different igneous suites emplaced at different times.
- The penetrative fabric development and amphibolite-facies metamorphism in the country rock to the *Hedesunda granite* close to Tierp formed prior to emplacement of the igneous rocks in this complex at 1863±16 Ma (or 1869±9 Ma according to the dating in Bergman et al. 2004). These results are consistent with the U-Pb (zircon) dating and intrusion–deformation relationships for the younger suite of GDG intrusive rocks (group C in Stephens et al. 2003) in the Forsmark area to the east (Hermansson et al. 2008).
- The younger titanite fractions represent a later metamorphic event around 1.8 Ga. These data are also consistent with the U-Pb (titanite) data in the Forsmark area (Hermansson et al. 2008).

ANATECTIC, GARNET-BEARING, LEUCOCRATIC METAGRANITOID (GP INTRUSIVE SUITE) IN MIGMATITIC PARAGNEISS, HANINGE

Rock	Anatectic, garnet-bearing, leucocratic metagranitoid (GP intrusive suite)
Sample number	MBS000132A
Coordinates (RT 90)	6562425/1633335
Map sheet	10I Stockholm SO
Locality	Haninge, southern part of Stockholm
Project	Regional project Bergslagen (code 2412)

The aim of this geochronological study was to date the igneous crystallization age of a garnet-bearing, leucocratic metagranitoid in a migmatitic paragneiss, in order to provide some constraints on the timing of migmatization in the south-eastern part of the Bergslagen region that belongs to the southern migmatitic metamorphic domain (see the section "Deformation, metamorphism and mechanism of emplacement of the 1.87–1.84 Ga GSDG suite of intrusive rocks" in the main text). The garnet-bearing leucogranitoid belongs to the Granite-pegmatite (GP) intrusive suite in the Bergslagen region.

Sample description

The dated sample at Haninge (see Fig. 14 in the main text) is a garnet-bearing, leucocratic metagranitoid (Fig. XIIa) that occurs as larger lenses and thinner sheets or veins in a migmatitic paragneiss. The leucocratic metagranitoid is interpreted as a product of anatexis in a region where both sedimentary rocks and GDG granitoids are affected by high-grade metamorphism (Stålhös 1969). The dated leucocratic metagranitoid is affected by a distinctive linear grain-shape fabric (Fig. XIIb) that plunges gently towards the east-northeast. The occurrence of similar leucocratic sheets or veins both along the axial surface traces of mesoscopic folds and as folded entities (Fig. XIIc) suggests that the leucocratic metagranitoid is broadly syntectonic in character, i.e. it formed during regional deformation. The migmatite consists of flattened inclusions of inferred metasedimentary rock in a diatexite that is partly gneissic in character (Fig. XIId).

Analytical results and interpretation of geochronological data

The garnet-bearing, leucocratic metagranitoid contains both zircon and monazite crystals and both these minerals were dated. Most zircons are pale to dark brown in colour. Length to width ratios are generally 1 to 5. Some zircons have sharp edges but most grains are more or less rounded, metamict and rich in fractures. The majority of zircons contain cores or overgrowths and the cores are either euhedral or rounded.

Three zircon fractions were analysed. The zircons in fraction 1 are magnetic. They were chosen since they were less rounded than the non-magnetic zircons and did not show any cores or overgrowths. The grains in this fraction are elongate with length to width ratios of 3 to 8 and are only slightly metamict. This fraction was not abraded, since the elongate shape of the crystals renders them more prone to breakage rather than abrasion. The zircons in fractions 2 and 3 are non-magnetic and the zircons in fraction 3 are partly metamict. Fractions 2 and 3 were strongly abraded prior to analysis.

Fig. XII. Field relationships at the sampled locality, Haninge, Stockholm. **A.** Garnet-bearing, leucocratic metagranitoid sampled for U-Pb (zircon, monazite) dating purposes. **B.** Linear grain-shape fabric in the sampled garnet-bearing, leucocratic metagranitoid. **C.** Leucocratic metagranitoid as both folded sheets or veins and as an occurrence along the axial surface trace to a mesoscopic fold in diatexite. **D.** Inclusions of inferred metasedimentary rock in diatexite.

Two monazite fractions were analysed. The monazite grains are greenish yellow, and both clear and turbid crystals are present. The majority of crystals are rounded and most are oblate in shape. The monazites in fraction 2 are smaller and paler than those in fraction 1. The monazites were not abraded prior to analysis.

The analytical results are presented in Table XI and a U-Pb concordia diagram that summarizes all the analyses is presented in Figure XIII. If a discordia line is constructed through the two data points defined by the zircon fractions 1 and 3 (Fig. XIII), the upper and lower intercept ages on the concordia are 1877±5 Ma and 258±94 Ma, respectively. If a discordia line is constructed through the essentially two data points defined by the zircon fraction 2 (single crystal) and the two monazite fractions (Fig. XIII), the upper and lower intercept ages on the concordia are 1838^{+9}_{-5} Ma and 339±350 Ma, respectively. The significance of such discordia lines is highly questionable, bearing in mind the occurrence of only two points along each line. It is apparent that the interpretation of the results of this study is uncertain.

One possible interpretation is that the older $^{207}Pb/^{206}Pb$ ages from zircon fractions 1 and 3 represent the formation of the garnet-bearing, leucocratic metagranitoid at or prior to 1.87–1.86 Ga, while the younger $^{207}Pb/^{206}Pb$ ages from monazites and zircon fraction 2 represent subsequent deformation and metamorphism around 1.8 Ga. A second possibility is that the zircons in fractions 1 and 3 represent grains inherited from the source rock to the leucocratic metagranitoid with ages greater than 1.86 Ga and that the leucocratic metagranitoid actually formed around 1.8 Ga during regional deformation and metamorphism, including migmatization, as represented by the monazites and zircon fraction 2. A third possibility, favoured here, is that the zircon and monazite ages are the result of a mix between different geological events prior to 1.86 Ga and around 1.8 Ga.

A protolith age of 1838^{+9}_{-5} Ma was presented on the structural, metamorphic and isotope age map for Bergslagen (Stephens et al. 2007b). Although the geochronological work has provided some constraints, the igneous crystallization age of this garnet-bearing leucogranitoid and the timing of migmatization are not

Table XI. U-Pb TIMS isotopic data for zircons and monazites from an anatectic, garnet-bearing, leucocratic metagranitoid in migmatitic paragneiss, Haninge.

Fraction	No. of crystals	Weight (µg)	U (ppm)	Pb_{tot} (ppm)	Common Pb (ppm)	$^{206}Pb/^{204}Pb$	^{206}Pb–^{207}Pb–^{208}Pb (atom %)	$^{206}Pb/^{238}U$	$^{207}Pb/^{235}U$	$^{207}Pb/^{206}Pb$ age (Ma)
Zircon										
1	12	9.5	943.2	283.5	1.20	11933	87.8–10.0–2.2	0.3055±17	4.798±27	1863±2
2	1	4.4	655.6	201.9	0.20	19689	88.9–10.0–1.1	0.3183±15	4.914±24	1832±2
3	3	7.3	640.7	201.8	0.52	15619	88.3–10.1–1.6	0.3228±13	5.094±22	1871±2
Monazite										
1	1	6.6	2082.5	5865.2	6.41	5025	10.0–1.1–88.9	0.3235±16	5.000±26	1834±2
2	4	7.1	1740.3	3972.8	1.50	18513	12.3–1.4–86.3	0.3234±13	5.002±21	1835±2

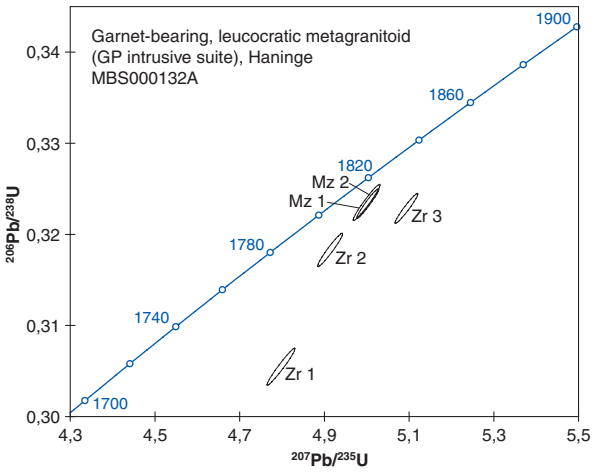

Fig. XIII. Concordia diagram showing the U-Pb TIMS data for zircons and monazites from an anatectic, garnet-bearing, leucocratic metagranitoid in migmatitic paragneiss, Haninge.

resolved. More detailed U-Pb SIMS work is needed to reduce the uncertainties recognized here.

REFERENCES

Allen, R.L., Lundström, I., Ripa, M., Simeonov, A. & Christofferson, H., 1996: Facies analysis of a 1.9 Ga, continental margin, back-arc, felsic caldera province with diverse Zn-Pb-Ag- (Cu-Au) sulfide and iron oxide deposits, Bergslagen region, Sweden. *Economic Geology 91*, 979–1008.

Bergman, S., Persson, P.-O., Delin, H., Stephens, M.B. & Bergman, T., 2004: Age and significance of the Hedesunda granite and related rocks, south-central Sweden. *Abstract 26th Nordic geological winter meeting, GFF 126,* 18–19.

Hermansson, T., Stephens, M.B., Corfu, F., Page, L.M. & Andersson, J., 2008. Migratory tectonic switching, western Svecofennian orogen, central Sweden: Constraints from U/Pb zircon and titanite geochronology. *Precambrian Research 161*, 250–278.

Lundström, I., 1995: Beskrivning till berggrundskartorna Filipstad SO och NO. *Sveriges geologiska undersökning Af 177, 185*, 218 pp.

Lundström, I., Allen, R.L., Persson, P.-O. & Ripa, M., 1998: Stratigraphies and depositional ages of Svecofennian, Paleoproterozoic metavolcanic rocks in E. Svealand and Bergslagen, south central Sweden. *GFF 120*, 315–320.

Magnusson, N.H., 1940: Herrängsfältet och dess järnmalmer. *Sveriges geologiska undersökning C 431*, 78 pp.

Persson, L. & Persson, P.-O., 1997: U-Pb datings of the Hedesunda and Åkersberga granites of south-central Sweden. *GFF 119*, 91–95.

Ripa, M., Kübler, L., Persson, L. & Göransson, M., 2002: Beskrivning till berggrundskartan och bergkvalitetskartan 11G Västerås NO. *Sveriges geologiska undersökning Af 217*, 70 pp.

Stålhös, G., 1969: Beskrivning till Stockholmstraktens berggrund. *Sveriges geologiska undersökning Ba 24*, 190 pp.

Stephens, M.B., 1998: Bedrock map 10E Karlskoga NO, scale 1:50 000. *Sveriges geologiska undersökning Af 184*.

Stephens, M.B., Lundqvist, S., Ekström, M., Bergman, T. & Andersson, J., 2003: Forsmark site investigation. Bedrock mapping. Rock types, their petrographic and geochemical characteristics, and a structural analysis of the bedrock based on stage 1 (2002) surface data. *Svensk Kärnbränslehantering AB P-03-75*, 133 pp.

Stephens, M.B., Ahl, M., Bergman, T., Lundström, I., Persson, L., Ripa, M. & Wahlgren, C.-H., 2007b: Regional geological and geophysical maps of Bergslagen: Metamorphic, structural and isotope age map. *Sveriges geologiska undersökning Ba 58:2*.

Geological Survey of Sweden
Box 670
SE-751 28 Uppsala
Phone: +46 18 17 90 00
Fax: +46 18 17 92 10
www.sgu.se

Uppsala 2009
ISSN 0373-2657
ISBN 91-7158-883-8
Tryck: AB Danagårds Grafiska, Ödeshög